THE UNIVERSITY OF NEWCASTLE UPON-TYNE

DEPARTMENT OF CIVIL ENGINEERING

THE FATIGUE CHARACTERISTICS OF PRECAST CONCRETE RAFT UNITS

A Thesis submitted for the degree of

DOCTOR OF PHILOSOPHY

by

YOUSEF BASHIR LUHESHI

B.Sc., M.Sc., MASCE.

OCTOBER 1997

Acknowledgments

The author wishes to thank the Secretary of Communications, Libya, for the financial support offered to him. He would like to thank all his past and present colleagues in the Civil Aviation Authority in Libya for their support and help.

The author wishes to express his deep gratitude to Mr. A. I. B. Moffat and his present supervisor Mr. A. H. Rhodes for their support and encouragement. I wish to offer my special thanks to them for their invaluable guidance and advice during the late stages of this work.

His thanks are forwarded to Professor M. Pescod, Head of Department, Dr. Evan K. S. Passaris, Postgraduate Sub-Dean, and Mr. D. J. Buck, Senior Assistant Registrar.

Grateful thanks are also due to Professor J. Knapton for his assistance and his expert guidance in technical matters during the correction stage. Also thanks to the secretary of the structure group Mrs D. Baty for her cooperation and help.

The author is also indebted to the following members of the technical staff Mr. J. Moor (superintendent), Mr. A. Jefferson, Mr. K. Scholefield, Mr. W. Gragie, Mr. G. Stacey and Mr. E. Armstrong (retired Superintendent). Also many thanks to Mr. R. Fern, Engineering Liaison Librarian and all the staff of the library for their help.

The author is grateful to Sir Alexander Gibb & Partners for their technical help and allowing him to use their library for this research.

The author is grateful to the Redland Aggregates and its general production manager Mr. P. Hastings, for supplying the Raft Units and some other relevant information.

Special thanks and gratitude are also due to the many friends who helped and encouraged me, in particular Abdulmoun, Abdulrauf, Ahmed, Amjad, Gamel, Karim, Otman, Paul, Sami and Talal. Many thanks to my friend Mr Essam Korban for his help and writting the computer programme of the emperical formula. Very special thanks and appreciation are due to my neighbors George & Wendy Stacey, who have become part of my family. They encouraged me in my work through very difficult circumstances.

The author is to acknowledge any early assistance offered to him by his initial supervisor Dr. J. W. Bull.

The author wishes to acknowledge that without the unfailing support of his parents, his brother and his wife, his sister, and his family in law, it would not have been possible to complete this work. He offers this work to them for their encouragement, love, sacrifices, and endurance.

And last but not least, the author wishes to express his deepest gratitude to his wife Wedad and his children Raaef, Mohamed Rifaee, Nuria and Bashir who have untiringly offered him the greatest support, encouragement and the patience in tolerating all the inconveniences he caused to them while he was carrying out this work.

ABSTRACT

This research project represents a continuation of the research programme into Precast Concrete Pavement Units, "P.C.P.U.", which is based in the Department of Civil Engineering at the University of Newcastle upon Tyne. The units were referred to as raft units throughout the thesis which focused on the use of raft units as a full concrete paving system for aircraft parking, taxiway, and other low speed areas, at airports.

The physical full scale test model was designed and constructed to represent the applied loading from one of the dual wheel legs of the design aircraft, a Boeing 727-200, when it is taxiing over a raft unit paving system. It was only possible for the test model to be provided with a contact area of 200 mm square compared to the real life of 400 mm square. A theoretical correction was applied to allow for this difference. Sixteen raft units were tested in pairs using the test model. The tests were divided into three modules to investigate the effect of the raft unit dimensions, Module(M1); the reinforcement design, Module(M2); and the raft thickness, Module(M3). The twin loading assembly applied a repetitive dynamic load which was moved manually between four different loading positions to represent the aircraft moving across the raft units.

The primary aim of the experimental programme was to identify for the first time the fatigue life and failure mechanisms of the raft units under the influence of twin dynamic moving loads, and provide experimental results to enable a more refined numerical design method to emerge for raft units, as well as to determine the causes of failures and to recommend remedial measures. Observations were made of vertical deflection, concrete strains, crack widths and crack patterns, failure load, and failure modes, each of which were described in detail.

The test observations showed that by increasing each of the following variables, namely, the aspect ratio, the amount of steel bar reinforcement and the thickness of the raft units, resulted in each case in an extension of raft unit life. It was found that some form of uplift restraint on the raft unit should be added to improve the fatigue life for one of the loading positions and that fibre reinforcement should not be used.

The ultimate load capacity of the raft units was influenced by the loading position, the applied load level and the number of load repetitions, together with the crack patterns. Using the results from the raft units that had failed within a specific module, it was

possible to predict the ultimate and reserve load capacity of raft units within the modules that were only partially fatigued.

Four important conclusions have been established during the research project. Firstly, based on the test results, an empirical relationship was derived using regression analysis, relating the number of load repetitions to the aspect ratio, the amount of reinforcement, the raft thickness, and the applied loading. This will need further verification, but it should eventually be very useful when estimating the fatigue life of these specific raft unit models. Secondly, a new design method has been proposed. The design methods for raft units proposed previously by Bull, Ismail, Annang, Ackroyd, and the British Port Association were reviewed. The test results enabled a new design method to be developed which was based on Bull's method but proposed new design charts and tables for each of the raft units considered in the research project which introduced the additional variables of contact pressure and the exact loading position. Thirdly, the measured strains were used to develop strain fatigue relationships for designing raft units and estimating the reserve design life in a raft unit paving system for the purpose of maintenance management by relating the accumulated number of load repetitions of a design load to the permissible concrete strain. The strain fatigue equations were generated for each of the raft units considered in this research project. Thus, the most realistic way to control raft unit distress is through the use of a predictive fatigue model. This should prove invaluable to those involved in the maintenance of raft unit paving systems. Finally, life cycle cost analysis was conducted for three types of construction pavement (paving blocks, PQC, and raft units). The analysis demonstrated that the precast concrete raft units will become a viable alternative to conventional pavement construction and a real competitive to the concrete paving blocks.

Notation

Unless otherwise defined, the meanings of the following symbols are as follows:

a	Radius of contact area.
b	Effective width of section.
MR	Modulus of rupture.
BM	Bending moment.
M_{uls}	Resistance bending moment at the ultimate limit state.
BPA	British Ports Association.
c	Constant which is a function of contact pressure.
CBR	California Bearing Ratio.
D	Pavement damage.
d_e	Effective depth.
E	Modulus of elasticity.
E_b	Modulus of elasticity of base material.
E_h	Allowable base horizontal tensile strain.
E_s	Modulus of elasticity of steel.
f_c	Characteristic compressive strength of concrete.
f_y	Steel yield strength.
H	Overall depth of section.
I	Second moment of area.
k	Modulus of sub-grade reaction.
h	Thickness of the raft.
L_x	Length of the raft.
L_y	Width of the raft.
LCI	Load classification index.
N	Number of load repetitions.
N_{calc}	Number of load repetitions from charts.
N_{exp}	Number of load repetitions from experiment.
N_m	Equivalent number of the maximumnumber of load repetitions.
N_{sg}	Number of load repetitionsbefore pavement needs relevelling.
N_{st}	Number of load repetitions before raft needs replacement.
N_{ed}	Ratio of equivalent load cycles to design load cycles.
P	Tyre pressure.
PAWL	Port are wheel load.
P_m	Maximum contact pressure.
PUS	Percentage ultimate concrete stress.
r	Radius.
SGBP	Sub-grade bearing pressure.
P_u	Ultimate pressure due to load W, in KN/m^2.
V	Shear stress due to applied load.
v	Shear stress.
vc	Ultimate shear stress.
W	Applied load.
W_m	Maximum applied load.

Z	Lever arm.
ν	Possion's ratio.
σ	Ultimate tensile stress of the concrete pavement.
$\sigma_{'L}$	Flexural tensile stress induced in a pavement by a load of magnitude L.
$\sigma_{'c}$	Concrete stress at corner.
$\sigma_{'e}$	Concrete stress at edge.
$\sigma_{'i}$	Concrete stress at interior.
ϕ	Bar size.
W_a	Ultimate punching shear load for raft/polystyrene.
W_b	Ultimate punching shear load for raft/Type 1 fill.
R	Stress ratio.
α	Angle of load dispersion.
$\varepsilon_{'f}$	Failure strain.
$\varepsilon_{'L}$	Strain corresponding to 1,000 cycles for a particular load.
t	Tonne, 1t = 10KN.
T	Total number of applied load cycles on the test raft model.
P1	Loading position one.
P2	Loading position two.
P3	Loading position three.
P4	Loading position four.
G	Strain gauge transducers.
LVDT	Linear variable differential transformer.
•	Locations of the LVDT's (0 to 15)
–	Locations of the G (a to P).
a.c.	Alternating current.
d.c.	Direct current.
F.O.S	Factor of safety

Units of Measurements

1ft = 30.48cm = 0.3048m
1in = 2.54cm = 25.4mm
$1ft^2$ = $0.0929m^2$

1tonne = 10KN.
1tonne = 1000kg.
2.2lb = 1kg.

$1lb/ft^3$ = $160.3kg/m^3$.
$1lb/in^2$ = $0.07031kg/cm^2$ =0.006895MPA.
$1N/mm^2$ = 1MPA.

TABLE OF CONTENTS

Chapter -one

INTRODUCTION

1.1 BACKGROUND

There are three phases involved in providing airfield pavements: the planning the pavement design and the construction works. Planning is the process of site selection and the design of the layout to meet the internationally accepted standards for the layout of airfields. Pavement design, the second phase, is the determination of the composition of the pavements to carry the tyres, movements and weights of aircrafts which are planned or expected to use the airfield. The construction phase is to ensure that the designed pavement is constructed according to the design specification. Pavement designs are broadly the same for both civil and military airfields; in detail however, there are some differences. Civil aircraft have lower tyre pressures and relatively slower landing speeds when compared to military aircraft; also, the aircraft movement rates are generally much higher than those at military airfields.

All trafficked areas must be surfaced in some form to keep aircraft maintenance to a reasonable level and to maintain all year operations. The essential qualities of the majority of paving systems are their strength, durability, and the ride-quality of their surface. For the safe operation of aircraft, pavements must not break up through over-loading, fuel spillage and jet blast attack, or by environmental effects, and in this way avoid loose materials that would create a hazard. The main aim for pavement design should be for the pavement to be as maintenance free as possible particularly at heavy trafficked airports with limited facilities such as a single runway. Major works extending over periods of weeks, for example, are so highly disruptive to traffic schedules that they should be avoided as far as possible. With such difficulties in mind, the designer attempts to provide pavements which will remain safe for the longest possible time, and a pavement life of at least 20 years initially without major maintenance works should be a prime objective. The length of the initial design life of 20 years, sometimes, is chosen to minimise the whole-life pavement cost. Some clients specify a design life up to 40 years, in this case, designers should bear in their mind the economic design life [see Section 4.7].

Precast concrete technology is well-established in many fields of construction which involves precast concrete pavement units being manufactured in a plant and then erected on-site. Concrete pavements typically consist of many slabs of identical dimensions

which make them ideal structural members for precasting. Precast concrete pavement units are normally prefabricated off-site and are commonly called raft units. The raft units are made of dense reinforced or unreinforced concrete, bound at the top edges by a steel angle frame, which protects the top edges from spalling. Some of the raft units are fabricated without the steel angle frame. Steel fibre reinforced concrete can be used as an alternative reinforcement. The combination of plan dimensions, thickness and weight is such that heavy surface loads can be evenly distributed through the lower pavement layers. Raft units vary in size from 1.0m square to 3.2m by 5.3m and occasionally even up to 10.0m by 2.29m. Aspect ratios, that is the ratio between the width and the length of a raft unit, have been between 0.25 and unity with a thickness of between 75 mm and 220 mm. Most practical work specifies raft units of 2m square in plan (Bull, 1991). A square raft unit of sufficient dimension (i.e. 2m and over) to allow two way bending to develop and designed with structural reinforcement, is structurally more efficient than a long, narrow raft that bends predominately in one direction like a beam. The size and shape of a paving area necessitates the provision of some special sized and shaped raft units which are designed to meet specific needs.

The use of raft units has developed rapidly since the early 1960's. Raft units have been used for temporary roads, airfield and highway repairs, port container terminals, and pavements subjected to heavy industrial traffic. Their use has been increasing, particularly where settlement is high due to low bearing capacity soils, and, also where rapid construction is required. Consequently, in these conditions, the raft units have distinct advantages over other forms of pavements as they can easily be laid, moved, and re-used. They offer major advantages for pavement repairs. Traffic is only interrupted during the repair period, and as soon as the repair is completed, the pavement can be reopened to traffic. A notable example of such a repair was in 1981 at San Diego's Lindbergh Field, USA. During this effort, 116 damaged slabs were replaced, at night, with raft units, while the airfield was kept open to traffic during the day. The use of the raft units minimises the operational disturbances and maintenance costs, and allows the airport to continue operation during period of maintenance. Other advantages include:

(i.) they can be easily re-levelled if there should be settlement of the sub-soil;

(ii.) they can be taken up and re-laid where required; for example, they allow easy access to underground services without damage to the paving system; and

(iii.) they provide easy replacement if damage occurs, eliminating the high cost and interference of excavation in-situ paving.

The shape of the raft units is predominantly rectangular, although hexagonal shapes have been cast. Steel fabric and steel fibre reinforcement as well as prestressed concrete have been used in Europe, and USA (Bull, 1991). Unreinforced precast concrete hexagons, of 1.25m long and from 100 mm to 140 mm thick; and for heavier aircraft 1.5m long and from 140 mm to 200 mm thick, were used for the first concrete airfields in the former Soviet Union in 1931-32. Orly airport, Paris, France, in 1947-1958 was the first airfield to use precast prestressed concrete pavement slabs of triangular shape with side lengths of 1m and a thickness of 160 mm. In 1956, a 61m square section of airport pavement was constructed at Finningley, England, UK, of 9.1m by 2.7m precast prestressed slabs that were 150mm thick. In 1958, a taxiway at Melsbroek, Brussels, was constructed of 1.25m by 12m precast prestressed slabs, that were 75 mm thick.

The raft units were laid using a fork lift truck. The sub-grade or soil was graded to the required profiles and then a granular sub-base, preferably in excess of 300 mm thick, particularly for high loads, was laid and compacted. A lean dry concrete sub-base could also be used as an alternative. A bedding course of sand, 50 mm thick was placed and compacted on the sub-base. The bedding layer was used to level the raft units and to ensure that there was support underneath them. The joints between the raft units were maintained by the use of steel spacers. The joints were then filled using dry sand, sand slurry, or similar materials. One unusual feature and an assumption made when designing the raft units, was the lack of a need for permanent load transferring joints connecting the raft units. In some cases, such as with high loads, connecting the raft units was desirable.

The essential qualities of the majority of paving systems was their strength, durability, and ride-quality of their surface. Due to the safety standard requirements in airport and highway pavements, the importance of these qualities were even more significant than in other areas. However, the properties of the surface of the raft units should include:

(i.) a skid resistance with good frictional characteristics;

(ii.) the capability of rapid repair and a low maintenance requirement;

(iii.) an adequate drainage system;

(iv.) a resistance to displacement, due to temperature or loading condition;

(v.) the control of the differential deflection;

(vi.) an ability to withstand high tyre contact pressures; and

(vii.) a resistance to chemical spoilage, and de-icing agents.

Finite element analysis has been used to establish design methods for raft units. Recent design methods that have been developed and based on the finite element analysis have been proposed by Bull (1986), Ackroyd (1985), Annang (1986), and Ismail (1990). Also, other design methods have been developed by the British Port Association [see chapters 3 and 7]. The finite element methods offer a more acceptable way of analysing raft units and avoid the assumption of an infinite slab which is necessary when the Westergaard models are used. Therefore, the existing design methods should not be used for a new paving system such as raft units without first checking to ensure that the basic assumptions used in the methods were not effected. The short but intensive use of raft units has shown that such a paving system should be treated as far as possible as a separate system from conventional paving design and construction.

This research project relates for the first time the fatigue life to the design parameters such as plan dimensions, thickness, and reinforcement of the raft units; the effects of these variables have to be considered in terms of fatigue effects under critical loading conditions. The critical loading conditions have been considered as the maximum take-off load of a Boeing B727-200 aircraft with one leg of its undercarriage applied to the surface and with a traffic width within which 100 per cent of the wheel paths fall; also the load distribution was considered to be uniform within the traffic width. The maximum take-off axial wheel load of B727-200 [i.e. 450kN] was chosen to be the design load for the raft units that was used in this research. The repair or failure criteria used for the raft units in this research project, were mainly when the raft unit was unable to accept additional loading conditions due to either fracture fatigue, punching shear, or uplift deflection equal or greater than 40 mm [see Section 4.7]. This state was called the ultimate limit state which the raft units could not sustain any further additional load repetitions, would mean that the raft unit would need to be replaced.

The feasibility study for a paving system is important, as it has financial implications on the final design. If the pavement becomes unserviceable at an early stage, maintenance costs become excessive, thus any savings in construction costs and time must ensure effective design and minimum maintenance costs throughout the pavement design life. The final selection of a type of pavement construction is based on both initial construction and future maintenance costs. Unfortunately these are difficult to assess accurately in a general appraisal since they are dependant on the variations in raw materials and labour costs, and different construction techniques.

In the future, there is scope for expanding and studying the use and design of raft unit paving systems as an alternative construction. The scope for civil and military use is

clear, where speed is critical for repair and maintenance works (Bull and Clark, 1991). Raft units may be considered for high speed traffic such as rapid exit taxiways, runways and highways but they would need properly designed load transfer devices and increased raft unit size, thickness, strength and durability. Load transfer devices should be cheap and simple to incorporate and use. Any increase in raft unit thickness has certain limitations due to the increased costs. However, a reduction of raft unit thickness reduces raft life; where the raft thickness is one of the major parameters which govern their use due to its effect on raft unit performance. So consideration must be given to a reduction in raft unit thickness without any negative effect on the allowable deflection and concrete stress. This can be maintained by introducing load transfer devices at joints to carry part of the applied load; also the additional reinforcement at the edges and the corners of raft units, using stabilised base materials; or by improving the raft supporting system, e.g. the sub-base, and sub-grade can have a similar effect.

1.2 NEED FOR THE RESEARCH

With this background, it is clear that there is a need to investigate the performance of the raft unit as a paving system. Raft units have been used in airfields mainly for damage repairs, but not as a full paving system. Usually, clients search for faster construction alternatives, that have a significant impact on reducing interruptions in air and ground traffic movement, and thus minimising the whole life costs. Currently, raft units and interlocking concrete paving systems are the construction alternatives to conventional pavements when expanding pavement facilities. Interlocking concrete pavement systems are beyond the scope of this research project and can be found elsewhere (Knapton and Emery CAA paper 96001, 1996; and Muir, 1996).

Despite the widespread use of raft units as a complete paving system or just as repair tools (Barber, 1980; Ismail, 1990; Salomo, 1990), their application in airports has so far been limited only to repairs. This research project focuses on the use of raft units on airside areas of an airport which are subjected to low-speed, and high load movements. There is a belief that the current use of raft units for the surfacing of heavy duty pavements, for example, in port areas and for repairing concrete pavements, will be extended to the airport industry. Recently, further properties of raft units have begun to be considered in order to develop their use more widely. For this project, it was decided to look at the fatigue strength of raft units and relate it to the failure mechanism under a simulated dynamic moving wheel load, and to investigate the effects of reinforcement, dimension and shape, and the thickness of the raft units on their fatigue life when

subjected to different loading configurations. The proposed test model included the sub-grade, sub-base, bedding sand, and the raft units [see Chapter 4].

1.3 OBJECTIVES

The aim of this research project was to clarify experimentally for the first time the fatigue life and the failure mechanism of the raft units under various loading conditions, and to provide experimental evidence for an analytical design method. The design parameters used in this research project for raft units were, the plan dimensions, reinforcement and thickness.

Usually, a model and its prototype are completely similar, but in some cases it is not feasible and impractical to impose complete similarity in a model test. Consequently, a full scale laboratory test programme for simulating the applied loading from the dual wheel leg of the design aircraft Boeing 727-200 taxiing over a raft unit paving system, was designed and constructed allowing only the contact area to deviate from its real size of 400 mm square to its laboratory size of 200 mm square for reasons discussed in Section 4.6.2, which required a theoretical correction to be applied [see Section 4.7.1]. The full scale laboratory test programme represented a major and novel test programme which has generated considerable interest for these working in this field

With this background, the following objectives were set for the research project:

(i.) to review and present a critical appraisal of the current design methods for raft units;

(ii.) to design and construct a test rig that would simulate the applied loading from a dual wheel leg of the design aircraft Boeing 727-200 taxiing over raft units paving system;

(iii.) to design an experiment using the test rig to investigate relationships, if any, between fatigue life and the design parameters for raft units;

(iv.) to determine the causes of failures and to recommend remedial measures for the design of raft units;

(v.) to develop, if possible, a more refined method for the design of pre-cast concrete raft units , and an empirical relationship between the design parameters tested;

(vi.) to develop a method for estimating the reserve life of a taxiway or an apron constructed of raft units paving system to improve the management of maintaining such system;

(vii.) to introduce cost benefit analysis for such a paving system; and

(viii.) to suggest further research to verify and extend the findings of this research.

A total of sixteen reinforced pre-cast concrete raft units were tested. The details of these raft units and the applied loading system were described in Chapter 4.

1.4 OVERVIEW OF THE THESIS

The various pavement systems were described in Chapter 2 as well as the loading system affecting their behaviour and failure criteria.

Some of the current design methods and analysis techniques were reviewed in Chapter 3. Also, the current practice carried out at the University of Newcastle upon Tyne on pre-cast concrete pavement raft units was described.

The author's experimental programme was described in Chapter 4, which included the details of the design parameters of the raft units, the test rig, the loading system, the instrumentation, the plate bearing test, and the general test procedures.

The test results showing the relationship between the design parameters of the raft units and their fatigue life were presented and discussed in Chapters 5 and 6, respectively.

A method was proposed in Chapter 7 to predict the fatigue life of raft units based on the experimental results. Predictions were made of the ultimate load capacity of the tested raft units in the light of the test results. Relationships for the magnitude of the load, the number of load repetitions, and the behaviour of the raft unit were developed using regression analysis. Experimental verification was provided for the design method proposed by Bull. Relationships for designing and estimating the reserve capacity of raft units were derived by relating the number of load repetitions to concrete strain, which would improve the management for maintaining such pavements. A brief appraisal for the total life costs of such a paving system including cost benefit analysis.

In Chapter 8, a summary of the principal conclusions and design recommendations were proposed together with suggestions for further research.

Chapter - Two
CHARACTERISTICS OF AIRPORT PAVEMENTS AND LOADING SYSTEMS

2.1 INTRODUCTION

The selection of suitable materials for pavement construction is usually ensured by the use of experimentally established specifications. The behaviour of pavement structures depends mainly on the ultimate strengths of the component materials. Materials used in pavement construction are normally non-isotropic and hold varying degrees of elastic, plastic and viscous characteristics. Material characterisation has been used to quantify their elastic, both linear and non-linear, and their visco-plastic behaviour. The elastic behaviour is used for the analysis of the resilient response of the pavement structure, and the plastic behaviour to long term deformation. Also, temperature variation is a parameter which influence the character of the basic material.

The rapid growth of airport operation during the 1940's led different international organisations to lay down standards and specifications in order to govern and achieve a uniform control of airport operation. These technical documents have been used as codes by operators and designers. The most widely used of these organisations are the International Civil Aviation Organisation (ICAO), the US Federal Aviation Administration (FAA), and the UK Civil Aviation Authority (CAA). The overall performance of aircraft and the performance of functional components (such as, for example, landing gear, tyres, brakes, speed, centre of gravity) are subject to federal regulation, which leads manufacturers to present detailed information for each aircraft using aeronautical terminology. Such information is published in National Aircraft Standard documents and disseminated by the aircraft companies (see Airbus Industries (1983) and Boeing Industries (1985)).

The advent of the heavy and wide body aircrafts has brought a new concern for pavements and pavement design. These aircraft, each weigh nearly one million pounds (i.e. 454, 545 kg). Therefore, it was necessary on the ground to support either the aircraft by providing more wheels within the main landing gear or by strengthening the pavement. Thus, the primary purpose of pavement deign is to provide adequate support for the imposed loads. The capacity of a pavement to carry an aircraft has been expressed by a single number using the appropriate standard load classification curves and/or a computer program such as Load Classification Number (LCN), Load Classification Group (LCG), or Pavement Classification Number (PCN). The PCN is a

number expressing the bearing strength of a pavement for unrestricted operations by an aircraft with a classification (ACN) of the same number. It is a component of the ICAO ACN-PCN method for reporting strength pavement.

The degree of pavement loading by individual aircraft is normally provided in a series of tables and figures designed to cover the requirements of pavement loading throughout the aircraft operation. The various phases of aircraft operation include static, slow taxi, steady-state turns at various speeds and turn radii, take-off roll, roughness, landing impact, and braking.

2.2 TYPES OF PAVEMENT CONSTRUCTION

Historically, pavements have been divided into two broad categories, flexible and rigid pavement . These two categories can be sub-divided further into one of the types shown in Figure 2.1. The paving materials and construction techniques vary from one type to another. There are two main elements in a pavement structure namely the surface material and the base. The former must be of a high durability and strength to resist severe surface loads, contact stresses and the relative fatigue damage; whereas the latter spreads the load so that the sub-grade is not over stressed. The sub-base layer is provided only when the pavement is constructed on a weak sub-grade and is subjected to high load and high fatigue life. Pavements derive their ultimate support from the underlying sub-grade and the behaviour of each of the other paving layers.

Pavement performance depends to a large extent upon the types of paving materials chosen. The basic requirements for a pavement structure to fulfil are:

(i.) to provide a comfortable and uniform riding quality for the passengers and the crew;
(ii.) to be strong enough for the pavement to spread the imposed traffic stresses through the underlying layers to the sub-grade;
(iii.) to control frost action by including frost resistant material in the pavement;
(iv.) to provide the pavement surface with a good drainage system and a skid resistant texture despite the extensive introduction of anti-skid brake units in the aircrafts; and
(v.) to provide a minimum capital and maintenance costs throughout its life.

Airport and road pavements have much in common in which the general principles applying to one apply also to the other. However, several distinct differences exist

between the two types of pavement regarding the quantitative values assigned to each factor; namely, the magnitude of the applied load, the tyre pressure, the geometric section of the pavement, and the number of load repetitions applied to the pavement during its design life. For instance, tyre pressures on aircrafts are higher than on trucks where the former may be as high as 2.76MPa and the latter are in the range of 0.42MPa to 0.825MPa. Lateral placement of the heavy traffic on roads is usually close to the edge of the pavement. In contrast, traffic on an airfield is concentrated primarily in the centre of the pavement. Other differences are the sub-grade characteristics and the required length of pavements for airports which relatively is much smaller than for roads. Thus, when designing a road, the designer has an additional decision to make, that is, whether to recommend a uniform design throughout the cross-section based on the weakest soil strength in the area, or a number of cross-sections tailored for different sub-grades, and which take account of the effect of economic and construction factors.

2.2.1 Flexible Pavements

The flexible pavement mainly consists of a relatively thin wearing surface constructed over a base and sub-base resting on the compacted sub-grade. Flexible pavements consist of a series of layers, with the highest quality materials at or near the surface. Hence, the strength of a flexible pavement is a result of building up thick layers and thereby distributing the load over the sub-grade, rather than by the bending action of the slab. The thickness design of the pavement is influenced by the strength of the sub-grade. The load-carrying capacity of a flexible pavement is brought about by the load-distributing characteristics of the layered system.

The two main design criteria which are used in flexible pavement design methods are the maximum tensile strain in the asphalt and the maximum compressive sub-grade strain [see Fig. 2.2.b]. In both cases, the maximum allowable values depend on the number of load repetitions expected in the design life of the pavement. The levels of strain will clearly depend on the magnitude of the wheel load. These design criteria have been set to limit the permanent deformation in the layers and the fatigue cracks. Prevention of excessive rutting is dealt with by limiting the maximum vertical strain on the sub-grade [see Fig. 2.2.b].

It is common practice to construct flexible airport pavements with either cement or bitumen-bound bases even though an unbound base or sub-base with good grading and a high level of compaction can provide the desired performance. This is particularly true on good and dry sub-grades, but not on wet sub-grades. The bound base materials

normally specified by the different agencies are rolled dry lean concrete (DLC), Portland Cement, dense macadam or Marshall base courses. The designed thickness of the base layer can be made up of any one or a combination of these materials. For instance, for the majority of UK sub-grades, it is advisable to use the DLC as the first layer above the formation.

The top layer placed on the base of the flexible pavement is normally called the bituminous surface. The standard minimum thickness for the bituminous surface over critical areas is 100mm, and 75mm for non-critical areas. The 100mm thickness is usually made up of a 40mm wearing course on a 60mm basecourse. Additionally a 20mm thick open macadam friction course is provided. The purpose of the surface is to provide:

(i.) an high stability to resist the shearing stresses induced by heavy wheel loads and high tyre pressures;
(ii.) a durable hard-wearing weatherproof surface free from loose material which presents a foreign object damage (FOD) hazard for the engine of aircrafts;
(iii.) a good readability and non-skid qualities; and
(iv.) a resistance to damage caused by jet blast (excessive heating) and/or fuel spillage.

The principal bituminous surfacing materials used by the different agencies are either a combined Marshall asphalt wearing and basecourse or an hot rolled asphalt wearing course on a macadam base course.

Failure in flexible pavements may result from full-depth fatigue cracking of the bituminous surfacing or permanent deformation in the pavement layers with an eventual shear failure (Shahin, 1994). The failure can be related to an excessive movement within the constructed pavement layers resulting from poor materials quality and poor construction of the sub-grade, sub-base, base, or surface course. The primary failure mode for pavements with bound bases is likely to be rutting with associated heave due to shear failure of the sub-grade. Rut depth at failure depends on a number of factors, including the magnitude and configuration of the load, the sub-grade and the base characteristics, the pavement thickness and the lateral distribution of the aircraft wheel paths. For pavements subject to channelised trafficking (e.g. taxiway) by medium to heavy single wheel geared aircraft the acceptable rut at the end of the design life is unlikely to exceed 15mm in depth and 1.5m in width. For pavements subject to less channelised trafficking (e.g. centre section of runway) by heavy multi-wheel geared

aircraft, the rut depth should be within the range of 20 to 40mm and the width may be in excess of 5m (Dept. of Transport, 1989), "Guide to Airfield Pavement Design and Evaluation".

Failure associated with overloading by the aircraft results in surface deformation and the formation of a network of cracks in the bituminous top surface, this progresses (accelerated by the ingress of water and possibly frost action) until small pieces of the surface or individual stones work loose. At this stage the pavement has failed, in that it cannot fulfil its main function of carrying aircraft safely. Assuming that the granular layers have been satisfactorily laid and compacted, the cause of failure is excessive deformation of the sub-grade which has led to the repeated imposition of unacceptably high stresses and strains within the surfacing and its final failure.

2.2.2 Rigid Pavement

The concrete pavement is a traditional form of construction used in airports, highways, harbours, and other industrial areas such as the storage of heavy containers. It provides a smooth and comfortable riding surface which is hard wearing and can sustain the oil spillages and the heat engine of an aircraft. Generally it rests on a relatively thin base and sub-base layers which distribute wheel loads over a wide area of sub-grade by the integrity of its rigidity and modulus of elasticity. The concrete pavement can provide the most convenient solution to the paving problem particularly for pavements subjected to high loads.

There are two forms of rigid construction, reinforced and unreinforced concrete pavements which may incorporate load transfer devices such as dowel joints, to share the load between adjacent slabs. The unreinforced concrete pavement is unsuitable for use in areas subjected to heavy and high movement of traffic and/or site settlement which can lead to severe cracking in the early stages of the fatigue life. It is not widely used and those that do exist are either severely cracked or not heavily loaded.

Reinforced concrete is more widely used. The steel content has to be designed to minimise the width of cracks, to increase fatigue life, and to reduce thermal cracks under the combined stresses of wheel loading and the substantial temperature gradient through the slab. The differential in the daily temperature at the top and bottom surfaces of a slab induces both hogging and sagging along both axes of the slab, hence top and bottom reinforcement in both directions are essential. Due to the overall expansion and contraction, the pavement is designed with an appropriate joint system.

A well designed concrete pavement can provide a very durable surface providing that sub-grade settlement is prevented. A differential settlement in the sub-grade layer will increase the induced bending moments under loading and therefore, cause rapid and severe cracks in the concrete surface. There are three significant causes of strain in a concrete slab, the applied load, warping of the slab due to temperature gradients through the concrete, partly or wholly resisted by boundary restraints and slab weight. Finally, the overall contraction and expansion due to temperature variations are partly or wholly resisted by boundary restraints. Heavy reinforcement ensures fine cracks, prevents cracks opening up, and shear load transfer is maintained by mechanical aggregate interlock. Reinforced concrete pavements that have been laid are generally 200mm to 250mm thick, with both top and bottom reinforcement. The thickness design of a concrete pavement depends on the loading conditions and the function of such a pavement (see Chapter 3).

The rigid pavement utilises flexural strength to distribute the load from the aircraft undercarriage to the sub-grade. Cracking of the concrete due to a high stress level for the material to withstand, may initiate pavement failure. It should be noted that a crack in the concrete pavement does not, in itself, constitute failure but may lead to it.

2.2.3 Precast Concrete Raft Units

Precast concrete slabs, commonly called raft units, have been used extensively for industrial pavements and roads as well as airfields. The raft units have been used to build new pavements and to repair existing pavements. They can be prestressed or can include fibre reinforcement to improve significantly their strength and load-carrying capacity, as well as to suit a particular purpose. As shown in Chapters 5 and 6, steel fibre reinforcement alone is not recommended for pavements subjected to high loads. The raft units have a steel angle along the top edges to prevent spalling and to maintain the unity of the raft unit after cracking. They are designed as single units with or without load transfer between adjacent rafts.

Several countries produce this type of pavement. The most widely known concrete raft units are manufactured by Stelcon which is based in the Netherlands. The Stelcon rafts are manufactured in the UK by Redlands Aggregates Limited under licence to Stelcon Precast and precast prestressed concrete pavement slabs have been used in different industries for a specific function in Europe, US, Japan, and the former Soviet Union. They have been used for temporary construction, highway and airfield repairs,

pavements subjected to heavy industrial traffic, airfield construction and port container terminals.

The use of raft units for particular solutions, such as container terminals which require a very high load capacity and good durability, is very common. Often these terminals are built on fill areas and are subjected to large sub-grade settlements. Precast concrete raft units provided the required strength for large concentrated loads and have been used for several container terminals in UK and in Europe (Barber, 1980, and Patterson, 1976). The early port pavements were designed for much smaller loads. For example, in the mid 1950's, the maximum gross weight of a four-axle rigid lorry was 22.35 tonnes. Currently, in container terminals, axle loads of up to 800kN are common with 450kN container corner casting loads (Barber, 1980).

The use and development of the raft units were demonstrated in detail in Chapter I. Also in the UK an extensive research and development programme at the University of Newcastle upon Tyne has been undertaken and produced design methods for reinforced concrete raft pavement units by different researchers [see Chapters 3 and 7].

2.2.4 Concrete Block Pavements

Concrete blocks are a relatively new form of pavement surfacing compared with conventional pavement systems. Concrete block pavements have been used for many years in Belgium, the Netherlands, Germany, Denmark, and used for road construction since the early 1970's. There was an obvious caution in applying such a form of pavement made up of small individual blocks of concrete and whether they would perform successfully.

A concrete block pavement usually comprises three different layers of construction (Barber, 1980). A granular sub-base is prepared according to the specification for road and bridge works (Dept. of Transport, 1976) and over this a screed of 50mm to 80mm of uncompacted sand is laid. The bedding sand layer is similar to that used for raft units and acts as a regulating layer to cover any surface unevenness of the sub-base. The finished surface combines the high strength concrete blocks. The base or sub-base is the critical factor in pavement design. For concrete blocks, it is generally found that a granular sub-base is sufficient for areas carrying loads of the same order as road traffic, but for heavy loading, such as container handling areas, a cement bound base is required (Barber, 1980).

Concrete blocks are manufactured by several firms and are available in a variety of shapes and colours. They are generally hand sized, having overall plan dimensions of 100 by 200mm, but when laid they form an integral pavement surfacing. The concrete blocks are generally available in three thicknesses, 60mm, 80mm, and 100mm. For general trafficking, including heavy loads, 80mm thick concrete blocks are usually adopted; 100mm thick are recommended by some manufacturers for heavy duty use and the 60mm blocks are considered to be suitable only for non-trafficked areas (Knapton and Barber, 1979).

The concrete blocks are laid by hand. They can be laid in either a stretcherbond or a herringbone pattern. It is generally accepted that the herringbone pattern should be used for rectangular blocks and for heavily trafficked pavements since it is not only increasing the strength, but also gives better resistance to horizontal braking and acceleration forces. If this pattern is used, with the line of blocks set either perpendicular to or at 45 degrees to the line of traffic, then there is no significant difference in the performance of rectangular and shaped blocks (Barber, 1980)

The interlock of the concrete blocks by filling the joints with compacted sand, gives the necessary structural rigidity. The blocks are laid with joint widths of between zero and 6mm. However, the vibration evens these out giving a typical joint width of 3mm. Adequate edge restraint is necessary since interlock will be lost if the blocks are allowed to move horizontally.

The essential qualities of any aircraft pavement are strength and durability with good frictional, rideability, and drainage characteristics. The concrete blocks provide a durable and tolerant form of construction. The riding quality is not as good as that from an asphaltic surface, but has proved adequate for straddle carrier operation, and traffic with static and low speed movement such as the three cross taxiways adjacent to the main runway 18R/36L at Dallas/Fort Worth International Airport DFW, USA (Faxwerthy, 1991) and at Luton Airport, UK (Emery, 1986). Most recent use of paving blocks, however, was the construction of a 1000m long and 20m width airstrip and a small apron for light weight aircraft in Thevenard Island -Western Australia (Muir, 1996).

Since the concrete blocks spread the applied loading, pavement thickness design is similar to that used for conventional flexible pavements. The concrete blocks and sand layer can be used in lieu of the same thickness of asphalt. The block surfacing constitutes an integral pavement course having elastic properties analogous to those of

conventional flexible paving materials. Therefore, design recommendations for the concrete blocks were developed in the UK based on the sub-base design curves of the design method Road Note 29 (Knapton, 1976). An extension to these design recommendations uses road-base design curves from Road Note 29 in a modified form to accommodate the block surfacing in heavily trafficked roads (Lilley and Walker, 1978; and Lilley, 1978). In this design method, wheel loads are converted to standard axles using equivalence factors given in Road Note 29. The sub-base and road-base are proportioned from the relevant design charts to allow for the load carrying capacity of the block surfacing.

A design solution based on the CBR value and the cumulative number of standard (8,200kg) axles which the pavement must withstand, was used to design the concrete blocks (Knapton et al., 1986). Other approaches for the design of a heavy duty concrete block pavement is that using the British Ports Association design method (Knapton et al., 1986), and the Civil Aviation Authority of UK, paper 96001 (Knapton and Emery, 1996).

2.2.5 Composite Pavement Construction

Pavements comprising flexible and concrete layers overlaying each other as well as an asphaltic surfacing over a cement bound base material are termed composite construction. The composite construction is widely used in container handling ports, highways, and airfields, and has performed well and demonstrates the feasibility of this type of construction (Barber, 1980, Burt and Bcc, 1986, and Westall, 1966), respectively. The pavement overlay is required when the existing pavement is no longer serviceable or when the pavement must be strengthened to carry greater loads than considered in the design. Therefore, the selection of a suitable surfacing is critical.

The method of designing and evaluating composite pavements depends on the pavement structure, and their behaviour and failure mode. Composite pavements are either flexible overlays on concrete slabs or concrete overlays on a flexible pavement. The first can be divided into three types which use relatively thin flexible overlays, thick flexible overlays or fall between the thin and thick flexible overlays (Dept. of Transport, 1989). The thin overlay is designed to convert the thickness of the overlay to an equivalent concrete thickness which is added to the underlying concrete thickness and then the pavement is treated as a rigid pavement. The thick overlays are designed to convert the thickness of the concrete slab to an equivalent thickness of bound base material which is then added to the thickness of the overlying flexible overlay; the pavement then is

treated as a flexible pavement. The third type which falls between the other two types and cannot be defined as rigid or flexible, is designed by interpolation. The design of a concrete overlay on a flexible pavement is the same as the design of a concrete pavement on a grade. The modulus of sub-grade reaction, "k", is determined by plate-bearing tests made on the surface of the flexible pavement. Several agencies specify that no "k" value greater than 500 lb. per cubic inch (135734.4 kN/m^3) be used when designing rigid overlays for flexible pavements (Packard, 1973).

2.2.6 Practical Experience - Field Trial Tests

There are two distinct types of test that can be used for the life-testing of a pavement. The first type involves tests using real traffic conditions and the other type using simulated loading conditions. The tests involving real traffic conditions are usually carried out in non-laboratory conditions, due to the size of the area required to achieve a full scale pavement test.

In the absence of full-scale test data and field experience of raft unit paving system, a series of full-scale raft unit pavement tests was set up for this research. The test programme of this research involved the simulation of the loading conditions of real aircraft operations applied to full-scale raft unit pavement (see chapter 4). Simulation was used because it was not possible to acquire a site where real traffic conditions could be observed passing over real raft units.

However, the field test has the advantage of giving results in a natural environment and under real traffic conditions. This validates the results greatly if the test was conducted over the pavement life which is usually equal to or greater than 20 years, and the traffic and environmental conditions were controlled. However, in most cases, a good pattern of future pavement life can be obtained in the first few years, and there may be no need for further periods. The field tests are costly and need a long time to undertake, particularly on sites with major climatic and sub-grade variations, and covering a wide variation of the materials and their thicknesses. Despite all these constraints, some field trials have been carried out to assess rapid repair systems for airport pavements.

During the late 1960s, tests were carried out at the Military Engineering Experimental Establishment at Christchurch to examine the use of raft units for rapid runway repair. The foundation used at Christchurch was 75 mm of 10 mm single size Lytag laid on shingle. A sand bedding layer was used and sand was brushed into joints. No compaction was used. The tested raft units were subjected to a wheel load of a fighter

aircraft and settlements up to 38 mm were recorded. This inadequate system was not developed further.

In the early 1980s, the US, German and Dutch airforces developed similar rapid runway repair system. The design comprised bulk ballast rock fill with geotextile lining in the crater bowl, and a base layer of fine gravel (10 mm single size) 100 -150 mm thick, laid on a geotextile layer. Compaction was used on the top of the ballast fill (two passes of a 10 tonnes vibrating roller), but not on the base layer, which was just screeded and levelled. The raft units were laid and bedded in with several passes of the vibrating roller per row of the raft units. In such repairs, bedding in settlements up to 40 mm were typical (Bull, 1990). The British airforce adopted a similar but more conservative approach, using a base layer of 20 mm single size stone and raft units of 200 mm thick.

In 1985, both US and UK research agencies developed these repair systems for military strategic transport aircraft (C5 Galaxy) and wide-bodied aircraft (Tristar). It was a major trial for developing such a system that was suitable for such large aircrafts. A large number of aircraft movements were made across the repair and no more than 25 mm settlement was recorded with the most critical area being at the interface between the repair and the original pavement. Clearly, great care is needed in this area. Also, a variety of gap-filling techniques were tried. These included special fast-curing cement mortars and asphalt mixes but the fibreboard strip was essential to permit raft unit movement under load.

2.3 TYPES AND CHARACTERISATION OF CONSTRUCTION MATERIALS

2.3.1 General

To design new pavement structures and to estimate the load carrying capacity or plan rehabilitation for existing structures requires definitions of the materials' characteristics and the dimensions of the various layers that are being considered for or actually comprise a pavement structure. The selection of appropriate materials depends on the design or rehabilitation methodology that is being used. The selection of the materials is usually ensured by the use of empirically established specifications, based on simple grading or proportion classifications. All materials used in pavement construction are non-isotropic and exhibit varying degrees of elastic, plastic and viscous characteristics.

Despite the diversity of paving materials and construction techniques, most pavement structures can be classified as one of the previous categories discussed in Section 2.2. There are two main elements in a pavement, namely surfacing material and the base. The soil foundation for both flexible and concrete pavements is termed the sub-grade. The surfacing material must be of high durability and strength in order to resist severe deteriorations. The base is the structural component of the pavement which distributes the load.

Modern flexible and rigid pavements consist of three main layers, surfacing, roadbase and sub-base. The bituminous surfacing in a flexible pavement is generally sub-divided into a wearing course and a base course, laid separately. The base and sub-base may also be laid in composite form using different materials which are designated the upper and lower road-base or upper and lower sub-base (Burt and B.C.C., 1986). The concrete pavement can be laid only with two layers, the concrete slab and the sub-base. In this section, a brief summary of the material characteristics which have been associated and adopted by the principal analysis and design methods, is presented.

2.3.2 The Base

The base is defined as the layer of material that lies immediately below the surface of a pavement, and the sub-base is a layer of material between the base and sub-grade. It may be constructed of stone fragments, slag, soil aggregate mixtures and stabilised soil, dry lean concrete, dense bituminous macadam, and Marshall asphalt. The prime requirement for the base is to increase the load supporting capacity of the pavement by distributing the load through the pavement. The basecourse must possess high resistance to deformation in order to withstand the high pressures imposed upon it. The stiffness or elastic characteristics of the materials are required in designing a pavement. For both road and airfield pavements, the base should be compacted to at least 100 per cent standard AASHO densities.

2.3.3 The Sub-base

The sub-base performs three functions, as a structural layer, a working platform, and an insulating layer against freezing where the sub-grade material might be weakened by the action of frost. It may be constructed of a granular material such as crushed rock, gravel, crushed concrete or well burnt non-plastic shales, and cement stabilised materials. It is agreed generally that an untreated granular layer of sub-base will develop moderate strength when compacted to a high density, thus providing additional strength to the pavement at relatively low cost. A firm underlying layer is required to achieve this level

of compaction. Therefore, the strength of the granular sub-base layer is a function of the strength of the underlying material and layer thickness.

Type 1 and Type 2 are granular sub-base materials defined by the Department of Transport (Dept. of Transport, 1976). The materials used for Type 1 sub-bases are crushed rock, crushed slag, crushed concrete. For Type 2 sub-bases, additional materials are used such as natural sands and gravels. The grading limits for Type 1 and Type 2 sub-bases are specified in the Department of Transport Specification (Dept. of Transport, 1976 and 1992). The grading and moisture content limits for Type 2 sub-bases were selected on the basis of laboratory research, so that the material would, under the specified moisture condition, have a laboratory CBR value of not less than 30 per cent (Croney, 1991). Other procedures are available for cohesive soils to estimate a design value from the plasticity index of the soil (Powell et al., 1984). In the UK conditions, a relationship was established to determine the elastic stiffness directly from the plasticity index (PI) (Black and Lister, 1979):

$$S_s = 70 - PI \tag{2.1}$$

where,

S_s is expressed in MPa and PI is expressed as a percentage.

Sometimes, the availability of good quality materials, with or without self-cementing properties, can make conventional granular base and sub-base construction a practical and economic choice. However, this type of construction is only recommended on good dry sub-grades, where it is possible to achieve the necessary high level of relative compaction which is not always the case in practice, for concrete airfield pavements, granular sub-base courses may be used if the sub-grade layer was weak and an improvement in the sub-grade support was provided by the granular sub-base. In this case, the cost of the sub-base layer should be weighed against the savings realised on the thickness of the base courses and the concrete surface.

The effective elastic stiffness of a granular layer depends to some extent on the thickness and stiffness of the other layers. It is more dependent on the type of material, state of compaction, water content, and grading of the granular material. In areas where acceptable base and sub-base materials are expensive, cement stabilised materials and asphalt bound materials offer important economic advantages.

2.3.4 Cement Stabilised Materials

Cement can be used to enhance the strength of granular material for the base or the sub-base layers. The material is defined basically as an aggregate of some kind, with low cement and low water contents added to give modest strength at low workability. The strength needs at least 7 days to develop. The cement stabilised sub-base provides a highly impermeable layer that reduces the amount of surface water reaching the sub-grade, as well as provides strong support for the pavement. The high strength of the cement stabilised sub-base permits the use of thinner concrete pavements for given loading conditions.

The current policy of the Department of Transport is to construct pavements with bound bases. The cement- or bitumen-bound bases have been used for flexible pavements while the dry lean concrete base has been used for rigid pavements. In general, the bound bases are highly recommended in the case of pavements subjected to regular trafficking by heavy aircraft with high tyre pressures. On the other hand, pavements with bound bases permit the use of a less stringent specification and give structural benefits over pavements built on unbound bases, allowing a saving in thickness over the granular base and sub-base requirement. The bound base designs provide an economic and practical solution and most significantly give reliable performance. (Dept. of Transport, 1989)

2.3.5 The Sub-Grade

The soil immediately below the formation is referred generally to as the sub-grade. The performance of the pavement is affected by the characteristics of the sub-grade especially for flexible pavements where the required thickness depends greatly on the shear strength of the soil. The function of the sub-grade is to provide a support to the pavement and the wheel load imposed on it. Desirable properties which the sub-grade should possess include strength, drainage, ease of compaction, and permanency of compaction and strength. The pavement structure must reduce the stresses on the sub-grade due to traffic loading to a level that ensures that there is only very limited deformation at the end of the design life. The magnitude of stresses in the sub-grade at formation level is strongly influenced by the stiffness of the sub-grade and the deformation caused by these stresses is related to the strength of the sub-grade. Thus both stiffness and strength of the sub-grade affect its performance and the level of stresses generated in all the overlying pavement.

For adequate sub-grade construction, several basic principles should be followed at all times, including proper compaction of the sub-grade, construction of adequate subdrains, and adequate field control. Both stiffness and strength of the sub-grade are strongly influenced by moisture conditions. Apart from its effect on the strength of the sub-grade, inadequate drainage can have adverse effects on the stability of granular foundation layers subjected to prolonged saturation and thus deny the normal basis of design. It has been shown that sub-grades that become very wet during construction subsequently reach lower equilibrium strengths than those that are kept dry and well drained (Black and Lister, 1979).

Sub-grade stiffness is a critical factor in defining pavement deformation and is usually characterised by the modulus of sub-grade reaction (k), or by the elastic modulus, (E_S).

Regardless of whichever factor is chosen to define and control the deformation, field measurements are required to maintain the necessary quality control over the construction. The assessment of sub-grade strength and stiffness is usually made in the field and can be applied to laboratory samples compacted at the appropriate field moisture content, by the CBR test, the plate bearing test for getting the modulus of sub-grade reaction (k), and in some cases the dynamic penetrometer (British Standards Institution, 1990). The CBR test, although giving unrealistically low results on wet cohesive soils near saturation, is generally accepted and practical measure that can be used to give an estimate of both stiffness and strength. In situ CBR values are not normally representative of the equilibrium sub-grade strength under a pavement. The equilibrium CBR value can be estimated from laboratory tests (Black, 1961, and Black, 1962). Sub-grade strength also needs to be measured when existing pavements are being reconstructed. This can be carried out by in-situ CBR testing in pits or by making boreholes and using the cone penetrometer (Black, 1963).

The sub-grade stiffness can be characterised by its resilient or elastic behaviour, and permanent or plastic behaviour. These are generally regarded as the relationships between applied stress and recoverable strain, and permanent strain and number of load repetitions, or design life. Relationships have been developed between the elastic modulus (E_S) and the CBR by several researchers. Since an elastic modulus is required for analytical design methods, the expression $E_s = 10\times(\text{CBR})$ N/mm^2 has been widely adopted (Heukelom and Foster, 1967). This relationship is purely empirical in form.

It has been observed that more pavement failures occur in locations where the pavement has been placed on sub-grade in cut sections and particularly where the sub-grade transitions from cut to fill sections. In these situations, it is necessary to provide a

transition zone at that section to preclude pavement break-up at these locations. A capping layer will be suitable for such a transition zone. The sub-grade of compacted fill material provides better support.

Sub-grades with a CBR value less than 5 per cent require a suitable capping layer of low cost, local material, as recommended by the Department of Transport, (1989) and Powell et al., (1984). This capping layer is designed to provide a working platform as well on which sub-base construction can proceed with minimum interruption from wet weather, and to minimise the effect of a weak sub-grade on pavement performance. The capping layer reduces the risk of damage to any cement bound materials above the capping layer during construction operations and can thus improve the structural contribution of these layers. It was observed that such capping layers also minimise any reduction in the strength of the sub-grade during wet weather and any consequential adverse effect on its final equilibrium strength (Black and Lister, 1979).

The Poisson's ratio of the sub-grade should be known although it does not have a large effect on the results from an analytical design method. This parameter has typical values ranging from 0.4 to 0.5 for cohesive soils and from 0.2 to 0.35 for granular soils, while for non-cohesive soils the value approaches 0.3 (Yoder and Witczak, 1975). In the British Port Association (BPA) manual, the following relationship proposed by Heukelom and Foster, (1960) has been used:

$$\mu = 0.82 - 0.1\log_e E_s \qquad (2.2)$$

where,

E_s = elastic modulus of the sub-grade (N/mm^2)

μ = Poisson's ratio

While most pavement designers believe stabilised materials will give better performance than their unstabilised counterparts, there is wide belief that a comparison of thicknesses, which would yield equal pavement performance, must depend on many factors such as the quality of materials, position in the pavement structure, load magnitude and climate. Details of material requirements and construction methods for quality stabilised and unstabilised bases, sub-bases and sub-grades are given in the appropriate references of this chapter.

2.4 LOADING SYSTEM

2.4.1 Introduction

Airport design and construction has become one of our modern day skills. Airport pavements, however, are related uniquely to the aircraft itself and its operating qualities. The considerations which tie the pavement and the aircraft together are simply, that the pavement must physically support the aircraft during all its ground phases with a minimum safety risk when taking-off and landing. Such risk includes ingestion of stones, slush and water into the engines of the aircraft due to the poor design of the corners, edges, and the drainage system of the pavement.

A conventional take-off involves an acceleration phase until the rotation speed is reached, whereupon the nose is lifted and the aircraft climbs away to a prescribed climb speed. The conventional landing involves descent on a controlled path, to cross the threshold at a speed which allows the pilot to round-out for an airborne touch-down. Once the aircraft has landed on the ground, the prerequisites for a prompt, safe stop and running on taxiways and aircraft parking, lie in the proper choice of the aircraft and airfield pavement characteristics.

The characteristics of the aircraft which affect pavement strength design are aircraft all-up weight, percentage load on the nose wheel, wheel arrangement, main leg load, tyre pressure, and contact area of each tyre. Table 2.1 shows these data for aircraft currently in use. The all-up weight of one of the largest civil aircraft in service, the Boeing 747, is now over 350 tonnes with tyre pressures of 1.30 N/mm^2. It retains, however, conventional dual-tandem (DT), four wheel bogies for the main undercarriage gear [see Plate 2.1c], but requires four main units to carry the increased weight.

At present 23.45 tonnes is about the maximum load carried on one wheel. A large number of wheels is, therefore, needed to bear the weight of large aircraft like the Boeing 747, the C-5A Galaxy, and the Douglas DC-10. A wide variety of wheel arrangements is possible. The standard and the most common undercarriage categories are single wheel (sin.), dual wheel (D), and dual-tandem (DT) units [see Fig. 2.3]. The airfield pavement designer may well have to consider a number of non-standard wheel arrangements such as complex wheels (COM) [see Plate 2.1d].

Aircraft loads are transmitted to the pavement through the landing gear. The portion of the load imposed by each leg will depend on the position of the centre of gravity with

reference to the main and auxiliary (nose) legs. The load supported by each leg is transmitted to the pavement by one or several rubber-tyred wheels.

A major consideration in the design and evaluation of a pavement is the effect of the traffic intended to use the pavement. For a particular aircraft or traffic mix, the following traffic information should be considered in pavement design and evaluation.

(i.) Gear configuration of the design aircraft.
(ii.) Contact (tyre) pressure of the design aircraft.
(iii.) Maximum take-off weight.
(iv.) Annual aircraft movements.
(v.) Lateral distributions of loads on taxiways and runways, and longitudinal distribution of loads on runways.
(vi.) The aircraft speed.
(vii.) Special loading considerations (e.g. braking, turning movements, and jacking).

2.4.2 The Effect of Aircraft Undercarriages

The choice and location of the landing gear is usually dictated by the particular layout of the aircraft; the final arrangement depending on the shape and volume of the space which is available to house the entire unit when retracted.

Most aircraft have a tricycle type undercarriage arrangement comprising two main wheel gears near the centre of gravity of the aircraft and a nose wheel gear which carries 5 per cent to 10 per cent of the total aircraft load. The number of wheels on the main gears varies with the type and weight of the aircraft [see Fig. 2.3]. The main gears with four or more wheels, for practical design purposes, are treated as dual-tandem. Tandem gears are not very common and can be treated as duals when using the design charts.

The concept of an equivalent single wheel load (ESWL) for a multi-wheel group is somewhat delicate. Equivalence can be based on one criterion only, it will be valid for that one aspect and only for some assumed part in the pavement. The pattern of strain and stress, for instance, which a multi-wheel undercarriage imposes on the pavement will differ from the pattern imposed by a single wheel. Computations for determining equivalent wheel and axle loads are based on equal deflection or the equal stress criterion. The validity of the equivalent single wheel load depends upon how dominant an influence the criterion selected affect pavement performance. The use of the ESWL

concept was introduced to simplify the design analysis of multiple wheels (Yoder and Witczak, 1975).

The stress within the surface of a pavement due to the applied load depends upon the load on the undercarriage unit, the spacing of the wheels within the bogie, the tyre pressure and the precise position of the undercarriage in relation to the pavement. These parameters have a potential effect on the magnitude and the behaviour of both the stress and deflection at the top surface of a pavement immediately under a twin wheel and at the bottom surface of a pavement (Yoder and Witczak, 1975). The average failure load for the two wheel arrangements was always less than twice that of one wheel, and about the same as half that of four wheels. This is to say, there is a strong presumption that if the corner of a slab is loaded by only two of the four wheels of a four wheel bogie, this is the worst case (Dawson and Mills, 1970).

In cases where separate undercarriage legs are so close that the effects of wheels from adjacent legs appreciably interact, the combined effect of the wheels from both undercarriage legs must be considered as a single complex undercarriage (ICAO, 1983). However, such cases result in load interaction and affect the calculations of obtaining the Aircraft Classification Number (ACN) which are based on one main wheel gear only. Therefore, a correction factor for adjacent gear load interaction should be applied. The procedure for assessing the loading effect of adjacent main wheel gears and the correction factors are stated in (Dept. of Transport, 1989).

In the following stages of aircraft design, the designer may wish to study the effect of various wheel spacing on pavement stresses. A computer programme developed by the PCA in 1967 , was used in a limited study for dual and dual-tandem gears (Packard, 1967). The data in the program was expressed as relative stress so that the relationship can be applied for any gear load. Generally, the programme shows for each inch (25.4mm) that spacing is increased, stress is reduced by slightly less than 1 per cent. Changing the dual spacing from 30in (762mm) to 36in (914.4mm) reduces the stress by about 5 per cent. Only minor effects are indicated for the other variables, namely, radius of relative stiffness and contact area. For dual-tandem gear, changing dual spacing changes stress at the rate of about 1 per cent per inch (25.4mm), changes in tandem spacing have slightly less effect. For equal loads, increasing the dual-tandem gear spacing from 30in (762mm) by 55in (1397mm) to 36in (914.4mm) by 60in (1524mm) decreases stress by about 9 per cent.

2.4.3 Selected Aircraft Loading

It is a general practice to design or evaluate a pavement based upon a design aircraft which will operate regularly from an airport.

In different design procedures, a pavement design chart or formula is prepared outlining the operational classification of the various pavements at the airport for the aircraft under consideration. Each method gives a slightly different pavement requirement in terms of overall depth and individual layer thicknesses.

Pavement design is always based on parameters of sub-grade strength, materials to be used in the pavement layers, type of trafficking and length of service required. Undercarriage configurations, individual wheel loads, and forecast frequencies of aircraft movements which may use the airport, are the most significant parameters which need special and delicate considerations during the design tasks. Since the traffic forecast is a mixture of a variety of aircraft having different landing gear types and different weights, the effects of all traffic must be accounted for in terms of the design aircraft. The loading conditions applied throughout the tests included in this thesis are a simulation for traffic mix with the same undercarriage or converted to the same landing gear of the design aircraft Boeing 727-200; and different take-off weight. The conversion to the equivalent annual departures and into the same landing gear configuration should be determined by the appropriate formula such as that used by FAA (FAA, 1978). For this computation 95 per cent of the gross weight of the aircraft is assumed to be carried by the main landing gear.

After all these considerations of the all-up weight, the next important factors are the landing gear configuration, and the operating frequencies of aircrafts. However, it was found that the heaviest aircraft which requires the greatest pavement thickness was the Boeing 727-200 and was thus used as the design aircraft [see Plate 2.1 b]. The total gross weight carried by the dual wheel landing gears of the design aircraft was 94.318 tonnes with a wheel spacing of 865 mm.

2.4.4 Aircraft Weight Limitation

The traffic mixture consists of a variety of aircraft having different landing gear types and different weights and tyre pressure with different frequencies. In order to assess their effect on the structural performance of pavements, all load contributions of the different aircraft sizes must be quantified and related to a specific characteristic. Attempts have been carried out to reduce mixed traffic to a single parameter such as

Load, Aircraft and Pavement Classification Numbers (LCN), (ACN), and (PCN) (Packard, 1967).

An economic analysis relating the cost of pavement upgrading to the penalty cost associated with adding gears and wheels to aircraft to provide adequate flotation for current pavement design criteria has been performed (Ledbetter, 1976). Adequate flotation implies distributing the total mass of the aircraft over a larger area to keep pavement stresses within acceptable limits. In this analysis, the question that had to be answered was, whether or not the FAA policy on pavement strength should be changed due to the advent of both wide body jets and the possible addition of an aircraft weighing up to 680 tonnes to air carrier fleets in the future. Of course, the basis for the answer was mainly economic. However, the basic assumption of the possible additional aircraft is unlikely to happen at least in the near future due to its compatibility with the existing airport facilities in general including pavement characteristics. Therefore, the cost analysis for aircraft and pavements recommended that the practical alternative of increasing the number of gear bogies to aircraft was more acceptable and economic than upgrading the existing airport pavement and changing the current FAA policy.

The effects of dynamic loading induced by aircraft performance on a pavement during landing and at the point of rotation for take-off as well as during low and high speed taxiing, braking, turning operations and surface unevenness are difficult to evaluate and need more research. A study of the responses of a typical flexible and rigid airport pavement to static and dynamic loading was undertaken by Ledbetter (Ledbetter, 1976). In this study, two series of full scale tests using B727 and C880 instrumented aircraft and runways were made. In general aircraft dynamic wheel loads have had a significant effect on airport pavements; specifically,

(i.) the increased magnitudes of aircraft wheel loads that result from aircraft modes of operation, pavement unevenness, and aircraft structural characteristics during moving ground operations, and

(ii.) the dynamic load phenomena associated with the materials used in the construction of both rigid and flexible pavements.

It was shown that none of the basic aircraft ground operating modes induced pavement responses (elastic plus inelastic) greater than those occurring for the static mass of the aircraft, even though the aircraft dynamic loads were as much as 1.2 times the static load. For landing performance, the measured aircraft loads showed that high horizontal

loads were applied to the pavement surfaces during turning. Where at the deepest layers monitored (i.e. 990 mm to 1300 mm for the flexible pavement and 380 mm to 610 mm for the rigid pavement) the responses to various modes of aircraft operation of the flexible and rigid pavements were 10 per cent and 30 per cent of their surface responses, respectively (Ledbetter, 1976).

Aircraft tyres treads which produce surface stresses higher than the tyre pressure due to the load concentration on the tread bars. For a given load, an increase in tyre inflation pressure reduces the net contact area, resulting in an increase in contact pressure. The contact areas are non-uniform with localised areas of high pressure, and the contact distribution can change with increases in tyre pressure. Without the treads, the contact distribution is uniform and equal to the tyre pressure. The contact area is then equal to the wheel load divided by the tyre pressure. it was found that near the centre of the tyre contact area, pressures were uniform and closer in magnitude to the tyre pressure (Okamoto and Pachard, 1989). Although this increases the stresses within the concrete surface, the stress concentrations are substantially dissipated through the pavement structure, and therefore, the effect on structural design parameters is negligible. Increasing the tyre pressure increases the pavement stresses in the surface which result in high stress concentration due to decreased surface curvature. For practical design, the tyre pressure produces the intensity of the applied load on pavement. Okamoto and Pachard (1989), showed that there was no significant difference in pavement response between the non-uniform pressure and uniform pressure net area distribution. The change in stress and deflection was less than 2 per cent and 1 per cent, respectively.

The thickness required for pavements subjected to parked or slow-moving aircraft should be based on the static mass of the aircraft, as is the current practice. This applies to the parking aprons, taxiways other than high speed exit areas, and runway ends. In high speed exit areas and other areas that are subjected to high speed aircraft operations only, design should be based on an analysis of the design loading to the pavement and the pavement response to dynamic loading. For an economic pavement design, in high-speed areas, high horizontal loads are applied to the pavement surface which requires high strength pavement surfaces rather than an increase in the overall thickness of the pavement.

2.4.5 Aircraft Traffic Mix

Among the most important factors to be evaluated in the structural design of airport pavements are the effects of aircraft type, traffic volume, and mode of operation of the

aircraft. The effect of aircraft traffic mix involves consideration of the various aircraft types expected to be encountered within the design life, the anticipated number of movements of each aircraft type within the design life, and the lateral wander effect of aircraft within the traffic mix. Also the mode of aircraft operation is primarily concerned with the speed at which the aircraft operates on the design pavement area. Other design criteria for airport pavements include the number of load repetitions that the pavement will receive during its fatigue life. The load repetition is an aircraft movement over a particular point on the pavement which normally constitutes a pass.

Pavements are often designed for operations by a specific type of aircraft, called standard or design aircraft, so the calculation of the loading system is relatively straight forward. Other approaches are adopted for mixed traffic operations. Although both methods consider the aircraft and traffic repetitions, the philosophy used in handling these affects are quite different. Normally, in the former design approach, only the heaviest or the most damaging aircraft is used and the damage effects of the other aircraft types are ignored. The procedure relying on a standard aircraft type within the aircraft traffic mix normally includes the use of determining the equivalent damage effects of all the aircraft types in the mix expressed in terms of the number of repetitions of the standard aircraft and thereby to calculate the number of equivalent coverages by the standard aircraft. While the magnitude and configuration of the wheel loads are the dominant factors in the design of airport pavements, therefore the forecast of aircraft traffic mix for an airport should be converted to the standard aircraft within the mix (see Section 2.4.2).

2.5 RANGE AND FREQUENCY OF LOADING

It is well established that heavier wheel or axle loads are more damaging to a pavement than lighter ones. The distribution of aircraft weights were described in sections 2.4.2 and 2.4.4 of this Chapter. In these sections, it was quite obvious that the magnitude and configuration of the wheel loads were the dominant factors in the design of airfield pavements. It is not the heaviest loads which are the most damaging to a pavement, but where magnitude and frequency combine to give a critical condition. The effect of fatigue caused by load repetition is an important concept for designing a pavement. However, pavements subject to high frequencies of trafficking have to be significantly thicker than those subject to low frequencies (Packard, 1974).

The appropriate frequency of trafficking depends on the number of coverages during the design life of a pavement. The coverages are effected by the design life, pattern of

trafficking and mixed traffic. An aircraft movement over a particular portion of the pavement normally counts for a pass or repetition. The total number of repetitions are considered as the total number of movements. The mixed traffic analysis is used to design the effect of aircraft operations at different gross weights. The details of mix traffic analysis are described in ICAO, FAA, DOT manuals, and others (ICAO, 1983, Dept. of Transport, 1978 and 1976, and Rada and Witczak, 1991). The relationship between passes and coverages depends on the main gear wheels, the width of the tyre contact area and the lateral distribution of the aircraft wheel paths relative to the pavement centre-line (i.e. lane channelling). The number of coverages which represent the number of times a particular point on the pavement is expected to receive a maximum stress as a result of a given number of aircraft passes, is calculated:

$$Coverage = \frac{Passes}{Pass - to - Coverage\ Radio}$$

In normal circumstances pavement deterioration is gradual, becoming noticeable over a period of a few years. This deterioration can be due to surface weathering or structural fatigue or both factors. It is recommended that the structural design life should be in a range of 20 to 40 years (Dept. of Transport, 1978 and 1989). More details about fatigue characteristics can be found in Chapters 3 and 7.

2.6 LANE CHANNELLING

Aircraft moving along an airport pavement possess some lateral wander associated with its movement. The net effect of this wander is that the number of aircraft passes is not equal to the number of coverages at a given point in the pavement. The coverages resulting from operations of a particular type of aircraft are a function of many factors that were stated in the previous Section 2.5. Fundamental to the current procedure for converting aircraft passes to coverages is the assumption that aircraft wheel-paths for 75 per cent of operations are uniformly distributed over a certain pavement width (Hosang, 1976). The wander varies significantly with the type of pavement characteristic under consideration. In some cases, the channelling is very important in pavement design; for example, vehicle movements in a highway are restricted within a lane width of the same order as the track width.

In airfield operations, the shapes of the lateral distribution patterns for take-offs are generally narrower than those for landings and both of them are different from the behaviour in taxiways particularly high speed taxiways. Relatively, the lateral

distributions of an aircraft on a runway are affected by crosswinds, wet pavements, and night operations.

The standard deviations for take-offs, landings, and taxiways are different. The standard deviation defines the distribution of wheels across a pavement and provides an estimate of the proportion of traffic covering a particular point on the pavement. A study carried out by Hosang, 1975, showed that the computed standard deviations for individual types of aircraft, compared at the various airports, generally varied from 0.91m to 2.4m for take-offs and from 1.2m to 2.7m for landings (Hosang, 1975). Also, there was no consistent correlation of the standard deviation with respect to type or size of aircraft. The standard deviations of the lateral distributions on high speed exit taxiways are generally greater than those on runways and are affected by the aircraft operational flow pattern and the exit configuration. It was found that the standard deviations of high-speed taxiways ranged from approximately 2.4m to 3.2m, with the upper limit probably more representative of typical exit configurations and their normal use (Hosang, 1975).

2.7 AIRCRAFT/PAVEMENT INTERACTION AND OPERATION

With the advent of the wide-bodied aircraft, and perhaps merely the stage of development that has been reached in aviation, there has been a strong interest in pavement behaviour on the part of aviation industry groups other than those directly concerned with pavement design. Major aircraft industries, as well as their Aircraft Industries Association (AIA), have shown a strong interest in pavement requirements for aircrafts. Similar interest in pavements has been evident on the part of the International Air Transport Association (IATA); the Aircraft Operators Council International (AOCI); the International Civil Aviation Organisation (ICAO); and the Air Line Pilots Association (ALPA).

The increase in the number of aircraft operations at the airports coupled with the continual growth of aircraft size and weight, are adding new dimensions of concern to airfield pavement design. This represents a broad concern for the interaction of aircraft and pavements, and points to the need for better understanding and definition of the effects of aircraft on pavements and of pavements on aircraft.

There has been a broad awakening to the problems of aircraft and supporting pavement interaction, particularly on the part of those concerned primarily with the aircraft. Through the years there has been a strong trend towards widening the concepts of pavement design. This began with little more than load, thickness, and some evaluation

of the in situ strength of the sub-grade. Concepts have been expanded to include material quality, climate effects, tyre pressure, frequencies, multiple wheels, mixed traffic, skid resistance and roughness.

The development and operation of an aircraft cannot be undertaken with safety in so far as ground handling is concerned, without full knowledge of the loading characteristics of the aircraft and the load bearing properties of the airfield pavement on which it is to operate. For instance, the aircraft classification number, pavement classification number (ACN, PCN) is the standardised ICAO method for reporting airport pavement strength. With this system, both the structural effect of an aircraft and the load carrying capacity of the pavement are expressed in terms of a standard single wheel load. The management of airport operations is greatly simplified by the fact that the effects of various gear configurations on a pavement can be compared directly in terms of the standard single wheel load. The PCN is based on a required design life, thus, operating an aircraft with an ACN larger than the pavement's PCN will shorten the design life of the pavement.

The problem of pavement unevenness is of concern to many operators in the airport and aircraft industries. Airport owners and operators are required to ensure that smoothness is maintained. Aircraft manufacturers are required to design their aircraft with a good ride quality and structural integrity for both air and ground operations. One of the objects of each is to minimise both aircraft structural damage and passenger and crew discomfort during ground operations.

2.8 ENVIRONMENTAL EFFECTS

Concern for the environmental effects of pavements is expanding, and significant research has been made in developing means of treating climatic variation. The response of a pavement is affected by the environmental conditions such as temperature and moisture in which it is situated. The design considerations associated with these factors are material stiffness, frost heave, and volume changes. Thermal stress depends on pavement temperatures.

The response of asphalt treated materials is temperature dependent, which influences their behaviour in pavement sections. Temperature changes cause thermal stresses in bituminous, asphalt concrete, and portland cement concrete pavements. The distribution of temperatures in pavement layers can be estimated from weather data as average air temperatures and their daily ranges by using various solutions such as the heat-

conduction equation (Barber, 1957, and Pretorius, 1969). Also temperature can be measured using a temperature sensor such as copper-constant thermocouples (Janoo and Berg, 1991). The surface and pavement temperatures are used for pavement analysis and design.

The water table is usually 3m or more below the surface. The soil generally is highly impervious to subsurface water flow and there is very little transmissibility of surface or subsurface water through the soil material. The water (i.e. moisture content) affects the responses of materials in pavement sections or layers to load and may cause undesirable volume changes like frost heave. Moisture content influences mainly the sub-grade and the unbound pavement materials. By increasing the moisture content of soil, its consistency can be varied from semi-solid to plastic to liquid.

For design purposes, the effect of moisture content can be evaluated by measuring the properties of untreated materials in the saturated condition using the soaked CBR test. The percentage of moisture content (i.e. Liquid and Plastic Limit (LL, PL), and Plastic Index (PI)), based on dry weight, at which each change in consistency occurs, can be determined using the Atterberg tests. It is widely known that soils with high plasticity indices are much less desirable for sub-grades or base courses than those having lower indices.

Frost and thaw depths can be determined using the surface temperature measurements. The frost and thaw depth can be accurately estimated for soil such as silty clay, sand, and silty sand by using the zero Celsius isotherm. It must be kept in mind that increasing thaw depths do not necessarily result in a drained layer above the frozen layer. In fact, observations indicated that trapped water in the sub-base layers during the early spring has a great impact on pavement performance during the thaw period (Janoo and Berg, 1991).

The load transfer efficiency is affected by temperature and the thaw depth. It was found that at the beginning of the spring thaw the load transfer efficiency followed the pavement temperature trend and then remained constant or underwent very small changes with pavement temperature (Janoo and Berg, 1991). Also, it was concluded that the initial high load transfer efficiency may be due to a frozen or partially frozen sub-base and/or sub-grade. As thawing progresses into the pavement structure, the load transfer efficiency decreases even though the pavement surface temperature increases. A pavement with a good drainage system, will drain the excess water and its load transfer efficiency will recover and increase with time.

2.9 Total Life Cycle Costs

The total life cycle cost concept is a means of comparing the total cost of different types of pavement. The components of the total life cycle cost comprise :

- Initial construction cost
- Maintenance cost
- Salvage cost

Since some of the components ,e.g. periodic maintenance, will be incurred at a future date, these future costs must be discounted to a present value using an appropriate discount rate and added to the initial construction cost in order to compare alternatives. Discount rate can be defined as the minimum attractive rate of return on an investment. It is difficult to predict the year on year discount rate over a design life of say forty years for a pavement but values of 5,10 and 15 per cent are often used in economic comparisons of pavements. By using a discount rate, it is possible to evaluate the present
worth of a future cost. The basic equation for determining present worth as stated in the CAA paper 9600, (Knapton and Emery, 1996) is:

$$PW = C + M_1\left(\frac{1}{1+r}\right)^{n_1} + \ldots\ldots\ldots\ldots\ldots\ldots\ldots\ldots + M_i\left(\frac{1}{1+r}\right)^{n_i} - S\left(\frac{1}{1+r}\right)^{z} \qquad (2.3)$$

where:

PW : Present Worth.

C : Present cost of initial design or rehabilitation activity.

M_i : Cost of the i^{th} maintenance or rehabilitation alternative in terms of present costs.

r : Discount rate.

n_i : Number of years from the present to the i^{th} maintenance or rehabilitation activity.

S : Salvage value at the end of the analysis period.

Z : Length of the analysis period in years.

$\left(\frac{1}{1+r}\right)^{n_i}$ = Single payment Present Worth Factor (PWF).

Salvage cost is a residual value at the end of the analysis period and should be expressed as a negative value in the whole life cycle cost analysis. It was considered that any salvage cost in a concrete pavement will be very small, say 10 per cent of its original value. Some other activities such as old sealant materials and overlay treatments to surface, were assumed to have no salvage value since there useful lives have been exhausted during the analysis period (FAA, AC150/5320-6C, 1978).

The life cycle cost of airfield pavement and similar paved areas was considered by different authorities in terms of initial construction cost, maintenance cost, salvage value and present worth value.

Three concrete block surfaced taxiways had been constructed at Dallas, Fort Worth International Airport (DFW) during 1990 (Larry et al, 1991). This type of pavement was selected due to its ease of construction, and its ability to shorten runway closures. The installation costs were comparable to the alternate Portland cement concrete pavement, and the maintenance costs were expected to be lower. A DFW study concluded that construction of Taxiways B and C, and other associated taxiways, significantly reduced delays and costs. By using concrete paving blocks instead of conventional concrete pavement, the DFW reduced its nightly construction runway closures from 14 to 12 hours. This two - hour reduction saved more than $37,000 (£25,000) daily in delays to the airlines. Over the 114 - night construction period that savings amounted to $4,232,000 (£2,821,334).

New development of a new international airport (DIA) in Denver, USA during 1990. Primary airfield elements included 6 - runways with associated taxiways and parking aprons (Loy and Warren, 1991). Life cycle cost analyses were conducted for both full-strength Portland cement concrete (PCC) and Asphalt concrete (AC), in accordance with FAA AC.150/5320-6C, 1978. Present worth economic analysis with a 4 per cent discount rate was used over 20-year and 40-year design lives. The results of the life cycle cost analyses were obtained as the life cycle costs over the 20 and 40 year design lives, of the PCC were less than the AC by 19 per cent and 37.7 per cent respectively. Based on these analyses, the full-strength pavement "PCC" was preferred.

A new 1 km (0.625 m) runway associated with a small parking apron (i.e. total area of 26,000 m^2) were completed on Thevenard Island, Western Australia, using concrete paving block in March 1995 (Muir, 1996). The consulting Engineers of this project investigated different pavement alternatives including concrete paving blocks. Life cycle cost analyses 15-year design life and construction period of 6-weeks indicated that the concrete paving blocks was the most suitable option. The initial construction cost for this option was AUD $2.4m, where for other options such as the cement stabilising sand; and prime and two coat seal were AUD $1.1m and AUD $1.5m respectively. Technically, however both these options required regular maintenance that increased the total life cost to values higher than that of the paving blocks. The asphalt concrete option of an initial construction of AUD $1.9m was considered but would still require

some maintenance. Based on the life cost analyses and pavement performance, it was decided that the concrete paving blocks presented the most attractive option.

With this brief in mind, it was felt that similar analysis should be carried out for the precast concrete raft units as a new paving system for airfields [see Section 7.8].

2.10 Summary of Chapter

A brief review on the interaction between the aircraft and pavement was presented. Airport pavement, however, are related uniquely to the aircraft itself and its operating qualities. The considerations which govern the pavement and the aircraft together are simply, that the pavement must physically support the aircraft during all its ground phases with a minimum safety risk when taking-off and landing.

Historically, pavements have been divided into two broad categories, flexible and rigid pavement. These two categories can be subdivided further into one of the types shown in Figure 2.1, which includes the conventional pavement (asphalt and PQC) the concrete block pavement, and the precast concrete raft units pavement. There are two main elements in a pavement structure namely the surface material and the base. The behaviour of pavement structures depends mainly on the ultimate strengths of the component materials. Material characterisation has been used to quantify their elastic and visco-plastic behaviour.

Pavement performance depends to a large extent upon the types of paving materials chosen. The basic requirements for a pavement structure to fulfil are:

(i.) to provide a uniform riding quality,
(ii.) to be strong enough to carry the traffic and control the environmental effects,
(iii.) to provide a good drainage system and a skid resistance, and
(iv.) to provide an economical life cost.

The increase in the number of aircraft operations at the airports coupled with the continual growth of aircraft size and weight, are adding new dimensions of concern to airfield pavement design. The rapid growth of airport operation during 1940's led different international organisations to lay down standards and specification in order to obtain a uniform control of airport operation. The advent of the heavy and wide body aircraft has brought a new concern for pavement design and airport operation. Therefore, it was necessary on the ground to support either the aircraft by providing more wheels within the main landing gear or by strengthening the pavement. However,

the characteristics of the aircraft which affect pavement strength design are aircraft all-up weight, wheel configuration, and contact pressure.

The total life cycle cost concept was introduced by comparing the total cost of airfield pavement and similar paved areas that considered by different authorities was illustrated in terms of initial construction cost, maintenance cost, salvage value, and present worth value.

Chapter - Three

DESIGN REVIEW: CONVENTIONAL PAVEMENTS AND PRECAST CONCRETE RAFT UNITS

3.1 INTRODUCTION

There are many pavement design methods which are based on past experience and on theoretical analyses. Neither of these two approaches are satisfactory within themselves. Complete reliance upon past experience of pavement performance needs a relatively long time before a new concept can be proven. On the other hand, theoretical equations are based upon simplified assumptions which cannot be universally applied. A balance between these two approaches would probably give a more comprehensive design solution. The methods vary from the use of charts to sophisticated computer analysis. It would appear that past research particularly in recent years contributed to the development of improved methods of pavement design which would have the potential impact to provide solutions to pavement problems as well as increasing the reliability of the design.

Elastic mathematical models have been developed for most design methods, and the majority of research has been based on this approach. Although pavement behaviour is not truly elastic, plastic behaviour is much more difficult to model and some of the relevant parameters are not known with sufficient accuracy.

Several complete design methods have been based on the multi-layer elastic model. The finite element theory provides a ready method of solution for plastic and elastic behaviour in a multi-layered system. In these methods all pavement materials are assumed to be homogeneous, isotropic with infinite horizontal dimensions.

The raft units have been widely used throughout the world as a paving system for highways, industrial cargo areas and as pavement repairs for airports. The complexities of either an analytical or an empirical solution to the design of raft units are due to the non-linear behaviour of the pavement components in terms of stress, strain and deflections, and the lack of information on fatigue performance. None of the analytical solutions which are used to design infinite pavements, are suitable for the analysis of raft units, where it is necessary to consider the finite size of the raft unit, the layered foundation, the loading positions, and the tyre contact area. Most of the design methods

for raft units are based on using finite element analysis combined with Westergaard's analysis for concrete pavements (Westergaard, 1926). The original Westergaard pavement analysis has been criticised in favour of finite element analysis due to some of its assumptions. Vesic and Saxena (1969) have shown that the combined tensile stress in a cement concrete pavement is the best indicator of pavement performance. They developed relationships which were used for developing a new design method for raft units namely the Bull design method (Bull, 1986). The maximum principle tensile strain in the raft units and the maximum compressive strain were used as the critical maintenance criteria for the pavement.

3.2 DESIGN METHODS FOR CONVENTIONAL PAVEMENTS

There are many design methods in current use and not all of them can be covered here. The major constraint in the development of a satisfactory theoretical basis for pavement design has been a lack of detailed information on the properties of the materials.

Many highway and airport test pavements have been constructed and monitored around the world in order to reach a sufficient advanced understanding of the behaviour of the materials. The following pavement trials were specifically relating to road pavements and represented the most popular and well known experiments.

(i.) W.A.S.H.O. Road Test (Western Association of State Highway Officials); and

(ii.) A.A.S.H.O. Road Test (American Association of State Highway Officials).

Both trials took place in USA toward the end of the 1950 decade.

The principal aim of these tests was to examine the effects of various axle loads and wheel configurations on the performance of both flexible and rigid road pavements. One of the major conclusions of the A.A.S.H.O. Road Test was the development of equivalence damage factors for different axle loads. The tests showed that damage sustained by a pavement was dependent on the vehicles axle load, but independent of pavement structure (see Section 3.11.3).

The development of empirical pavement design methods has been investigated widely. American design methods have been reviewed extensively by Yoder and Witczak, (1975). The different design methods used in Europe were discussed by Peattie, (1975), and details of several specific methods can be found elsewhere. An empirical design

method that has been used widely in the UK is Road Note 29 (Road Research Laboratory, 1970; Powell et al, 1984; and DOT-HD26/94, 1994).

There are several airport pavement design methods in common use. There is no universally accepted method available at present although a great deal of research has and is being carried out on a world wide basis. The I.C.A.O. Pavement Design Manual lists the following alternative design methods without any particular recommendation (ICAO, 1977):

- Canadian Practice
- US (FAA) Practice
- LCN Method
- French Practice
- UK (DOE) Practice

In addition, various other design methods such as Portland Cement Association (PCA) and Corps of Engineers. A brief discussion for the American specifications can be found in Westergaard, (1926). The design method used for airport pavements in the UK was issued by the Department of the Environment (DOE), (1989). When these methods are used, then, each give a slightly different pavement requirement in terms of overall depth and individual layer thicknesses. Designers prefer to check the design of a pavement by two or more of the methods including their own favoured method. Then a decision on the pavement construction is made on the basis of the calculated layer thicknesses coupled with experience of the performance of airport pavements at the particular airport itself or elsewhere that offers a similar environment.

The main feature of these design methods is the use of empirical design charts. Due to the variation in the stress distribution of single, dual, and dual tandem gear aircraft, separate flexible pavement design charts for each of these landing gear arrangements have been used in designing airport flexible pavements.

Two of these design methods have been chosen to outline briefly their procedure; they are the Portland Cement Association (PCA) and the Federal Aviation Administration (FAA).

PCA Design Method:

This method is based on design charts produced for several specific aircraft. The modulus of elasticity of the concrete is assumed to be 4,000,000 psi (27590 N/mm$^{2)}$ and Poisson's ratio for the concrete was 0.15. The variations in E and μ, have only a slight effect of about 5 per cent and 8 per cent on thickness design, respectively (Packard, 1973).

The basis of these charts was developed from;

(i.) the performance of existing pavements on both civil and military airfields;

(ii.) the full-scale pavement loading tests such as those conducted by the US Army Corps of Engineers during and since World War II;

(iii.) the controlled laboratory tests of pavement sections and models; and

(iv.) the theoretical studies of pavement stresses and deflections by H. M. Westergaard, Gerald Pickett, Gordon K. Ray, Donald M. Burmister, and others.

Bending of the concrete pavement under wheel loads produces both compression and flexural stresses. Ratios of flexural stress to flexural strength are often exceeding values of 0.5 and therefore the design charts for pavement thickness are based on the modulus of rupture (MR) of the concrete. It was recommended by (PCA) that the final design should be based on MR test data at 90-days, but in the absence of this data the following approximate relationship between flexural and compressive strength can be used in the preliminary design stages (Packard, 1973).

$$MR = K\sqrt{f_c} \tag{3.1}$$

where,

MR = Modulus of Rupture (psi)

K = a constant between 8 and 10

f_c = compression strength (psi)

A safety factor, which is represented as a ratio of design modulus of rupture to working stress, is used when specific data on trafficking and frequencies of aircraft movements are not available.

Flexural fatigue research on concrete has shown that, when the stress ratio is not more than about 0.55, concrete will withstand virtually unlimited stress repetitions without loss in load-carrying capacity (Packard, 1973). Rest periods also increase the flexural fatigue resistance of concrete.

The PCA used two methods to develop its own coverages and fatigue design procedure. The first is the coverage method developed by the US Army Corps of Engineers as part of their pavement design methodology for both rigid and flexible pavements (Packard, 1973). The following equation relates coverages to the number of operations for a specific aircraft:

$$C = D \times \frac{0.75NW}{12T} \tag{3.2}$$

where,

C = coverages

D = number of operations at full load

N = number of wheels on one main gear

W = width of contact area of one tyre, inches

T = traffic width, feet

The second is the fatigue method used for highway pavement design and based on concrete fatigue research (Portland Cement Association, 1966). The percentage fatigue used by any given load can then be determined by dividing the actual repetition of load by the allowable repetition of load. If the sum of the ratios is equal to the number given in the following equation, the pavement will not fail (Yoder and Witczak, 1975):

$$\frac{n_1}{N_1} + \frac{n_2}{N_2} + \ldots\ldots\ldots + \frac{n_n}{N_n} \leq 1.0 \text{ } to \text{ } 1.10 \tag{3.3}$$

where,

n = actual repetitions

N = allowable repetitions

FAA Design Method:

In 1958, the FAA adopted a policy of limiting Federal participation in aircraft pavements to pavement sections designed to serve at least a 160 tonnes aircraft with a DC-80-50 series landing gear configuration. With the increasing gross weight of aircraft, and the number and spacing of landing gear wheels, the FAA has adopted a method of designing and reporting aircraft pavement strength in terms of gross aircraft weight for each type of landing gear. The FAA made some changes to the previous design charts in the 1970's (FAA, 1978) to include:

(i.) the main under-carriages of the aircraft were assumed now to support 95 per cent instead of 90 per cent of the total weight of the aircraft; and

(ii.) the gross aircraft weights would be used instead of single wheel loads.

The pavement design charts were developed using the California Bearing Ratio (C.B.R.) method for flexible pavements and the Westergaard edge loading analysis for rigid pavements. Also, when designing jointed rigid airport pavements, the edge loading stresses were reduced by 25 per cent to account for load transfer across joints.

The design charts proposed by the FAA were used in the same manner as all charts of this type, including the PCA charts. As an input to these charts, the 90 day flexural strength of the pavement concrete was required. The design thickness values (T) obtained from these charts were for critical areas. Criteria for the FAA state that the thickness of non-critical areas should be 0.9, 0.8, or 0.7 times the critical pavement thickness (T) depending on traffic type and relative location.

The revised edition of the FAA Pavement Design Manual in 1980 adopted new design charts and as a result the new design procedures required relatively thicker pavement sections.

The use of stabilised bases under a concrete pavement was recommended by the FAA for the heavy loads of dual-tandem aircraft.

Fatigue effects are taken into consideration by converting annual departures to coverages assuming a 20 year design life (FAA, 1978).

3.3 DEVELOPMENT OF WESTERGAARD'S SOLUTIONS

3.3.1 Introduction

The analytical work of Professor Harald Malcom Westergaard (1888-1950) has been at the heart of pavement design since the 1920's. Every code of practice published since then makes reference to the "Westergaard solutions". These solutions are only available for three particular loading conditions (interior, edge and corner), and assume a slab of infinite or semi-infinite dimensions. For some circumstances, the Westergaard equations have often been misquoted or misapplied. Therefore, much research has been undertaken to reconsider these solutions using different analytical design methods (Ioannides et al., 1985); for example, the finite element method. Several investigators, however, have noted repeatedly that although the original Westergaard solution agreed fairly well with their observations for the interior loading condition; Equation (3.4), failed to give even a close estimate of the response in the case of edge and corner loading, Equations (3.5 & 3.6), for the conventional concrete pavement (Ioannides et al., 1985) and precast concrete rafts (Bull, 1991).

$$\sigma_i = \frac{3P(1+\mu)}{2\pi h^2}\left[\ln\left(\frac{2l}{a}\right) + 0.5 - \gamma\right] + \sigma_2 \tag{3.4}$$

$$\sigma_{e\,(semi\,-circle)} = 0.529(1+0.54\mu)\frac{P}{h^2}\left[\log\left(\frac{Eh^3}{Ka_2^4}\right) - 0.71\right] \tag{3.5}$$

$$\sigma_c = \frac{3P}{h^2}\left[1 - \left(\frac{12(1-\mu^2)K}{Eh^3}\right)^{0.15} \times (a\sqrt{2})^{0.6}\right] \tag{3.6}$$

where,

P = total applied load

E = slab Young's modulus

μ = slab Poisson's ratio

h = slab thickness

K = modulus of subgrade reaction

γ = Euler's constant (= 0.577)

σ_2 = supplementary stress =

$$= \frac{3P(1+\mu)}{64h^2}\left[\left(\frac{a}{l}\right)^2\right] \tag{3.7}$$

a = radius of circular load

a_2 = radius of semi-circle

l = radius of relative stiffness $= 4\sqrt{\frac{Eh^3}{12(1+\mu^2)K}}$

Investigators have put in a substantial effort since the 1920's to evaluate and examine the Westergaard solutions (Westergaard, 1926) in their different forms, namely, the theoretical background, the limitations and applicability of these Equations (3.4, 3.5, and 3.6). Several empirical adjustments to the Westergaard solutions and slab size requirements for the development of Westergaard responses have been considered.

3.3.2 Interior Loading

As defined by Westergaard, it is the case where a wheel load at a considerable distance from the slabs edge, with contact pressure assumed to be uniformly distributed over the area of a small circle with radius "a" (Westergaard, 1926).

Equation (3.4) includes a supplementary stress, σ_2, which was first derived by Westergaard (1939), Equation (3.7). This additional term was introduced to account for the effect of the finite size of the loaded area, and it was found that it was satisfactorily applicable when "a" does not exceed "l", [see Section 3.3.6]. Some changes to Equation (3.4) were proposed by Westergaard (1926), in which the radius "b" replaces the true radius "a" of the loaded area.

$$\sigma_{i(special\ theory)} = \frac{3P(1+\mu)}{2\pi h^2}\left[\ln\left(\frac{2l}{b}\right) + 0.5 - \gamma\right] + \sigma_2 \tag{3.8}$$

where,

$b = \sqrt{1.6a^2 + h^2} - 0.675h \rightarrow a\langle 1.724h$

$b = a \rightarrow a\rangle 1.724h$

NOTE:

Equation (3.8) shows the relationship between a, b, and h.

$$\sigma_{2(special\ theory)} = \frac{3P(1+\mu)}{64h^2}\left[\left(\frac{b}{l}\right)^2\right] \tag{3.9}$$

This was introduced to account for the effect of shear stresses in the vicinity of the load, neglected in Equation (3.4). The validity of Westergaard's semi-empirical adjustment and of the resulting special theory, Equation (3.8), has been debated by various investigators Bull (1991), BPA (1983), and Ackroyd and Bull (1985). It was recommended, that when comparisons with finite element results were made, with ordinary theory, Equation (3.4) should be used (Ioannides et al., 1985).

3.3.3 Edge Loading

Westergaard defined edge loading as the case when the wheel load was at the edge away from any corner. The contact pressure was assumed by Westergaard (1926) to be distributed uniformly over the area of a small semi-circle with the centre at the edge.

The first equations for a circular load at the edge were presented in 1948, by Westergaard (1947). In this presentation, generalised solutions for maximum stress and deflection were produced using elliptical and semi-elliptical loaded areas placed at a slab edge.

Setting the lengths of both the major and minor semi-axes of the ellipse to "a" or "a_2" led to the corresponding solutions for a circle radius "a", or a semi-circle radius "a_2", given by the following equations.

circle:

(New formula)

$$\sigma_e = \frac{3(1+\mu)P}{\pi(3+\mu)h^2}\left[\ln\left(\frac{Eh^3}{100Ka^4}\right) + 1.84 - \frac{4\mu}{3} + \frac{1-\mu}{2} + 1.18(1+2\mu)\left(\frac{a}{l}\right)\right] \tag{3.10}$$

semi-circle:

(New formula)

$$\sigma_e = \frac{3(1+\mu)P}{\pi(3+\mu)h^2}\left[\ln\left(\frac{Eh^3}{100Ka_2^4}\right) + 3.84 - \frac{4\mu}{3} + 0.5(1+2\mu)\left(\frac{a_2}{l}\right)\right] \quad (3.11)$$

circle:

(New formula)

$$\delta_e = \frac{P\sqrt{2+1.2\mu}}{\sqrt{Eh^3K}}\left[1-(0.76+0.4\mu)\left(\frac{a}{l}\right)\right] \quad (3.12)$$

semi-circle:

(New formula)

$$\delta_e = \frac{P\sqrt{2+1.2\mu}}{\sqrt{Eh^3K}}\left[1-(0.323+0.17\mu)\left(\frac{a_2}{l}\right)\right] \quad (3.13)$$

where,

σ_e = maximum bending stress for edge loading

δ_e = maximum deflection for edge loading

Further work was presented by Losberg (1960) to simplify these Equations (3.10, 3.11, 3.12, and 3.13), by introducing simplifications of the same type as introduced by Westergaard (1923) in his original formula, Equation (3.5), to eliminate the complicated functional relationship in which μ appears in these equations. So, the simplified new formulae were

circle:

(Simplified new formula)

$$\sigma_e = \frac{-6P}{h^2}(1+0.5\mu)\left[0.489\log\left(\frac{a}{l}\right) - 0.012 - 0.063\left(\frac{a}{l}\right)\right] \quad (3.14)$$

semi-circle:

(Simplified new formula)

$$\sigma_e = \frac{-6P}{h^2}(1+0.5\mu)\left[0.489\log\left(\frac{a_2}{l}\right) - 0.091 - 0.027\left(\frac{a_2}{l}\right)\right] \tag{3.15}$$

circle:

(Simplified new formula)

$$\delta_e = \frac{1}{\sqrt{6}}(1+0.4\mu)\frac{P}{Kl^2}\left[1 - 0.76(1+0.5\mu)\left(\frac{a}{l}\right)\right] \tag{3.16}$$

semi-circle:

(Simplified new formula)

$$\delta_e = \frac{1}{\sqrt{6}}(1+0.4\mu)\frac{P}{Kl^2}\left[1 - 0.323(1+0.5\mu)\left(\frac{a_2}{l}\right)\right] \tag{3.17}$$

In the formulae proposed by Losberg (1960), which are given by Equations (3.16 & 3.17), the Westergaard's original equation, Equation (3.18) for edge deflection Westergaard (1926) can be derived by setting the radius of the loaded area to zero.

$$\delta_e = \frac{1}{\sqrt{6}}(1+0.4\mu)\frac{P}{Kl^2} \tag{3.18}$$

Comparisons were made between the general Equations (3.10 & 3.11) and the Losberg's simplified Equations (3.14 & 3.15), which showed that the latter led to results which were typically about 1 per cent greater than those obtained by the first (Ioannides et al., 1985).

It was pointed out above, as well as by other investigators (Losberg 1960, and Bergstrom et al. 1949), that in the case of interior deflection, stress, and edge deflection, when the "new" formulae were specified for a circular and a semi-circular loaded area, they became identical to the corresponding Westergaard's original Equations (3.6 & 3.13). It was shown that edge stresses calculated from the "new" formula were considerably different from those computed using the original formula (Ioannides et al., 1985).

It was shown that the "new" formulae, Equations (3.11 & 3.13), typically led to stresses that were 55 per cent higher and deflections 8 per cent lower than the values obtained using the original formulae, Equations (3.5 and 3.18) (Ioannides et al., 1985). A comparison was carried out between Equations (3.11 & 3.13) and Equations (3.10 & 3.12), and indicated that the semi-circular load was more severe than the circular load, i.e. led to higher stress and deflections. This difference was due to the argument of where the centre of gravity was located in both cases semi-circle and circle loads. This argument led also to a conclusion that the difference in response from a circular and semi-circular load should be fairly small, and was proportional to the difference in the distance between the respective centres of gravity and the slab edge.

It was found that the difference between Equations (3.11 & 3.13) and Equations (3.10 & 3.12) was about 1 per cent, and the deflection differences were about 5 per cent (Ioannides et al., 1985). These differences were more compatible with expected values, than the stress difference obtained using the original equations.

Ioannides et al. (1985), performed a comparison between Westergaard's Equations (3.10 & 3.12), Illi-SLAB, and H-51 (Kreger, 1967). The latter was a computerised version proposed by Pickett and Ray (1951) in a form of chart for edge loading. It suggested that stresses exhibit almost perfect agreement, even at the low $\left(\frac{L}{l}\right)$ values, and deflections were more sensitive to the effects of slab size. Furthermore it found an excellent agreement between Illi-SLAB and H-51 results and the "new" formula, which confirms Losberg's observation that the original formula for edge loading according to Westergaard (1926) is, at least theoretically, completely erroneous.

The Pickett and Ray charts (Pickett and Ray, 1951) for the edge loading condition on a dense liquid sub-grade were based on a pair of integral equations identical to those presented by Westergaard (1947). The results from these charts, therefore, agree with the "new" formulae as stated above. It is interesting to note that although in several design codes reference is made to the original equation, the fact that multiple-wheel loads were often considered implies that design charts in these codes have been obtained using the Pickett and Ray charts, i.e. the “new" formulae. It was stated that, the question of the source of the discrepancy between Westergaard's original and "new" formula for edge loading remains unanswered, and was too early to dismiss the original formula as altogether false.

Bergstrom et al. (1949) reported that values calculated using these equations were "in relatively close agreement with test results". They furthermore suggested that there were no reasons to use the new formula for edge loading. On the other hand, Scott (1981) suggested that experimental indications are that the edge stresses experienced in practice are higher than the Westergaard original equation indicates.

Laboratory model tests by Carlton and Behrmann produced edge stresses 10 per cent to 12 per cent lower than the "new" formula predicts, supporting the expectation that in-situ values probably lie between the two Westergaard equations (Goldbeck, 1919).

3.3.4 Corner Loading

Corner loading is undoubtedly the most obscure and debatable case when compared to the interior and edge loading cases. The initial attempts to solve the problem of the corner loading case was carried out by Goldbeck (1919), and Older (1924). By assuming that in the corner region the slab acted as a cantilever of uniform strength, i.e. that in this region the subgrade reaction was negligible compared to the applied loads, Equation (3.19).

$$\sigma_c = \frac{3P}{h^2} \tag{3.19}$$

The semi-empirical and approximate nature of the determination of the maximum corner stresses and deflection have led to revisions and modifications in the years following their original publication by Kelley (1939) and Pickett (1946). They attempted to discuss the behaviour of observed slabs with theory. Westergaard took up this point trying to account for the effect of a load "P" distributed over an area at a small distance a_1 from the corner, along the bisector of the corner angle of Westergaard (1926). Using a simple approximation process, such as the use of the principle of minimum potential energy, an improved approximation to the corner deflection and stress was reached, Equations (3.20 & 3.21) of Westergaard (1926). Furthermore, the distance "X_1" to the point of maximum stress along the corner angle bisector was found to be given "roughly" by Equation (3.22) of Westergaard (1926).

$$\delta_c = \frac{P}{Kl^2}\left[1.1 - 0.88\frac{a_1}{l}\right] \tag{3.20}$$

$$\sigma_c = \frac{3P}{h^2}\left[1-\left(\frac{a}{l}\right)^{0.6}\right] \tag{3.21}$$

$$X_1 = 2\sqrt{a_1 l} \tag{3.22}$$

$$X_1 = 1.8C^{0.32}l^{0.59} \tag{3.23}$$

A new equation was developed by (Ioannides et al., 1985) for the location of the maximum stress, Equation (3.23). This equation indicated that the influence of the radius of relative stiffness, l, was much greater than that of the size of the loaded area, and suggested that these two parameters contributed equally in the determination of "X_1".

3.3.5 The Effect of Slab Size

Westergaard solutions assume a slab size of infinite dimensions. In practice empirical guidelines have been developed for the least slab dimension (L) required to achieve the Westergaard "infinite slab" condition. Westergaard-type equations are applicable only for an infinite slab size and simplifying assumptions need to be imposed to analyse small slabs (Bull, 1990).

Ioannides et al. (1985) analysed a slab with a radius of relative stiffness "l" of 23.16in (588.3 mm) and a mesh fineness ratio (i.e. $\frac{2a}{h}$) of 1.8 using F.E.M. for establishing similar guidelines. It was pointed out that for the interior loading, both the maximum deflection and bending stress converge as slabs become bigger. The same patterns were observed for the other loading conditions (i.e. edge and corner loading). The rate of convergence was defined as the slab size at which the infinite slab solution should be used. The maximum deflection and bending stress converge $\left(\frac{L}{l}\right)$ were varied between the three loading positions and ranged between 8.0 and 5.0; and 3.5 and 5.0 respectively.

It was found that deflection appeared to be much more sensitive to slab size changes for $\left(\frac{L}{l}\right)$ values of less than 3, whereas bending stress was less sensitive to changes in $\left(\frac{L}{l}\right)$ (Ioannides et al., 1985). The limiting value which was approached by maximum deflection $\left(i.e.\ \frac{L}{l}=8.0\right)$ was the Westergaard solution, Equation (3.24). On the other hand, the value to which bending stress converged upon slab size expansion was slightly lower than the Westergaard's solution, Equation (3.4). Design methods based on the

Westergaard analytical solutions include the assumption of infinite slab size. Nevertheless, model studies (Ioannides et al., 1985; and Behrmann, 1964) have found that this assumption can be met for slabs having dimensions not less than three to five times the radius of relative stiffness.

$$\delta_{i(circle)} = \frac{P}{8Kl^2}\left[1+\left(\frac{1}{2}\pi\right)\left(\ln\left(\frac{a}{2l}\right)+\gamma-\frac{5}{4}\right)\left(\frac{a}{l}\right)^2\right] \qquad (3.24)$$

3.3.6 Equation for the Corner Loading Condition based on a F.E.M.

An analysis was reported by Ioannides et al. (1985) using a F.E.M. to establish a set of equations that would predict accurately the response of a slab, in full contact with a winkler foundation, to a single load distributed over a small area at its corner similar to those proposed by other investigators Westergaard (1926), Goldbeck (1919), Older (1924), Kelley (1939), and Pickett (1946). A special effort was made to keep the general form of the equations the same as that of the Westergaard formula. Thus, a straight line was used to describe corner deflections, δ_c, which were obtained using the F.E.M. Equation (3.25).

$$\delta_c = \frac{P}{Kl^2}\left(1.205-0.69\left(\frac{C}{l}\right)\right) \qquad (3.25)$$

where,

C = the side length of the square loaded area

The similarity to Westergaard's equation indicated that Westergaard's approximation was fairly good. The finite element results obtained by Ioannides et al. (1985) were typically about 10 per cent higher than those predicted by Westergaard. This was explained to be due to the lack of a theoretical solution for a square loaded area, as well as the limitation of the finite element solution with respect to mesh fineness and slab size.

In the case of the maximum corner stresses, σ_c, this analysis suggested an equation represented these stresses, Equation (3.26).

$$\sigma_c = \frac{3P}{h^2}\left(1.0-\left(\frac{C}{l}\right)^{0.72}\right) \qquad (3.26)$$

Assuming that finite element results give a fairly accurate view of the theoretical solution, the Westergaard equation, Equation 3.21, represents a considerable improvement over the Goldbeck-Older equation, Equation (3.19).

The F.E.M. gave results which fell between those predicted by Westergaard (1939) and those predicted by Bradbury (1938). Most of the empirical modifications to the Westergaard formula have tended to increase the discrepancy between calculated and theoretical stresses. As a result, discrepancies between measured responses and theory may be expected. Scott (1981) pointed out that experimental indications showed that the corner stresses experienced in practice were higher than that indicated by the Westergaard equation.

3.3.7 Effect of the Size of the Loaded Area

An attempt to develop equations for a loaded area of finite size was performed by Westergaard. Westergaard (1947) suggested that his equations were valid for any size of loaded area and assumed that the average width and length of the footprint of the tyre was greater than the thickness of the slab in all significant cases. Losberg (1960) showed that stress and deflection equations presented by Westergaard, are only the first one or two terms of a rapidly converging infinite series. The rate of convergence can be expected to vary depending, among other things, upon the size of the loaded area.

The effect of the size of the loaded area was investigated by Ioannides et al. (1985) using the F.E.M. It was observed that Westergaard stress values, Equation (3.4), agreed with finite element results for a loaded area whose side length, C (if square) was about 0.2 times the radius of relative stiffness, "*l*", and if the loaded area was circular, its radius, "a", must be about 0.1 *l*. As $\left(\frac{c}{l}\right)$ or $\left(\frac{a}{l}\right)$ increase, finite element stresses become progressively higher than Westergaard's. Therefore, the consequences of Westergaard's limitation mentioned above, should be borne in mind when attempting such comparisons.

Responses, for the corner loading case, were generalised with respect to the values obtained using the proposed best fit equations (3.25) and (3.26) [see Section 3.3.6] (Ioannides et al., 1985). Accordingly, it was observed that deflections were not very sensitive to changes in $\left(\frac{c}{l}\right)$, but stresses diverge from the theoretical values as $\left(\frac{c}{l}\right)$ exceeds about 0.2. The trend exhibited by corner stresses is the reverse of that for

interior loading. The effect of $\left(\frac{c}{l}\right)$ on corner stresses is less clear than for interior stresses.

A study was conducted by Portland Cement Association (Packard, 1973), using B727 aircraft with different contact areas, to determine the magnitude of this effect and whether significant error resulted. The results were expressed as changes in stress by referring these stresses for different contact areas under equal load to a stress for specific contact area. The conclusion of the study showed that, the stress level was not particularly sensitive to changes in contact area, and the stress change was about 5 per cent as contact area varied over a wide range of 190 sq. in (0.12258 m^2) to 240 sq. in (0.15484 m^2).

The finite element analysis run by Bull and Clark (1991), found that for centrally loading, by increasing the loaded contact area from 200mm×200mm to 400mm×400mm (the contact area for the design load B727-200) reduced the concrete stress and the total faulting deflection by 23.4 per cent and 21.8 per cent respectively. The same for the corner loading where the centre of the loaded area moved toward the raft unit centre as the loaded area increased, the concrete stress and the total faulting deflection were reduced by 19 per cent and 19.1 per cent respectively.

Fukuda (1977), found that the stress components in the lower part of the concrete slab were hardly affected by the contact pattern of load. Therefore, the contact pattern of wheel load can be approximated in engineering design to a circular or rectangular pattern of uniformly distributed load. In the majority of pavement design, circular and rectangular tyre imprints and the uniform distribution of the contact pressure over the imprint area are assumed.

From this brief review, it was concluded that the stress and deflection levels were not particularly sensitive to changes in the size of contact area, as the changes in stress and deflection levels were in an average of 20 per cent. These changes have given a conservative and safe parameter design. with this brief in mind, the laboratory contact area of this research was designed (see Section 4.6.2).

3.4 BULL'S ANALYTICAL DESIGN METHOD

There were no direct methods or charts revealed in the literature survey which could be used to design precast concrete raft unit pavements. Bull (1984) has investigated

theoretically the factors affecting the behaviour of raft stresses, subgrade bearing pressure and developed design charts which were claimed as a new design method for raft units (Bull, 1986). In this analysis, Westergaard's principles and a model of the raft unit lying on a liquid subgrade were used. It was assumed, the raft unit would act as a homogeneous elastic solid and that the reactions of the subgrade were purely vertical and directly proportional to the deflection of the raft unit; (i.e. "k" the modulus of subgrade reaction). The analysis also assumed that there was only one layer underneath the raft unit.

The finite element package PAFEC Ltd. (1978) was used together with the eight-node, three-dimensional brick element number 37100, to develop the numerical design method for raft units (Bull, 1986). From this output data, the stresses and ultimate stress (PUS) were found. The criteria considered were the maximum combined tensile stress in the concrete raft unit and the maximum compressive stress developed in the subgrade. In this design method, the point at which the serviceability limit state was reached was defined as the criterion of the combined maximum tensile stress that would be induced in a plain concrete pavement (Vesic and Saxena, 1969), Equation (3.27).

$$N = 225000\left[\frac{\sigma_c}{\sigma_Q}\right]^4 \qquad (3.27)$$

where,

σ_c = tensile stress of the concrete

σ_Q = maximum combined tensile stress induced in the raft unit due to load Q

N = number of load applications to the point where the raft unit pavement may require repair or replacement.

Equation (3.27) was used in the analysis to determine the number of load applications; the stress was found from the three-dimensional finite element stress field. From the vertical centre point load applied downward on a raft unit, a stress value due to a 10kN load was obtained (Bull, 1986) and expressed as a percentage of its ultimate stress (PUS) which was found to be of 5.55N/mm^2 (Vesic and Saxena, 1969, and Highway Research Board, 1962).

The number of load repetitions predicted by the Bull design method was investigated experimentally (Bull et al., 1986). These laboratory tests showed that the number of load repetitions predicted by using the design charts associated with the Bull method

represented a critical condition when the raft unit required maintenance, but despite serious cracks the raft unit continued to sustain loading to a number of load repetitions more than those predicted by the design charts. Furthermore, as the load increased, the design charts showed a reduction in the predicted number of repetitions. The design charts which were based on an analytical investigation were used as a design method for the raft units (Bull, 1986). But further work, both theoretically and experimentally, was needed to validate this method.

The design method has been updated since 1984 by Annang (Bull et al., 1986) and Ismail (1990). The first investigated and modified the design method by including the size of the loaded area. The second has developed and refined numerically Bull's design method by using a more accurate element in the Finite Element Method and including different sizes of loaded areas [see Section 7.5].

3.5 BRITISH PORTS ASSOCIATION DESIGN METHOD

The British Ports Association (BPA) (now changed to the British Ports Federation, BPF) method is based on design charts which were produced using assumptions based upon the fatigue orientated elastic analysis, using the concept of a port area wheel load (PAWL), the load classification index (LCI), and on infinite pavement (BPA, 1983). These charts can be used for the design of the pavement layers in a pavement trafficked by port handling equipment and similar vehicles. They can be used for the design of rigid and flexible pavements. In this publication, the design of raft units using the BPA manual was discussed. The design method was based on an equation proposed by Hukelom and Klomp (1978), [equation 3.28], giving pavement damage D in terms of maximum load W_m and its contact pressure P_m for calculating the applied loading condition

$$D = \left[\frac{W_n}{W_m}\right]^{3.75} \times \left[\frac{P_n}{P_m}\right]^{1.25} \qquad (3.28)$$

Where

W_m = Maximum load to cause failure after a design life represented by *N*, the number of cycles

W_n = Applied load

P_m = Contact pressure of the maximum design load.

P_n = Contact pressure of the Applied load

The loading conditions considered in the BPA method, were the load classification index (LCI) and the damaging effect which was represented by calculating the "Port Area Wheel Load" (PAWL). Therefore the damaging effect of the PAWL was calculated from the following from that based on equation 3.28:

$$D = \left[\frac{W}{12000}\right]^{3.75} \times \left[\frac{P}{0.8}\right]^{1.25} \qquad (3.29)$$

where,

D = pavement damage

W = wheel load (kg)

P = tyre pressure (N/mm^2), not more than $2N/mm^2$

"D" was measured in Port Area Wheel Load (PAWL) units and a damage effect of one PAWL was defined as the damage inflicted on a pavement by one repetition of a 12,000kg wheel applying a contact pressure of $0.8N/mm^2$.

Relatively, the maintenance criterion which was considered in Bull's design method was used in the "BPA" design method. Excessive vertical compressive strain in the sub-grade and excessive horizontal tensile strain in the raft units were the causes of serviceability failure in the pavement.

The analysis technique used in the BPA method for designing a pavement was that each course within the pavement was transformed into an equivalent thickness of pavement sub-grade material (Odemark, 1949).

As the original pavement has now been replaced by a pavement in which each course has the properties of the sub-grade, the strains due to applied load can be calculated using the Boussinesq analysis technique (Heukelom and Foster, 1960). The strains were calculated at the boundary of each layer and were compared with limiting strains for the actual layer of the pavement. The sub-grade was characterised by its C.B.R. value, and the charts were produced accordingly. The C.B.R. values ranged to represent the very weak to the good sub-grade strengths. The sub-grade was assumed to be semi-infinite and its elastic modulus was equal to ten times its C.B.R. value (Croney, 1977). In this

method (BPA), the sub-base was optional and the charts were produced for a certain depth of the sub-base namely 600mm, 300mm, 150mm, and no sub-base. The elastic modulus for this course was calculated from the thickness of the sub-base and the elastic modulus of the sub-grade (Shell International Petroleum, 1978).

Some other work has shown that two of the assumptions upon which, this design method was based may invalidate its use for raft units; namely the use of the equivalent single wheel load to represent multiple wheel loading and the assumption that the pavement was continuous (Knapton, 1986).

3.6 ACKROYD DESIGN METHOD

This design method was based on using the finite element method combined with Westergaard (Westergaard, 1926) analysis for concrete pavements (Ackroyd and Bull, 1985). It used square raft units of 2m×2m for heavy duty pavements on low bearing capacity sub-grades. It used a series of interrelated graphs to determine the required sub-base thickness, raft thickness, allowable concrete tensile stress, and allowable sub-grade bearing pressure to satisfy the required number and type of loadings.

The maintenance criteria for the raft units was considered to be the maximum tensile stress in the raft unit (Vesic and Saxena, 1969), and the maximum compressive strain in the sub-grade (Shell International Petroleum, 1978). The raft unit serviceability state, expressed as the number of load application which can be related to the concrete tensile stress due to the applied load (Vesic and Saxena, 1969), while the subgrade compressive strain can be related to the sub-grade stress due to the pavement loading (Croney, 1977).

As stated in Section 3.3, the first complete theoretical design method for rigid pavements was developed by Westergaard (1926). Further work allowed the slab tensile stress for any shape of loaded area to be deduced for the system analysed by Westergaard (Pickett and Ray, 1951). A layered pavement system solution forms the basis of multilayer elastic pavement analysis computer programmes. These analyses are mainly used for infinite pavements, but they are used for non-infinite slabs as an approximation, where it is necessary to consider the small size of the raft unit, the layered foundation, the load positions, and contact area. Therefore, as a trial to solve these difficulties, a work carried out by Ackroyd and Bull (1985) using finite element analysis of individual raft units and an experimental verification of the design method was performed. This experimental verification has shown that raft units must be

designed as individual units, and the use of the equivalent single wheel load concept must be discounted.

In this design method, design charts were produced using finite element models with the corner and edge loading as the most critical positions. The chosen model was based on work performed by Taylor (1982) which found that there are three critical load cases for raft units that were analogous to those investigated by Westergaard (1926). The variables investigated in this design method were ten in number. Two (Young's modulus and thickness) in each layer of the raft unit, sand bedding, sub-base, and subgrade plus the contact area (A) and the applied load (P). The Poisson ratio's, of all the materials were set at standard values due to its small effect on the stresses (*i.e.* about 1 per cent).
A series of comparative trials were conducted to determine the most suitable combination of elements based on a simply supported plate and a plate with free edges on a Winkler foundation (Ackroyd and Bull, 1985). This foundation was composed of either spring elements, or in later models, a thin layer of brick elements overlaying a rigid base. It has been shown that provided the elastic layer was thin, the latter model can represent accurately a Winkler foundation (Vesic and Saxena, 1969). This was confirmed by running equivalent models on each foundation and obtaining identical results for the stresses and deflections of the plate (Ackroyd and Bull, 1985).

A set of twelve design charts have been produced which enables raft units to be designed for the maximum tensile stress in the raft unit and the maximum compressive stress in the subgrade due to a single wheel load. The first four charts were used to determine a modulus of subgrade reaction "k" for a raft unit loaded at the centre of an edge. The value of "k" for a given foundation may be inserted into Westergaard's original formula (Westergaard, 1926) to determine the maximum tensile stress in the raft unit. The second four charts have been prepared from Westergaard's original formula and are used to determine the maximum tensile stress in the raft unit for a standard 10kN load at the centre of one edge. The last four charts are used to determine the maximum subgrade bearing pressure "SGBP" due to the standard 10kN load placed at the corner of the raft unit. In this design method, the authors concluded that closely spaced wheels can be considered by using the equivalent wheel load concept, but further development is required to deal with more than one wheel on the raft unit.

3.7 RECENT WORK AT NEWCASTLE

Analytical and experimental work has been carried out recently in the Department of Civil Engineering, University of Newcastle Upon Tyne by different researchers studying the behaviour of raft units (Ismail, 1990, and Salmo, 1990).

Ismail, (1990) reports the analytical validation of the method to design Precast Concrete Pavement Units (see section 7.5). The work included the effect of repeated loading on the design life of the raft pavement, load transfer and raft interlock, infinite element analysis of the raft units, and the use of raft units as a partially supported medium. Also, the design life of raft units with different contact pressures were investigated.

The research conclusions were as follow:

(i.) it was found that the contact area of the applied load affects the design life of the raft by increasing the contact area the ultimate load and the design life increased;

(ii.) the punching shear was not the main cause of the failure of the raft unit and there was no need for shear reinforcement;

(iii.) yield lines on the failed raft unit that had been loaded at the centre, were found to be perpendicular to the sides of the raft unit. These were due to the upward deflection of the four corners which did not allow the diagonal yield line pattern to form, as assumed by different theories;

(iv.) computer analysis of the raft units, has produced design charts which can be used in conjunction with Bull's design method (Bull, 1986), to design a precast concrete pavement. In these analyses the effects of the various design parameters (i.e. raft design properties, sub-base and sub-grade thickness, and sub-grade C.B.R.) on both the ultimate concrete stress (PUS) and the sub-grade bearing pressure (SGBP) were included in the charts;

(v.) using PAFEC software (Pafec Ltd., 1978), an attempt was made to overcome the problem of the raft unit lifting upwards when loaded at the corner or at the edge, by modelling the gap or separation between the raft and the bedding layer using the beams module and a partial solution was obtained; and

(vi.) it was suggested that raft units could be used on a partial medium such as covers for services and drainage gullies; it was shown that the 2m square by 200mm thick and the 1.3m x 2m rectangle by 140mm thick raft units were suitable as simply supported covers.

Salmo, (1990) included experimental and analytical investigations on "Precast Concrete Pavements Used in Port Areas" catering for the large imposed loadings from the stacked containers. The finite element method of analysis was used in the investigation and an experimental programme was carried out on raft units of 2m x 2m x 140mm thick, under one and two point static and dynamic loading conditions. These raft units were tested on a polystyrene layer and on rock fill.

The research findings are summarised below:

(i.) the static loading revealed that the vertical load capacity of raft units were controlled by the position and magnitude of the applied loads; and influenced by the composition and spacing between the loaded areas of the applied load;

(ii.) it was found that the horizontal distributions of the principal stresses through the depth of the raft unit of 140mm, were non-linear;

(iii.) it was found that the most stable position of two point load was when the loaded areas were at one metre centres and the ultimate load was up to 60 tonnes. The ultimate load for longer spans between the loaded areas namely 2m and diagonally opposite corner positions were 58 per cent and 42 per cent of the ultimate load of 1m centres, respectively; and

(iv.) a relationship between the induced tensile strain (crack width) in a raft unit, and the predicted number of load repetitions using the formula developed by Vesic and Saxena (1969), to render a raft unfit for service, was established for one point load at the centre and two point load at 1m centres. The equation was in the following form:

$$N = C\alpha^{n}$$

where,

N = predicted number of load repetitions

C = constant

$$\alpha = \frac{\varepsilon_f}{\varepsilon_L}$$

ε_f = failure strain

ε_L = strain corresponding to 1000 cycles for a particular load.

Using the plotted curve of the experimental results, the final formula was;

$$N = 1000 \times \left[\frac{\varepsilon_f}{\varepsilon_L}\right]^3 \tag{3.30}$$

3.8 CONCLUSIONS DRAWN FROM THE THREE DESIGN METHODS

The maintenance criteria assumed for the design methods proposed by Ackroyd and Bull were the maximum compressive strain in the subgrade and the maximum tensile stress in the raft unit. The BPA method assumed that the maintenance criteria were the allowable subgrade vertical compressive strain and the allowable horizontal tensile strain in the concrete.

The BPA method uses the Port Axle Wheel Load (PAWL), where Ackroyd uses a 10kN load acting at the centre, at the corner or in the middle of an edge; and Bull uses 10kN single or multiple wheel load at any position on the raft.

The design methods developed by Bull, (1986), and Ackroyd and Bull, (1985) indicated that the maximum stress within the raft unit could be in the top or bottom surface depending upon the multiple wheel position, and the maximum stress "PUS" in the raft; the maximum "SGBP" did not occur simultaneously. The "SGBP" stress was always a maximum when the raft unit was loaded at the corner. The maximum stress in the raft unit occurred when loaded at the middle of one edge which was confirmed experimentally by Taylor, (1982) which indicated that Westergaard's corner formula was not applicable to the raft unit. The reason was that the raft unit rotates about a horizontal axis as the corner is loaded, and the support for the corner loading was principally by cantilever action which caused large tensile stresses in the concrete.

For the British Ports Association design method, there were two contradictions for the design of raft units, namely the use of the equivalent single wheel load to represent multiple wheel loading and also the assumption that the pavement is continuous.

It was found that the loading of a raft unit affects adjacent raft units whether there is a physical connection through a gap filler, or not (Pickett, 1946, and Ismail, 1990). The reason for this was that the load was transferred to the lower pavement layers forming a depression and, causing adjacent raft units to deflect. The present approach of designing rafts, assumes no load transfer between rafts. This assumption is valid and will give a conservative design.

3.9 LOAD TRANSFER FOR CONVENTIONAL CONCRETE PAVEMENT

3.9.1 Joint Types

Joints for rigid pavements can be divided into four basic groups:

(i.) contraction joints;
(ii.) expansion joints;
(iii.) construction joints; and
(iv.) hinge or warping joints.

Each type of joint has a distinct function and thus is used only at certain sections of the pavement. The function of these joints follow below.

A variety of jointing layouts can be used for different types of concrete pavements depending upon a number of factors. These layouts may include short slabs with no reinforcement and longer slabs with reinforcement distributed through the slab along with the use of load transfer devices. It is necessary to provide load transfer across all joints. This can be accomplished in short non-reinforced slabs by aggregate interlock, whereas for longer slabs, load transfer must be provided by means of dowel bars, key ways or perhaps the use of a stiff sub-base such as cement treated or asphalt-treated gravel.

3.9.2 Load Transfer Across Joints

Theoretically, if the dowel was 100 per cent efficient, the dowel would transfer one-half of the applied load from one slab to another (PCA, 1966). This is true if each slab at the joint deflects an equal amount and the designer assumes that one-half of the applied load bears on each slab. Therefore, if a load was applied just a small distance from the joint, the design load for the dowel bar should be one half of the design load. However, looseness that develops in the dowel embedment under the action of repeated load tends to reduce the load transfer. The following types of joints [see Fig. 3.1] and load transfer devices are generally used in concrete pavements.

(i.) Contraction Joints

Contraction joints are intended to relieve only tensile stresses resulting from contraction and warping in the concrete. The joint does not relieve expansion stresses. In some cases, load transfer from aggregate interlock may be questioned, and thus a dowel bar is placed across the joint. The dowel bar is used to transfer the load across the joint. Due to the movement of the slabs in the longitudinal direction, at least one-half of the dowel bar must be lubricated to permit freedom to slide.

(ii.) Expansion Joints

Expansion joints must be constructed with a gap throughout the depth of the slab to permit expansion to take place. Since the joint has no aggregate interlock, it is necessary to provide some type of load transfer. Expansion joints for highways are highly susceptible to pumping action, and therefore, their use is minimised. Their structural adequacy is determined to a large extent by the load transfer device. High expansion stresses result primarily from certain types of concrete aggregates. Field studies have indicated that the frequency of occurrence of blow ups is a function of the source and type of course aggregate (Yoder and Witczak, 1975). Thus, if due caution is used in selecting course aggregate, distress due to blow-ups can be minimised. This relieves the necessity of using expansion joints for most construction.

(iii.) Construction Joints

Construction joints are usually of the butt type and contain dowel bars for transferring the load across the joint. They are used at the transition from old to new construction.

(iv.) Hinge or Warping Joints

Hinge and/or warping joints are used to control cracking along the centreline of the pavement. The type of joint used depends primarily upon the method of pouring the concrete slabs. For instance, if lane-at-a-time construction is used, keyed joints are generally built. In some cases, the keyed joint are tied together with tie bars to make certain that the key functions in load transfer.

3.9.3 Joint Shape Factor

The importance of the joint shape factor is to provide an adequate seal at all joints. The purpose of sealing joints is to keep all material out of the joint and to provide resistance against infiltration of water through the joint.

3.9.4 Jointing at Intersections

The jointing of pavements at intersections becomes critical particularly, as it is well known that the concrete expands and contracts primarily in the direction of its longest dimension. For instance, if a taxiway is perpendicular to a runway, the runway will tend to move in the direction perpendicular to the paving lanes of the taxiway. Therefore, an expansion joint at the junction of the two pavements must be provided.

3.10 PRECAST CONCRETE PAVEMENT INTERLOCK

The extent of site preparation required for laying raft units will depend on the applied loads and the bearing capacity of the underneath layers. Precast concrete pavement joints must allow for concrete expansion and contraction from temperature changes and must be sealed to prevent debris from entering the joint. Additional to that, slab separation under traffic must be considered. It is necessary to provide restraint against this movement even if the pavement design does not require load transfer across the joints. In this case, tie and dowel bars at certain spacing can be used. Smooth male and female curved surfaces representing the sides of the slabs interlock and the edge restraint prevent slab separation. The edge anchor includes surface and subsurface drainage systems, kerbs, edge beams, or similar related structures.

In Eastern Europe, some precast raft units have been placed both with and without load transfer devices at the joints between the raft units. The latter contains additional

reinforcement at the edges and corners of the raft units instead of using load transfer across the joints to resist the high stresses at the edges of the raft units. The other type of raft units have two brackets along the short, transverse side of the raft unit, and brackets between adjacent raft units which are welded together to resist the high stresses. Furthermore, other jointing methods reported, in use are keyed joints, epoxy filled joints, and sand-cement grout filled joints (Mednikov et al., 1974). Joints every 18m to 20m are left unwelded to allow for raft movements.

A special type of joint was used in a test section of a precast, prestressed concrete slab pavement built on US Highway, South Dakota, and the research was conducted by the South Dakota State University (Gorsuch et al., 1962). A grout key as shown in Figure 3.2.b was used on the longitudinal sides to provide load transfer between adjacent slabs. An optional connection joint [see Fig. 3.2.c] was formed by widening the grout key at the slab longitudinal one-quarter and three quarter points and welding the protruding No. 3 reinforcing bars (10mm diameter) together. The South Dakota test was used as an example for recommending precast construction for strengthening airport pavements (Hargett, 1969).

Welding two points per slab side, as was the case with some of the East European slabs and the South Dakota slabs mentioned above, will help maintain the alignment of the slabs but in some cases will not provide load transfer except possibly when the load is immediately adjacent to the welded point (Rollings and Chou, 1981). The optional connection [see Fig. 3.2.c] could be provided on all the slab sides for load transfer, but this would require a significant amount of welding in the field. It was suggested that the preferred welded joint for reinforcing steel is a butt joint due to the alignment and welding requirements, but this would not be practical for precast pavement construction (Rollings and Chou, 1981). Furthermore, a single-lap welded splice [see Fig. 3.3.a, b] would be compatible with the South Dakota joint. However, the eccentricity of this joint can cause distortion when loaded, which tends to split the concrete cover. An improvement for the single-lap splice is the double-lap welded splice [see Fig. 3.3.c], but the work of welding is increased. It is possible to design a load-transferring welded joint using some variation to the South Dakota, or East European slabs design such as bar size, and spacing. It was advised that welded joint connections should be avoided due to the required large number of field welds under awkward conditions, and the difficulties in fabricating the preferred butt splice joint (Rollings and Chou, 1981).

A grouted shear key such as shown in Figure 3.2.a is relatively simple to fabricate and construct. The inclined faces of the key ensures mechanical interlock as well as adhesion of the grout to the slab face. Some special material grouts which have higher adhesion strengths can be used in this type of joint, but a mechanical interlock would still be required particularly for heavy loading. It seems that more tests are needed to evaluate grouted shear keys for heavy loading and large numbers of load repetitions such as for aircraft, and container handling vehicles.

The load transferring joints for precast concrete pavements are many and have different advantages and disadvantages for their use. Some of these types are,

(i.) a thin steel plate is inserted from the side between two slabs after they are placed, and a grout is injected beneath the plate [see Fig. 3.4.a];

(ii.) a tie or dowel bar is placed in a preformed faces of the slabs and grouted into place [see Fig 3.4.b];

(iii.) a sleeper slab is placed under the joint, and the joint is sealed with Bitumen [see Fig. 3.4.c]. This type thickens the edge of the slab at the joint and needs special preparation of the subgrade to accommodate the sleeper slab; and

(iv.) Figure 3.5 shows a joint load transfer device developed in France which consists of a steel deformed tube that allows expansion and contraction within the elastic range of the steel; it transfers the load between the rafts through shear, preventing relative displacement of the raft unit surfaces, and allowing the raft unit to expand without excessive restraint forces from the steel tube.

A series of tests were performed by Ismail (1990) at the University of Newcastle upon Tyne, using 2m square by 150mm thick precast concrete pavement raft units, to determine the amount of load transfer between the raft units. The construction gap between the raft units was 10mm, but one case was left without a gap (i.e. the raft units are touching and no gap filler had been used). Different filler materials (plywood, sand, polystyrene) were used to assist load transfer. One of these tests were performed with an empty gap of 10mm and a 600mm×600mm steel plate embedded in the layer under the converging corners of four raft units. The three Westergaard loading cases; interior, edge, and corner, were used. The results of these tests showed that whether there is physical contact through a gap filler or not, load was transferred to the lower pavement layers forming a depression and causing adjacent raft units to deflect. The results also

showed that using a gap filler in the corner loading case, reduces the deflection under the loaded point. The greatest reduction was achieved using the steel plate which stopped the corner of the raft unit punching into the lower layers.

3.11 RESEARCH INTO THE FATIGUE BEHAVIOUR OF CONCRETE PAVEMENTS

3.11.1 Fatigue Behaviour

Structural elements must sustain the development and application of stress or strain that produces permanent damage cumulatively during their service lives. The fatigue process in a certain condition may be governed by stress or strain levels. The life of a structure may be increased with decreasing levels of stress, and below a certain stress level it may possess infinite fatigue life. The fatigue process has usually three distinct stages, initiation, propagation and final failure. In case of defects, the initiation stage will be shortened and as a result a potential reduction in fatigue life becomes inevitable. The fluctuations of strain or stress (crack width) is the most important effective parameter to gauge the fatigue performance of a structure or any material. Additionally, the level of the maximum and minimum induced strains are also important.

The fatigue performance of concrete under a constant cyclical loading is usually dependent on both the stress amplitude and, to a lesser extent, on the mean stress level. The stress level may be expressed as a stress amplitude, or more usually as a stress ratio, R = min stress/max stress. Many researchers have dealt with the fatigue phenomena of concrete pavements under bending and different formulae have been proposed giving scattered results dependent on their own original assumptions. Research work has been undertaken on the fatigue of a highway pavement in Spain by Faraggi et. al. (1981), taking into account the ratio between the maximum and minimum applied stresses "R". The research has shown that for a given stress level "R" there was an increase in load repetitions to failure as the age of the concrete increased. As a result of this research, the following formula was produced;

$$\log_{10} N = \frac{11\left(1 - \frac{\sigma_{max}}{MR}\right)}{(1 - R)} \tag{3.31}$$

where,

N = Number of cycles "fatigue life" to failure.

R = Stress level.

MR = Modulus of rupture of concrete.

σ = Maximum applied stress.

The numerical coefficient (11) was adjusted to match the field fatigue behaviour of several Spanish concrete pavements. The numerical coefficient differs slightly from that proposed by Domenichini (1986). In practice, service loading of a pavement subjected to traffic, is not applied in a regular cyclical pattern over a period of hours or days. Traffic loads vary in both magnitude and intensity and depend on the time periods between successive load repetitions over the whole life of the pavement. Also, pavement loading varies with the speed of the traffic.

3.11.2 The Combined Effects of Traffic Loading and Temperature Variations

The combined effect of traffic loading and temperature changes on pavements is an important parameter when designing a pavement structure. In some cases, it has been proved by measurements on existing pavement that stresses calculated by adding values obtained individually compared to the simultaneous application of traffic loading and thermal gradients are not the same. The individual stresses are less than the combined stresses. Consequently, research was undertaken in order to calculate the combined effect of traffic loading and thermal gradients on concrete pavements by Faraggi (1986). The finite element method was used to analyse the results. The load positions which were used in the study were similar to those used by Westergaard. The concrete slabs were assumed to be resting on an elastic layered structure.

Among the various cases that could be used to combine traffic loads with zero temperature gradients were the results provided by the F.E.M. (Faraggi, 1986) and those obtained by Pickett and Ray (1951) influence charts. It was found that both solutions were in good agreement. Moreover, combinations of thermal gradients and zero traffic loading were employed to compare their results with those obtained by means of the Westergaard (1947), Bradbury (1938) and Kelley (1939) theories. It was found that the solutions resulted from the classic theory which normally underestimated such stresses.

It must be pointed out that with these particular combinations, it was possible to make a comparison between the stresses resulting from the addition of these values which were obtained separately, (as is assumed in some design procedures), and those calculated by considering the simultaneous presence of the same traffic load and thermal gradient. It was found that the stresses obtained due to a traffic load and a thermal gradient applied

at the same time were clearly greater than the sum of those calculated by considering each factor separately.

From this study, different formulae for these combinations were obtained at central and joint load positions. These formulas give the maximum values of stresses as a function of load, thermal gradient, slab dimensions L, h, and stresses σ. For further information about these formulae, the reader should refer to Faraggi et. al. (1986).

3.11.3 The Effect of Overloading on Fatigue Life

Historically, the analysis of traffic mix when designing airfield pavements have been based on the use of the critical or most damaging aircraft. The damage effects of other aircrafts are either ignored or incorporated empirically into the analysis. A major consideration in the design and evaluation of airfield pavements is the effect of traffic [see Section 2.4, Chapter 2]. For a particular aircraft type, such factors as the main gear configurations, tyre spacings, tyre loads and tyre pressures should be incorporated. Pavements seldom fail under the application of one heavy load. Damage generally results from an accumulation of small plastic deformations brought about by the passage of aircrafts operating broadly within the design standard under consideration. The heavy traffic loads have a well known impact on the performance of pavements particularly when the pavement was not designed to withstand such overloads, and, therefore, this potentially effects the pavement fatigue life.

To quantify the influence of any overloaded traffic repetitions, some preliminary evaluations should be made to include the effect of the maximum allowable load repetitions and temperature variation throughout the year together with the characteristics of the pavement. An investigation was carried out by Domenichini (1986), who considered the influence of overloads on concrete pavement fatigue life. Reference was made to a plain concrete pavement with dowelled joints. The number and the value of the overloads, and the changes in temperature were considered to be variables in the calculations. The traffic induced stresses were computed according to Westergaard (1926), with an allowance of 25 per cent for load transfer across the joint. The temperature induced stresses were computed according to the approach by Thomlinson (1940) and Eisenmann (1970) for each month of the year and for each hour of the day respectively. The fatigue analysis was based on the Miner fatigue rule and on the design fatigue relationship of the stress level of the load cycles (R) and the number of load repetitions to failure, Eqns. 3.32 and 3.33.

$$\frac{\sigma_{max}}{MR} = 1 - 0.0954(1-R)\log N \tag{3.32}$$

$$R = \frac{\sigma_{min}}{\sigma_{max}} = \frac{\sigma_{temperature}}{\sigma_{temperature} + \sigma_{traffic}} \tag{3.33}$$

In this investigation, it was found that contrary to experience, such a slab thickness must be increased by 20 per cent to assure the slab resists the influence of the overloading and to have a fatigue life comparable to the design life.

Other research was carried out in the late 1950's which formed part of the A.A.S.HO Road Test. One of the major conclusions of this research, was the development of equivalence damage factors for different axle loads. The tests showed that the induced damage was dependent mainly on the applied load, not on pavement structure. Therefore, a relationship was developed between pavement damage (D) and axle load (W) which was found to be

$$D \propto W^4$$

This relationship has been verified by results from other pavement tests, which have studied the subject in more detail and included tyre pressure (P) as an additional variable. Thus, Heukelom and Klomp (1978), proposed the following relationship [Eq. 3.28, Section 3.5];

$$D \propto W^{3.75} \times P^{1.25}$$

3.11.4 Assumptions Relating to Material Behaviour

An investigation into the fatigue analysis of plain concrete was carried out, taking into account the influences of traffic and temperature among other factors, by Cornelissen and Leewis (1986). The analysis was based on assumptions relating to the S-N (stress-number) curves which were used in the "VNC" design method, and the applicability of Miner's rule. The principles of this design method (Vereniging Nederlandse Cementindustrie, VNC) have been dealt with in Leewis and Van Der Most (1986).

The S-N curves give the relationship between the magnitude of the load variation and the number of variations (loading repetition) to failure. In this investigation, the slope of the S-N curves were estimated and the following formula was derived:

$$\log N = 12.6\left[1 - \frac{0.8\left(\frac{\sigma_{max} - \sigma_{min}}{f_{bk}}\right)}{0.8 - \left(\frac{\sigma_{min}}{f_{bk}}\right)}\right] \tag{3.34}$$

where;

f_{bk} = flexural tensile strength of the concrete

From Equation 3.34, as long as the number of cycles was lower than N (cycles to failure), the material would not fail, but it would undergo changes as a result of formation and propagation of different cracks. The load cycles cause different degrees of damage to the pavement.

Miner's linear damage accumulation rule assumes that the damage due to "n" cycles is equal to n/N. A loading group "i" comprising (n_i) the material would occur if;

$$\sum_{i=1}^{j} \frac{n_i}{N_i} = 1 \tag{3.35}$$

The results of this investigation were compared with the starting points of the so-called VNC-guideline for a concrete pavement. This guideline has been developed by the Vereniging Nederlandse Cementindustrie (VNC) (Dutch Cement Association) Leewis and Van Der Most (1986). This guideline is a recommendation of the VNC design method for concrete pavements which is based on determining the contribution of each traffic load and the temperature variation on the fatigue life of the pavement. The actual fatigue behaviour of concrete in a pavement was verified with reference to the results of comprehensive fatigue research carried out by the Stevin Laboratory, in which the effect of pulsating tensile stresses and of alternating tensile-compressive stresses was studied (Cornelissenen and Timmers, 1981). These stresses corresponded to those which occur in a concrete pavement under the influence of traffic and temperature. The conclusion of this investigation was:

(i.) the formula (Eqn. 3.34) which was used in the "VNC" design method for determining the number of load repetitions that can be resisted at a given temperature stress was a safe approximation; and

(ii.) Miner's rule (Eqn. 3.35) for determining the life of a pavement structure could be applied justifiably.

3.11.5 Prediction of the Fatigue Life of Concrete Pavements using Fatigue Cracking Models

Fatigue has become increasingly important as a design condition for pavement subjected to repeated loads during its service life. Cracking occurs in a concrete pavement slab when the tensile stress caused by wheel loading exceeds the tensile strength of the concrete. Therefore, cracking of concrete pavement can occur as a result of repetitive stresses. The number of repeated loads (N) that concrete pavement can sustain in flexure prior to fracture depends on the ratio of the applied stress to the ultimate static flexural strength of the concrete. A number of relationships between "N" and "R" are available (Portland Cement Association, 1966; and Darter, 1977). Further appraisal of the performance of concrete pavement has been made in terms of the effect of the major pavement variables, namely slab thickness, concrete strength, amount of reinforcement and foundation support. Equations have been established relating pavement life, in terms of standard axles, to these major variables (Vesic and Saxena, 1970; and Mayhew and Harding, 1987).

In 1962, a large amount of test data became available due from the AASHO Road Test results. Some of these results were analysed and two different relationships for single and tandem loads were derived to relate the rigid pavement performance directly to the edge stress (Hudson and Scrivner, 1962). They concluded that the edge stress was not the critical stress for slabs subjected to tandem loads. A complete stress and deflection analysis was performed for all rigid pavements slabs of the AASHO Road Test and a relationship between the critical stresses and the number of load repetitions for all slabs, regardless of type of loading , was derived (Eq. 3.27). The same principals were used for raft units (see Sections 3.4, 3.6, and 3.7). In these sections, it was found that concrete damage was not related linearly to the applied load but was usually related to the fourth power law.

The derived relationship, such as Eq. 3.27, has additional general implications regarding rigid pavement design. Considering the fact that the pavement stress was found to be proportional to wheel load "Q", and inversely proportional approximately to the 1.25 power of the slab thickness "h", a general relationship between the principle variable in the AASHO Road Test was established as:

$$N_{25} = Cf_c^4 h^5 Q^{-4} \tag{3.36}$$

This equation relates the ultimate number of axle-load applications, $N_{2.5}$, to the flexural strength of pavement material, f_c, the thickness of pavement slab, h, and the magnitude of axle load, Q. The term "C" is a constant. The equation showed the importance of these major variables, for example, the quality of pavement materials. A 10 per cent increase in strength of the concrete means a 50 per cent increase in pavement life. Also the equation gave a base for evaluation of effects of overload and mixed traffic on pavement life.

In 1987, Mayhew and Harding analysed performance data for a reinforced and an unreinforced pavement from seven experimental concrete road sites. The support offered by the foundations to the concrete slabs of the experimental roads was evaluated in terms of the Young's modulus of an equivalent uniform elastic foundation of infinite depth. A range of design variables was incorporated into each of the various experimental roads with a consequent and essential influence on pavement life. Data were available for these experiments and had a wide range of design variables namely, slab thickness, H in mm, concrete strength at 28 days, S in MPa, the foundation equivalent modulus, M in MPa and slab reinforcement, R in mm^2/m. The multiple regression analysis technique was used to examine the effect and significance of the variables that were thought most likely to influence pavement life in terms of cumulative traffic (msa). The regression estimate of cumulative traffic (L) in msa, that can be carried before failure is given by:

For Unreinforced slabs

$$ln(L) = 5.094ln(H) + 3.466ln(S) + 0.4836ln(M) + 0.08718ln(F) - 40.78 \tag{3.37}$$

where F→is the percentage of failed bays.

For Reinforced slabs

$$ln(L) = 4.786ln(H) + 1.418ln(R) + 3.171ln(S) + 0.3255ln(M) - 45.15 \tag{3.38}$$

The regression analysis indicated that slab thickness was the most significant variable; it accounted for 67 per cent of the variation in observed performance. The remaining

variables in order of significance were the amount of reinforcement, the concrete strength, and the foundation stiffness; these four variables accounted for 91 per cent of the variation in observed performance.

3.12 Summary of Chapter

There are many pavement design methods which are based on past experience and on theoretical analyses. Neither of these two approaches are satisfactory within themselves. A balance between these two approaches would probably give a more comprehensive solution.

Elastic mathematical models have been developed for most design methods, although pavement behaviour is not truly elastic, and the majority of research has been based on this approach. Several design methods have been based on the multi-layer elastic model. In this respect, the finite element theory provided a ready method of solution for plastic and elastic behaviour in a multi-layered system as pavement materials were assumed to be homogeneous, isotropic with infinite horizontal dimensions.

It was shown that none of the analytical solutions which are used to design infinite pavements (conventional pavement), are suitable for the analysis of raft unit pavement, where it is necessary to consider the finite size of the raft unit, the layered foundation, the loading positions, and the tyre contact area. The design methods for raft units pavement are based on using finite element analysis combined with Westergard's analysis for concrete pavements. In these design methods, the maximum compressive strain were used as the critical maintenance criteria for the raft units pavement.

The original Westergaard pavement analysis developed in 1926, has been criticised in favour of finite element analysis due to some of its assumptions which are not applicable on the finite size of the raft units.

The basic assumptions of Westergaard's analysis are:

(i.) the loading positions are at interior, edge and corner,

(ii.) the pavement is infinite or semi-infinite dimensions,

(iii.) the concrete slab is at all times in full contact with the underneath layers, and

(iv.) the foundation material is elastic.

The effect of the size of the loaded area was investigated by Westergaard (1947) using his original equations and Ioannides et al (1985) using the finite element method. It was observed that Westergaard stress values, Equation (3.4) agreed with the finite element results for a loaded area whose side length "C" (if square) was about 0.2 l, and if circular, its radius "a" must be about 0.1 l.

A detailed discussion was presented for the current design methods of raft units. As a result of the detailed discussion, the following conclusions were drawn:

(i.) the current design methods have little experimental back up. The experimental evidences are needed to validate and verify the assumptions of these methods,

(ii.) the maintenance criteria assumed for the design methods proposed by Ackroyd (1985), Bull (1986), Annange (1986), and Ismail (1990) were the maximum compressive strain in the subgrade and the maximum tensile stress in the raft unit, but for the BPA method were the allowable tensile strain in the concrete slab,

(iii.) the BPA method used the Port Axle Wheel Load (PAWL), where Ackroyd used 10 kN load acting at the centre of the raft unit, and Bull and Ismail used 10 kN single or multiple wheel load at any position on the raft unit,

(iv.) the design methods developed by Bull, Ackroyd, and Ismail indicated that the maximum stress within the raft unit could be in the top or bottom surface depending upon the multiple wheel position, and the maximum stress in the raft unit always occurred when loaded at the middle of one edge, and

(v.) there were two contradictions in the BPA method for the design of raft units, namely the use of the equivalent single wheel load (PAWL), to represent multiple wheel loading and also the assumption that the pavement is continuous.

The comparison of the current design methods has shown a great variation in design requirements of the raft unit and therefore, the need for a more powerful design method that can take into account most or all the various parameters of the raft unit pavement.

The load transferring joints for conventional and precast concrete pavements have been illustrated showing the advantages and disadvantages of their use particularly for the precast concrete raft units.

The fatigue performance of concrete pavement under repeated loads was reviewed. The fatigue process has usually three distinct stages, initiation, propagation, and final failure. The fluctuations of strain and final failure. The fluctuations of strain or stress (crack width) is the most important effective parameter to gauge the fatigue performance of the concrete pavement. Additionally, the level of the maximum and minimum induced strains are also important. The number of repeated loads (N) that concrete pavement can sustain prior failure depends on the ratio (R) of the applied stress to the maximum stress in the concrete. Further appraisal of the performance of concrete pavement has been made in terms of the effect of the major pavement variables, namely slab thickness, concrete strength, amount of reinforcement and foundation support. Thus, Equations have been established relating pavement life (N), in terms of standard axle load, to these major variables (Vesic and Saxena, 1970; and Mayhew and Hardin, 1987).

Chapter Four

EXPERIMENTAL PROGRAMME

4.1 INTRODUCTION

The fatigue characteristics of precast concrete raft units are determined normally by a full scale field test until complete failure occurs. This type of test usually is not practical due to the length of time needed to conduct such a test. A facility to test full scale precast concrete pavement raft units, has been built in the heavy structure laboratory of the Department of Civil Engineering at the University of Newcastle upon Tyne. The applied loading system was designed by the author and built in the Department Workshop to simulate the traffic loading applied by the undercarriage of a design aircraft Boeing B727-200.

This particular research project formed part of the long term research programme in the Department. A total of sixteen raft units were tested under two-point repeated loadings [see Table 4.1]. The raft units were constructed in the form of different sizes and different levels of reinforcement. The aim of this experimental programme was to determine the fatigue life and fatigue failure mechanism of reinforced precast concrete pavement raft units under two-point repeated loadings.

Physical models of structures are used often for design and study purposes. A model can be built and tested. Usually, the prime motivation to conduct experiments on structures at reduced scale is to reduce the cost of the experiments. Modelling in structures usually requires the utilisation of an equivalent material, whereby a much softer material replaces the prototypes in such a manner as to satisfy the condition of similarity (i.e. similitude). These are based on mathematical considerations where the scale of time, dimensions, and force are varied without changing the governing equations of a particular criteria. In practice it is almost impossible to attain perfect similitude, but the model may still be sufficiently accurate to yield valuable quantitative results.

The reliability of the results from a given physical modelling study is perhaps the single most important factor to the user of the modelling approach. Therefore, the precise structural modelling and the accuracy of measurements should be as close as possible to the prototype of the true structure. Although model studies have some limitation, they

have never the less been useful in some cases where the full scale model is not possible, in establishing several relationships describing the general behaviour patterns of structures.

As a general rule, one cannot devise a suitable model test incomparating the most significant variables, nor can the results of the model, unless the basic theory of the phenomenon is understood. Even though the general nature of the phenomenon may be known, it is often impracticable to build the exact model that would furnish directly the desired information. In other words, the model and the prototype would be completely similar. Obviously, complete similarity is impossible without geometric similarity. Usually it is not feasible and impractical to impose complete similarity in a model test. Consequently, some of the independent dimensionless variables are allowed to deviate from their correct values and then theoretical corrections have to be applied to compensate for them.

With this brief definition of structural modelling, and the facilities available in the Department of Civil Engineering, University of Newcastle upon Tyne, the full scale physical model approach was chosen except for the contact area of the design aircraft B727-200. The true contact area had to be scaled down from 400mm×400mm to 200mm×200mm in order to maintain different contact pressures related to the expected traffic mix and however, needed for analysing the raft units performance, by applying the load increments over a smaller fixed contact area [see Sections 4.6.2 and 4.7]. Therefore, the effect of using small fixed contact area instead of the exact size on the damage effect (i.e. fatigue life) of raft units could be corrected by means of the pavement damage concept proposed by Heukelom and Klomp, 1978. It was decided not to scale down the test model due to the availability of the laboratory facilities in the Department such as a high strength loading frame, loading equipment, and space; and the lack of funds to pursue alternative strategies. Also, due to the ability of the full scale model to portray the true behaviour of the full structure of the raft units with actual boundary conditions, it was decided to monitor the actual behaviour of the raft units and compare the results with numerical design methods. The full scale physical model was designed to meet the design criteria of the raft units subjected to the passage of the Boeing 727 design aircraft. The effect of the contact area being one-quarter of the full-scale size would mean significantly higher contact stress for a given applied load. This effect had to be accounted for in the subsequent analysis (see Chapters 5, 6, and 7).

The solution of this phenomenon (i.e. the raft unit performance) was expressed by means of dimensionally homogenous relationships in terms of the specified variables namely the plan dimensions, thickness, and reinforcement of the raft units, the applied loads, and the contact pressure. The measured variables were determined at the outset, on the basis of the understanding of the literature review of the raft units performance and raft unit design methods (see Chapter 3). Also the nature and constraints (*i.e.* cost and time) of this type of test programme did not allow for minor adjustments to be practical.

As the structural modelling approach was not used in this research project, any detailed discussion about the characteristics of structural modelling are beyond the scope of this thesis. In this Chapter, the engineering properties and dimensions of the full scale physical model are described together with the experimental procedures adopted for the project.

4.2 GENERAL DETAILS OF THE TEST RAFT UNITS

In the absence of full-scale test data and field experience of raft unit paving system, a series of full-scale raft unit pavement tests was set up for this research. The test programme of this research involved the simulation of the loading conditions of real aircraft operations of the loading conditions of real aircraft operations applied to full-scale raft unit pavement. The aim of the experimental programme was to determine the fatigue life and fatigue failure mechanism of the reinforced precast concrete raft units pavement under two point repeated loadings.

The full scale physical model was designed to meet the design criteria of the raft units subjected to the passage of the Boeing 727-200 design aircraft (see Section 4.1). Thus, the actual behaviour of the raft units can be monitored and compare the acquired results with the numerical design methods (see Chapter 3). The solution of the raft unit performance was expressed by means of relationships between the specified variables.

The criteria used to design the dimensions and reinforcement of raft units were based on durability and practicality of using the raft units in terms of how simple it would be to manufacture, to transport, to lay and most important to be economic.

In practice the weight and, therefore, the dimensions of the raft units was considered to be a main concern when designing the raft units in order to optimise their performance and yet achieve their advantages for use in constructions and repairs (see Chapter 1).

The standard design of the raft units (i.e. 2m square and 140mm thick) used for developing the numerical design method by Bull (1986) (see Chapter 3), was able to satisfy some but not all needs of constructions and repairs using the raft units. Therefore, different raft unit sizes were designed with different aspect ratios ranging from 0.25 to 1.0, to meet the different needs such as design layout for a raft unit paving system; and clarify their practical and economic use.

In order to study the effect of reinforcement on the performance of raft unit pavement, various forms of reinforcement [steel fabric and steel fibre] have been used. These forms of reinforcement were similar to that used in the numerical design method proposed by Bull (1986) for a range of 85 mm^2 / m to 314 mm^2 / m. The reinforcement was designed within the range set up relationships between the fatigue life "N" and the other parameters including the reinforcement, and to examine experimentally the effect of using various amount of reinforcement on the performance of the raft units pavement as well as to verify the numerical design method proposed by Bull (1986). Therefore, the steel mesh was designed with two layers at each of the top and the bottom that spaced 100mm and 200mm (see Section 4.3.3). From the literature, Chapter 3, a typical design for heavy aircraft loading would be to have reinforcement in both directions at the top and the bottom of the concrete pavement to cater for both the hogging and sagging moments. The other type of reinforcement namely the steel fibre, was designed to compare its performance with steel fabric reinforcement using the recommended quantity (i.e. 10% by weight) by the manufacturer.

To sum up, the design criteria of reinforcement and the raft unit dimensions used in the test raft units models were designed within the ranges that used in the numerical design method proposed by Bull (1986), see Chapter 3, in order to verify and modify the numerical design method and produce a new empirical design method. Thus, the laboratory experimental design and the results could be related to the numerical design method.

The simulated loading criteria was designed to include the basic aircraft ground operating modes of the design aircraft Boeing 727-200, for loads from 100kN to the standard design load of the design aircraft B727-200 (i.e. 450kN) and its gear configuration. The aircraft B727 -200 was determined to be the design aircraft by different international organisations (FAA,1978 and ICAO, 1983, 1984, and 1991).

The repeated moving load applied over the raft units test model in the laboratory was regarded as a simulation of moving the design aircraft B727-200 wheel load over a taxiway or an apron paved with raft units. The raft units test model was simulated in the form of moving wheel loads being applied at four most critical positions P1, P2, P3, and P4 which positions P1/P3 and P4 represent the classic loading positions (interior, edge, and corner) used in the classic and original pavement design method developed by Westergaard (1926) as well as used in the numerical design method proposed by Bull (1986). Loading position P2 represents a new position introduced by the author in order to clarify differences (if any) between this position P2 and position P4.

The real passages of the design aircraft B727-200 was considered during the experiment design stage. It was found technically and economically, that the erection of the real wheels of one leg of the design aircraft with a load of maximum take off weight, in a laboratory was not practical, despite its advantage of representing the real passage of the design aircraft (ie sequentially one passage at each of the four loading positions). Therefore, an economic and practical alternative was designed which represented a simulation of the dual wheels of one leg of the design aircraft B727-200.

The laboratory tests had a dominant loading direction and the applied loading was moved manually from positions P1 to P2 to P3 to P4 and then back to P1 to repeat the sequence. The repeated moving load was carried out by changing cyclically a loading position after 600 load cycles at each of the four loading positions and was considered to represent 600 passages of the applied load over the raft units test model. Such a loading procedure was adopted to simulate the continuous passage of wheel loads of the design aircraft Boeing 727-200 over a raft unit paving system.

The simulation of the passage of the aircraft over the raft units test model on critical assumptions that the tracking load was considered the critical wheel path and that the aircraft wheel paths followed that path for 100 per cent of operations and were uniformly distributed over the tracking load (see Section 2.6).

The loading direction was designed to represent the critical case for design the raft units pavement by creating a layout that produces maximum bending moments which usually appears along the longest span. The raft units were laid along their longer edges as to be perpendicular to the loading direction so as to obtain variations of the maximum bending moments along the longest span of the raft unit.

4.2.1 Test Series and Modules

Due to the length of time needed to complete one test and the time taken to load the test raft units to complete failure, only sixteen raft units were chosen for this research project. The raft units were tested in pairs, [see Tables 4.1 and 4.2]. A total of eight tests were performed. Each test occupied an average thirty working days, with ten working hours a day; in addition there were seven days for preparations and the final dismantling of each of the tests. Any breakdowns during the test are not included in these estimates of time.

The raft units were designed to cope with loads that arise during manufacture, transportation, stockpiling, construction, and of course, the required traffic loading. With raft units designed for airfield use, the heavy loads due to aircraft undercarriages were the predominant and ruling loading condition.

The test raft units were divided into three different modules, namely modules M1, M2, and M3 [see Table 4.2]. Module M1 consisted of five test raft units to investigate the effect of different raft dimensions on fatigue life; M2 consisted of three test raft units for investigating the effect of different reinforcement design on fatigue life; and M3 consisted of two test raft units for investigating the effect of different thickness design on fatigue life. Tables 4.1 and 4.2 show the detailed dimensions of the raft units.

4.2.2 Raft Notation

Most of the raft units used in the experimental programme have a prefix (R) followed by the initial of the raft shape, r or s, and then two numbers separated with a hyphen and followed by a letter D; the exceptions were the three raft units in Module M1, which have a prefix (R) followed by two numbers separated by hyphens and finally a letter D. The first and second numbers denote respectively the thickness and the serial number of the raft unit and the letter D denoted a two-point loading. Therefore, RS-14-1/D, for instance [see Table 4.1], denoted a raft unit (R) of square shape (S), and thickness 140mm with serial number (1), and loaded for two-point loading (D). R6-2/D, denoted a raft unit (R) with width 0.6m, serial number (2), and loaded for two-point loading (D). Raft RSF-14-3/D was the same as the previous reference apart from the extra letter F, which denoted a raft unit with a fibre reinforcement (F).

4.3 CONCRETE AND REINFORCEMENT DETAILS

4.3.1 Concrete Mix Design

The concrete mix was designed with properties similar to that used by the manufacturer of these raft units, namely "Redland Aggregates Limited". The concrete mix was designed to achieve a cube strength of 60 N/mm^2 at 28-day. The concrete mix used in the experimental programme was established by trials and had the following properties:

(i.) 28-day cube strength of 65 N/mm^2.

(ii.) Water/cement ratio of 0.35

(iii.) Cement (O.P.C.) 400kg/m^3

(iv.) Aggregate:
Granite 20mm. 400kg/m^3
Granite 10mm. 1100kg/m^3
Granite fine (5mm and less) 1500kg/m^3

(v.) Sand 1930kg/m^3

(vi.) Type of admixture, super plasticiser 4.2 litres, i.e. 10ml/kg of cement.

The above constituents, were weight/m^3 of fully compacted concrete. The use of admixtures or plasticiser was to improve the workability of the mix.

4.3.2 Concrete Strength

Due to the significant effect the proportions of these constituent materials have on the properties of high strength concrete, it was important to have trial mixes to obtain the correct mix proportions. A series of cubes were cast at the same time as the raft units for each batch of concrete. These cubes were tested in the manufacturer's laboratory by their engineers in order to determine the real strength of the concrete from which the Young's Modulus 'E' was obtained. The Young's Modulus 'E' and the Poisson's ratio 'v' were found as 34000MPa and 0.15 respectively. The concrete compressive strengths f_{cu} were taken as the average of three cube strength tests, determined after 7-days and 28-days after casting. The 7-day and 28-day cube strengths were found to be 62.3 N/mm^2 and

66.35 N/mm^2 respectively. The concrete strength of 65 N/mm^2 was used for the analysis of the test results.

4.3.3 Reinforcement Design

The test raft units have a number of different reinforcement characteristics [see Table 4.3]. Series 1 and 2 were reinforced with two layers at each of the top and bottom, and Series 3 was reinforced with fibre steel. Each layer was arranged in two directions, longitudinally and transversely. Longitudinal and transverse bars were spaced 100mm apart in Series 1, and 200mm apart in Series 2. End and side clearances were 100mm to allow for nearly complete reinforcement and yet achieve adequate concrete cover. The top and bottom cover was 50mm and 40mm respectively. Welded deformed bars with 6mm diameter were used for series 1 and 2 reinforcement. High yield strength reinforcing steel was used, series 1 and 2 were reinforced with steel of strength 480 N/mm^2. The range of the percentage of the steel was between 0.05 per cent and 0.3 per cent of the cross-sectional area of the pavement.

The steel fibre reinforcement used in Series 3, was a glued fibre type of Dramix stainless steel. The steel fibres were glued together in compact bundles which made it easier to add the fibres to the concrete and to obtain a homogeneous mixture. The fibres had hooked ends that allowed a strong mechanical anchorage in the concrete. The fibres were made of cold drawn steel wire with a minimum tensile strength of 1,100 N/mm^2. The fibre steel reinforcement of Series 3 was designed with round stainless steel hooked fibre, comprising, 0.65mm diameter/ 60mm length, aspect ratio $\frac{l}{d} = 92$, and a weight of 240 kg/m^3 (i.e. 10 per cent by weight) with aligned fibre steel. The reinforcement was closely spaced fibres to improve the tensile strength. The concrete mix design was the same for all the raft units prepared for the experimental programme.

4.4 THE MANUFACTURE OF PRECAST CONCRETE PAVEMENT RAFT UNITS

The manufacture of these raft units was carried out in the "Redland Aggregates Limited" factory. It was not possible to manufacture raft units in the laboratory of the Department due to their size, weight, volume, and the need for a large space, heavy duty special equipment, large concrete mix plant, plus special tools for formwork, casting, and handling. The following general brief description of the manufacture of the raft units was drawn from Bull (1990).

4.4.1 Formwork

The casting of the raft units was carried out as a wet cast process in large open pan moulds. The finish and accuracy of the moulds employed was critical if consistent and accurate products were to be made. There are different types of mould materials (wooden, steel, glass-reinforced plastic) in which their use depended largely on the number of components to be manufactured and their sizes.

A glass-reinforced plastic (G.R.P.) mould was used to produce the 2 metre square test raft units. Due to the cost of G.R.P., commercial measures must be taken to ensure the most effective use of the glass and resin. G.R.P. is a composite material consisting of filaments of glass impregnated with a polymeric binding agent, usually a polyester or epoxy resin.

A master wooden pattern or plug had to be produced providing an exact replica of the required raft unit; this was fixed face down onto a rigid flat board. Shuttering was then fixed around the edges of the base board. A thin resin/glass laminate shell was laid up over the pattern and base board so that an accurate and highly defined surface skin was formed. A series of ties or layer of steel mesh was bonded to the sides and edges of the skin using glass fibre laminated strips. At this stage, steel lifting point inserts were attached to the inside faces of the side shuttering together with any other steel locating plates or inserts, such as the lift tube mountings on the finished mould skin.
The void space between the shutter and the pattern was now filled with concrete and any additional required reinforcement were inserted. Once the concrete was adequately cured, the side shuttering was removed and the lift point inserts or a vacuum lift pad used to draw the concrete backed mould skin off the master pattern

Figure 4.8(a) and (b) shows the typical raft profile sections for framed and frameless raft units. Figure 4.9 shows the main components of the G.R.P. mould for construction and assembly.

4.4.2 Casting

Prior to the commencement of casting, the mould cavity had to be thoroughly cleaned and be lightly sprayed with release oil. The raft must be positioned on an accurately levelled, rigid bed so that no distortion occurred when the 1000 kg to 2000 kg of concrete was poured. The level of the bed must be true in both planes. To ease the

manual finishing operations it was advantageous to have the mould supported such that the top face was about 600mm above floor level.

The bottom mesh was supported with spacers to ensure its correct location in the mould. The lift tubes, with the rubber plugs set into their tops, were then set onto their locators. The steel top frame, if used, was planed into its seating and clamped securely in place, the second mesh then being inserted and tied to the anchor wires of the frame. In the case of frameless raft units, the two meshes were held in relative position to each other with welded stirrups. The whole mesh assembly was lowered into the mould and its position determined by the spacer elements which was clipped onto the lower face of the mesh. The mould, was now ready to accept the concrete.

Considerable care had to be exercised to ensure that the quality of the concrete supply was high and repeatable. The concrete was initially distributed across the mould by shovelling and was then vibrated into place with manually operated pokers. Due to the close pitched mesh used in the raft units the poker vibrators must be withdrawn and repositioned in the mould on a controlled pattern so as to ensure even compaction.

The screed bar was able to produce a rather smooth finish which is sometimes inappropriate for the intended duty. It is necessary for raft units intended for vehicular traffic to have a textured top face to maximise skid resistance. This texture was applied by drawing a stiff bristle brush strip across the raft face, this device was located off the top edge of the mould face.

4.4.3 Curing and Handling

In the initial twenty four hours of curing, the raft units remained in their moulds covered with damp hessian and protected by polythene sheets or a similar material.
After twenty four hours of curing, the raft units were lifted out of the moulds and transferred to the stockyard. The lifting operation is most critical as the raft unit in its `green' state is weak and therefore prone to accidental damage. The best way of lifting was by vacuum pads mounted on a lift truck. The use of lifting keys is not recommended for stripping raft units from their moulds as very severe local stresses, higher than the allowable green stresses, are imposed on the raft units and failure may result.

When the moulds were removed, the raft units were of low strength (i.e. about 15MPa), and had to be stacked no more than three high. After seven days, when strengths in

excess of 40MPa were achieved, the raft units were restocked, this time by using an ordinary fork lift truck.

4.5 THE TEST RIG

The test rig has two main parts, the steel tank and the loading frame [see Plate 4.2]. The steel tank shown in Figure 4.1 was constructed using three layers of 300mm high grade steel channel sections and has internal dimensions of 4.5m by 4.5m by 0.9m deep. These channel sections were drilled and bolted at the corners and mid-span, to restrict the horizontal movement of the support layers. The test rig has a rigid concrete floor 1000mm thick (i.e.: the base of the steel tank)

4.5.1 Raft Units and the Foundation

Figure 4.2 shows the simulated paving model which contained a fabricated steel tank, with internal dimensions of 4.5m by 4.5m by 0.9m deep. The base of the tank was laid with 100mm of polystyrene which represented a weak 2.0 per cent C.B.R. sub-grade (Taylor, 1982). Overlaying the polystyrene, a 750mm thick layer of Type 1 granular sub-base was laid, levelled, watered, and compacted according to the specification of Road and Bridge works Clause 802 (Dept. of Transport, 1976). A bedding sand layer of 50mm thick was placed, screeded, and tamped on top of the sub-base. The two raft units of the test pavement model (Raft I and II) were then placed beside each other leaving a 10mm gap [see Fig. 4.4]. All raft units were partially restrained horizontally by means of timber packing pieces and heavy iron block weights placed between the outer sides of the raft units and steel bars which were hammered through the pavement layers. The packing was to ensure that the raft units did not move vertically relative to the applied loading. It was assumed that there was no provision for load transfer between the raft units; and also between the outerside of the raft units and the surrounding steel tank. The boundary condition on the vertical sides of the steel tank allowed no horizontal movement, while on the base of the steel tank, no vertical movement was allowed. Therefore, the raft units could be considered to have no significant structural support from adjacent raft units, and the ultimate capacity of the raft unit could be assessed. The absence of the physical connection between the raft units disallowed any reduction in the free edge stress. For the purpose of design, it was considered to be reasonable to reduce the free edge stress, calculated by the Westergaard analytical model, by 25 per cent to account for the load transfer that would be achieved in practice across joints or when designing an airport pavement where the free edge of the pavement would not be trafficked.

If the raft units were joined together they would provide structural support for one another. However, by joining the raft units together some flexibility of the paving system would be lost. It would no longer be possible to remove the raft units and re-use them after correcting for say settlement, obtaining access to underground services, or relocating the raft units. Efforts to achieve high levels of load transfer would add significantly to the overall cost of the paving system. Some investigators have elected to use simple connectors to maintain the alignment of raft units, and others have chosen to leave the raft units unconnected. Open joints between raft units are sometimes useful because the joints allow water to percolate to and drain through the sub-base. The gap between raft units can be filled with a variety of materials including sand, sand slurry, cement and sand mixtures, elastic fibre board materials, and epoxy.

4.5.2 Loading Frame

Figure 4.1 shows the loading frame of the test rig. Outside the edges of the steel tank were four (i.e. two pairs) loading columns, and between each of the pairs spanned a deep loading beam orientated in the direction that the applied load would be moved. The loading beam was so stiff that bending was negligible; in addition an I-beam section was placed at right angles over the two loading beams to prevent any tilting. The repeated moving wheel loads of the aircraft were simulated by using a 100 tonne double acting jack fixed to a jack carrier which was rail mounted and ran along the loading beam at the centre of the tracking load. The location of the simulated wheel loading relative to the raft unit could be varied manually between four different loading positions P1, P2, P3, and P4 [see Section 4.6.3], by sliding the rail over the loading beam in the longitudinal direction of the applied load (i.e. in the transverse direction of the test raft units) [see Plate 4.2].

4.6 LOADING APPLICATION AND LOADING SYSTEM

The design of a new pavement requires information on different design parameters including the frequency of trafficking. This is derived from a number of factors, as follows:

(i.) the design life,

(ii.) the pattern of trafficking and assessment of passes,

(iii.) coverages and pass-to coverage ratio, and

(iv.) the aircraft traffic mix.

Aircraft wheel arrangements can be divided into several basic categories, such as, single, dual, and dual tandem wheel landing gear [see Section 2.4]. In the design of airport pavements, the design wheel load may be either for the largest aircraft that will use the pavement or assessed by accounting for mixed traffic with varying loads and wheel arrangements. The latter is dependent on the frequency of trafficking and the occasional operations of the largest aircraft within the traffic mix. The characteristics of the aircraft loading system were discussed in detail in Sections 2.4 to 2.7.

To compare fatigue relationships with the design parameters of the raft units, the effects of variables such as traffic width and aircraft gear configuration have to be translated into terms of fatigue effects. The traffic mix analysis for the experiment was based upon the conversion of the proposed traffic mix into an equivalent number of load repetitions of the design aircraft. The equivalent number of load repetitions was calculated using the formula developed by Heukelom and Klomp (1978). The analysis had been based upon the design aircraft B727-200 which was considered to be the critical aircraft. The damage effects from other load increments were incorporated into the analysis.

One of the most important tasks in the test programme was to apply the load accurately to the raft units. The loading system used for this test programme was the HI-Force system supplied by H.E.S. Group Limited. The system consisted of a 100 tonne double acting hydraulic jack, a hydraulic power pack and an electronic control console [see Plate 4.2]. The function of these components is described below.

4.6.1 Aircraft Traffic Mix

According to the brief review presented in Section 2.4.5, Chapter 2, aircraft traffic mix for this research project was chosen [see Table 4.5], to represent a typical aircraft traffic mix experienced by Tripoli International Airport (TIA), Libya, over a 20 year design life (1980-2000). The aircraft traffic mix information and the annual movements used to develop the concrete pavement raft units design was provided by the TIA. Table 4.5 shows the aircraft types which have been operated within the fleet mix over the design life. The B727-200 was determined to be the design aircraft with a maximum take-off dual wheel load of 450 kN [see Table 2.1]. Since the traffic mix was a mixture of aircraft having different landing gear types and different weights, the effects of all the traffic were related to the design aircraft using the conversion factors published by the

FAA, 1978. The conversion factors were used to convert from one landing gear type to another.

Therefore, for this research project, to fulfil the simulation requirements of the design aircraft, a full scale physical model simulating the undercarriage of one bogie of the design aircraft B727-200 was constructed providing a two-point loading system spaced at 865mm centres using a high grade steel I-beam section. The characteristics of the design aircraft were shown in Table 2.1.

A range of load increments were chosen for the laboratory test programme representing the typical traffic mix shown in Table 4.5, that would use the test paving model. The simulate loading criteria for the traffic mix included the range of wheel loads from 100kN to the standard design load of 450kN, the gear configuration of the design aircraft B727, and a range of tyre pressures from 1.25 to 8.75 MPa. The load increments of 600kN and 700kN were used to accelerate failure after the test model had been subjected to 100,000 load cycles, due to time constraint.

4.6.2 The Loaded Contact Area

The effect of the size of the loaded area was investigated by different researchers (see Section 3.3.7, Chapter 3). The effect of varying the contact area is apparent in the design number of load repetitions before the raft unit needs maintenance. Aircraft wheel contact areas and tyre pressures are readily available [see Chapter 2]. The design aircraft Boeing 727-200 with an all up mass of 94,318kg, has 47.5 per cent of the mass on one main gear leg comprising dual wheels with tyre pressure of 1.42MPa. The aircraft traffic mix discussed in Section 4.6.1 and Section 2.4.5 had a wide range of contact pressures. In view of this fact it was important for the experiment to incorporate a similar range of tyres pressure

As shown in Section 3.3.7, Chapter 3, the stress level was not particularly sensitive to changes in contact area and the total deflection was well within the factor of safety normally used in pavement design (*i.e.* less than a 23 and 19 per cent as the contact area increased from 200mm square to the contact area for the design aircraft B727-200 of 400mm square respectively). Also it was shown that there was no significant difference between non-uniform and uniform contact pressure; a load uniformly distributed over a gross contact area was used in the experimental programme. Also, it was assumed that the contact pressure between the tyre and pavement was equal to the tyre pressure, ignoring the effect of the tyre wall pressure; this provides a conservative analysis. As the

contact area was constant at 200mm by 200mm, the contact pressure increased with increasing applied load.

The contact area of the test model was designed to allow for different tyre pressures, varying from 1.25MPa up to 8.75 MPa, depending upon the load increment. Relationships were established between the tyre pressure and the fatigue life of the raft units [see Section 7.2]. The load increments were chosen to achieve different contact pressures applied through a fixed contact area of 200mm×200mm by applying different load increments. It was found, more practical to change the applied load increments rather than the contact area in each test. The latter was found to be not economical as well as inconvenient where a better alternative solution was available and more practical. However, the design of the contact area led to conservative results and therefore, the raft unit design method would incorporate a higher factor of safety.

The loads were applied through steel plates measuring 200mm square by 12mm thick. A 12mm thick rubber pad was placed under the steel plate to prevent the steel plate punching into the concrete surface at an early stage of loading. The rubber pad was intended to represent the tyre wall. As a result, the contact pressure between the tyre and the raft units were considered to be equal to the tyre pressure.

In summary, this experiment has applied full-scale wheel loads to full-scale raft units using a contact area that is one- quarter of the size of the full-scale contact area. Researchs have shown that the stresses induced into the raft units will be 19 percent higher due to the smaller contact area.

4.6.3 The Loading Arrangement

Dynamic Load tests using the B-727 aircraft on pavement structures showed that none of the basic aircraft ground operating modes induced pavement responses (elastic and plastic behaviour) greater than those occurring for static and low speed load conditions (Ledbetter, 1976). It was assumed therefore that the dynamic effects induced by the test rag were similar to those of the B-727 aircraft and were neglected (see Section 2.4.4, Chapter 2). Therefore, the loading system used in this experiment was based on the maximum take-off weight of the design aircraft Boeing 727. Static loads can cause very high stresses in the pavement. If the pavement was designed to carry repetitive wheel loads, it will usually be able to carry the associated static loads without structural failure.

As mentioned in Section 2.4.2, Chapter 2, the location and direction of the maximum bending moment applied to an airport pavement are dependent on the type of aircraft landing gear. They are related to the intersection (original position) of the longitudinal axis of the aircraft, and the transverse axis of the axial wheel of the landing gear. They are represented by the shift and the rotation of the gear imprints from the original position. As was given in the manual of the design aircraft B727-200 , the maximum position of the bending moment was when the dual-wheel gear was moved 76.2mm downwards and at a rotation angle of zero (*i.e.* in the direction of the moving applied load of these experiments).

From field and laboratory observations (Bull and Luheshi, 1989; and Kiyoshi et al 1978) a difference has been observed in the effect on fatigue failure of the pavement between a fixed point load and a moving repeated load. The fixed point load was not sufficient to reveal the real fatigue life characteristics of raft units subjected to moving loads. The effects of moving wheel loads on fatigue life appeared to be highly significant. In the fixed point load, initial cracks occurred beneath the loaded point and then extended along the principal moment trajectory. In the moving repeated load, the bending moment diagrams at adjacent loading positions overlapped each other and the cracking pattern had a grid-like form. Movement of the loads sequentially changed the principal moment directions, and consequently, the cracks spread over the entire top and bottom surfaces of the raft units, as well as widened up the crack width in the vicinity of the loading positions through the entire depth of the raft units.

As an aircraft moves along the raft units, it must follow certain wheel paths within a pavement width. The pavement width was simulated in the laboratory in the form of a load being applied at four different loading positions, P1, P2, P3, and P4. The applied loading was moved manually from P1 to P2 to P3 to P4 and then back to P1 to repeat the sequence. At each point a prescribed number of load applications were applied to simulate the passage of aircrafts passing over the raft unit. The simulation was based on critical assumptions that the tracking load was the critical wheel path and that the aircraft wheel paths followed that path for 100 per cent of operations and were uniformly distributed over the tracking load.

In the laboratory tests, consideration was given to the direction of the traffic flow across the raft units test model. The laboratory tests had a dominant direction and the loading followed the sequence of positions P1, P2, P3, and P4. The distances between the four loading positions P1, P2, P3, and P4 varied depending on the geometry of the test raft

units [see Fig. 4.4]. As explained in Section 4.7.1, the moving load used in this test programme was carried out by changing cyclically a loading position after 600 load cycles at each of the four loading positions. Such a loading procedure was adopted to simulate the continuous movement of wheel loads of the design aircraft Boeing 727-200. The outline of the loading frame and loading arrangement are shown in Fig. 4.1. All raft units were tested symmetrically under two-point repeated loading at four locations along the transverse direction of the raft units. The raft units were tested in pairs. The two loading points were called outer and inner loaded areas. The outer loaded areas were located at the edge of the test raft unit with the inner loaded areas at a transverse distance of 865mm centres away from the outer loaded areas. The movement of the loads was carried out manually; the railcarrier jack was moved every 600 cycles of loading progressively to each loading position P1, P2, P3, and P4 in the transverse direction of the raft units. The applied load was recorded by the appropriate load cells which gave a numerical display in tonnes.

4.6.4 The Range of Applied Load

Real traffic is mixed in composition. It consists of aircraft having different weights and undercarriage configuration. To assess the effect on the structural performance of pavements, the contributions made by loads of different sizes must be quantified. A range of loadings were applied, from 100kN. For each test the load started with 3 runs of 600 cycles each at each loading position, with 100kN load. The load was increased in 50kN load increments up to a load of 400kN; with three runs of 600 cycles for each load increment at each loading position. Then the design load of 450kN was applied and the total number of laboratory cycles was increased to 100,000 cycles unless complete failure occurred. If the pavement did not fail, the load was increased to 600kN and 700kN, in order to accelerate failure, with different numbers of cycles dependent on the test condition, until complete failure. The increments of 600 cycles up to 1800 cycles for each load application at each loading position were considered a practical limit for the laboratory tests, due to the time it took to complete each load level before applying the design load of 450kN.

The load increments used in this test programme were chosen to provide a range of contact pressures applied through a fixed contact area (see Section 4.6.2). The damage effects of these load increments were related to the design load of 450 kN, using the pavement damage concept (Heuklom and Klomp, 1978).In this way, it would be possible to estimate a fatigue life for a raft unit in terms of the number of applications of the design load of 450 kN using a range of applied load during the test programme.

The frequency of loading was maintained in a fixed range throughout the test programme. The average loading speed of the hydraulic jack (travelling distance) during the test was 10mm/second.

4.6.5 Dynamic Loading Equipment

Due to the nature of the experiments, accurate load applications to the raft units were extremely important. The repeated loading equipment used was the HI-Force system supplied by H.E.S. Group Limited. The system consisted of a heavy duty electric/hydraulic pump, cooler system, high pressure hydraulic valve, 23 gallon reservoir with a low level oil sight gauge, H.D.R 10045-100 tonne double acting jack fitted with special wear resistant seals for high performance, and an electronic control console. The control console system regulated and controlled the loading level, loading frequency and the number of load applications. It consisted of load control valves and a meter control panel which enabled the user to select the required number of load repetitions, counting the total load repetitions, and to set up the required frequency of the applied load.

The one hundred tonne jack was calibrated up to 78 tonne using a 100 tonne load cell supplied by Strainstall Ltd. A straight line fit was achieved for the load cell readings versus the applied loads, which were controlled by a loading control valve on the repeated loading equipment. The jack was found to be working satisfactory.

During the pre-test checking of the system, there was a build up of back pressure in the retract hose which was reported to the supplier. Modifications were made to the system after discussions with the suppliers engineers, by introducing a bypass relief pressure and safety valve mounted on the jack.

4.7 Performance and Failure Criteria

The design life of a pavement is determined as the length of time between the day the pavement becomes operational and the time when the pavement has deteriorated to a predetermined condition. The length of initial design life, is chosen to minimise the whole-life pavement cost, including construction and maintenance costs. When the pavement life is specified, the economic design life should be considered. This can result in different optimum design lives for different types of pavement and operation. With this brief and Section 4.6.1 in mind, the design life of these raft units was chosen as 20 years.

The concept of pavement design life is to ensure that the pavement will carry the expected volume of traffic associated with that life without deteriorating to the point where reconstruction or major structural repair is necessary within the design life. The pavement should be designed and constructed to provide, during the design life, a riding quality and skid resistance acceptable for the users. Pavement can show signs of distress in many forms, for example, cracks, distortion, and disintegration.

Reinforced concrete generally remains uncracked, or with a limited amount of early-life cracking, for a period of time and then starts to develop cracks at a fairly constant rate. The main cracks propagated through the full depth of the tested raft units and contributed most to failure were the longitudinal, transverse, and cross-corner cracks. The longitudinal cracks run perpendicular to the loading direction at the centre line of the raft unit, where the transverse cracks run at approximately right angles to the centre line of the tracking load *i.e.* parallel to the loading direction. The cross-corner cracks are a diagonal crack forming a triangle with the corner of the raft unit. The formation of the main failure criteria would be when the tested raft units failed in either punching shear or/and fracture fatigue modes. At this point the raft unit would be considered to have failed safely.

Other failure criteria that was considered in this research, included the uplift deflection of the free edge of the loaded raft unit. The uplift deflection or faulting is a difference in elevation of two adjacent raft units. Faulting between a loaded raft unit and an adjacent unloaded raft unit is particularly significant. Surface deformation of approximately 50mm could be accommodated in ports due to the large diameter wheels and the low speed of the container handling equipment (British Port Association, 1983). Modern aircraft have an operational requirement of fault free runways and high speed taxiways, with projections of no more than plus or minus 30 mm and sometimes plus or minus 15 mm. for low speed areas such as for example a prons, holding areas, and taxiways, where faulting up to 40 mm. is acceptable (DoT, 1989).

It is well known that a pavement may exhibit failure in the classical sense of structural mechanics and still perform its function. failure associated with high moving loads may result in surface deformation and the formation of wide cracks in the raft units. With this purpose in mind, a complete analysis was performed for performance and modes of failure of the test raft units, for which the ultimate state data was required. The failure criteria was judged by achieving complete failure where the raft unit pavement cannot carry aircraft movement safely and if any of the following defects occurred:

(i) the width of the top main cracks were equal or greater than 3 mm;

(ii) the inability to accept additional load when the steel bars snapped;

(iii) when the punching shear cracks developed in the vicinity of the loaded areas, through almost the entire effective depth of the raft unit;

(iv) the increasing deflection without an increase in applied loads;

(v) the uplift deflection and faulting between adjacent raft units equal or greater than 40 mm.

4.7.1 Compensation for the Raft Unit Damage

The effect of using a contact area that was one-quarter of the full scale size would be compensated by means of the damage concept (see Section 4.1). The concept of raft unit damage would be assessed by using an equation proposed by Hukelom and Klomp (1978), giving pavement damage, D, in terms of wheel load, W, and contact pressure, P (see Eq. 3.28, Chapter 3). The parameters that would be used to quantify the real damaging effect would be wheel load and contact pressure characteristics of the traffic mix used in the experiments (see Section 4.6.1), including the design wheel load of the B727-200 aircraft and its contact pressure of 1.42 N/mm^2. Therefore, the average damaging effect of each aircraft within the traffic mix would be calculated using Equation 3.28, Chapter 3.

Table 4.5 showed the aircraft traffic mix used in this research. Tables 2.1 and 4.5 formed the basis for calculating the average damaging effect of an aircraft within the mix. Equation 3.28 that proposed by Heuklom and Klomp, 1978, was used for the calculations to give raft units damage, D, in terms of wheel load, W, and contact, P,. The units used to quantify the damaging effect were the loading characteristics of the design aircraft B727-200 (i.e.: the design dual wheel load of 450 kN and contact pressure of 1.42 MPa). The procedures are:

(i) Calculate the wheel load for the aircraft and the associated contact pressure.

(ii) Calculate the Laboratory contact pressure as the applied load devided by the contact area, for each wheel load of the traffic mix.

(iii)Calculate the damaging effect of each wheel load using Equation 3.28 and tabulate the results in a Table (see Table 4.6).

(iv)Calculate the average damaging effect and tabulate the result in Table 4.6

(v) Multiply each of the damaging effects or their average by the appropriate laboratory fatigue life to obtain the real fatigue life for that particular wheel loads.

Due to the similarity in loading characteristics it was necessary to show one calculation for the aircraft mix to demonstrate the calculations of the damage effect. The following calculations show the damage effect of the design load of 450 kN applied on raft units RS1 :

Test raft units = RS1

Design load (W_m)= 450 kN

Applied laboratory load(W_n)= 450 kN

Laboratory load repetitions for 450 kN load (N_{Lab})= 116269 repetitions

Laboratory contact pressure (P_n)= 5.625 MPa

Real contact pressure (P_m)= 1.42 MPa

Using Equation 3.28 as:

$$D = \left[\frac{W_n}{W_m}\right]^{3.75} \times \left[\frac{P_n}{P_m}\right]^{1.25}$$

The pavement damage "D" is an arbitrary quantity related to the induced strains and stresses caused by the applied load repetitions throughout the pavement life. It "the D" is a dimensionless unit used to quantify the relative damaging effect due to one pass of a given wheel load "W" and its contact pressure "P". In other word, the relative damaging effect represents the partial damage contributed by one load repetition. The unit used to quantify the total damaging effect is the number of load repetitions applied throughout the raft unit pavement life. However, the relative damaging effect is multiplied by the number of load repetitions of that wheel load "W" to given fatigue life time "N" of the raft unit pavement and represent the total pavement damage (i.e. complete failure) after this fatigue life time "N".

Complete failure means that when raft unit pavement cannot carry aircraft movements safely and if any of the failure criteria shown in Section 4.7 occurred such as fracture fatigue associated with a top crack width equal or greater than 3.0 mm.

The damage effect in the laboratory " D_{Lab} " due to applying the design load of 450kN is

$$D_{Lab} = \left[\frac{450}{450}\right]^{3.75} \times \left[\frac{5.625}{1.42}\right]^{1.25} = 5.59$$

Similarly the damage effect in the real life is

$$D_{Real} = \left[\frac{450}{450}\right]^{3.75} \times \left[\frac{1.42}{1.42}\right]^{1.25} = 1.0$$

Thus, if the damage created in the laboratory is to be equivalent to that in the field the ratio of the D_{Lab}/D_{Real} must be 5.59.

The real fatigue life (N_{Real})[i.e. the total damage] related to the design load of 450kN and its real contact pressure of 1.42 MPa can be obtained as:

$$N_{Real} \times D_{Real} = N_{Lab} \times D_{Lab}$$

$$N_{Real} \times 1 = 116269 \times 5.59$$

$$N_{Real} = 649943 \text{ load repetitions.}$$

4.8 SUPPORTING LAYERS

The components of the paving system layers used in this test programme are shown in Figure 4.2 and discussed below.

4.8.1 Sub-Grade Layer

A subgrade layer was needed as part of the pavement system used in this test programme which would represent a weak subgrade layer in the field and give sensible results. It was found that polystyrene foam could represent a weak subgrade due to the similarity in its behaviour, strength and response under load (Taylor, 1982). Taylor

(1982) carried out tests on a 100mm thick polystyrene material at the University of Newcastle Upon Tyne, and showed that the values obtained for the Young's Modulus and yield stress were 3.33N/mm^2 and 0.09N/mm^2 respectively. The C.B.R. value for 100mm thick sheets was approximately 2.0 per cent. Based on these results, a 100mm standard thickness of polystyrene materials was used to represent a weak subgrade of 300mm thick layer of around 2.0 per cent C.B.R. The polystyrene of 100mm thick sheets were laid on the rigid foundation which comprised a 1m thick, prestressed concrete floor in the heavy structures laboratory.

4.8.2 Sub-Base Layer

The sub-base layer was very important to the pavement system it supported and transferred the applied load from the above layers to the sub-grade layer. Also, it was crucial to the performance of the paving system particularly with high loads. Laboratory experiments had shown that to ensure the raft unit did not displace vertically to an excessive extent, the minimum sub-base CBR and thickness had to be 20 per cent and 300mm respectively (Bull and Clark, 1991). In the light of this role and the fact that the sub-base layer was not the parameter to be investigated in this research project, it was decided to use a sub-base layer of 750mm thick, which can achieve a minimum CBR value of 20 percent.

The most popular sub-base materials recommended for use in UK highway pavements are Type 1 sub-base, soil-cement, cement treated granule material, and Type 2 sub-base with C.B.R. values higher than 30 per cent. Type 1 limestone sub-base was chosen because it was recommended by the manufacturer "Redlands Aggregate Limited" and was available in the Department.

The sub-base layer was laid on top of the subgrade and compacted according to the Specifications for Road and Bridge Works Clause 802 (Dept. of Transport, 1976). The sub-base material was laid in 150mm thick layers and compacted with eight passes of a heavy duty vibrator (i.e. for a plate mass of 2,000kg/m^2 for each layer).

The elastic parameters for the sub-base were needed for the analysis of the test results and later publications of this work using Finite Element analysis. There is an empirical relationship between the Modulus of Elasticity (E) and California Bearing Ratio (C.B.R.) which can range from $E = 9.3\ CBR$, to $E = 20\ CBR$, where E was measured in N/mm^2 and CBR as a percentage (Heukelom and Foster, 1960). Most soil materials are expressed by the lower limit of the relationship such as $E = 10\ CBR$. Plate bearing tests were conducted before and after each test to determine the Modulus of Sub-grade

Reaction "k" and C.B.R. values of the sub-base layer [see Section 4.11]. The plate bearing test results showed a marginal rate of change (an increase) throughout the tests in "k" and C.B.R. values.

It should be obvious from the definition of rigid and flexible pavements that, the essential difference between the two types of pavement is the way in which the applied load is distributed. A major portion of the structure capacity of the rigid pavement is supplied by the slab itself while in flexible pavement it is supplied by the result of building up thick layers and, thereby, distributing the load over the sub-grade rather than by the bending action of the slab. It is evident that the limited depth of the compressible support layer has very little effect on bending moment and stresses in a concrete slab as long as the depth of the support layer, H, exceeds about two stiffness radii of the slab. Even when the support layer thickness is only one stiffness radius thick, the difference in bending moments and stresses is, for practical purposes, small (Highway Research Board, 1962).

For raft pavement, it was found that as the load position changes from the centre to the centre of the edge to the corner, the percentage of surface displacement that takes place in the sub-base layer changes from 11, 18.1, and 22.81 per cent respectively (Bull, 1992). It is clear from these results that the corner loads produced the highest displacement in the sub-base, where the case is reversed with the subgrade layers due to the nature of load distributions in the deeper ground support layers.

The effect of the variation in the average CBR values shown in Table 4.4 on the raft unit pavement performance was found to be small and could be neglected. This was confirmed by applying different analysis techniques. Westegaards analysis (1926) showed that the concrete raft unit tensile stress reduced by 2 per cent when the CBR value of the sub-base layer was increased from 20 to 100 per cent. On the other hand, the finite element analysis shows a reduction in concrete raft unit stress of only 5 per cent by increasing the CBR value of the sub-base layer from 20 to 50 per cent (Bull and Singh, 1990).

Numerical analysis carried out by Ismail (1990) shown that varying the design parameters of raft units affected the concrete stress (PUS) rather than the sub-grade bearing pressure (SGBP), and varying the CBR values of sub-base and sub-grade affected the sub-grade bearing pressure rather than the concrete stress. For example the range of sub-base thickness is usually between 300mm and 600mm but varying the

thickness up to 2100mm would result in a 90 per cent reduction in the SGBP and a 20 per cent reduction in the PUS. Also, he found that increasing the CBR value from 30 per cent to 100 per cent reduced the concrete stress by only 10 per cent.

A chart has been developed by Knapton (1996) from experience and experiments, which shows that the remarkable effect of CBR values between 1 and 7 per cent. The 7 per cent level was classified as strong ground that a truck could be driven over and would provided concrete pavement design that was relatively straightforward. CBR values over 7 per cent have little effect on stress behaviour and therefore on concrete pavement performance.

For CBR values greater than 20 per cent, the additional support offered by the underlayers to the raft unit pavement does not provide a significant additional structural condition. Therefore, in order to avoid complications in the design process, the additional support offered by stronger underlayers should be disregarded thus resulting in identical raft unit thickness and an additional conservatism in raft unit pavements over foundations with CBR values exceeding 20 per cent. These effects have to be considered during the design of raft units and therefore, the raft units can be designed to suit the design deformation so that no over stressing or faulting occurs in the concrete to cause raft unit failure at an early stage.

4.8.3 Sand Bedding Layer

The best construction practice for raft units was to prepare carefully the foundation for the raft unit. However, one of the requirements when using the raft unit construction was that a minimum time should be spent on each work phase. The material normally used for the bedding course was sand, fine cold asphalt, or a similar material that possesses an unconfined compressive strength enhancing its capacity to resist repeated loading. The bedding course was used to ensure full contact between the raft unit base and the sub-base layer. The manufacturer of the raft units, Redland Aggregates Ltd., recommended a sand bedding layer that consisted of a moist clean sharp sand in accordance with Table 2 BS882, Zone 2 or similar laid to a thickness of 50mm. The results of a small scale trial carried out in the Department of Civil Engineering in 1991 suggested that a thinner layer (30mm) of fine cold asphalt (Bitucrete) would be a more suitable material.

The material used for the bedding course contributed significantly towards the stability of the raft units; if the material was difficult to compact or it might permit sideways

movement due to shear failure under load this could affect the durability of the pavement structure. Generally the sand layer did produce settlement and the bulk of the permanent deflection during the initial loading application [see Chapters 5, and 6]. The bedding sand layer forms a critical part of a raft unit pavement system and, therefore, needs significant attention during the design and construction stages. The sand layer was required to have a uniform moisture content to achieve the required dry density in order to increase the stability and to decrease settlement. In selecting a design moisture content, consideration was given to seasonal variations where the post-construction moisture content was likely to be higher than the pre-construction in-situ value, and therefore, a good drainage system for the raft unit pavement was essential.

Therefore, in the test model, a sand bedding layer of 50mm. thick was placed, watered, tamped and screeded on top of the sub-base [see Plate 4.4]. The sand was well-graded clean sharp builders' sand, with a maximum size of 5mm to BS12, part2, 1986. The moisture content of the sand was determined by means of a "Speedy" moisture tester [see Fig 4.3]. In each test, the moisture content was controlled at 5 per cent, as recommended by the manufacturer of the raft units (Redland Aggregates Limited).

4.8.4 Precast Concrete Raft Layer

Tables 4.1 and 4.3 and Figure 4.2 show the details of different design properties of the raft units tested. Each raft unit was a precast unit having a concrete strength of $65N/mm^2$ and a density of $2,400kg/m^3$.

The raft units were doubly reinforced top and bottom with high yield strength steel. Rafts RSF-14-3/D were reinforced with stainless steel glued fibre type. Cover to the reinforcement was 50mm and 40mm, top and bottom, respectively.

The raft units could be lifted by special keys inserted into the precast elongated steel eyes through the full depth of the raft unit which were welded into the main reinforcement. Each raft unit had two steel eyes.

The two raft units were laid down and placed on a 50mm bedding sand layer, a gap (joint) of 10mm was maintained between the raft units by the use of a special steel spacer. The pair of raft units in the test pavement model (Rafts I and II) were placed beside each other leaving the 10mm wide gap empty [see Fig. 4.4.]. Special tools for laying raft units were provided by the manufacturer (Redland Aggregate Limited). In practice, the 10mm wide gap between the raft units was filled with sand and sealed.

Although the sand filler was not designed to transfer load between the raft units, the ingress of water or oils strengthens the joint such that raft unit uplift was, in the long term, often reduced.

4.9 INSTRUMENTATION

The objectives of the instrumentation were to monitor the upward and downward displacements of the raft units and the concrete strains in the raft units at various locations. Crack widths were also measured.

4.9.1 Measurement of Displacement

Sixteen LVDT displacement transducers were used to monitor the upward and downward deflection of the test raft units, and numbered from N_i0 to N_i15 [see Figure 4.4]. LVDT's were fixed into a specifically adjustable aluminium frame which mounted and screwed into three 5.5m long steel hollow box-sections. The steel box-sections were erected in three rows across the whole length of the steel tank [see Plate 4.1].

All the LVDT displacement transducers used in the first four tests in Module M1 and were connected to Solartron Interface Measurement System, which had a d.c. input and output and were of type D2/2,000A supplied by RDP Electronics Limited. With the purchase of new data logging equipment, of the E500 type, new a.c. displacement transducers were used for the remaining tests and were of the type ACT 2,000 A supplied with the E-500 system by RDP Electronics Limited. The use of a.c. transducers was due to the shortage of the d.c. card interfaces. Two cards were available and accommodated sixteen transducers, eight transducers in each card. The required number of d.c. transducers for the test was seventeen (16 LVDT and 1 load cell).

The displacement transducers were calibrated individually with the new E-500 data logger for a working range of ±50mm.

4.9.2 Measurement of Strains

A total of fifteen electrical demountable strain transducers were used throughout the tests to monitor the strains at various locations on the top, and sides of the raft units. The transducers were fixed on the raft unit surfaces at the expected critical sections for both tension and compression in relation to the loading arrangement [see Figure 4.4]. Research has suggested that the free edge and corner loading are the most critical

loading positions (Bull, 1990). The stresses around the tracking load are, therefore, critical. Critical tensile stresses are also found at the top of the raft unit between the wheel loads (Salmo, 1990), and due to cantilever action caused by loss of support under the loaded area (Bull, 1990).

The demountable strain transducers were developed by Cook (1980) of the Cement and Concrete Association. The general arrangement, dimensions and details of the strain transducers used in the test programme are shown in Figure 4.5(a). The components of the transducers were a flexible aluminium strip and six aluminium blocks labelled as N, U, T, glued to the strip by the recommended adhesive cyanoacrylate (Cook, 1980). The lower blocks N, each had a conical pin for locating into the Demec stud. The other blocks, T and U, were to provide sufficient height to extend the fixing springs, which held the transducer in place. Four Showa foil strain gauges labelled A, B, C, and D in Figure 4.5(a) and (b), Type N11-FA-5-120-23 with a gauge length of 5mm were used on each of the strain transducers. The gauges were glued in pairs on either side of the flexible strip using the cyanoacrylate. The four gauges were wired up in a full-bridge circuit [see Fig. 4.5 (b)], which was sensitive to the bending strain induced in the strip, but insensitive to any axial strain.

The strain transducers were calibrated individually using an extensometer calibrator [see Figure 4.6], on which the transducers were mounted in the same manner as mounted on the test raft using Demec studs and restraining springs. The Demec stud at one end of the strain transducer was stuck on a fixed section, while the other end could be moved. The mounted transducer, which was energised by 6 volt d.c., was cycled over a range of ±8,000 με and the output voltages were recorded by a data logger [see Section 4.9.4]. The output voltages for each transducer were taken by averaging the +ve and -ve range and a calibration factor for each of them was obtained. The average of these two calibration factors were taken in order to obtain the calibration factor as accurately as possible.

4.9.3 Measurement of Crack Widths

The crack widths were measured using the Ultra Lomara 250b microscope, supplied by Wexham Developments Limited. The microscope has a 4mm range of measurement and a lower scale divided into 0.2mm divisions.

4.9.4 Data Logging Equipment

As stated previously, two data logging systems were used in the tests, a 3510B Master Measurement Unit (M.M.U.) supplied by Solartron Limited connected to a micro-computer Apple II plus, and an E-500 Translog supplied by RDP Electronics Limited connected with an IBM compatible computer system the NIMBUS AX40 (see Plate 4.5).

The 3510B (M.M.U.) Solartron

The data logging system comprised an external power pack, a Master Measurement Unit and an Apple II plus micro-computer.

(a) External Power Pack.

The external power pack provided a constant 6 volt d.c. supply to energise the displacement and strain transducers.

(b) Master Measurement Unit.

The 3510B Master Measurement Unit (M.M.U.) was interfaced between the transducers and the Apple II plus 64K micro-computer. Two major components of the M.M.U. were an analogue-to-digital convertor (A.D.C.) and multiplexer (with reed-relay switching). Since the A.D.C. could only take one reading at a time, the multiplexer with reed-relay switching was required to connect the A.D.C. sequentially to each transducer. The capacity of the M.M.U. was 64 input channels.

(c) Micro-Computer and Operation System.

The Apple II computer sent programming information to the M.M.U. and commanded a measurement to be obtained and then accepted the measurement results from the M.M.U.. The software, supplied by Solartron Limited, made the computer generate and transmit the necessary data to the M.M.U. In response to the data received, the multiplexer scanned the selected channels sequentially for analogue output of the transducers, which was then converted into binary form by the A.D.C. and sent to the computer. The output measurement was in the form of a voltage and could be sent to a printer, a floppy disc and/or a V.D.U.

The Translog E500

The E500 Translog was a new and advanced system introduced to the Department of Civil Engineering, University of Newcastle upon Tyne, for this test programme (see Plate 4.5). For various reasons it arrived late and the old system 3510B M.M.U. Solartron had to be used initially. The main data acquisition mechanisms were similar for the two systems. Therefore, a general description for the new system is presented below.

In general the E500 was an all purpose, medium speed, Data Acquisition System (D.A.S.), designed for use with a Personal Computer. The Base Unit (Type E505) comprises a power supply, Computer Module (Type E504) 8 slots for signal conditioning Modules, and a standard 19" industrial enclosure for table top or rack mounting.

The E504 computer Module was an intelligent instrumentation front end, designed to turn any personal computer with an RS232 serial port into a powerful D.A.S.. This Module supervised the operation of the signal conditioning Modules, and performed a variety of Data Logging tasks.

A variety of Signal Conditioning Modules were available, each module having 8 channels. The system accommodated 32 modules in four separate racks, allowing a total of 256 channels in total, but only one rack was available allowing only 64 channels to be used. Each Module was a complete signal conditioning unit, capable of providing amplification and excitation for LVDT (a.c. and d.c.), strain gauges, and d.c. output transducers. The available Modules were:

E510 LVDT scanner, E511 Strain gauge scanner

E512 DC-DC scanner, E514 Relay output

To operate the different modules in the E500 system incorporating the E510 LVDT Modules, the system required an E510 Module in SLOT1, then the E510 called the Master Module. This prevented numerous Module oscillators causing beat-frequency problems.

4.10 PLATE BEARING TEST

The plate bearing test was used to evaluate the support of the sub-grade and the sub-base. The following equipment was used in the test [see Plate 4.6a & b];

(i.) Hydraulic jack.

(ii.) A load cell with a digital load indicator.

(iii.) A 450mm diameter, 15mm thick, circular steel plate.

(iv.) Other smaller plates 15mm thick for stacking.

(v.) Four dial gauges or LVDT.

The plate bearing test was carried out using the usual plate bearing test procedure. Incremental loads were applied and the corresponding displacements were measured. The displacements were measured at four points at the edges of the 450mm diameter plate, along two diameters perpendicular to each other. The loading was carried out in increments of 5kN up to the total applied load of 45kN.

Based on the plate bearing test results, a graph of load versus displacement was plotted for each test [see Figure 4.7].

The modules of sub-grade reaction "k" were stated in terms of a load in kN per square m per m of deflection obtained under a rigid plate diameter of 760mm. The 760mm diameter plate was used as the basic diameter for the plate bearing test and results from any plate diameter can be related to it (Croney, 1991). The use of the modules of sub-grade reaction (k) in the analysis assumed that the sub-grade and sub-base layers were elastic foundations and therefore their support was directly proportional to the deflection.

The modulus of sub-grade reaction was taken as the reaction due to stresses causing 1.25mm deflection of the plate. The modulus of sub-grade reaction k was calculated from the relation;

$$k = \frac{P}{\Delta}$$

where,

P = Pressure (kN/m^2)

Δ = Deflection of the plate (m)

4.11 MODULUS OF SUB-GRADE REACTION

The modulus of subgrade reaction "k" is a measurement of the stiffness of the sub-grade. Usually it is stated in terms of load in kN per square metre of deflection measured under a rigid plate of 760mm in diameter. The value of the modulus of sub-grade reaction depends critically on the size of the plate used. Clearly plates smaller than the standard diameter of 760mm are easier to use and they require a smaller loading rig. However, the plate used in this test programme had a 450mm diameter which was available in the Department [see Section 4.10] and the modulus of sub-grade reaction was taken as the reaction due to a stress causing 1.25mm deflection of the plate.

Since the plate bearing tests were carried out using a plate of 450mm diameter, a conversion factor of 1.5 was used in all the calculations (Croney, 1991). The conversion factor was obtained from the curve based on American experimental evidence relating the measured k-value with plates of various sizes.

From the same reference (Croney, 1991), the equivalent C.B.R. values for the calculated k values were obtained using the empirical relation between k-value and C.B.R. The corrected values of the various modulus of sub-grade reaction and the equivalent values of C.B.R. are shown in Table 4.4.

4.12 GENERAL TEST PROCEDURES

4.12.1 Before the Test

The test raft units were painted with white emulsion to facilitate the detection of cracks. A 300mm. square or rectangular grid was marked (i.e. dependent on the raft dimensions) [see Figure 4.4.], so cracks could be accurately and easily located and recorded. The load positions were marked at locations P1, P2, P3, and P4 for the required contact area 200mm×200mm [see Plate 4.3]. Demec studs and restraining springs for the demountable strain transducers were fixed to the top and sides of the raft units using a quick setting glue (Araldite Rapid) at the required locations [see Figure 4.4.].

A wooden frame with internal dimensions of 4.30m, by 2.45m, by 100mm deep was erected on the test rig of the fabricated steel tank. A sharp sand was laid on top of the sub-base, tamped and screeded to the required level of 50mm by means of the prepared screeding board bearing on the edges of the wooden frame [see Plate 4.4].

The moisture content of the sand was determined using a "Speedy Moisture Tester" which is a specially designed piece of equipment to determine the moisture content of fine soils [see Figure 4.3]. Immediately before laying the test raft units, four samples were taken from various locations of the surface of the sand bedding layer. The moisture content was found to be 5 per cent, as recommended by the manufacturer of the raft units (Redland Aggregates Limited).

Before the raft units were lifted into the test rig, the reference lines were drawn onto the top edges of the wooden frame and the test rig. The raft unit was lifted into the test rig by placing the lifting keys into the precast two eyes for handling and using the overhead travelling crane. The raft units were laid on the screed sand and were lined up with the reference lines. Initially, a 1 tonne load was applied and then increased to 2 tonnes at each loading position, to bed the raft units into the sand layer and to ensure a better compaction to the bedding sand.

The centre of the tracking load was aligned with the centre of the hydraulic jack. A joint between the raft units was maintained by using a spacer of 10mm thick plywood board. It was easier to use the plywood rather than the steel spacer. The raft units were restrained partially horizontally using timber packing pieces and iron block weights around the outer sides of the raft units.

4.12.2 During the Test

During the test, checks were made to ensure that:

(i.) the hydraulic equipment gave the required initial applied load of 100kN;

(ii.) the jack was aligned with the centreline of the tracking load and on position P1;

(iii.) LVDT and strain transducers were fixed in their places [see Plate 4.1];

(iv.) load cell of 100kN was connected; and

(v.) data logging was switched on and programmed.

The data logging scanner was then commanded to scan the LVDT displacement and strain transducers for initial readings. The required initial applied load was set up using

the load control value on the control console of the hydraulic equipment. Then the load was increased incrementally [see Section 4.7].

The moving repeated load was applied in a sequence of 600 cycles at each loading position P1, P2, P3, and P4 for every run. The movement of loading position was carried out manually after each completed run in the traffic (longitudinal) direction [see Figure 4.4]. Each loading position received 3 runs at each load increment starting with 100kN and in 50kN increments up to 400kN inclusive. Therefore, the load was applied for 3×600 =1,800 cycles at each load value of 100,150, 200, 250, 300, 350, 400kN. The next increment was the design load of 450kN which was applied in the same manner as previous loads but continued until the total number of cycles on the whole pavement model (i.e. at four loading positions P1, P2, P3, and P4) received one hundred thousand cycles or failed whichever was first. Due to the time constraints, the load was then increased to 600kN and finally 700kN in order to accelerate failure of the test specimens. The test had to be stopped somewhere due to either failure or that one hundred thousand cycles or more were achieved. At each load increment and after each 600 cycles of applied load, the marking of the cracks (if any), the measuring of the critical crack widths, and the recording of the test observations, were undertaken and checked.

The rate of loading was maintained in a fixed range throughout the tests. The range presented the real low speed of an aircraft moving across different areas of an airfield. Therefore, each load cycle was in a range of three and six seconds for low and high loads respectively and the load itself was applied for one second.

The following measurements were taken at the end of each run (i.e. 600 cycles), and at each load increment.

(i.) The applied load was read from the digital load indicator, and recorded directly by the data logging interface when the new E500 Translog was used.

(ii.) The data logger was commanded to scan the LVDT displacement and strain transducers. For the old data logging "Solatron", the output was in the unit of volts and was printed on a hard copy, where as for the data logging E500, the output was directly in mm and microstrain for deflections and strains respectively. The results in volts needed time to convert them to mm. and microstrain. The time was estimated to be about 600 working hours providing a computer programme was written. The computer programme was written using Lotus 3.0 software.

(iii.) Cracks were detected and marked on the raft unit, and recorded on a "to scale" sketch of the raft unit.

(iv.) Using the crack detector device (microscope), the crack widths were measured every 1,800 cycles and every load increment and recorded on a pre-prepared table. The device had a 4mm range of measurement which had a lower scale divided into 0.2mm divisions.

The purposes of these measurements were as follows:

(i.) to investigate the variation of strains along the longitudinal and transverse axes of the raft unit, for each loading position;
(ii.) to investigate the variation of strains at each of the loading areas;
(iii.) to monitor the strains at the centreline of the tracking load at each loading position;
(iv.) to monitor the upward deflection at the free edges and corners of the raft unit;
(v.) to monitor the downward deflection at the loaded areas and compare the differences between the inner and outer loaded areas;
(vi.) to monitor the deflection and strain on the unloaded part of the raft unit; and
(vii.) to investigate the maximum deflection and strains, and their relation to the design of the raft units tested.

4.12.3 After the Test

The time needed to run a two-point moving repeated load test was in the order of, thirty working days, ten working hours per day, plus seven days for the preparation and the dismantling of the test. Any equipment breakdowns were not included in this estimation.

Immediately after the completion of the test and dependent on the time of the day, the data file was saved in the computer. The data logging and the hydraulic equipment were switched off and disconnected. Displacement and strain transducers were removed from the raft unit. Springs and demec studs were removed from the tested raft unit for re-use. The high grade load I-beams section (at each loading position) and the raft units were then removed from the test rig using the overhead travelling crane.

The bottom cracks of the raft units were drawn onto a “to scale” sketch and photographed. The plate bearing tests were conducted on the sub-base layer in three

different locations, and performed both before and after each test to assess the variation in the strength of the sub-base due to the test.

4.13 Summary of Chapter

The fatigue characteristics of precast concrete raft units are determined by a full scale laboratory test until complete failure occurred . The full scale physical model approach was chosen except for the contact area of the design aircraft B727-200, due to economic and practical reasons shown in Section 4.1. The true contact area was scaled down from 400mm x 400mm to 200mm x 200mm in order to maintain different pressures related to the expected traffic mix. The effect of using small fixed contact area instead of the exact size on the fatigue life of raft units, was corrected by means of the pavement damage concept proposed by Heukelom and Klomp, 1978. The full scale physical model was designed to meet the design criteria of the raft units pavement subjected to the passage of the Boeing 727-200 design aircraft.

A total of sixteen raft units were tested in pairs. The test raft units were divided into three different modules, namely modules M1, M2, and M3 [see Table 4.2] which were designed to investigate the effect of different raft unit plan dimensions, reinforcement design, and thickness design on their fatigue life, respectively.
The raft units were designed for 20 years design life, to cope with loads that arise during manufacture, transportation, stockpiling, construction, and of course, the predominant and ruling loading condition of the design aircraft B727-200.

The test rig that used in the experiment, has two main parts, the steel tank which includes the raft units and the foundation layers, and the loading frame [see Figs. 4.1 and 4.2]. The passage of the design aircraft B727-200 over the raft unit pavement, was simulated by moving manually the applied loads, sequentially from loading position P1 to P2 to P3 to P4 and then back to P1 to repeat the sequence. The load was applied from 100 kN in 50 kN load increments up to a load of 400 kN, with three runs of 600 cycles for each load increment at each loading position. Then the design load of 450 kN was applied and the total number of laboratory cycles was increased to 100,000 cycles unless

complete failure occurred. If the raft unit pavement did not fail, the load was increased to 600 kN and 700 kN, in order to accelerate failure due to time constraints, until complete failure.

The failure criteria that was considered, was judged by achieving complete failure where the raft unit pavement cannot carry aircraft movement safely and if any of the following defects occurred :

(i.) top main cracks width equal or greater than 3mm;
(ii.) snapping of the steel reinforcement bars;
(iii.) development of the punching shear cracks through the entire depth of the raft unit;
(iv.) increasing deflection without an increase in applied loads;
(v.) uplift deflection equal or greater than 40mm.

The primary aim for the experimental stage of this research was to investigate both experimentally and theoretically the fatigue strength and failure mechanism for a range of raft units with different design parameters [see Table 4.2]. Attention was directed towards the study of the following criteria:

(i.) the mode and mechanism of failure;
(ii.) the value of the failure load;
(iii.) the deflection and strain development;
(iv.) the crack patterns and crack widths at various stages of loading; and
(v.) the fatigue life and estimation of the consequent degree of damage.

Chapter - Five

PRESENTATION OF THE TEST RESULTS

5.1 INTRODUCTION

To study the effect of the plan dimensions, different reinforcement designs, and the thickness designs of raft units on their performance, a series of experimental tests were carried out under repeated two-point moving wheel loads representing one leg of the main landing gear of the design aircraft B727-200. They included five different raft unit sizes with varying raft unit lengths and widths, three different systems of reinforcement, and two different thickness, which called modules M1, M2, and M3, respectively [see Chapter 4].

Precast concrete raft units are generally small in area and thin compared to conventional concrete pavements, which makes them easy to handle during construction and transportation. Although the raft unit can be square, rectangular, hexagonal, or other shapes, the rectangular shape is predominant. For practical use, the side length varies normally from 1.0m to 4.5m for square rafts and from 1.2m to 3.6m for rectangular rafts (Bull, 1990). The width for rectangular raft units normally varies from 0.6m to 1.8m and the thickness from 0.14m to 0.25m. Larger sizes can be manufactured but, due to the limitations imposed by the practical considerations of handling and transporting the raft units, make this undesirable [see Chapter 1].

Most raft units in use today are reinforced at either the bottom or both the top and the bottom, to withstand high stresses due to a high number of heavy wheel loads passing over the pavement, and the stresses induced during handling. Raft units with reinforcement in the bottom only can be used for light loads and less important functions, such as warehouse floors, but for airfield use where safety and fatigue life are important, reinforcement in the top and bottom is necessary.

Raft units can be reinforced with steel fibre when light loads are considered, e.g. warehouse floors. It was claimed that steel fibre improves the flexural strength of concrete and increases the load capacity of the raft units. The manufacturers of Dramix steel fibre have claimed that their product offers a high flexural strength combined with high crack resistance, high fatigue resistance and an increase in shear strength.

Raft units are usually reinforced according to their use and function in order to improve their performance. Also the performance could be improved further by increasing the thickness of the raft unit. However, to achieve a prescribed fatigue life, a designer has to compromise between the thickness of the raft unit and a reduction in the amount of steel reinforcement or vice versa. It must be remembered that the reinforcement does not make a significant contribution to the flexural capacity of the raft unit, and therefore, a minimum thickness design for a particular boundary condition should be maintained without affecting the fatigue life of the raft unit.

In Chapter 4, the author's experimental programme was described in detail, including the loading arrangement and the design of raft units. The raft units under consideration in this thesis were designed for airfield use in low speed sections (*i.e.* taxiways, aprons). In this Chapter, the results from sixteen of these raft units that were tested are presented. The measured deformation characteristics were crack widths, strains, and deflection. The fatigue characteristics and fatigue failure mechanism of the raft units were also examined. The fatigue life represented by the laboratory number of load repetitions for a particular load, which was obtained by adjusting the damage effects of the various load levels to that load using the equation (Eqn.5.1) proposed by Heukelom and Klomp (1978) [see Section 5.5].

For convenience of discussion, the term "loading conditions" should be read as the applied load and Equivalent number of Load Repetitions (ELR). The applied load means, the actual load intensity applied in the laboratory. The ELR means, the equivalent number of laboratory load repetition for the design load of 450 kN owing to applied various load cycles of the applied loads in the laboratory using Equation 5.1.

The test programme has been divided into three modules M1, M2, and M3, the test observations of the three modules will be presented for each of the four loading positions P1, P2, P3, and P4. The raft unit notations and modules were shown in Table 4.2 of Chapter 4.

The effect of the size of the loaded area was discussed in sections 3.3.7, 4.6.2 and 4.7.1. The effect of varying the contact pressure is apparent in the number of load repetitions before raft unit needs maintenance or replacement. As shown in section 3.3.7, the stress and deflection loads were reduced by 23 per cent and 19 per cent as the contact area increased from 200mm ◈ 200mm to 400mm ◈ 400mm, respectively, therefore, the contact area of 200mm square used in this experimental programme led to conservative results and incorporated a high factor of safety equal to the changes in strain and

deflection levels. With this brief and sections 3.3.7, 4.6.2 and 4.7.1 in mined, the test results will be presented in this chapter and discussed in chapter 6.

5.2 Observation of Crack Propagation

5.2.1 General observation

The application of the initial load of 100kN for the first run, produced flexural cracks which formed at the bottom of the raft units. They were not clearly visible in some cases, but as the applied load and load repetitions increased, the flexural cracks became visible and could be measured. The flexural cracks were visible at 1438 equivalent load repetitions of load 150kN. They developed along the main transverse and longitudinal centreline of the raft units.

The most common crack patterns observed during the tests were longitudinal along the main centreline of the raft unit, transverse, delta, cross-corner cracks or a combination of some of them. The combination of these types of crack were observed on most of the raft units [see Fig. 5.1, 5.2 and Plate 5.1].

On further loading up to 200kN and then to 250kN, more bottom cracks appeared around the loaded part of the raft unit (*i.e.* in the vicinity of the tracking load) which followed the patterns of the previous flexural cracks. Whereas thicker raft units (RS7) developed a few bottom cracks at a loading in excess of 450kN. As the applied loading conditions increased further, the flexural cracks at the bottom developed throughout the entire depth of the raft unit and eventually appeared on the top surface of the raft unit at 3113 equivalent load repetitions of load 350kN except for raft unit RS7 which was at 5563 equivalent load repetitions of load 600kN. The first top surface crack to appear in most of the raft units was the main crack along the transverse centreline of the raft units.

The cross-corner cracks were initiated at the joints and edges of the raft units, under different loading conditions. The cross-corner cracks appeared in RS2 at load of 300kN, whereas in RS1 with a higher percentage of reinforcement [see Section 4.4], at load of 450kN. On the other hand, by increasing the thickness of RS1 to RS7 (*i.e.* from 140mm to 175mm), the cross-corner cracks appeared in RS7 at load of 600kN.

Because of space limitation, the detailed propagation of cracks around the loaded areas (*i.e.* outer and inner) and the development of punching shear failure has been shown in Figures 5.1 and 5.2. The general observations for each module are summarised below

5.2.2 The Plan Dimensions : Module M1

The crack propagation depended on the plan dimension of the raft unit. There were no cracks along the main centreline of the narrower raft units R6 and R9 (*i.e.* longitudinal direction of the raft unit), while the main cracks in these raft units were across the whole width within the tracking load (*i.e.* between the wheel loads) in the transverse direction of the raft units. The main cracks along the longitudinal direction of the wider raft units R12, RR, and RS2 were similar. However, two significant differences were observed, first, the main cracks in the wider raft units developed along the entire main centreline of the raft unit with loads lower than 400kN and, second, the main cracks in the narrower raft unit developed at loads above 450kN with no cross-corner cracks for R6 and R9, and had an angle (ϕ) with the horizontal when the cracks deviated from the inner loaded area towards the joint or the free edge [see Plate 5.2]. The angle ϕ varied between tests and depended on the propagation and development of cracks in that vicinity. The value of the angle ϕ was not considered important in the formation of crack patterns, but just gives an indication of the anticipated failure mode of a punching shear in that section under the inner loaded area as was, for example, the case with R9, and R12.

The form of the cracks around the loaded areas depended on the dimensions of the raft units (*i.e.* depended on the aspect ratio of the side length to the side width), and on the positions of the loaded area, whether at the outer or at the inner contact area. The cracks spread and developed around the loaded areas of loading positions P1, P2, and P3 for R9, R12, and RR through the entire depth of the raft unit as the applied load was increased up to 700kN; and due to the movement of the applied loads sequentially (*i.e.* loading positions P1, P2, P3, and P4). Raft units R9, R12, RR, and RS2, indicated the beginning of punching shear failure under both loaded areas at loads of 400kN and 450kN.

5.2.3. The Reinforcement : Module M2

In all respects of different reinforcement of the raft units, the main cracks were similar. When the applied loading condition was increased up to failure, the cracks spread and scattered widely, with new cracks forming in the steel fabric raft units, RS2 and RS1, at a late stage of loading, while in the steel fibre, RSF, very few new cracks developed but instead the existing flexural cracks widened up to 5.52mm in position P1 at a failure loading condition of 4289 ELR of 450kN loads. It can be seen that the crack patterns of the steel fibre RSF were less scattered than for the steel fabric raft units [see Plate 6.1].

As the applied loading condition increased further, few new cracks appeared and the flexural cracks widened and extended through the full depth of the raft units.

However, three significant differences were observed: the main top surface cracks appeared in the steel fabric raft units at a load of 300kN while in the steel fibre raft units they appeared at a load of 250kN. The second difference concerned the crack patterns in the steel fabric raft units where there was an increase in the flexural crack width with very few new cracks. The third difference to note was that the cracks spread and developed around the loaded areas through the full depth of the steel fabric raft units due to an increase in applied load up to 700kN and formed the punching shear failure, while in the steel fibre raft units the main transverse and longitudinal cracks widened and formed a fracture failure at 450kN [see Plates 6.2 and 6.7].

5.2.4 The Thickness : Module M3

The development of cracks in raft unit pavements depends on the thickness as well as the plane dimensions and reinforcement of the raft units as explained above. The development of flexural cracks of the thinner raft units RS1 was faster than the thicker raft unit RS7. The first top surface crack appeared in RS1 at a load of 300kN, where as with RS7 the first top surface crack was the cross-corner cracks, at the outer loaded area of positions P1 and P2 for applied load of 600kN. As the applied loading conditions were increased to failure, the cracks spread and scattered widely with the formation of new cracks at a late stage of loading in the thinner raft unit, RS1. Apart from the initial flexural cracks in the thicker raft unit RS7, no new major cracks developed except for the cross-corner crack in the area around loading position P2 [see Plate 7.1]. It can be seen that the crack patterns of the thicker raft units were less scattered than the thinner raft units. The post cracking behaviour of RS7 was much better than RS1 as the thickness of RS1 increased from 140mm to RS7 of 175mm.

In general, the behaviour of a certain type of crack in the raft unit was similar to the previous modules M1 and M2 [see Figures 5.1 and 5.2] However, four significant differences were observed; firstly, the crack patterns spread over the whole surface of the thinner raft units RS1, but in the thicker raft units RS7, appeared only under the loaded areas for most of the loading positions. The second was, that the main top surface cracks appeared at 300kN and 600kN for RS1 and RS7 respectively. The third was, the cracks spread and developed around the loaded areas through the entire depth of RS1 due to an increase in the loading conditions to failure at 700kN and formed a punching shear failure in the area of loading positions P2 and P3, while RS7 did not fail apart from loading position P4, and the test was stopped when the laboratory number of

load repetitions reached 201,800 cycles. The last difference observed was, that the maximum crack widths were 4.68mm (bottom) and 3.08mm (top) for RS1 and RS7, respectively.

The relationship between the characteristics of the cracked surface and the number of load repetitions, particularly for the main cracks, were clearly observed and recorded [see Figs. 5.3 to 5.5]. The most critical section (*i.e.* the main cracks) produced severe cracking at the bottom of the raft unit at loading positions P1 and P3 [see Plate 5.1]. As an example, the maximum bottom cracks and residual bottom crack widths in these sections of R9 at P1, and P3 were 5.07mm and 2.36mm at failure load of 700kN, respectively. The formation of these cracks or slits affected the continuity of flexural rigidity and also the shear strength of the raft units.

Figures 5.1 and 5.2 show the crack patterns in the area of different loading positions for different increments of loading conditions as they occurred. The bold lines indicate the main cracks that contributed most to failure.

5.3 Strain Behaviour

In all the tests, extensive Demec gauge readings were taken at each load increment and each run at the four loading position P1, P2, P3, and P4 on the top and vertical surfaces of the raft units at different locations [see Fig. 4.4]. The measured strain locations represent the strains under the loaded areas, at the middle of the tracking load (*i.e.* between the loaded areas), and at remote sections such as point I, in the longitudinal and/or transverse directions.

It was not possible to monitor the strains at the bottom surfaces of the raft units due to the nature of the study which concentrated on the ultimate fatigue life of the raft units associated with high loads (*i.e.* ultimate stage). The applied load for this particular study provided for up to 700kN and about 150,000 laboratory load cycles for each test. Therefore, any bonded strain gauge at the bottom surface of the raft unit would not sustain this loading condition and the associated friction in the interface between the raft units and the bedding sand. On the other hand, major cracks can break a gauge and subsequently the readings from that gauge were lost. However, to overcome this problem, the induced strains at the vertical sides of the raft units were measured instead of the bottom strains with a positive margin factor in mind. All locations of the vertical measured sections were at one-third of the raft unit depth, measured from the bottom surface. However, that was the closest possible location in which a demountable gauge

could be mounted and function safely, giving a margin to the downward deflection at that section.

The variation in the strain gauge readings at different locations changed in magnitude and alternated between compression and tension. The variations depended mainly on the thickness plan dimensions and reinforcement of the raft units, the applied loading conditions, the loading position, and whether the section was cracked or uncracked. The fluctuations in the induced strains on the top surface of the raft unit were observed mainly at the loaded areas and at the centreline of the tracking load. For example, the fluctuations in the measured tensile strain on the top surface of the raft unit were small in the raft units with a low aspect ratio i.e. R6 and R9, but slightly higher in raft units with higher aspect ratio i.e. R12 and RS2 [see Fig. 5.7]. The average tensile strain before cracking was in the region of 550 microstrain, where raft units with a higher percentage of steel reinforcement RS1 than their counterpart RS2, the maximum induced strain just before cracking was 1753 (comp) microstrain [see Figs. 5.8 to 5.10]. The induced strains at remote sections (*i.e.* away from the tracking load) were fairly low unless a crack extended to these sections, and were lower than those around the tracking load. Even though the remote section was cracked, the magnitude of the strains were still small.

When the applied loading conditions were increased particularly to loads over 450kN, the variation in the strains was observed where most of the flexural cracks occurred [see Figs. 5.7]. It was observed that the strain readings at the cracked section were reduced as soon as other cracks developed in the same or near the cracked sections, and some cases caused a sudden sharp increase in strains. The average tensile strain that was measured at 550 microstrain before cracking, was increased up to 2105.26 microstrain due to a crack's appearance in that section. In some cases where the crack width was very wide, the strain transducer was disregarded in that cracked section because it had been stretched beyond its limit (i.e. ± 6000 microstrains). For example the maximum induced compressive strain was recorded for a section in raft unit RS2, was well over the limit of the transducer due to an applied load of only 250kN. It was found that the strain transducers beyond this limit were unreliable.

The rate of increase of strains as the number of cycles increased was steady, especially with loads of 350kN and over. The rate of increase of strains owing to increasing applied loads was steady and small with the middle range of loading [i.e. between 400kN and 450kN] but there was a sharp increase in the first stage of fatigue life, associated with loads up to 350kN. Under load repetitions of the design load 450kN,

the measured strains were steady and slightly increased as the load repetitions increased [see Figs. 5.7 and 5.11].

Figures 5.12 and 5.13 show the relationship between the raft unit sizes and the development of strain and deflection. The figures show that by increasing raft unit size increases the induced strain levels and decreases the induced deflection levels.
Figures 5.8 to 5.10 and 5.14 to 5.16 show the variation of the induced strains in the longitudinal and transverse reinforcement at the loaded areas and at the centreline of the loading track (points B, E, and F) [see Fig. 4.4]. The maximum compressive strains at the outer loaded area just before this section cracked, were 301, 1052.63, and 1753 microstrains for raft units RSF, RS2, and RS1 respectively. Also the figures showed that the maximum induced tensile strain levels in the thicker raft unit RS7 were relatively low compared with that of the thinner raft unit RS1.

As observed during the tests for the three modules M1, M2, and M3, the rate of increase in the induced strains due to the applied loads was steady and small with low loads and rose sharply with high loads of 450kN and over. On the other hand, the rate of increase in the induced strain levels changed slowly and steadily with increasing load repetitions. However, the maximum strains recorded always increased as the applied loads increased. The highest induced top and bottom surface strain levels were around the loaded areas and in the centreline of the loading track (*i.e.* between the loaded areas) for the four loading positions [P1, P2, P3, and P4].

5.4 Deflection Behaviour

Detail of the LVDT transducers used in the experimental work and their function were described in Section 4.9.1. At the initial loading conditions of 100kN and 150kN and around loading positions P1 and P3 for each test, the raft units settled almost uniformly with average downward deflections at the inner and outer loaded areas of 4.04mm and 4.72mm respectively. Similarly for loading positions P2 and P4, the free edges of the raft unit deflected upward with average deflections of 2.80mm and 4.89mm, respectively. The initial deflection was relatively high and deflected downwards and upwards, depending mainly on the compaction of the bedding sand and then on the plan size and thickness of the raft units. The test results showed that the initial deflections for all the tests took place in the bedding sand layer. This phenomenon was supported by discussion in Section 4.8.2, where an increase in the CBR values of the sub-base layer for each test was shown to have a negligible effect on the induced strains and deflection within the raft unit pavement model.

As the applied loading conditions increased, the deflections started to increase linearly until the flexural cracks grew to wider cracks and/or new cracks developed at the section. As loads were applied throughout the test, the bedding layer of sand gradually gained strength which effected the deflection levels particularly at the free edges of the raft units due to loading positions P2 and P4. The rate of increase in the deflection levels with higher loads than the flexural loads of 100kN and 150kN, was steady and slower than those of the initial deflection. For instance, Fig. 5.17 shows the trend of the induced deflection due to loading positions P3 for RS2 and RSF and how the deflection started to decrease gradually when the crack width had reached 2.28mm at 40900 ELR and 2.96mm at 8500 ELR, respectively.

It was observed that with high loading conditions such as the design load of 450kN, the loaded raft unit affected the adjacent raft unit even without any physical connection particularly at areas close to the loading position. This phenomenon was related to the relatively small response of the layers under the raft units particularly the response of the bedding sand layer to the high applied load. The deflection on the adjacent raft unit was only 1.5mm at 24689 ELR of the design load 450kN.

The maximum downward deflections recorded at the loaded area of loading position P1 for the low aspect ratio of R6 and R9 and the high aspect ratio of RR and RS2, were 27.16mm and 16.05mm respectively [see Fig. 5.18]. The same trend occurred with loading positions P2 and P4 but in an opposite direction *i.e.* upward deflection. The maximum uplift deflection recorded was at the free edge of the raft unit due to applying the load at position P4, this measured -13.99mm at 1032 equivalent load repetitions of 200kN, and -11.90mm at 2512 equivalent load repetitions of 350kN for the raft units of low and high aspect ratios, receptively.

Table 5.1 shows the maximum downward and upward deflections for all the raft units tested in modules M1, M2, and M3, at the design load of 450kN and the corresponding fatigue lives. The permanent deflection which was measured as a residual deflection was recorded and was in the range of 40 per cent to 50 per cent of the total measured deflection. The magnitudes of the deflection at certain loading conditions were different depending on the applied load, the compaction of the bedding sand, and the plan size and thickness of the raft units, but the form of deflection for a specific location was similar. By comparing the deflection curves and Table 5.1, it was found that,

(i.) the maximum downward deflection was always at the loaded areas,

(ii.) the maximum upward deflection was always at the free edge (*i.e.* the joint interface) of the raft unit due to loading position P4;

(iii.) the trend of deflection behaviour was affected by crack patterns. In general, the relation between the deflection and the applied loading was linear;

(iv.) the initial deflections for all the tests took place in the bedding sand layer;

(v.) the induced deflection decreased with the increasing plan size of the raft units (i.e. inversed proportional relationship); and

(vi.) the rate of increase in deflection for the same loading conditions was higher in the thinner raft units than in the thicker raft unit.

5.5 Fatigue Life

The raft unit pavement performance was represented by the mean value of the number of load repetitions to failure under a particular applied load. The fluctuation in strain level at the top and bottom surfaces of the raft units, the width of the main cracks at loading positions P1 and P3; and the width of the cross-corner cracks at loading position P2, affected potentially the fatigue life of the raft units. For instance, the fatigue life of the raft units in the area of loading positions P1, P2, and P3 was controlled by strain level (*i.e.* fatigue cracks) which affected crack width and crack patterns; whereas in the area of loading position P4 it was controlled by uplift deflection.

The fatigue occurred at loading positions P1, P2 and P3 when the raft units had reached their ultimate state and were unable to sustain any further load repetitions. Loading position P4 failed by uplift deflection without the raft units showing sign of fatigue failure, in fact the raft unit could be lifted and replaced again after relevelling the bedding sand layer. Figures 5.19 to 5.26 show the relationships between the actual number of load repetitions for a particular load and the value of the failure loads for the tested raft units, at each of the loading positions P1, P2, P3, and P4.

The applied load is mixed in composition. It represents a mix of aircraft types having different weights [see Section 4.6.1]. To assess the effect of these weights on the structural performance of the raft unit pavement, the contributions made by loads of different sizes was quantified. The actual number of load repetitions for a particular load was calculated to relate the damage effects at various load levels to that load, using the following equation, proposed by Heukelom and Klomp, (1978).

$$N_m = N_n\left[\frac{W_n}{W_m}\right]^{3.75}\left[\frac{P_n}{P_m}\right]^{1.25} \qquad (5.1)$$

As indicated by Equation (5.1), to relate the damage of a load to another involves consideration of both the applied load and the contact pressure. Where the contact pressure for this test programme was constant for a particular load increment, *i.e.*,

$$\left[\frac{P_n}{P_m}\right]^{1.25} = \left[\frac{\frac{W_n}{A}}{\frac{W_m}{A}}\right]^{1.25} = \left[\frac{W_n}{W_m}\right]^{1.25}$$

then the equation could be rearranged as:

$$N_m = N_n\left[\frac{W_n}{W_m}\right]^{5.0} \qquad (5.2)$$

where:

W_m = Maximum load.

W_n = Applied load.

N_m = Actual number of the maximum load repetitions.

N_n = Number of repetitions of the applied load.

P_m = Contact pressure of the maximum load.

P_n = Contact pressure of the applied load.

A = Contact area.

The contact area of the applied load was scaled down from 400mm to 200mm squares for reasons discussed in Section 4.6.2, Consequently, the fatigue life resulted from the experiments should be compensated by multiplying the laboratories load repetitions by the compensation factor of 5.6 [see Section 4.7].

It was observed that the fatigue life of the square raft units (*i.e.* aspect ratio = 1.0) was longer than the rectangular raft units. By increasing the steel fabric reinforcement from 142mm^2/m as RS2 to 283mm^2/m as RS1, the fatigue life of the raft units increased by about 2.5 times. On the other hand, a combination of an increase in steel reinforcement and thickness of raft units, would improve the performance of the raft unit pavement. By increasing the thickness of RS1 from 140mm to 175mm (RS7), the fatigue life of the raft units (RS7)increased by 2.02 times, before showing any sign of failure. It was concluded that the fatigue life of RS7 could last longer up to 3.5 times the fatigue life of

RS1 [see Section 7.2]. At failure, it was observed that the steel fibre reinforcement (RSF) could not hold the raft unit together with the result that it fell into three parts [see Plate 6.4]. Generally, the performance of steel fabric raft units was not comparable to that of steel fibre raft units.

Table 5.2 shows the fatigue life of the raft units related to the design load of 450kN, except for some tests at loading position P4 where the fatigue life of the raft unit related to the applied load in which the raft unit failed.

5.6 Failure Mechanism and Failure Modes

The failure mode and failure mechanism of the raft units test were different depending on the loading position, the crack patterns, and the design of raft units. Table 5.2 shows the failure load and failure mode of the raft unit tested in the three modules M1, M2, and M3. The observed failure modes were punching shear, fracture fatigue, and uplift deflection. The crack patterns that developed spread all over the raft units. The main cracks propagated through the full depth of the raft units and contributed most to failure namely along the transverse and longitudinal centrelines of the raft unit, and the cross-corner.

In general, the failure modes were similar to a specific load position with differences in failure load and fatigue failure. Considering the post-cracking behaviour, observations throughout the test programme showed that cracked raft units can sustain high loads and high load repetitions. Also, it was observed that the reinforcement held the raft units together and bridged across the opening of the cracks until failure occurred. The formation and widening of the main cracks in RSF were the main failure criteria for the steel fibre reinforcement [see Plates 6.1 and 6.2].

Around the inner and outer loaded contact areas, shear cracks were developed and punching shear failure took place at the areas of high loads and at the late stage of the life of the raft unit. On the other hand, due to applied loads at position P4 (*i.e.* edge load) failure occurred by uplift deflection at the free edge of the raft [see Table 5.2].

With reference to the three modules M1, M2, and M3, as expected loading position P4 always failed by uplift deflection apart from RSF in Module M2 which failed in fatigue fracture for reasons already discussed in Section 5.2. The loading position P4, failed in uplift deflection but at different failure loading conditions. It was concluded by the

author that uplift restraints should be introduced in order to improve the fatigue life caused by the edge loading [see Chapters 2, 6 and 7].

5.7 Summary of Chapter

(i.) The initial fine cracks (flexural cracks) first appeared at a flexural load of 100kN. These cracks enlarged due in part to friction at the crack faces, as the applied loading conditions increased.

(ii.) Cracks developed mainly in the loaded parts of the raft units, *i.e.* at and near to the tracking load, and then extended to the remote parts.

(iii.) The main crack formed along the longitudinal and transverse centrelines of the raft units; and were the main cause of fatigue failure.

(iv.) The maximum induced strain always occurred under the loaded areas and at the centre of the tracking load. The remote sections (*i.e.* the unloaded parts) of the raft units developed low strain levels.

(v.) The maximum downward and upward deflections always occurred under the loaded areas and at the free edge of the raft units.

(vi.)The behaviour of strain and deflection were affected by the crack patterns.

(vii.) The response of the raft units tested to the loading condition varied between the loading positions and depended on the design of the raft units (*i.e.* plan size, thickness, and reinforcement).

(viii.) An increase in the plan size of raft units decreased the deflection and increased the strain levels. In other words, the plan size of raft units is directly related to strain behaviour and inversely related to deflection behaviour.

(ix.) Increasing the amount of steel fabric reinforcement increased the fatigue life of the raft units. Also, the combination of increasing the number of steel fabric reinforcement bars and the raft unit thickness increased the flexural capacity and the fatigue life of the raft unit.

(x.) It was found that the steel fibre reinforcement can enhance the flexural capacity of the concrete. Further, the inclusion of only fibre reinforcement allows the raft unit to break into independent parts and fail by fatigue fracture.

(xi.) Failure of the raft units was cumulative and gradual. The uplift deflection was considered as a result of this test programme, as a maintenance criteria at loading position P4. The observed failure modes in this test programme were punching shear, fatigue fracture, and uplift deflection.

Chapter - Six

Discussion of the test results

6.1 Introduction

Precast concrete raft units are generally small in area and relatively thin for easy handling during construction. The design parameters of the raft units such as plan dimensions, thickness, reinforcement and applied loads were briefly explained in Section 5.1.

Concrete has a high resistance to compressive forces, but a low resistance to tensile forces. Consequently, reinforcement is added to overcome these tensile forces. In the case of raft unit pavements, the reinforcement and thickness designs are important as they can control the tensile forces and effect the long-term life expectancy of the raft unit pavement.

The test observations of this research were presented in the previous chapter. From these observations and related theories, and other design methods for pavement engineering in general, the performance of the raft units will be discussed below. Also, comparison will be made of the changes in the behaviour of concrete strains, deflections and cracks as well as the loading conditions and fatigue life, as the design parameters of the raft units were varied.

The purpose of the discussion of the test results was to reveal the effect of the design parameters of the raft units on their fatigue life characteristics. In the previous chapter, the test observations showed that significant trends in the behaviour of raft units were discovered such as the change of crack patterns with changes in the width, thickness and type of reinforcement in the test raft units. However, the test results showed that as the aspect ratio, thickness and reinforcement of raft units increased, their life performance improved. Also, the response of the tested raft units to different loading positions were analysed in the light of their performance.

In Chapter 4, the author's experimental programme was described in detail. In Chapter 5, the test observations of sixteen raft units tested in pairs were presented. In this Chapter, these test observations are discussed following the same pattern as the previous chapter in order to assist the comparison and appraisal of the test results.

The definition of the term loading conditions is the same as in Section 5.1. It is expressed in terms of the actual load intensity and the equivalent number of load repetitions (ELR) for the design load of 450 kN applied in the laboratory. Also, the effect of using a sealed down version of the contact area in the laboratory instead of using the real life-size contact area of the design aircraft B727 200 will be included in the discussion of this Chapter as was the case with the previous chapter (see Section 5.1). It showed that the scaling down of the real contact area in the laboratory led to conservative results and incorporated a high factor of safety equal to the changes in strain and deflection levels by less than 23 and 19 per cent, respectively.

6.2 Crack characteristics

6.2.1 Flexural Cracks

In the absence of values for the modulus of rupture, the flexural strength of the concrete raft units was related to its compressive strength. An approximate relationship between flexural and compressive strength suggested by Portland Cement Association PCA was used (Packard, 1973),

$$MR = K\sqrt{f_c'} \qquad (6.1)$$

where,

MR= flexural strength (Modulus of rupture), psi

K= a constant between 8 and 10

f_c' = compressive strength, psi ≡ 65N/mm^2

$$MR = 10\sqrt{9427.121} = 970.934\,psi \approx 6.7\ \text{N/mm}^2$$

The concrete strength obtained should be increased by 10 % to give the 90 day strength (Packard, 1973). Therefore, the MR was 7.4 N/mm^2.

Flexural cracks developed at the bottom and/or at the top surface of the raft units, depending on the loading conditions and the design of the raft units. The raft units were initially loaded with 600 cycles of applied load of 100 kN for each loading position, then the load was increased in 50 kN increments (see Section 4.6). As the loading conditions were increased, the flexural cracks appeared at the vertical side of the raft units. Despite the differences in the design parameters of the raft units, these loading conditions cracked all the raft units and cracks were just visible at the 100 kN and 1200 equivalent load cycles, except for the thicker raft units. In the thicker raft units (RS7), the cracks were first visible at higher load of 150 kN and 838 equivalent load cycles.

However, it was clear that the increase in thickness of the raft units from 140 mm to 175 mm made a significant positive contribution to their flexural capacity, to increase the flexural load capacity by 50 per cent.

Despite the different reinforcement provision (i.e.: type, quantity and arrangement), the concrete cracked at the same flexural loading condition. However, it was concluded that the presence of steel reinforcement on its own has not made any significant contribution to the flexural capacity of the raft units. On the basis of the design of the raft units, the flexural capacity of the raft units can be obtained as follows:

(i.) if the presence of steel reinforcement was ignored, then the flexural capacity of the raft unit is given by:

$$M = MR\left(\frac{bh^2}{4}\right)$$

$$= 7.4 \times 10^3 \times \frac{140^2}{4}\ 10^{-6}$$

$$= 36.26 \text{ kN m/m}$$

(ii.) according to BS8110, part 1, 1985 and the following properties of the raft units,

Steel yield strength (f_y) = 480 N/mm^2

Effective depth (d_e) = 140-30 = 110 mm

Lever arm factor = 0.95 d_e

Design area of steel (A_s) = 283 and 142 mm^2/m

Then the resistance moment of the reinforced concrete, at the ultimate limit state is given by:

$M_{uls} = A_s * 0.85 f_y * 0.95 d_e$

$= 283 * 0.85 * 480 * 0.95 * 110 * 10^{-6}$

$= 12.34$ kN m/m

Therefore, as a reinforced concrete section, ignoring the tensile strength of the concrete, the resistance bending moment at the ultimate limit state represents one third of that for the concrete (36.26 kN m/m). At the bending moment of 12.34 kN m/m, the modulus of rupture (MR) of the concrete was 2.52 N m/m. In the same manner the figures for the thicker raft units (RS7) were 56.66 kN m/m and 15.91 kN m/m, respectively. Therefore, when the raft units were considered to be a reinforced concrete section, ignoring the tensile strength of the concrete, the resistance bending moment at the ultimate limit state

were 34.03 per cent and 28.1 per cent of that for the concrete of RSI, and RS7 respectively. At the bending moment of 12.34 kN m/m and 15.91 kN m/m for RS1 and RS7, the moudulus of reputure (MR) of the concrete was 2.52 kN m/m and 2.08 kN m/m, respectively.

From the above calculations, it was seen that the presence of steel reinforcement did not make a significant contribution to the flexural strength of the raft units but carried the tensile strains in the bottom and top of the raft unit as a result of the high load repetitions. The combination of an increase in the amount of steel reinforcement and the thickness of the raft unit contributed significantly to increase the flexural strength and improving the postcracking behaviour of the raft units particularly at high load repetitions.

The visible bottom and top surface flexural cracks appeared in the raft units tested at different applied loading conditions. The flexural cracks developed along the full length of the main longitudinal and transverse centreline of the raft units. The development of the flexural cracks depended on the design parameters of the raft units and the applied loading conditions.

The development of bottom and top surface flexural cracks occurred after 2638 equivalent load repetitions of 150 kN load for a low aspect ratio of 0.25 (R6), and 2535 equivalent load repetitions of 250 kN load for a higher aspect ratio of 0.5 (R12). The average top and bottom crack widths at a load of 300 kN, for example, were 0.12 mm and 0.36 mm respectively. The crack widths in larger sizes or higher aspect ratios, were wider than that of smaller sizes. This argument was supported by the proportional relationship with the strains (see Section 6.3).

Generally, the steel fabric and the steel fibre raft units showed a limited amount of early flexural cracks up to 300 kN and 250 kN respectively. As the applied loading conditions increased, new cracks started to develop at a fairly constant rate up to the design load of 450 kN. The rate of propagation of new cracks in low percentage steel fabric RS2 was higher than that of higher percentage steel fabric RS1.

Of course this should be the case, where the increase in the amount of reinforcement from 142 mm^2/m in RS2 to 283 mm^2/m in RS1 made a significant contribution to maintaining the raft unit as a unit and narrowing crack widths. Reinforcement does not stop cracks to occurring but controls cracks by resisting the induced tensile strains. On the other hand, the rate of propagation in steel fabric RS2 and RS1 was much higher

than that of the steel fibre RSF. In contrast, the rate of increase in crack widths of RSF was higher than that of RS1 and RS2, at specific loading conditions.

Some of the bottom cracks in the thinner raft units RS1 developed through the entire depth of the raft units at loads from 300 kN along the main longitudinal and transverse cracks. In the thicker raft units RS7, there was no sign for top surface cracks until the very late stage of loading. The top surface cracks appeared for loading conditions of 700 kN and 97825 ELR., at the outer loaded areas of loading positions P1 and P2 (see Figs. 5.1 and 5.2). Figures 5.5, 5.6; and 6.1; to 6.5 show the development of the top and bottom flexural cracks.

6.2.2 Crack Pattern

Figures 5.1 and 5.2 show the crack pattern at failure for the tested raft units, together with the loading conditions applied at each position in which each crack was first observed and the extent of the crack at that loading condition. These cracks which contributed to the failure of the raft units were marked boldly. Most of the cracks that appeared on the vertical sides of the raft units were extensions of the cracks developed at the bottom surface.

The propagation of the cracks was slow, and new cracks developed at a fairly late stage of the test with high loading conditions as an average from 450 kN and 4000 ELR. The crack patterns were developed in different forms dependent on the design parameters of the tested raft units. For instance, the main cracks developed in the low aspect ratios of 0.25 and 0.375 (R6 and R9 respectively) were at the transverse centreline of the raft unit (i.e. between the two loaded areas) where in the high aspect ratios of 0.65 and 1.0 (RR and RS2 respectively) were at the longitudinal and transverse centreline of the raft unit (see Fig.5.1a). also, the crack pattern in the steel fibre raft units were very limited even with the high loading conditions, instead the flexural crack patterns remained almost the same and widened up with increasing the applied loading conditions (see Plate 6.1).

On the other hand, these cracks developed through the entire depth of the raft units and along the longitudinal and transverse centreline of the raft units dividing it into three separate pieces (see Plate 6.4). The crack pattern of the steel fabric raft units RS1 and RS2 had a wide grid-like form which propagated through the entire depth of the raft units at the most critical sections (i.e. The main cracks along the longitudinal and transverse centreline of the raft units) (see Figs. 5.1 b, 5.2 b and Plate 6.3)

Although few cracks initiated in the thicker raft units, RS7, at the early stage of the loading compared to that of the thinner raft units, RS1, the crack patterns and widths were limited and very narrow in RS7 (see Fig.5.1 c). Figures 6.3 and 6.4 show the relationship between the applied loading conditions and the crack and the residual crack widths for both RS1 and RS7. The combination of increasing the reinforcement and thickness of the raft units (RS7) made a significant contribution to limiting the crack propagation compared with the high applied loading conditions and demonstrated a long fatigue life of over 234475 ELR.

In addition to the effect of the design parameters of the raft units on the crack patterns, other effects due to the applied load movements were observed. A series of tests had been undertaken for one point load (Bull and Luheshi, 1989). It was observed during these tests that the initial cracks occurred beneath the loading point and then extended along the principal bending moment trajectory. In contrast, the crack patterns observed for the moving wheel loads had a grid-like form. This can be related to the movement of the applied loads between the four loading positions P1, P2, P3 and P4. Movement of the applied loads sequentially changed the principal bending moment directions and consequently the cracks spread over the top and bottom surfaces of the raft units. This change caused a double curvature bending moment along the main longitudinal and transverse centreline of the raft units. The double curvature bending moment was in a direct proportional relationship with the aspect ratio of the raft units due to the increase in the induced strains as the raft units size increased (see sections 5.3 and 6.3) at the same time the double curvature was in an inverse proportion to the thickness of the raft units.

The relationships between the characteristics of the cracked surface and the number of cycles were clearly observed, particularly at the critical sections (along the main centreline of the raft unit). Along the main crack, due to the actions of alternate compression and tension, the crack faces were clamped together and rubbed against each other. Consequently, the crack faces were worn away and then a slit forming a fairly wide opening appeared in the cracked section. It was observed during the test that fine concrete powder fell from the slit to the ground. This slit contributed significantly to the fracture failure which took place at load positions P1 and P3, of the tested raft unit. The formation of such a slit impaired the continuity of the flexural rigidity and reduced the shearing strength of the raft units. The discontinuity of flexural rigidity is shown in Figure 6.5 for the design load 450 kN at the different loading positions. Figure 6.5 shows the relation between crack widths and loading positions for the design load, where cracks beneath the load open wider than those of the other positions which are in

slightly remote positions from the applied load. In general, the crack widths for the remote position were almost equal to the residual crack widths. Such phenomena was observed in the three modules (i.e. M1, M2 and M3) with different crack widths at different loading conditions. Furthermore, the discontinuity developed alternate stresses due to the applied moving wheel load and eventually resulted in penetration of the cracks across the entire depth of the raft unit.

The punching shear cracks developed gradually around loaded areas of the loading positions P1, P2, and P3 for high loading conditions from 450 kN. The punching shear crack patterns developed more when the applied loading conditions increased further up to 700 kN. The punching shear crack patterns of loading position P2 were different from that of loading positions P1 and P3. The forms of punching shear cracks at loading positions P1 and P3 were the same at the inner loaded areas as full circles and half circles for the outer loaded areas. The punching shear cracks patterns of loading position P2 were due to the cross corner-cracks at the outer loaded areas and formed a quarter of a circle centred at the corner of the raft unit (see section 6.2.3). Plate 6.7a and b show the total punching shear failure of loading positions P1 and P2 of RS1 as they occurred.

Figures 5.3, 5.4, 6.6, and 6.7 show the relationship between the top and bottom crack widths of the raft units and the laboratory number of load cycles for the design load of 450 kN. Figures 6.3 and 6.4 show the relationship between the applied loading conditions and the crack and the residual crack widths for both thinner and thicker raft units RS1 and RS7 respectively.

6.2.3 Cross-Corner Cracks

The cross-corner cracks only occurred at loading positions P2 and sometimes, but very rarely at P4. Loading position P2 represents the applied load acting on the joint between the two raft units simultaneously. Loading position P4 represents the edge load at the long side of the raft unit. The initiation of cross-corner cracks appeared usually at a load between 300 kN and 350 kN. Typically, these cracks initiated at the corner under the outer loaded area, through the entire depth of the raft unit.

It was observed that the raft units with relatively small width (i.e. R6 and R9) had not developed cross-corner cracks. In contrast, raft units with longer width (higher aspect ratio between 0.5 and 1.0) developed cross-corner cracks and failed in punching shear (see plate 6.7b). This typical behaviour in terms of thickness effect was observed at failure for the thinner raft units RS1 and the thicker raft units RS7. The former (RS1)

failed in punching shear at loading positions P2, but the latter (RS7) did not show any sign of failure in the P2. It was observed that the rapid increase in the main longitudinal and transverse crack widths affected the crack patterns around P2 and caused a degradation in the flexural rigidity of the raft unit (see Plate 6.2).

The maximum cross-corner crack widths were always at the top surface rather than at the bottom. For example, the maximum top surface crack widths were recorded as 2.96 mm and 3.88 mm for RS1 and RS2, respectively. This difference in crack widths showed the effect of having more reinforcement in RS1 than in RS2, and hence improved the fatigue life.

The development of the cross-corner cracks further due to the applied loading conditions, caused a punching shear failure at that section. In general, the design of the corner sections in concrete pavement needs more attention than some other sections during the design and construction stages because they represent weak sections within the pavement system and cause spalling to the section. In this research, it was found that the combination of the reinforcement and raft unit thickness contributed positively in improving the behaviour of these sections and the fatigue life of the raft units and there was a clear contrast between RS2, RS1 and RS7 (see Table 5.2, Chapter 5).

6.2.4 Crack Control

It was observed that the width of the first main cracks along the centreline of the raft unit (i.e. loading position P1 and P3) and the cross-corner cracks (i.e. loading position P2), failed either by punching shear and/or fatigue fracture, and were always the widest cracks, even at initiation.

It was observed that the maximum crack widths at given loading conditions tended to vary and depend on the raft unit parameters and crack patterns on the top and bottom surfaces. For instance, within the plan dimension of these test raft units, the growth of cross-corner cracks could be controlled by maintaining a low aspect ratio, but that will be at the expense of the fatigue life of the raft units. Also, they can be controlled by increasing both the raft unit thickness and steel fabric reinforcement, and by designing close-spaced reinforcement bars. The steel fibre reinforcement should be superseded by the steel fabric reinforcement when raft units were subjected to high loading conditions. On the other side, by increasing the raft unit thickness from 140 mm to 175 mm, an average reduction in crack width of 60 per cent was achieved for RS7.

6.3 Strain Characteristics

6.3.1 General

As explained in Section 4.9.2, concrete strains were measured at different locations (see Fig. 4.4), on the raft units. The measured strain points represent the strains under the loaded areas, at the middle of the tracking load (i.e. between the loaded areas), and remote sections such as points I and H, in the longitudinal and/or transverse directions.

For the top surface, the initial induced strains were mainly compressive under the loaded areas and at the centreline of the tracking load (i.e. between the loaded areas), until a concrete section cracked. Figures 5.14; 6.8 and 6.9 show that the strain at the centreline of the tracking load and at the edges of the raft unit which alternated from compression to tension, depended on the cracks behaviour. In all the raft units tested, the centre of the tracking load behaved similarly in compression in the initial stage of loading (i.e. up to 250 kN) at the four loading positions. For the bottom surface, the induced strains were mainly compressive particularly under the loaded areas unless a large crack at the section occurred (see Fig. 6.10). The results of the strain measurements are discussed below.

6.3.2 The Plan Dimensions: Module M1

Figures 5.7, 5.11, 5.13, and 6.11 to 6.21 show the typical strain variations on the top and bottom surfaces of the raft units, for the four different loading positions.

It can be seen from Figure 5.7 that the induced tensile strains under the loaded areas increased with increasing applied loading conditions. The increase in the induced tensile strain levels depended on the plan dimensions of the raft units. As was presented in Chapter 5, as the plan dimensions of a raft unit increased, the induced strains increased (see Fig. 5.13).

The maximum induced strains occurred always under the outer loaded areas (i.e. at the middle edge) of the raft units. Generally speaking, the maximum induced strains at the outer loaded areas could be related to two reasons. First, the possibility of the percentage of shear transfer across the joint interface (i.e. at loading position P2 only). Second, for such a small range of side length of the raft units (i.e. between 0.6 m to 2.0 m) while one wheel load was placed next to the edge (i.e. at the outer loaded area) and the other wheel load was near to the centre of the raft unit (i.e. at the inner loaded area) for loading positions P1, P3, and P4. As there was no physical connection between the

raft units, the mixed action of both the centre and edge loads may contribute together to increase the induced strains at the outer loaded areas. The maximum induced strains increased from 935.67 to 1169.59 microstrains when the aspect ratio increased from 0.5 (R12) to 0.65 (RR), respectively. The rate of increase in the induced strains reduced as the aspect ratio increased particularly along the longer side of the raft unit (i.e. the remote sections, see Fig. 6.14). The induced strains at the remote sections were lower than those around the tracking load. This phenomenon could indicate that if the raft units were joined together by means of a load-transfer device and thus behave as a larger raft unit, this would not significantly affect the strain behaviour of the raft units.

Figures 6.12, 6.15, 6.18, 6.19 show the induced strains at the centreline of the tracking load (i.e. between the loaded areas). The trend of the strain variation was similar for the four loading positions. The initial induced strains at the centreline of the tracking load were mainly compressive strains at the top surface and tensile at the bottom of the raft unit. The smaller raft units R6 and R9 initially developed tensile strains at the top which was not expected, but then followed similar trends as for the other raft units. This could be related to their low aspect ratio. Work carried out by Salmo (1990) using low applied load up to 300 kN suggested that, for a two-point load up to 1.0 m centres, the raft unit sagged and developed tensile strains at the bottom and compressive strains at the top surface. Beyond 1.0 m centres, the raft unit hogged and developed tensile strains at the top and compressive strains at the bottom surface. This has been confirmed by the author as the load spacing was 0.865 m centres, at the initial stage before flexural cracks developed. As the loading conditions increased new cracks developed and some of the induced strains were alternated and then reduced gradually.

The fluctuation in strain behaviour could be related to the crack patterns at the section and/or the double bending moment of the raft unit surface along the main longitudinal and transverse centrelines of the raft units particularly for raft units with high aspect ratio RR and RS2 (see Section 6.2). The tendency to double curvature bending depended on the length of both sides of the raft units (i.e. aspect ratio) and on the position and magnitude of the loading conditions.

Figures 6.16 and 6.17 show the variation in the strain behaviour at loading positions P1 and P3 due to load applied at loading position P2. The induced strains at positions P1 and P3 followed the same trend as that of position P2 particularly for raft units with low aspect ratio R6, R9 and R12. The magnitudes of the induced strains at P1 and P3 were less than that measured at P2 due to the distance from the centreline of position P2 which was under loading to the centrelines of positions P1 and P3 for the raft units. The

distance between the centrelines depended on the breadth of the raft unit (i.e. the aspect ratio), as the breadth of the raft unit increased, the magnitude of the induced strains reduced. It was very obvious that the induced strains reduced gradually towards the unloaded sections and depended on how far these sections were away from the loaded section. This indicated that the loading positions with others such as raft unit parameters governed the state and magnitude of induced strains, and thus, the significance of including the effect of loading positions in raft unit design.

The maximum induced compressive strains were recorded at 6,500 microstrain. As the aspect ratio for R9, RR and RS2 increased from 0.375 to 1.0, the maximum induced compressive strains increased from 5,856 to 7,955 to 8,604 microstrains, respectively. These maxima occurred at the same applied load levels of 600 kN, but at different fatigue lives: 36731 ELR, 34203 ELR, and 32274 ELR for R9, RR and RS2 respectively. The induced tensile strains had the same trend as its counter part, the induced compressive strains. For example, the maximum induced tensile strains for raft units with aspect ratios of 0.5 (R12) and 0.65 (RR) were recorded as 935.67 and 1169.59 microstrains at loads of 400 kN and 1889 ELR; and 600 kN and 31674 ELR, respectively (see Fig. 5.7). However, these results confirmed the finding shown in Figure 5.13, with the induced strains at any section in the raft unit increased as the raft unit size increased.

6.3.3 The Reinforcement: Module M2

Figures 5.14, 5.16, 6.8 to 6.10, and 6.22 to 6.24 show the typical variations in strain behaviour on the top and bottom surfaces of the raft units for the four loading positions. The strain behaviour in the three different reinforced raft units RS1, RS2 and RSF (module M2) followed the same trend as that of module M1 discussed in section 6.3.2. The trend of strain behaviour for a particular section at a specific loading position was similar for the two modules. In all respects, the strain variations were affected by the reinforcement design of these raft units. The steel fabric reinforcement RS1 and RS2 performed better than the steel fibre reinforcement RSF in controlling the crack width (i.e. fatigue crack) (see Section 6.2), and the induced strains. Figure 5.14 show that the induced strains under the outer loaded area varied in the three different reinforcement in both the magnitude and state (tension or compression). The strain behaviour was influenced remarkably by the crack widths and crack patterns. The increase in steel fabric reinforcement from 142 mm^2/m (RS2) to 283 mm^2/m (RS1) improved the flexural strength of the raft units and resisted the additional tensile strains that occurred due to applying high loading conditions.

From the calculations of the flexural capacity in Section 6.2.1, it was found that the steel fabric reinforcement did not make a significant contribution to the flexural capacity of the raft unit as that of the steel fibre reinforcement. The steel fibre reinforcement enhanced the flexural capacity of the raft unit in the serviceability limit state. In the initial stage of loading, the flexural cracks were limited in the RSF than in RS1 and RS2. In contrast, in the ultimate limit state when loading conditions were increased, there was a thorough control in crack widths in RS1 and RS2 than in RSF. However, the design of RS1 and RS2 with top and bottom reinforcement in both direction contributed significantly to resisting the double acting bending moment and controlling the cracks behaviour at the ultimate limit state.

The initial induced strains on the bottom surface of the raft units were mainly tensile and tended to alternate between tensile and compressive due to the formation and the growth of the flexural cracks when the raft units were subjected to the higher loading conditions. In some cases, the fairly high induced strains recorded during the test would not be only due to an increase in the loading conditions but also to the increase in the main crack widths and the crack patterns in the raft units. The main cracks along the longitudinal centrelines of the raft unit were wide particularly the RSF (see Section 6.2), and behaved as a hinge tied joint due to the reinforcement producing an alternating compressive and tensile strain in this section. This fluctuation in the induced strains impaired the continuity of the flexural rigidity and also caused a remarkable reduction in the shearing strength of the raft units that was mainly relying upon the steel reinforcement and the aggregate interlock. The discontinuity of the flexural rigidity was shown in Figure 6.5.

In this respect, the steel fabric reinforcement (RS1 and RS2) performed and resisted the discontinuity of the flexural rigidity significantly and better than the steel fibre reinforcement (RSF). Also the test results showed that increasing the steel fabric reinforcement from 142 mm^2/m (RS2) to 283 mm^2/m (RS1) reduced the induced strains and controlled the crack widths, therefore improved the long-term life expectancy of the raft units. The behaviour of these main cracks at the ultimate limit state caused fatigue fracture failure for the three different reinforcement, but at a different load capacity and fatigue life. By increasing the steel reinforcement from RSF to RS2, then RS1, the performance of the raft units improved from 400 kN and 1889 ELR to 600 kN and 32274 ELR then to 700 kN and 116269 ELR, respectively (see Table 5.2).

It is believed that the increase in the steel reinforcement would lead to a reduction in the induced strains and an associated improvement in the performance and fatigue life of the raft unit pavement.

6.3.4 The Thickness: Module M3

In Section 6.3.3, for module M2, the effect of using the steel fabric and the steel fibre reinforcement on the performance of the raft unit was discussed; it was found that increasing the steel fabric reinforcement increased the flexural rigidity and shearing strength of the raft units and hence, improved their life performance. In this section, the effect of the combination of reinforcement and thickness design on the performance of the raft units will be discussed.

Figures 5.8 to 5.10 and 6.25 to 6.30 show the typical variations in strains behaviour on the top and bottom surfaces of the raft units for the four loading positions.

As shown in these figures, the induced strains varied between the thinner (RS1) and the thicker (RS7) raft units. The initial induced top and bottom strains in RS1 and RS7 were measured at 100 and 53 microstrains, respectively. The induced strains suddenly increased and changed their trends as soon as flexural cracks initiated at particular sections. As the applied loading conditions increased, the induced strains increased and thus new cracks developed particularly in RS1. In RS1 the flexural cracks widened as the loading conditions increased further and caused a fluctuation in the behaviour of the induced strains, where in RS7, the flexural cracks which were very few (see Section 6.2.2) remained steady and the induced strains progressed very slowly. The variation of crack widths in RS7 was small, particularly the top surface cracks, but in RS1 was relatively high especially the residual crack. The variation in the residual crack width is associated with a degradation in the flexural rigidity and the shearing strength of RS1. The residual bottom crack width was 2.92 mm which was correspondent to the induced tensile strains of 3370 microstrains at loading conditions 700 kN and 116269 ELR. In contrast, the RS7 developed a residual crack width of only 1.08 mm at a loading conditions of 700 kN and 234475 ELR (when the test stopped before any sign of failure), associated with induced tensile strains of 1093 microstrains. The maximum induced compressive strains were 1513 and 558 microstrains at loading conditions similar to that of the residual bottom cracks.

It was found that by increasing the raft unit thickness from 140 mm (RS1) to 175 mm (RS7), the induced strains reduced by 6o per cent and the fatigue life increased by 2.02

times. The combination of increasing the steel fabric reinforcement (see Section 6.3.3) and the thickness increased the stiffness of the raft units and hence the induced strains and deflection for particular plan dimension reduced. Also, as the stiffness of the raft units increased, their load carrying capacity and the life performance improved.

The variations in the distribution of the induced strains on the top and bottom surfaces of the raft units were related to the double curvature bending along the main longitudinal and transverse centrelines and to cracks behaviour of the raft units. The double curvature bending was reduced remarkably as the thickness of the raft units increased from 140 mm (RS1) to 175 mm (RS7) and therefore, the induced strains reduced.

To sum up, generally, the trend of the induced strains in the raft units followed likewise for all the loading positions. The sequential movement of the applied loads changed the principal bending moment directions and caused a double curvature bending in both directions along the main longitudinal and transverse centreline of the raft units. It was found that the double bending moment in both directions increased as the plan dimensions (i.e. aspect ratio) of the raft units increased, and thus, the induced strains increased. The combination of increasing the steel fabric reinforcement and the thickness of the raft units improved their resistance to the double bending moment and therefore reduced the induced strains. Also, this combination improved the flexural rigidity and shearing strength of the raft units RS1 and RS7.

6.4 Deflection Characteristics

The deflection behaviour exhibited by the test raft units were of two types, upward (uplift) and downward deflection. The test observations of the deflection behaviour were presented in Section 5.4. It was observed graphically that, the relationship between the induced deflection and the applied loading conditions was linear in the elastic state. Basically, the deflection behaviour of the raft units in modules M1, M2, and M3 was similar to each other, but with a few exceptions due to the crack behaviour that was governed by the raft units parameters. Figures 5.12, 5.13, 5.17, 5.18, and 6.31 to 6.44 show the deflection behaviour of the raft units at the most critical sections due to the four loading positions (see Fig. 4.4).

6.4.1 The Bedding Sand

As mentioned earlier in Section 5.4, the source of the initial high deflection was the bedding sand layer. The sand was difficult to compact; instead it was screeded to give a

levelled surface and more controlled tolerances. The bedding layer was used to ensure full contact between the raft unit base and the sub-base layer. Thus, the 50 mm thick sand bedding layer, could be reduced or an alternative material to the sand course could be used such as a Bitucrete (see Section 4.2.3) in order to minimise the initial deflection caused by the bedding sand layer of 50 mm. The significance of this reduction was found numerically, to be in reducing the induced strains associated with a slight increase in the induced deflection in the raft unit (Bull and Clark, 1991).

6.4.2 The Plan Dimensions: Module M1

For a low aspect ratio, the raft unit has a small plan area of the underneath layers support and therefore, the raft unit will be subjected to a large downward deflection into the bedding sand with relatively small bending moment in the raft unit. In other words, the bending action within the raft unit was not fully developed and the applied loading conditions were mainly supported by the layers underneath. When the aspect ratio increased from 0.25 to 1.0, the bending action of the raft unit started to develop and a larger area supporting the raft unit, thus the induced strains increased and the induced deflection decreased.

As expected, the loading positions P1 and P3 which represent almost the central load, produced downward and upward deflections (see Fig. 6.31 and 6.32). In contrast, the loading position P4 which represents the edge and corner loads, produced uplift deflections (see Fig. 6.33). These figures show that the maximum deflection levels were in inverse proportional relationship with the aspect ratio of the raft units. For instance, the maximum downward deflections at loading position P1 for the low aspect ratio R6 and R9 and high aspect ratio RR and RS2 were 27.16 mm and 16.05 mm, respectively (see Fig. 5.18). The same trend occurred with loading position P4 but in an uplift deflection at the free edge of the raft unit. This range of the aspect ratio from low to high influenced the uplift deflection levels as the maximum uplift deflection for the bottom range was -13.99 mm at 1032 equivalent load repetitions of load 200 kN, and for the top range was -11.90 mm at 2512 equivalent load repetitions of load 350 kN.

It was clear that the uplift deflection increased with an increase in the loading conditions. With reference to the crack behaviour, the development of the main longitudinal and transverse cracks affected the trend of the induced deflection. As the aspect ratio increased, the corners of the raft unit tended to lift up away from the bedding sand due to the applied load at position P1, but gradually decreased as soon as the main cracks developed. Figure 6.32 shows the induced deflection at the corners of

the raft units tested in the module M1 (i.e. with different aspect ratio). RS2 has an aspect ratio equal to unity and the largest width in the module. It deflected upwards at its corners for a maximum uplift deflection of 3.71 mm at loading conditions of 250 kN and 139 ELR. Due to the widening in the main crack from 0.24 mm to 3.92 mm which associated with top crack of 2.39 mm, this maximum was reduced to 2.47 mm at loading conditions of 450 kN and 14489 ELR. Obviously, this variation in the maximum could be related to the effect of the crack behaviour in general. On the other hand, the maximum downward deflections always occurred around the loaded areas. Figures 5.18 and 6.31 show the induced deflection around the loaded areas of position P1 and shows that the induced deflection was in an inverse proportional relationship with the size of the raft unit. The variation in the induced deflection at different locations on the raft units, was affected drastically by the cracks behaviour particularly with high loading conditions and the appearance of the punching shear failure cracks. The development of the failure cracks caused a rapid increase in the induced deflection and significantly influenced the ultimate load carrying capacity.

Figure 6.34 shows the behaviour of the middle tracking load section near to the free edge. The distance from the section to the free edge varied between the raft units and depended on their aspect ratio. The distance increases with increasing the aspect ratio. The section was deflected downwards as expected for all the tested raft units except for the raft unit RS2 that was with the highest aspect ratio (i.e. a unity), deflected upwards. Such behaviour confirmed the complexity of the distribution of the induced strains and deflection as a function in their aspect ratio. In other words, this phenomenon could be related to the double bending of the raft unit due to its aspect ratio.

The same principles were observed for the applied load on the joint (i.e. Loading position P2). Figures 6.35 shows the general trend of the induced deflection of the free edges due to loading position P2 which was mainly uplift deflection after the raft units had settled down at the early stage of the test. The maximum deflection at the free edge was 8.36 mm due to loading position P2.

It was observed during the tests that the loaded raft unit affected the adjacent raft unit even without any physical connection. This effect was negligible with low loading conditions and relatively high with higher loading condition at positions P1 and P3. The average deflection on the adjacent unloaded raft unit was only 1.5 mm at loading conditions of 450 kN and 24689 ELR. In this case, if the applied loads were right on the joint (i.e. Loading position P2), the effect was even higher. This effect was related to the

response of the underneath layers of the raft unit particularly the response of the sand layer to the high applied loading conditions.

This phenomenon led to an assumption that various per cent shear-transfer values occurred along the joint interface despite, there was no physical connections between the raft units. The per cent shear-transfer was defined as the ratio, as a percentage, of the induced deflections along the joint interface between the unloaded or less heavily loaded and the adjacent loaded raft units. The two raft units were assumed to have the same dimensions. Also, zero bending moment transfer across the joint interface has been considered as there was no physical connections at the joint during the tests. The shear transfer for loading positions P1 and P3 was neglected as the average deflection on the unloaded raft unit was low (i.e. 1.5 mm) compared with the loaded raft unit and therefore the ratio in percentage was low (i.e. around 12.5 per cent). However, shear transfer for loading positions P2 was considered as both raft units demonstrated close deflection levels. The one hundred per cent shear transfer means that the induced deflections induced along the joint interface were equal. The test results for strain and deflection behaviour showed that the percentages of shear transfer due to loading position P2 were in the range of between 46 per cent and 96 per cent. The induced strains were reduced compared with their counter part around loading positions P1 and P3. The highest level of this range (i.e. 96 per cent) means that the applied load was distributed almost equally (i.e. nearly 100 per cent) at the joint interface and produced an equal deflection level on the two adjacent raft units. On the other hand, at a fatigue life of 14200 ELR for the design load of 450 kN, the induced deflection levels at the joint interface (i.e. loading position P2) reduced from 28.69 mm down to 19.21 mm as the aspect ratio increased from 0.25 to 1.0, respectively (see Fig. 6.36). This phenomenon confirmed two main points in the design of raft units.

(i) as shown in figures 5.12 and 5.13, as the raft unit size (aspect ratio) increased, the induced strains increased and induced deflection decreased for any loading position, and

(ii) the applied load at position P2 has not been shared equally between the adjacent raft units as suggested by the design method developed by Bull (1986) (see Section 7.7).

the uplift deflection due to loading position P4 was the most critical loading position as far as the uplift deflection was concerned. Figures 6.33 and 6.37 show that the initial induced uplift deflection increased as the applied loading conditions increased. It can be seen that the form of the induced deflection (uplift) along the free edge of the raft unit

was similar but with a different magnitude. This variation in the uplift deflection was due to the crack behaviour particularly the main cracks along the longitudinal and transverse centrelines of the raft unit. The maximum uplift deflection due to the loading position P4 for all the tested raft units were shown in Table 5.1. With these values, loading position P4 was considered to have failed in an uplift criteria (see Table 5.2), and to be unsafe to carry on the tests at this loading position.

6.4.3 The Reinforcement: Module M2

Generally speaking, the behaviour of the induced deflection due to the four loading positions was mainly similar in the three different modules. The effect of different design reinforcement on the deflection behaviour was to eliminate the effect of the crack behaviour on the induced deflection.

Figure 5.17 shows the trend changed due to the crack behaviour. The effect of cracks behaviour was very clear, the induced deflection levels declined gradually when the crack widths had reached to a level over 2.0 mm. The behaviour of fatigue cracks depended on the induced strain levels at a section. The development of the crack width and crack patterns usually associated with an increase in the induced strain levels due to the applied loading conditions. In this respect, the relationship between the behaviour of strains and deflection was clear, as they are in an inverse proportional relationship (see Section 6.3).

Figures 6.38 and 6.39 show the general trend of the induced deflection at the free edges of the raft units due to applied load on the joint (i.e. position P2). Generally, the induced deflection tended to deflect downwards which was different from the predictions for such sections, particularly with high loading conditions. The variation in the induced deflection could be related to the crack behaviour of the three different reinforced raft units RSF, RS2 and RS1. The additional reinforcement increased the stiffness of the raft units and thus controlled the crack behaviour and maintained the unity of the raft unit.

Figure 6.40 shows typically the induced downward deflection at the outer loaded area due to loading position P2. It was observed that, the sudden increase in the induced deflection was due to the formation of the two cross-corner cracks in the joint interface of the raft units, for RS2 and RS1 at the design load of 450 kN. The corner section always represents one of the most critical sections in concrete pavement design and therefore, designers have to take this into their considerations. Usually, the designers

treat this section by increasing the steel reinforcement, raft unit thickness or combination of both of them (see module M3).

Despite the high initial deflection in the steel fibre reinforcement RSF, the rate of increase in the induced deflection for RSF was lower than that for the steel fabric RS2 and RS1 at a particular loading condition. These observations could be related to the lack of compaction in the bedding sand for the steel fibre test and to the flexural capacity of the steel fibre reinforcement at a particular fatigue life. Although it is understandable that the increase in the induced deflection was dependent mainly on the applied loading conditions, but the main crack widths contributed significantly in the deflection behaviour particularly the uplift deflection. The difference between the steel fabric and steel fibre reinforcement in controlling the cracks behaviour was discussed in section 6.2 and showed that the former controlled the crack widths better than the later which controlled the crack patterns and failed to minimise the crack width (see plate 6.5 and 6.7). Therefore, the widening of the main crack to act as a joint and thus reduced the uplift deflection along the free edge of the raft unit due to loading position P4 from 37.4 mm for RS1 down to 12.0 mm for RSF (see Table 5.1).

At the end of the fatigue life, a rapid increase in the induced deflection was observed. This rapid increase was due to the development of cracks at the last phase in the fracture fatigue and punching shear failure mechanism, which significantly influenced the ultimate load carrying capacity particularly for the RSF and RS2. These induced deflection levels should not be considered.

6.4.4 The Thickness: Module M3

The general trend of the induced deflection of the raft units in Module M3 was similar to that of modules M1 and M2. Figure 6.41 shows typical variation in the induced deflection at the corners of the raft units due to the loading positions P1 and P3. It can be seen that the thinner raft units RS1 produced uplift deflection at their corners, but the thicker raft units RS7 produced downwards deflection at the same sections. Although the RS1 and RS7 behaved differently, the rate of increase in the induced deflection of RS1 was higher than that of RS7 for particular loading conditions. These differences could be related to the increase in the stiffness of RS7 by increasing its thickness from 140 mm to 175 mm which controlled the deformation characteristics by reducing the double bending curvature as a result of the combination of an increase in the steel reinforcement and the thickness of the raft units (RS7). The induced deflection levels increased as the loading conditions increased particularly for the corners close to the

tracking load. The variations in the trend of the induced deflection of RS1 were higher than that of RS7 due to the crack behaviour in both raft units. The crack behaviour of RS7 was improved remarkably in respect of limiting crack patterns and crack widths, due to the increase in its stiffness (see Section 5.2).

The trend of the uplift deflection was similar to that discussed above for modules M1 and M2. Figure 6.42 shows typical variation of the induced uplift deflection at the free edges of the raft units due to the applied loading conditions at position P4. The maximum induced deflection for RS1 and RS7 were close to each other (see Table 5.1) but the rate of increase in RS1 was higher than that of RS7 particularly if the initial induced deflections were excluded. The initial induced uplift deflection along the free edge of the raft units were 2.84 mm and 10.15 mm for RS1 and RS7 respectively. However, the difference in the initial induced deflection could be related mainly to the lack of compaction of the bedding sand (see Fig. 6.43).

It was observed that there were differential deflections between the edge and the centre of the raft unit which contributed to cause a larger bending particularly with high aspect ratio of raft units such as RS2. By increasing the thickness of the raft units from 140 mm (RS1) to 175 mm (RS7), the induced strains and deflections were reduced remarkably (see Section 6.3 and Fig. 6.44), due to the associated increase in the relative stiffness of the raft unit (RS7). The reduction in the induced deflection reduced the differential deflections both between the adjacent and within the raft units, and thus improved their life performance and riding quality.

To sum up, from the above detailed discussions on the deflection characteristics [see Section 6.4], it can be seen that the general trend of the induced deflection of the raft units in the three modules M1, M2 and M3 were similar for a particular loading conditions.

The maximum induced deflections always occurred under the loaded area in general and under the outer loaded area in particular, while the maximum uplift deflection always occurred at the free edges of the raft units due to loading applied at position P4 [see Table 5.1]. the variation in the induced deflection levels of the raft units could be due to firstly, the crack pattern and crack width of the main and the cross-corner cracks, secondly, the lack of compaction of the bedding sand layer, and finally, the double curvature bending of the surface of the raft unit.

The induced deflection is in direct proportional relationship with the applied loading conditions. The rate of increase in the induced deflection was influenced more by the applied load increments than by the applied load repetitions.

The induced deflection was influenced dramatically by the design parameters of the raft units. It was shown that as the raft unit size (i.e. aspect ratio) increased, the induced deflection decreased [see Figure 5.12]. The steel reinforcement bars controlled the crack behaviour more efficiently than the steel fibre reinforcement. The combination of increasing the steel reinforcement and the thickness of the raft units (RS7), increased their stiffness and thus the induced deflection reduced.

The induced strains were increased and the induced deflections were decreased as the aspect ratio of the raft units increased. These changes reduced remarkably for remote sections away from the tracking load. The changes can be expected to cease when the raft unit rigidity and the side length were increased beyond 3 m., and become insignificant.

The applied load at position P2 has not been shared equally between the adjacent raft units as suggested by the design method developed by Bull, 1986.

It was observed that the uplift deflection could be considered as a maintenance criteria for loading position P4, where all the raft units failed in the early stages of the test with an average load capacity of 350 kN with the exception of RS1 and RS7 [see Table 5.2]. The uplift deflection can be controlled and then the fatigue life will improve, by providing surrounding beams or retaining strips at the edges of the raft unit pavement system to allow this position to act in a similar way to loading position P2.

6.5 FATIGUE LIFE CHARACTERISTICS

Fatigue performance is usually expressed by the mean value of the number of load repetitions to failure for a particular loading conditions. The fatigue behaviour of concrete pavements is influenced by several factors such as loading intensity and cumulative fatigue damage, the rate of loading and frequency, and the residual deformation. The range of strain fluctuations is the parameter which has a potential impact on the fatigue performance. Also, the progressive growth of cracks and fracture of steel and concrete has a significant effect on the fatigue life. The major cracks that develop under repeated wheel load are referred to as concrete fatigue cracks.

One of the main objectives of this research was to develop relationships between the fatigue life "N" and the corresponding deformation of the raft units [see Chapter 7]. The measured deformation under various loading conditions have been used to develop and validate the relationships.

It was observed throughout the tests that fatigue developed in three stages which were initiation, propagation, and final failure. Failure of the raft units was not sudden, but they gradually deteriorated by forming major cracks due to punching shear and fatigue fracture which were accompanied by permanent deformation due to the residual deflection, strains and cracks. However, the cracked raft units performed satisfactorily, in fact, well past their serviceability limit state and continued to sustain high load conditions up to their ultimate limit state. The failure criteria adopted required complete failure of the raft unit at each loading positions and that the raft unit could not sustain any additional loading conditions due to cracking, spalling, snapping of the steel reinforcing bars, and/or a differential deflection exceeding 40 mm [see Section 4.7,].

Figures 5.19 to 5.26 show the relationship between the applied loads and the actual laboratory load repetitions from the three modules M1, M2 and M3 at different loading conditions. The actual laboratory load repetitions related to a certain applied load were calculated using Equation 5.1 [see Section 5.5]. As discussed in Section 4.7 the actual laboratory load repetitions should be compensated by the compensation factor of 5.6, due to using a contact area smaller than the real contact area for the design load. Therefore, the actual laboratory load repetitions obtained from these figures should be multiplied by the compensation factor in order to obtain the real design life of a raft unit.

For the sake of discussion of the fatigue characteristics, the actual laboratory load repetitions were used and related to the design load of 450 kN and called the equivalent load repetitions (ELR).

The behaviour of the raft units to failure varied depending on the deformation that occurred during their fatigue life. Table 5.2 shows the actual laboratory fatigue life for each test at each loading positions P1, P2, P3 and P4

Loading positions P1, P2 and P3 failed in the same manner either by punching shear and/or fatigue fracture in the three modules (see Plates 6.6, 6.7, 7.2 and 7.3). There were no failure for these loading positions in the thicker raft units RS7 and the test of these raft units stopped at 234475 ELR due to the time constraints. Loading position P4

always failed in uplift deflection and was the most critical loading position and produced the lowest fatigue life compared to the other loading position for the reasons discussed in section 6.4.1. Fatigue life for loading position P4 could be improved by constructing an edge beam or retaining strips around the pavement system and/or a physical connection at the joint in order to allow position P4 to perform as/or similar to loading position P2 and thus reduce the differential deflection in the pavement system.

The performance of the steel fabric reinforcement was better than that of the fibre reinforcement. However, the raft units RS1 with the highest percentage of steel fabric reinforcement maintained the highest fatigue life. Table 5.2 showed the effect of using different types and amounts of reinforcement on the fatigue life. For instance, by using steel fibre reinforcement RSF and increasing the steel fabric reinforcement from 142 mm^2/m (RS2) to 283 mm^2/m (RS1), the fatigue life of loading position P1 improved from 4,289 to 32,274 to 116,269 ELR, respectively. On the other hand, the combination of increasing the steel fabric reinforcement and the raft unit thickness from 140 mm (RS1) to 175 mm (RS7) improved the fatigue life of both RS1 and RS7, and the load capacity of the thicker raft units RS7 (see Section 7.2). By increasing the thickness of raft units, the fatigue life of RS1 increased from 116,269 ELR to failure; to 234,475 ELR to the end of the test.

As discussed in sections 6.3 and 6.4, there were strong relationships between the induced strains, deflections and the aspect ratio of raft units. The aspect ratio is in direct proportional to the induced strains and inversely proportional to deflections. However, with a low amount of reinforcement of 142 mm^2/m and a minimum thickness of 140 mm for raft units subjected to heavy wheel repeated loads, as the aspect ratio is increased the induced strains increased, thus, the fatigue life was affected relatively as is the case with RS2. With the same aspect ratio as RS2 (i.e. equal to unity), and an improvement in thickness and reinforcement design RS7 and RS1, the fatigue life improved drastically (see Table 5.2).

It was observed that the widening of the main transverse and longitudinal cracks impaired the flexural rigidity of the raft units and caused a remarkable reduction in the shear strength. Such behaviour affected the fatigue life and reduced the pavement life of the raft units (see plate 5.7 and 6.2). Also, it was found that the increase in steel fabric reinforcement would not prevent the raft unit from cracking, but increased the fatigue life and strength of the raft unit by resisting the tensile strains and thus controlling the cracks. The steel fibre reinforcement should not be recommended for use on its own for raft unit paving system if it is likely to be subjected to high loading conditions and to

long fatigue life. The fatigue life could be improved by a feasible combination of increasing the steel fabric reinforcement and raft unit thickness, constructing an edge beam at the end of the pavement system, and/or a physical connection at the joint in order to reduce the differential deflection due to loading position P4 and at the joints.

6.6 Failure Load and Failure Modes

The most common failure mode for a concrete pavement in the ultimate limit state is punching shear and/or fatigue fracture. Some of the punching shear failures are preceded by a partial flexural failure. The value of failure loads was influenced by the existence of extensive cracks, loading conditions and the crack patterns. The raft units failed in different modes of uplift deflection, punching shear and/or fatigue fracture dependent on the loading position, crack widths, and crack patterns. Table 5.2 shows the failure load and failure mode for every raft unit at each loading position. The failure mechanism for a specific mode is similar for all raft units, but the values of the failure loads are different. The main observed failure criteria were fracture and punching shear. The uplift deflection failure mode was a limited criterion. Since the raft failure was mainly due to both fracture and punching shear, the ultimate load capacity of the raft units can be predicted (see Section 7.2).

Loading positions P1 and P3 are similar and failed either by fatigue fracture or punching shear (see Plate 6.6). Loading position P2 is a new loading position introduced by the author in this research, and different from other loading positions by being located right on the joint, but failed in the same manner as loading positions P1 and P3. In some cases, with raft units that have low aspect ratios (i.e. RS6, RS9 and RS12) the area around loading positions P1 and P3 passing through loading position P2, failed by the same failure criteria and interacted with each other which could have been due to the close proximity of the loading positions on those raft units. Loading position P4 maintained an early failure in uplift deflection before making a real contribution in crack behaviour, and low failure load levels of 350 kN were recorded with an exceptional case of a raft unit with the highest percentage of reinforcement (RS1) which maintained a high failure load levels of 600 kN.

Clearly, the additional loading position P4 on the adjacent raft unit affected the failure mechanism and the fatigue life of the raft units. The loading applied at position P4 affected the behaviour of the induced strains in the area around load position P3; also, the variation in strain was affected by the distance away from other loading positions.

It could be concluded that a long fatigue life and high failure load level at loading position P4 contributed and affected the failure mechanism of loading position P3, by accelerating the fatigue fracture and punching shear failure. The mechanism of the failure was though the alternating compressive and tensile forces at the main cracks along the main transverse and longitudinal of the raft units and the development of the punching shear cracks at high loading conditions (see Fig. 5.1 b).

Generally speaking, fatigue failure at a loading position was affected primarily by the loading intensity at that position and secondly by the applied loading cycles at other loading positions. However, the effect of the loading cycles of other positions was significant compared to that of the applied load.

6.6.1 Punching Shear

Punching shear calculations shown in Section 7.2 were carried out for both the failure case for different failure loads and for the non-failure case for RS7. Also an allowance was made for the effect of using a small size contact area 200 x 200 mm in the laboratory instead of using the real contact area of 400 x 400 mm, when assessing the failure mechanism of punching shear.

The mechanism of punching shear failure using the real contact area could be predicted by relating it to the laboratory punching shear failure loads. By using the real contact area, the predicted failure mode due to just the applied wheel load was not punching shear, as the shear strength (ϕ Vc) was always higher than the shear force (Vu) acting on a critical section. The critical section of the real contact area was larger than that of the laboratory contact area and therefore, the shear strength was higher, thus the punching shear failure due to only the applied wheel load was denied. However in some cases during the laboratory tests, punching shear failure occurred. Despite this difference, the punching shear failure would occur with the real contact area as a result of applying the wheel load and the real load repetitions shown in section 4.7.

As the applied loading conditions increased, the punching shear cracks around the loading areas started to develop due to the accumulation and concentration of the local induced strains around these areas towards the end of the fatigue life of the raft units (see Section 6.2). due to these cracks the top surface of the raft unit deteriorated and was accompanied by further snapping of the reinforcement and partially penetrating shear cracks with large residual crack widths. These shear cracks impaired the flexural rigidity of the raft unit and caused a severe reduction in the shearing strength which mainly

relies upon the steel reinforcement and the aggregate interlock. At this stage the total punching shear failure occurred around loading positions P1, P2 and P3 of the raft units (see Plate 6.7). Punching shear failure has not occurred in raft units with low aspect ratios (R6) and with a combination of higher reinforcement and thicker thickness (RS7). As the aspect ratio increased, the punching shear failure occurred even when the steel reinforcement increased from 142 mm^2/m (RS2) to 283 mm^2/m (RS1), but at different failure load levels. However, the extra reinforcement improved the load carrying capacity of the raft units as both the raft units RS2 and RS1 failed in punching shear mode at different failure load levels of 450 kN and 700 kN, respectively (see Table 5.2)

Punching shear failure at the outer loaded area of loading position P2 was mainly due to the development and the enlargement of the cross-corner cracks in the adjacent raft units at the joint interface (see Plate 6.7b). The residual crack widths at punching shear failure for loading position P2 were 2.08 mm and 2.83 mm for RS1 and RS2, respectively. The punching shear failure at the outer loaded area of loading position P3, for example, was due to the crack patterns in general and the cross-corner cracks at loading position P4 in particular (see Fig. 5.1b).

6.6.2 Fatigue Fracture

Fatigue fracture is one of the criteria observed during the test programme. Fatigue fracture failure occurred always at loading positions P1 and P3. The fatigue fracture resulted from the bending action of the raft unit and the additional bending due to differential deflections between the centre and the edge of the raft unit. Thus, the fatigue fracture was due to fatigue of the tensile reinforcing bars at the top and bottom of the raft unit at different failure loads (see Plates 6.4 a to d). Table 5.2 shows the failure load and failure mode.

The main cause of fatigue fracture was similar in all the raft units and was due to the form of the main transverse cracks along the centreline of the raft units. With an increase in applied loading conditions; and the sequential movement of the applied load, the main cracks propagated and developed through the entire depth of the raft units (see Plate 6.3). The relationships between the characteristics of the cracked surface and the number of load cycles were clearly observed (see Section 6.2). Due to the actions of alternating compression and tension, these crack faces were clamped together and rubbed against each other. Consequently, the cracks were worn away and the crack widths enlarged; the shear resistance of the raft units was reduced remarkably. This was confirmed during the test by observing a sequential falling of a fine concrete powder

from the wide opening (see Plate 6.6). The residual top and bottom crack widths at failure were recorded as 2.86 mm and 4.86 mm and 2.09 and 3.86 mm for RS1 and RSF at load levels of 600 kN and 450 kN respectively.

As discussed in Section 6.3 and 6.4, the raft units with lower aspect ratio had smaller induced strains and larger induced deflections. The induced strains in raft units (R6) were small due to the development of small bending along the short span of the principal moment trajectory. In other words, when the aspect ratio of the raft unit increased, not only the bending action of the raft units started to develop but the strains due to a large area of foundation support and the larger differential deflections between different locations on the raft unit, started to build up. As a result, a large bending moment developed and the induced strains in the raft unit increased.

With this phenomenon in mind, the increases in steel fabric reinforcement (RS1) resisted partially the increases in the induced strains and resulted in an increase in the failure load levels from 450 kN for RS2 to 600 kN for RS1. Following this increase in steel fabric reinforcement, the raft unit thickness was increased from 140 mm (RS1) to 175 mm (RS7). The combination of increases in the reinforcement and the thickness had a potential impact on the performance of the raft unit which rose to the predicted ultimate load capacity of RS7 up to 937.5 kN (see Section 7.2.1).

It can be concluded that the formation of such a wide opening reduced the flexural rigidity and the shear strength, particularly for the steel fibre reinforcement RSF. The steel fabric reinforcement bars contributed significantly to minimising the crack widths and resisting the tensile strains in the cracked section particularly when combined with an increase in raft unit thickness (RS7). The steel reinforcement limited and reduced the development of cracks rather than prevented them.

6.6.3 Uplift Deflection

As discussed in Section 4.6.2, the effect of using the small laboratory contact area (200 mm square) instead of the real contact area (400 mm square) on the performance of the raft units should be considered. It was shown that the effect of increasing the loaded area where the centre of the loaded area moved towards the centre of the raft unit as the loaded area increased, had reduced the strains and deflection levels which resulted in conservative results by an average of 20 per cent more than would be the case in reality.

Uplift deflection is a failure criterion considered in this research due to the nature of the loading arrangement used for loading position P4. Position P4 acted as a middle edge or a corner load in which the free edge lifted remarkably (see Section 6.4.1). The magnitude of the uplift deflection was not very high during the test but was unsafe to continue with the tests due to the differential deflection between the loaded edge and the free edge of the raft unit. Loading position P4 produced failure by uplift deflection at an early stage of fatigue life without damaging the raft unit, enabling the raft unit to be lifted and reused again after relevelling the bedding sand layer. Table 5.2 shows the uplift deflection of the tested raft units due to loading position P4. For example, the maximum uplift deflections of loading position P4 were 37.4 mm and 32.4 at 23274 ELR and 28331 ELR for the thinner (RS1) and the thicker (RS7) raft units, respectively. Most of the differential deflection occurred in the bedding sand under loading position P4 which contributed potentially for lifting up the free edge of the raft unit.

The differential deflection due to loading position P4 varied and depended on the compaction of the bedding sand layer, the aspect ratio and the thickness of the raft units. The test results showed that uplift deflection is inversely proportional to the aspect ratio and the thickness of the raft units (see Table 5.1). It was quite obvious that as the aspect ratio and thickness of the raft units increased, the self weight of the raft unit increased and, therefore could resist the uplift deflection at the free edges of the raft units.

The fatigue life of loading position P4 for the raft units tested was low compared with the other loading positions (see Table 5.2). The fatigue life of position P4 could be improved by designing an edge beam or retaining strips around the pavement system to allow this position to act in a similar way to loading position P2, increasing the strength of the bedding sand and by a physical connection at the joints.

6.7 Summary of Chapter

(i) The sequential movement of the applied loads changed the principal bending moment directions and caused a double curvature bending in both directions along the main longitudinal and transverse centreline of the raft units. The double bending increased as the plan dimensions (i.e. aspect ratio) of the raft units increased and thus, the induced strains increased and the induced deflection decreased for any of the loading positions.

(ii) The induced strains were increased and the induced deflections were decreased as the aspect ratio of the raft units increased. These changes reduced remarkably for

remote sections away from the tracking load. The changes can be expected to cease when the raft unit rigidity and side length are increased beyond 3 m, and become insignificant.

(iii) The percentage of shear transfer between adjacent raft units varied and depended on the differential deflection at the joint interface (i.e. at loading position P2). Therefore, the applied load at position P2 has not been shared equally between the adjacent raft unit as suggested by the design method proposed by Bull (1986). The one-hundred per cent shear transfer means the deflections along the joint are equal and hence the applied load shared equally.

(iv) Clearly from the literature review (see Chapter 3), the design method proposed by Bull (1986) did not predict the uplift deflection criteria. The uplift deflection resulting from this research could be considered as a maintenance criteria for loading position P4. It has been suggested that the uplift criteria should be constrained on site by different means such as constructing an edge beam or retaining strips around the paremant system.

(v) The combination of increasing the steel fabric reinforcement and the thickness of the raft units improved their flexural rigidity and shearing strength and hence increased their resistance to the double bending curvature. The test results confirmed the thickness design principle of the concrete pavement for achieving the required fatigue life performance with appropriate design properties for the steel reinforcement and the thickness of the raft units. Also, they have shown that a significant reduction in the thickness can be achieved without violating the required life performance of the raft units. Therefore, such design made the use of raft unit pavement more practical and hence, proved some of its advantages (see Section 1.1).

(vi) The use of steel fabric reinforcement demonstrated a superior post-cracking performance particularly for high loading conditions, over the steel fibre reinforcement. Thus, it would appear that there was an advantage in using steel fabric rather than the steel fibre reinforcement. In view of this advantage, the steel fabric reinforcement should be designed in the top and bottom of the raft unit and uniformly spaced.

(vii) The combination of increasing the number of steel fabric reinforcement bars and the raft unit thickness improved the performance and increased the life expectancy of the raft unit.

Chapter - Seven

THE FATIGUE LIFE OF RAFT UNITS: METHOD OF PREDICTION

7.1 INTRODUCTION

Fatigue means that failure occurs as a result of the repeated applications of strain below the level which causes rupture in a single application. Traffic and temperature changes can cause material fatigue, leading to cracking at stresses which are lower than the static strength. When concrete is subjected to tensile stress of around 50 per cent of the static failure stress, the initial stress-strain relationship becomes non-linear.

Fatigue performance is usually expressed in terms of the endurance curve, which is known as the S-N curve. This curve is a relationship between the mean value of the number of cycles to failure under a particular loading condition (N) and the stress level induced by the applied loads (S). The stress level can be expressed as a range of stress or as a stress ratio between the fatigue failure stress and the failure stress due to static load.

Pavement fatigue can be considered to be a damage factor, which can be used as a design criterion for a concrete pavement. The damage generally results from an accumulation of structural damage caused by the passage of vehicles. For this reason the cumulative traffic carried by a certain type of pavement is important in determining its present condition and its life expectancy. In addition to the behaviour of the pavement material, the fatigue life of the pavement is controlled also by the foundation on which the pavement rests. Cracking of the pavement arises from repeated tensile strain and propagates as the number of load cycles increases. This increase causes a gradual weakening of the pavement structure.

This Chapter focuses on the prediction of the fatigue life of raft units. It shows how the number of load repetitions can be related to the dimensions and reinforcement of raft units; and also to the strain induced within the raft unit due to an applied load. Thus, fatigue equations have been derived in the following sections. Other design restrictions that can be placed on pavement loading, such as, a combination of wheel loads, loss of sub-grade support and environmental conditions, can be related to a specified design life. Therefore, the most realistic way to control the fatigue life and distress of raft unit pavements is through the use of such a prediction fatigue model.

Until the early 1980's there was no method available for the design of raft unit pavements. In response to this need a Finite Element analysis and a laboratory test programme were initiated at the University of Newcastle Upon Tyne, to develop design procedures for raft units [see Chapter 3]. In Chapter 3, the attempts by Bull (1986), Ismail (1990), and Salmo (1990) to predict fatigue life were described. The limitations of Bull's method are discussed below in Section 7.5. On the other hand, Ismail (1990) has developed and refined analytically the Bull method, using a more accurate element in the Finite Element Method and then following a similar way to the Bull method. The fatigue relationship developed by Salmo (1990) was limited to the use of raft units in port areas and the number of load applications applied to the test raft units were very low compared to the number of load applications applied to the raft units tested during the experimental programme which provided the base data for this thesis.

The experimental results discussed in chapters 5 and 6 were used in the following sections to develop a fatigue model. In Section 4.7, it was made clear that a compensating factor had to be applied to the fatigue life results to allow for the relatively small contact area used in the test compared to the size of the contact area of a real Boeing 727-200. A compensation factor of 5.6 was used (see Section 4.7).

7.2 PREDICTION OF THE ULTIMATE LOAD CAPACITY OF RAFT UNITS

All the raft units tested, apart from RS7 at loading positions P1, P2, and P3, failed in either punching shear, fatigue fracture or uplift deflection. RS7 and RS1 of Module M3 were identical apart from their thickness, RS7 is 175mm thick, and RS1 is 140mm thick. Raft RS7 did not fail and the test was stopped due to time constraints [see Chapters 5 and 6]. Therefore, the ultimate load capacity of RS7 could be predicted using the results of the failed raft unit RS1. Along with the predicted ultimate capacity of RS7, calculation of the punching shear for the other raft units is presented and discussed below.

7.2.1 Flexural Failure

The bending moment of a structure (i.e. raft unit) is a function of its Young's modulus, and therefore, the structural capacity in bending is dependent on the square of its depth. For RS7 and RS1 which have the same section properties apart from their thickness, the ultimate load capacity of RS1 was reached when the test load was 600kN and 700kN at loading positions P1 and P3, respectively. Then, the predicted ultimate load capacity of RS7 was equal to $600\times\left(\frac{175}{140}\right)^2 = 937.5$kN. If the ultimate load capacity of RS1 at loading

position P3 was considered, then the predicted ultimate load capacity of RS7 was equal to 1093.75kN.

The loading position P1 of RS1 performed a low fatigue life compared with its counterpart position P3, that could be related to a poor casting of the raft unit [see Section 5.5]. With the exception of loading position P1 of RS1, the fatigue life achieved (72,296 repetitions) for RS1 at loading position P3 due to load capacity of 700kN, can be predicted for RS7 at the higher load capacity of 1093.75kN. In other words, if a load of just 700kN was applied to RS7 and RS1, RS7 would offer a longer fatigue life than RS1, before complete failure occurred.

7.2.2 Punching Shear Failure

A heavy load applied to a slab or a footing within a specified loaded area may cause a shear failure by punching or punching out part of the effected shear area (i.e. punched zone) [see Fig. 7.7]. The shape of the shear failure surface depends on the loaded area, rectangular loaded areas tend to create pyramid shaped failure surfaces, whereas circular loaded areas cause conical failure surfaces (Nilson and Winter, 1979).

There were many different methods available for dealing with punching shear (Nilson and Winter, 1979; Hulse and Mosley, 1986; Hughes 1980; and Kong and Evans, 1987). The method of calculation of the critical parameter varied among these methods. Some assumed that the critical shear area was one and a half times the effective depth (1.5 d_e) of the slab, (Hulse and Mosley, 1986), others assumed it was half the effective depth $\left(\frac{d_e}{2}\right)$ of the slab (Nilson and Winter, 1979).

Raft units that were supported by a multilayer structure underneath do not really act as a simply supported slab, but it can be assumed that the general principles for the shear strength of beams can be applied to slabs. In the test rig, the localised support due to the bedding sand was pressurised by the shear area core at the base of the raft unit; the sand support would be unable to resist the applied load and would allow the concrete core to act as a simply supported slab, but with some support which would depend on the strength of the base layer. Since the punching shear criterion is not the main objective to investigate, and most of the shear design methods give similar results, the formulae of Nilson and Winter (1979) were used for the punching shear calculations. Punching shear calculations were carried out for the failure case for different failure loads and for the no-failure case for RS7 as well as for the effect of using small size contact area 200mm×200mm in the laboratory instead of using the real contact area of

400mm×400mm, on the failure mechanism of punching shear. Punching shear failure for RS7 could be predicted using the failure load of the similar raft unit, RS1. Also the mechanism of punching shear failure using the real contact area could be predicted by relating it to the laboratory punching shear failure loads. The main principles of shear stress were used, with the punching shear area subjected to a heavy load, (Salmo, 1990).

(i) NO FAILURE CASE

(a) Raft Unit RS1 - Module M3

ultimate pressure (P_u) = $\frac{W_a \times 10^3}{2000 \times 2000} = \frac{W_a}{4000}$

where,
W_a = ultimate load causing punching shear failure (kN).

Area outside punched zone = $2000 \times 2000 - (200 + 2h \cot \alpha)^2$

where,

α = angle of load dispersion = 45 [see Fig. 7.7]

h = thickness of raft unit in mm. = 140mm.

Punching shear stress,

$$\upsilon = \frac{W_a}{4000} \times \frac{2000^2 - (200 + 2h\cot\alpha)^2}{4 \times (200 + 2h\cot\alpha)h} \tag{7.3}$$

$$\upsilon = 0.003506 W_a \tag{7.4}$$

(b) Raft Unit RS7 - Module M3

Using the same procedure for raft unit thickness of 175mm,

$$\upsilon = \frac{W_b}{4000} \times \frac{2000^2 - (200 + 2h\cot\alpha)^2}{4 \times (200 + 2h\cot\alpha)h}$$

where, W_b = ultimate load capacity causing punching shear failure for raft RS7.

$$\upsilon = 0.002401 W_b \tag{7.5}$$

Equating equations 7.4 and 7.5 for the punching shear stress of raft units RS1 and RS7, gives:

$$\frac{W_b}{W_a} = \frac{0.003506}{0.002401} = 1.460225$$

where the failure wheel load of RS1 (W_a) was 350kN

Therefore the ultimate wheel load capacity of RS7 (W_b) will be 511kN (i.e. the axial load is 1022kN).

The ultimate load capacity of RS7 in punching shear was very close to that obtained for the flexural failure criterion, which was in a range between 937.5 and 1093.75kN. Therefore, with the exception of loading position P1 of RS1 which offered a low fatigue life due to the poor casting of the raft unit, it can be expected that the ultimate load capacity obtained for the punching shear criterion, would maintain a similar fatigue life to that of the flexural failure criteria [see Section 7.2.1].

The same principles for calculating the punching shear stress were used with real contact area. Punching shear stresses v are:

- The laboratory contact area 200mm×200mm and h = 140mm

$$v_{Lab} = 0.003506 W_a$$

- The real contact area 400mm×400mm and h = 140mm

$$v_{Real} = 0.0023225 W_a$$

$$\therefore \quad v_{Lab} = 1.51\ v_{Real} \text{ (i.e. } v_{Lab} > v_{Real})$$

(ii) FAILURE CASE

Punching shear failure occurred at different loading positions apart from loading position P4 throughout the test programme. The failure load for punching shear failure was always 700kN, except for loading position P2 for RS2 which was 450kN [see Table 5.2]. Punching shear calculations for the two different failure loads are shown below:

(a) Failure Load of 700kN

wheel load = $\frac{700}{2}$ = 350kN

Loaded area = 0.2 × 0.2 m

L_y, L_x = 2.0 × 2.0 m

Raft thickness, h = 140mm, effective depth = d_e = 100mm

Concrete strength = 65 MPa

Ultimate pressure = $P_u = \frac{W}{L_x L_y} = \frac{350}{2 \times 2} = 87.5 \text{kN/m}^2$

Shear force acting on the critical section is,

$$V_u = P_u\left(L_x L_y - \left(a \times b + \frac{\pi \times d_e^2}{4}\right)\right)$$

$$= 87.5 \times \left(2 \times 2 - \left(0.2 \times 0.2 + \frac{\pi \times 0.1^2}{4}\right)\right) = 345.8\text{kN}$$

Shear strength of concrete = V_c

$$V_c = \frac{(\sqrt{f_{cu}} \times b \times d_e)}{3}$$

where, b = critical perimeter = $2a + 2b + \pi \times d_e$ = 1.114m

$$V_c = \frac{(\sqrt{65} \times 1.114 \times 0.1)}{3} = 299.38\text{kN}$$

Using the strength reduction factor for shear (ϕ) = 0.85

$$\phi V_c = 0.85 \times 299.38 = 254.47\text{kN}$$

$$V_u = 345.7 > \phi V_c = 254.47$$

Therefore, punching shear occurs in the tests.

(b) Failure Load of 450KN

wheel load = $\frac{450}{2}$ = 225kN

Following the same procedures as paragraph a) above with new failure wheel load of 225kN:

$$V_u = 222.3\text{kN}$$

$$\phi V_c = 254.47$$

Therefore,

$$V_u < \phi V_c$$

Therefore, no punching shear would occur which is different to the test results.

(iii) Punching Shear for the Real Contact Area

A rupture surface which generally has a curved generatix, is often claimed to take place when the tensile strength of concrete is reached. This contradicts the test observations, where the punching shear cracks appeared around the loaded areas at the late stage of the test i.e. beyond the flexural state of the concrete. The experimental results showed that despite serious concrete cracks, the raft units continued to sustain the applied loads up to the load repetitions given in Table 7.1. The punching shear failure was not a phenomenon of chance, but it has a definite mechanical cause which was dependent on the applied loads, the applied load repetitions, and the loaded contact area.

Following the same procedures as Section (ii) above, the punching shear calculations for the real contact area subjected to failure wheel loads used in Section (ii) are:

a) Wheel load = 700/2 = 350kN

Loaded area = 0.4m ◈ 0.4m

The ultimate pressure = P_u = 87.5kN/m^2

The shear force acting on the critical section is

$$V_u = 335.32\text{kN}$$

The shear strength = ϕV_c = 437.3kN

$$\therefore \qquad V_u < \phi V_c$$

Therefore, no punching shear would occur.

b) Wheel load = 450/2 = 225kN

Loaded area = 0.4m ◈ 0.4m

The shear force = V_u = 215.56kN

The shear strength = ϕV_c = 437.3kN

$$\therefore \qquad V_u < \phi V_c$$

Therefore, no punching shear would occur.

By using the real contact area, the predicted failure mode due to just the applied wheel load was not punching shear. In other words, with the real contact area, the shear strength (ϕV_c) was always higher than the shear force (V_u) acting on a critical section. The critical section of the real contact area was larger than that of the laboratory contact area and therefore, the shear strength was higher. Thus, the shear stresses had to be distributed over the larger critical section which denied the punching shear failure to occur due to just the applied wheel load. However, in some cases during the tests, punching shear failure occurred with the laboratory contact area.

Despite this difference and the differences in shear stresses, the punching shear failure would occur with the real contact area as was the case with the laboratory contact area, due to not only the applied wheel load but also due to the real applied load repetitions. The real applied load repetitions were obtained by relating the damaging effect of the laboratory contact area to the real contact area using the concept of pavement damage [see Section 4.7]. This argument can be supported by the test observations as the induced strains increased by increasing the applied wheel loads and the number of load repetitions [see Figures 5.3, 5.4, 5.11, 6.6, and 6.7].

For instance, in Case (ii, b) and (iii), the predicted failure mode due to the applied wheel load of 225kN and using the real contact area, was not punching shear. However, the predicted failure mode was different from that of the test result, which failed by punching shear. This can be related to the process of the fatigue mechanism in the raft units which produced progressive, permanent, internal, structural damage within the raft units due to the repetitive stresses; also there was the progressive growth of cracks, particularly shear cracks, and the fracture of steel bars and concrete which resulted eventually from the applied load repetitions and the range of cycling stress. Therefore, the cause of the actual punching shear failure which occurred during the test, was due to a combination of the effects of the applied load and the load repetitions.

7.3 Loading position P4 as a design criterion

Once the raft unit paving system is built, the most direct structural response is the deflection or vertical displacement of the raft units due to the moving load. With reference to the three modules M1, M2, and M3, the loading position P4 always failed by uplift deflection apart from raft unit RSF in module M2 [see Section 5.4 and 6.4}.

Uplift deflection is a failure criterion considered in this research due to the nature of the loading arrangement used for loading position P4. Loading position P4 acted as a middle edge or a corner load in which the free edge lifted remarkably [see Section 6.4.1]. The magnitude of the uplifted deflection was not very high during the test but was unsafe to continue with the tests due to the differential deflection between the loaded edge and the free edge of the raft unit. Loading position P4 produced failure by uplift deflection at an early stage of the fatigue life without damaging the raft unit, enabling the raft unit to be lifted and reused again after re-levelling the bedding sand layer.

Loading position P4 was abandoned due to reasons given in chapter 5 and 6. This meant that the loading conditions applied at position P4 produced the shortest fatigue life and it was found that it would be unsafe to carry on the test at that loading position. It was demonstrated by Ismail(1990) that the effects of including joint filler material in improving the performance of the raft units, and the contribution this would make to the lateral distribution of loading. Also, it was clear that proper boundary constraints would improve the performance of the edge and corner of the raft units. For these reasons, it was felt that the results from loading position P4 could be considered as the subject for further research.

In airfields, the uplift deflection causes pumping. The term pumping is usually associated with the movements of infiltrated rainwater that can saturated the base material and the raft unit / base interface. Due to the action of the wheel loads at loading position P4, the interface cab be open due to the uplift deflection, at the free edge of raft units. Therefore one of the essential condition that prevent pumping is the sealing of joint and crack discontinuities with flexible mastic or inorganic compounds such as silicon, polysulphide, polyurethane, and PAVESEAL. Also, a good drainage system is required. As the laying of the raft units proceeds, the joints should be filled using treated sand or alternatively, using some of the elastic material stated above. It is essential that the joints is to minimise the loss of joint material and pumping as well as to resist the shear deformation at the joints.

For design purpose of the loading position P4, the edges of the raft unit paving system should be designed with an edge beam or retaining strip to prevent the sliding of the raft units under dynamic loading (i.e. traffic movement). The joint between the edges of the raft unit paving system and retaining strip or the beam should be treated in a similar way as that of the interior joints discussed earlier. This design considerations allow loading position P4 to behave in a similar way to loading position P2, and thus improve the

performance of the paving system. Other major consideration in raft unit design is the load transfer devices between raft units and at the interface between raft units and the surrounding structure (e.g. Edge beam) to the paving system. Therefore, it should be investigated thoroughly to assess its effect on fatigue life and cost. For this reason, it was felt that loading position P4 should be considered as the subject for further research.

7.4 DEVELOPMENT OF THE STRAIN FATIGUE RELATIONSHIP

7.4.1 Strain Fatigue Characteristics

The principal criteria for most approaches to the structural design of rigid pavements is based on considerations of either tensile stress or tensile strain in the pavement slab. Therefore, the thickness of raft units should be designed so as to keep this strain within certain limits. These limits would be set by either the ultimate tensile strength of the concrete material in bending (MR), as this represents the serviceability limit state, or the maximum tensile strain corresponding to the anticipated design load which would represent the ultimate limit state. When repetitive loading exceeds the tensile strength of the concrete, a crack starts to develop in the pavement slab even though the raft unit continues to function in service. The cyclical life of a pavement slab increases with decreasing strain levels, and with a very low strain level, it seems to posses infinite life; that is fatigue failure does not occur.

The strain level may be either expressed as a strain amplitude or, more usually, as a strain ratio; that is the ratio of the minimum strain to the maximum strain. For this analysis and for the graphical representation of the cyclical strain parameters, the strain ratio concept has been adopted. The maximum strain is assumed to be the strain that corresponds to the anticipated design load assumed for the paving system and the minimum strain is the strain in the raft unit caused by different traffic loads. The result of fatigue loading is to over stress the concrete raft unit and to cause fracture. For this research, the design load was chosen to be 450kN which was the same as that expected in practice [see Section 4.6].

Three stages have been found in the fatigue life of a precast concrete raft unit [see Sections 5.5, and 6.5], as follows:

(i.) crack initiation;

(ii.) crack propagation; and

(iii.) fatigue fracture.

The second stage begins with slow crack growth which is followed by steady crack growth leading to eventual fatigue fracture.

This research has confirmed the work carried out by Salmo (1990), that is tensile strain can occur at either the top or bottom of the raft units depending on the loading conditions. Relationships have been developed between tensile strain and the number of load repetitions for raft units up to both the serviceability limit state, where the raft unit requires maintenance, and the ultimate limit state, where the raft unit requires replacement. At the serviceability limit state, a raft unit pavement may exhibit fine cracks yet still continue to sustain heavy loads and perform its function.

The analyses of strain measurements discussed in chapters 5 and 6 have brought to light several important features of the structural behaviour of the raft units. It was found, for example, that at the early stage of loading for a given raft unit and given loading conditions, the strain varied linearly with the applied loads, and increased with an increasing aspect ratio.

In previous sections 7.6 and 7.7, the analyses of fatigue life has been related empirically to the plan dimensions, the thickness, and the reinforcement of the raft units and their loading conditions. Using the same basis, an attempt was undertaken to relate the raft unit performance directly to the maximum induced strain. Thus, a relationship could be derived between the maximum strain under moving loads and the number of load repetitions to failure.

In this section the analysis has been extended to establish the relationship between the predicted number of load repetitions and the induced tensile strain in the raft unit. The raft unit fatigue life has been related directly to the strain ratio (R). It has been concluded that the critical strains are generally under the outer loaded area for loading positions P1 and P3 [see Chapters 5 and 6]. Therefore, the measured strains at various stages of loading with an increasing number of load repetitions at positions P1 and P3 were used to establish the relationship. The equivalent number of load repetitions "N" to failure was calculated by relating the lower applied loads to the maximum applied load and the damaging effect of the laboratory contact area to the real contact area using the formulae proposed by Heukelom and Klomp (1978) [see Section 4.7 and 5.5], and then related the result to the strain ratio.

It was noted that, generally, there was a difference in strain measurements between the thinner raft unit (RS1) and the thicker raft unit (RS7). The probable explanation for this

lies in a greater susceptibility of the thinner raft units toward partial loss of the support from the sand layer due to the raft unit warping resulting from the applied loads, and the effect of the thickness on the behaviour of raft units. Also, it was noted that the induced strains in the thinner raft units were much more sensitive to variations of the loading positions in the transverse direction, due to the crack patterns that developed during the loading stage [see Section 6.3]. As discussed earlier in chapters 5 and 6, the development of strain was a function of the distance from the loaded area. This observation could be seen very clearly during the tests as the first cracks appeared around and under the loaded areas particularly around the outer loaded areas where, the highest strains occurred. It appeared that the edge strains that were measured around the outer loaded areas recorded the maximum strains that were induced due to loading and the number of load repetitions. However, in developing the fatigue relationships [see Figs. 7.8 to 7.10], the induced strains at remote distances from the outer loaded areas when the load was applied at the middle edge of the raft units, were excluded from consideration relying instead on the induced edge strains around the outer loaded areas.

The relationships between the strain ratios for each of the load increments in each test, and the equivalent number of load repetitions can be found in figures 7.8 to 7.10. The relationship between the strain ratio "R" and the predicted number of load repetitions was obtained for all the test raft units through the multiplicative regression analysis. The equation of the relationships has the following form:

$$N = CR^t \tag{7.6}$$

where,

N = the predicted number of load repetitions,

R = strain ratio = $\frac{El}{Edl}$ = greater or less than 1.0,

$E\,l$= maximum induced tensile strain for a particular applied load,

Edl = maximum tensile strain corresponding to the design load of 450kN,

C and t = both constants.

The coefficients "C" and "t" are constant for each raft unit and for a general relationship for each module, and were determined by regression analysis (i.e. the best fit curve).

Design curves have been presented relating the fatigue life of the raft units to their strain ratios for different aspect ratios, reinforcement, and thicknesses of raft unit. The strain ratio was controlled by the induced strains at particular load levels which depended on the aspect ratio and thickness of the raft unit.

Also, the induced strain was restrained by the amount and type of steel reinforcement holding the raft unit together. Thus, there was a relationship between the fatigue life ``N" and the aspect ratio, the steel reinforcement, and the thickness of the raft unit. Therefore, equations have been established that are based on the experimentally developed relationships shown in figures 7.8 to 7.10. Using the appropriate curve and equation, the fatigue life "N" can be predicted for the raft unit. The equation of the best fit curve for each test was stated in the relevant figure.

Cracking of the raft unit can occur as a result of repetitive strains smaller than the tensile strength of the concrete. This type of cracking is referred to as concrete fatigue cracking. In the fatigue method, the number of load repetitions "N" to failure was related to the strain ratio "R". The load repetitions that the raft unit could sustain in flexure prior to fracture (i.e. the serviceability limit state) depended on the strain ratio of the applied strain to the flexural strength of the concrete (i.e. Modulus of rupture, MR). Laboratory tests during this research showed that fatigue still has an effect on concrete, even up to 100's of millions of load repetitions to failure (i.e. the ultimate limit state).

The relationships derived are shown in figures 7.8 to 7.10, and were generalised by establishing correlation between the strains measured around the loaded area (i.e. the maximum tensile strain) under moving loads and the raft unit performance. The maximum strains for each load increment and for each raft unit in the three modulus M1, M2, and M3 were plotted in the form of a strain ratio versus the equivalent number of load repetitions for a particular load increment, and thus, a general relationship for each module was derived [see Figs. 7.8 to 7.10]. The general relationships (Eqns. 7.6a to 7.6c) were derived for all the raft units tested, relating the fatigue life "N" to the plan dimensions, the reinforcement, and the thickness of the raft units regardless of the type of loading. The equation of the best fit curve for each module was obtained as follows:

Module M1:

$$N_{eq} = 150\,000R^{-3.3} \qquad (7.6a)$$

Correlation Factor = 84.34 per cent

Module M2:

$$N_{eq} = 200\,000R^{-1.4} \qquad (7.6b)$$

Correlation Factor = 73.45 per cent

Module M3:

$$N_{eq} = 380\,000R^{-2.65} \qquad (7.6c)$$

Correlation Factor = 91.97 per cent

The appropriate combination of these parameters is very important for a good raft unit pavement design, as well as for maintaining a minimum whole life cost including both construction and maintenance costs. In this design procedure, the load repetitions (fatigue life) were related to the strain ratio (R). To design a raft unit pavement system for a required design life using this design procedure, a good combination between these parameters namely, aspect ratio, thickness, and reinforcement of raft units can be achieved. Figures 7.8 to 7.10 are used for design, by entering the required fatigue life and the strain ratio that related to the allowable strains level, until cross the most suitable combination of curves that represent the raft unit design parameters and satisfy most, the required fatigue life.

It must be noted that in equations 7.6a to 7.6c, the induced tensile strain "E_t" due to the applied loading is not now limited to a maximum value equal to the modulus of rupture or to an expected maximum strain due to the design load that was intended for the raft unit pavement. In other words, the strain ratio "R" could be greater or less than 1.0. Based on the experimental results of this research, equations 7.6a to 7.6c should be considered as the fatigue design equation for raft units that will be used for airfield pavement. Also, the fatigue analysis showed that these equations have a physical significance to raft unit pavement. For example, in Equation 7.6c, when R=1.0, the load repetitions "N" to failure for a particular design load = 380,000. In other words, when the strain ratio attains this value corresponding to the design load, the 380,000 load repetitions could cause fatigue failure. Furthermore, instead of using maximum tensile strain corresponding to a required design load, the concrete strength (MR) could be used as a maximum allowable tensile strain, and thus, the number of load repetitions that caused fatigue cracking could be predicted (i.e. the serviceability limit state).

The constant coefficient "C" included in Equations 7.6a, b, and c; and 7.7a, b, and c (below) are different from those proposed by AASHO Road Test 1970, Salmo 1990, and others [see Section 7.4]. They were determined by regression analysis for each test

module and were adjusted in order to maintain closer results to that acquired experimentally for each individual test. The adjustment process in all the equations was within a range of ±3 per cent.

This significant finding confirmed the soundness of a rational, mechanistic approach to the design of raft units. Furthermore, it confirmed the results discussed in chapters 5 and 6, and demonstrated clearly that failure in raft unit performance was not a phenomenon of chance but a phenomenon which has a definite mechanical cause. Moreover, it becomes possible to predict the potential life of raft unit pavements subjected to traffic having different wheel configuration. Thus, the empirical findings presented in this Section have a potentially great practical importance.

7.4.2 Raft Unit Pavement Management

7.4.2.1 Introduction

Historically, pavement engineers have used various techniques to evaluate in-situ pavements during their operational phase. Generally, these techniques can be divided into two basic types of procedures namely, structural evaluation and the performance or condition surveys (i.e. function performance). The major objective of a structural evaluation of an airport pavement is to obtain specific quantitative measures of relevant insitu structural properties of the paving system. In contrast, performance surveys have as their main objective the monitoring of the degree of deterioration of a paving system (such as rideability) at a specific time. To be effective, routine condition surveys should include both structural and functional measurements. The variables to be measured are directly dependent on the design model being used. These principles are also applicable to a raft unit pavement.

For an airport raft unit paving system, structural evaluation and performance surveys are important because they provide the following input data:

(i.) the determination of the rideability of the system by measuring the differential deflection between the adjacent raft units;

(ii.) the estimation of the remaining life of the system at any specified time together with an estimate of the air traffic flow during the life of the paving system; and

(iii.) to assess the strength of an existing system when strengthening (e.g. replacing the damaged raft units) programmes or future overlay requirements were being considered.

7.4.2.2 Performance Evaluation

To assist the engineer in deciding what to do and when to perform pavement maintenance and/or rehabilitation, the performance of a raft unit pavement should be measured on a systematic and continuing basis. In the performance evaluation both functional and structural performance of the pavement system should be considered. The functional performance describes how well the raft unit pavement serves the operator while the structural performance is related to its ability to sustain traffic loads which in turn influences the capacity of the raft unit pavement to serve the operator. The definition of structural distress and functional performance vary and depend on the type of aircraft (i.e. the size of the wheel configuration and tyres), and the facilities (i.e. taxiway or apron) being considered.

It is appropriate to consider two phases in the performance evaluation process. The first is termed network monitoring and the second phase is detailed investigations. In the first phase, condition surveys provide a basis for segregating those raft units which clearly do not require maintenance from those that may and for which further information is required. In the second phase detailed investigations provide the data required to determine an appropriate strategy for maintenance which include measurements of physical conditions such as surface characteristics, structural response, and drainage difficulties. Also, additional information is required such as details of maintenance and construction history, traffic flows and loading, and accident records due to the ground movements within the airfield. The measurement of the structural performance of a raft unit pavement is an attempt to anticipate the remaining life of the raft unit pavement and when maintenance or rehabilitation should be considered so that the functional performance would be maintained at a reasonable and economical level.

It is important to appreciate that the concept of planned airfield pavement maintenance can be achieved only if there exists accepted design criteria and intervention levels, and if the airfield network is monitored regularly to define its physical condition and to obtain measurements that can be used both to describe the existing state of the raft unit pavement condition and to predict the rate of deterioration.

The procedures being used these days to perform a pavement evaluation include destructive and non-destructive testing. The destructive testing comprises two phases; field and laboratory testing. The non-destructive testing is carried out in the field with minimum disturbance. Non-destructive pavement test devices have been developed. Their procedures provide the advantages of rapid evaluation for a paving system with minimum disturbance to normal traffic operations. There are a number of devices

available to measure the response of the pavement to loads. Measurement devices in current use include the Benkelman beam, Deflectograph, Falling Weight Deflectometers and others being used in different countries. Using suitable analysis, the magnitude of stresses or strains generated in raft unit pavement and the deformation behaviour of the supporting layers are measured and direct correlation between these parameters and the performance is investigated using an appropriate technique.

The proposed procedure for raft unit pavement evaluation has been summarised briefly below.

(i.) Deflection measurements would be made at the edges, corners, and centres of the raft units along the pavement length, both in and between the wheel tracks as well as at the joint interfaces. Also, the differential deflection between the loaded end of a raft unit and the free edge of the raft units, should be measured. From the measurements and type of traffic (i.e. heavy or light aircraft), engineers can then decide whether the raft unit in question needs replacement, or the sand layer needs relevelling. The type of traffic identifies the maximum accepted level of deflection (e.g. for heavy wheel traffic at low speed areas, deflection of 40mm would be an accepted level).

(ii.) Unless the raft unit was badly damaged (e.g. widely cracked); the design life of the raft unit could be estimated. With cracked raft unit pavements, strain measurements should be made in the undamaged raft units, e.g. between the wheel track, to permit an estimate of the remaining life from Equations 7.6 and 7.7. The remaining life would be predicted by comparing the actual number of load repetitions experienced by the raft unit pavement to the allowable (design) number of load repetitions.

(iii.) In some cases engineers would recommend an overlay when two separate thickness designs should be made. The first, an overlay thickness to satisfy the sub-grade strain criteria. The second, an overlay thickness to satisfy the criteria of the fatigue strain of the raft unit taking into account the life already used by the traffic to date.

7.4.2.3 Development of the Performance Model

Based on Equation 7.6, a second fatigue relationship between the strain ratios and the accumulated number of load repetitions (N_{acc}) has been developed for each test in the three Modules M1, M2, and M3 [see Section 4.2]. The accumulated number of load

repetitions represented the equivalent number of load repetitions applied to the test raft units at each load increment [see Section 4.6], which were converted to the equivalent design load of 450kN. The accumulated number of load repetitions meant the summation of all load repetitions applied for each load increment including the failure load, after they had been converted to the required standard design load. The equations and design curves have been established by relating the accumulated load repetitions to the strain ratio, on the assumption that these load repetitions would produce the same deformation as that produced by a particular loading condition [see Figures 7.11 to 7.13]. This relationship would enable at any stage in the life of a raft unit paving system the prediction of the remaining life of the raft units before complete failure would occur. This would improve the management of such a paving system where the raft units were used, and would be more cost effective for the operator. The equation of the relationship has a similar form and the same assumptions to that of Equation 7.6, using the accumulated number of load repetitions (N_{acc}) to represent the predicted number of load repetitions for a particular design load. The general form of the equation was:

$$N_{acc} = CR^t \qquad (7.7)$$

where:

N_{acc} = The accumulated number of load repetitions.

R, C, and t = as Equation 7.6.

The derived fatigue relationships (Eqn. 7.7) could be used to calculate the remaining life of a raft unit paving system. To predict the critical load associated with cracking (fatigue life) in raft unit pavements, the relationship could be utilised using the strain induced by the wheel loads and the maximum allowable strain. Maintenance charts have been presented relating the accumulated load repetitions of a particular design load to strain ratios caused by traffic loads, for different aspect ratios, reinforcement, and thicknesses of raft unit [see Figures 7.11 to 7.13]. The equation of the best fit curve for each test was stated in the relevant figure. Similar general relationships derived for the design fatigue life of raft units [see Section 7.4.1], were generated for the maintenance charts (Eqns 7.7a to 7.7c). The maximum strains for each load increment and raft unit in the three modules M1, M2, and M3 were plotted in a form of strain ratio versus the accumulated number of load repetitions for a particular load, and thus a general relationship for each module was derived [see Figures 7.11 to 7.13]. The equation of the best fit curve for each module was obtained as follows:

Module M1:

$$N_{acc} = 100\,000R^{4} \qquad (7.7a)$$

Correlation Factor = 89.57 per cent

Module M2:

$$N_{acc} = 100\,000R^{2.15} \qquad (7.7b)$$

Correlation Factor = 71.36 per cent

Module M3:

$$N_{acc} = 50\,000R^{3.6} \qquad (7.7c)$$

Correlation Factor = 95.18 per cent

The constant coefficients "C" are as Equation 7.6 [see Section 7.4.1].

In the maintenance charts, the fatigue life was represented by the accumulated number of load repetitions applied by the standard design load. Using the same results, similar charts could be developed for other loads within the loading range used in this experimental programme. The maintenance charts would be used by using either the strain ratio measured at a certain stage in the life of a raft unit or the number of load repetitions applied, based on the statistical aircraft-traffic data at that stage. Then engineers could readily derive the remaining life of that raft unit pavement. Consequently, it would be necessary to ascertain the maintenance required for the life of the raft unit pavement and establish a maintenance programme. From this programme, schedules could be arranged to minimise disruptions to the aircraft movements in an airfield.

7.4.2.4 Application of the Performance Model

The results of strain fatigue relationships discussed above suggest that the raft unit pavement management system could be accomplished using these relationships as a remaining life approach. In this method the induced tensile strain due to loadings within raft units was used together with the maximum allowable tensile strain of the raft unit. The induced tensile strain was computed using the results of the detailed investigation of the pavement layer properties [see Section 7.4.2.2] and an appropriate method such as Finite Element method. Accordingly, for a required design load and strain level, the

design fatigue life (N_{eq}) and accumulated load repetitions (N_{acc}) were determined from the charts [see Figures 7.14 to 7.16]. Then, the remaining life corresponding to the required design life can be calculated as defined below:

Remaining life for a particular load = $N_{eq} - N_{acc}$

where,
N_{eq} and N_{acc} were as defined above [Eqns 7.6 and 7.7] and must be for the same load that the remaining life was calculated for.

Referring to the charts [see Figures 7.14 to 7.16] for a certain strain ratio ``R" on the abscissa, a line was drawn vertically from the required strain ratio to intersect all curves in the appropriate figure. From each intersection point for a specific design raft unit or for the general design curve (i.e. the general equation) a line is drawn horizontally to the left hand side to intersect with the first ordinate to obtain the design life (N_{eq}) for a particular design raft, and the second ordinate to obtain the consumed life (N_{acc}) related to the same design raft unit. The difference between N_{eq} and N_{acc} was equal to the remaining life of the raft unit pavement for that particular load and strain level.

From a comparison between the remaining life and the design fatigue life a decision can then be made to apply the appropriate remedial measures. This method becomes a performance model to indicate when maintenance or rehabilitation should be performed.

For raft unit paving systems, the differential deflection or edge movements was found to be a major cause for deterioration in rideability which could be directly related to the traffic load, the loading position, the strength of the support layers, and the joint filler material.

A similar process to that used for designing raft units, is applicable to the evaluation of an existing raft unit pavement using the accumulated load repetitions (N_{acc}) at a certain stage of the raft unit life. The procedure can be used to estimate the remaining life of a raft unit pavement under investigation, using the performance model, which in turn, permits the engineer to make a decision relative to the appropriate maintenance strategy to follow.

A general framework, which represents a number of procedures in this performance model, is summarised below.

(i.) The condition of an existing raft unit pavement, including the nature and extent of distress, would be first ascertained. Information of the condition of the existing raft unit pavement should be shown on a large-scale plan of the airfield facilities. This information, together with the deflection measurements, would be used in the sampling and field test phase as well as assisting in establishing sections considered to be uniform for the purposes of analysis.

(ii.) Concrete cores, layer samples, and undisturbed sub-grade samples would be obtained for analysis. Laboratory testing would consist primarily of determining representative stiffnesses and establishing distress criteria where appropriate.

(iii.) The measured values would be compared with their counterpart values resulting from laboratory tests, and these values would be adjusted until predicted and measured values were in reasonable agreement. For example, utilising the laboratory determined stiffnesses, comparison between the estimated deflections under a certain loading and those measured would be made until an acceptable agreement between them was achieved.

(iv.) With detailed traffic data, critical performance parameters such as fatigue fracture and differential deflection, would be determined by suitable analysis techniques and related to the resulted performance determined in the condition surveys as well as to the laboratory results.

(v.) The remaining life in the existing raft unit pavement would be obtained using the performance model as discussed above.

The damaged raft units due to fracture fatigue, edge movements, or differential deflection can be maintained. The structural failure of the raft units is maintained by removing the damaged raft units, and compacting and relevelling the support layers; and then replace them by new raft units. In the case of differential deflection, where the raft units were still able to sustain loads, the raft units can be used again by lifting and relevelling the raft unit pavement. The final surface level of the raft units can be achieved using an appropriate heavy roller.

7.5 PREDICTION OF THE FATIGUE LIFE OF A RAFT UNIT BASED ON THEORETICAL AND EXPERIMENTAL RESULTS

7.5.1 Introduction

As explained in Chapter 3, the major publications that provide guidance on the design of raft units were Bull (1986), British Ports Association (1983), Ackroyd (1985), Bull and Annang (1986), and Ismail (1990). The design procedures for these methods had to be based on theoretical studies and engineering judgement, due to the lack of experimental data which had been conducted specifically on raft units.

In this Chapter, apart from Ackroyd's method, the above four design methods were used to predict the fatigue life of the raft units tested during modules M1, M2, and M3 (see chapter 4). Due to the limitations of Ackroyd's method particularly when compared with the author's experimental model, the method was not included in the calculations but was used only in the discussion for the sake of comparisons. The design charts of the BPA manual were limited when they were used for high levels of the Load Classification Index (LCI) and, therefore, direct calculations for the fatigue life could not be carried out. Instead, the experimental results of the number of cycles "N" were used in the equation (see Appendix C), to obtain the allowable base horizontal tensile strain "E_h". The calculated value of E_h was used with the appropriate chart and the LCI. The corresponding thickness was obtained and compared to the performance of the raft units that had been tested in M1, M2, and M3.

These predicted fatigue lives were then checked and discussed in relation to the experimental results. The author's experimental results were used to verify the original design method by Bull (1986) and recommendations were made to improve the predictions further.

7.5.2 Comparison of the Current Design Methods with the Experimental Results

A general comparison was made in Chapter 3 between the design methods which dealt specifically (apart from the BPA method) with discrete finite sized raft units, in the light of the assumptions made and the method of analysis. These design methods were now used to predict the fatigue life of the raft units that had been tested during the experimental programme.

(i) Design Examples.

In order to compare the design methods with the experimental results, the test model configurations shown and discussed in Chapter 4 were used as worked examples. Table C.1 in Appendix C contains the details of configurations of the test models. The comparison was for the number of load cycles (i.e. fatigue life) the raft units could sustain before replacement was required. The calculation procedures are shown in Appendix C for the design methods. The results obtained from the appendix are shown in Tables 7.1 and 7.2.

The number of load repetitions at a particular load, after taking into account the damage effects of using a small contact area instead of a full size contact area for the design aircraft Boeing 727-200 tyre at a range of load levels [see Section 4.7], was calculated to give the number of load repetitions to failure at that particular load. A relationship developed by Heukelom and Klomp (1978), was used to relate the applied loads to the design load of 450kN. The laboratory number of load repetitions shown in Table 7.1, were calculated using this relationship [see Section 5.5].

(ii) Appraisal of the Prediction Methods.

The design examples shown in Appendix C, Section 7.5.2i, and Tables 7.1 and 7.2, were worked out to compare the design methods with the experimental results in the light of the tested models. Tables 7.1 and 7.2 show the fatigue life of the raft units predicted by the design methods and the actual laboratory load repetitions.

The experimental assessment of the design methods will follow the same manner as chapters 5 and 6. In other words, the assessment will be carried out for modules M1, M2, and M3, which represent the variables of raft unit plan dimensions, reinforcement, and thickness respectively, at different loading positions P1 and P3, P2, and P4. To facilitate the following discussion, the design methods were arranged in a way where each of them could be compared with Bull's original design method, as follows:

(i.) Bull and British Port Association (BPA) methods;

(ii.) Bull and Annang methods; and

(iii.) Bull and Ismail methods.

The Bull design method was the first numerical design method derived specifically for designing raft units. The new versions of the design method were for raft units developed according to the basic assumptions of Bull's original method [Annang, 1986 and Ismail, 1990]. Therefore, the Bull method was used in this discussion as a base maker for comparison with the experimental results.

(a) Bull and BPA Methods:

As explained in the previous Section 7.3.1, it was not possible to calculate the predicted number of load repetition (i.e. fatigue life) using the BPA manual for the tested models. However, raft unit thicknesses were calculated and predicted instead, using the second edition of the manual [see Table 7.2]. The Bull design method predicts the fatigue life of a raft unit pavement at its serviceability limit state which is expressed as the minimum number of load repetitions before the raft units relevelling or some other minor maintenance is required. Also the design calculations of Bull's method were used to determine the maximum and minimum number of load repetitions by assuming one wheel load and two wheel loads on a raft unit at a time, respectively. Therefore, for the sake of this discussion the average of these maximum and minimum load repetitions was considered. The characteristics of the tested raft units and the number of load repetitions obtained for all the tests were used as far as possible for both methods.

Tables 7.1 and 7.2 show the different values obtained using the two design methods. The results showed considerable differences in the fatigue life of the raft units produced by different thicknesses. For all the tests apart from the steel fibre raft unit(RSF), the BPA gave almost the same thickness design at each loading position, that is 300mm, despite the broad differences in the number of test cycles. The thickness design for the steel fibre raft unit was 250mm. The fatigue life of the tested raft units ranged from 77,778 to 1,313,060 load repetitions apart from RSF which was from only 10,578 to 24,018 load repetitions.

RS1 and RS7 were identical raft units apart from their thickness. RS1 was 140mm thick and RS7 was 175mm thick. Using the Bull design method, by increasing the raft unit thickness for RS1 from 140mm to 175mm resulted in an increase in the raft unit fatigue life from 1,616 cycles to 12,236 load repetitions for loading positions P1, P3 and P4, and from 25,848 to 338,684 load repetitions for position P2 (i.e. increasing the raft thickness by 25 per cent produced an increase in the raft unit fatigue life by an average of 10 times that of 140mm thick). Due to the limitations of the charts for the BPA manual, the calculation of raft fatigue life was not possible for the tested raft. The BPA

design method produced a raft thickness of 300mm. for the actual number of load receptions that lay within the broad range of the actual load receptions for all load positions. The number of load receptions obtained by the Bull method were within the range, and were used in the raft thickness calculation. Again the same raft thickness of 300mm was obtained, which eased the comparison between the two methods. Therefore, the raft thickness for the same fatigue life requirement which resulted from the two design method was significantly different; that is 175mm for the Bull method and 300mm for the BPA method.

The fatigue life predicted by the two design methods were very conservative and very much lower than those from the experimental results. The Bull design method predicted the serviceability limit state of the raft units and showed a linear relationship between the number of load receptions and the raft thickness.

The use of the BPADM charts required specific input data and certain combinations of load, CBR and a number of load repetitions that allowed a design to be produced. Using the charts to design the tested raft unit models was not straight forward, due to differences in the parameter levels from that used in the BPA design manual, such as high wheel loads, that is over 200kN, a concrete strength over 50MPa, and a sub-base thickness more than 600mm thick.

A major design consideration was how to interpret the LCI values which were based on the Port Area Wheel Load (PAWL) value. The PAWL concept is very similar to the Equivalent Single Wheel Load (ESWL) concept which has been abandoned for designing raft units (Bull and Salmo, 1987). The LCI value allocated a single letter, "A" for a low load up to "H" or unclassified for heavy load, for a single wheel or multiple wheel load. For raft units the actual wheel loading must be used (Salmo, 1990 and Bull, 1991). The extent of the base tension and sub-grade compression charts were limited particularly for the lower limit of load repetitions of 10^4, as heavy wheel loads of 450kN or more can cause failure at low load repetitions as was the case for RSF (see Table 7.1). The assumption of single wheel loads (PAWL), has been shown to lead erroneously to high raft thickness results.

The BPA design method required an excessive thickness for the raft unit compared to Bull's method and the experimental results. Although, both results for the two methods were well below the fatigue life demonstrated in the experimental results, the above analysis and the following evidence have shown that Bull's method was more acceptable than the BPA method. It was observed that the conservative prediction from the two

methods depended strongly on their original assumptions. The BPA does not allow for variable reinforcement, and different shapes and sizes. It used the principle of the (PAWL) and assumed the load positions to be anywhere on the pavement. These were found to contradict the experimental results. On the other hand, the original Bull method did not allow for contact pressure, reinforcement of less than 314mm^2/m, and a raft unit aspect ratio of less than unity.

Based on the author's observations and the above discussion, it could be concluded that the experimental findings may be used as evidence of certain shortcomings in the BPA design procedure and shows where further research is needed. The results show the advantages of Bull's method over the BPA design method. The following evidence can be drawn:

(i.) the BPA design manual does not consider pavement thickness less than 150mm for a sub-base thickness higher than 600mm and high grade's of LCI(F). With this shortcoming, the advantages of the Bull method increased; also, it was able to predict for load repetitions below the BPA's minimum limit of 10^4 repetitions;

(ii.) for all the experimental and the predicted load repetitions using the Bull method, the tested raft thicknesses were 42 per cent less than those predicted by the BPA method;

(iii.) the BPA method overestimated the raft thickness, and thus, the fatigue life, compared with the experimental results. It does not take into account the influence of load position and the centres of the wheels on the raft unit. The method implicitly applies the equivalent single wheel load concept. Therefore, the use of PAWL is misleading to designers and the actual wheel loading should be used; and

(iv.) the sensitivity analysis has shown that the Bull design method was more acceptable than the BPA method. Although the two methods agreed that reduced concrete strain can be achieved by increasing the raft unit thickness, the BPA method would give a very wide difference in fatigue life compared with Bull's method and the experimental results when using both methods for designing raft unit fatigue life by increasing the raft unit thickness from 140mm to 300mm. The BPA well underestimated the fatigue life of the raft unit corresponding to the 300mm thickness.

(B) Bull and Annang Methods

Work was carried out at the University of Newcastle upon Tyne to investigate the effect of high contact pressure on the design of the raft units, by Annang (1986). This work included a series of repeated loading tests carried out on 2m by 2m square raft units that were 140mm and 200mm thick and tested to the ultimate limit state. The contact areas were 300mm, 450mm, and 600mm in diameter. The loading positions were at the centre and at the centre of one edge of the raft unit. The actual load receptions were related to equivalent load receptions for the maximum applied load, using Equation C.1, Appendix C.

Annang had compared his experimental results with other research and with the fatigue life of the raft unit calculated using the original Bull design method. It was found that a raft unit can carry more load repetitions when it is loaded by large contact areas. The reason behind this could be due to the high stresses concentrated around the edge of the loaded area when high contact pressure was applied.

Table 7.1 shows the fatigue life of the raft units tested using Bull, and the Annang and Bull methods. It shows that there was a considerable difference in fatigue life when contact pressure was considered by Annang. The variation, however, does indicate an inverse relationship between the fatigue life and contact pressure. In other words, the ratio was high when the contact pressure was low and was low when the contact pressure was high.

The Bull design method was developed on the assumption that the maximum applied contact pressure was less than 2MPa. Annang extended the Bull design method from the serviceability limit state to the ultimate limit state and included the effect of the applied contact pressure using the following formula (Annang, 1986 and Bull et. al., 1987).

$$N_{exp} = N_{cal} \times \left[\frac{P}{0.875}\right]^{C} \qquad \textit{(see C.2, Appendix C)}$$

Accordingly a modified formula was introduced (Eqn. 7.2) to determine the load repetitions that a raft unit can carry before the ultimate limit state was reached. A chart was introduced showing the relationship between the constant C and the contact pressure P with a cut-off point at a contact pressure of 2MPa. This chart was then used as an additional parameter to the Bull method. Therefore, the predicted fatigue life of the raft models tested were obtained using Annang's modified formula (see Table 7.1).

$$N_{ult} = N \times \left[\frac{Contact\ Pressure}{0.875}\right]^{C}$$

$$N = \frac{22.5 \times 10^{12}}{(PUSF)^4}\left[\frac{P}{0.875}\right]^{C} \qquad (7.2)$$

where;

N_{ult} = the number of load repetitions to failure.

N = the number of load repetitions to the serviceability limit state.

P = the loaded area contact pressure in MPa.

C = a constant which is a function of P.

The value of 0.875 was the basic tyre contact pressure assumed for Equation (7.2).

Annang's work used the original Bull method procedures for predicting fatigue life and added a further parameter for the effect of the contact pressure on the design of the raft units. Therefore, any differences in the predicted fatigue life of the raft unit using the two methods would only be due to the applied contact pressure. However, the following discussion would be concentrated on the effect of the new parameter.

The results obtained using the modified formulae gave a better prediction of the load repetitions up to the ultimate limit state than the original Bull method for the tested raft units. Bull's design method underestimated the number of load repetitions and showed that using the serviceability limit criterion, the raft units would be only serviceable for these lower number of load repetitions. This contradiction between the original Bull method and Annang's modified formulae gave the latter an advantage over the former by producing more acceptable results and showed that by including the contact pressure parameter in the Bull design method a result closer to the experimental result could be achieved. Comparing the predicted fatigue life using Annang's modified formulae and the experimental results, it was found that Annang's formulae underestimated the load repetitions of the raft units for all the applied contact pressure [see Table 7.1]. However, the difference between the experimental and the predicted fatigue life was reduced slightly by including the contact pressure in the original Bull's method (Annang's formulae), and provided a more acceptable prediction.

Based on the experimental results and the above discussion, the author concluded that other variables such as different types and amounts of reinforcement, contact area and pressure, different aspect ratios, should be included and investigated analytically and

experimentally in the original Bull design method. The inclusion of such parameters in the design method would increase the accuracy and the reliability of the design method. Additionally, by using the experimental results, any discrepancies that may occur in the assumptions of the design method would be compensated.

(c) Bull and Ismail Methods

Ismail (1990) has developed and refined Bull's design method by using a more accurate finite element programme, type 37110 in PAFEC, with more degrees of freedom involved and by including the effect of contact area or pressure as a new variable to the design procedures. Ismail's design method adopted procedures that were the same as that of Bull's design method except that the contact area or contact pressures were introduced. Comparing the predicted fatigue life results using the two design methods, has shown that a much higher number of load repetitions were predicted by Ismail's method than those from the Bull method, which could be due to the effect of using element 37110 and including the contact area in the design. The difference between the two methods widened when the thickness of the raft unit increased from 140mm to 175mm for RS1 and RS7 respectively [see Table 7.1]. Apart from the differences due to using a concrete grade that was higher than the basic model of 50N/mm^2, the variation in the design results caused by the alteration in the design parameters between the two elements were similar and thus showed that the behaviour of element 37100 was acceptable.

Reducing the raft unit thickness would increase the stresses in both the concrete raft unit and the sub-grade while increasing the raft unit thickness would reduce both these stresses i.e. would give a better fatigue life. Using the Bull and Ismail methods, it was shown that the fatigue life of RS1 could be increased by 13 times and 7.53 times respectively when the raft unit thickness was increased from 140mm to 175mm (i.e. RS7), [see Table 7.1]. In other words, Ismail's method gave a number of load repetitions higher and closer to the experimental results than those obtained by Bull's method. However, due to this increase in the raft unit thickness the experimental results for the thicker raft RS7 were only twice as high as those for the thinner raft RS1 when it was 140mm thick. Thus, the accuracy level of Ismail's method compared to Bull's method enables a better prediction to be made for the fatigue life of raft units.

An increase in the Young's modulus of the concrete (i.e. concrete strength), would increase the stresses within the concrete raft unit and reduce the stresses within the sub-grade. There were wide differences between the results obtained using the design

methods due to the alternative percentage in PUS and SGBP for concrete grades higher than that used in the basic model of 50N/mm^2. For instance, a reduction in the alternative percentage in PUS from 8.626 per cent in Bull's method to 4 per cent in Ismail's method resulted in an average increase in load repetitions of 12 times higher for loading positions P2 and P4, and 16 times higher for positions P1 and P3, when compared to those obtained by the Bull method. These wide differences do suggest that the variation in PUS and SGBP due to changes in concrete grades in Ismail's method which were higher than that used in the basic model, should be checked again carefully. This could be supported by the wide deviation between the experimental results and those obtained by Ismail's method [see Table 7.1]. Also it could be confirmed by the results obtained by Annang's work which included the original Bull's method and the effect of contact pressure on the fatigue life of raft units. The work of both Annang and Ismail included the effect of contact pressure on fatigue life, but Annang's results were found to move closer towards the experimental results.

The variation in the value of the PUS and SGBP induced by varying the size of the raft units were mainly for square-size raft units in both methods. However, there was an inverse relationship between the size of the square raft units and PUS and SGBP stresses. Comparing the fatigue life predicted by Ismail's method and the experimental results, it was found that Ismail's method overestimated the load repetitions for square, and rectangular raft units at loading position P2 only; and underestimated the load repetitions for both sizes at loading position P1 and P3.

These broad differences in the predicted fatigue life using the two methods and the experimental results suggest that the loading position of a single wheel or multi-wheels affects the maximum stresses and deflections. The total load should be used whether it is on a single or multi-wheel. Therefore, the twin wheel loads at loading position P2 should not be divided between the two raft units. By dividing the applied load at loading position P2 between the two adjacent raft units, the behaviour of loading position P2 was assumed implicitly to be the same as that for loading position P4, which was not the case during the test. This argument was supported by the experimental evidence which showed the wide differences in the fatigue life between the experimental results and the predicted results particularly when the effect of contact pressure was included [see Table 7.1]. Loading position P2 was a new position introduced by the author and has its own characteristics. Thus, if the wheel moves about the raft unit, then the maximum value must be used in the design when considering the allowable differential deflection at loading position P2.

Comparing the results obtained from both design methods, it can be shown that there is an increase in the percentages of PUS and SGBP due to the variation in the raft parameters concrete strength and loading positions. Apart from these two parameters, the results of these two methods were similar and thus they can be used in the design method where additionally Bull's design method should include Annang's modified formulae. Loading position P2 should be included in the analytical design method as its effect is different from that of loading position P4. It should be treated as a new loading position when designing the raft unit.

As a result of the previous discussion [see paragraphs a, b, and c] for the different design methods, it could be concluded that the most important maintenance criterion used in the finite element analysis were the ultimate concrete stress (PUS), and the sub-grade bearing pressure (SGBP). The author has introduced a new criterion, namely the differential deflection due to loading position P2 as a result of the experimental observations. The most critical parameters affecting this criterion were the thickness, size and shape of the raft unit, concrete strength, sub-base strength, sub-grade strength, loading position, and contact pressure.

The effect of varying the contact pressure was apparent when predicting the number of load repetitions of the models tested to failure. The effect of varying the shape and size of the raft units needs more computer analysis and further empirical tests; also the raft units must be simple to manufacture and transport. The new loading position P2 should be included in the finite element analysis methods. The analysis of raft pavements needs a new approach which would incorporate a more accurate simulation of the pavement model.

The results produced by Annang's modified formula were closer to the actual experimental results than those using the Bull original method, and the Ismail method. The design values attributed to variations in the concrete grades that were higher than those used in the basic model should be checked again due to the wide differences between the predicted load repetitions using Ismail's method and the actual experimental results. The modified Bull method (i.e. Annang, 1986 and Ismail, 1990) have shown, in general, better results than those predicted by the BPA which has been supported by the experimental evidence of this research.

7.6 DEVELOPMENT OF AN EMPIRICAL DESIGN METHOD

7.6.1 Introduction

One of the aims of this research programme has been to develop and propose a suitable design procedure for heavily loaded raft units used in airfield pavements. In recognition of the fact that each design situation is unique, the design method should be capable of accommodating a variety of variables. Also, it was considered to be essential that the design procedure should be formulated in a way which preserved the designer's freedom to specify the characteristics of the variables within the ranges discussed below. The basic requirement, therefore, was for a simple presentation which could be followed easily, with an emphasis on the designer following the design procedure. The derived design procedure should allow for the designer to arrive at a series of designs which can then be taken forward for an economic appraisal.

In the previous chapters, it has been shown that the fatigue life, "N", was dependent on several variables representing the wheel load and raft unit characteristics [see sections 5.5 and 6.5]. The aim of this section was to find whether a particular relationship existed between fatigue life, "N", and the characteristics of raft units, namely raft unit dimensions and steel reinforcement; and loading conditions. The effect of the aspect ratio (i.e. the ratio of width to length of the raft unit), the thickness, the reinforcement and the loads applied onto the raft units were examined. These variables were designed in relation to the concrete strength, the foundation layers strenght, contact area, and contact pressure, all of which were most likely to influence raft unit life because of their influence on the way in which raft unit paving system responds to traffic movements. This relationship could then be used to predict values for "N" using different values of the raft unit, traffic movements, and the foundation layers characteristics. The multiple regression analysis technique was then used to examine the effect and significance of these variables, and to derive a non-dimensional empirical equation relating "N" to the raft units characteristics, and the applied load. The experimental results discussed in chapters 5 and 6 were used; and the range of design variables covered by these experiments is described in detail in Chapter Four. The conclusion of this part of the project was to develop a non-dimensional empirical design model in order to simulate and apply the basic design procedures that had been developed to design raft units for a specified design life.

7.6.2 Regression Analysis

(a.) General

Regression analysis is a statistical method used to find whether a relationship existed between a "dependent variable" and one or more "independent variables". The simplest

regression equation encompasses only one independent variable while multiple regression comprises more than one independent variable. Simple or multiple regressions can be linear or non-linear.

Specific input data were normally used in a regression model to derive particular relationships. These relationships can then be used to predict and optimise values of the dependent variable from other input data Montgomery (1984) and Demings and Morgan (1987).

(b.) Empirical Equation for Design

The analyses in chapters 5 and 6 show that the dependent variable, N, was a non-linear function of the following independent variables:

(i.) the aspect ratio [see Figs. 5.19 to 5.22, Chapter. 5];

(ii.) the thickness of the raft unit [see Figs. 5.24 and 5.25, Chapter.5];

(iii.) the area of steel reinforcement [see Figs. 5.26, Chapter. 5]; and

(iv.) the applied load.

As seen in the previous chapters, the minimum applied load was 100kN while the maximum load was 700kN. This non-linearity between N and the above variables suggested that the regression method to be used for this case was the non-linear regression analysis. Two different statistical software packages were used namely STATGRAPHICS, 1987; and MINITAB; Release 10 for Windows, 1994, to develop the best possible model for these variables. This analysis has been carried out as follows:

(i.) the statistical software packages (STATGRAPH and the MINITAB) were used;

(ii.) the multiple non-linear regression model was chosen;

(iii.) the input data used for this model comprised all the data drawn from the experimental tests described in Chapter 4 (i.e. the raft units' dimensions, steel reinforcement, applied load , concrete strenght, the foundation layers strenght, contact area, and contact pressure); and

(iv.) the regression model was run providing the empirical equation presented later in this section.

The multiple regression analysis technique was then used to examine the effect and significance of the variables that were thought most likely to influence raft unit fatigue life. The multiple regression of these data gave the regression estimate of cumulative fatigue life (N), in the form of a number of passes of a required design load or combination of design loads.

The present state of designing raft unit paving systems was to a large degree based on numerical analysis and empirical relationships developed during laboratory experiments [see Chapter 3]. As long as the designer was dealing with foundation soils, material properties, construction techniques, and traffic loading conditions that are similar to those for which the relationships have been determined, the performance of raft units can be reasonably well predicted. Based on the experimental results, the evidence of the relationship between loading conditions; raft unit plan dimensions, thickness and reinforcement; and fatigue life was so strong that the findings should have some direct practical application.

The equation expressing the relationship would provide an opportunity for quantitative evaluation of the effect on fatigue life of variations in plan dimensions, reinforcement, and the thickness of raft units; and thus strongly supports the need for quality control during casting and construction. The equation would offer also a reasonable rational basis within the load range for evaluation of an equivalent number of design load repetitions for the raft unit paving system subjected to mixed traffic.

Three different regression forms were tried following similar models developed by AASHO ROAD TEST, Vesic and Saxena, 1970; and MAYHEW and HARDING, 1987 [see Section 3.11.5, Chapter III]. The regression forms were logarithmic, power, and polynomials. However, the two softwares, Statgraphics and Minitab, were used and run for each of the three regression forms. Thus six regression forms were obtained and examined in the light of the experimental results. The trials in these regression forms were adopted to exploit the advantages of the software in this regard and thus provide better performing and easier-to-use design model. As a result of this exercise, the polynomial regression form was selected to represent the required design model [see Eq. 7.1].

The following equation has been derived to provide a basis for design. The designer would then be able to use the equation to estimate the dimension and reinforcement characteristics of raft units corresponding to required loading conditions that would provide a fatigue life for a specified number of applications of specified loads. The derived non-dimensional empirical design model is:

$$N = -16\left(\frac{W}{L}\right)^5 - 0.33\left(10 \times \frac{P}{HK}\right)^5 + 36.8\left(10 \times \frac{R\sigma_t H}{Q}\right)^4 + 4.22\left(\frac{Q}{Af_c}\right)^{-\frac{1}{2}} \qquad (7.1)$$

where:

N = the ultimate number of repetitions at which the raft units expected to fail, in million.

L = slab length (m)

W = slab width (m)

H = raft unit thickness (m)

W/L = the aspect ratio

R = area of steel in m^2/m

Q = applied load (kN)

P = contact pressure (kN/ m^2)

k = modulus of subgrade reaction (kN/ m^3)

σ_t = strength of steel reinforcement (kN/ m^2)

f_c = strength of concrete (kN/ m^2)

A = contact area

Correlation Coefficient = 87 per cent.

It should be noted that the above equation was derived for a range of applied loads between 100kN and 700kN on the basis that the ultimate number of load repetitions for a certain load at which raft unit was expected to fail would account for the load repetitions applied by the other loads (if any) within the traffic mix. Further, it is important to note that the derived equation presented in this section is applicable mainly for the following ranges:

(i.) the range of applied loads from 100kN to 700kN;

(ii.) two-point loading spaced up to and including 1m [see Section 2.4]; and

(iii.) the range of CBR values of the sub-base should not be less than 20 per cent.

[ie. minimum modulus of subgrade reaction "k" is 50,000 (kN/ m^3)]

From the data presented in previous chapters and the literature, the following primary steps were used for combining this data to form the required relationship. The steps were:

(i.) selecting the aspect ratio, thickness and reinforcement of the raft units as well as the loading conditions, concrete strength, foundation layers strength, contact area, and contact pressure with fatigue life of raft units;

(ii.) taking the characteristics of the equation parameters from the literature (Vesic and Saxena, 1970; and Mayhew and Harding, 1987) [see Section 3.11.5]. It was found, the life of the raft units should increase in proportion to the fifth power of the aspect ratio and the thickness of raft units, to the fourth power of raft unit reinforcement; and decrease in inverse proportion to the square root of the applied load;

(iii.) including the concrete strength and CBR values of the foundation support, implicitly within the range described above;

(iv.) including the load repetitions applied by other loads (if any) e.g. in case of mixed traffic design when specifying the ultimate number of load repetitions applied for a certain load to failure;

(v.) to develop a non dimensional empirical solution for loads between 100kN and 700kN was generated with respect to the 700kN load as an ultimate loading limit in the test programme,

(vi.) to move the applied load between the three loading positions P1, P2, and P3 for one cycle was considered to be one passage of the applied load over the three loading positions (e.g. P1), or one pass for the effect on the fatigue life [see Section 4.6],

(vii.) assuming that the uplift deflection due to loading position P4 had been effectively prevented, and

(viii.) the non-dimensional design model derived with a factor of safety of 25 per cent.

The multiple regression analyses indicated that 87 per cent of the variability in performance of these raft units was accounted for by the chosen tested variables (i.e.

aspect ratio, thickness, reinforcement, and applied loads) and that the thickness and aspect ratios of raft units were the most significant variable examined. The remaining variables in order of significance were, applied load, concrete strength, and the amount of reinforcement. The model fitting results showed that the variable describing the amount of reinforcement produced a low significant t-value. Based on the experimental results, this does not mean that this variable should be dropped from the model, since from the engineering point of view the amount of reinforcement was an important factor for increasing the fatigue life of the raft units, and the t-statistics measure the marginal contribution of each variable as if it was the last to be entered into the model. The non-dimensional variables accounted for 90 per cent level of confidence (i.e. P-value should be less or equal to 0.1) or of the variation in observed performance. From the experimental results and the statistical runs, it was clear that the selected variables were normally distributed.

It is important to draw attention to the following points while reading the results of the regression model:

(i.) the range of the data used was that obtained from the real experimental modules [see Chapter 4]; this equation, with care, could be used to predict values of the load repetitions (N) for raft units characteristics and loading conditions within the ranges considered in the test programme;

(ii.) the whole idea behind this statistical exercise was to demonstrate the possibility of regressing the experimental results by writing them in explicit non-dimensional empirical formulations. Also, this non-dimensional empirical equation could be developed further by increasing the number of tests and including various ranges of strength of the foundation layer, and concrete strength. The statistical exercise was an attempt to develop a non-dimensional empirical design method for raft units which would be taken as the base for further research by others to include all these variables. Due to the time needed for running one test which was estimated to be up to forty five working days [see Section 4.12.3], it was not practical for one researcher to carry all these required tests within a PhD programme; and

(iii.) for the non-dimensional empirical equation, the correlation coefficient was 87 per cent. It can be shown that the results obtained from this non-dimensional empirical equation does not deviate significantly from the real experimental results for the applied loads between 200kN and the design load of 450kN (see Table 7.8). It can also be shown that the amount of variation of the results

obtained from the non-dimensional empirical equation agree with the general trend of the variation in the experimental results which were discussed in chapters 5 and 6.

(c.) Design Method

The design procedures were written as a computer programme using FORTRAN 77 code, and run on a personal computer system. The computer programme is available for use on desk top computers. The FORTRAN 77 code developed in this study aimed at simulating the life of a raft unit. The complete programme was split into a series of subroutines, each covering a particular segment of the design process. These were called by the main programme in the order required by the designer (see Appendix D). The execution of the programme took the following steps;

(i.) answer the questions about the the strength of concrete and the foundation layer of the pavement;

(ii.) answer the question about the reinforcement arrangements. Specifically, the programme asks, "what is the strength of steel reinforcement (kN/ m^2) ?";

(iii.) then, the programme asks, about the purpose of conducting this particular simulation. As an example, it would ask "specify the design load and its contact pressure to which the fatigue life (N) is related". Also, the programme requires the loading conditions of the aircraft traffic mix prior to the design load (if any) within the proper design range; and

(iv.) the programme then will start the calculation of the fatigue life (N) as a loop operation corresponding to different combination of plan dimension, thickness, and the reinforcement of raft units, until the best combination of these variables which satisfy most the required design fatigue life, obtained,and

(v.) if for practical reasons, a specific raft unit dimensions are required, the programme allows for preference in chosen a particular dimension(s) for a raft unit paving system.

.

The computer proramme shown in Appendix "D" represents a simple design procedures for the design of raft units. If the fatigue life or the raft unit dimension(s) was found not acceptable, it could be modified by changing the values of the variables mentioned

above until the derived results were obtained and they satisfy the specified design criteria. If adjustments are required, a practical iteration, for example, to raft unit thickness can be considered (e.g. in 10mm increments). The desired result can be checked using the author's design charts discussed below in Section 7.7, to insure that the fatigue life considered is critical or allows for some overload repetitions or for a safety margin to a tolerable level for the selected design life. The use of the author's design charts permits increased confidence in the selected design life.

The stages of a typical design are shown in Appendix "D".

(d.) Validation

At this stage, the proposed design method should be limited to the different ranges of raft units paving system investigated in the test modules, until the work was extended and validated by further experimental evidence. If the design method was used with other ranges, then, the designed criteria should be used carefully and compared with similar design method such as the design Charts discussed in Section 7.7. In order to validate and generalise the design method, further tests should be designed to include a wider range of raft unit dimensions and reinforcement, as well as concrete strength, where each of these variables revealed new areas for further investigation. The effect of these parameters should be researched further using numerical methods in association with the experimental investigations. The results of this further investigation would complement the design procedures and would be of material assistance in the development of the design method.

7.7 THE EXPERIMENTAL VERIFICATION OF THE BULL NUMERICAL DESIGN METHOD

7.7.1 Introduction

The use of the Finite Element Method has led to a wide ranging study of the different parameters affecting the design of raft unit. The recent design methods for raft units that have been developed since the late 1970's, were briefly described in Chapter Three.

The numerical design method proposed by Bull (1986) is the first original method available specifically for designing raft units. Although Bull's method was refined numerically by Ismail (1990) and a new version was presented, the basic assumptions for the version have remained the same as that of Bull's original method [see Section 3.4]. Also, it has yielded better results than those of Ackroyd and the BPA, and appeared to need refining and verifying experimentally to validate the method.

For these reasons, the Bull method was used as a basis for comparison with the experimental results. Also, further experimental verification for the design method should be considered including introducing other design parameters.

The author's experimental results have shown that the raft units tested [see Tables 7.3 and 7.4] carried successfully repeated loading up to 700kN with associated loading pressures ranging between 1.25MPa to 8.75MPa at failure. As explained above in Paragraph 7.5.2-ii(a), this was in direct contrast to the BPA design manual that suggested the raft units need to be 300mm thick to carry just 350kN. The range of the contact pressure was used to compensate for the real number of load repetitions (i.e. fatigue life) of the raft unit corresponding to the real range of contact pressure (i.e. 0.31MPa to 2.19MPa) of the applied loads [see Sections 4.6.2 and 4.7]. The minimum figure was assumed to be the basic tyre contact pressure for the test programme in order to represent the contact pressure of the light aircraft [see Table 2.17]. Bull's design method assumed that the tyre contact pressure was below 2MPa and made no allowance for higher pressures. Bull's design method was described in Chapter 3 and Section 7.5.2 . The test programme was described in detail in Chapter 4

In order to verify the finite element results of the design method proposed by Bull, a series of experimental tests were carried out by the author on selected design parameters of the raft units namely plan size, thickness, and reinforcement [see Chapter 4]. The applied load was a two-point loading, 865mm apart which was designed to simulate one leg of the main landing gear of the design aircraft, a B727-200. The four most critical loading positions were considered, namely P1, P2, P3, and P4. Loading positions P1 and P3 were similar and gave almost the same fatigue life. Loading position P2 was considered differently because this was a new loading position [see Section 7.5]. Loading position P4 was abandoned due to the early uplift deflection which caused failure. It was suggested that loading position P4 should be designed with an edge beam and thus, it would behave in a similar way to loading position P2 [see Chapters 5 and 6].

Research into pre-cast concrete raft units has been undertaken at the University of Newcastle upon Tyne, since 1980 and as a result, different design procedures have been produced initially for square raft units as a basic model (Bull, 1990). It was logical to proceed to research using different sizes and shapes of raft units to meet the industries demands and to investigate the performance of these new types. This research project has investigated a design method for rectangular raft units and to investigate the effect on fatigue life of different raft unit sizes and shapes, i.e. different aspect ratio, different thicknesses, alternative steel reinforcement and various contact pressure. This has been

done using the numerical method proposed by Bull together with the experimental results. Therefore, the experimental verification and updating of the method proposed by Bull could be provided, enabling new parameters to be included. The design characteristics of the test raft units are shown in Table 7.3 and were described in detail in Chapter 4.

7.7.2 The Bull Method: Theoretical Considerations

The first analytical design method for infinite rigid pavements was developed in the 1920's by Westergaard [Section 3.3]. Later, layered pavement design solutions became available and formed the basis of the multi-layer elastic pavement analysis (Burmister, 1943 and BPA, 1983). Bull's design method considered two maintenance criteria that were similar to those used in flexible pavement design. These were the ultimate tensile stress (PUS) developed within the raft unit and the sub-grade bearing pressure (SGBP). The design method was first developed for interactive computer programs, using elastic parameters, for a basic pavement model of a 2 square metre raft unit (Bull, 1985a and Bull, 1985b). For more details please, refer to Chapter 3.

Relating the finite element output to a basic model, a series of design charts were developed where, for each chart, one variable was altered. The resulting alteration in PUS and SGBP was then related to the basic model. Using the charts, the known site conditions, maximum load and the required number of load repetitions, the designer could specify the required combination of the pavement system to limit the sub-grade settlement and predict the serviceability limit state. The repair or replacement of raft units were directly related to the combined maximum tensile stress developed in the concrete. The maximum principal concrete tensile stress was used, through the fourth power law [Eqn. 3.27, Chapter 3], to predict both the serviceability limit state at which raft unit maintenance would be required and the ultimate limit state at which the raft unit required replacement (Bull, 1990 and Bull et. al., 1987).

The accuracy of the finite element analysis can only be assessed by carrying out full scale controlled tests [see Chapter 4]. Previously published papers together with laboratory test results confirmed that for a single wheel load, the design life of raft units could be predicted for both the serviceability limit state and the ultimate limit state using finite element determined stresses, [see Appendix A for Bull and Luheshi, 1989 and Bull et. al., 1986].

7.7.3 The Experimental Programme

As explained in Chapter 4, the purpose of the laboratory experimental programme was to investigate the fatigue life and failure mechanisms of the raft units and provide laboratory data for a design method. The experimental programme was described in detail in Chapter 4. Single wheel load and Module M4 tests were carried out but are not discussed in this thesis [see Appendices A and B, Bull and Luheshi, 1989, and 1993 respectively].

The equivalent number of load receptions shown in Tables 7.1 and 7.4 were calculated to relate the applied loads to a specified load using Equation 5.1, Chapter 5, which was developed by Heukelom and Klomp (1978).

The load increments, the real contact pressure, and the ratio of the real equivalent load repetitions at each load increment to the equivalent load repetitions of that load increment using the Bull method (N_{ed}) are shown in Table 7.4. A factor of safety of 25 per cent was included in the calculations of the load repetitions [fatigue life] as a safety margin .Table 7.5 shows the equivalent load repetitions at each loading of each test for the design load of 450kN, the average and the range of CBR values for each test and each module, respectively, as well as the total range of the CBR value throughout the test programme.

7.7.4 Discussion

The laboratory test results were used to validate the design method proposed by Bull. Table 7.3 shows all the test modules. As discussed in Section 7.5.2, consideration of loading position P2 should be included in the design method, where the load distribution between the two adjacent raft units was unlikely to be equal which was assumed by Bull (1986). The relationships between the ratio of the observed fatigue life to the predicted fatigue life using Bull method (N_{ed}) and contact pressure for the three modules, are discussed below. By using the new charts [see Figs. 7.1 to 7.6], the design life of the raft unit pavement units at the most critical loading positions (i.e. P1/P3, and P2) and contact pressure, can now be related to the total applied loading conditions that occur in practice for airport pavements enabling the point at which the ultimate limit state can be predicted.

Tables 7.1 and 7.4 show the number of design load repetitions using the Bull design method and the experimental number of load repetitions. In all loading positions apart from loading position P4, the experimental number of load repetitions well exceeded

that predicted by the Bull method, which indicated that the analytical method gave very conservative results [see Section 7.5.2]. The sub-base CBR varied throughout the tests due to the sequence of the test programme, and therefore, the results of this variation were not discussed explicitly but were included in the fatigue life results [see Table 7.5]. This was based on the known practice that, by increasing the CBR of the sub-base tended to reduce the effects on the pavement layers, and so reduced both stresses in the concrete and the sub-grade. Ismail (1990) reported that by varying the sub-base thickness, sub-grade CBR, and the sub-grade thickness affected the Sub-Grade Bearing Pressure (SGBP) rather than the concrete stress (PUS) of the raft units. As he found that by increasing the CBR value of the sub-base to 100 per cent would reduce the stresses in the concrete raft unit by 10 per cent and in the sub-grade by 30 per cent [see Section 4.8.2].

(a) The Effect of the Loading Position

Bull's original design method did not consider either the exact location of the wheel loads or the new loading position P2. Table 7.1 shows the predicted and the experimental load repetitions achieved with the design load of 450kN. The predicted load repetitions using the original Bull design method gave the same load repetitions for loading positions P1, P3, and P4 but much higher for loading position P2 due to dividing equally the twin wheel loads between the two raft units. These results were in direct contrast to the results achieved in the laboratory, which gave different fatigue lives for the four positions particularly P1 + P3, P2, and P4.

In each test, the fatigue life was predicted for the four different loading positions at both the serviceability and ultimate limit states. With the exception of loading position P4 in Module M1, the experimental fatigue life in all tests exceeded the predicted fatigue life by variable percentages [see Tables 7.1 and 7.4]. For loading position P4 of Module M1, the case was different where the predicted fatigue life was higher than that recorded in the experimental programme and showed some form of inverse relationship with the aspect ratio of the raft units. The Bull method 1986, did not predict the uplift deflection criteria and therefore, overestimated the fatigue life of the raft unit where the uplift deflection was the limiting criteria. However, raft unit uplift was the limiting failure criterion, and thus the raft units themselves had not failed as was the case with loading position P4 in RS7; it was the bedding sand movement that caused the failure.

The experimental fatigue life for the proposed most critical loading positions gave the best indication of the expected life and showed that the actual wheel loading positions

must be used when designing raft units for airport pavements. Using the Bull design method, suggests that the realistic fatigue life should be modified to that shown in Table 7.4 and figures 7.1 to 7.6, to take into account the significance of using the actual and most critical loading positions rather than assuming the load was anywhere on the raft unit. The actual loading positions have affected the behaviour of the stresses within the raft units [see Chapters 5 and 6], and therefore, the alteration in the raft unit stress should be taken into consideration.

As explained and proposed earlier in chapters 5 and 6, some uplift restraint should be considered to enable loading position P4 to behave similarly to position P2, and thus the fatigue life would improve for the raft pavement system. Therefore, using Table 7.4 and figures 7.1 to 7.6 in conjunction with the design method, the designer would be able to know the likely life expectancy of the raft units.

(b) The Effect of Contact Pressure

It can be seen from Table 7.4 that contact pressure ranges from 0.313MPa at the initial load of 100kN to 2.19MPa at failure load of 700kN. The results of the equivalent number of load repetitions for a particular load were related in this project to the applied loads and contact pressures, while the predicted number of load repetitions using the Bull method were related only to the applied loads. Figures 7.1 to 7.6 show the relationships between the ratio of the experimental number of load repetitions to the design number of load repetitions using the Bull method (N_{ed}), and the real contact pressure for the three modules. The ratio of load repetitions corresponding to contact pressure higher than 2.19MPa were obtained using the resulting equations of the best fit curves.

The deviation between the results of the experimental number of load repetitions and the predicted number of load repetitions using the Bull method, is neither constant nor linear, but depends on contact pressure, loading position, aspect ratio, reinforcement, and thickness. The variations, however, do indicate some form of inverse relationship with contact pressure. The ratio of load repetitions varied with contact pressure, and was high when the contact pressure was low and decreased as the contact pressure increased.

New design charts and tables [see Figs. 7.1 to 7.6 and Table 7.4], were introduced which can be used in conjunction with the design method to predict the ultimate limit state for raft units. By using the new modification to the Bull method, the design fatigue life of the raft unit pavement at a specified loading condition and contact pressure, can be

related to the total number of applied loads and their respective contact pressures that occur in practice and, in this way, provide a more realistic prediction.

(c) The Effect of the Aspect Ratio

The aspect ratio was defined as a ratio of the width (W) to the length (L) of a raft unit. Table 7.5 shows the equivalent number of load repetitions for each raft unit size and each loading position. Table 7.4 shows the relationship between the ratio of experimental to the predicted number of load repetitions (N_{ed}) and the corresponding contact pressures. Generally speaking, as the aspect ratio increased from 0.25 to less than unity, the fatigue life of the raft units increased for almost all loading positions with few exceptions [see Table 7.5], together with the ratio of the experimental to the predicted number of load repetitions [see Table 7.4]. From the results in Tables 7.4 and 7.5, it can be seen that the 2 metre square raft unit (RS2) with an aspect ratio of unity, gave the smallest number of load repetitions in Module M1. The rectangular raft unit (RR) was the most efficient and achieved the best fatigue life in Module M1. But, square raft units with an aspect ratio of unity and an increase in both steel reinforcement (RS1) and raft unit thickness (RS7) showed that a better performance of a raft unit pavement can be achieved. Bull's design method does not consider non-square raft units and therefore, the alterations in PUS and SGBP for non-square raft units assumed the basic model (i.e. 2 metre square raft). The relationships between the aspect ratios and the actual fatigue lives were introduced at different loading positions in the form of charts and Table [see Figs. 7.1 and 7.2 and Table 7.4].

(d) Effect of the Steel Reinforcement

As concluded in Chapters 5 and 6, by increasing steel reinforcement the life of the raft unit increased. Tables 7.3 and 7.5 show that as the amount of steel reinforcement reduced from 283mm^2/m to 142mm^2/m to fibre reinforcement, the total number of load repetitions to failure for loading positions P1 and P3, for instance reduced from 651,106 to 180,734 to 24,018, respectively. Further, the inclusion of fibre reinforcement alone allowed the raft units to break into three independent pieces (one-half along the transverse centreline and two quarters) and they failed by fracture fatigue, which delayed the uplift failure for loading position P4 for RSF and produced more load repetitions before failure compared to RS2 for the same loading position.

The design spacing of the reinforcement bars should, in accordance with the elastic bending moment distribution, increase raft stiffness, reduce crack widths, and increase the fatigue life of the raft units. The amount of reinforcement in the raft units was

restricted by the practical limits of concrete cover to the bars and the physical ability of placing the bars and achieving the required vibration to provide the required modulus of rupture. Bull's method did not consider steel reinforcement less than 314mm^2/m. As a result, with the other reasons discussed earlier in this Section, the design method well underestimated the number of load repetitions to failure of the raft units. Table 7.4 shows that as the area of steel reinforcement increased from 142mm^2/m to 283mm^2/m, the ratio of the experimental to the predicted number of load repetitions (N_{ed}) increased by an average of 3.8 times. In general, the point at which the raft unit would need to be replaced ranged between 15.76 times to 71.95 times more than the serviceability load repetitions predicted by Bull for the design load of 450kN at loading positions P1 and P3.

By using the new charts and Table, the design fatigue life of the raft unit pavement at specified loading conditions and contact pressure could now be related to the actual applied loading conditions that occur in practice and then, significantly, a better fatigue life prediction could be achieved.

To test the validity of the new charts, the raw test results [see Section 7.7.3] were used and showed that the difference between the experimental and the predicted number of load repetitions was reduced. Module M4 [see Appendix B] was used to validate the new charts. The best match with the experimental results was at loading positions P1 and P3 where the difference between the experimental and the predicted number of load repetitions using the new charts and Bull's method, was in range of ±7 per cent, and ±68 per cent for loading position P2 when adjusted to the design load of 450kN.

7.8 APPLICATION OF THE DESIGN METHOD

7.8.1 Introduction

The development of raft unit pavement design methods have been described in Chapter 3. The new design procedures for airport raft unit pavements developed by the author have been illustrated in sections 7.6 and 7.7. In Section 7.6 an empirical model was developed using regression analysis where fatigue life was expressed as a function of aspect ratio, thickness, and reinforcement of raft units; and loading conditions. The other procedure developed by the author was the modified method proposed originally by Bull using the author's charts discussed in Section 7.7. This Section endeavours to demonstrate the application of the new design procedures to raft unit pavement design. The new design procedures can be used for designing raft unit pavements and can provide a check on the results obtained from other design methods. To ease the

following discussion, the new design procedures are designated as the design formula for the empirical model and the design charts for the modified method proposed originally by Bull. The design example compares and appraises four approaches, namely: the methods proposed by Bull and Ismail, the design formula; and the design charts. The example is based on raft unit pavements for use in taxiways and aircraft parking areas. The fatigue life which resulted from the first three methods will be compared with the results derived from the fourth method (i.e. the design charts) for the relevant design parameters.

The multiple regression analysis has established an equation relating raft unit life to the major variables for raft unit pavement. The design formula, the design charts, and the other design methods discussed in Section 7.5, have made it possible to predict the fatigue life of a range of different raft unit pavements, provided that the variables affecting raft unit performance are within a range that was not significantly different from the range of variables considered during the experimental programme of this research. In addition to the previously described potential for practical application of the design procedures (sections 7.6, 7.7, and 7.4); the research findings contribute substantially to the progress made in the design of raft unit pavements [see Chapter 3] of more rational approaches to raft unit pavement design. Using the design formula and the design charts, designers should be able, by utilising the results of this research, to predict with more certainty the potential fatigue life of raft unit pavements.

Each design method was shown to give a different fatigue life. In some cases, it is the policy of the designer to check the design by different design methods and the decision on which to specify was made on the basis of the required fatigue life intended to service a particular traffic mix coupled with the experience of similar airfields operating in the area under similar environmental conditions. Another factor which is vital when making such strategic decisions is the probability of the fatigue life being fulfilled. In general, pavement design including the design of raft units is based on the following parameters of sub-grade strength, the materials to be used in the pavement layers, the type of trafficking and the required fatigue life. The appropriate combination of these parameters is very important for good pavement design, otherwise, a substandard or over designed pavement may result with far reaching consequences which airfield operations cannot afford. Probably the most important factor when producing an effective and economic aircraft raft unit pavement is a high standard of both the manufacturing of the pre-cast raft units and the site supervision during construction. The raft unit pavement design must satisfy the following requirements:

(i.) sufficient strength for all aircraft types likely to use the airfield,

(ii.) sufficient fatigue strength,

(iii.) a capacity to accept temperature movements throughout the design life of the raft unit pavement,

(iv.) the absence of loose surface particles (debris), and good surface drainage,

(v.) resistance to jet blast, heat from jet engines and fuel spillage,

(vi.) provide a skid resistant but smooth riding surface for good rideability, and

(vii.) a minimum whole life cost including both construction and maintenance costs.

7.8.2 Safety Factors to be Considered in Raft Unit Design

The new design procedures (i.e. the design formula and charts) contained a safety factor of 25 per cent; the Bull and Ismail design methods contain no safety factor. The new design procedures are the straightforward application of the results from the experimental programme of this research project. Accordingly, the new design procedures are valid provided the entry parameters are within the ranges used in the research [see sections 7.6, 7.7, and 7.4]. In practice, this means that the designer needs to incorporate certain safety factors when estimating the value of the entry parameters which might be different from that used in this research or wishes to modify the assumed safety factor. For example, the new design procedures are based on average CBR values of the sub-base layer. Experience has shown that some conservatism in this respect is an appropriate measure particularly when high safety standards and reliability are essential.

The expected traffic intensity expressed either in terms of a design aircraft or mixed traffic loads is a major input parameter for the design procedure. The design procedure allows the use of both ways for traffic analysis, but uncertainties in this parameter can be accounted for by using the highest estimate. In this research, aircraft Boeing 727 is the design aircraft. Therefore, the weights and departure levels of an aircraft mix must be converted to a design aircraft and thus to an equivalent annual number of departures of the design aircraft.

The fatigue relationships represented a load repetition factor of 1.0, i.e. each pass is a full-load repetition [see Section 4.6]. The fatigue life can be adjusted, based on an appropriate traffic wander width, for specific aircraft which convert the number of aircraft passes to fatigue repetitions analogous to coverages.

Since the raft units which in this experimental programme were designed for use in critical areas where aircraft move slowly on aprons, taxiways, and holding areas at

runway ends, the observed fatigue life of the raft units tested were considered to represent the most severe conditions for the raft unit paving system. Therefore, it seems appropriate to take this into consideration when a factor of safety rather than the chosen factor of safety for this research (i.e. 25 per cent) is considered.

7.8.3 The Design Method

In recognition of the fact that each design situation is unique, the design method in question should be capable of accommodating a variety of variables. Also, it was considered to be essential that the design method should be formulated in a way which preserved the designers freedom to specify the characteristics of the variables within it's limitations.

Raft unit pavements can be designed to meet the design principles relating to serviceability maintenance criteria (Bull, 1986) or the ultimate limit state (Ismail, 1990; and the new design procedures from this research). In these two design approaches, the load repetitions were related to the maximum concrete strains developed within the raft unit. It must be remembered that the maximum concrete strain within raft units is one of the main parameters for measuring the failure of raft unit pavements. To consider the total required raft unit paving system and the combined factors that cause the most serious damage then it must be noted that the raft parameters are most critical in any design followed by the sub-base and the sub-grade thicknesses. By including the effect of contact pressure it has been possible to predict raft unit life more accurately and to show a better understanding and clearer picture of the loading characteristics. The design methods Bull, 1986, Ismail, 1990, and the design procedures developed in this research [see Sections 7.6, 7.7, and 7.4] were discussed in detail in Chapter 3 and in the relevant sections of this chapter.

In order to determine the accuracy and to quantify the differences in terms of fatigue life from each of the four design methods, the results of the load repetitions for the following design example using the four methods [see Table 7.8] were used in the following discussion. The resulting load repetitions using Bull, Ismail, and the design formula are compared to the results from the design charts.

7.8.4 Design Example

The design example is for an aircraft parking area and an apron taxiway, to be designed to meet the following design criteria:

1) Site Conditions

(i.) Sub-grade: - 1m thick a weak sub-grade layer,
- CBR value 2 per cent

(ii.) Sub-base: - 600mm thick,
- Type 1 aggregate, compacted limestone
- CBR of 22 per cent to 45 per cent, average value 30 per cent

(iii.) Sand bedding: - 50mm thick
- Medium compacted dense sand
- CBR of 5 per cent

2) Design Life
- 15 years

3) Traffic Loading

(i.) Due to the interruption which occurred to air transport in Libya during the late 1980s and the first half of the 1990s, it was assumed that the forecast for the annual aircraft movements between 1980 and the year 2000 discussed in Section 4.6, remains valid for the next twenty years (i.e. 1995 to 2015). The annual forecast aircraft movements is shown in Table 7.6.

(ii.) Calculate the average annual movement (AAM) for the period 1995 to 2015 from Table 7.6 as follows for each aircraft type and tabulate in Table 7.7.

$$AAM = \frac{1}{15} \diamondsuit 5\,(\,1995T + 2000T + 2005T + 2010T\,)$$

where:

T = total traffic movements in the year noted

N_5 = five year intervals for airtransport traffic forecast

N_{15} = design life.

(iii.) Calculate maximum design take-off weight (MTOW) and tabulate in Table 7.7.

(iv.) From points (ii.) and (iii.) above; and the aircraft wheel load characteristics [see Table 7.7], the design aircraft was obtained (i.e. B727-200).

(v.) In this example the design aircraft is equipped with dual wheel landing gear so all traffic was grouped into the dual wheel configuration using conversion

factors published by FAA 1978, and the equivalent annual movements of the design aircraft was calculated [see Table 7.7].

(vi.) The raft unit pavement would be designed for 30315 equivalent annual movements of the design aircraft of a dual wheel configuration, and weighing 94,318 kg.

Using the known site conditions, the maximum load and the required number of load repetitions for a variety of design options, combinations between raft unit characteristics and the design fatigue life were obtained. The thickness of the layers were continually modified until the required fatigue life had been satisfied. Although, the concrete strain was found to be smaller in the larger raft units [see Section 5.3] and thus the fatigue life increased, but the dimensions of raft units should be chosen practically in terms of how simple it would be to manufacture, to transport, to lay and most important to be economic. Accordingly, the final design was shown below. It was optimised by choosing the most suitable and economic design. It should be noted that using stabilised sub-base will improve the fatigue life of the raft unit pavement and lead to the most economical cross-section. Therefore, several thicknesses of stabilised sub-bases should be tried to determine the most economical cross-section.

The final trial raft unit pavement design:

Design aircraft is B727-200
Design T.O.W. is 94,318 kg
Total equivalent annual design traffic 30,315 movements
Tyre pressure 1.42 MPa

LAYER No. 1 Raft Unit
Plan dimensions = 2 m × 2 m
Thickness = 175 mm
Concrete strength = 60 MPa
Reinforcement= top and bottom,
= 283 mm^2/m in each direction

LAYER No. 2 Sand Bedding
Thickness = 50 mm
CBR = 5 per cent
Medium compacted dense sand

LAYER No. 3 Sub-base

Thickness = 600 mm

CBR = average 30 per cent

Type 1 aggregate, compacted limestone

LAYER No. 4 Sub-grade

Thickness = 1.0 m

CBR = 2 per cent

Design fatigue life - see Table 7.8

It is normal good practice to adjust the theoretical design thicknesses of pavement layers to practical construction thicknesses. The effect of this adjustment is generally to increase slightly the overall pavement thickness and hence to provide a small additional factor of safety.

- Jointing and Edge Conditions:

As the laying of the raft units proceeds, the joints should be filled using treated sand or alternatively, using some other elastic material property such as PAVESEAL. It is essential that the joints are kept full. For example, in the case of when dry sand is used, a soil stabiliser sealant should be placed in the joint on the top surface of the sand. The soil stabiliser sealant is used to minimise the loss of joint material and to prevent foreign object damage.

The edges of the raft unit paving system should be restrained horizontally. However, to prevent sliding of the raft units under dynamic loading (i.e. traffic movements), an edge retaining strip or an edge beam should be laid. The joint between the edges of the raft unit paving system and the retaining strip or the beam should be treated in a similar way to the interior joints discussed above.

- Opening the Paving System to Traffic:

It is recommended that raft unit paving systems subjected to heavy loads are given a running on period using normal or middle range of take off weight before maximum take-off weights are employed. From the test observation, the running on period could be suggested to be in a range of 2000 movements of middle range aircraft.

- Drainage System:

A well designed airfield pavement drainage system is a prime requisite for operational safety and efficiency, as well as pavement durability. Inadequate drainage facilities may result in costly damage due to flooding, as well as constituting a source of serious hazards to air traffic. In many respects, the design of an airfield drainage system is similar to highway drainage design. However, airfields often have special drainage problems which were usually characterised by vast expanses of flat areas and a critical need for the prompt removal of surface and sub-surface water. In such cases, the gradiation of a pavement plan makes it possible to direct the storm water to selected locations for drainage ditches, inlets, and manholes. The drainage system of an airfield pavement could include the following:

(i.) design of the underneath pipe system within the pavement layers,

(ii.) design of open channels, and

(iii.) design of inlets, and manholes.

7.8.5 Discussion

The four design methods were then compared in terms of the number of load repetitions at the ultimate limit state [see Table 7.8] when the raft units need to be replaced, for the design example described in Section 7.8.4. It was clear from this comparison that the results from the design formula were similar for middle range wheel loads but there was wide variation for the lowerer wheel loads such as for those applied by the F27 and F28 when they were compared with the results from the design charts developed by the author. For the design aircraft B727-200, the variation in fatigue life was less wider than those applied by the low wheel loads.

In view of the wide variation of the results particularly for the Bull method, it was suggested that designers should use the author design charts which were shown to be much more accurate than those of the other three methods. The results obtained by the design formula and the Ismail methods should be checked always against the results obtained using the design charts. The Bull method gave results that were very much lower than the design charts. The Bull method showed that as the applied load increased, there was a reduction in the predicted number of load repetitions and the differences widened between the Bull method and the results obtained from the other three methods particularly the design charts method. As shown in Table 7.8 the variation between the results of the design charts and the Bull method decreased from

about 505 times to about 270 times as the contact pressure increased from 0.55 MPa to 1.42 MPa respectively. In other words, the difference between them does suggest some form of inverse relationship with the contact pressure as was discussed in Section 7.7. The Bull method was designed for the serviceability limit state and did not include the effect of contact pressure. However, the laboratory test results showed that the number of load repetitions predicted by the Bull method could represent a condition when raft units were likely to require maintenance in the near future, the serviceability limit state, but that despite some concrete cracking, the raft units continued to sustain loading up to the number of load repetitions given by the experimental results [see sections 5.5 and 6.5], and in this example [see Table 7.8]. The Ismail method which is a revised form of the Bull method [see Section 7.5] gave an average of six times the design life produced by Bull and closer to that produced by the design charts and the design formula which suggests that the Ismail method (1990) was more accurate than the Bull method (1986). It was found that the Bull method could not be used for designing a raft unit pavement up to the ultimate limit state unless it was refined both numerically and experimentally. Ismail (1990) refined and revised numerically the Bull method by using a more accurate element in the finite element method and by including the effect of the contact area. Ismail's work represented an improved version of the Bull method as was shown in Section 7.5 and in Table 7.8 which gave the nearest results in terms of a raft unit's life to those obtained by the author.

The design charts and the design formula methods that have been developed from this research produced better results than those produced by the Ismail and Bull methods when the results were compared to the experimental results [see Section 7.7]. By using the design charts, the design fatigue life of raft unit pavements can now be related to the applied loading conditions that occur in practice for airport pavements enabling the point at which the ultimate limit state can be predicted. The results obtained using the design charts gave a more accurate method of predicting the ultimate limit state for a raft unit pavement and therefore, it could be used to predict the reserve life before a replacement of the raft unit was required. This suggests that the new design procedures produced by the author should be recommended for the design of raft unit pavement systems for airfields (i.e. aprons and taxiways). Furthermore, the method can be used to manage the maintenance of a raft unit pavement system.

7.9 COST BENEFIT ANALYSIS

7.9.1 Introduction

As illustrated in Section 2.9, the decision of selecting the best viable alternative pavement structure was based on the life cycle cost analysis and the performance of the

pavement structure. The life cycle cost concept is a means of comparing the total cost of different types of pavement structure which includes the initial construction cost, maintenance cost, user cost, and salvage cost. Since some of these factors, for example maintenance, will be incurred through the whole pavement design life, the future costs should be discounted to a present worth value using an appropriate discount rate and added to the initial construction cost in order to compare alternatives.

This section compared the initial construction cost, maintenance and other relevant costs of an extension of the existing aircraft parking project at Tripoli International Airport (TIA), Tripoli-Libya, surfaced with concrete paving blocks, pavement quality concrete (PQC), and precast concrete raft units [see Fig. 7.17]. This project was developed as part of a complete project, aircraft parking extension Phase I and represented phase II of the project. The phase I included sixteen remote stands for Boeing 737 aircraft size and a new taxiway "Y". The Phase II involved construction of 10,000m^2 of aircraft parking pavement plus paved shoulders, lighting, drainage, high pressure fuel main, and fire main.

The conventional pavement quality concrete has been used in TIA as the material of choice for so long time. The new development in pavement materials for airport industries such as paving blocks and most recent findings of this thesis, the precast concrete raft units encouraged Airport Authorities to select the best possible pavement alternative to achieve their requirements as well as being compatible with aircraft operations. Therefore, these three different alternatives were used for this comparison as the decision between their use could be based upon cost and the safety margins of an operational airport.

The main concern for the airport management was to minimise aircraft delays and enhance aircraft utilisation. Flight schedules are usually compromised because aircraft have to queue for approach and departure slots, or use of taxiway and airterminal gates. The results of delay are increased operating costs for the airlines, and passenger inconvenience.

The present worth of a future cost represented the basis of the cost comparisons. The life cost analysis presented, relates all costs to those appertaining at the time of the initial construction of the pavement. To reduce costs to a single present worth figure, pavement sections need to be postulated and a realistic future maintenance programme assumed. In economic comparisons of pavements, discount rate over a long design life, e.g.: over 20 years, can not be predicted but average values of 5, 10, and 15 per cent are

often used CAA paper 96001,(Knapton and Emery, 1996). In this analysis discounting of anticipated future cost was used. Discount rate has introduced into the computation as an average value of 5 per cent over a design life of 20 years. The design life of 20 years was chosen for the same reasons stated in Section 4.7. Salvage costs are likely to be a small proportion of the other costs, so only an approximate value was assumed.

In the light of this brief, the CAA-Libya (the responsible body for airports in Libya) search for faster and economic construction alternatives. The following subsections that deal with the aircraft operational analysis, was introduced in order to allow constructions to be drawn. After weighing these factors, a decision has to be taken by the CAA-Libya to proceed with the best alternatives.

7.9.2 Aircraft Operational Analysis

Tables 7.6 and 7.7 showed forecasts of aircraft movements for TIA [see Section 7.6.1]. The airtraffic forecasts were used for year 2015 corresponding to 20 years design life. Average annual aircraft movements of the design aircraft Boeing 727-200 was projected at 30315. The design aircraft was based on the airtraffic analysis of the TIA as the B727-200 was the most dominant and the best representative design aircraft for the TIA traffic (see Table 7.6). However, the total weight of each of these aircraft mix require less pavement thickness than the B727-200 would require. As a result, all aircraft movements were converted to equivalent annual movements for the design aircraft B727-200 using conversion factors published by FAA 1978, at maximum take-off weight of 94, 318 kg [see Table 7.7]. Since the Master Plan of the TIA did not anticipate any aircraft not currently in production, future aircraft types were not included in this analysis.

Tripoli International Airport is a hub airport with hub and spoke operations. Simply stated, a hub and spoke operation means that an airline has a number of flights from different cities arriving within a short period of time at a hub city such as Tripoli inbound aircraft are on the ground long enough to allow passengers time to connect to other departing flights. This type of operation happens several times during early morning and late evening and is known as a complex or bank of flights.

With the completion of the phase one of the aircraft parking extension project, which included new aprons and a new taxiway "Y", the operational activities on the existing Taxiways reallocated from one to another included the use of the new taxiway "Y". In other word, the aircraft ground operations were diverted from Taxiway A to B, B to C,

and C to Y. On the other hand, the new sixteen remote stands allowed the closure of taxiway A and stands number 1 and 2 which are close to the construction site of phase II. The continuous closure procedure involves low risk, controllable construction and is preferable to a nightly closure/daily re-opening, if that was necessary.

Generally speaking, the closure cost of any part of an operational aircraft would cause severe impact on the airport users. The closure would reduce the design capacity of the airfield and result in delay costs for operators. For reasons mentioned in Section 4.6.1, the growth in airtraffic movements at TIA was reduced. Therefore, the closure of Taxiway A and stands number 1 and 2 will not cause any losses and thus excluded from the life cycle cost analysis.

7.9.3 Pavement Thickness Design

Pavement quality concrete, concrete paving blocks, and precast concrete raft units are to be designed for a design life of 20 years. The design methods that were used to develop the required pavement cross-section were the FAA (1978), FAA modified design charts, CAA paper 96001 (Knapton and Emery, 1996), and the author's design charts developed in this thesis for the three types of pavement, respectively. To use these design methods, the following pavement design parameters must be determined:

Subgrade CBR	5 per cent
Concrete Pavement Strength	50 N/mm^2
Concrete Flexural Strength	5.7 N/mm^2

30315 annual movement of the dual wheel design aircraft B727-200 at 250 kN wheel load and 1.42 N/mm^2 contact pressure.

Using the traffic and soil information described above, the design pavement cross-sections were determined and shown in Fig. 7.17. In paving blocks section, the original design of the overall pavement construction thickness was 1435 mm. To optimise the design and reduce the cost of excavation works in deep layers, material conversion factors were introduced as given in Section 2.10 of reference CAA paper 96001, 1996. The optimisation was achieved by providing additional base material and less sub-base material using the currently factored amount of 1.0 for the Cement Bound Material (CBM3) and 0.3 for type 2 granular sub-base. The CBM3 base thickness was increased by 100 mm and thus, the reduction in type 2 granular sub-base thickness was 100/0.3= 333mm (say 330 mm). Therefore, the overall section of paving blocks was reduced by 230 mm (i.e. reduced to 1205 mm) and shown in Fig. 7.17.

7.9.4 Life Cycle Cost Analysis

The life cycle cost concept is a means of comparing the total cost of different types of pavement. The components of the life cycle cost analysis are:

- Initial constructive costs,
- Maintenance costs,
- Salvage costs,

Life cycle cost analyses were conducted for the three types of construction pavements that designed in Section 7.9.3 and shown in Figure 7.17, in accordance with FAA Advisory Circular 150/5320-6C, 1978; and the CAA paper 96001,(Knapton and Emery 1996). Present worth economic analysis with a five per cent discount rate was supplied over a design life of 20 years.

(a) Initial Construction Costs

The initial construction costs per square metre of the three pavement alternatives shown in Fig.7.17, were calculated below, using the present day costs (i.e. in 1996). The initial costs did not include subgrade grading and compaction, and any other underground services such as fuel main, fire main, and ducts, which were considered equal in all cases. The unit cost of raft units was based on the mass production. The current costs (i.e. 1996) of raft units revealed by the manufacturer Redland Precast, showed that a mass production over a thousand units reduces the unit cost by almost 50 per cent. The initial construction costs are:

• Concrete Paving Blocks	£/m^2
80 mm pavers &	
30 mm laying course sand	12.00
pavement sealer	1.40
550 mm CBM3	26.00
540 mm Type 2-granular material	9.00
	48.40
• Pavement Quality Concrete (PQC)	
320 mm PQC	26.40
150 mm DLC	7.50
300 mm Type 2-granular material	5.00
	38.90

• Precast Concrete Raft Units	
Size 2.0m * 2.0 m * 140 mm thickness &	
30 mm laying course sand	10.75
Grouting Raft Unit Joints	2.50
300 mm CBM3	14.20
450 mm Type2-granular material	7.50
	34.95

(b) Maintenance Costs

Maintenance costs were developed from the current costs of existing pavements in TIA and other airports in Libya, as well as CAA paper 96001, (Knapton and Emery ,1996); and the current costs of the manufacturer of raft units, Redland Precast 1996. Repair type and interval were based on the design consultant's experience with similar pavements in TIA (CAA-Libya, 1982). The maintenance was divided into three categories, routine, urgent (i.e. an emergency condition), and non-urgent. The maintenance programmes have been carried out at regular intervals dependent on the category of the maintenance. The intervals are varied from weekly, monthly, quarterly, half-yearly, to yearly. The frequency of the intervals may need to be varied as dictated by reports from field inspections.

Pavement maintenance costs of TIA are included in the airport's overall operations and maintenance budget under separate section together with other associated Engineering works. It is often difficult to identify specifically annual and periodic maintenance costs for airport pavements and therefore, engineering judgements, based on their previous experience in the TIA and other airports within the region, should be inherent in estimating these costs. The maintenance standard levels in the TIA have been carried out according to the manufacturers recommendations by maintaining safe and adequate surface integrity. Meanly, the regular maintenance was limited to inspection and repair for paving blocks and raft units where inadequate compaction has resulted in surface defects. As the paving blocks and raft unit pavements have not been used in Libya, such as maintenance costs were not experienced in Libya. Therefore, similar experience in the UK was used and indicated figures of £0.08/m^2/annum and £0.20/m^2/annum have been suggested for paving blocks and raft units (Knapton and Cook, 1995; and Redland Precast, 1996), respectively. Using the data discussed above, the maintenance costs were:

	Activity	Frequency	Costs £/m^2
• Concrete Paving Blocks	Regular Maintenance	Yearly	0.08
	Reapply Sealant	5 years	0.40
	Replace Pavers	5 years	0.90
• Pavement Quality concrete	Regular Maintenance	Yearly	0.10
	Reseal Joints	5 years	0.80
	Cracks Seal	5 years	1.20
•			
• Precast Concrete Raft Units	Regular Maintenance	Yearly	0.20
	Reapply Sealant	5 years	0.80
	Replace Raft Unit (i.e. 10% of the original)	10 years	1.325

(c) Salvage Cost

Salvage cost is a residual value in a pavement over its design life and expressed as a negative cost in whole life cycle cost analysis. It is usually considered in a concrete pavement as a very small compared with its original value (say 10 per cent). However, the less trafficked areas of concrete paving blocks and raft units are likely to remain sound (i.e. remaining life) and thus have a salvage. Due to the on ground clearances required for an aircraft ground movements, the less trafficked areas were estimated in this example by 50 per cent and had 10 years of life remaining at the end of the analysis period original costs.

The Salvage cost = remaining life / design life * original cost

- Concrete paving blocks = 10 years / 20 years * £ 12/m^2 = £ 6.0
- Pavement Quality Concrete = 0.1 * £ 26.40 / m^2 = £2.46
- Precast Concrete Raft Units = 10 years / 20 years * £10.75 / m^2 = £ 5.375

These figures take into account the damage which may occur during the removal of the pavement units and the man power and equipments required to prepare them for reuse. All other activities are assumed to have no salvage value since their useful lives have been exhausted during the analysis period.

(D) Present Worth

The present value of this example can now be determined using the present worth formula shown in Section 2.9 (Eqn. 2.3). a discount rate of 5 per cent over a design life

of 20 years was used. The present worth life cycle costs for each alternative were calculated and shown in Table 7.9.

To sum up, the present analysis of the three alternative pavements shown that the paving blocks and raft units were of similar total life cost and the PQC was the highest in life cycle costs [see Table 7.9]. The total life costs of both paving blocks and raft units were closely comparable to each other. The paving blocks and raft units appeared to be the most promising alternatives in this analysis.

The decision to select one of the most promising alternatives should also be based on such factors as speed of construction and weather conditions. Both alternatives paving blocks and raft units, offered the speed of construction and the ability of shortening closure times of airside facilities. From recent experience, two different teams of three skills labours laid 20.8 m^2/ hr. of paving blocks and 37.6 m^2/ hr. of raft units sized of 2 square metre (Muir, 1996; and Redland Precast, 1996), respectively. In this respect, the precast concrete raft units exhibited a superior and potential for their application over the paving blocks, despite their similarity in the total costs. Also, for a future expansion to an airfield and when operational constraints are critical, the out put of the life cycle cost analysis demonstrated that the raft units will become a viable alternative to conventional pavement construction and a real competitive to the paving blocks. Based on the analysis, it was anticipated that many airport authorities and the governing bodies for airport standards such as the ICAO, CAA, and FAA, will consider raft units as an alternative option for airfield pavement construction.

7.10 SUMMARY OF CHAPTER

(i.) Regression equation was derived for the design of test raft unit models using non-linear regression analysis. The design equation was based on the experimental results and included the major design variables (plan-dimensions, thickness, and reinforcement) generally thought to control the performance of raft units. The design equation relating the ultimate number of design load repetitions to these variables, and the magnitude of the design load, indicated that the raft unit fatigue life should be proportional to the fifth power of the aspect ratio and the thickness of the raft unit, to the fourth power of the raft unit reinforcement, and inversely proportional to the square root of the design load.

(ii.) The fatigue life of a raft unit has been defined as the traffic carried by the pavement up to a well defined condition of deterioration where the raft unit

cannot sustain any additional load repetitions. The fatigue life was sensitive to changes in raft unit plan dimensions, thickness, and the amount of steel reinforcement.

(iii.) The British Port Association (BPA) design method generally specified a raft unit thickness significantly in excess of the other design methods [see Section 7.5]. It used the PAWL concept which was similar to the equivalent single wheel load concept. Therefore, it was concluded that the BPA method was not appropriate for the design of raft units.

(iv.) The sensitivity analysis has shown that the new design methods developed by Bull and Annang (1986) and Ismail (1990) were more acceptable than both the design methods proposed by Bull (1986) and the BPA (1989).

(v.) The experimental test results have been used to validate the existing methods for designing raft units and to refine these methods where possible. The predicted number of load repetitions to failure determined by using Bull's design method produced conservative results.

(vi.) The ratio (N_{ed}) of the experimental number of load repetitions to failure, to the predicted number of load repetitions before maintenance of the raft unit, was determined for each individual load position, except for loading position P4, for all the three test modules. Loading position P4 was abandoned due to reasons given in chapters 5 and 6. This meant that the loading conditions applied at position P4 produced the shortest fatigue life and it was found that it would be unsafe to carry on the test at that loading position. It was demonstrated by Ismail (1990), that the effects of including joint filler material in improving the performance of the raft units, and the contribution this would make to the lateral distribution of loading. Also, it was clear that proper boundary constraints would improve the performance of the edge and corner of the raft units. For these reasons, it was felt that the results from loading position P4 could be discounted at this stage though it should be considered as the subject for further research. Due to this premature failure, it was suggested that the fatigue life could be improved by means of an edge beam or retaining strip to the pavement system and the strengthening the sub-base and the bedding sand layers in order to reduce the differential deflections between the loaded and the free edges of the raft units.

(vii.) The experimental verification of Bull's method demonstrated that the actual loading position should be used in design rather than assuming that the load acted anywhere on the raft unit. Therefore, the author's proposed charts should be used for predicting the fatigue life for appropriate conditions.

(viii.) The calculation of the number of load repetitions for loading position P2 should consider the full applied twin wheel loads and should not divide them equally between the two adjacent raft units. The evidence for this can be seen by the differences in the test results for loading positions P2 and P4 [see chapters 5 and 6]. It should be considered in design as a new loading position which could be treated according to the author's charts.

(ix.) The proposed design method predicts not only the serviceability limit state of the raft units, but also the ultimate limit state can be predicted using the relationships shown in the new charts. An inverse relationship has been established between the fatigue life and the applied contact pressure.

(x.) Using the author's charts, the design life of the raft units at specified loading conditions can now be related to the total applied loading conditions that occur in practice, and therefore, the fatigue life of the raft units can be predicted more accurately. The author's charts confirm the proposed design method and provide a means of including the design life variations discussed in Section 7.7.4.

(xi.) Strains within the raft units that were obtained using the experimental results, which gave a relationship between the fatigue life and the ratio of strain caused by traffic loading to the strain of a design load or the concrete strength (MR) used in the raft units. This suggested a possible criterion for design in terms of the strain ratio. Design curves have been presented relating the fatigue life of the raft units to their strain ratios for different aspect ratios, reinforcement, and thicknesses of raft units. The experimental results from this research have confirmed that the tensile strain in the raft unit caused by the moving loads represented the best indicator of raft unit pavement performance. Also, such a correlation confirmed the basic philosophy of existing rigid pavement design methods, which are mostly based on considerations of maximum tensile stress or strain in the pavement slabs.

(xii.) Using the derived design fatigue relationship, the induced tensile strain due to the applied loading is not now limited to a maximum value equal to the modulus

of rupture (MR). In other words, the strain ratios could be greater or less than 1.0. It is highly recommended that these relationships should be used for the fatigue design of airfield raft unit pavements.

(xiii.) General design fatigue relationship were derived for each of the design parameters: that is, plan dimensions, reinforcement, and the thicknesses of the raft units. This significant finding confirmed the soundness of a rational, mechanistic approach to the design of raft units. Furthermore, it confirmed the results discussed in chapters 5 and 6; and demonstrated clearly that failure in raft unit performance was not a phenomenon of chance but a phenomenon which has a definite mechanical cause. Moreover, it becomes possible to predict the potential life of raft unit pavements subjected to traffic having different wheel configurations. Thus, the empirical findings presented in this Chapter have a potentially great practical importance.

(xiv.) Similar relationships to that derived for fatigue design, were derived for the raft unit maintenance model by relating the accumulated number of load repetitions experienced by raft units for a design load to the strain ratio which is not now limited to a maximum value equal to the modulus of rupture, MR, (i.e. strain ratio is greater or less than 1.0) and thus maintenance charts were presented. These relationships would be the basis for the prediction of the remaining life of the raft unit pavement. A performance model was presented for these relationships which linked the design life (N_{eq}) and the accumulated load repetition (N_{acc}) for a particular load condition to the strain ratios caused by traffic load. The difference between the N_{eq} and the N_{acc} represents the remaining life of a raft unit pavement for that particular loading condition. The performance model would improve the management of such a paving system which would be more cost effective for the operator.

(xv.) The structural and functional evaluation of an existing raft unit pavement were essential requirements for its management using the performance model. The procedures for the performance model enabled a raft unit pavement to be maintained at an acceptable level of operation by estimating the remaining life of the existing raft unit pavement. These procedures provide the potential for new materials to be considered as an alternative to the sand bedding layer and joint fillers which would improve the fatigue life of the raft unit pavement. Any remedial measures would extend the life of a raft unit pavement for a specified period usually expressed in terms of the chosen design load.

(xvi.) In this chapter, the development and the application of the design methods proposed by the author, for raft unit pavements in airfields, have been described in detail. It was clear that the strain fatigue relationships were not solely restricted to raft unit pavements in airfields, and could be extended readily to include other industrial or highway pavements. The same could be said for the authors design charts which provided a range of wheel configurations that could be considered in design.

(xvii.) While there were limitations in these methods, their use is highly recommended and would improve the ability to design and evaluate raft unit pavements. It would be unwise to wait for the perfect method before using these new developments. The potential for using these methods has been demonstrated adequately. It should be apparent that the design methods provided extremely useful tools to permit the designer to expand the scope of the design and evaluation with considerable confidence. In addition to the previously described potential for the application of the above design methods in practice [see Sections 7.6, 7.7, and 7.4], this research has contributed substantially to the progress made in more rational approaches to raft unit pavement design.

(xviii.) Life cost analysis was conducted for three types of construction pavement (paving blocks, PQC, and raft units), in accordance with FAA, AC 150/5320-6C, 1978, and CAA paper 96001, 1996. Present worth value of 5 per cent discount rate was applied over 20 years design life. The analysis showed that the paving blocks and raft units were of similar total life costs and closely comparable to each other while the PQC was the highest in total life cost. Despite their similarity in total costs, the precast concrete raft units exhibited a superior and potential for their application over the paving blocks as the speed rate of construction per hour of the raft units (i.e. 37.6 m^2/hr) was higher than that of the paving blocks (i.e. 20.8 m^2/hr).

Chapter - Eight

CONCLUSIONS, RECOMMENDATIONS AND SUGGESTIONS FOR FURTHER RESEARCH

8.1 INTRODUCTION

Precast concrete technology is well-established in many fields of construction. This potentially provides a better product than would be obtained by in-situ casting and may ease and speed construction in the field. Such construction has included precast concrete pavement units (i.e. raft units), which are manufactured normally 10m long down to 1.2m by from 2.29m down to 0.6m wide by 0.3m down to 0.14m thick. For many years, raft units were used in the rapid emergency repair for roads and airfields. Reinforced and unreinforced raft units have been used of different shapes such as small and large hexagonal, triangular, and square shapes [see Chapters 5 and 6].

The use of raft units has developed extensively throughout the world, to accommodate very low sub-grade CBR values by having the required strength, flexibility and durability to carry loads as high as 900kN.

Aircraft pavements have the most demanding performance criteria of any other pavement application. The raft units must be durable, stable, skid resistant and provide an even running surface. Also, they must resist thermal movement, jet blast, thermal shock, fuel and oil spills, and de-icing agents. The advantages of the use of raft units over conventional rigid pavements are the ready access to underground utilities by removing the raft units, enabling rapid repairs and then the reinstatement of the same units. The raft units provide a structural, load bearing surface. Additionally, they are ready for aircraft traffic immediately after installation.

Aircraft pavements are designed normally to serve adequately a predicted traffic load for a required design life at the lowest possible annual cost. Therefore, the designer must be aware constantly that the prime objective is to achieve a minimum whole life cost, which includes the costs of both construction and maintenance.

With the expected advances in materials technology, raft unit designers will find it possible to design efficient cross-sections. The earliest pavements were designed using

empirical knowledge to determine the most economic pavement cross-section. In the early 20th. century there have been many analytical methods which correlate sub-grade types with pavement performance [see Chapter 3]. With the development of computers, the multi-layer elastic solution was combined with the Finite Element method and used in concrete raft pavement structures [see Chapter 3].

At the time of developing the design methods for raft unit pavements mentioned above they could not be validated because there was no experimental data available, and therefore, the design recommendations had to be based on theoretical studies and engineering judgement. The lack of experimental data in this topic was probably due to the difficulties associated with the experimental testing of raft units particularly for heavy duty pavements [see Chapters 4, 5 and 6].

The primary aim for the experimental stage of this research project was to investigate both experimentally and theoretically the fatigue strength and the failure mechanism for a range of raft units with different design parameters [see Chapter 4]. Attention was directed towards the study of the following criteria:

(i.) the mode and mechanism of failure;

(ii.) the value of the failure load;

(iii.) the deflection and strain development in the raft units;

(iv.) the crack patterns and crack widths at various stages of loading; and

(v.) the fatigue life and estimation of the consequent degree of damage.

In the light of this study, an empirical relationship was developed using regression analysis. The design methods proposed by Bull, Bull and Annang, Bull and Ismail, and the British Ports Association were compared with the actual experimental results. Experimental verification for the design method proposed by Bull was provided in Chapter 7. Those investigations have led to a more refined design for specifying raft unit pavement construction based on the size and reinforcement of the raft units and the expected dominant loading positions.

In view of the need for further development, some recommendations have been made below for the extension of the research programme.

8.2 CONCLUSIONS

A parametric analysis was carried out to investigate the relationship between the design parameters of raft units [plan dimensions, reinforcement, and thickness] and their life performance as a paving system for airports, under repeated slow-speed wheel loads applied by the design aircraft, a Boeing 727-200. The following points summarise the principal conclusions.

(i) **Development of Test Rig.** A full-scale laboratory test rig for simulating the applied loading from the dual wheel leg of the design aircraft Boeing 727-200 taxiing over raft units paving system, was designed and constructed. It is believed that this is the first attempt to test full-scale raft units in this way.

(ii) **New Use for the Raft Units.** The results of this research have demonstrated that it would be possible to use raft units for airfields pavements in slow-speed areas such as aprons, taxiways, holding areas, maintenance areas, and shoulders.

(iii) **Review of Literature.** The current design methods [Bull, 1986; Ananang, 1986; BPA, 1989; and Ismail, 1990] were compared and appraised with the actual empirical experimental results. These design methods were found to be inadequate when dealing with the design of raft unit pavements that were subjected to variable aircraft loading.

(iv) **Development From the Literature.** The author has proposed major modifications to the numerical design method first proposed by Bull (1986), by introducing new design charts. The new design charts provide a means of including design life variations which were related to the applied load contact pressure, and the exact position of the applied loading.

(v) **A New Approach to the Design of Raft Units.** A new empirical design method has been proposed for raft units using multiple regression analysis. The design equation showed that the ultimate fatigue life was sensitive to changes in design parameters particularly the thickness of the raft units.

(vi) **A New Method to Manage Raft Unit Pavements.** Design equations have been developed relating the fatigue life of a raft unit to its strain ratio. Such a correlation confirmed the basic philosophy of existing rigid pavement design methods, which were mostly based on considerations of maximum tensile stress

or strain in the pavement slab. Moreover, it becomes possible to predict the potential life of raft unit pavements subjected to traffic having different wheel configurations. The new performance model for the assessment of the reserve life within a raft unit pavement system has been proposed for maintenance management. It represents the basis for predicting the remaining fatigue life in a raft unit at any stage before complete failure occurs. The performance model would improve the management of such a paving system which would be more cost effective for the operator.

(vii) The new approach to design enables the designer to propose a unique combination of the design parameters [i.e. plan dimensions, steel fabric reinforcement, and thickness] of raft units for particular loading conditions to satisfy a prescribed fatigue life. Therefore, a significant reduction in some of the design parameters, for example the thickness, can be achieved without violating the required life performance of the raft units. The use of steel fabric reinforcement demonstrated a superior performance over the steel fibre reinforcement and thus the steel fabric reinforcement should be designed in the top and bottom of the raft unit and uniformly spaced.

(viii.) **Life Cycle Cost Analysis.** It was conducted for three types of construction pavements (paving blocks, PQC, and raft units) in accordance with FAA, AC 150/5320-6C, 1978; and CAA paper 96001, 1996. The analysis showed that the paving blocks and raft units were of similar total life costs and closely comparable to each other while the PQC was the highest among them in total life cost. Despite their similarity in total costs, the raft units exhibited a superior and potential for their application over the paving blocks as the speed rate of construction per hour of the raft units (i.e. 37.6 m^2/hr) was better than that of the paving blocks (i.e. 20.8 m^2/hr). However, the analysis demonstrated that the raft units will become a viable alternative to conventional pavement construction and real competitive to the paving blocks.

8.3 DESIGN RECOMMENDATIONS

A general set of design recommendations are set out below for a raft unit paving system for the slow-speed passage of mixed aircraft.

8.3.1 Design Considerations

(a.) On the basis of the various raft unit design methods and the experimental results discussed in Chapter 7, the following methods could be recommended for the design of raft units:

- The author's new design charts and ;
- The design formula

(b.) It was suggested that for thin raft units not less than 140mm thick with aspect ratios of 0.25 to 0.49 or up to 1.00 with a side length of 2m or more, a minimum steel fabric reinforcement of 283mm^2/m should be used.

(c.) The use of closely spaced steel reinforcement at the top and bottom of the raft units, with a spacing between 50mm and 100mm particularly at the edges of the raft unit, is recommended and increased the fatigue life. Therefore, there is no need to use shear reinforcement. The use of fibre reinforcement only is not recommended.

(d.) The author's tests showed that a third design criteria should be included, namely, the uplift deflection. Depending on the type of sub-grade and sub-base available, the raft unit can be designed to suit the three main design criteria to avoid early failure due to an over stressing in the concrete raft unit and an excessive deformation in the layers underneath. The minimum sub-base thickness and CBR value should not be less than 300mm and 20 per cent respectively.

(e.) The author has recommended a combination of design parameters which affect the design fatigue life and, how to achieve the best combination for the most economic results; for example, reducing the thickness of the raft unit in favour of increasing the amount of reinforcement.

(f.) The paving system should be designed with an edge beam to allow loading position P4 to behave in a similar way to loading position P2, and by filling the joint with elastic materials such as plywood, treated sand or polystyrene to restrain the raft units and keep them in place

(g.) Casting and assembly tolerances for raft unit pavements must allow economical construction and operation, but, they must provide the design fatigue life with

safe performance. Generally, in terms of whole life costing, raft units become increasingly competitive.

8.4 SUGGESTIONS FOR FURTHER RESEARCH

(i.) The overall dimensions of the author's raft units tested were shown in Table 4.1, Chapter 4. Further experimental work is required on larger raft units (i.e. larger than 2m by 2m) and shapes other than rectangular and square to confirm the results of the present experimental programme.

(ii.) The author's experimental programme investigated the effect of different aspect ratios, different thicknesses and different levels of reinforcement on the failure mode and the fatigue life of raft units. The effect of other parameters should be studied:

(a) various raft dimensions and thicknesses in 25mm increments;

(b) different reinforcement arrangements;

(c) concrete strength;

(d) loading arrangements (e.g. different wheel configurations and spacing);

(e) different contact areas for the applied loading;

(f) different base course material rather than sand bedding; and

(g) different sub-base thickness and CBR.

Such a parametric study would be an important extension to this research area to identify and quantify the parameters which have a significant effect on the failure mode and the fatigue life of raft units. Based on these studies and the results of the present experimental programme, the empirical relationship developed by the author, could be extended and validated further by increasing the number of tests and including new and wider ranges of the design parameters listed above, to predict the fatigue life of the raft units.

(iii.) Load transfer between raft units is a major consideration in raft unit design and, therefore, should be investigated thoroughly to assess its effect on fatigue life. For this reason, it was felt that loading position P4 should be considered as the subject for further research.

(iv.) The raft units have been tested under repeated loading to assess their use in slow-speed areas such as taxiways, and aprons. Their use in high speed areas like touch down zones in runways should be tested under heavy impact loading.

(v.) There is a need to extend the research programme to monitor the performance of raft units in service, providing a relationship between experimental, analytical and on-site characteristics of raft units.

(vi.) The use of raft units as gully covers for airport pavements, gives a major concern to designers, and therefore should be investigated very carefully.

(vii.) The potential for cost savings and improved performance is great. Therefore, a whole life cost model should be developed to consider the total costs associated with a raft unit paving system.

REFERENCES

ACKROYD, R. F. and BULL, J. W., (1985) "The design of precast concrete pavements on low bearing capacity sub-grades." Computers and Geotechnics 1, pp, 279-291

AIRBUS INDUSTRIE, (1983) ,National Aircraft Standard, Airplane Characteristics, Airport Planning Manual for Airbus A300-600, France.

ANNANG, R. B., (1986) "The effect of high contact pressure on the design of precast concrete pavements." M.Sc. thesis, Newcastle upon Tyne university.

BARBER, E. S., (1957) "Calculation of the maximum pavement temperatures from weather reports." HRB, Bull l68, pp. 1-8.

BARBER, S. D., (1980) "Pavement design in port areas." Ph.D. Thesis, De-partment of Civil Engineering Newcastle upon tyne university.

BEATTY, A. N. S., (1992) "Predicting the performance of bedding sands." Proc. 4th Int. Conf. Concr. Block Paving. Porirua, Pave New Zealand.

BEHRMANN, R. M., (1964) "Small scale model study to determine minimum horizontal dimensions for infinit slab behaviour." Technical Report No. 4.32, Ohio River Division 1aboratories, U.S Army Engineer.

BERGSTROM, S. G., FROMEN, E. and LINDERHOLM, S., (1949) "Investigation of wheel load stresses in concrete pavements." Swedish Cement And Concrete Research Institute, Proc. No. 13, Royal Institute Of Technology, Stockholm.

BLACK, W. P. M. and LISTER, N. W., (1979) "The strength of clay fill sub-grades: its prediction in relalion to road performance." TRRL Report LR 889

BLACK, W. P. M., (1961) `'The calculation of laboratory and in-situ values of CBR for bearing capacity data." Geotechnique. London, pp. 14-21.

BLACK, W. P. M., (1962) "A method of estimating the CBR of cohesive soils from plasticity data." Geotechnique, London. pp. 271-282.

BLACK, W. P. M., (1963) "The strength of clay sub-grades:Its measurement by a penetrometer." Department of the Environment and Department of Transport, TRRL Report LR 901, Crowthorne.

BOEING INDUSTRIE., (1985) National Aircraft Standard, Airplane characteristics, Airport Planning; Manual For B767-Series, Jan., U.S.

BONNAURE, F., GEST, G., GRVIOUS, A. and UGIE, P., (1977) "A new method of predIcting the stiffness of asphalt paving mixtures." Proc. Assoc. Of Asphalt Paving Technologists (AAPT), vol. 46, San Antonio, Feb.

BRADBURY, R. D., (1938) "Reinforced concrete pavements." Wire Reinforcement Institute, Washington DC.

British Ports Association (BPA), (1983) "The structural design of heavy duty pavement for ports and other industries." , BPA, London.

British Ports Association (BPA), (1996) 'the structural design of heavy duty pavement for ports and other industries." , BPA London.

BRITISH STANDARDS INSTITUTION, (1973) Specification for coated macadam for roads and other paved areas." BS 4987. BSI. London.

BRITISH STANDARDS INSTITUTION, (1985) "Specification for rolled asphalt (hot process) for roads and other paved areas. BS 594. BSI. London.

BRITISH STANDARDS INSTITUTION, (1990) "Methods of test for stabilzed soils." BS 1924, Part1 and 2, London.

BRITISH STANDARDS INSTITUTION, (1990) "Methods of testing soils for civil engineering purposes." BS 1377 Part 9. London.

BRITISH STANDARDS INSTITUTION, (1992) " Guide for structural design of pavements constructed with clay or concrete block pavers." BS7533.

BRITISH STANDARDS INSTITUTION. (1986) "Methods for sampling and testing of mineral aggregates sand and fillers part 2, sampling, size, shape and classification." BS 812, London.

BROWN, S. F. and BRUNTON, J. M., (1986) "An introduction to the analytical design of bituminous pavements." 3rd edition, Univ. of Nottingham, England.

BROWN, S. F. and PEATTIE, K. R., (1974) "the structural design of bituminous pavements for heavy traffic." Proc. Inst. Civil Eugineers. Vol. 57, March, pp. 83-97.

BROWN, S. F., (1978) "Material charateristics for analytical pavement design." Developements in High way Pavemenent Engineering, Applied Science pp.41-92.

BROWN, S. F., (1978) "Mechanical properties of bituminous materials." Journal Inst. of Asphalt Technology, No.25, pp. 10-17.

BULL, J. W. and LUHESHI, Y. B., (1989) "The experimental and finite element analysis of non-square raft type concrete pavements." 3rd. Int. Sym. Num. Models in Geotechnics, Canada, pp. 707-715.

BULL, J. W. and SALMO, S. H., (1987) "The use of the equivalent single wheel load concept for discrete raft type pavements." Computers and Geotechnics, pp. 29-35.

BULL, J. W., (1985a) "The analysis of the interaction between precast concrete pavement units and soils using three dimensional elastic analysis." App. Solid. Mech. Conf, University of Strathclyde, Glasgow.

BULL, J. W., (1985b) "The design analysis of raft type concrete pavements using finite element." Proc. of the 10th. Canadian Congress Applied Mechanics, University of Western Ontario, Canada., Vol. 1, A319.

BULL, J. W., (1986) "An analytical solution to the design of precast concrete pavements." Jour. Num. And Anal. Meth. In Geomechanics, Vol. 10,pp. 115-123.

BULL, J. W., (1990) "Precast concrete raft Units." Blackie and Sons.

BULL, J. W., (1991) "Thickness design of heavy duty precast concrete units using the British Ports Federations pavement design manual." Structural Engineering Review, pp. 31-39.

BULL, J. W., ANANG, R. B. and ISMALL, M. H., (1986) "The conditions of fracture of heavy duty precast concrete pavement units and the relationship between serviceability and ultimate limit state." Proc. 3rd Int. Conf. On Creep And Fracture Of Engineering Matrials and Structure.Institute of Metals.

BULL, J. W., ISMAIL, M. H. H. M. and SALMO, S. H., (1986) "The expermental verification of two new numerica.l clesign metllods for very heavy duty industrial pavements." 2nd.Int. Sym. Num. Models in Geotechnics. Ghent, pp. 569-576.

BULL, J. W., LUHESHI, Y. B. and WOODFORD, C. H., (1993) "The finite element analysis of precast. Concrete pavement units and the laboratory verification for aircraft over-running" 5th. Int. Conf. on Civil an Structural Engineering Computing, Developement in Structural Engineering Computing, Edinburgh , Scotlan, U.K.

BULL, J.W., (1991) "The violation of westergaard's full contact assumption and it's efect on raft unit pavements." Computers and Ceotechnics 12, pp. 133-147.

BULL,J.W and CLARK,J.D., (1991) "Rapid runway and highway repair using precast concrete raft units, Proc. Int. Conf. on Rapidly Assembled structures, Southampton, UK, pp 139-149.

BULL,J.W. and SINGH, A. (1990) " A comparsion between the stresses computed for finite sized precast concrete pavement units using Westergaard s' equations and a numerical design method. Computers and Geotechnics, 9, pp 325-340

BURMESTER, D. M., (1943) "The theory of stresses and displacements in layered system and applications to the design of airport runways." Proc. High Research Board.

BURT, A. and BERKSHIRE COUNTY COUNCIL (BCC), (1986) "M4 Motorway, a composite pavement, the mechanism of failure."Proc. 2nd. Int. Conf. on The Bearing Capacity of Roads and Airfields, 16-18 Sept., Plymouth England.

CAA- LIBYA, (1982)" Construction of new airfield pavement at Tripoli International Airport (TIA) " Maintenance Procedure report, unpublished.

CARLTON, P. F. and BEHRMANN, R. M., (1956) "A model study of rigid pavement behaviour under corner and edge loadings. Proc, 35th Annual Meeting, Highway Research Board.Washington D.C.

chemometric approach." Elsevier, Amsterdam.

CHILDS, L. D., (1960) "Effect of granular and soil cement, sub-bases on load capacity of concrete pavement slabs." Journal of the PCA Research and Dcveleopement Laboratories. Vol. 2,. No. 2,May

CHOU, Y. T., (l981) "Structural analysis copmuter programs for rigid multicomponent pavement strctures with discontinuities- WESLIQID and WESLAYER: program developement and numerical presentations." Technical report, GL-81-6, Report 1, US Army Eng. waterwavs Experiment Station, CE. Vicksbury. Miss.

COOK, C. F., (1980) "An electrical demountable strain transducer." Journal of the British Society for Strain measurement, vol. 16, No. 3, .July, pp 113-119.

CORNELISSEN, H. A. W. and LEEWIS, M., (1986) "fatigue experiments for the design of plain concrete pavements." Workshop on Theoretical Design of Concrete Pavements, Netherlands Centre for Research and contract Standardization in Civil and Traffic Engineering, Epen Netherlands.

CORNELISSEN, H. A. W. and TIMMERS, G., (1981) "Fatigue of plain concrete in uniaxial tension and in alternating tension-compression." Report No. 5-81-7, Stevin Laboratory, Delft University of Technology.

CRONEY, D., (1977) and 2nd. edition (1991) "The design and performance of road pavements." Dept. of the Environment," TRRL,HMSO,London.

DARTER,M.I. , (1977) " Design of zero-maintenance plain jointed concrete pavement : Vol.I- Development of design procedures" Federal Highway Administration, Report No. FHWA-RD-77-111, Washington, D.C.

DAWSON, J. L. and MILLS, R. L., (L970) "Undercarriage effects on rigid / flexible pavements." Proc. lnst. Civil Engineers Aircraft Pavement Design. London, Nov.

DEMINGS, S. N. and MORGAN, S. L., (1987) "Experimental design: a chemometric approach" Elsevier, Amsterdam.

DEPARTMENT OF ENVIRONMENT. (1989) "Design and evaluation of aircraft pavements." Civil Engineering and public works Review, Pt. 1 Dec.,PP 1305-1316, Pt. 2 Jan. 1972,pp.33-40.

DEPARTMENT OF TRANSPORT (I). (1978),Tehnical memorandum, H10/71, London, HMSO.

DEPARTMENT OF TRANSPORT (II). (1978), Tehnical memorandum, H6/78, London, HMSO.

DEPARTMENT OF TRANSPORT, (1976) "Specificatin for road and bridge works." London, HMSO. This now replaced by Departement of Transport Manual of Contract Documents for High works. Volume 1 Specification for highway Works, 1993.

DEPARTMENT OF TRANSPORT, (1986) "Desgin standards for rigid and flexible pavements." This now replaced by Departement of Transport Manual for Roads and Bridges - Volume 7 Pavement Desigin and Maintenance. 1992

DEPARTMENT OF TRANSPORT, (1987), Departmental Standard HD14 / 87, "Structural design of new road pavements." London, England.

DEPARTMENT OF TRANSPORT, (1989) " A guide to airfield pavement design and evaluation." London, HMSO.

DEPARTMENT OF TRANSPORT, (1992) "Specification for highway works." London, UK.

DEPARTMENT OF TRANSPORT, (1993) 'Road design manual." Volume 7, London.

DEPARTMENT OF TRANSPORT, (1994) "Design manual for roads and bridges." Volume 7 HD 26/94, London. UK.

DOMENICHINI, L. and MARCHIONA, A., (1981) "Influence of stress range on plain concrete pavement fatigtue design." Proc. 2nd International Conference on Concrete Pavement Design, Purdue.

DOMENICHINI, L., (1986) "lnfluence of overloads on concrete pavement fatigue life." Workshop on Theoretical Design of Concrete Pavements, Netherlands Centre for Research and contract Standardization in Civil and Traffic Engineering, Epen Netherlands.

DUBROVIN, E. M. et.al., (1962) " Precast reinforced concrete slabs in road construction." Giorodskie Khozayaisto Moskvy. 36, No. 9

EISENMANN, J., (1970) "Bemessung Von Zementbetondecken" Forschungsarbeiten ans des Strassenwesen, No. 82, Luglio.

EMERY, J. A., (1986) "Strengthening of aircraft pavements using concrete blocks." Proc. 2nd. Int. Conf. on The Bearing Capacity of Roads and Airfields, 16-18 Sept., Plymouth England.

FARAGGI,V., JOFRE, C. and KRAEMER, C., (1986) "Combined effect of traffic loads and thermal gradients on concrete pavement design." Workshop on Theoretical Design of Concrete Pavements, Netherlands Centre for Research and Contract Standardization in Civil and Traffic Engineering, Epen Netherlands.

FAXWERTHY P.T., (1991), Aircrat./pavement Interaction. An Integrated System, Proceeclings of the conference, ASCE,4-6 Sept.

FEDERAL AVIATION AUTHORITY (FAA), Department of Transport (1978), Advisory Circular AC 150/ 5320-6C, Airport Pavement Design and Evaluation, Washington DC, July.

FOSTER, C. R., (1972) "Strength of bases and sub-bases." Proc. 3rd. Int. Conf. on the Struc., Design of Asphalt pavements Ann Arbor, Univ. Michigan, pp. 226-232.

FUKUDA, T., (1977) "lnfluence of load contact patterns on stress distribution in concrete pavements." Technology Report. Vol. 42, No. 1. Tohoku University, Japan.

GLUSHKOV, G. I. and RAYEV-BOGOSLOVSKII, B. S. (1970) "Construction and maintenance of air fields." Transporation into English, Moscow Wright-Patterson Air Force Base, Ohio

GOLDBECK, A. T., (1919) "Thickness of concrete slabs." Public Roads Vol. 1. ,No. 12. April.

GORSUCH, R. F., KRUSE, C. G., and JACOBY, G. A., (1962) "Test section of precast, prestressecl concrete slabs on US highway." Conducted at South Dakota State University, Brookings.USA.

HANNA, A. N. et.al. (1976) "Technological review of prestressed pavements" Federal Highway Adminstration. Washington D.C,, FHWA-RD-77-8.

HARGETT, E. R., (1969) "Structral reinforcement for airport pavement." Transportation Engineering Journal. 95, No. TE4.ASCE. pp. 629-637.

HARRIS, A. J., (1956) "Prestressed concrete runways: History practice and theory, Part 1." Airports and Air Transportation, Vol. 10, No. 121 ,London.

HEUKELOM, W. and FOSTER, C. R., (1960) "Dynamic testing of pavements." Journal of Soil Mechanics and Fonudations Division, Vol. 86, No. .5M1, Proc. paper 2368, Feb.

HEUKELOM, W. and KLOMP, A. J. G., (1978) "Consideration of calculated strains at various depths in connection with the stability of ashalt pavements" Proc. 2nd Int. Conf. on the Structural Design of Asphaltic Pavementsl.University of Michigan, Ann Arbor, pp. 158-186.

HIGHWAY RESEARCH BOARD. (1962) "The AASHO road test." Report. 5: Pavement Research ,Special Report 61E, Publication No. 954. Nat. Acad. Sci., Washington DC.

HoSANG, V. A., (1975) "Field survey and analysis of aircraft distribution on airport Davements." FAA, Report FAA-RD- 47-36, NTlS Springfied, Feb.

HoSANG, V. A., (1976) "Field survey and analysis of aircraft distribution on airport pavements." Special Report 175, Proc. FAA, Atlanta, Georgia. 15-17 Nov.

HUDSON,W.R> and SCRIVNER,F.H., (1962) "AASHO Road Test Principal Relationships- Performance with stress, Rigid Pavements. HRB Spec. Rep. 73, pp.227-241.

HUGHES, B. P., (1980) "Limit state theory for reinforcecl concrete design." 3rd. ed.

HULSE, R. and MOSLEY, W. H., (1986) "Reinforced concrete designed by computer."

INTERNATIONAL CIVIL AVIATION ORGANISATION (ICAO). Part 1 2nd edition (1984), Part 2 3rd edition (1991). and part 3 2nd edition(1983) Aerodrome Design Manual, DOC 9157 -AN/901 .Pavement, Montreal.

IOANNIDES, A. M., THOMPSON, M. R. and BARENBERG, E. J., (1985) "The Westergaard's solutions reconsidered." Presented a the Annual Meeting Of The Transportation Research Board, Washington DC, Jan.

ISMAIL, M., (1990) "Research into and the validation of precast concrete pavement units design method." Ph.D. THesis, Department of Cvil Engineeing. Newcastle Upon Tyne University.

JANOO, V. C. and BERG, R. L., (1991) "Performance of airport PCC pavement during spring thaw periods." Aircralt/Pavement Interaction, An Integrated System, Proceeclings of the conference, ASCE. 4-6 Sept., edited by P.T.FAXWERTHY.

JONES, S. A. and IVERSON, J. P., (1971) "Use of precast slabs for the repair of faulted joints in concrete pavements." Federal Highway Administration, Washington DC, Special Report.

KELLEY, E. F., (1939) "Application of the results of research to the structural design of concrete pavement." Public Roads, Vol. 20, No. 5, July; Vol. 20, No. 6, August 1939. Also in Journal of American Concrete Institute,June 1939.

KIYOSHI, O.; HIROKAZU, O.; and KEIICHIRO, S., (1978) "Fatigue failure mechanism of reinforced concrete bridge deck slabs." Proc. Conf. Conducted by the Transportation Research Board, Sept. 25-27, 1978

KNAPTON, J. and BARBER, S. D., (1979)" The behaviour of a concrete block pavement." Proc. Instn. Civil Engineers Part l, Vol. 66. May.

KNAPTON, J. and EMERY, J. A., (1996) "The use of pavers for aircraft pavements." CAA paper 96001, Civil Aviation Authority, London, UK, March 1996.

KNAPTON, J. K., (1986) "The structural design of heavy industrial pavements." Discussion Proc. Inst. Civ. Eng., Part I, April, pp .559-573.

KNAPTON, J., (1985) "The structural design heavy industrial pavements." Proc. Instn. Civil Engineers Part 1. No. 8841, Feb., pp. 179-194.

KNAPTON, J., (1976) " The design of conrete blocks roads." (Cement and Concrete Association, Wexham Springs, 'I'ech. Report 42.515.

KNAPTON, J., (1984) "The structural design of heavy duty pavements for ports and other industries." London, British Ports Authority.

KNAPTON, J., COOK I. D., (1995) " Whole life costs of flexibly bedded clay pavements " Proc. of the forth Int. Masonary Conf., British Masonary Society, No. 7 23-25 Oct. 1995 Vol. 1 pp- 183-187.

KNAPTON, J., NIGEL NIXON and PARTNERS., (1986) "'Ihe structural design and performance of concrete block roads." Proc. 2nd . Int. Conf. On The Bearing Capacity of roads and Airfields, 16-18 Sept., Plymouth England.

KONG, F. K. and EVANS, R. H., (1987) "Reinfoiced and Prestressed Concrete. " 3rd . ed., V. N . R . (UK) .

KREGER, W. C., (1967) "computerized aircraft ground flotation analysis, edge loaded rigid pavement." Reseach Report, No. ERR-FW-572, General Dynamics Corporation, Fort Worth, TX, January.

LARY, J., PETIT R, AND SMALLRIDGE, (1991) "DFW Concrete block pavement taxiway construction " Proc. of Int. Conf. On Aircraft/Pavement Interaction, an Integrated System, ASCE, 4-6 Sept. 1991.

LEDBETTER, R. H. (1976) "effects of dynamic loads on airport pavement" Research in airport pavement, Special Report 175; proc. FAA,Atlanta, Georgia, 15-17 Nov.

LEDBETTER, R. H., ULERY, H. and AHLVIN, R. G., (1972) "Traffic tests of airfield pavements for the jumbo jet." Proc. 3nd. Int. Conf. On the structure design of Asphalt pavements,Ann Arbor, Univ. Michigan, Vol.1, pp. 876-902.

LEEWIS, M. and Van Der MOST, H. E. (1986) "The design of concrete pavement." Proc. 5th. International Symposium on Concrete Road, Aachen.

LEIGH, J. V. and CRONEY, D., (1972) "The current design procedure for flexible pavements in Britain." Proc., 3rd Int. Conf. on the Structural Design of Asphalt Pavements, Ann Arbor, University of Michigan, pp 1039-1048.

LILLEY, A. A. and WALKER, B. J., (1978) "Concrete block paving for heavily trafficked roads and paved areas." Cement and Concrete Association, Wexham Springs, Tech. Report 46.023.

LILLEY, A. A., (1978) "Concrete block pavements for specialised traffic - a design method." Cement and Concrete Association, Wexham Springs, Advisory Document ADS/36.

LOSBERG, A., (1960) "Structurally reinforced concrete pavemens." Doktor-savhandlingar Vid Chalmers Tekniska Hogskola, Gotesborg, Sweden.

LOY, F. and WARREN, M. (1991) "Pavement design for the new Denver International Airport (DIA) " Proc. of Int. Conf. on Aircraft/Pavement Interaction, an Integrated System, ASCE, 4-6 Sept. 1991.

MAIDEL, V. G. and TIMOFEEV, A. A., (1962) " Precast concrete roads and footways." Giorodskie khozayaisto Moskvy,26(3), pp. 26-29.

MAYHEW, H. C. and HARDING, H. M., (1987), Transport and Road Research Laboratoly, Research Report RR87, "Thickness design for concrete roads." Department of Transport , London, England.

MEDNIKOR, I. A., MALCHANOV, Y. A. and GORODELSKII, L. V., (1974) "Analysis and jointing of polygonal round slabs." Osnovaniya. Fundamently i Mekhanika Giruntov, Vol. 11, No. 5, Translated by consultants Bureau. New York.

MELLINGER, F. M. and AHLVIN, R. G., (1959)" Pavement design for commercial jet aircraft." ASCE, Jounal of Air Transport Division, Vol. 85. NO. AT2, May, pp. 29-43.

MICHIGAN UNIV., (1977), Proc. 4th. lnt. Conf. on the Struc., Design of Asphalt Pavements, Ann Arbor,vo. 1 and 2.

MITCHELL, J. K., (1976) "The properties of cement stabilized soils in matrials and methods for low cost road, rail, and reclamation works." Univ. of south Wales, Sydney, Australia., Sept., pp .365-404.

MONISMITH, C. L., (1978) "Consideration In Airport Pavement Managementt." Dept. Of Civil Engineering and Inst. Of Transport Studies, Univ of California , Berkeley, U.S.

MONTGOMERY, D. C., (1984) Design and analysis of experiments." 2nd ed ., john Wiley & sons, New York.

MUIR, I., (1996) "The use of concrete segmental paving for construction of an aircraft landing airstrip on Thevenard Island, Western Australia." Proc. Of the 5th Int. Conf. on concrete Block Paving, Tel-Aviv, June 1996.

NILSON, A. H. and WINTER, G., (1979) " Design of concrete structures." 10th ed.

ODEMARK, N., (1949) "Investigations to the elastic properties of the soil and design of pavements to the theory of elasticiy." Stockhlolm.

OKAMOTO, P. A. and PACKARD, R. G., (1989) "Effect of high tyre pressure on concrete pavement performance." Proc. 4 th Int. Conf. On Concrete Pavement Design and Rehabilitation, Purdue University, India 47907 , USA, pp. 61-74.

OLDER, C., (1924) " Highway research in Illinois."Trans .. ASCE. Vol 87. Also in Proc. , ASCE, February 1924.

PACKARD, R. G., (1967) "Computer program for aircraft pavement design." Portland Cement Association.

PACKARD, R. G., (1973) "Design of concrete airport. pavement.." Engineering Bulletin, Portland Cement. Association PCA.

PACKARD, R. G., (1974) "Fatigue concepts for concrete aircraft pavement design." Journal of Transport Engineering.

PAFEC Ltd., PAFEC 75, (1978) Theory Results, Pafec Ltd. Nottingham.

PATTERSON, W. D. O., (1976) " Functional pavement design for container terminals." Proceedings, Australian Road Research Board , Vol. 8, part 4.

PEATTIE, K. R., (1975) " flexible pavement design procedures in Europe." Proc. Amer . Soc. Civil Engineers. Volume 103. No. TE1, June.

PICKETT, G. and RAY, G. K., (1951) "Influence charts for concrete pavements." Trans. ASCE, Vol. 116.

PICKETT, G., (1946) "Concrete pavement design - Appendix III. A study of stresses in the corner region of concrete pavement slabs uder large loads."

PORTLAND CEMENT ASSOCIATION, (1966), Thickness Design For Concrete Pavements.

PORTLAND CEMENT ASSOCIATION, (1969), Suggestecl Specifications for Soil Cement Base Course, Skokie, IL.

Portland Cement Association, 1951.

PORTLAND CEMENT ASSOCIATION. (1969), Soil Cement Construction Handbook , Skokie, IL.

PORTLAND CEMENT ASSOCIATION. (l971). Soil Cement Laboratory Handbook, Skokie, IL.

POWELL, W. D., POTTER, J. F., MAYHEW, H. C. and NUNN, M. E., (1984) "The structural desin of bituminous roads." TRRL Report LR1132.

pp. 279-291.

PRETORIUS, P. C., (1969) "Design consideration for pavement containing soil cement bases." Ph.D. Thesis. Berkeley, California.

RADA, G.R. and WITCZAK, M.W., (1991) " Aircraft traffic mix analysis Damage factors and coefficients." Aircraft/Pavement, Interaction. An Integrated System, Proceedings of the conference, ASCE, 4-6 Sept., edited by P.T.FAXW-ERTHY.

REDLAND AGGREGATE LIMITED, (1996), Redland Precast Division, Personal communication, England, UK.

ROAD RESEARCH LABORATORY, (l970) "A guide to the structural design of pavements for new roads." Road Note 29 (3rd Ed.) HMSO. London.

ROAD RESEARCH LABORATORY. (1970) "A guide to the strctural design of pavements for new roads." 3rd edit!ion, London, HMSO, Road Notes 29. This now replaced by Transport Research laboratory Report, LR 1132 and Research Report 87 and Department of Transport Design Manual for Roads and bridges, volume 7 HD 26/94.

ROLLINGS, R. S. and CHOU, Y. T., (1981) "precast concrete pavements." Geotechnical Laboratory , US Army Eng. , Waterways Experiment Station.

SALMO, S. H., (1990) "Precast concrete pavements used in port areas." Ph.D. Thesis, Department of Civil Engineering , Newcastle Upon Tyne University

SCOTT, R. F., (1981) "Foundation analysis." Prentice-Hall.

SHAHIN,M.Y., (1994) "Pavement management for airports, roads and parking Lots, Chapman & Hall New York and London.

SHAHIN, M. Y., (1994) "Pavement management for airports, roads, and parking Lots, Chapman & Hall New York and London

SHELL INTERNATIONAL PETROLEUM Co. Ltd., (1978) "Shell pavement design manual." London.

SONODA, K. and HORIKAWA, T., (1982) " fatigue strenght of reinforcement concrete slabs under moving loads." Procs. Internatioal Association for Bridge and Structural Engineering (IABSE), Colloquium, Lausanne.

TAYLOR, S. N., (1982) "Aspects of rigid pavement design with particular reference to stelcon slabs." Ph.D Thesis, Newcastle Upon Tyne University.

THOMLINSON, J., (1940) "Temperature variations and consequent stresses produced by daily and seasonal temperature cycles in concrete slabs." Concrete and Construction Engineering, Vol. 35.

THOMPSON, M. R., (1966) "Shear strength and elastic properties of lime-soil mixtures." HRB, Highway Research, Record 139, pp. l-14.

THOMPSON, M. R., BARENBERG, E. J., IOANNIDES, A. M. and FISCHER, J. A., (1983) "Developement of a stress dependent finite element slab model." US Air Force Office Of Scientific Research, Report No. TR-83-1061, Air Force Systems Command, USAF, Bolling AFB. D. C. 20332, May.

TRANSPORTATION RESEARCH BOARD., (1976) "Research into airport pavement systems." Special Report 175, Proc. FAA, Atlanta, Georgia. 15-17 Nov.

U.S. ARMY CORPS OF ENGINEERS., (1958), Flexible Airfield Pavements. EM1110-45-302, part 12.

VAN de LOO, P. J., (1978) "The creep test: a key tool in asphalt mix evaluation and in the prediction of rutting" Shell Int. Pet. Co. Ltd., London.

VAN Der POEL, C., (1954) "A general system describing the visco-elastic properties of bitumens and its relation to routine test data." Journal App. Chem. 4, Pp. 221-236

VESIC, A. C. and SAXENA, S. K., (1969) "Analysis of structural behaviour of road test rigid pavements." Highway Researd Record No. 291.

VESIC, A. S. and SAXENA, S. K., (1970) "Analysis ol structural behaviour of AASHO road test rigid pavements." NCHRP, Report 97.

WALSH, I. D. and GARRETT, C., (1984) "A comparative study of concrete paving blocks." Proc. 2nd Int. Conf. Concr. Block Paving. Delft, University of Technology, 1984

WESTALL, W. G., (1966) "Concrete overlays on asphalt pavements" Highway Research News (22), Highway Research Board, Feb., pp.52-57.

WESTERGAARD, H. M., (1926) "Stresses in concrete pavements computed by theoretical analysis." Public Roads Vol. 7, No. 2, April 1926. Also in Highway Research Board, Proceedings, 5th Annual Meeting (1925, published 1926), Part I, under the title "Computation of stresses in concrete roads."

WESTERGARRD, H. M., (1923) "Om beregning of plader paa elastik under-lag med saerlight henblik paa sporgsmaalet om spaedinger i betonveje" (On the design of slabs on elastic foundation with special reference to stresses in concrete pavements) Ingenioren. Vol. 32. Copenhagen.

WESTERGARRD, H. M., (1947) "New formulae for stresses in concrete pavements of airfields." ASCE.Transactions, Vol. 113, 1948. Also in ASCE Proc., Vol. 73, No. 5 May.

WESTERGARRD, H. M., (1937) "What is known of stresses." Engineering News Record,.January.

WESTERGARRD, H. M., (1939) "Stresses in concrete runways of airports.' Proc., 19th Annual Meeting, Highway Research Board, Washington D.C. Also in "Stresses in concrete runways of airports." Portland Cement Association, Chicago, IL, December 1941.

WILLIAMS, R. J., (1988) "Maintaining the roads to carry the loads." J. Inst. Highways and Transport 35, No. 4, April,pp. 28-35.

WITCZAK, M. W., (1973) "Prediction of equivalent damage repetitions for aircraft traffic mixtures for full depth asphalt airfield pavements." Proc. AAPT. Vol, 42, pp. 277-299.

WITCZAK, M. W., (1974) "Asphalt pavement performance at Baltimore Washington International Airport." Asphalt Institute, College Park; Res. Report. 74-2.

YODER, E. J. and WITCZAK, M. W., (1975) "Principles of pavement design." 2nd edition, New York, Wiley.

Appendix A

THE EXPERIMENTAL AND FINITE ELEMENT ANALYSIS OF NON-SQUARE RAFT UNIT TYPE CONCRETE PAVEMENTS

A brief description of a paper by Bull and Luheshi (1989) published in the proceedings of the 3rd International Symposium Numerical Models in Geomechanics (NUMOGIII), Niagara Falls, Canada:

ABSTRACT:

A series of research papers have been published since 1985, describing the numerical and laboratory research into precast concrete raft unit type pavements. This paper reports on the current work into centrally loaded rectangular raft unit type pavements ranging in length from 2.0 metres to 2.44 metres and in width from 0.608 metres to 2.44 metres. The effect of adding steel reinforcement to the bottom and the top and bottom of the raft units is also investigated. The paper concludes, that the square raft is the most efficient rectangular shape in terms of the number of load applications it can sustain and proving reinforcing steel in the top and bottom of the raft unit increases the raft unit life more than reinforcing steel placed only in the bottom. Laboratory test results designed to validate the numerical design method that developed by Bull (1986), are also included.

INTRODUCTION:

The use of precast concrete raft type pavement units ranging in size from 10.0 metres by 2.29 metres down to 300mm square is a frequently used method of road and pedestrian surfacing. With the increasing requirement of the operators of very heavy duty industrial pavements to continuously reorganise their pavements to accommodate changing storage and transport patterns, it is becoming necessary to purchase ``off the shelf'' precast concrete raft units in a variety of rectangular sizes. The raft units are also used in tunnels and mines and are being investigated for their possible use in relation to the Channel Tunnel Project where the fast track laying of pavements and immediate access to the services laid beneath them, has large financial implications.

In the early 1980's a major research effort was initiated at the University of Newcastle upon Tyne to research and develop design methods for square precast concrete

pavement units ranging in size from two metre square down to 300mm square, subjected to vehicular over-run.

CONCLUSIONS:

The conclusions that were drawn for a raft unit pavement, centrally loaded with a single, variable, repeatedly applied load are:

(i.) the shape of the raft unit affects the life of the raft unit. The relationship between the raft unit shape and its life has been determined,

(ii.) the affect of introducing steel bar reinforcement is to increase the life of the raft unit. Proving reinforcing steel in the top and the bottom of the raft unit increases the raft unit life more than reinforcing steel placed only in the bottom, and

(iii.) the available laboratory test results for the 600mm × 2440mm by 140mm thick raft unit confirm the proposed design method and provide a means of including design life variations related to the applied load contact pressure. Further research is proceeding into alternative single and multiple wheel load positions. Further laboratory validation of the design method on non-square raft units is proceeding.

Appendix B

THE FINITE ELEMENT ANALYSIS OF PRECAST CONCRETE PAVEMENT UNITS AND THE LABORATORY VERIFICATION FOR AIRCRAFT OVER-RUNNING

A brief description of a paper by Bull, Luheshi, and Woodford (1993) was published in the proceedings of the 5th. International Conference on Civil and Structural Engineering Computing (CIVIL-COMP93), Edinburgh, Scotland.

ABSTRACT:

Precast concrete pavement units (raft units), reinforced with steel bars have been used for road pavement surfacing and for surfacing heavy duty industrial areas. The industrial areas included ports used for the trans-shipment of containers and storage areas for heavy industrial materials. With the use of raft units for aircraft hard standing and for temporary highways, the UK Ministry of Defence initiated research into their use for rapid runway repairs. Part of this research has been reported elsewhere, but another part led to further investigations. This paper reports on some of those further laboratory and numerical investigations and concludes that; fibre only reinforcement should not be used, increasing the amount of steel bar reinforcement increases raft unit life, increasing raft unit thickness increases the raft unit life more than the design method Bull (1986) predicts, the use of steel angle around the top edges of the raft unit increases raft unit life, and some form of uplift restraint on the raft unit should be added. Further, the way in which a movable load traverses the raft unit effects raft unit life and failure mechanisms.

INTRODUCTION:

The purpose of the laboratory experimental programme was to clarify the fatigue life and failure mechanisms of the raft units and provide the laboratory data for the raft unit design method. For this purpose, the experimental programme was divided into two parts. Part one consisted of eighteen tests for the twin wheel load, divided into four modules: module M1, five tests to investigate the effect of raft unit size, module M2, three tests to investigate raft unit reinforcement, module M3, two tests to investigate raft unit thickness and module M4, two tests to investigate the effect of the steel angle around the top edges of the raft unit. Part two consisted of seven single wheel load tests which with module M1, is not discussed in this paper.

The experimental work was performed in the Heavy Structures Laboratory of the University of Newcastle upon Tyne. The test arrangement was shown in Fig. 1 and 2.

The raft units were placed on a 50mm thick sand layer to ensure raft unit bedding. Under the sand layer was a granular sub-base 750mm thick and a sub-grade 100mm thick. Concrete cubes were taken to find the raft unit concrete compressive strength for the fatigue calculations. High strength reinforcing steel with a series of reinforcement arrangements as described in Table 2 was used. Further, some raft units were manufactured with a steel angle frame around their top edges. The steel angle frame was anchored into the concrete and welded into the main raft unit reinforcement. Initially the steel angle frame was incorporated to prevent concrete spalling if the raft unit were to be subject to impact. However, from the test observations, the steel angle frame had the additional benefit of increasing raft unit fatigue life.

CONCLUSIONS:

(i.) The use of only fibre reinforcement is not recommended as the raft unit breaks into pieces.

(ii.) Increasing steel bar reinforcement increases raft unit life, until the bar itself breaks.

(iii.) Increasing raft unit thickness increases the raft unit life, to a greater extent than the design method predicts.

(iv.) The use of steel angle around the top edges of the raft unit increases raft unit life by not allowing the raft unit to break into pieces.

(v.) Some form of uplift restraint on the raft unit should be added. Allowing the raft unit to lift of the bedding layer increases the stress on the lower layers, increases the surface displacements and reduces the life of the pavement layers. The effect on the raft unit life depends upon the location of the load. For an edge load, the stress is reduced by about 25 per cent. This latter effect is the subject of further research.

(vi.) The way in which the load traverses the raft unit effects raft unit life and the failure mechanism.

The results presented in this paper are preliminary. When the full laboratory test program results and the computer analysis of the laboratory tests are available a more rigorous comparison can be made. From the comparison will flow a more refined design method which will be subsequently published.

Appendix C

DESIGN EXAMPLES

Design Examples Relating Particularly To Chapter Seven.

The following test model configurations used in this thesis were described in detail in Chapter Four. These models were used as design examples to demonstrate the design methods described in Chapter Three, namely the design methods proposed by the BPA, Ackroyd, Bull and Annang, Bull and Ismail. The author's experimental results were compared with these design methods and were used to verify the original design method proposed by Bull (1986). The basic details of the pavement layers were shown in Chapter Four, and the data required in the design examples were listed in Table C.1. It was decided that it was only necessary to show one calculation for the three modules (i.e. 8 tests) to demonstrate the design method. Therefore, RS-14-2/D (i.e. RS2) in Module M1 was chosen. In Chapter 7, Section 7.7, the method for predicting the fatigue life of raft units was described based on the test results. The experimental number of load repetitions and the load repetitions predicted by the original design method proposed by Bull (1986) were discussed and used to validate the Bull method [see Chapter 7, Section 7.7 and 7.2].

The calculation procedures for the Bull and Annang's design method and the modified Bull's design method were based on the original method proposed by Bull, (1986). The original method contained twenty tables which showed the results obtained when using the F.E.M. to investigate the effects of the various pavement parameters on concrete stress and vertical sub-grade stress. Therefore, in the following calculations, the appropriate tables for the calculations will be referred to rather than included in the thesis.

Calculation Procedures.

(a.) The Design Method Proposed By Bull:

Section A: Design PUS = $2177.9/N^{0.25}$ assume N = 750 cycles	DPUS 416.17
Section B: Not Applicable	
Section C: Grade of concrete f_c = 65 MPa	PUS % 8.626
Section D: Load on each wheel 225N $\frac{225}{10} \times$PUS % = 194.09	PUS (A) 194.09
Section E: Load conditions Two loaded wheels 0.865m. apart, the alteration value = 1.1423 2×PUS(A)×1.1423 = 443.42	PUS(C) 443.42
Record the largest of the PUS values from PUS(A) to PUS(C) and call it PUS(I)	PUS(I) 443.42
Section F: Alterations due to soil conditions	
Section G: Sub-grade CBR 2% Value of PUS -0.085 Alteration in PUS = PUS(I)×-0.085	PUS (K) –37.69
Section H: Sub-grade thickness = 0.3m. Value of PUS -0.03 Alteration in PUS = PUS(I)×–0.03	PUS(L) –13.3

Section I: Determine the PUS value to the site conditions and the load PUS value = PUS(I) + PUS(K) + PUS(L) = PUS(M)	PUS(M) 392.43
Section J: Determine the difference between the design PUS and the values due to the site and load conditions. PUS value = PUS(M) – DPUS = PUS(N) = 392.43 – 416.17 = –23.74 DPUS is greater than PUS(M), therefore the standard design of the raft pavement is satisfactory.	PUS(N) –23.74
Section K: Sub-base The raft pavement design which can be altered by the designer for the most suitable sub-base type. The sub-base in the models Granular Type 1 sub-base CBR 40.77% Value of alteration –0.055 Alteration in PUS = PUS(I)×–0.055	PUS(O) –24.39
Section L: Sub-base thickness = 0.75m. Value –0.147 Alteration in PUS = PUS(J)×–0.147	PUS(P) –65.18
Section P: Alteration in PUS due to Type 1 sub-base Alteration in PUS = PUS(O) + PUS(P)	PUS(T) –89.57
Section R: Sand bedding layer 50mm. The raft pavement is not covered, value 0.00 Alteration in PUS = PUS(I)×0.00	PUS(V) 0.00

Section S: Steel reinforcement - top and bottom Area of reinforcement = 142mm^2/m, value 0.00 Alteration in PUS = PUS(I)×0.00	PUS(X) 0.00
Section T: Raft size 2000×2000mm., value 0.00 Alteration in PUS = PUS(I)×0.00	PUS(Y) 0.00
Section U: Raft thickness 140mm., value 0.100 Alteration in PUS = PUS(I)×0.100	PUS(Z) 44.342
Section V: Alteration in PUS actually achieved PUS(T) + PUS(V) + PUS(X) + PUS(Y) + PUS(Z) –89.57 + 0.00 + 0.00 + 0.00 + 44.342	PUS(ZA) –45.23
Section W: To check designed PUS PUS(M) + PUS(ZA) 392.43 + (–45.23) = 347.2 Hence, the number of cycles that the raft can sustain before maintenance is required. $N_{min} = \frac{22.5 \times 10^{12}}{[PUS(ZC)]^4} = 1548$ cycles $PUS(ZC) \times \left[\frac{PUS(C)}{PUS(I)}\right] = 347.2$ Therefore; $N_{max} = \frac{22.5 \times 10^{12}}{[PUS(ZD)]^4} = 1548$ cycles Therefore, N = 1548 cycles for 2 point load of the design load of 450KN	PUS(ZC) 347.2 PUS(ZD) 347.2

(b.) The Design Method Proposed By Bull And Annang:

Bull's design method was developed on the assumption that the maximum applied contact pressure was less than 2MPa. Annang used the ultimate limit state criterion, and introduced Equation C.2 (Bull et al., 1986), which was produced from the original formula C.1, developed by Heukelom and Klomp (1978).

$$N_w = N_m \left(\frac{W_m}{W_w}\right)^{3.75} \left(\frac{P_m}{P_w}\right)^{1.25} \qquad (C.1)$$

$$N_{\exp} = N_{cal} \left(\frac{P}{0.875}\right)^{C} \qquad (C.2)$$

where,

N_{exp} = Expected no. of cycles at which the ultimate limit state is reached.

N_{cal} = The calculated no. of cycles from Bull's design method.

P = Contact pressure (N/mm^2).

C = Constant which is a function of P.

0.875 = A basic pressure to be consistent with the value used to derive the equation.

By incorporating the C-P chart and the modified formula (Eq. C.2) into the design example in Bull's design method, then the actual number of cycles at the ultimate state is;

P = applied contact pressure = 5.625 (N/mm^2)

N_{cal} = 1548 cycles

C = constant, using C-P chart = 1.5

hence;

N_{exp} = 25,237 cycles.

(c.) The Design Method Proposed By Ismail:

A similar design method to the one proposed by Bull has been developed by Ismail (1990), in which the contact area was included and the type of PAFEC element was different to that used by Bull (1986). As a result, the alterations in PUS and SGBP due to sub-base CBR, raft thickness, and concrete strength have been changed slightly. The calculation procedures of Ismail's method follow Bull's procedures for calculating the load cycles but with reference to the modified design charts produced by Ismail.

Applying the contact area results into the design example in Ismail's method, the life expectancy was:

$$N_{exp} = N_{cal}\left[\frac{\sigma_1}{\sigma_2}\right]^4$$

where,

N_{exp} = The expected fatigue life.

N_{cal} = The calculated no. of cycles using Ismail's design method.

σ_1 = Max. concrete stress PUS due to a certain loading position, centre, corner or edge.

σ_2 = Concrete stress due to pressure load (σ_1 – %Alteration*σ_1).

hence ;

$N_{exp} = 33495*\left[\frac{0.44}{0.43}\right]^4$

= 36721 cycles.

(d.) British Ports Association Design Method:

The BPA design method was based on a concrete strength of 30N/mm^2. The concrete strength of the raft units tested was 65N/mm^2. Therefore a corresponding line of 65N/mm^2 must be drawn in Chart "B" of the BPA design manual which was almost the same as the line for fibre reinforcement in the chart. This line represented the horizontal strain, by using the following equation [see Section 3.5, Chapter 3]:

$$E_h = \frac{f_c \times 993500}{6 \times E_b^{1.022} \times N^{0.0502}}$$

where,

E_h = allowable concrete horizontal tensile strain (microstrain).

$E_b = 16800 \times f_c^{0.25}$

f_c = concrete compressive strength = 65 N/mm^2 therefore:

E_b = 47702 N/mm^2

N = Number of load repetitions.

Due to the limitations of the charts for high loads, the backward calculation, for the thickness of the tested raft models was required and entered onto the appropriate charts. This calculation was not possible. Therefore, it was substituted by the experimental number of load cycles for all the tests in order to obtain the corresponding allowable concrete horizontal tensile strain E_h enabling the equivalent raft unit thickness to be read from the charts. These procedures were carried out at each loading position P1, P2, P3, and P4 and the maximum concrete thickness was selected.

Using the E_b value of $E_b = 16800 \times 65^{0.25} = 47702$ N/mm^2 with the number of repetitions 10^4 to 10^8 as the limiting values, the line corresponding to 65 N/mm^2 grade concrete could be drawn on Chart "B".

From the data listed in Table C.1, the PAWL value can be calculated as follows:

$$PAWL = 2 \times \left[\frac{22.5 \times 1000}{12000}\right]^{3.75} \times \left[\frac{5.625}{0.8}\right]^{1.25}$$

$$PAWL = 2 \times 10.56 \times 11.45 = 241.824$$

Using Table 2.5 of the BPA design manual (BPA, 1983), the Load Classification Index L.C.I. is "H".

The experimental number of load cycles for test RS-14-2/D at loading position P1 = 14489 cycles.

Therefore $$E_h = \frac{65 \times 993500}{6 \times 47702^{1.022} \times 14489^{0\,0502}}$$

$$= \frac{178.02}{14489^{0.0502}} = 110.05 \text{ N/mm}^2$$

From Chart 42 in the BPA manual, the design raft unit thickness, h = 300mm.

Appendix D

THE COMPUTER PROGRAMME FOR THE NONE-DIMENSIONAL EMPIRICAL DESIGN MODEL

```
      PROGRAM FATIGUE
      REAL Q,FC,ST,A,K,P
      REAL NMIN,NMAX,NP
      CHARACTER*16 , OUTFN
1      WRITE(6,*)"FATIGUE LIFE"
      READ(5,*) NMIN
      WRITE(6,*)"PREVIOUS FATIGUE LIFE"
      READ(5,*) NP
      WRITE(6,*)"APPLIED LOAD (kN)"
      READ(5,*) Q
      WRITE(6,*)"STRENTH OF CONCRETE (kN/m2)"
      READ(5,*) FC
       WRITE(6,*)"STRENTH OF STEEL (kN/m2)"
      READ(5,*) ST
      WRITE(6,*)"CONTACT AREA (m2)"
      READ(5,*) A
      WRITE(6,*)"MODULUS OF SUBGRADE REACTION (K) (kN/m3)"
      READ(5,*) K
      WRITE(6,*)"CONTACT PRESSURE (P) (KN/m2)"
      READ(5,*) P
      WRITE(6,*)"ENTER OUTPUT FILENAME"
      READ(5,*) OUTFN
      OPEN(UNIT=13 , FILE=OUTFN)
      WRITE(6,*)
      WRITE (13,*), " PREVIOUS FATIGUE LIFE(million)=",NP
      NMIN=NMIN-NP
      NMAX=1.15*NMIN
      WRITE (13,*), " MINIMUM FATIGUE LIFE (million)=",NMIN
      WRITE (13,*), " MAXIMUM FATIGUE LIFE(million)=",NMAX
      CALL FAT(NMIN,NMAX,Q,IM,FC,ST,A,K,P)
      IF (IM.EQ.1) THEN
      WRITE (13,*), " TRY ANOTHER FATIGUE LIFE "
```

```
GOTO 1
ENDIF
END
SUBROUTINE FAT(NMIN,NMAX,Q,IM,FC,ST,A,K,P)
INTEGER IW,IR,IH,IM
REAL Q,W,R,H,FC,ST,A,K,P
REAL ZN,NMIN,NMAX
IM=0
W=0.25
R=0.000085
H=0.12
ZN=-16*W**5+0.33*(10*P/H/K)**5 + 36.8*(10*R*ST*/Q)**4 +
+4.22*(Q/A/FC)**(-.5)
IF (ZN.GT.NMAX) THEN
WRITE (13,*), " MINIMUM PARARMETERS ARE USED"
WRITE (13,*), "FATIGUE LIFE (million)=",ZN
WRITE (13,*), "APPLIED LOAD (KN)=",Q
WRITE (13,*), "ASPECT RATIO=",W
WRITE (13,*), "AREA OF STEEL (m2/m)=",R
WRITE (13,*) ,"THICKNESS (m)=",H
WRITE(6,*)"STRENTH OF CONCRETE (kN/m2)",FC
WRITE(6,*)"STRENTH OF STEEL (kN/m2)",ST
WRITE(6,*)"CONTACT AREA (m2)",A
WRITE(6,*)"MODULUS OF SUBGRADE REACTION (K) (kN/m3)",K
WRITE(6,*)"CONTACT PRESSURE (P) (KN/m2)",P
IM=1
RETURN
ENDIF
I=0
DO 30 IW=25,100,5
DO 20 IR=85,345,10
DO 10 IH=12,25,1
W=IW/1E2
R=IR/1E6
H=IH/1E2
ZN=-16*W**5+0.33*(10*P/H/K)**5 + 36.8*(10*R*ST*/Q)**4 +
+4.22*(Q/A/FC)**(-.5)
```

```
      IF  (ZN.GE.NMIN.AND.ZN.LE.NMAX) THEN
      I=I+1
      WRITE(13,*),"CASE NO=",I
      WRITE (13,*), "FATIGUE LIFE (million)=",ZN
      WRITE (13,*), "APPLIED LOAD (KN)=",Q
      WRITE (13,*) ,"ASPECT RATIO=", W
      WRITE (13,*) ,"AREA OF STEEL (m2/m)=",R
      WRITE (13,*) ,"THICKNESS m=", H
      WRITE(6,*)"STRENTH OF CONCRETE (kN/m2)",FC
      WRITE(6,*)"STRENTH OF STEEL (kN/m2)",ST
      WRITE(6,*)"CONTACT AREA (m2)",A
      WRITE(6,*)"MODULUS OF SUBGRADE REACTION (K) (kN/m3)",K
      WRITE(6,*)"CONTACT PRESSURE (P) (KN/m2)",P
      ENDIF
   10   CONTINUE
   20   CONTINUE
   30   CONTINUE
      RETURN
      END
```

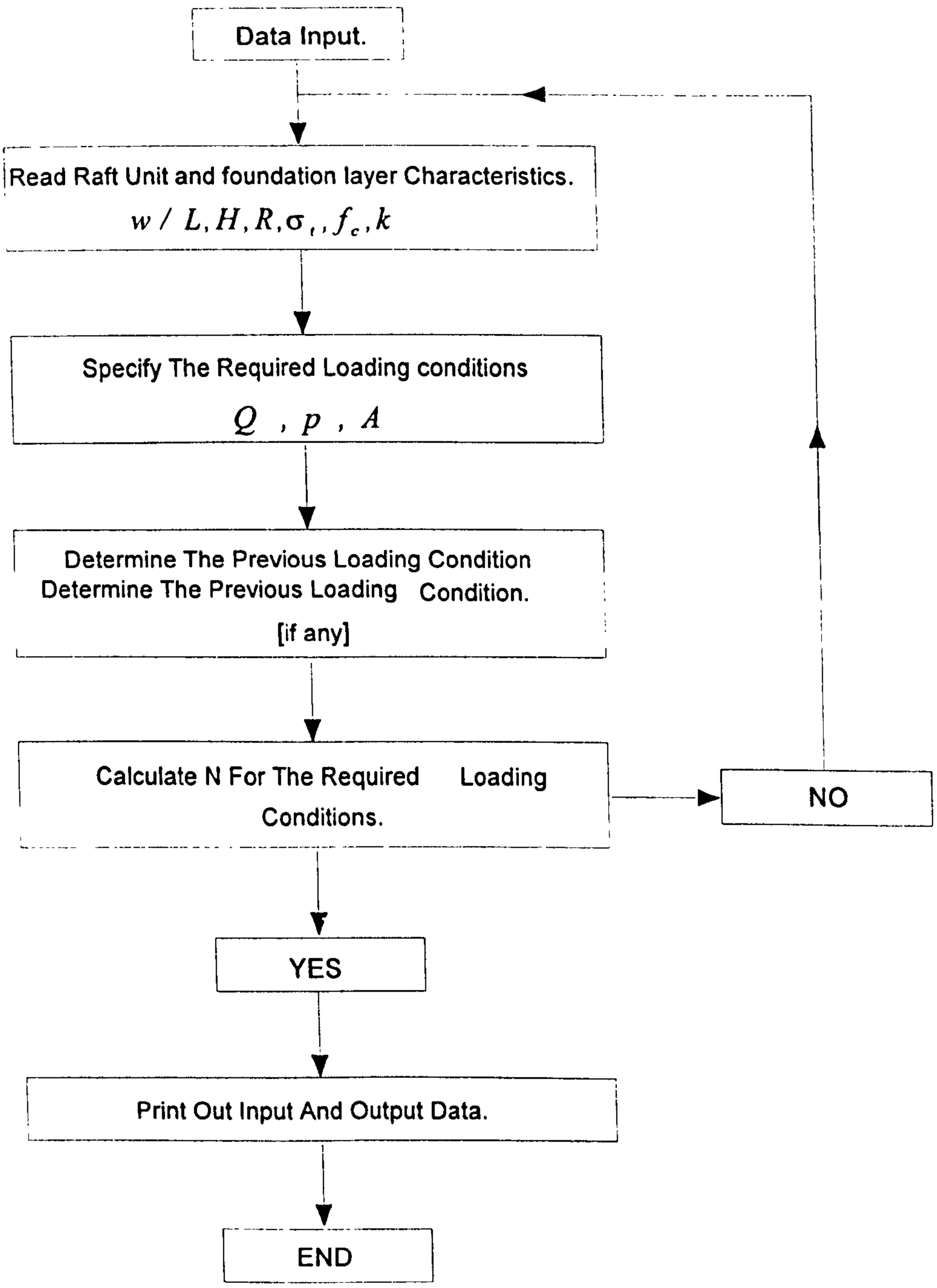

Design Flow Chart

TABLE C.1 : THE CONSTRUCTION AND PROPERTIES OF THE TESTED MODELS.

Modules	M1					M2			M3	
Raft Units	R6	R9	R12	RR	RS2	RS1	RS2	RSF	RS1	RS7
Concrete strength (MPa)	65	65	65	65	65	65	65	65	65	65
Raft size (m)	2.4×0.6	2.4×0.9	2.4×1.2	2.3×1.5	2.0×2.0	2.0×2.0	2.0×2.0	2.0×2.0	2.0×2.0	2.0×2.0
Raft thickness (mm)	140	140	140	140	140	140	140	140	140	175
Reinforcement mm^2/m (top & bottom)	142	142	142	142	142	283	142	240	283	283
Load (kN)	450	450	450	450	450	450	450	450	450	450
Contact area (m)	0.2×0.2	0.2×0.2	0.2×0.2	0.2×0.2	0.2×0.2	0.2×0.2	0.2×0.2	0.2×0.2	0.2×0.2	0.2×0.2
Contact pressure (MPa)	5.625	5.625	5.625	5.62	5.625	5.625	5.62	5.62	5.62	5.62
Sub-base CBR (%)	30.85	34.11	35.81	38	40.77	46.04	40.77	43.73	46.04	51.12
Sub-base thickness (m)	0.75	0.75	0.75	0.75	0.75	0.75	0.75	0.75	0.75	0.75
Sub-grade CBR (%)	2	2	2	2	2	2	2	2	2	2
Sub-grade thickness (m)	0.3	0.3	0.3	0.3	0.3	0.3	0.3	0.3	0.3	0.3
Sand CBR (%)	5	5	5	5	5	5	5	5	5	5
Sand thickness (mm)	50	50	50	50	50	50	50	50	50	50

TABLE 2.1 : AIRCRAFT CHARACTERISTICS FOR DESIGN AND EVALUATION OF PAVEMENTS

Aircraft Type	Maximum Take-off Weight Kg	% Load on Nose Wheel	Wheel Arrangement	MAIN LEGS OF LANDING GEAR							
				Load on Each Leg Kg	Contact Pressure MN/m^2	Contact Area cm^2	Wheel Spacing				Additional Data for Complex Arrangements
							S	S_T	S_D	d	
A300 B4	150.500	11.00	DT	66.773	1.26	1.294	93	140	168.1	63.16	
A300-600	165.900	12.87	DT	72.276	1.25	1.412	92.7	139.7	-	-	
B707-320C	151.480	4.3	DT	72.558	1.26	1.440	88	142	167.1	56.52	
B720 B	106.220	4.0	DT	50,985	1.00	1.250	81	124	148.1	51.67	
B727-200	94.318	5.0	D	44.801	1.42	1.586	86.5	-	-	52.96	
B737-200	50.260	6.5	D	23.494	1.04	1,130	78	-	-	50.12	
B747C	351.785	3.6	COM	84,780	1.30	1.618	112	147	184.8	78.63	
B767-200ER	159,700	12.27	DT	70,050	1.24	1,432	114	142	-	-	
Concorde	176,450	6.0	DT	82.933	1.27	1.595	68	167	180.3	34.87	
DC-3	11.420	0.0	SIN	5.709	0.31	1.784	-	-	-	-	
DC-4	33.130	0.0	D	16.565	0.52	1.563	78	-	-	45.21	
DC-6A1B	48.520	12.0	D	21.350	0.73	1.443	78	-	-	46.49	
DC-8-55	147.400	5.0	DT	70.015	1.28	1.336	76	140	159.3	45.68	

TABLE 2.1 (cont.) : AIRCRAFT CHARACTERISTICS FOR DESIGN AND EVALUATION OF PAVEMENTS.

Aircraft Type	Maximum Take-off Weight Kg	% Load on Nose Wheel	Wheel Arrangement	MAIN LEGS OF LANDING GEAR							
				Load on Each Leg Kg	Contact Pressure MN/m^2	Contact Area cm^2	Wheel Spacing				Additional Data for Complex Arrangements
							S	S_T	S_D	d	
DC-8-63	161.060	3.0	DT	78.114	1.38	1.415	81	140	161.7	49.79	
DC-9-32	49.030	4.5	D	23.413	1.05	1.094	64	-	-	36.56	
DC-9-41	51.680	3.5	D	24.937	1.12	1.094	66	-	-	38.56	
DC-10-10	195.000	6.0	DT	91.652	1.23	1.833	137	163	212.9	101.48	
DC-10-30	251.784	5.8	COM	97,248	1.14	2.096	137	163	212.9	99.02	Classification based on wing DT. Main U/C induced central D
F27	19.780	5.0	D	9,394	0.54	854	45	-	-	20.76	
F28	29.460	6.0	D	13,846	0.69	989	55	-	-	28.91	
Lloll-385	195.000	5.2	DT	92.432	1.24	1.834	132	178	221.6	96.47	

*NOTE

SIN = Single Wheel, D = Dual Wheels

DT = Dual Tandem. COM = Complex Wheels

TABLE 4.1 : DETAILS OF TEST RAFT UNITS AND LOADING

RAFT		$\frac{L}{H}$ ratio	$\frac{W}{L}$ ratio	TYPE OF REINFORCEMENT	TYPE OF DYNAMIC & No. OF RAFT		
Notations	Dimensions L × W × H*				Single-Wheel	Twin-Wheel	Total
Rs-14-1/D	2.0*m* × 2.0*m* × 140*mm*	14.3	1	Distributed Steel	0	2	2
Rs-17-1/D	2.0*m* × 2.0*m* × 175*mm*	11.43	1	Distributed Steel	0	2	2
Rs-14-2/D	2.0*m* × 2.0*m* × 140*mm*	14.3	1	Distributed Steel	2	2	4
Rr-14-2/D	2.3*m* × 1.5*m* × 140*mm*	16.43	0.65	Distributed Steel	2	2	4
R6-2/D	2.4*m* × 0.6*m* × 140*mm*	17.14	0.25	Distributed Steel	1	2	3
R9-2/D	2.4*m* × 0.9*m* × 140*mm*	17.14	0.375	Distributed Steel	1	2	3
R12-2/D	2.4*m* × 1.2*m* × 140*mm*	17.14	0.5	Distributed Steel	1	2	3
RsF-14-3	2.0*m* × 2.0*m* × 140*mm*	14.3	1	Fibre Steel	0	2	2

* L = Length of the raft units
W = Width of the raft units
H = Thickness of the raft units.

TABLE 4.2: MODULES OF THE TEST RAFT UNITS

Module Number	Raft Units	Descriptin
M1	R6-2/D (R6) R9-2/D (R9) R12-2/D (R12) RR-14-2/D (RR) RS-14-2/D (RS2)	Discuusses the influence of the rafts shapes and sizes on their behaviour (see chapters 5 and 6)
M2	RS-14-1/D (RS1) RS-14-2/D (RS2) RSF-14-3/D (RSF)	Discusses the inluence of different reinforcement of the rafts on their behaviour (see chapters 5 and 6)
M3	RS-14-1/D (RS1) RS-17-1/D (RS7)	Discusses the influence of the raft thickness on their behavious (see chapters 5 and 6)

TABLE 4.3 : DETAILS OF REINFORCEMENT

MODEL-RAFT	REINFORCEMENT						NUMBER OF BARS		EFFECTIVE DEPTH	REMARKS
Notation	Bar-Size	% of steel in each direction		area of steel (mm^2/m)		yield strength				
		top	bottom	top	bottom	(N/mm^2)			(mm)	
Rs-14-1/D	D6	0.202	0.202	283	283	480	10	10	100	10cm space. top & bottom. each direction
Rs-17-1/D	D6	0.162	0.162	283	283	480	10	10	135	10cm space. top. bottom. each direction
Rs-14-2/D	D6	0.11	0.11	142	142	480	5	5	100	20cm space. top & bottom. each direction
Rr-14-2/D	D6	0.11	0.11	142	142	480	5	5	100	20cm space. top & bottom. each direction
R6-2/D	D6	0.11	0.11	142	142	480	5	5	100	
R9-2/D	D6	0.11	0.11	142	142	480	5	5	100	
D-12-2/D	D6	0.11	0.11	142	142	480	5	5	100	
RsF-14-3/D	Fibre	*round stainless steel fibre with hooked fibres. see section 4.3.3 *0.65mm diameter × 60mm length aspect ratio l/d = 92 *Quantity 240 kg/m^3 (10% by weight) with aligned fibre steel								

TABLE 4.4 : MODULUS OF SUB-GRADE REACTION & EQUIVALENT CBR VALUES			
Rafts	Modulus of Sub-Grade Reaction, k (kN/m^3)	CBR Value % & The Average	
Before testing	59230.77	22	
R6-2/D	76192.31	28.3	25.15
R9-2/D	89923.10	33.4	30.85
R12-2/D	93746.15	34.82	34.11
RR-14-2/D	99076.92	36.80	35.81
RS-14-2/D	105538.5	39.2	38.0
RSS-14-2/D	113992.31	42.34	40.77
RSF-14-3/D	116846.20	43.40	42.87
RS-14-1/D	118596.20	44.05	43.73
RS-17-1/D	129284.62	48.02	46.04
After testing	145976.92	54.22	51.12

TABLE 4.5 : AIRCRAFT TRAFFIC MIX - TIA								
	Annual Movements					Load on	Wheel	Conversion
Aircraft	1980	1985	1990	1995	2000	each leg kg.	arrangement	factor
F27	780	830	850	970	1200	9349	D	1.0
F28	820	850	850	970	1200	13846	D	1.0
B747C	42	624	1093	1555	2205	84780	DDT	1.7
B737-200	780	624	705	818	1040	23494	D	1.0
DC9-41	234	187	141	164	380	24937	D	1.0
A300B4	84	1248	2186	3110	4410	66773	DT	1.7
B707-320C	936	312	88	103	156	72558	DT	1.7
DC-8-63	936	312	88	103	156	78114	DT	1.7
B727-200	9256	10452	11278	11666	11856	44801	D	1.0
DC-10-30	84	1248	2186	3110	4410	97248	DDT	1.7

TABLE 4.6: THE AVERAGE DAMAGING EFFECT "D"

Load	Laboratory Contact Pressur (MPa)	Real Contact Pressure (MPa)	Damaging Effect " D "
100	1.25	0.32	5.492
150	1.875	0.47	5.6381
200	2.5	0.63	5.601
250	3.125	0.78	5.6682
300	3.75	0.94	5.64
350	4.375	1.10	5.62
400	5.0	1.25	5.66
450	5.625	1.42	5.59
600	7.5	1.88	5.64
700	8.75	2.19	5.65

The calculated average damaging effect " D " = $\frac{56.1993}{10}$ = 5.61993 ≅ 5.6

TABLE 5.1: MAXIMUM DEFLECTIONS AT FATIQUE LIFE OF THE DESIGN LOAD 450 KN

Fatgue Life* (N)	Deflection at Loading Positions (mm)				Raft Unit Type	Locations (see Fig. 4.5, Chapter IV)
	P1	P2	P3	P4		
62262	36.9				R6-2/D (R6)	At the outer loaded area (point 0)
62262		38.2				At the outer loaded area (point 2)
62262			42.7			At the outer loaded area (point 3)
36				-10.8		At the free edge (point 7)
102323	29.7				R9-2/D (R9)	At the outer loaded area (point 0)
64061		30.9				At the outer loaded area (point 2)
80459			38.6			At the outer loaded area (point 3)
198				-10.2		At the free edge (point 7)
62262	17.8				R12-2/D (R12)	At the outer loaded area (point 0)
51329		19.2				At the outer loaded area (point 2)
40397			27.2			At the outer loaded area (point 3)
889				-18.9		At the free edge (point 7)
94811	12.8				RR-14-2/D (RR)	At the outer loaded area (point 0)
94811		19.9				At the outer loaded area (point 2)
94811			17.6			At the outer loaded area (point 3)
1889				-13.5		At the free edge (point 7)
14489	13.0				RS-14-2/D (RS2)	At the outer loaded area (point 0)
13889		19.5				At the outer loaded area (point 2)
32274			19.2			At the outer loaded area (point 3)
889				-18.0		At the free edge (point 14)
4289	10.2				RSF-14-3/D (RSF)	At the inner loaded area (point 6)
4289		7.8				At the outer loaded area (point 2)
1889			10.6			At the inner loaded area (point 8)
1889				-12.0		At the free edge (point 14)
18217	12.5				RS-14-1/D (RS1)	At the outer loaded area (point 0)
116269		20.5				At the outer loaded area (point 2)
116269			19.6			At the outer loaded area (point 3)
23274				-37.4		At the free edge (point 14)
234475	4.7				RS-17-1/D (RS7)	At the outer loaded area (point 0)
234475		11.8				At the outer loaded area (point 2)
234475			6.4			At the outer loaded area (point 3)
28831				-32.4		At the free edge (point 14)

*Note: -ve measns an uplift deflication

* Equivalent number of laboratory load rebetitions of the design load (450 k N)

TABLE 5.2 : FAILURE LOAD, FAILURE MODE, AND FATIGUE LIFE FOR THE TEST RAFT MODELS

Test Raft	Fatigue Failure	Loading Positions			
		P1	P2	P3	P4
R6-2/D	Failure Mode	MODE 2	MODE 2	MODE 2	MODE 3
	Failure Load (kN)	700	700	700	150
	FATIGUE LIFE	62262	62262	62262	2038*
R9-2/D	Failure Mode	MODE 1	MODE 3	MODE 1	MODE 3
	Failure Load (kN)	700	700	700	200
	FATIGUE LIFE	102323	64061	80459	1032*
R12-2/D	Failure Mode	MODE 2+1	MODE 2	MODE 1	MODE 3
	Failure Load (kN)	700	700	700	350
	FATIGUE LIFE	62261	51329	40397	1912*
RR-14-2/D	Failure Mode	MODE 1	MODE 1	MODE 1	MODE 3
	Failure Load (kN)	700	700	700	400
	FATIGUE LIFE	94810	94810	94810	2207*
RS-14-2/D	Failure Mode	MODE 2	MODE 1	MODE 2	MODE 3
	Failure Load (kN)	450	450	600	350
	FATIGUE LIFE	14489	13889	32274	2511*
RS-14-1/D	Failure Mode	MODE 2	MODE 1	MODE 1	MODE 3
	Failure Load (kN)	600	700	700	600
	FATIGUE LIFE	18217	116269	116269	23274
RSF-14-3/D	Failure Mode	MODE 2	MODE 2	MODE 2	MODE 2
	Failure Load (kN)	450	450	400	400
	FATIGUE LIFE	4289	4289	1889	1889*
RS-17-1/D	Failure Mode	No Failure	No Failure	No Failure	MODE 3
	Failure Load (kN)	700	700	700	600
	FATIGUE LIFE	234475	234475	234475	28331

(1) MODE 1 = Punching Shear, MODE 2 = Fatigue Fracture, and
MODE 3 = Uplift Deflection

(2) Fatigue Life Are Related to the Laboratory Load Repetitions of the Design Load 450 k N

*Fatigue Life for the Failure Load

TABLE 7.1: THE PREDICTED AND THE EXPERIMENTAL LOAD REPETITIONS, N, TO CAUSE FAILURE USING THE DESIGN LOAD.*

	THE DESIGN METHODS				THE DESIGN METHODS			
Loading Position	Ismail's (a)	Annang's (a)	Bull's (b)	Experimental (a)	Ismail's (a)	Annang's (a)	Bull's (b)	Experimental (a)
Test : R6-2/D (R6)					Test : RS-14-2/D (RS2)			
P1	35,201	15,764	1,400	348,667	36,721	17,431	1,548	81,138
P2	402,657	587,190	22,386	348,667	451,997	649,857	24,786	77,778
P3	35,201	15,764	1,400	348,667	36,721	17,431	1,548	180,734
P4	25,177	15,764	1,400	23	28,269	17,431	1,548	4,020
Test : R9-2/D (R9)					Test : RSF-14-3/D (RSF)			
P1	34,636	16,553	1,470	573,008	37,676	17,825	1,583	24,018
P2	426,436	617,503	23,542	358,741	463,972	664,424	25,331	24,018
P3	34,636	16,553	1,470	450,570	37,676	17,825	1,583	10,578
P4	26,670	16,553	1,470	112	29,004	17,825	1,583	10,578
Test : R12-2/D (R12)					Test : RS-14-1/D (RS1)			
P1	34,729	16,620	1,476	348,661	38,555	18,197	1,616	102,015
P2	427,611	618,818	23,592	287,442	474,775	391,902	25,848	651,106
P3	34,729	16,620	1,476	226,223	38,555	18,197	1,616	651.106
P4	26,738	16,620	1,476	3063	29,687	18,197	1,616	130,334
Test : RR-14-2/D (RR)					Test : RS-17-1/D (RS7)			
P1	36,161	17,206	1,528	530,936	290,182	137,778	12,236	1,313,060
P2	445,328	641,190	24,445	530,936	3,572,769	5,135,073	338,684	1,313.060
P3	36,161	17,206	1,528	530,936	290,182	137,778	12,236	1,313,060
P4	27,838	17,206	1,528	6843	223,384	137,778	12,236	158,653

*The design load = 450kN.
(a) Design method at ultimate limit state.
(b)Design method at serviciability limit state

TABLE 7.2 : THICKNESS DESIGN USING BPA METHOD AND THE TESTED MODELS

Raft Units	Test No. of Cycles Related to 450 kN	Max. Thickness (mm)	
		B.P.A	Tested Model
R6-2/D	see Table 8.1	305	140
R9-2/D	see Table 8.1	305	140
R12-2/D	see Table 8.1	305	140
RR-14-2/D	see Table 8.1	305	140
RS-14-2/D	see Table 8.1	300	140
RSF-14-3/D	see Table 8.1	250	140
RS-14-1/D	see Table 8.1	300	140
RS-17-1/D	see Table 8.1	300	175

TABLE 7.3 : TEST RAFT UNIT DESIGN CHARACTERISTICS

Raft Notation	Module (M)	Raft size m * m	Raft thickness mm.	Aspect ratio W/L	Raft mass kg.	Area of steel mm^2/m	% of steel in each direction top & bottom
R6-2/D	M1	2.4 * 0.6	140	0.25	484	142	0.11
R9-2/D	M1	2.4 * 0.9	140	0.375	726	142	0.11
R12-2/D	M1	2.4 * 1.2	140	0.5	968	142	0.11
RR-14-2/D	M1	2.3 * 1.5	140	0.65	1160	142	0.11
RS-14-2/D	M1	2.0 * 2.0	140	1.0	1344	142	0.11
RS-14-1/D	M2	2.0 * 2.0	140	1.0	1344	283	0.202
RS-14-2/D	M2	2.0 * 2.0	140	1.0	1344	142	0.11
RSF-14-3/D	M2	2.0 * 2.0	140	1.0	1344	Fibre stainless steel hooked 0.65mm dia/60mm long, 240kg/m^3	
RS-14-1/D	M3	2.0 * 2.0	140	1.0	1344	283	0.202
RS-17-1/D	M3	2.0 * 2.0	140	1.00	1344	283	0.162

TABLE 7.4 :RATIO BETWEEN THE OBSERVED LOAD REPETITIONS TO CAUSE FAILURE USING A DESIGN LOAD OF 450KN TO THAT PREDICTED BY THE BULL METHOD FOR SERVICIABILITY ALLOWS FOR A 25 % REDUCTION IN THE OBSERVED LOAD REPITITIONS TO REPRESENT A F.O.S., AND THE CONTACT PRESSURE (N_{ed})

Load	Real Contact Pressure	Ratio of The Observed to Predicted Load Repetitions (N_{cd})															
		R6-2/D (R6)		R9-2/D (R9)		R12-2/D (R12)		RR-14-2/D (RR)		RS-14-2/D (RS2)		RSF-14-3/D (RSF)		RS-14-1/D (RS1)		RS-17-1/D (RS7)	
kN	Mpa	P1/P3	P2	P1/P3	P2	P1/P3	P2	P1/P3	P2	P1/P3	P2	P1/P3	P2	P1/P3	P2	P1/P3	P2
100	0.32	586	53.30	624	51.18	642	41.40	686	13.12	315	10.59	68	4.25	810	84.42	386	22.64
150	0.47	408	35.58	483	34.56	478	27.62	498	8.75	210	7.07	45	2.41	540	55.41	258	15.12
200	0.63	324	26.66	380	25.90	443	20.70	461	6.44	157	5.26	34	2.03	432	42.23	193	11.32
250	0.78	273	21.33	321	20.72	347	16.60	376	5.25	126	4.24	27	1.66	324	33.81	155	9.07
300	0.94	227	17.78	282	17.27	310	13.81	313	4.37	105	3.53	22	1.07	306	28.17	129	7.55
350	1.10	256	15.30	268	14.84	262	11.87	265	3.76	88	3.04	19	0.92	276	24.20	109	6.47
400	1.25	167	13.34	234	12.95	235	10.35	231	3.28	75	2.65	16	0.80	265	21.12	95	5.66
450	1.42	149	11.68	209	11.43	205	9.14	208	2.91	70	2.36	15	0.72	241	18.90	86	5.03
600	1.88	114	8.93	159	8.67	160	6.94	157	2.19	53	1.79	11	0.54	180	14.10	65	3.78
700	2.19	102	7.75	141	7.54	134	6.05	139	1.89	49	1.61	10	0.47	158	12.05	57	3.21

$$N_{cd} = \frac{75\% \text{ of the observed load repetitions}}{\text{The predicted load repetions using Bull method}}$$

The design Table 7.4 includs 25% F.O.S.

TABLE 7.5 : THE EXPERIMENTAL LOAD REPETITIONS OF LOAD 450kN TO CAUSE FAILURE AND THE RANGE OF CBR VALUES.*

Test Raft	No. of cycles at position (Pn)				CBR %		
	P1	P2	P3	P4	at the test	Range during the test module	Total range of the CBR
Module M1							
R6-2/D	348,667	348,667	348,667	23	30.85		
R9-2/D	573,008	358,741	450,520	112	34.11		
R12-2/D	348,662	287,442	226,223	3063	35.81	9.92%	
RR-14-2/D	530,942	530,942	530,942	6843	38.00		
RS-14-2/D	81,138	77,778	180,734	4020	40.77		
Module M2							20.27%
RS-4-2/D	81,138	77,778	180,734	4020	40.77	5.27%	
RSF-14-3/D	24,018	24,018	10,578	10,578	43.73		
RS-14-1/D	102,015	651,106	651,106	130,334	46.04		
Module M3							
RS-14-1/D	102,015	651,106	651,106	130,334	46.04	5.08%	
RS-17-1/D	1,313,060	1,313,060	1,313,060	158,653	51.12		

* For the range of CBR values, see Section 4.8.2.

TABLE 7.6: AIRCRAFT TRAFFIC FORECAST

Aircraft	Forecast Annual Aircraft Movements					Average Annual Traffic
	1995	2000	2005	2010	2015	
F27	780	830	850	970	1200	1158
F28	820	850	850	970	1200	1173
B747C	42	624	1093	1555	2205	1380
B737-200	780	624	705	818	1040	992
DC9-41	234	187	141	164	380	277
A300B4	84	1248	2186	3110	4410	2760
B707-320C	936	312	88	103	156	399
DC-8-63	936	312	88	103	156	399
B727-200	9256	10452	11278	11666	11856	13627
DC-10-30	84	1248	2186	3110	4410	2760

TABLE 7.7: AIRCRAFT TRAFFIC CHARACTERISTICS					
Aircraft	Average Annual Traffic	Load on Each Leg. kg.	Wheel Arrangement	Conversion Factor	Design Traffic
F27	1158	9349	D	1.0	1158
F28	1173	13846	D	1.0	1173
B747C	1380	84780	DDT	1.7	2346
B737-200	992	23494	D	1.0	992
DC9-41	277	24937	D	1.0	277
A300B4	2760	66773	DT	1.7	4692
B707-320C	399	72558	DT	1.7	679
DC-8-63	399	78114	DT	1.7	679
B727-200	13627	44801	D	1.0	13627
DC-10-30	2760	97248	DDT	1.7	4692
Total	24925				30315

TABLE 7.8: COMPARISON OF THE PREDICTED NUMBEROF CYCLES FROM THE FOUR DESIGN METHODS [see design example in Section 7.8.4]

Aircraft	Contact Pressure MPa	Number of Load Repetitions "N"			
		Bull method(b)	Ismail method(a)	The design (a) formula (Eq 7.1)	The design Charts(a)
F27	0.55	156,734	2,184,964	663,240,000	79,150,670
F28	0.70	32,604	454,299	180,400,000	13,041,600
B747C	1.31	1,492	5,172	5,050,000	414,776
B737-200	1.04	4,669	54,825	22,260,000	4,430,038
DC9-41	1.14	1,559	43,186	17,640,000	3,375,228
A300B4	1.29	3,597	13,442	7,670,000	1,007,160
B707-320C	1.26	2,580	9,641	6,880,000	730,140
DC-8-63	1.38	1,921	7,175	4,991,000	524,433
B727-200	1.42	1,110	4,145	3,830,000	299,700
DC-10-30	1.16	1,287	2,987	9,540,000	373,230

(a) Design method at ultimate limit state.
(b) Design method at serviceability limit state.
(c) The number of load repetitions was factored by 25%.
(d) **NOTE**: The number of cycles to reach the design fatigue life for RS1 is 406,250 which compares to 651,106 to reach failure, this suggest a factor of safety. This means that the design Charts still conservative but safe. It is more economic than the Bull method which predicted 1625 cycles.

Table 7.9: PRESENT WORTH LIFE-CYCLE COSTS
a/ Concrete Paving Blocks

Year	cost (£/m^2)	PWF*, 5%	PW**, (£)
0 initial cost	12.00	1.0000	12.000
1 regular maintenance	0.08	0.9524	0.076
2 ~ ~	0.08	0.9070	0.073
3 ~ ~	0.08	0.8640	0.070
4 ~ ~	0.08	0.8230	0.066
5 replace blocks & sealant	1.38	0.7835	1.080
6 regular maintenance	0.08	0.7462	0.060
7 ~ ~	0.08	0.7107	0.057
8 ~ ~	0.08	0.6768	0.054
9 ~ ~	0.08	0.6446	0.052
10 replace blocks & sealant	1.38	0.6139	0.850
11 regular maintenance	0.08	0.5847	0.047
12 ~ ~	0.08	0.5568	0.045
13 ~ ~	0.08	0.5303	0.042
14 ~ ~	0.08	0.5051	0.040
15 replace blocks & sealant	1.38	0.4810	0.664
16 regular maintenance	0.08	0.4581	0.037
17 ~ ~	0.08	0.4363	0.035
18 ~ ~	0.08	0.4155	0.033
19 ~ ~	0.08	0.3957	0.032
20 ~ ~	0.08	0.3769	0.030
Sub Total Salvage Value	- 6.00	0.3769	- 2.26
Total	11.50	-	13.183

PWF* = Present Worth Factor [5% represents the discount rate]

PW** = Present Worth value

Table 7.9 (cont.)
b/ Pavement Quality Concrete

Year		cost (£/m^2)	PWF, 5%	PW, (£)
0	initial cost	26.40	1.0000	26.40
1	regular maintenance	0.10	0.9524	0.095
2	~ ~	0.10	0.9070	0.091
3	~ ~	0.10	0.8640	0.086
4	~ ~	0.10	0.8230	0.082
5	cracks & joints seal	2.10	0.7835	1.650
6	regular maintenance	0.10	0.7462	0.075
7	~ ~	0.10	0.7107	0.071
8	~ ~	0.10	0.6768	0.068
9	~ ~	0.10	0.6446	0.065
10	cracks & joints seal	2.10	0.6139	1.290
11	regular maintenance	0.10	0.5847	0.059
12	~ ~	0.10	0.5568	0.056
13	~ ~	0.10	0.5303	0.053
14	~ ~	0.10	0.5051	0.051
15	cracks & joints seal	2.10	0.4810	1.010
16	regular maintenance	0.10	0.4581	0.046
17	~ ~	0.10	0.4363	0.044
18	~ ~	0.10	0.4155	0.042
19	~ ~	0.10	0.3957	0.040
20	~ ~	0.10	0.3769	0.038
Sub Total Salvage Value		- 2.64	0.3769	- 1.000
Total		31.76	-	30.412

Table 7.9 (cont.)
c/ Precast Concrete Raft Units

Year		cost (£/m^2)	PWF, 5%	PW, (£)
0	initial cost	10.75	1.0000	10.75
1	regular maintenance	0.20	0.9524	0.191
2	~ ~	0.20	0.9070	0.181
3	~ ~	0.20	0.8640	0.173
4	~ ~	0.20	0.8230	0.165
5	reapply sealant	1.00	0.7835	1.784
6	regular maintenance	0.20	0.7462	0.150
7	~ ~	0.20	0.7107	0.142
8	~ ~	0.20	0.6768	0.135
9	~ ~	0.20	0.6446	0.129
10	reapply sealant	1.425	0.6139	0.875
11	regular maintenance	0.20	0.5847	0.120
12	~ ~	0.20	0.5568	0.110
13	~ ~	0.20	0.5303	0.110
14	~ ~	0.20	0.5051	0.100
15	reapply sealant	0.20	0.4810	1.481
16	regular maintenance	0.20	0.4581	0.092
17	~ ~	0.20	0.4363	0.087
18	~ ~	0.20	0.4155	0.083
19	~ ~	0.20	0.3957	0.079
20	~ ~	0.20	0.3769	0.075
Sub Total Salvage Value		- 5.375	0.3769	- 2.03
Total		12.21	-	12.98

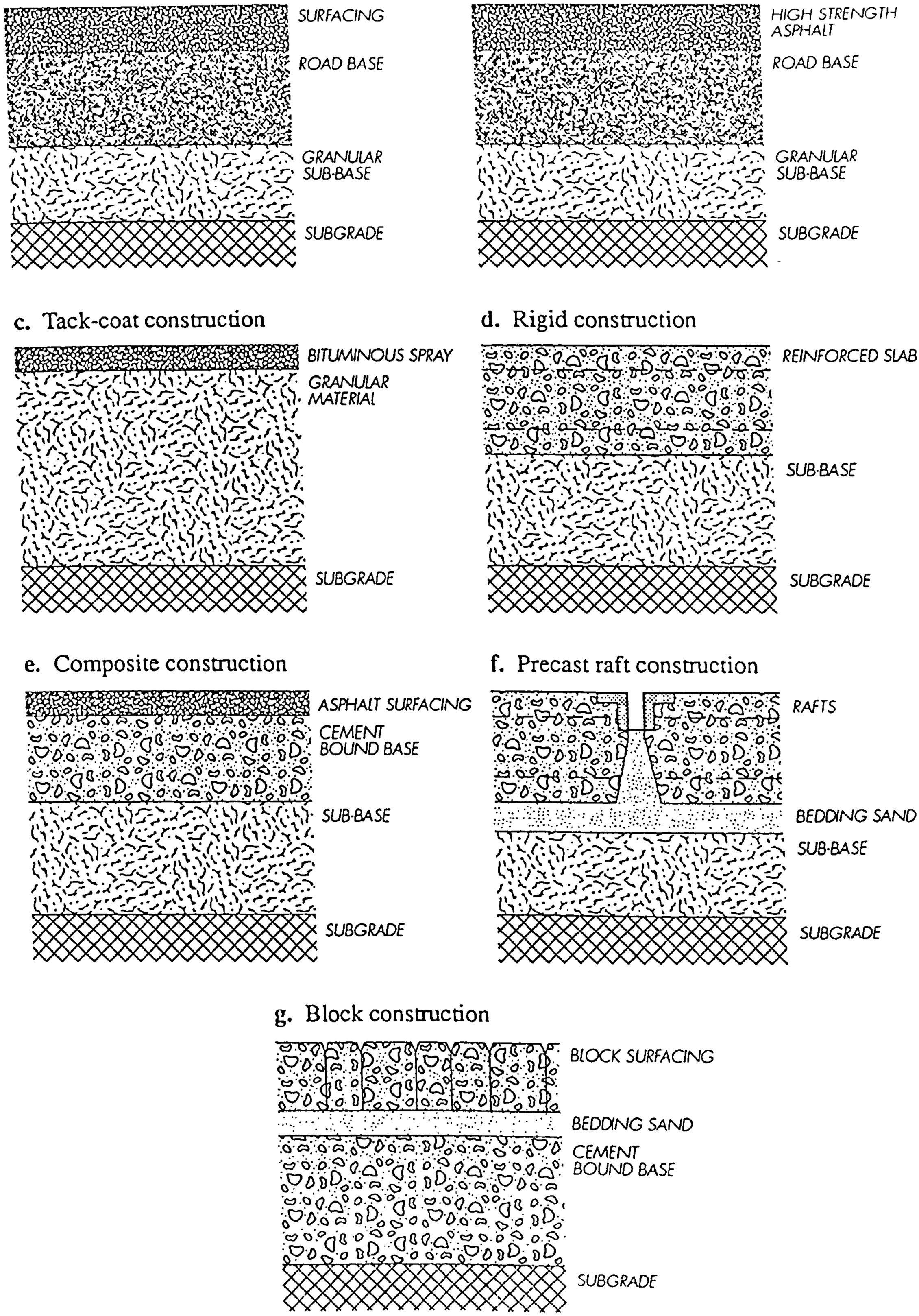

Figure 2.1: Types of Pavement Construction

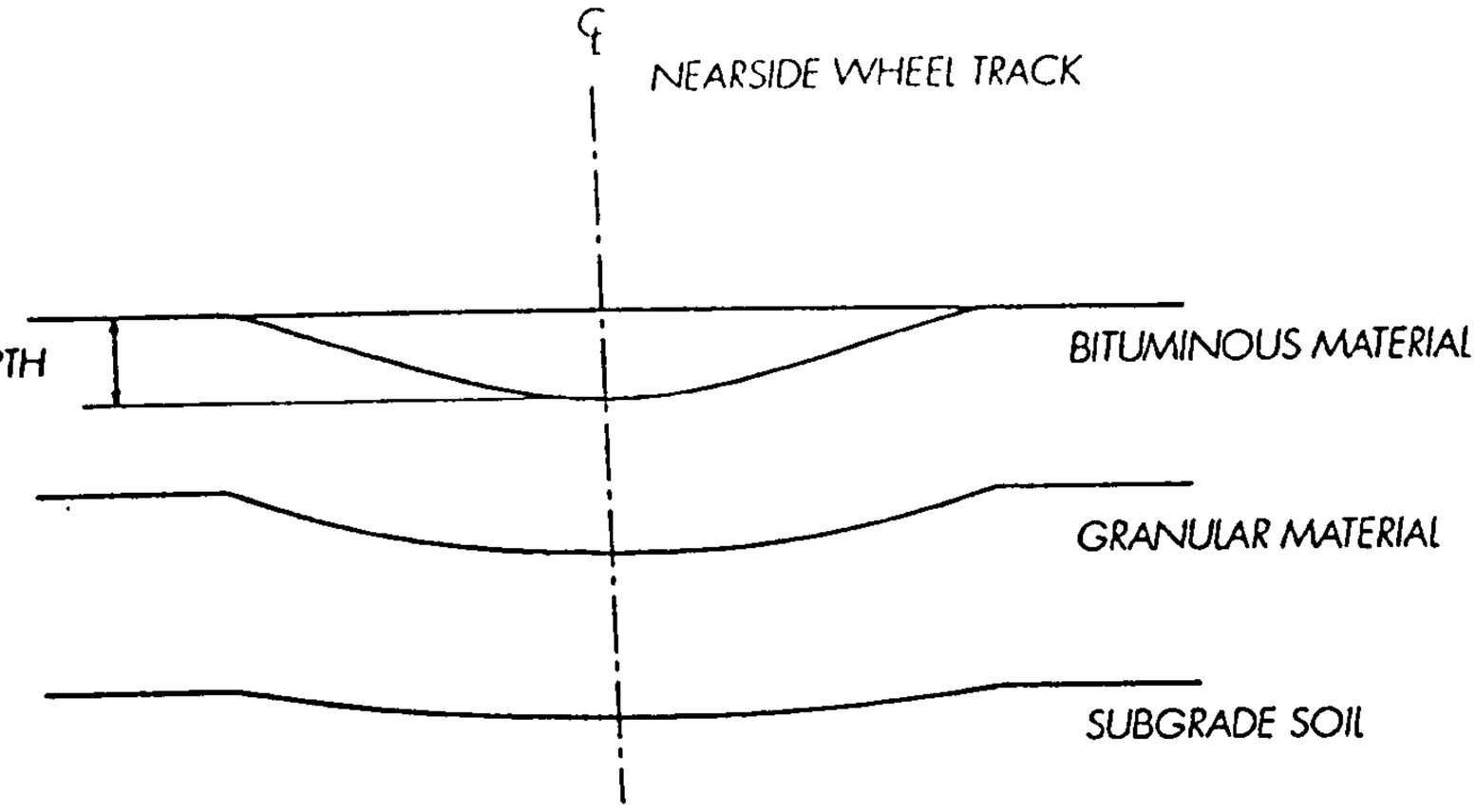

a. Permanent deformation

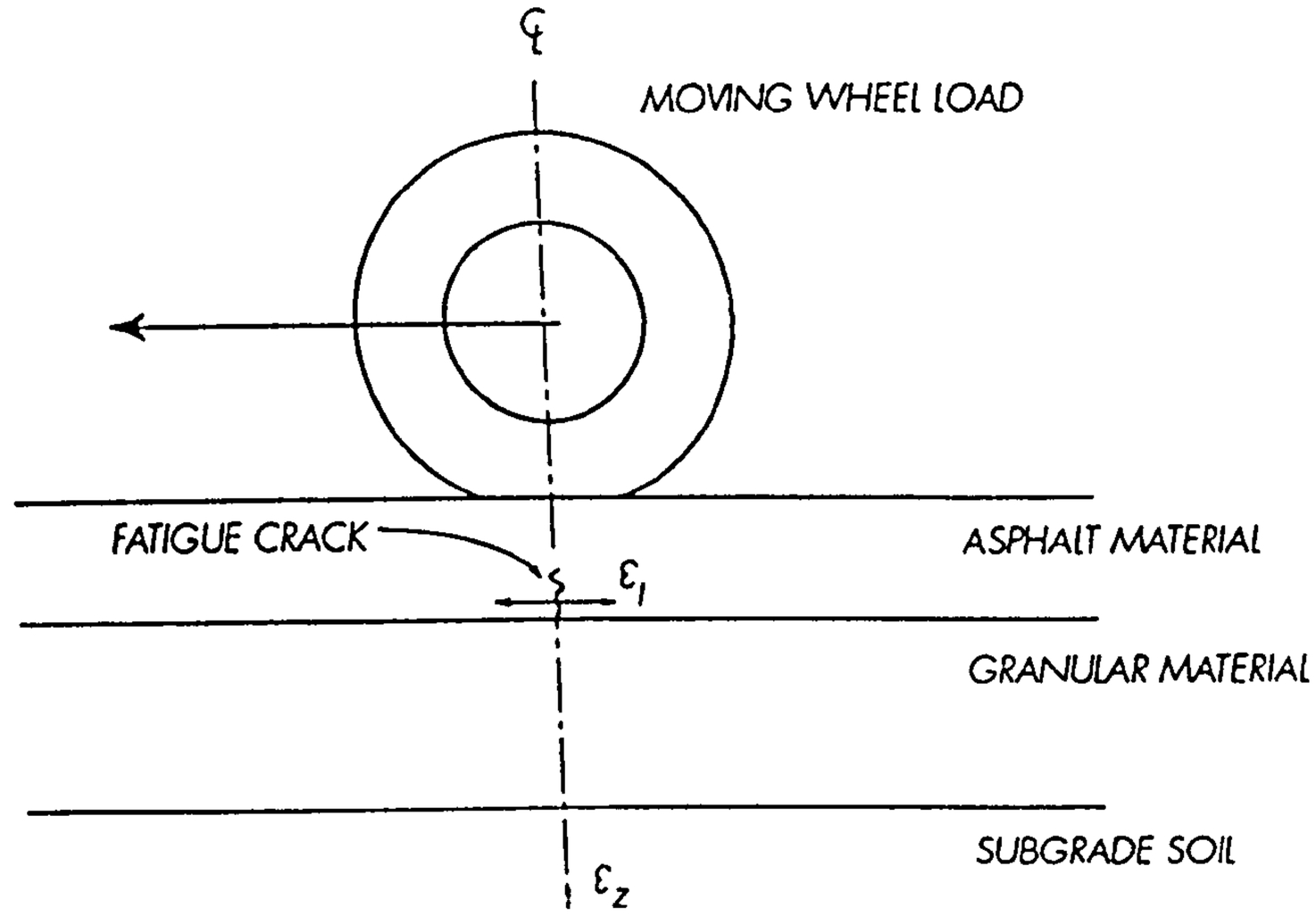

b. Fatigue cracking and critical strains

Figure 2.2: Failure Modes and Critical Strains in Asphalt Pavements

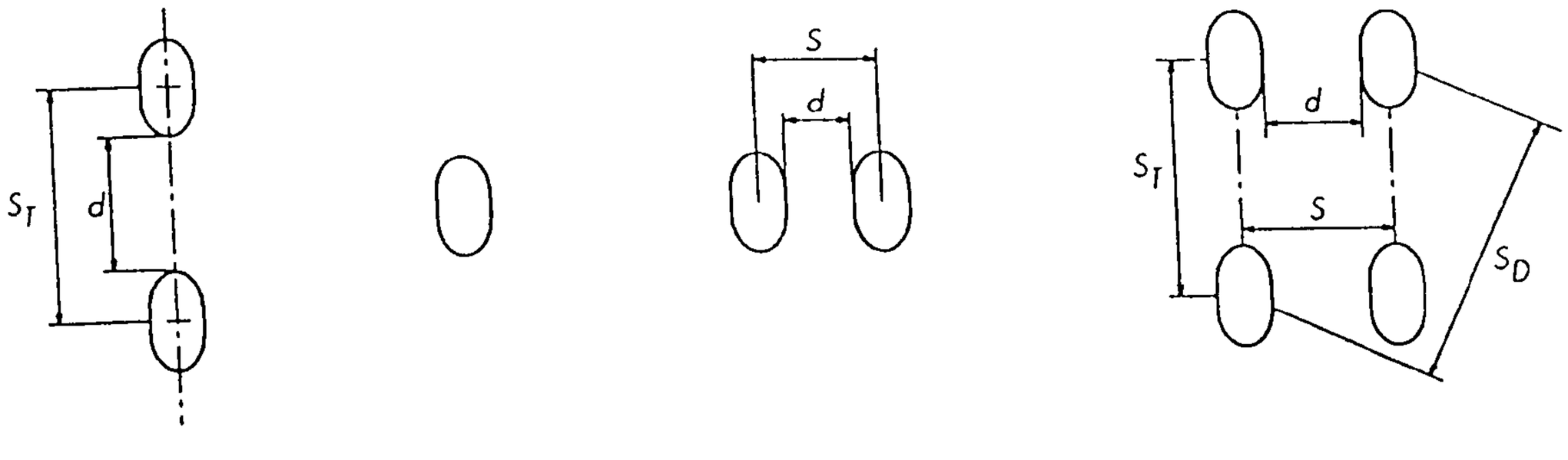

Typical undercarriages wheel arrangements

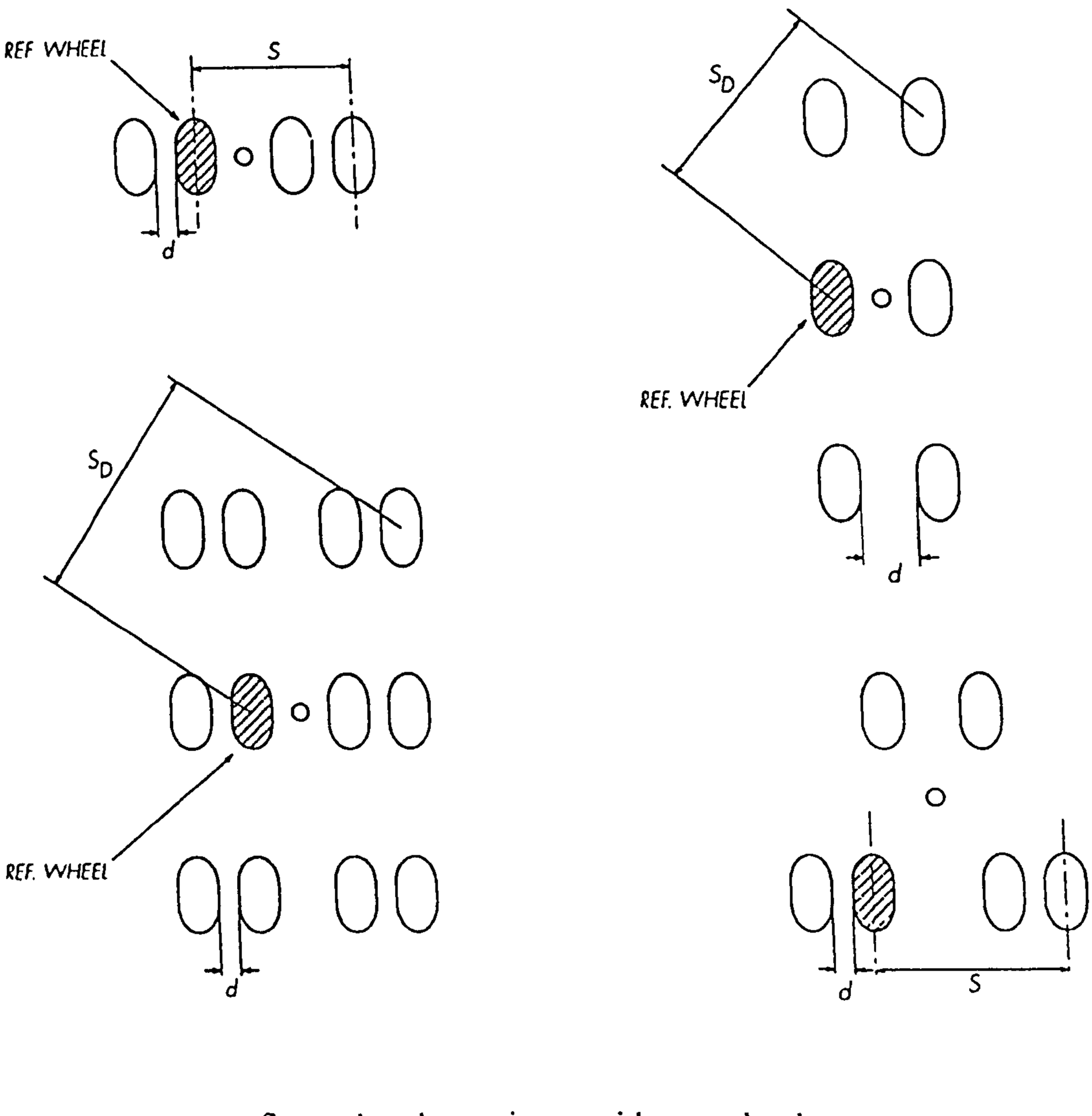

Several undercarriages with complex layouts

Figure 2.3: Several Wheel Arrangements on the Main Legs of Landing Gear

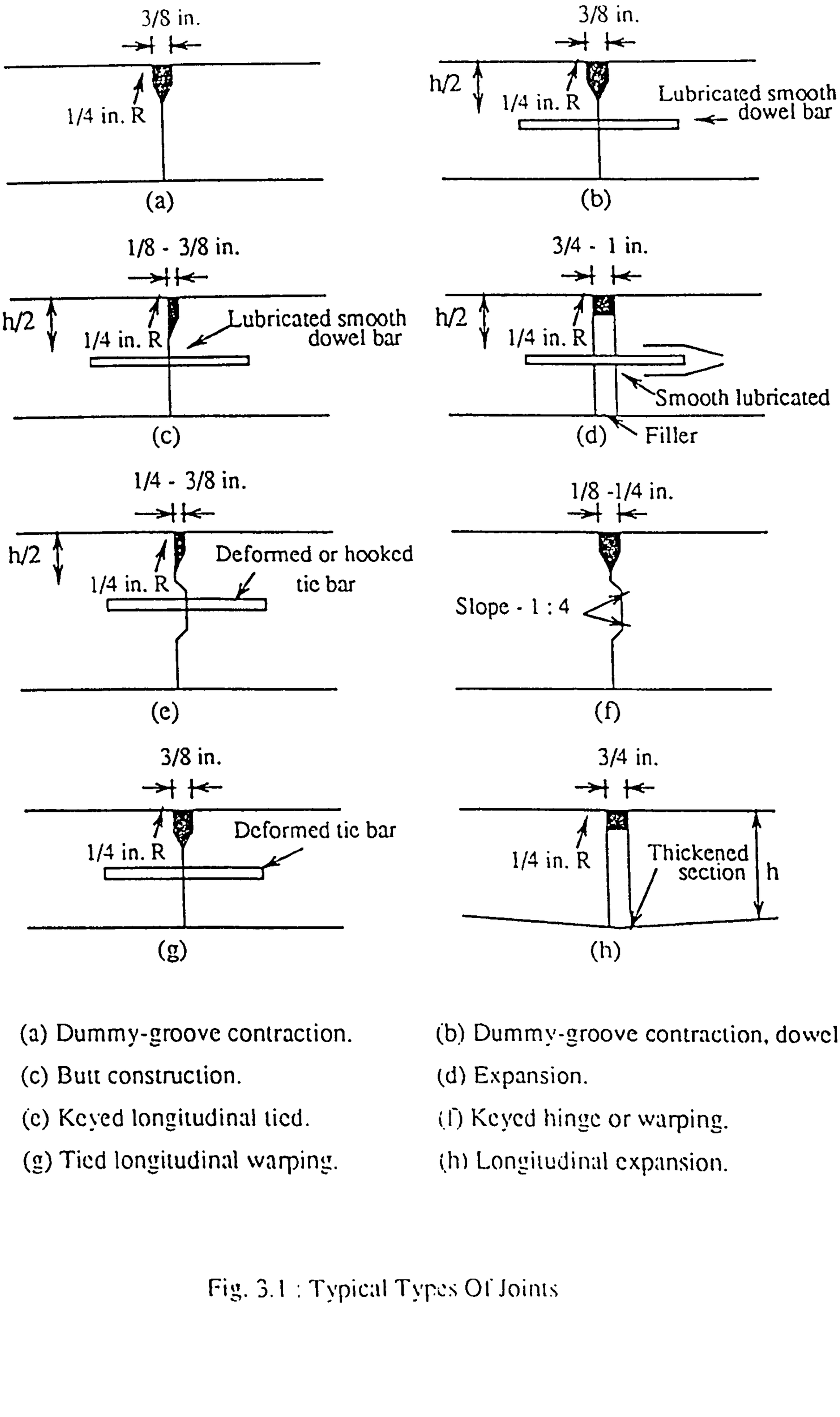

(a) Dummy-groove contraction.

(b) Dummy-groove contraction, dowelled.

(c) Butt construction.

(d) Expansion.

(e) Keyed longitudinal tied.

(f) Keyed hinge or warping.

(g) Tied longitudinal warping.

(h) Longitudinal expansion.

Fig. 3.1 : Typical Types Of Joints

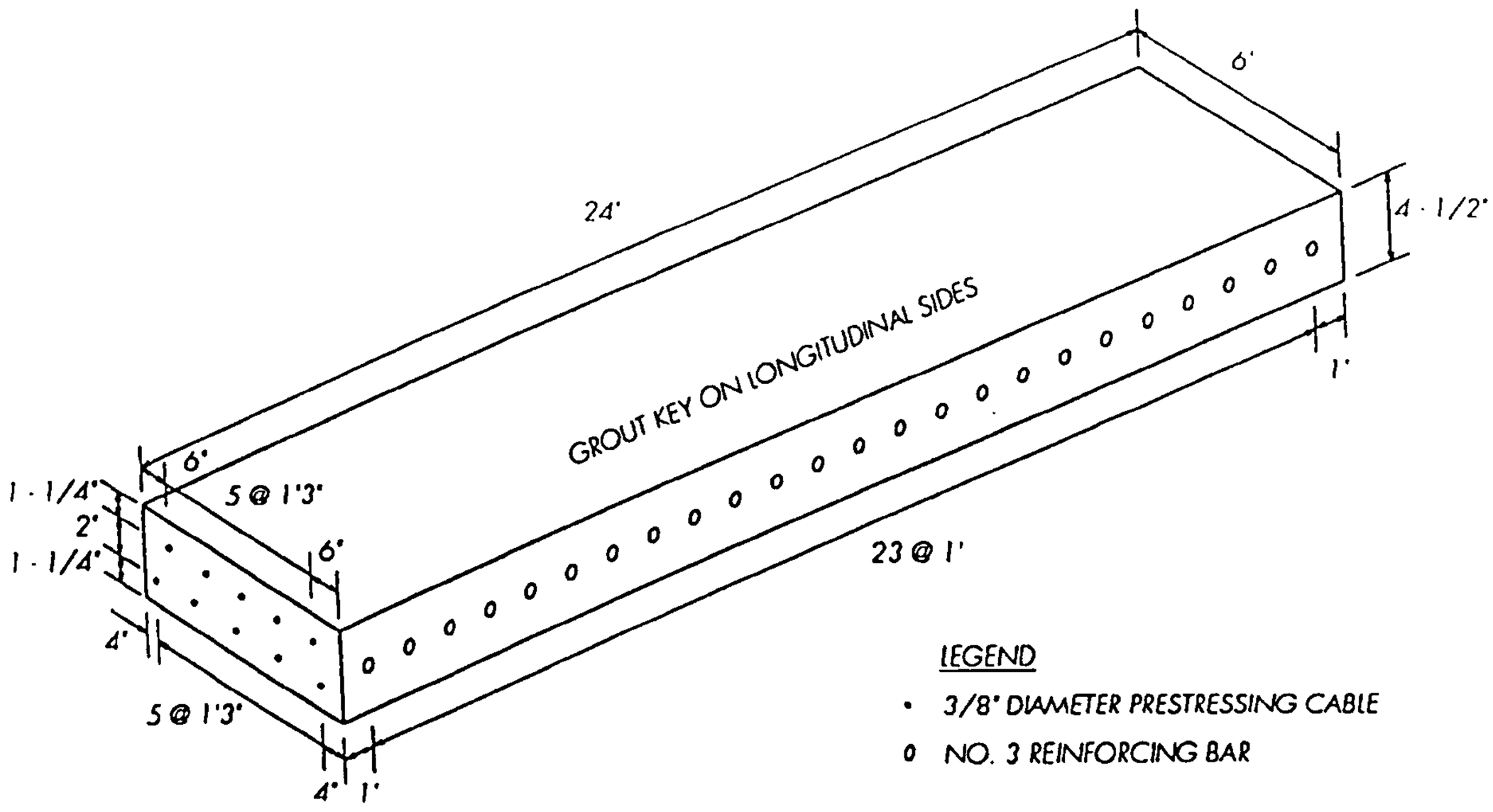

a. Dimensions and reinforcing

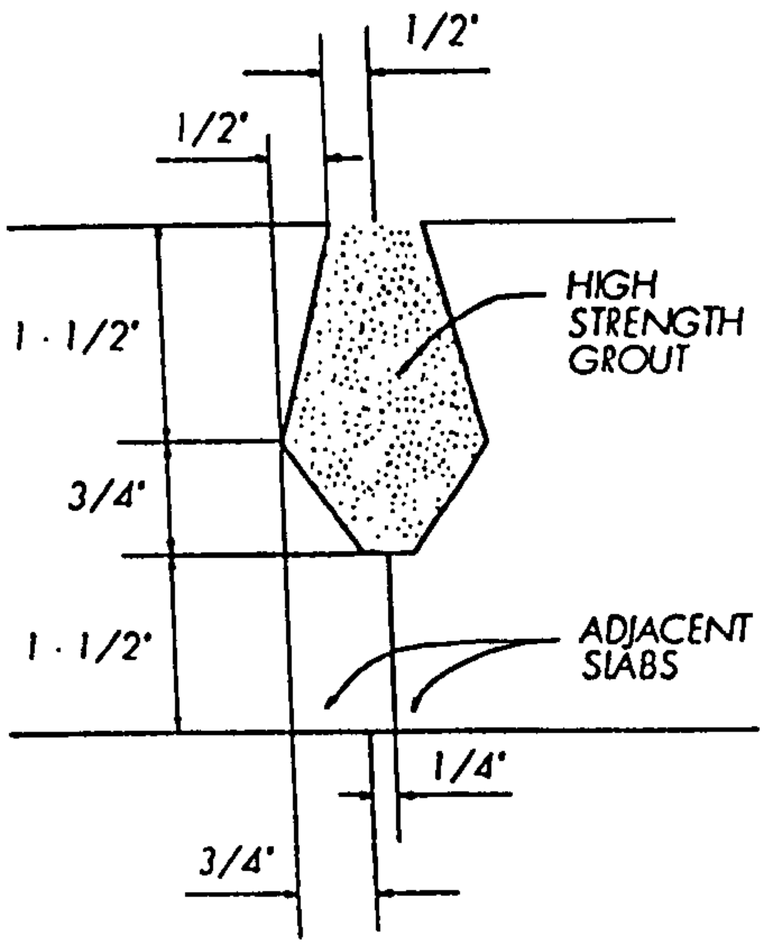

b. Group key

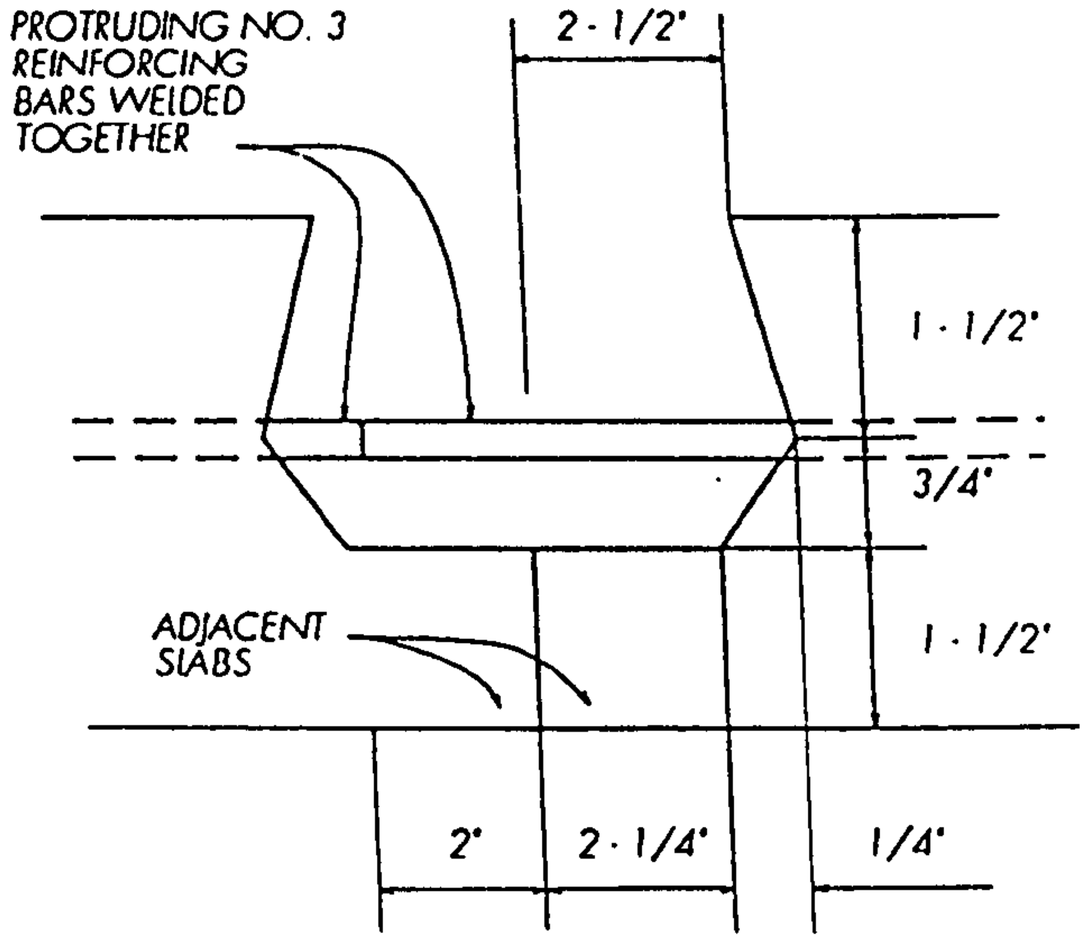

c. Optional connection joint at slab 1/4 and 3/4 points

Figure 3.2: Final Slab Design for Test Pavement Section, Brookings, South Dakota

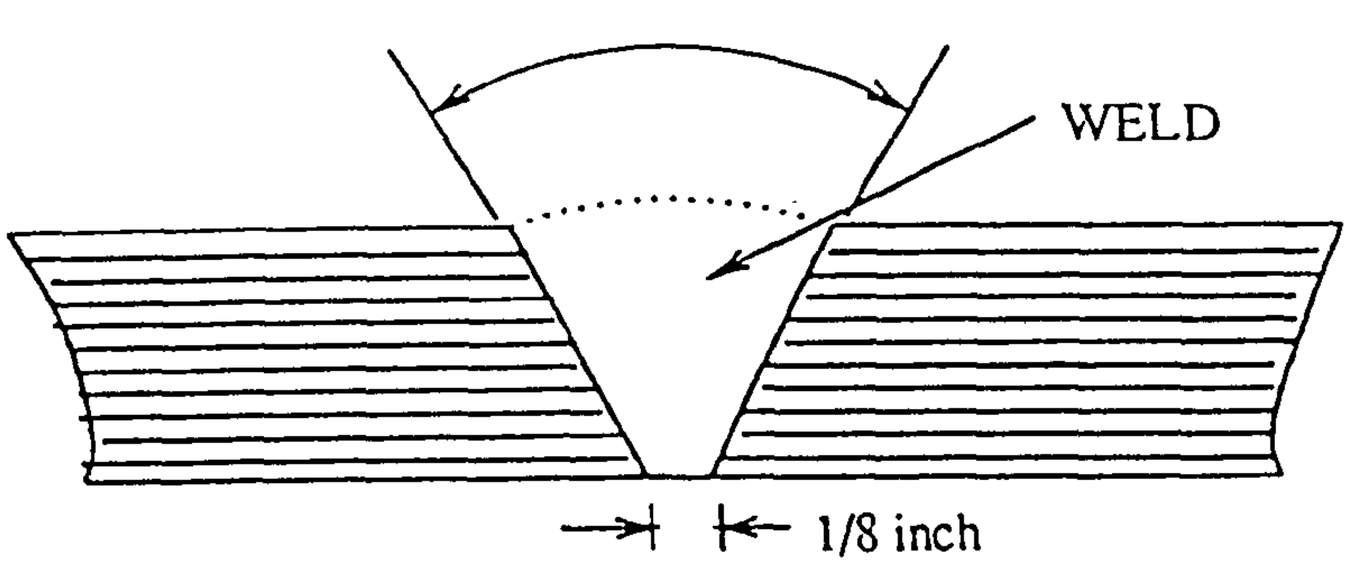

a. SINGLE - V WELDED BUTT SPLICE

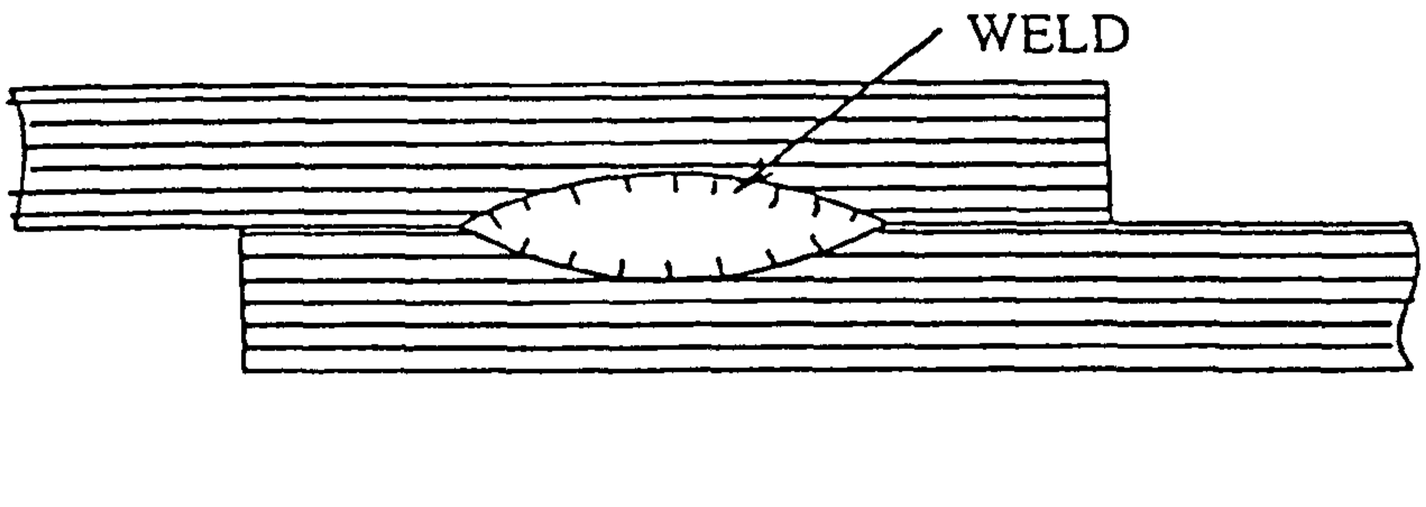

b. SINGLE - LAP WELDED SPLICE

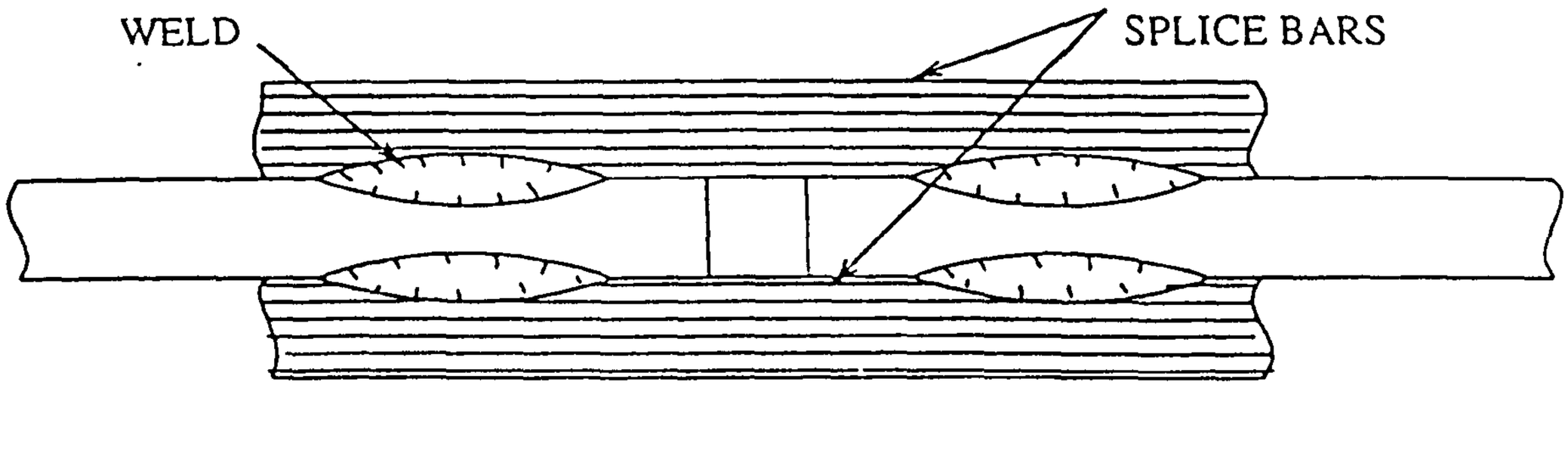

c. DOUBLE - LAP WELDED SPLICE

Fig. 3.3 : Example Weld Splices For Reinforcing Bars.

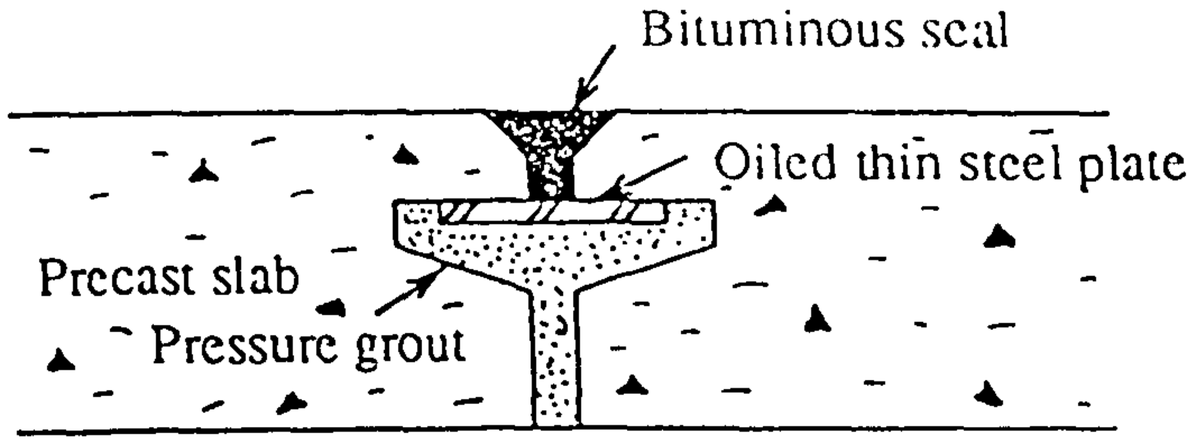

a. STEEL PLATE

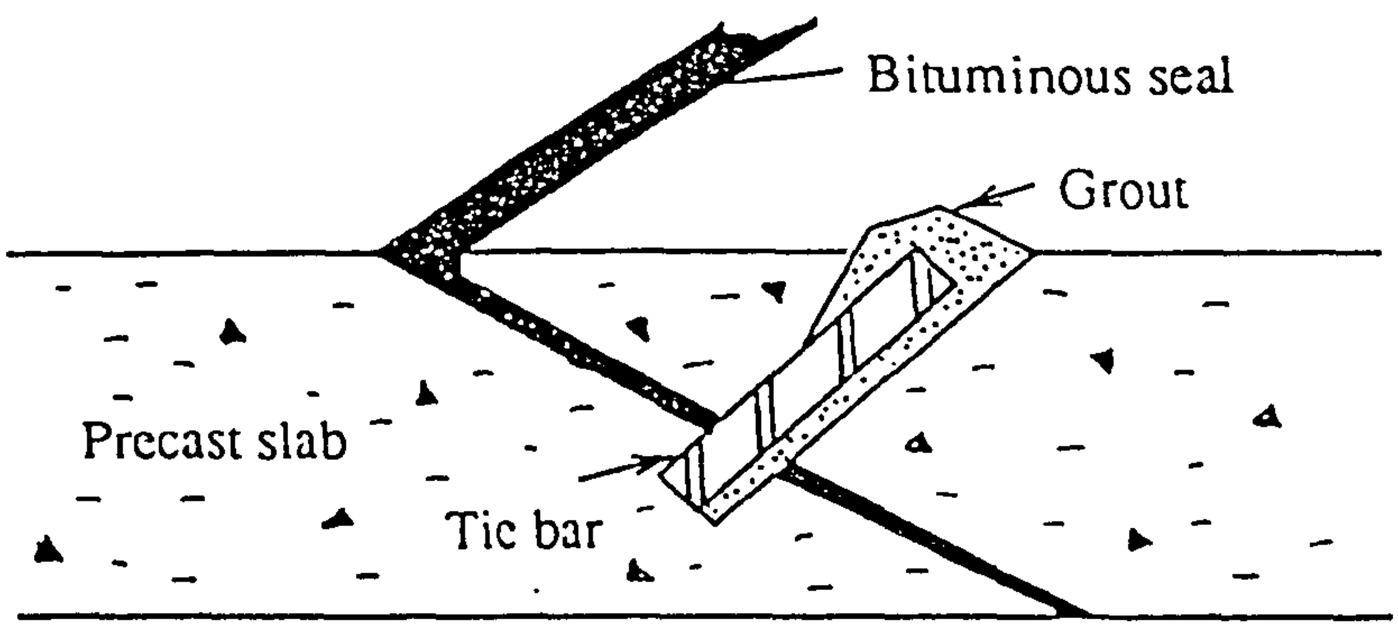

b. INCLINED FACE

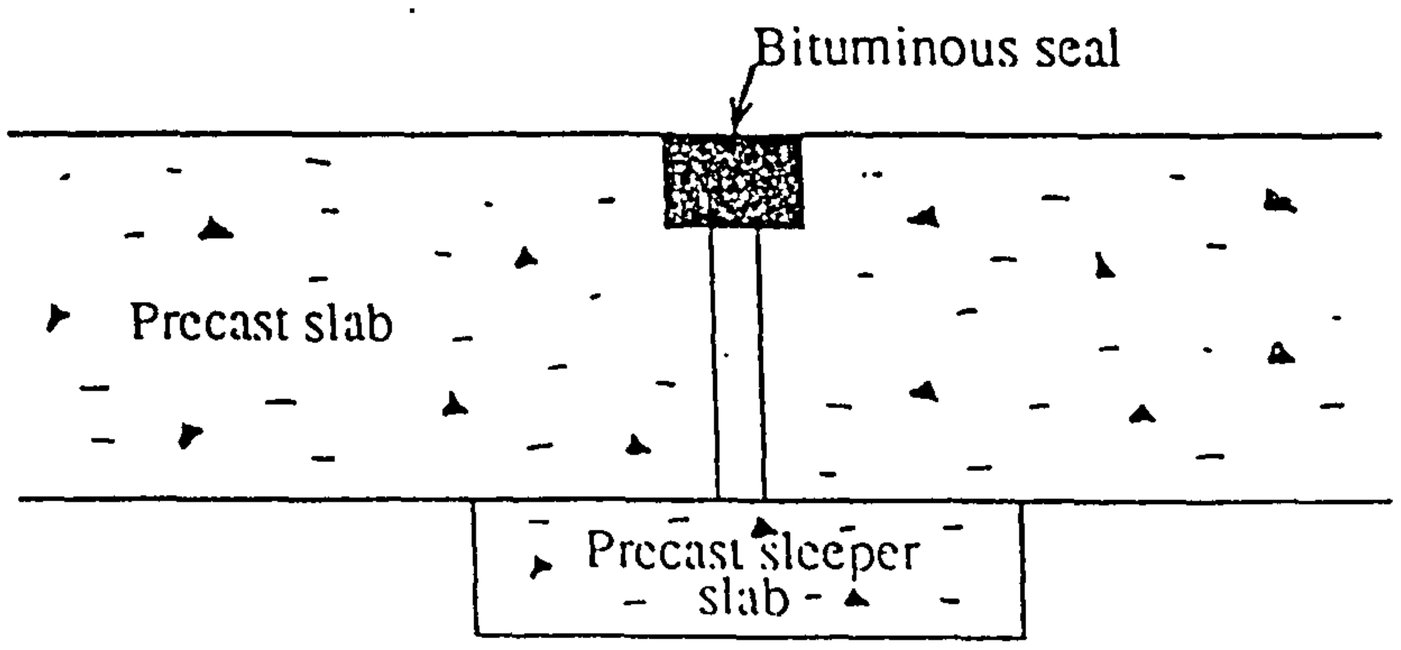

c. SLEEPER BAR

Fig. 3.4 : Load Transferring Joints For Precast Slabs

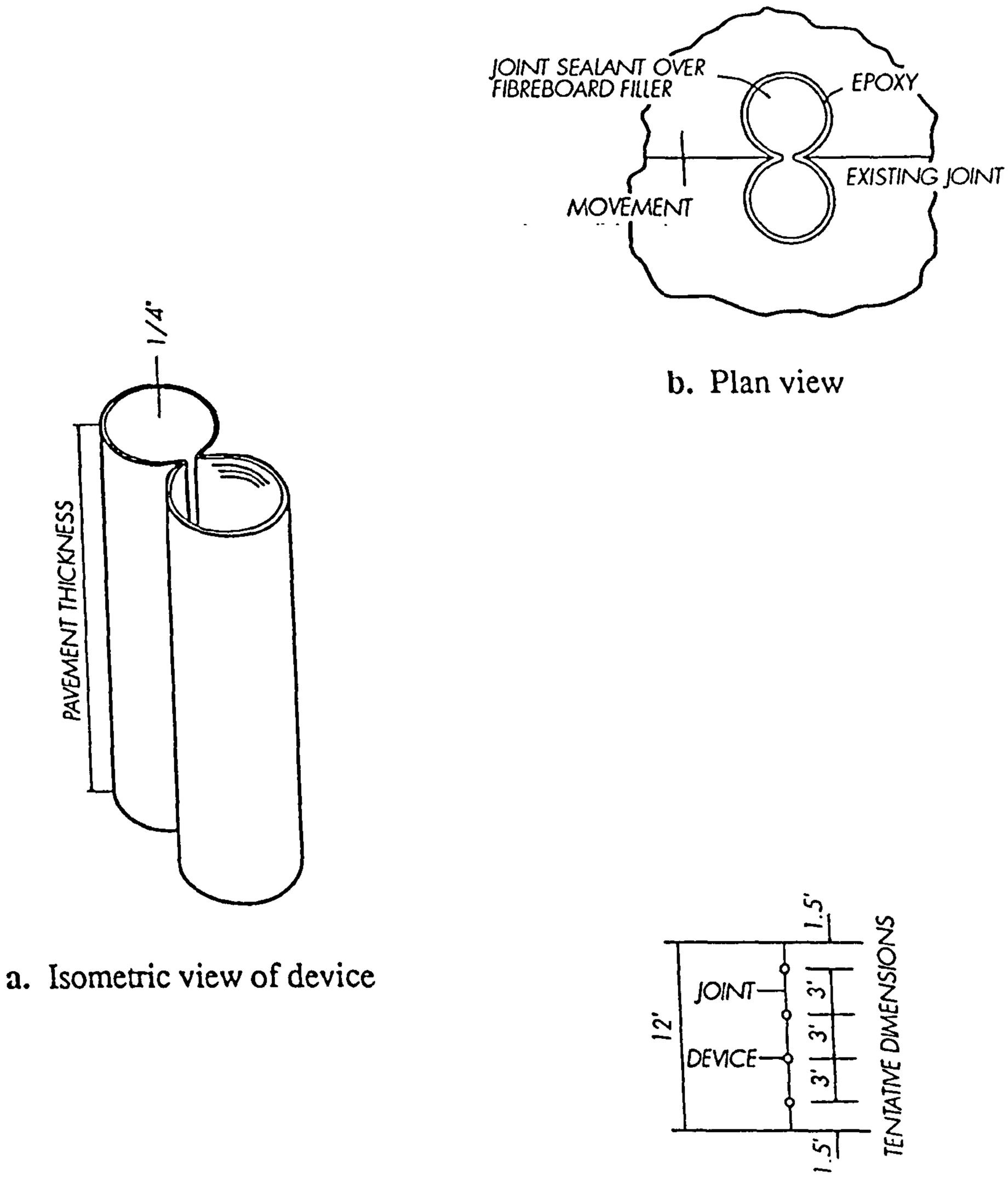

a. Isometric view of device

b. Plan view

c. Proposed layout for highway

Figure 3.5: Deformable Steel Tube Load Transfer Device (after Barenberg and Smith 1979)

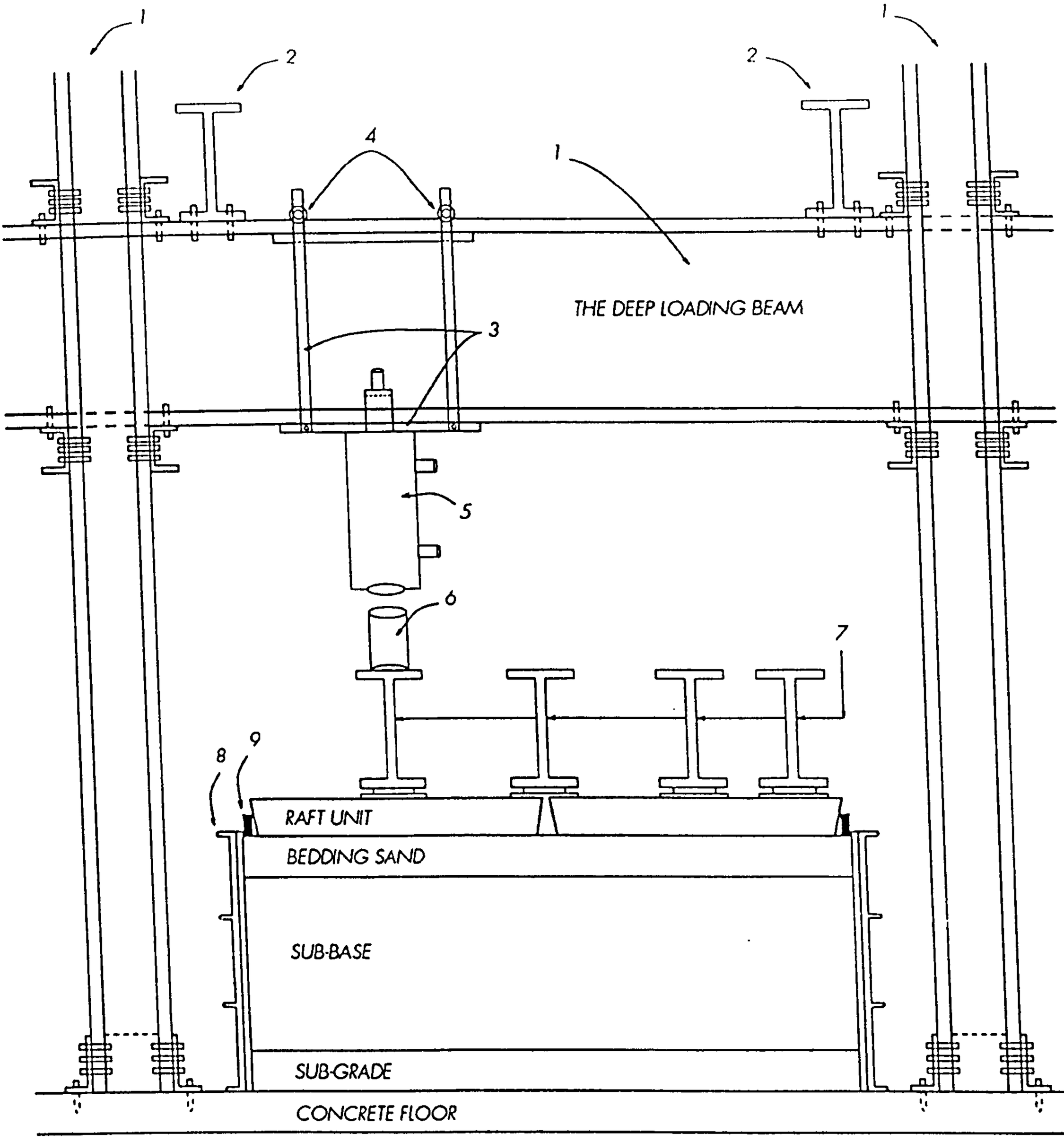

LEGEND

1. THE MAIN LOADING FRAME, DEEP LOADING BEAMS AND FOUR LOADING COLUMNS
2. THE TWO CROSS I - BEAM SECTION
3. THE JACK CARRIER RAIL
4. THE TWO WHEELS OF THE CARRIER
5. THE HYDRAULIC JACK
6. THE LOAD CELL - 100 TON
7. THE LOADS DISTRIBUTING HIGH GRADE STEEL I - BEAM SECTION
8. THE STEEL TANK, 3-STEEL CHANNEL SECTIONS
9. THE HORIZONTAL RESTRAINTS

Figure 4.1: Layout of Loading Frame and Test Area

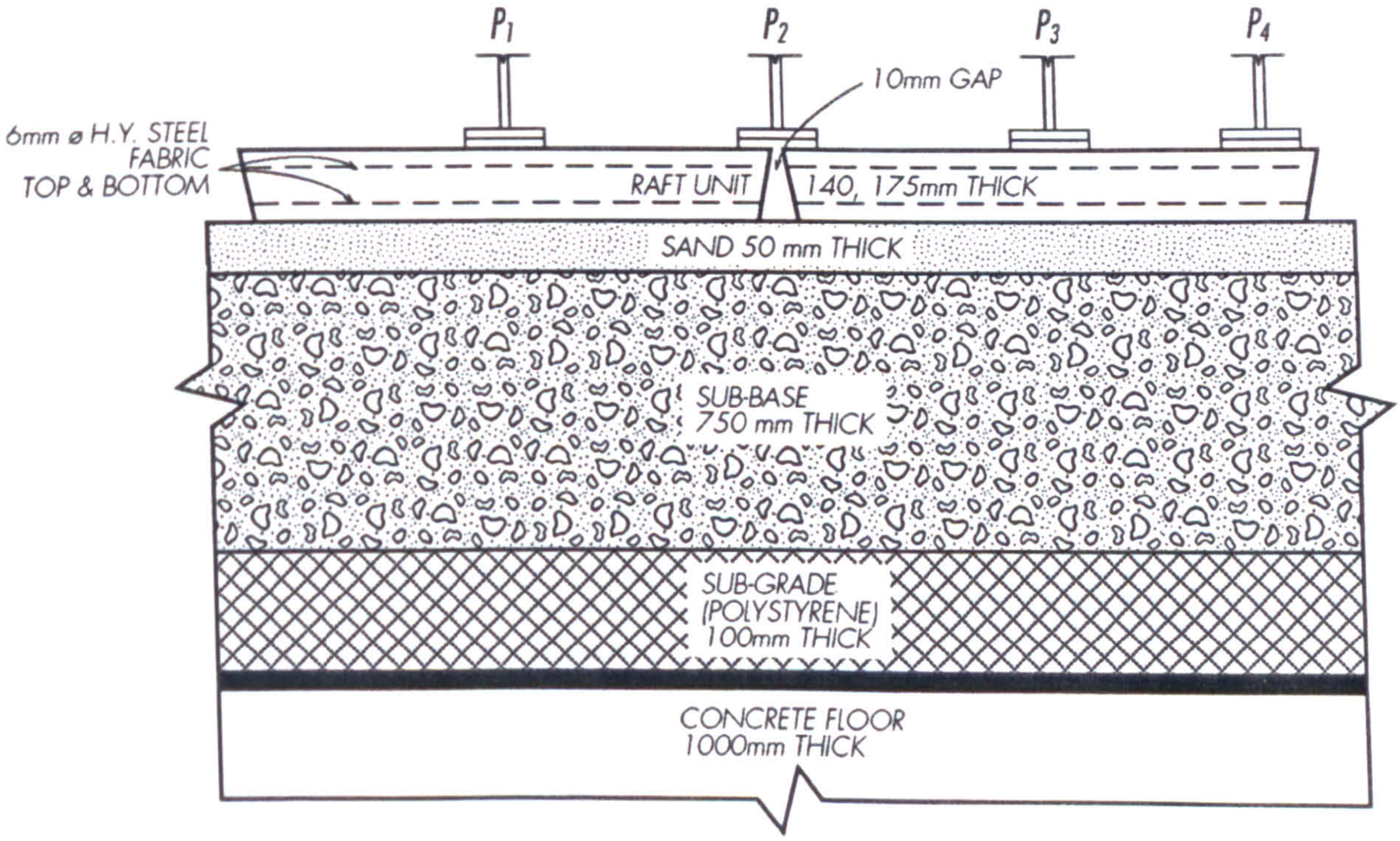

Fig.4.2: The Test Raft Model Layers

Fig.4.3: "Speedy" Moisture Tester

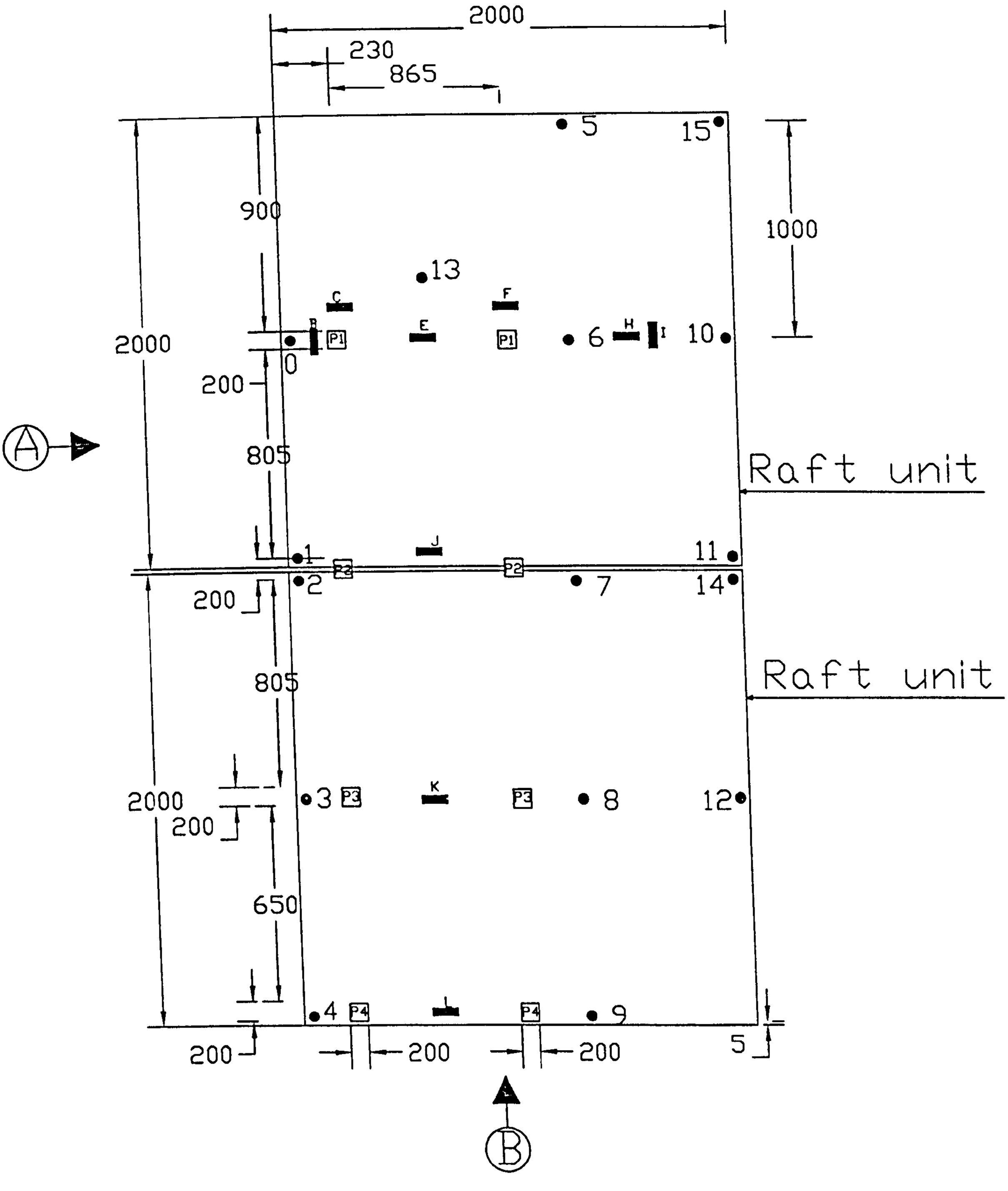

P1 P1 Loading positions number one.
P2 P2 Loading positions number two.
P3 P3 Loading positions number three.
P4 P4 Loading positions number four.
Not to scale: Raft unit 2000x2000 on plan

Strain gauges(B,C,E,F and H-L)
LVDTs (0-15)
Dimensions in mm

Fig. 4.4(a):GENERAL LAYOUT OF LOADING POSITIONS AND INSTRUMENTATION

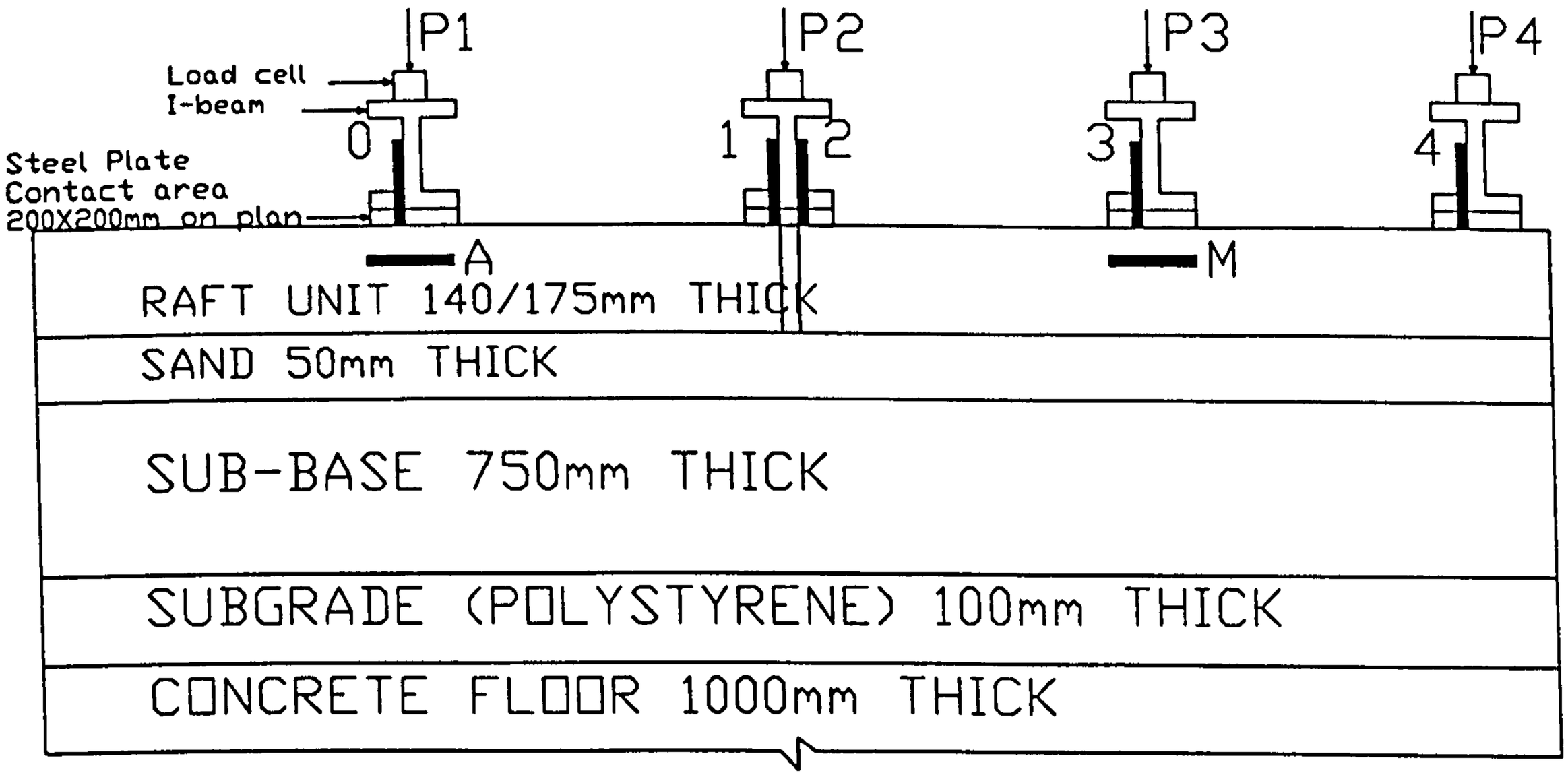

(b) Side View A

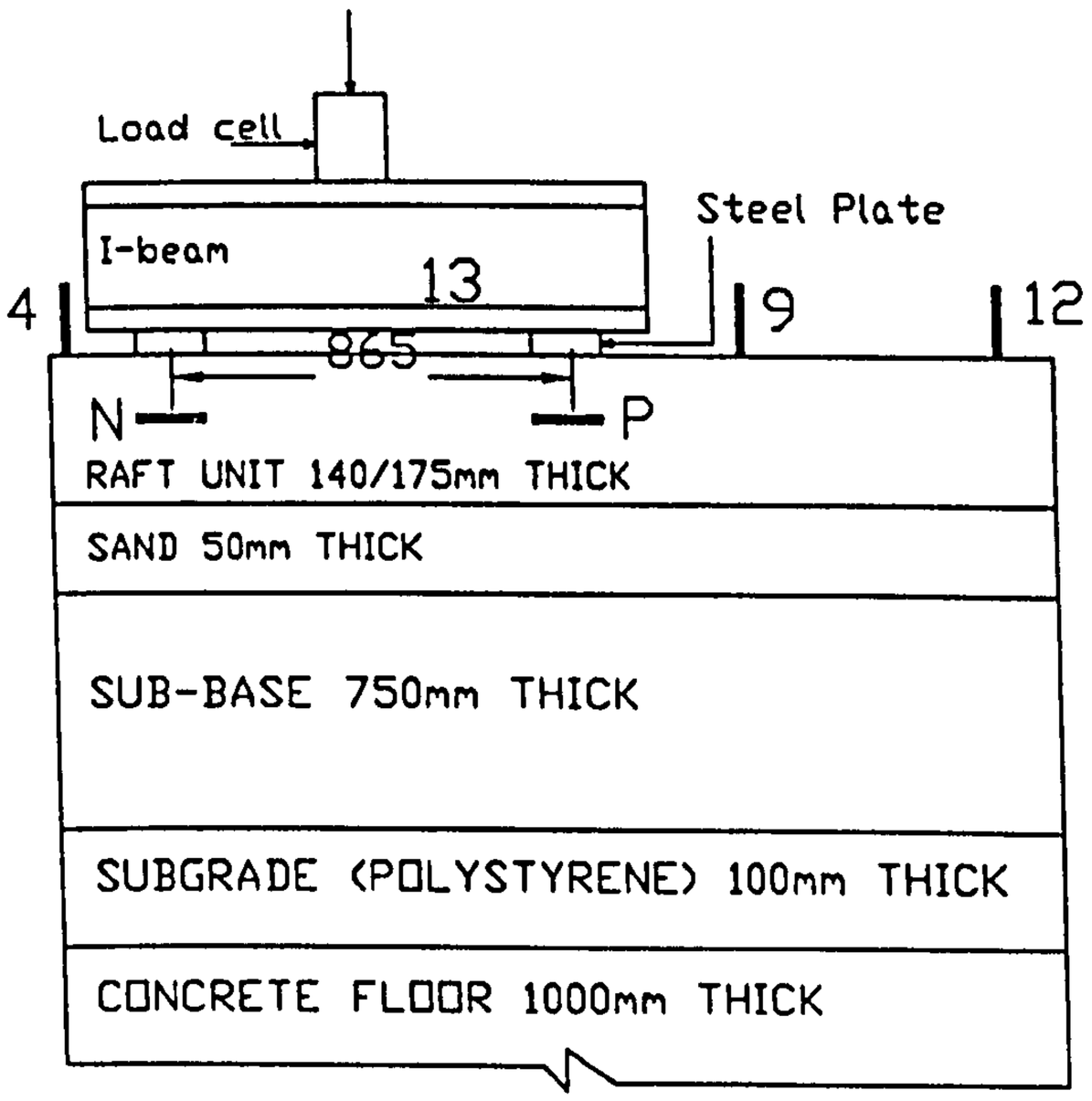

(c) End Elevation B

— (A,M,N and P) Strain gauges

| (0,1,2,3,4,9,12 and 13) LVDTs

P1,P2,P3 and P4 are the loading positions

Not to scale Raft unit 2000x2000 on plan

Dimensions in mm

Fig. 4.4 (b and c) SIDE AND END ELEVATION OF LOADING POSITIONS AND INSTRUMENTATION

(a) Load at position P1

(b) Load at position P2

(c) Load at position P3

(d) Load at position P4

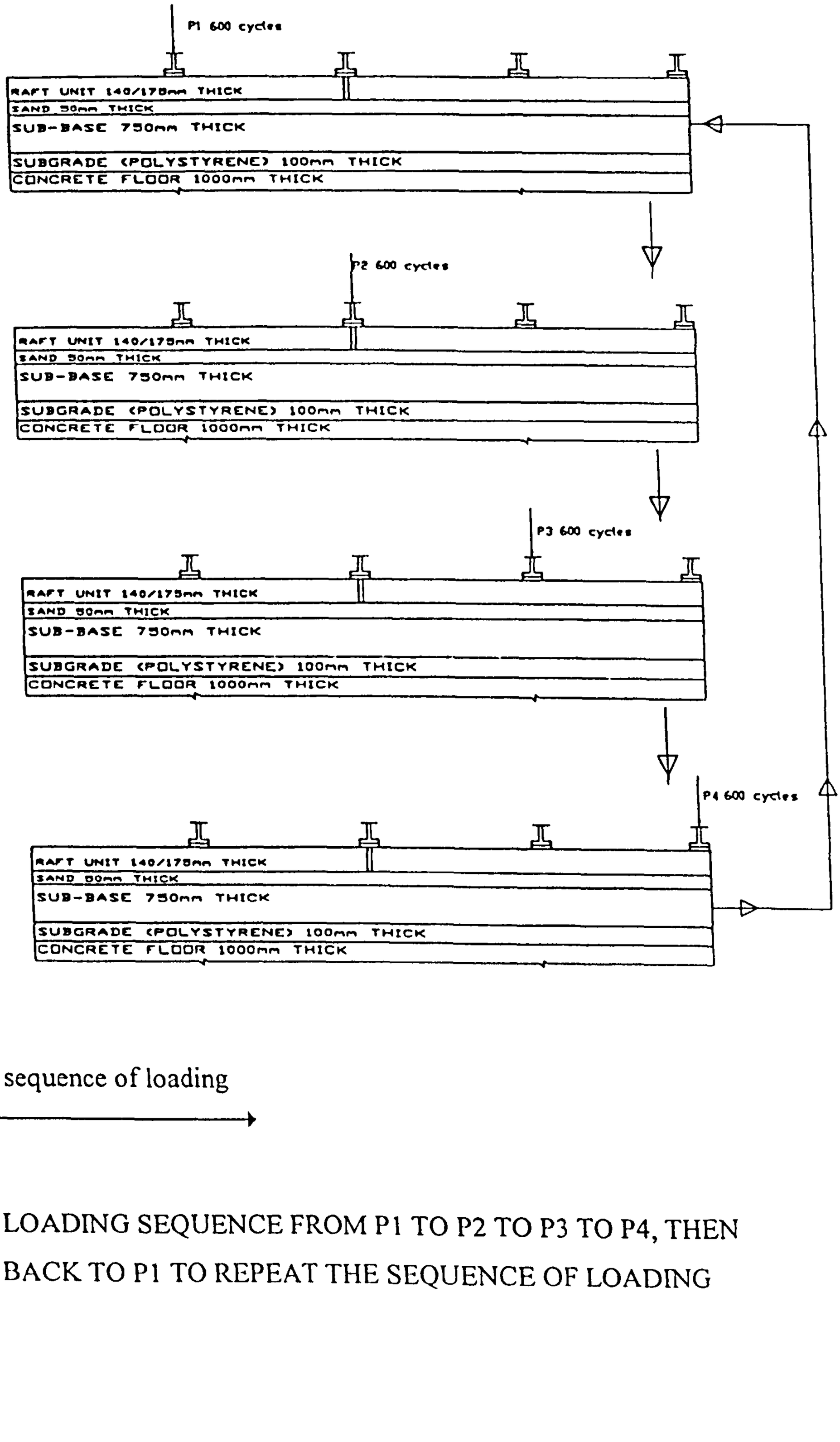

Direction of the sequence of loading

Fig. 4.4(d) LOADING SEQUENCE FROM P1 TO P2 TO P3 TO P4, THEN BACK TO P1 TO REPEAT THE SEQUENCE OF LOADING

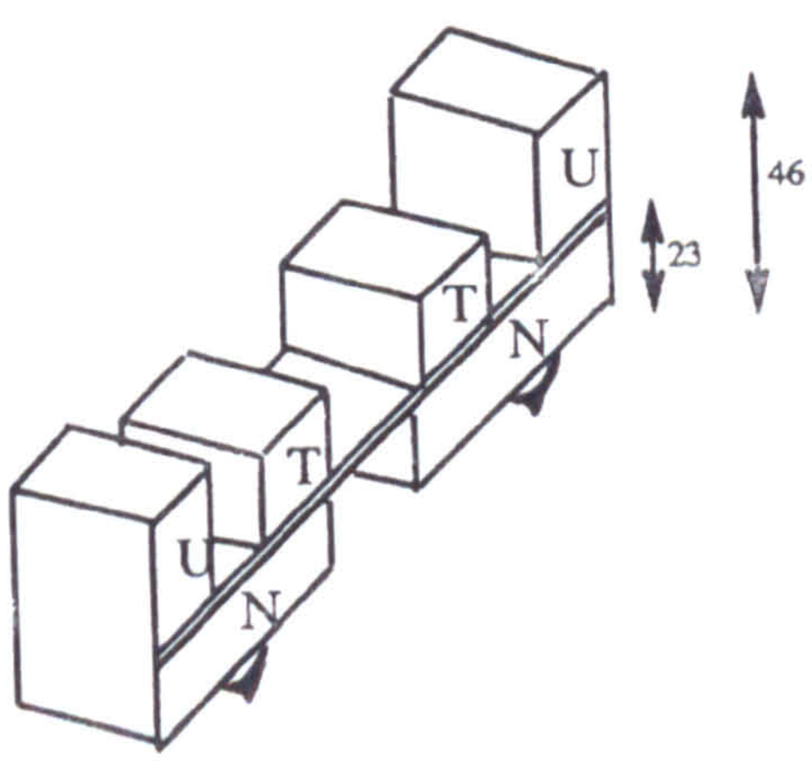

(a) General Arrangement

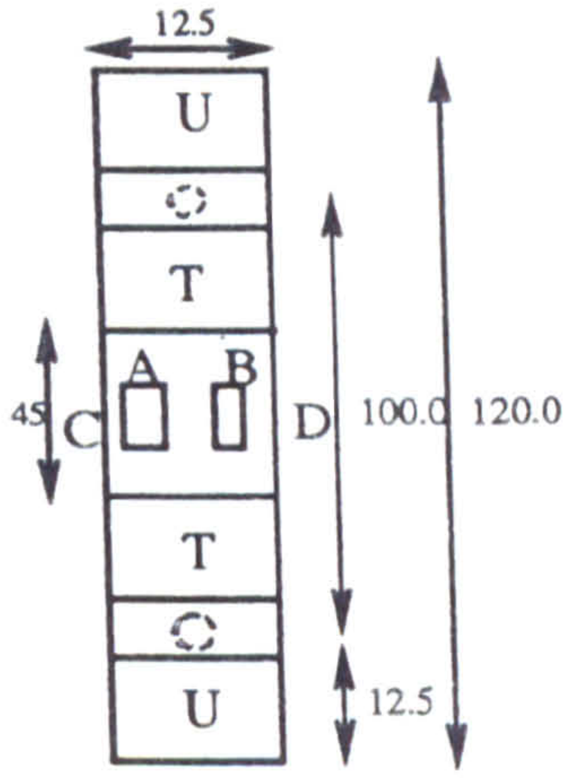

Plan View

(Dimensions in mm.)

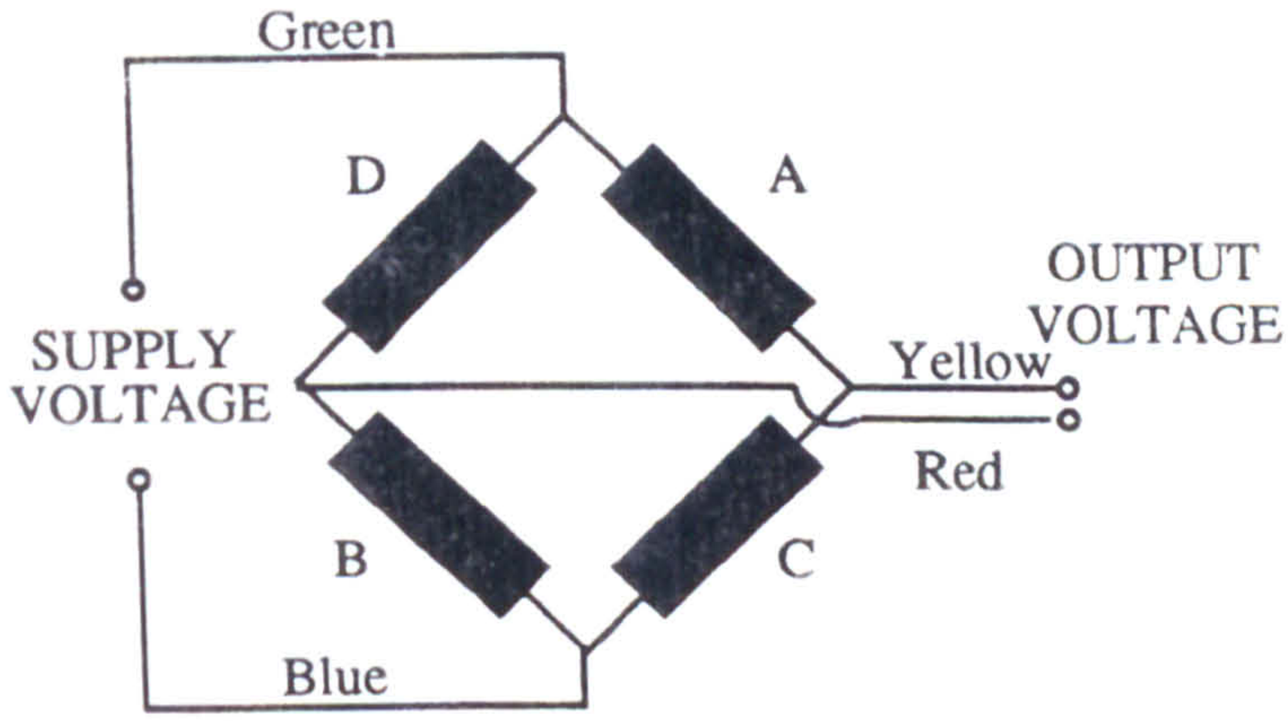

(b) Electrical Connection

Fig. 4.5 : Details of Demountable Strain Transducer.

Fig. 4.6 : Extensometer Calibrator For Strain Transducers

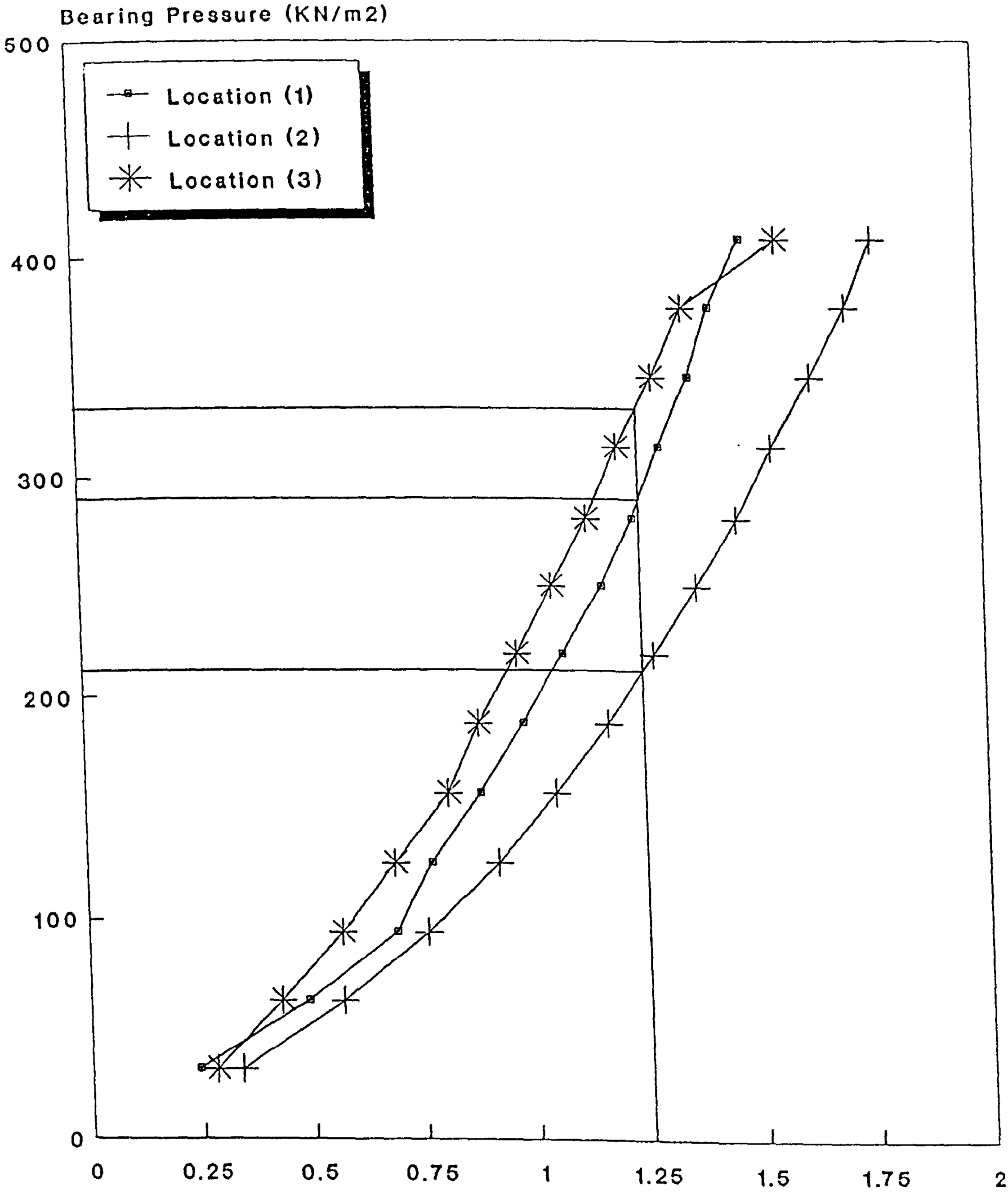

Fig 4.7: Plate Bearing Tests on Sub-base

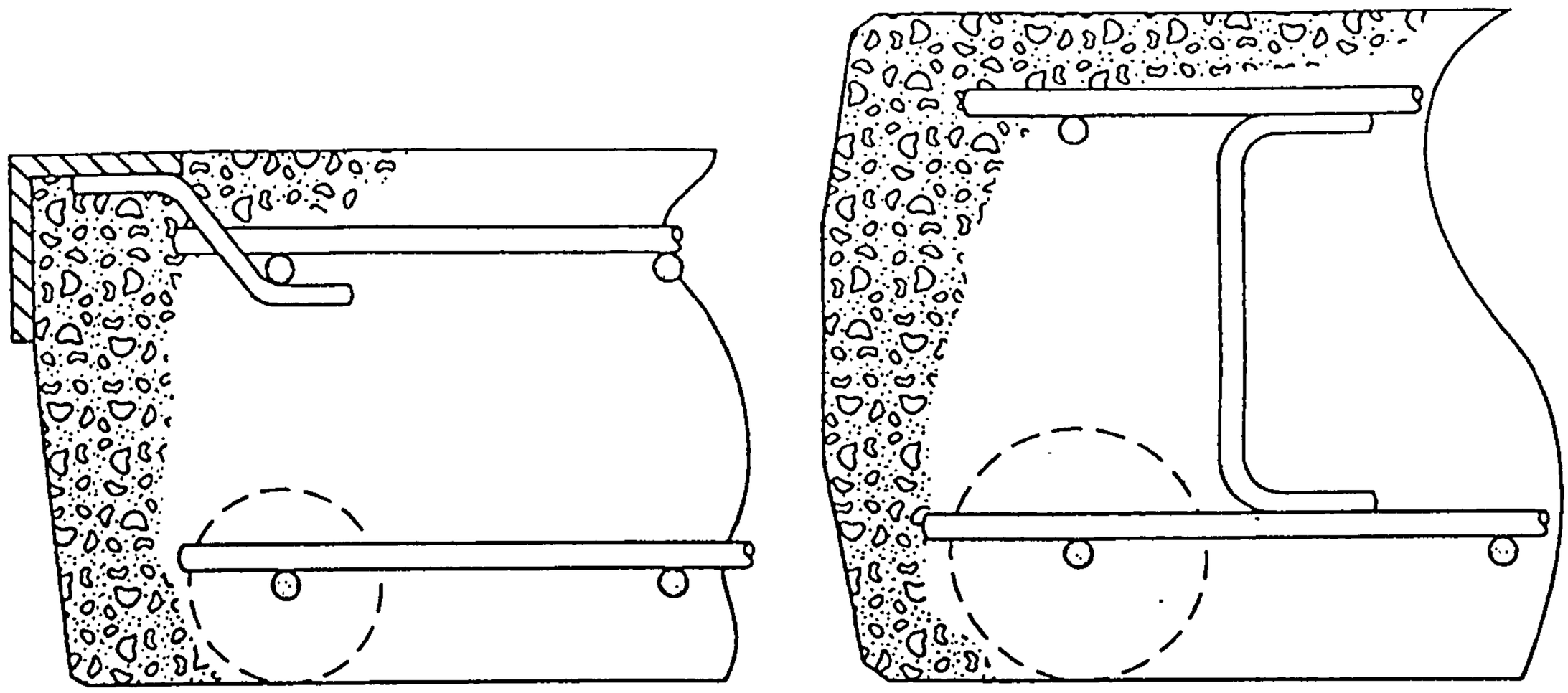

a. Profile section of framed raft

b. Profile section of frameless raft

Figure 4.8: Typical Raft Sections

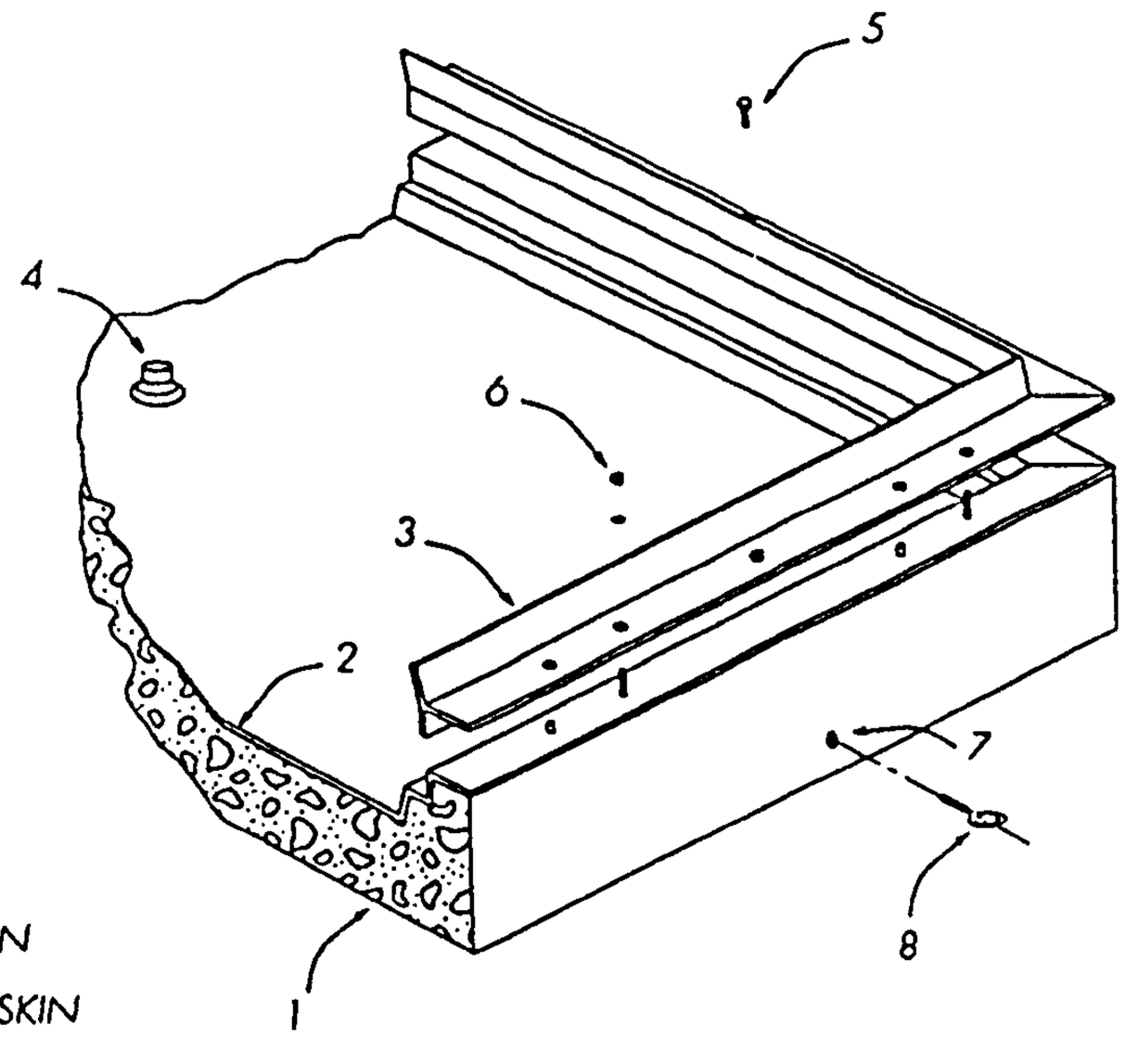

LEGEND

1. CONCRETE BACKING TO MOULD SKIN
2. GLASS REINFORCED PLASTIC MOULD SKIN
3. PROFILED STEEL UPPER MOULD FRAME
4. VOID FORMER AND TUBE LOCATOR
5. JACKING BOLT FOR STRIPPING UPPER MOULD FRAME
6. NUT FOR HOLDING DOWN UPPER FRAME DURING MOULDING
7. CAST-IN THREADED INSERT FOR MOULD HANDLING
8. MOULD LIFTING EYE

Figure 4.9: Part Section Indicating Mould Construction and Assembly

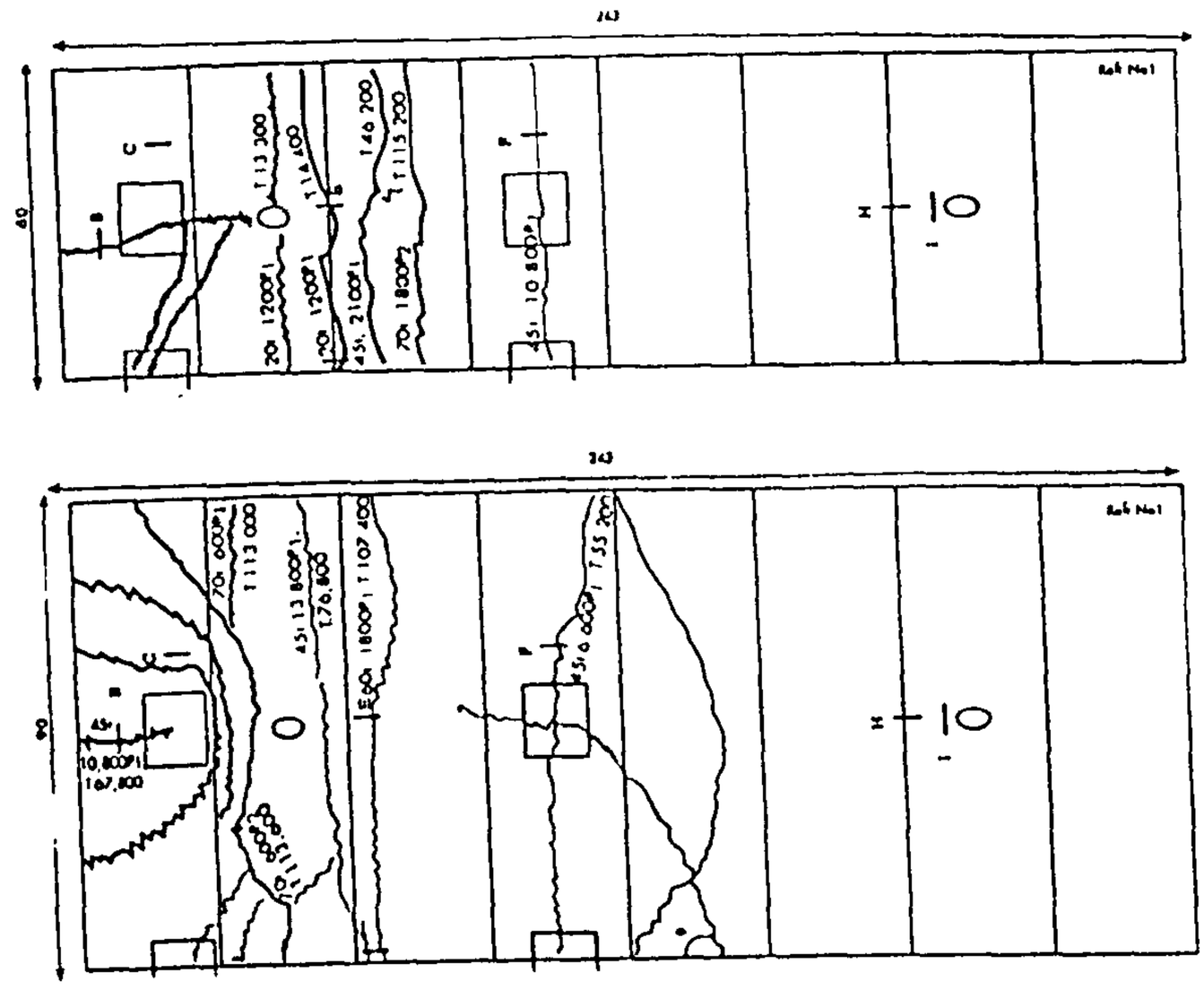

Raft Unit- R6 (Aspect Ratio = 0.25)
2430 ×600 mm on plan

Raft Unit- R9 (Aspect Ratio = 0.375)
2430 ×900 mm on plan

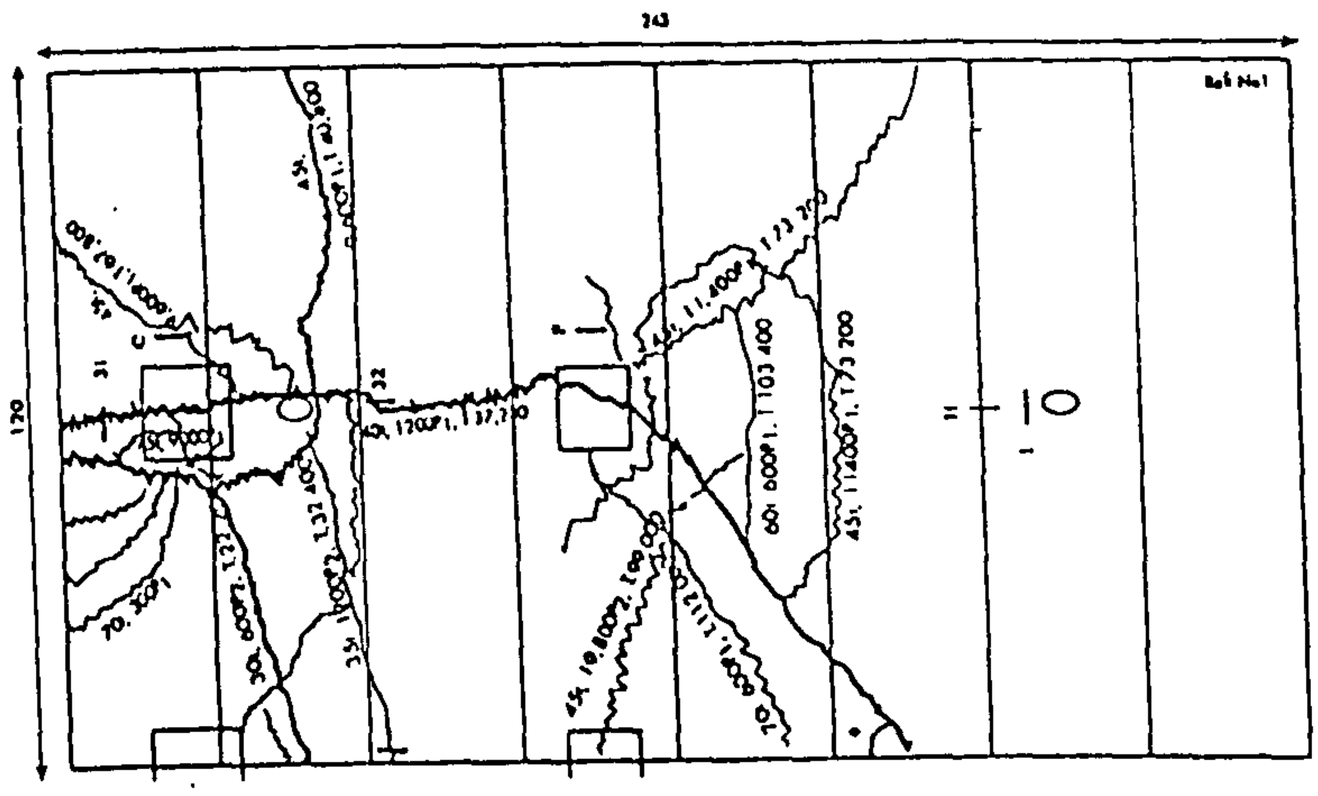

Raft Unit- R12 (Aspect Ratio = 0.5)
2430 ×1200 mm on plan

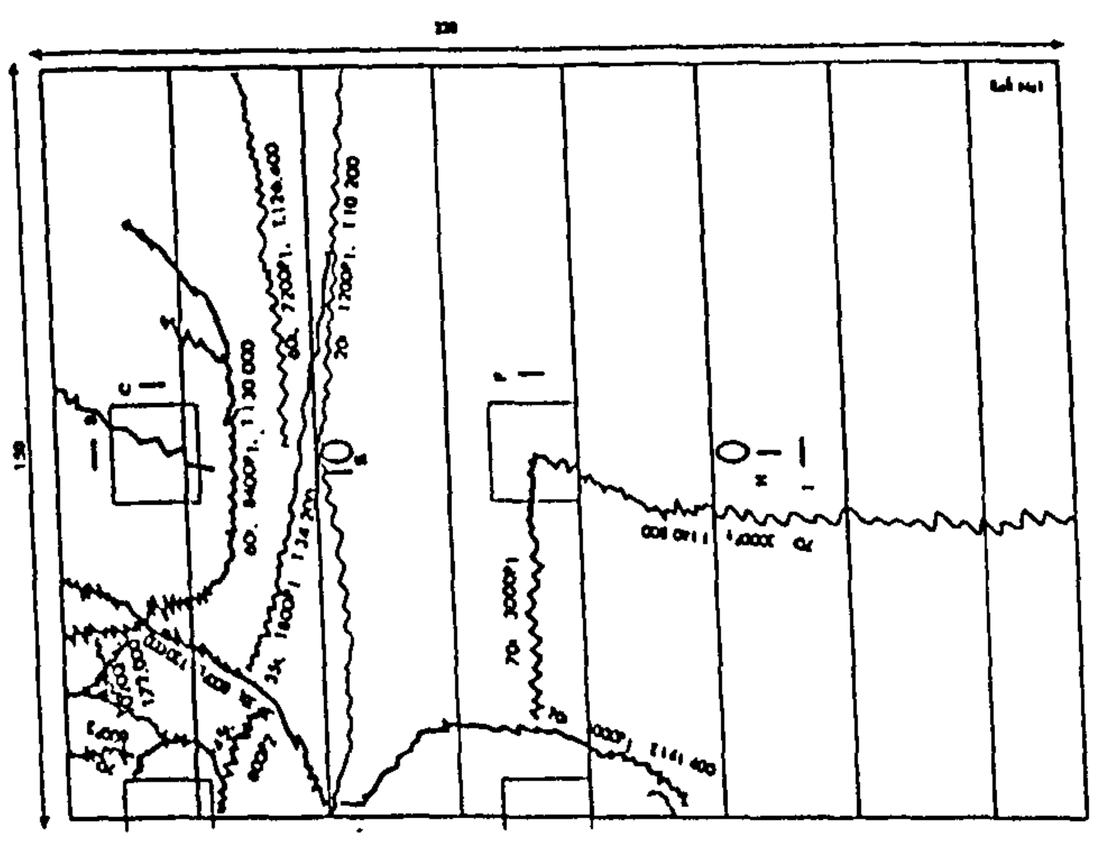

Raft Unit- RR (Aspect Ratio = 0.65)
2300 ×1500 mm on plan

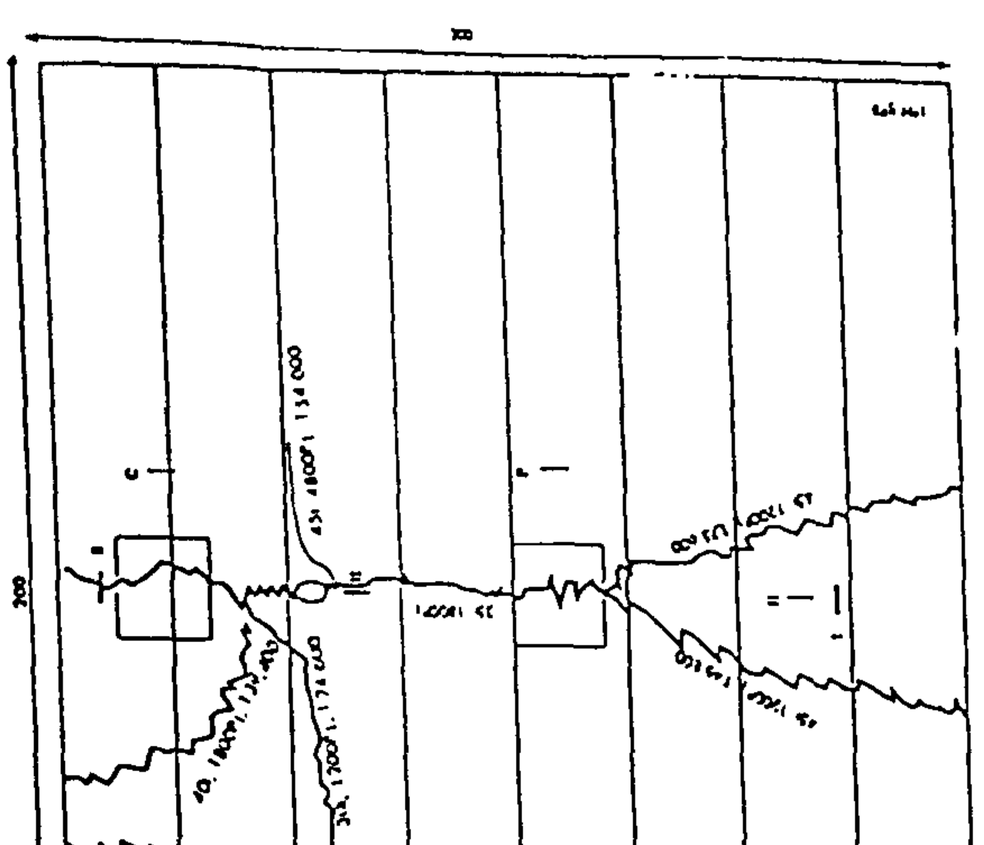

Raft Unit- RS2 (Aspect Ratio =1.0)
2000 ×2000 mm on plan

Fig.5.1 a: Top Crack Patterns to Failure - Module M1

| For Test Rig Notations see Table 4.2 and Fig 4.4|

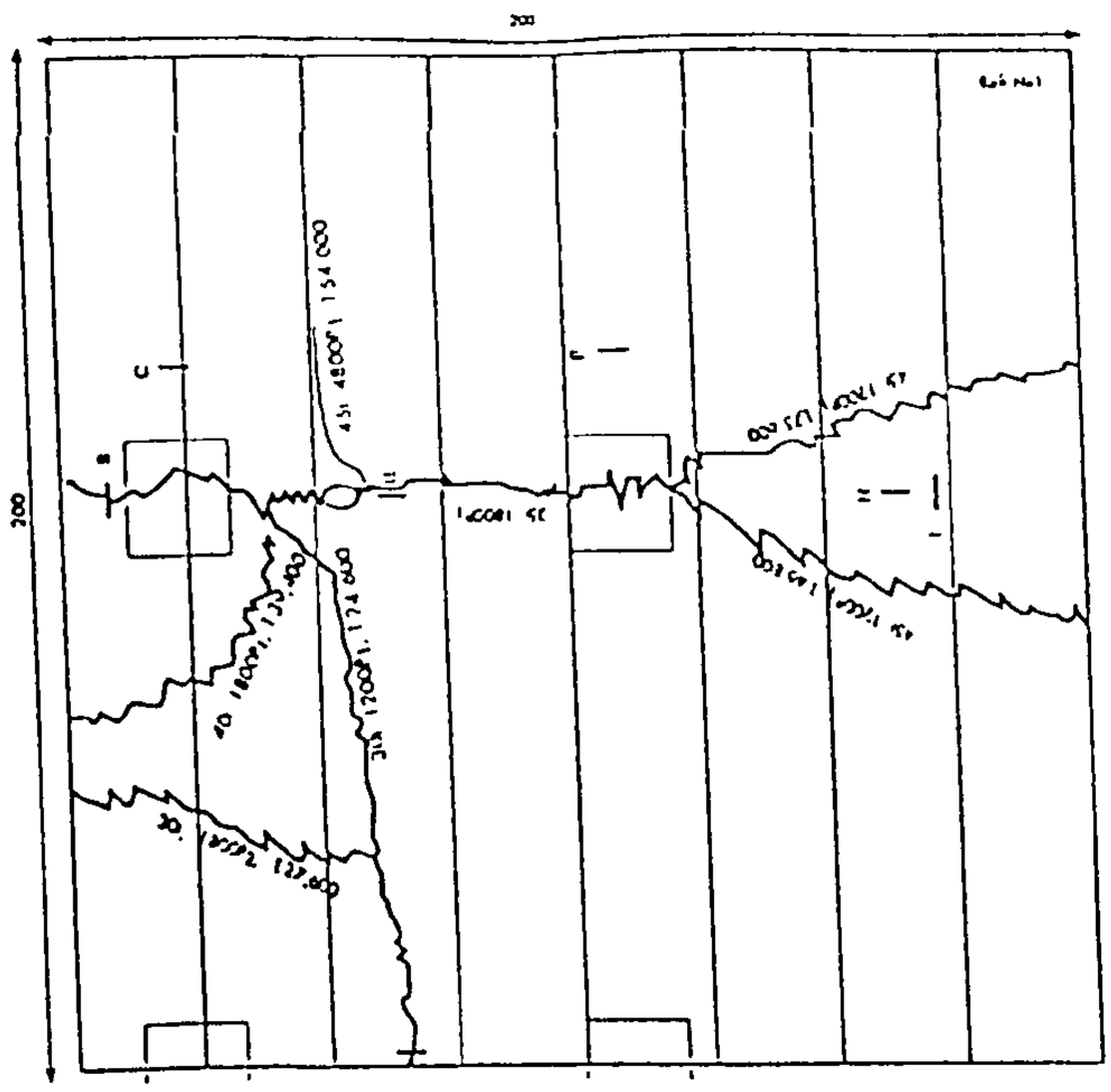

Raft Unit- RS2, Steel Fabric Reinforcement
142 mm^2/m, 2000 ×2000 mm on plan

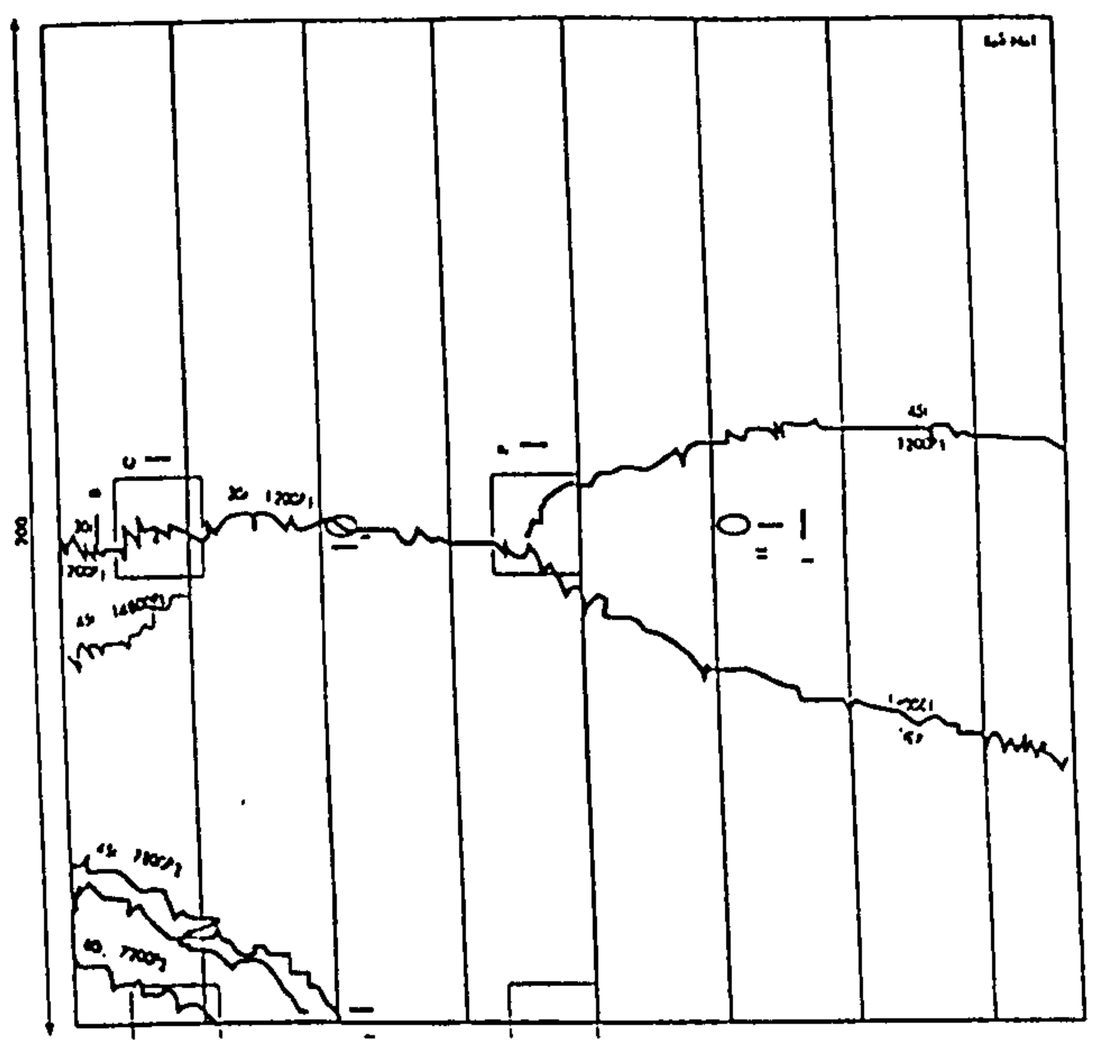

Raft Unit- RS1, Steel Fabric Reinforcement
283 mm^2/m, 2000 ×2000 mm on plan

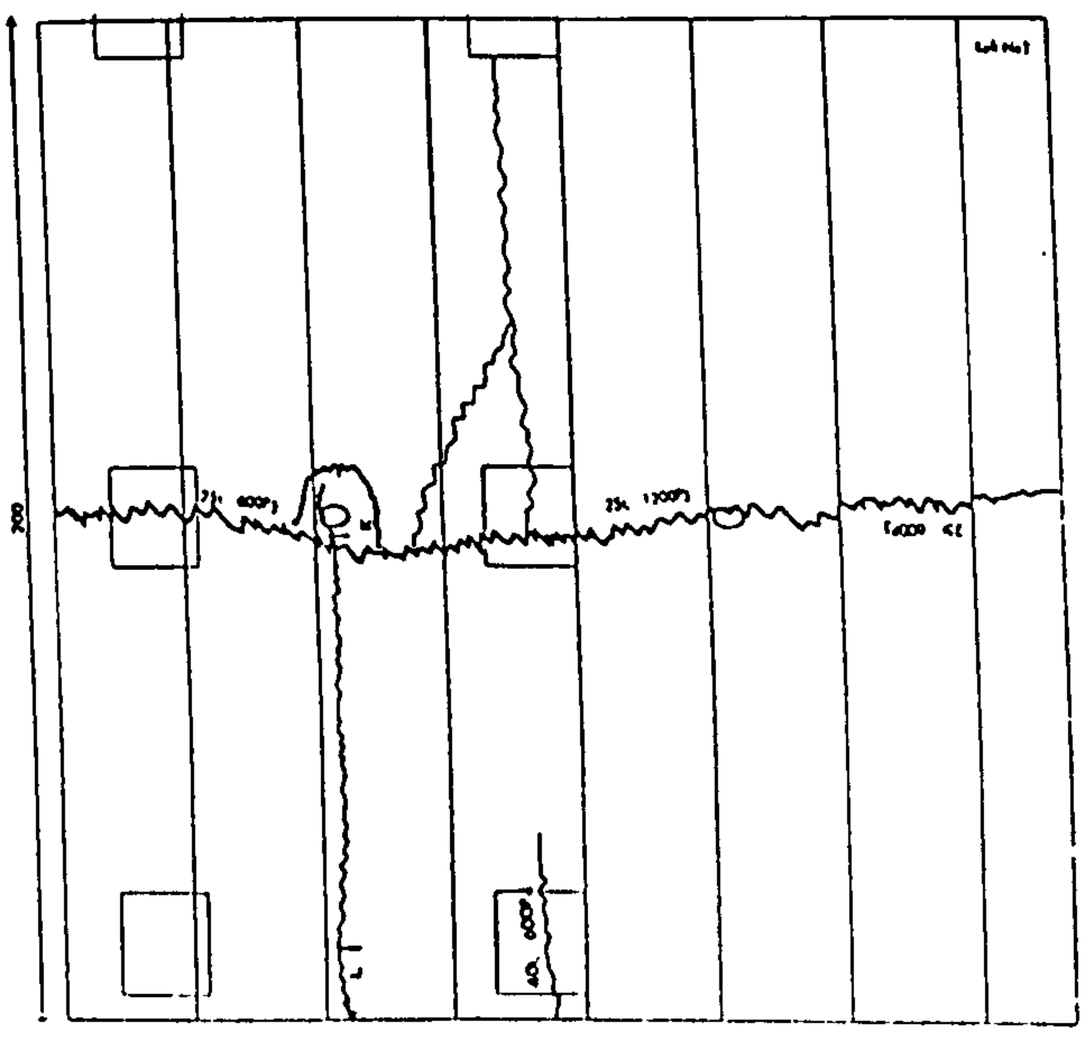

Raft Unit- RSF, Steel Fibre Reinforcement
240 kg/m^3 (ie 10%by weight)
2000 ×2000 mm on plan

Fig.5.1 b: Top Crack Patterns to Failure - Module M2

| For Test Rig Notations see Table 4.2 and Fig. 4.4|

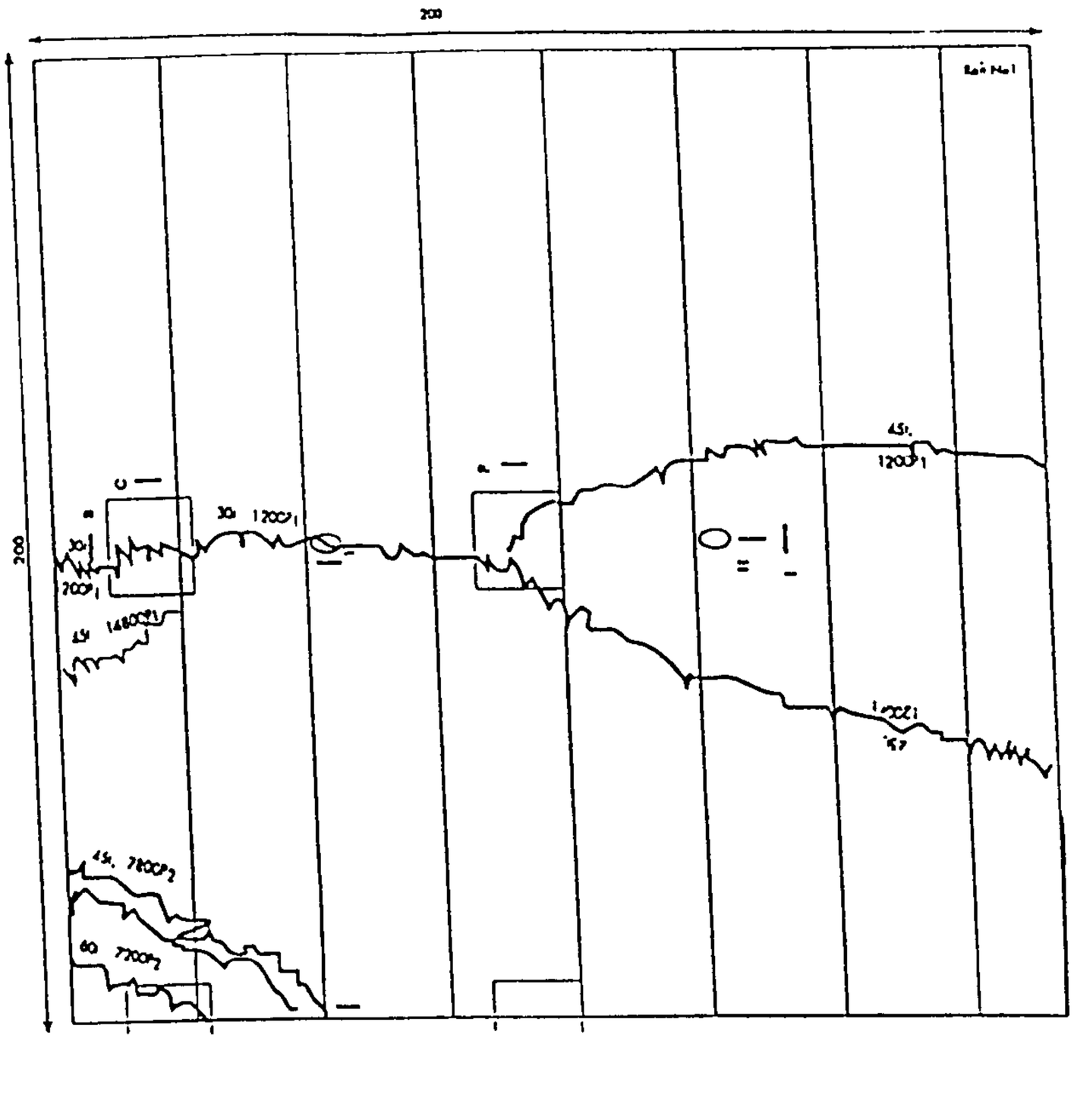

Raft Unit- RS1, Thickness 140 mm
2000 ×2000 mm on plan

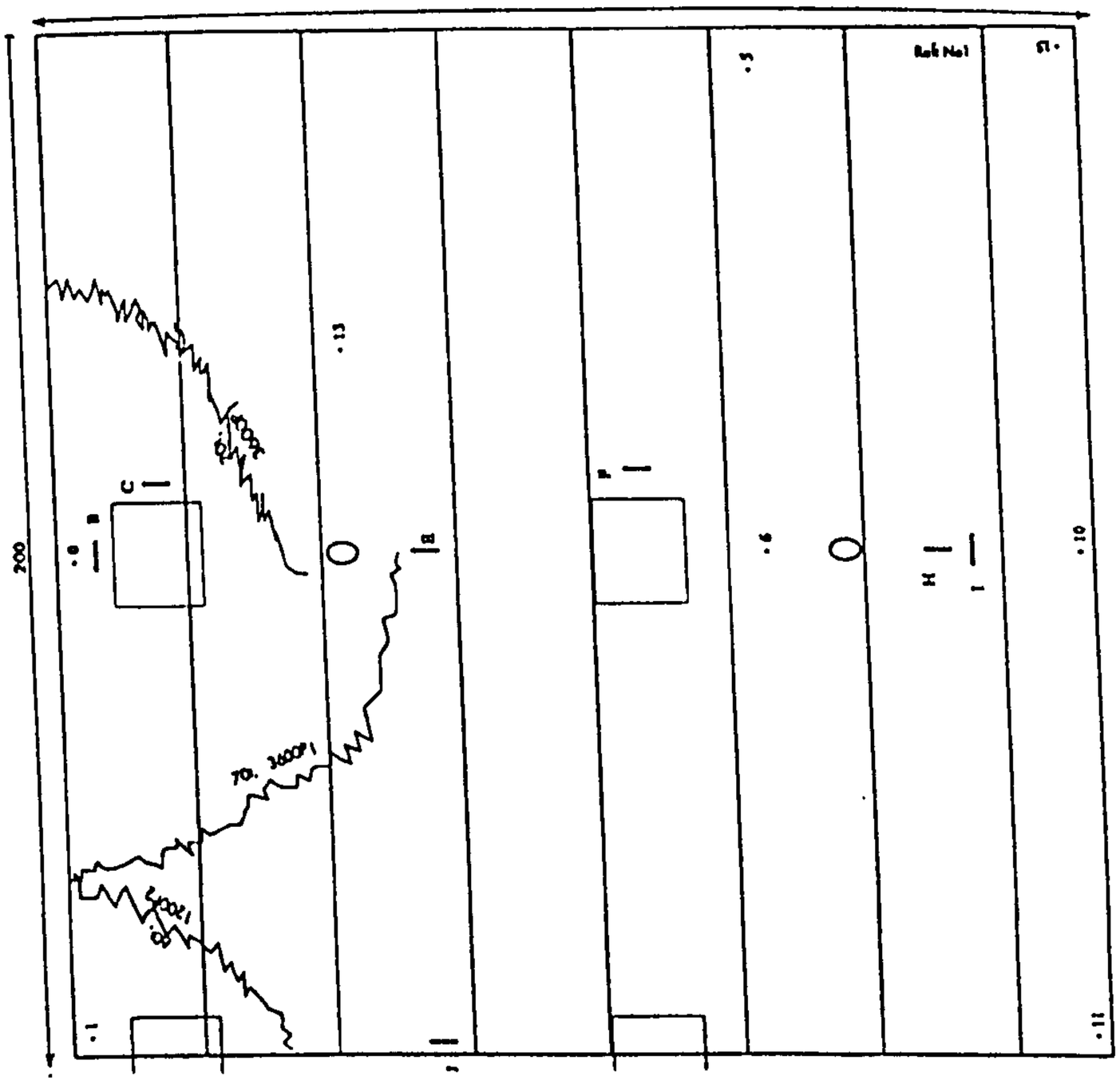

Raft Unit- RS7,Thickness 175 mm
2000 ×2000 mm on plan

Fig.5.1 c: Top Crack Patterns to Failure - Module M3

[For Test Rig Notations see Table 4.2 and Fig. 4.4]

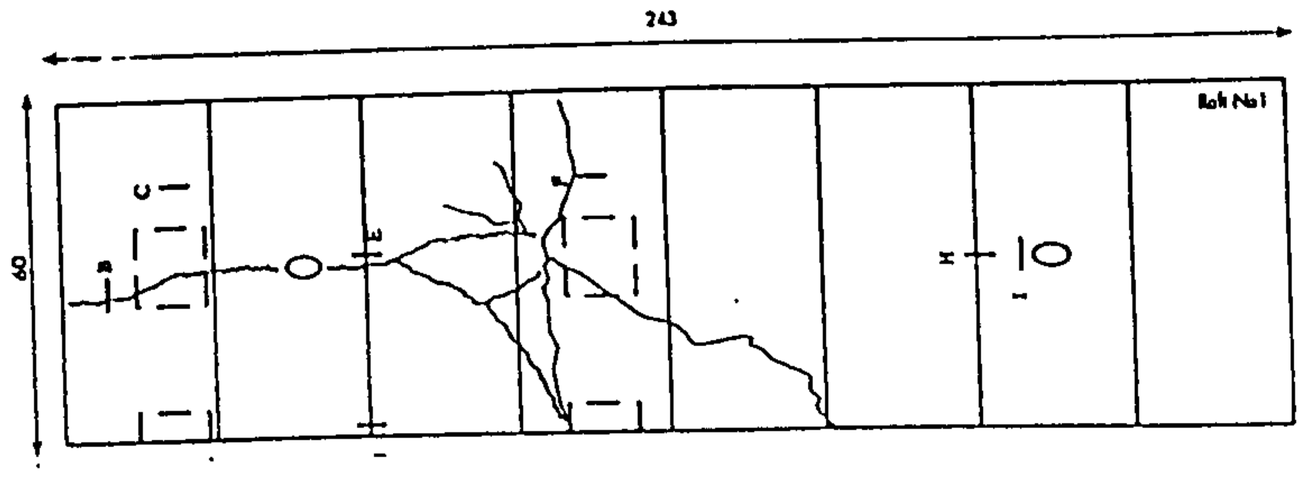

Raft Unit- R6 (Aspect Ratio = 0.25)
2430 ×600 mm on plan

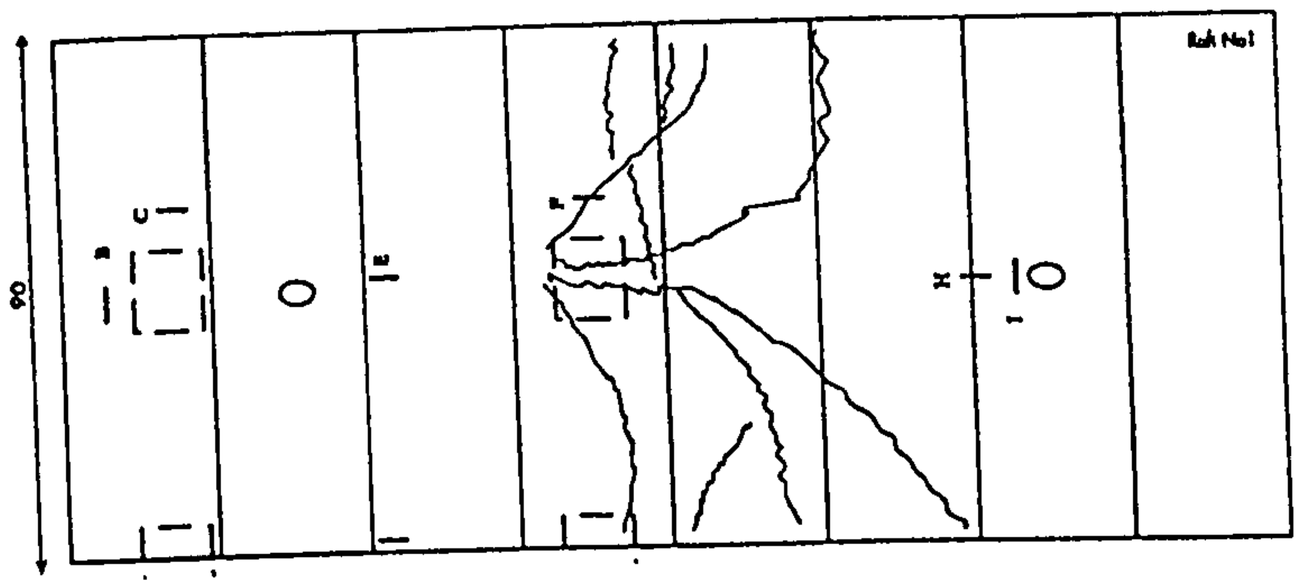

Raft Unit- R9 (Aspect Ratio = 0.375)
2430 ×900 mm on plan

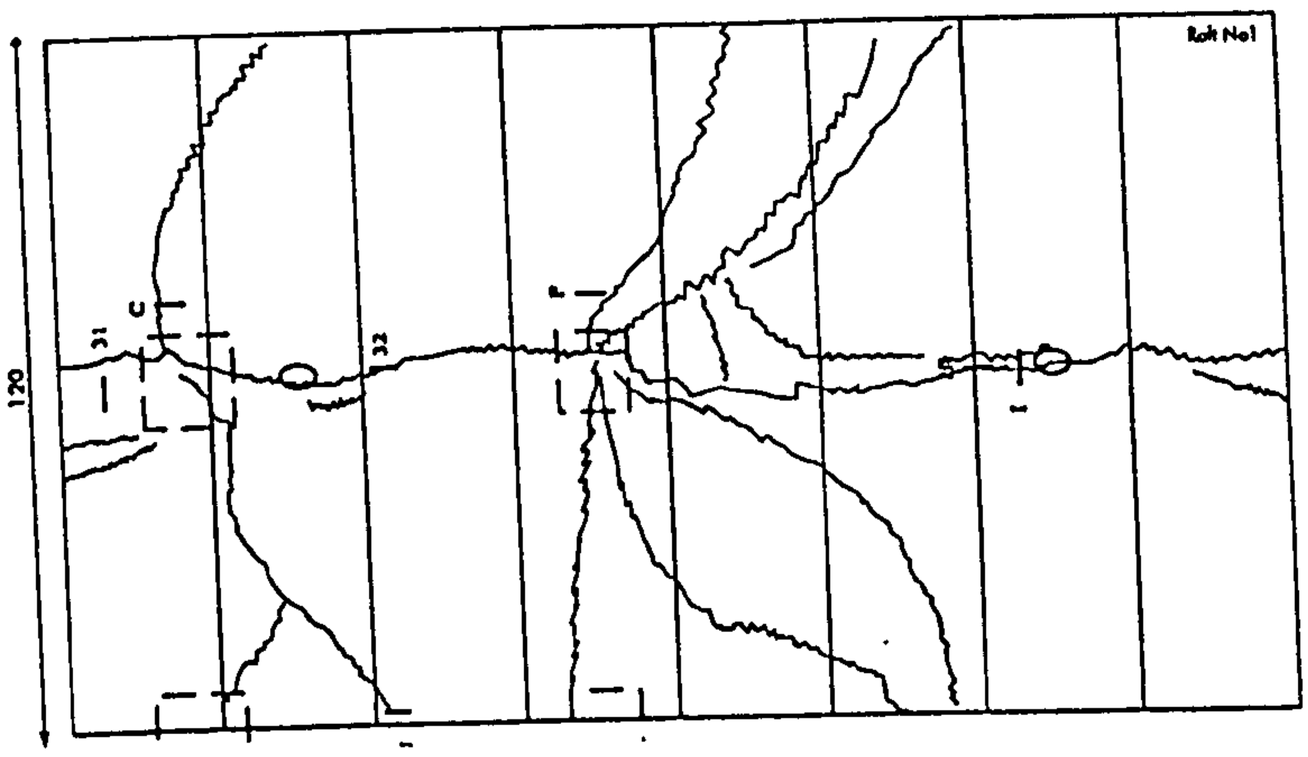

Raft Unit- R12 (Aspect Ratio = 0.5)
2430 ×1200 mm on plan

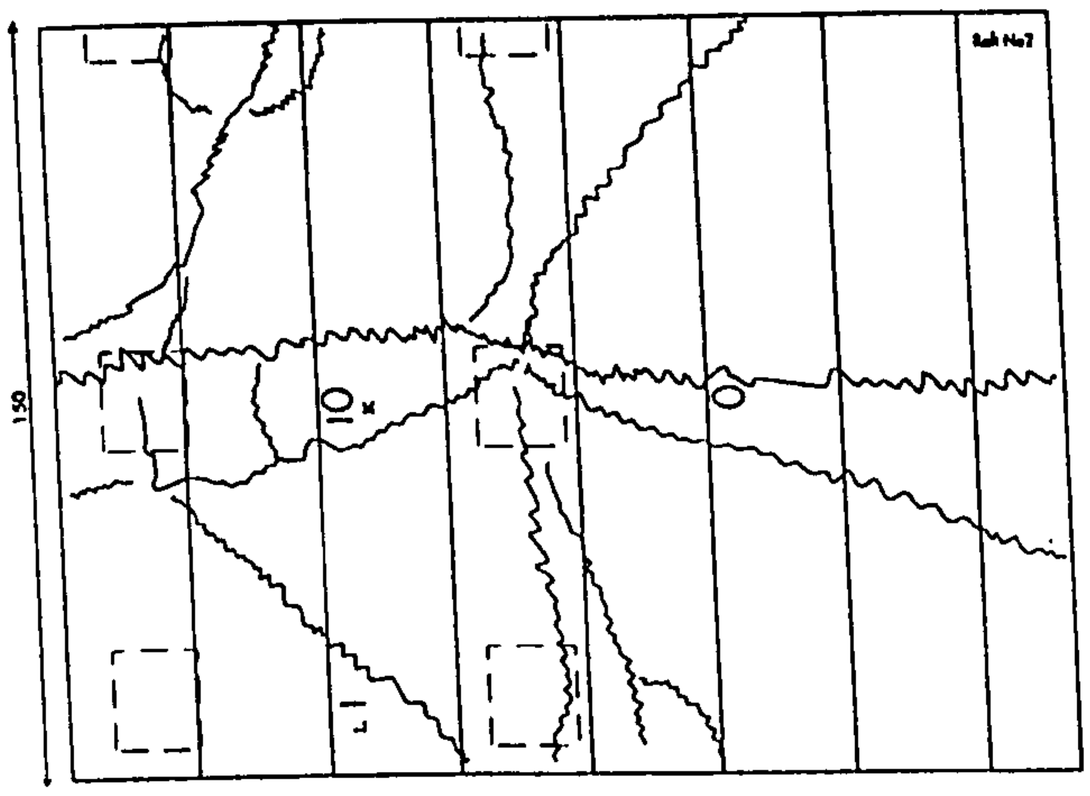

Raft Unit- RR (Aspect Ratio = 0.65)
2300 ×1500 mm on plan

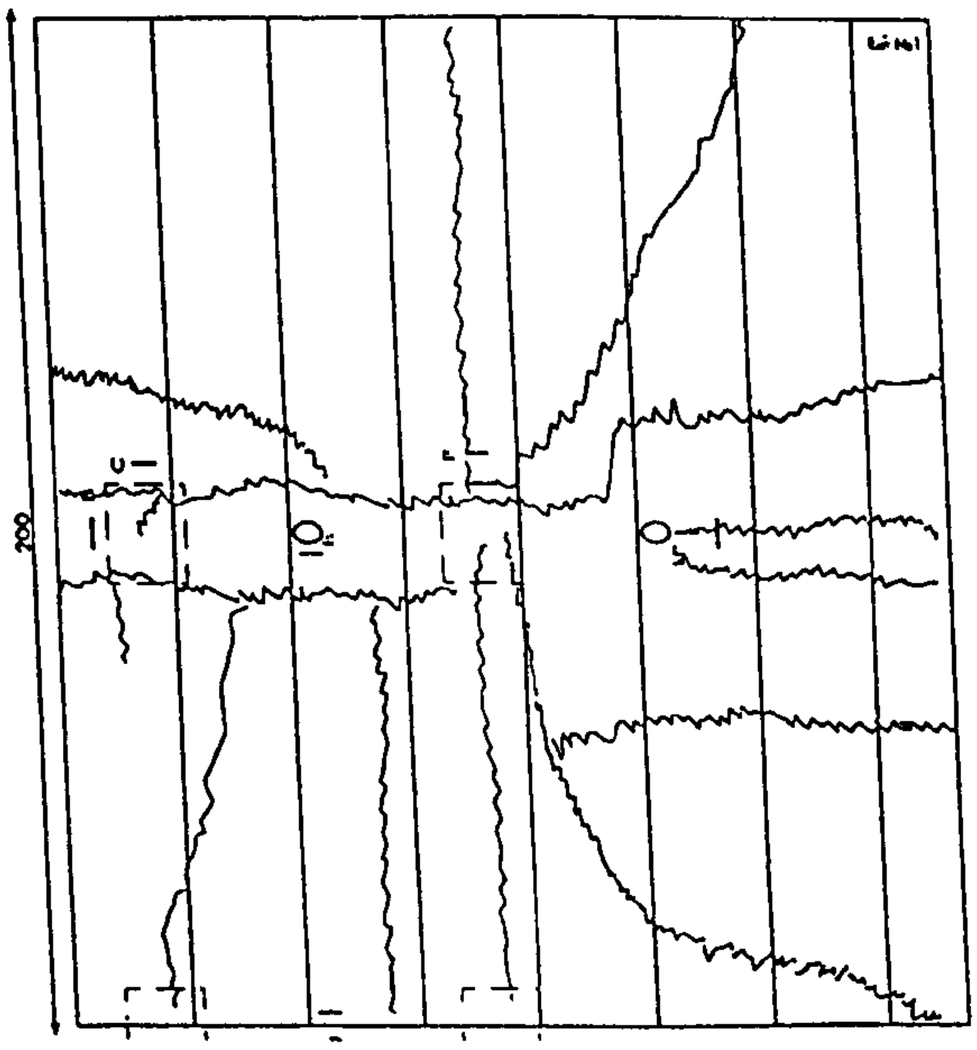

Raft Unit- RS2 (Aspect Ratio =1.0)
2000 ×2000 mm on plan

Fig.5.2 a: Bottom Crack Patterns to Failure - Module M1

[For Test Rig Notations see Table 4.2 and Fig 4.4]

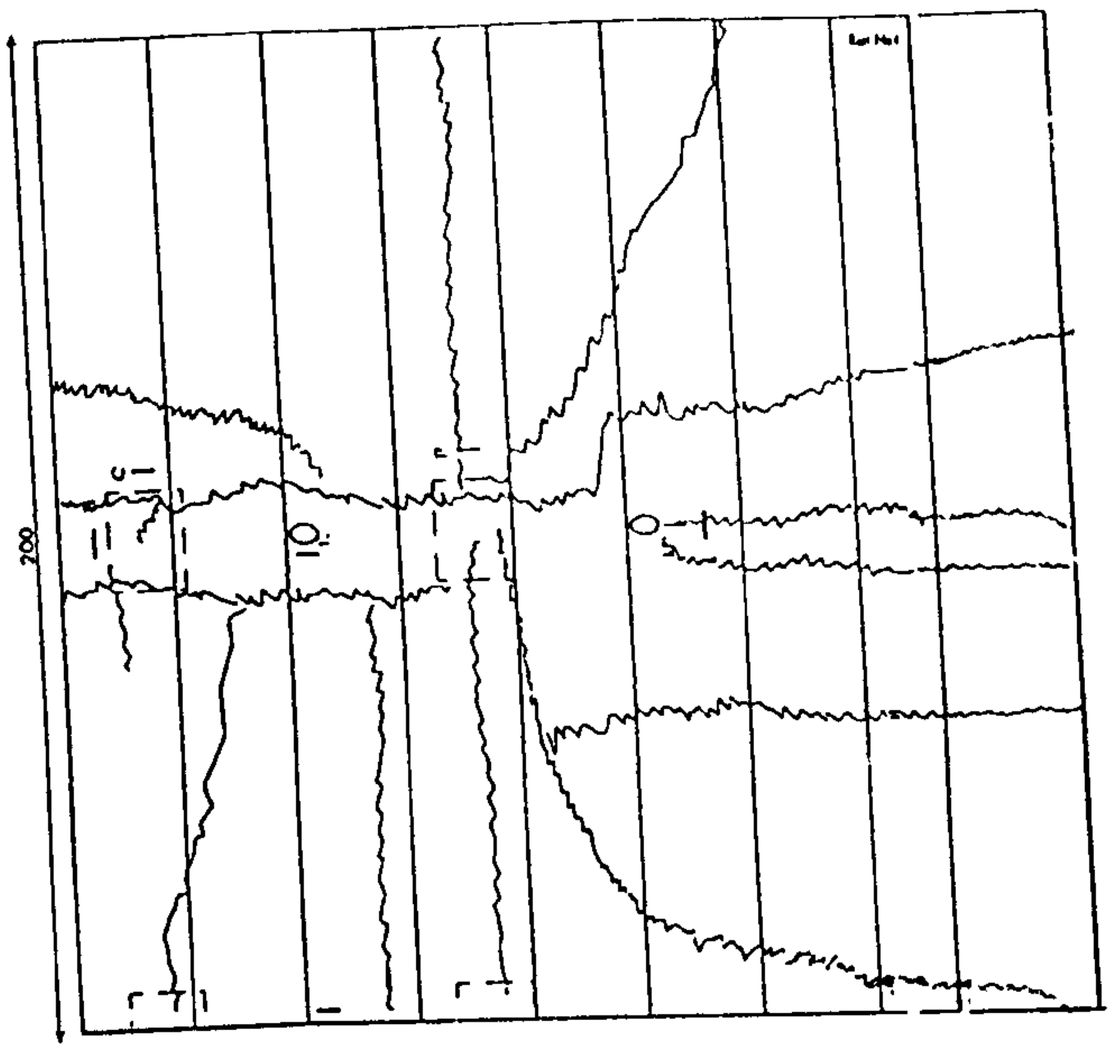

Raft Unit- RS2, Steel Fabric Reinforcement
142 mm^2/m, 2000 ×2000 mm on plan

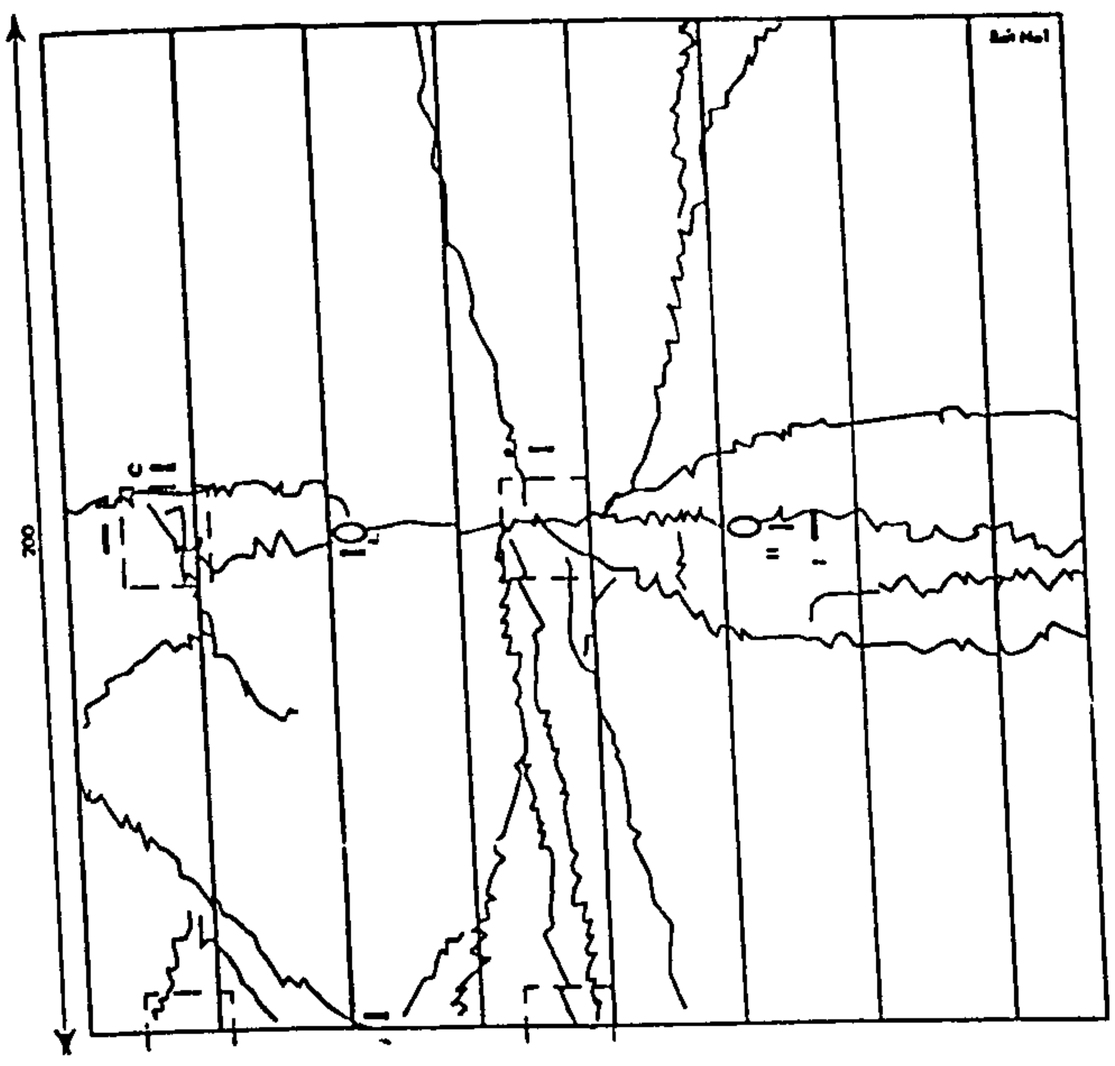

Raft Unit- RS1. Steel Fabric Reinforcement
283 mm^2/m, 2000 ×2000 mm on plan

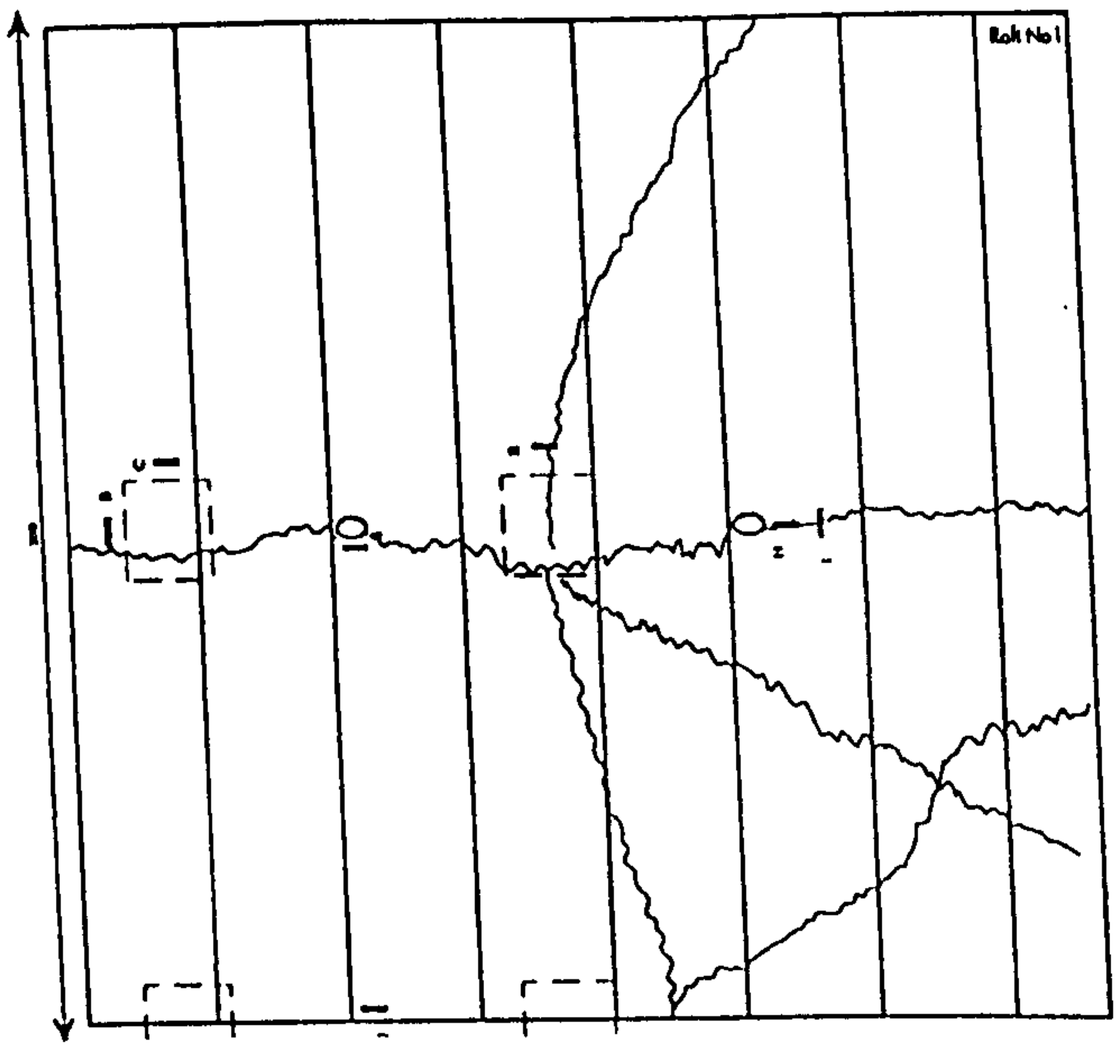

Raft Unit- RSF, Steel Fibre Reinforcement
240 kg/m^3 (ie 10%by weight)
2000 ×2000 mm on plan

Fig.5.2 b: Bottom Crack Patterns to Failure - Module M2

[For Test Rig Notations see Table 4.2 and Fig. 4.4]

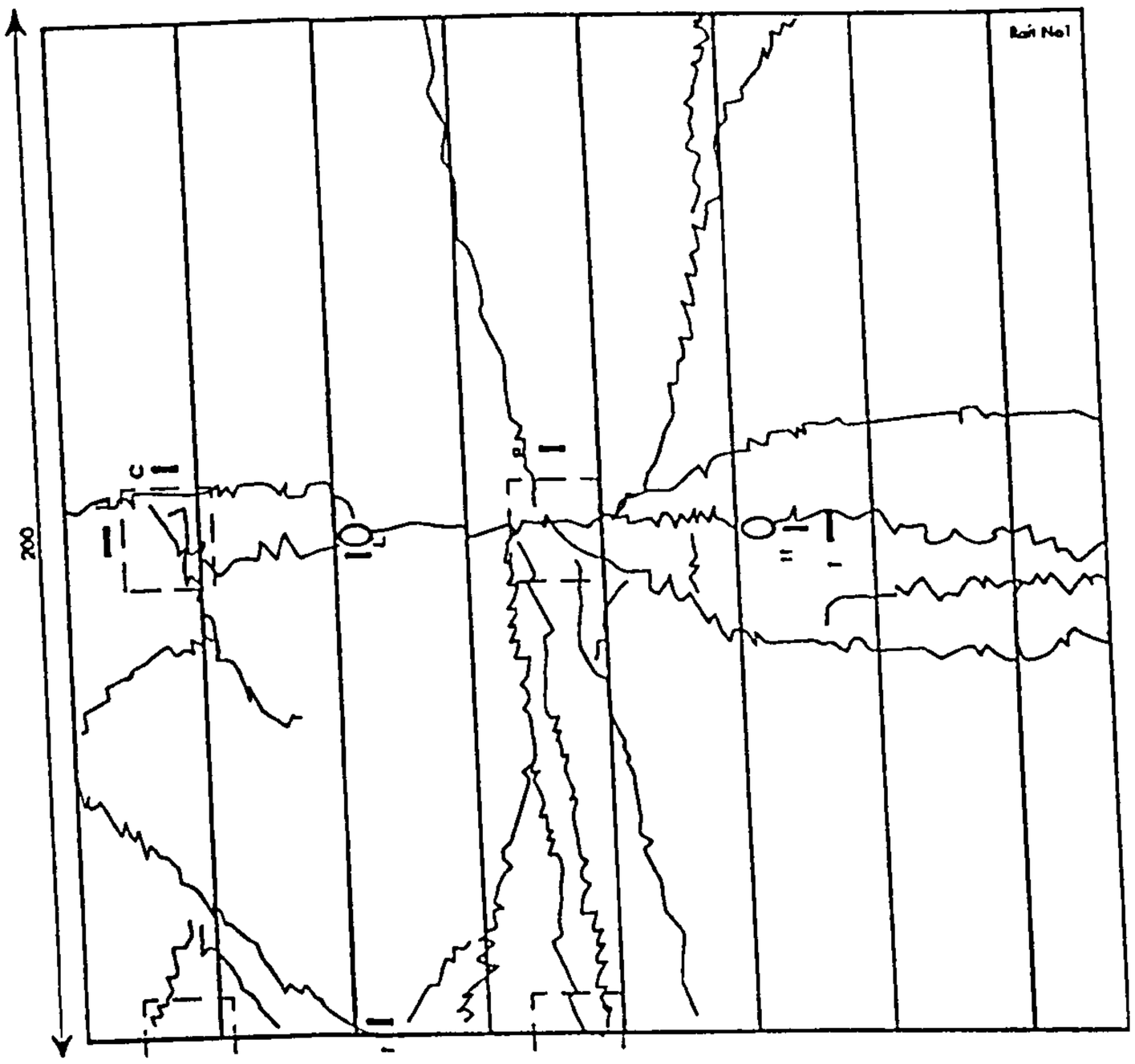

Raft Unit- RS1, Thickness 140 mm
2000 ×2000 mm on plan

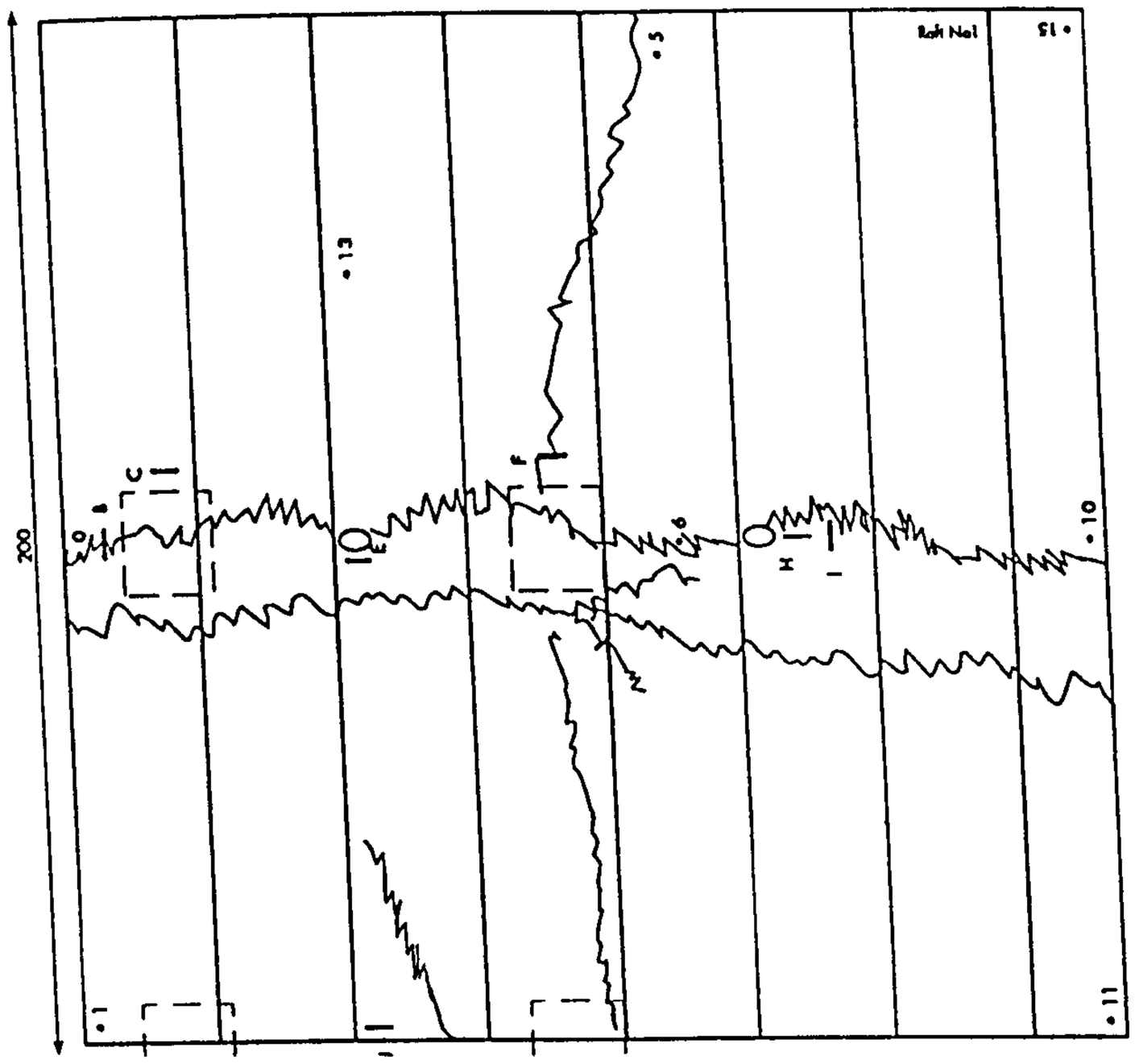

Raft Unit- RS7.Thickness 175 mm
2000 ×2000 mm on plan

Fig.5.2 c: Bottom Crack Patterns to Failure - Module M3

[For Test Rig Notations see Table 4.2 and Fig. 4.4]

Fig.5.3: LOAD CYCLES Vs BOTTOM CRACKS
For Load 450 kN
Due to Loading Position P3- For M1

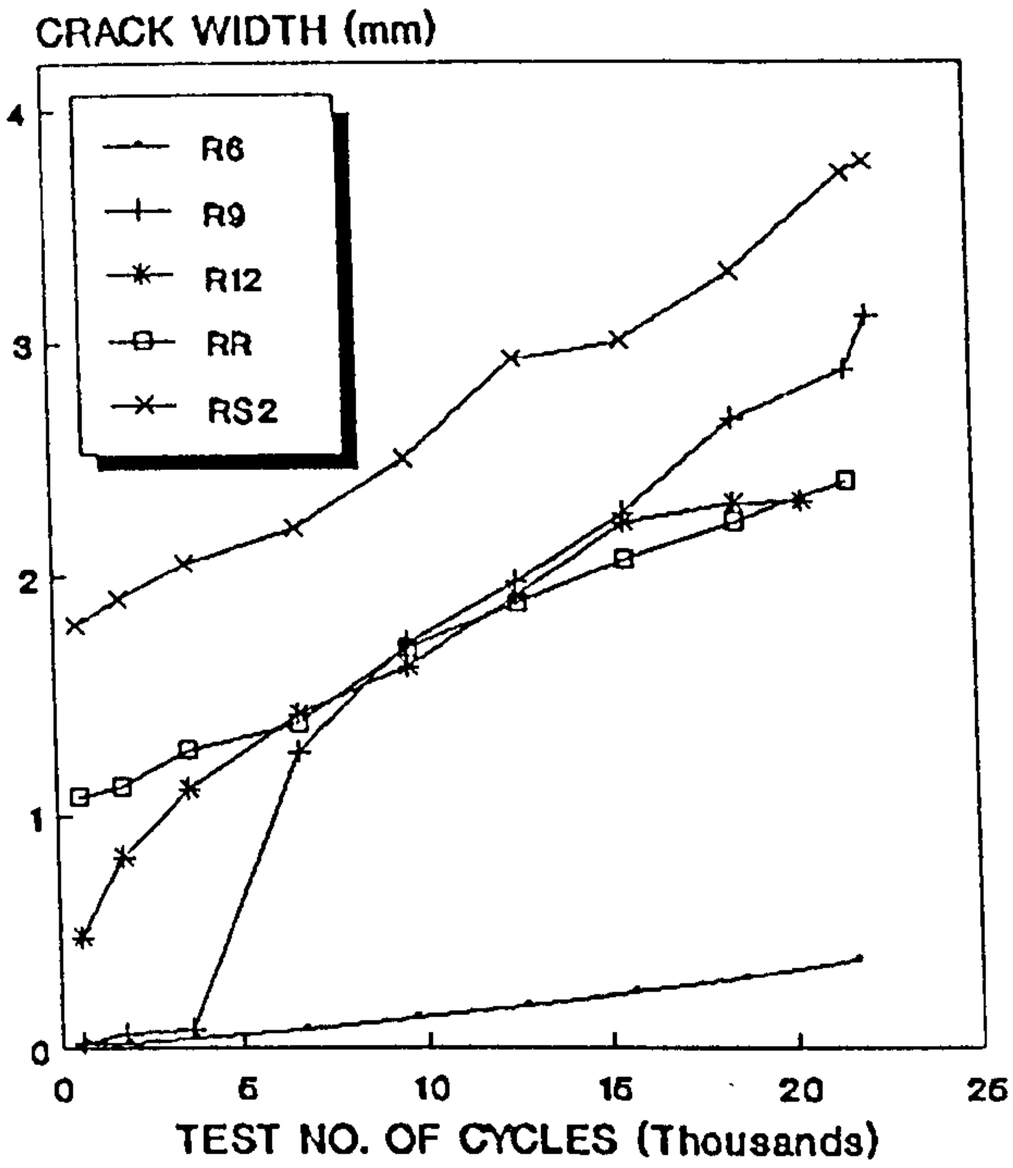

Fig.5.4: LOAD CYCLES Vs TOP CRACKS
For Load 450 kN
Due to Loading Position P3-For M1

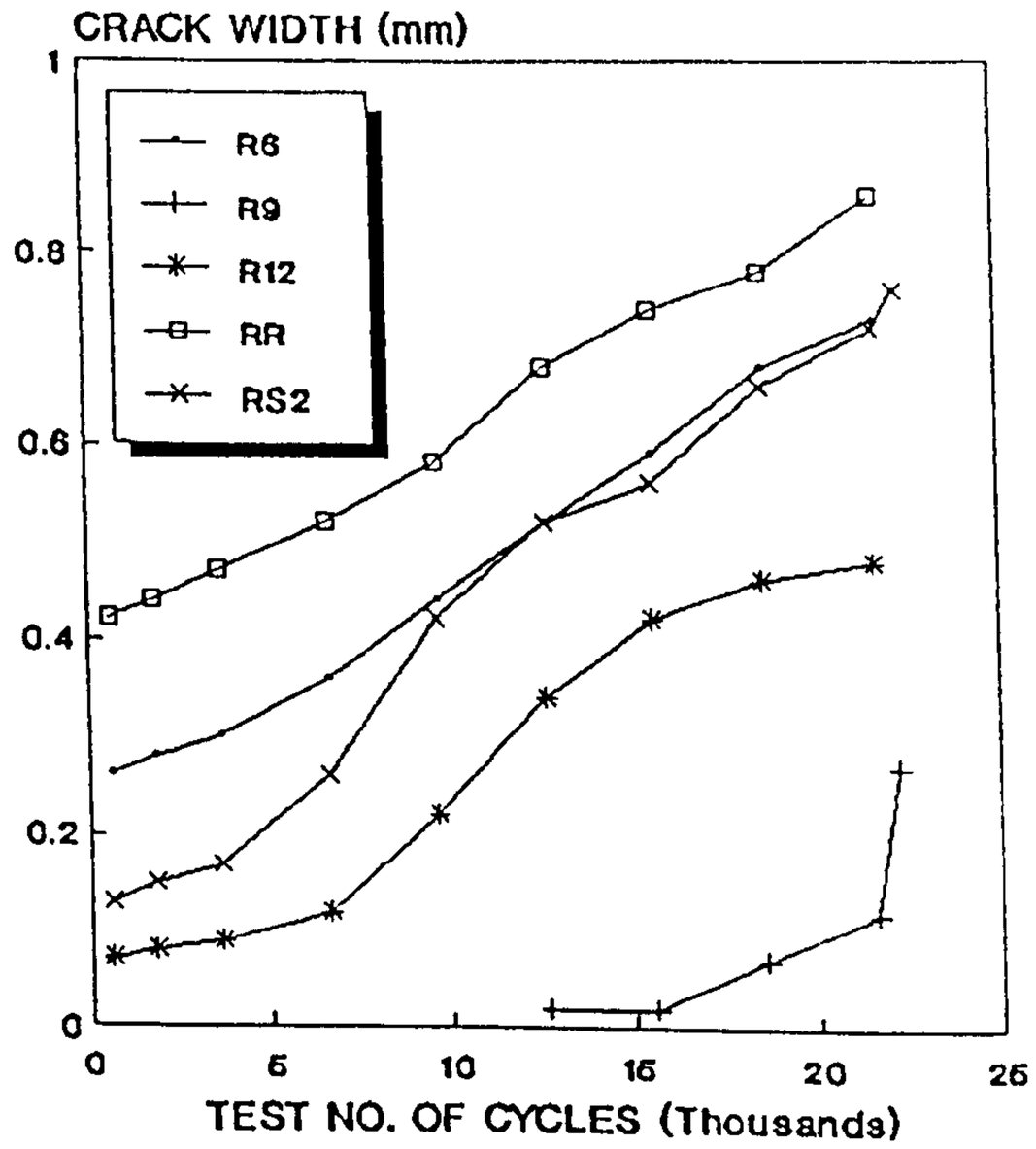

Fig.5.5: LOAD Vs TOP CRACKS
Due To Loading P1-For M1

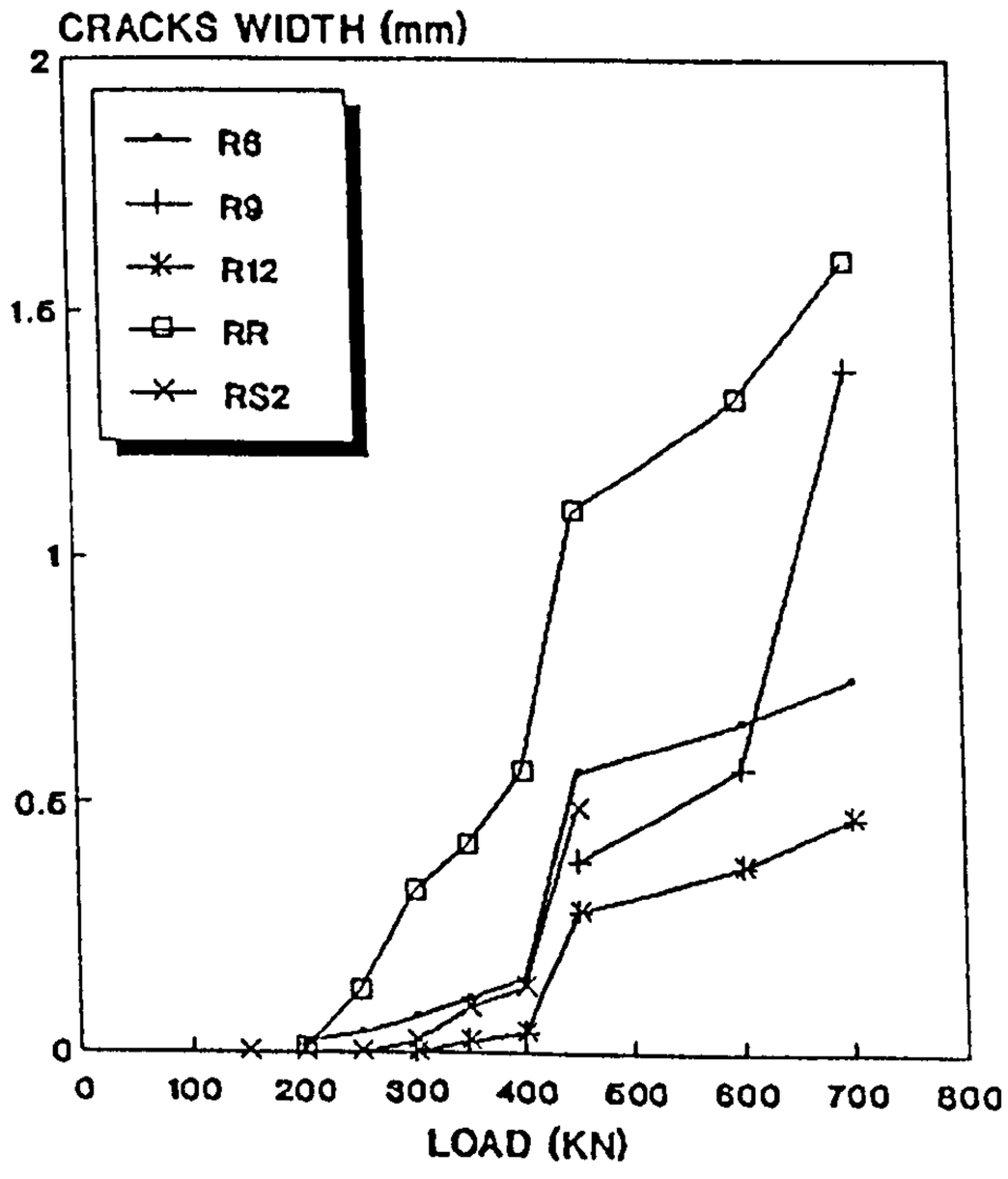

Fig.5.6: LOAD Vs BOTTOM CRACKS
Due to Loading P1-For M1

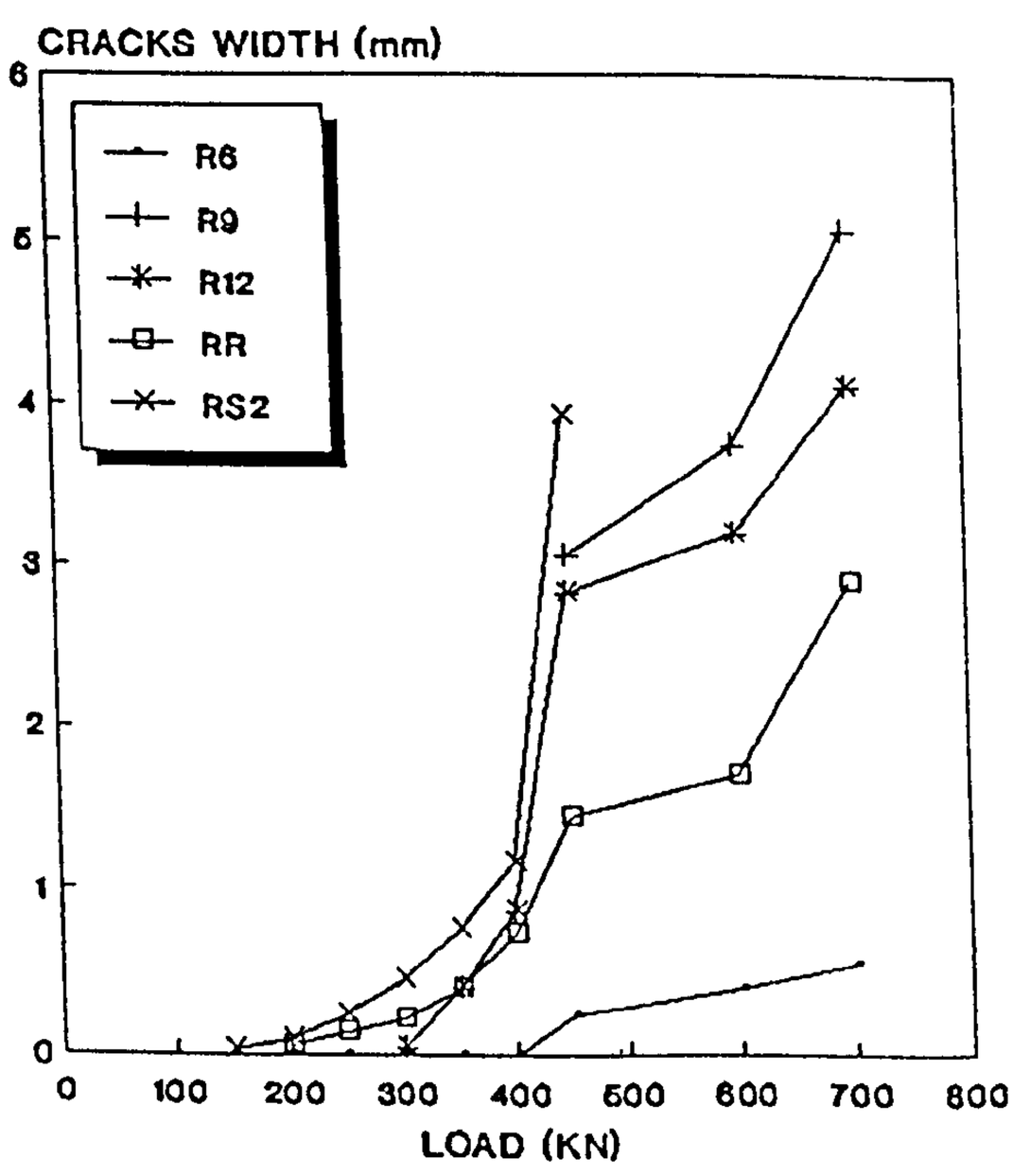

[For Test Rig Notations See Table 4.2 and Fig. 4.4]

Fig. 5.8: LOAD Vs STRAIN
Outer Loaded Area, Point B
Due to Loading P1- For M3

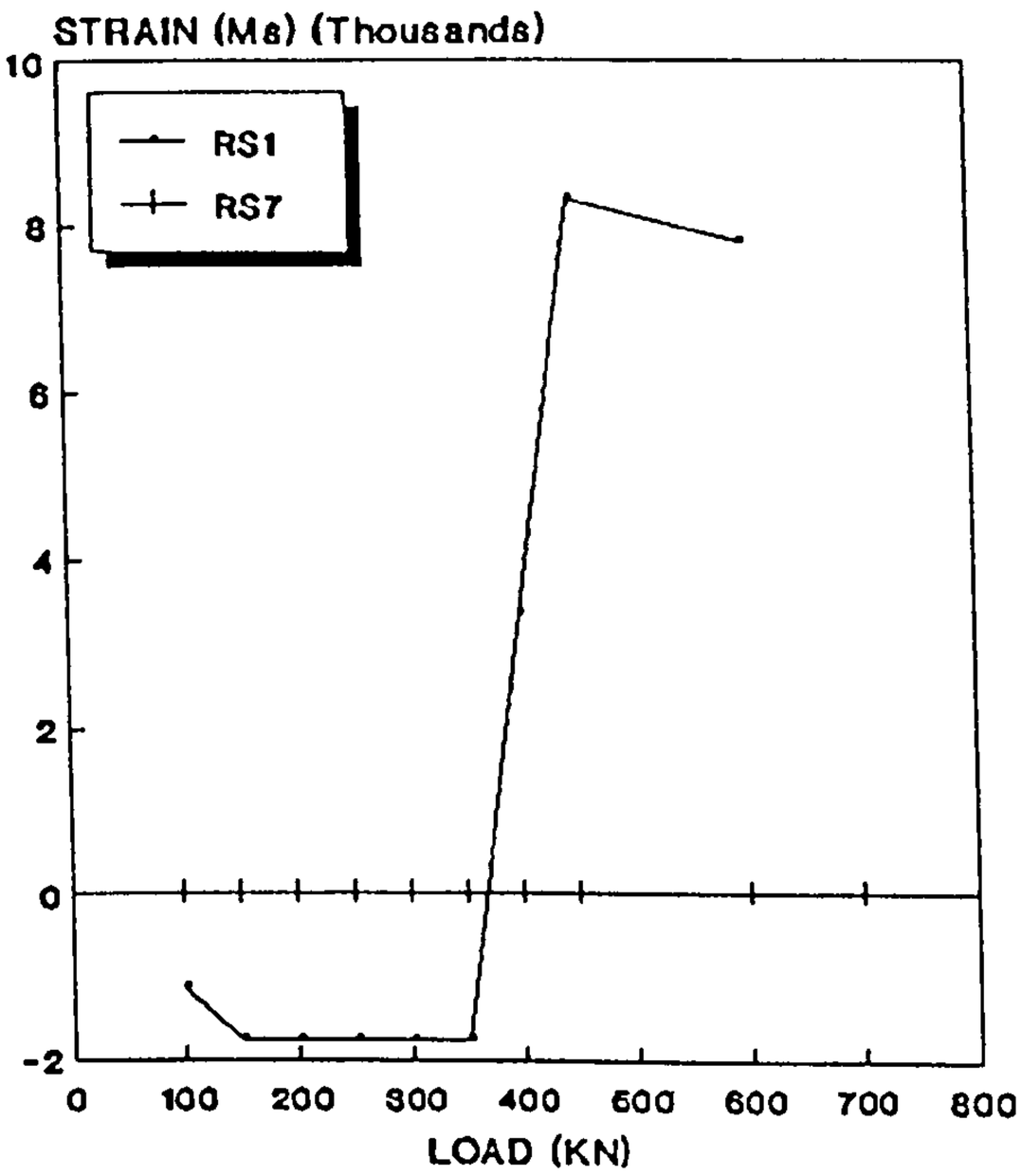

Fig .5.9: LOAD Vs STRAIN
Inner Loaded Area, Point F
Due to Loading P1-For M3

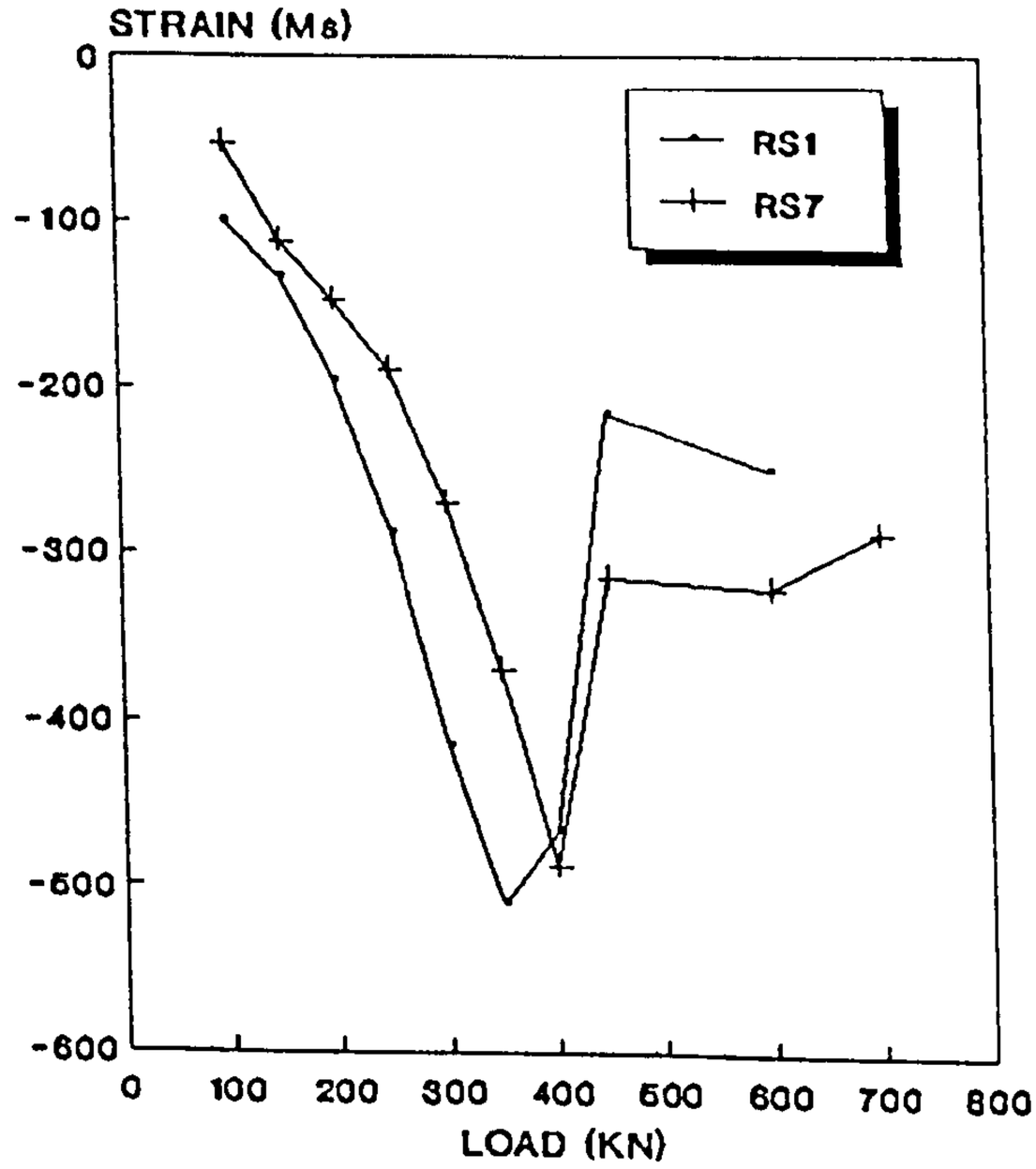

Fig.5.10: LOAD Vs STRAIN
Between Loaded Areas, Point E
Deu To Loading P1- For M3

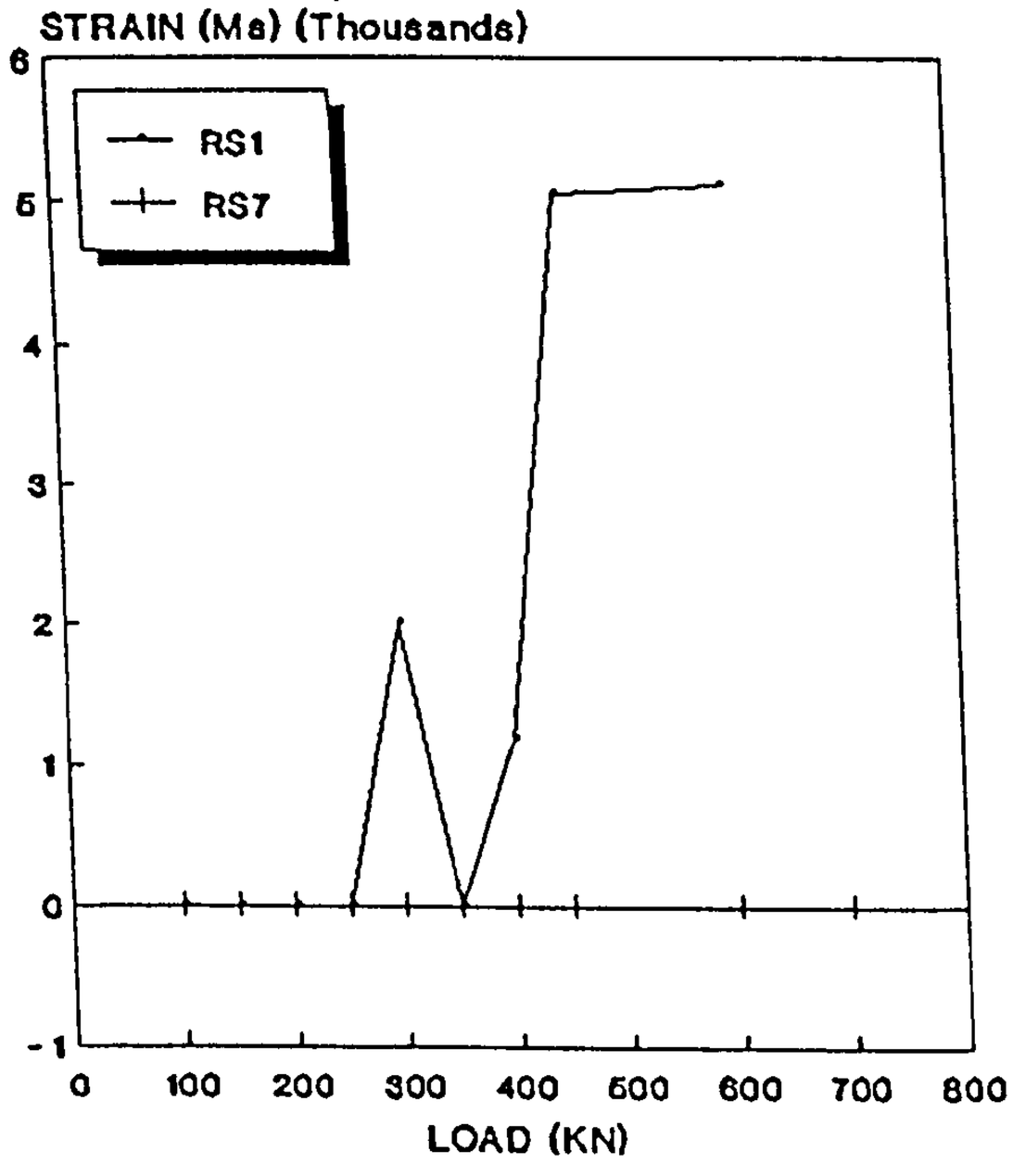

[For Test Rig Notations See Table 4 2 and Fig. 4.4]

Fig.5.7: LOAD Vs STRAIN
Outer Loaded Area ,Point B
Due to Loading Position P1- For M1

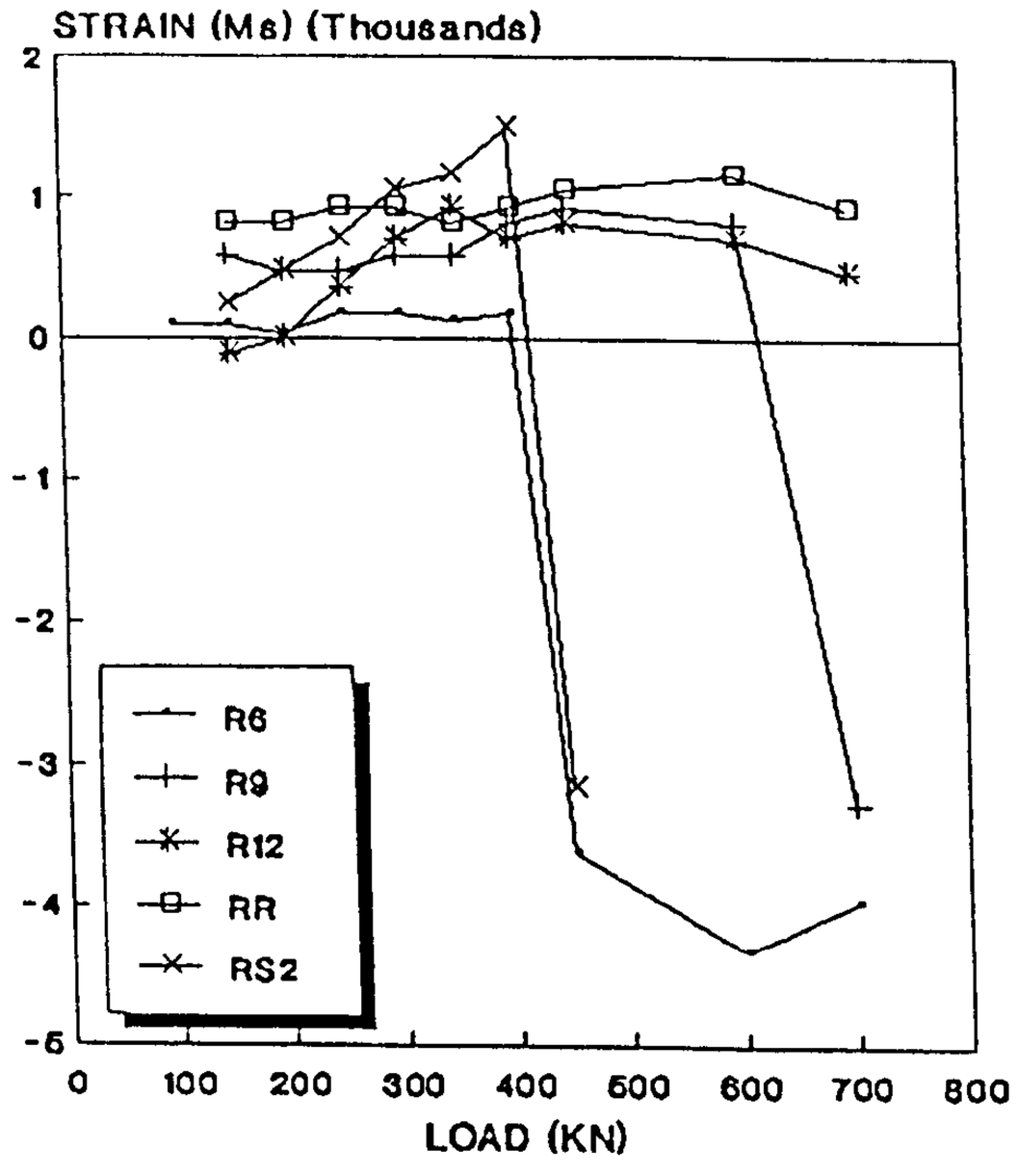

Fig. 5.11: LOAD CYCLES Vs STRAIN
For Load 450 kN, Point A
Due to Loading P1- For M1

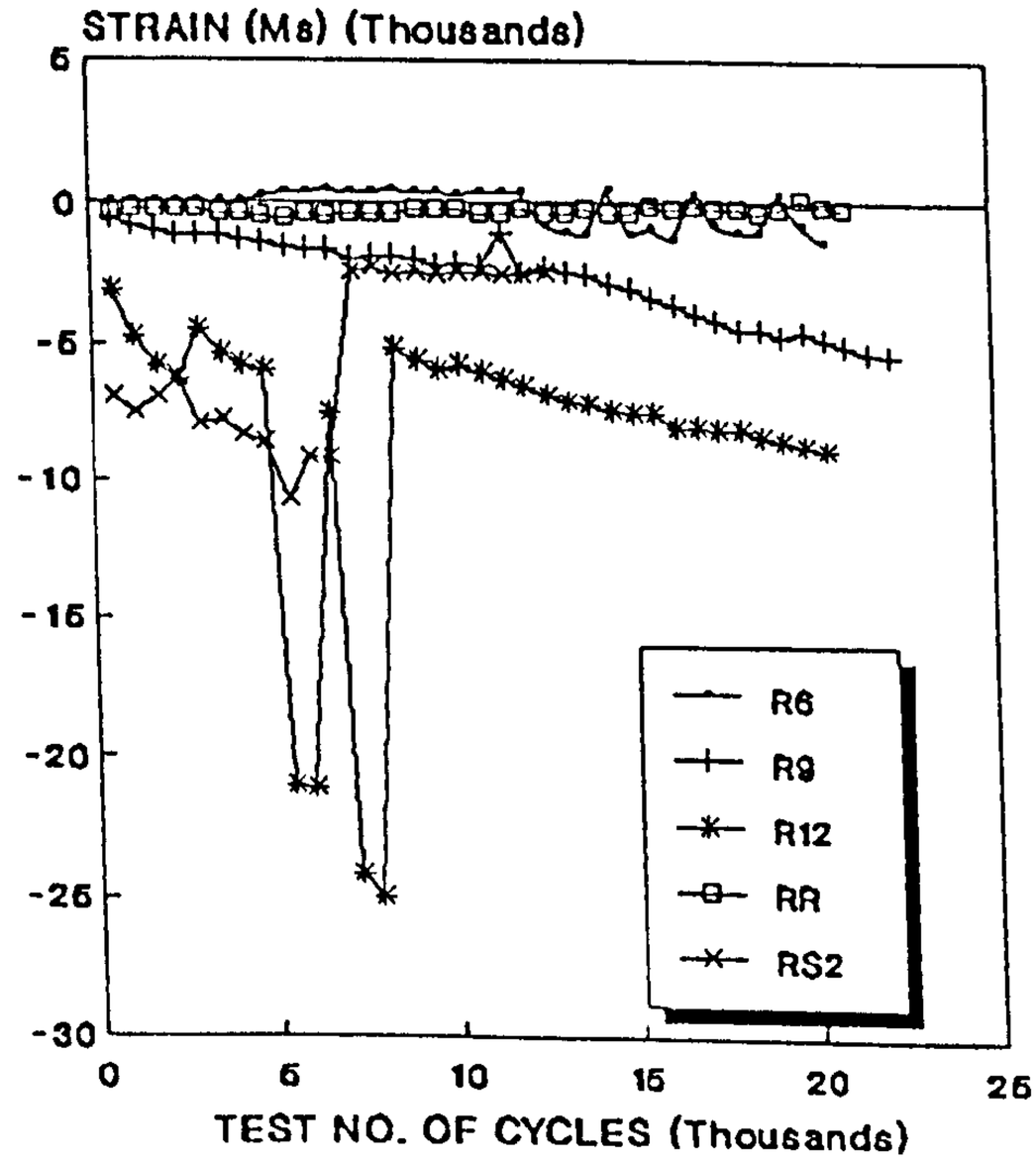

[For Test Rig Notations See Table 4.2 and Fig. 4.4]

Fig. 5.12: Relationship Between Max. DefL, &Raft Sizes For Load 450kN.

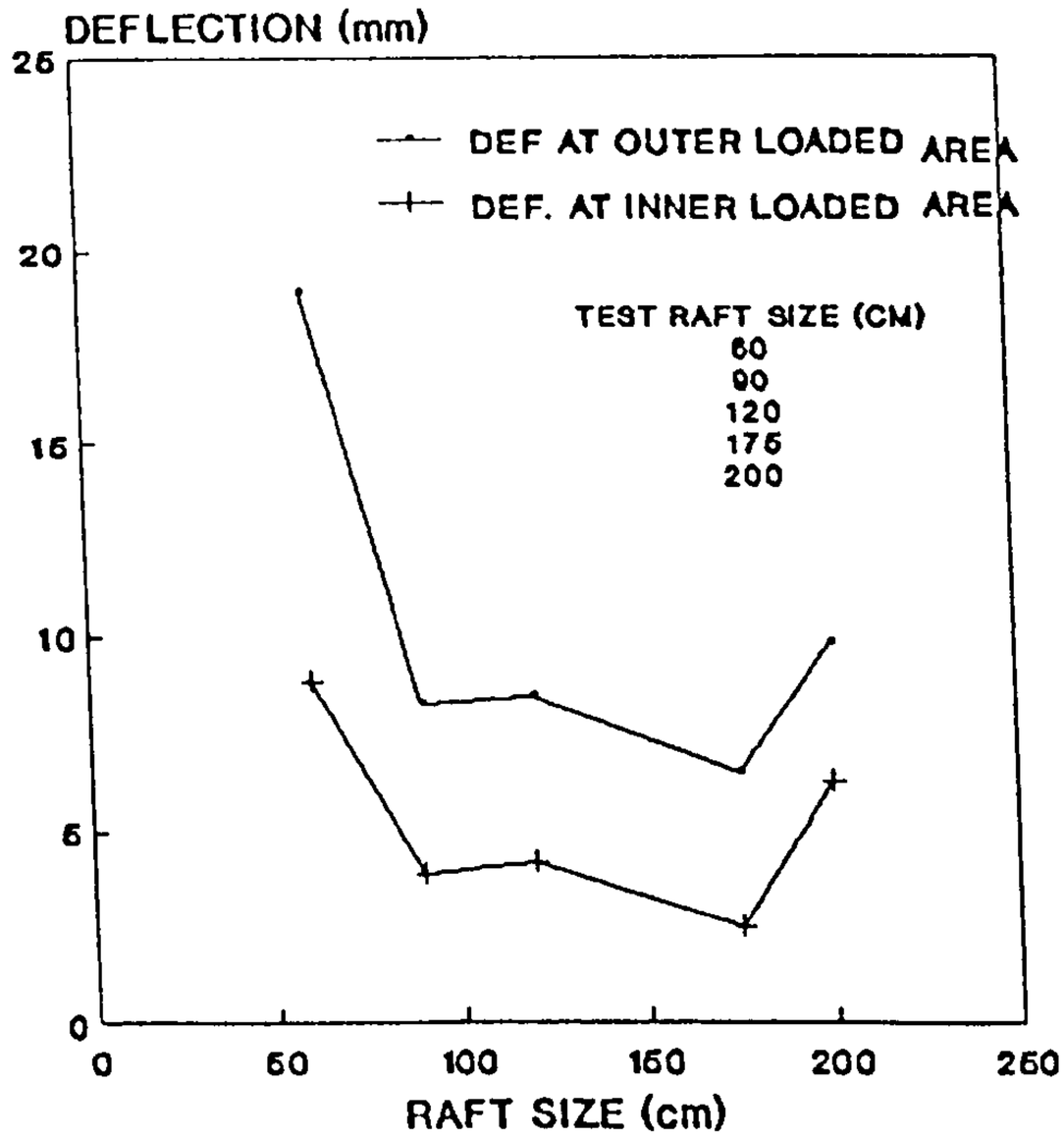

Fig. 5.13: Relationship Between Max. Strn.&Raft size For Load 450kN

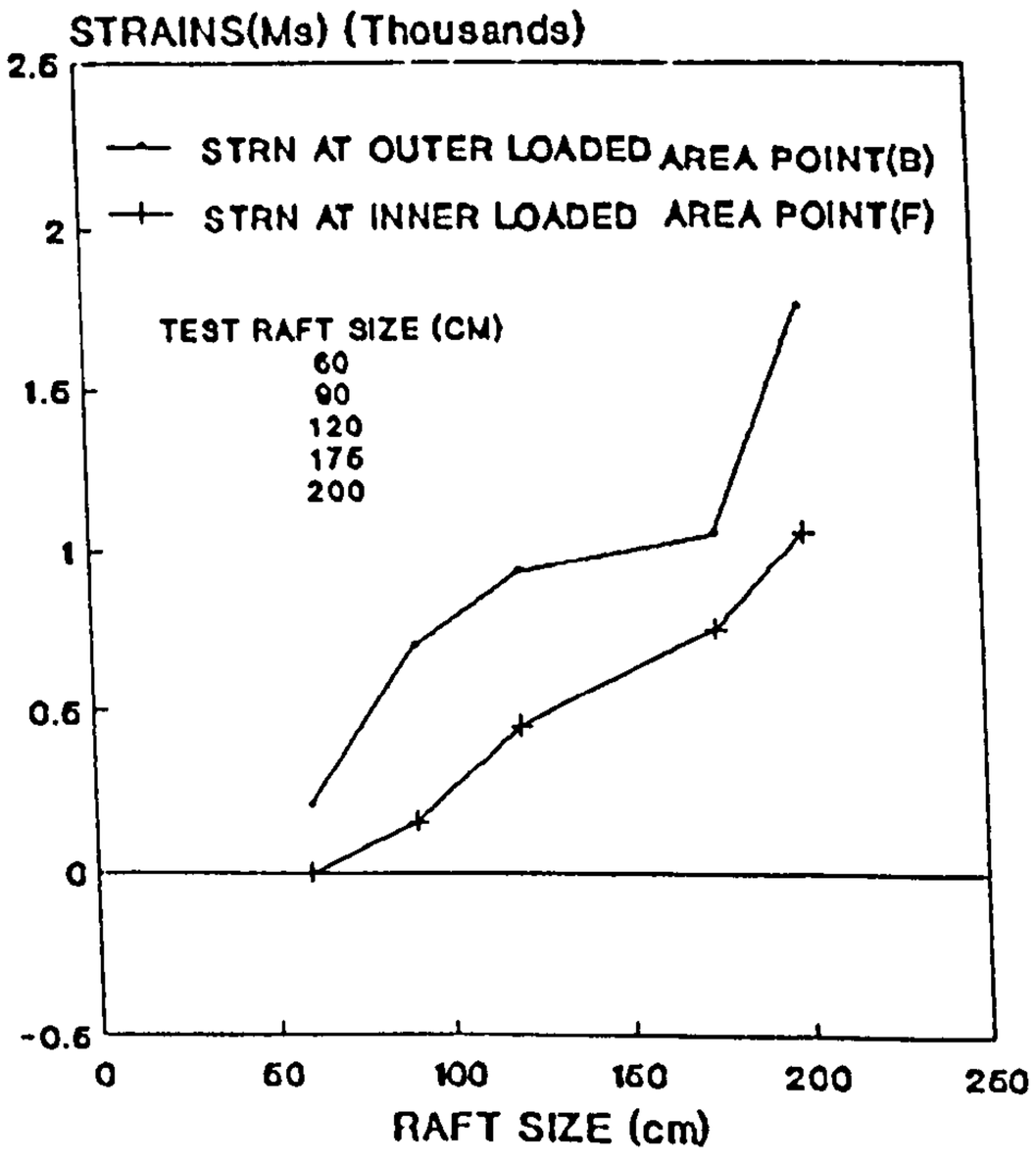

[For Test Rig Notations See Table 4.2 and Fig. 4.4]

Fig. 5.14: LOAD Vs STRAIN
Outer Loaded Area, Point B
Due to Loading P1- For M2

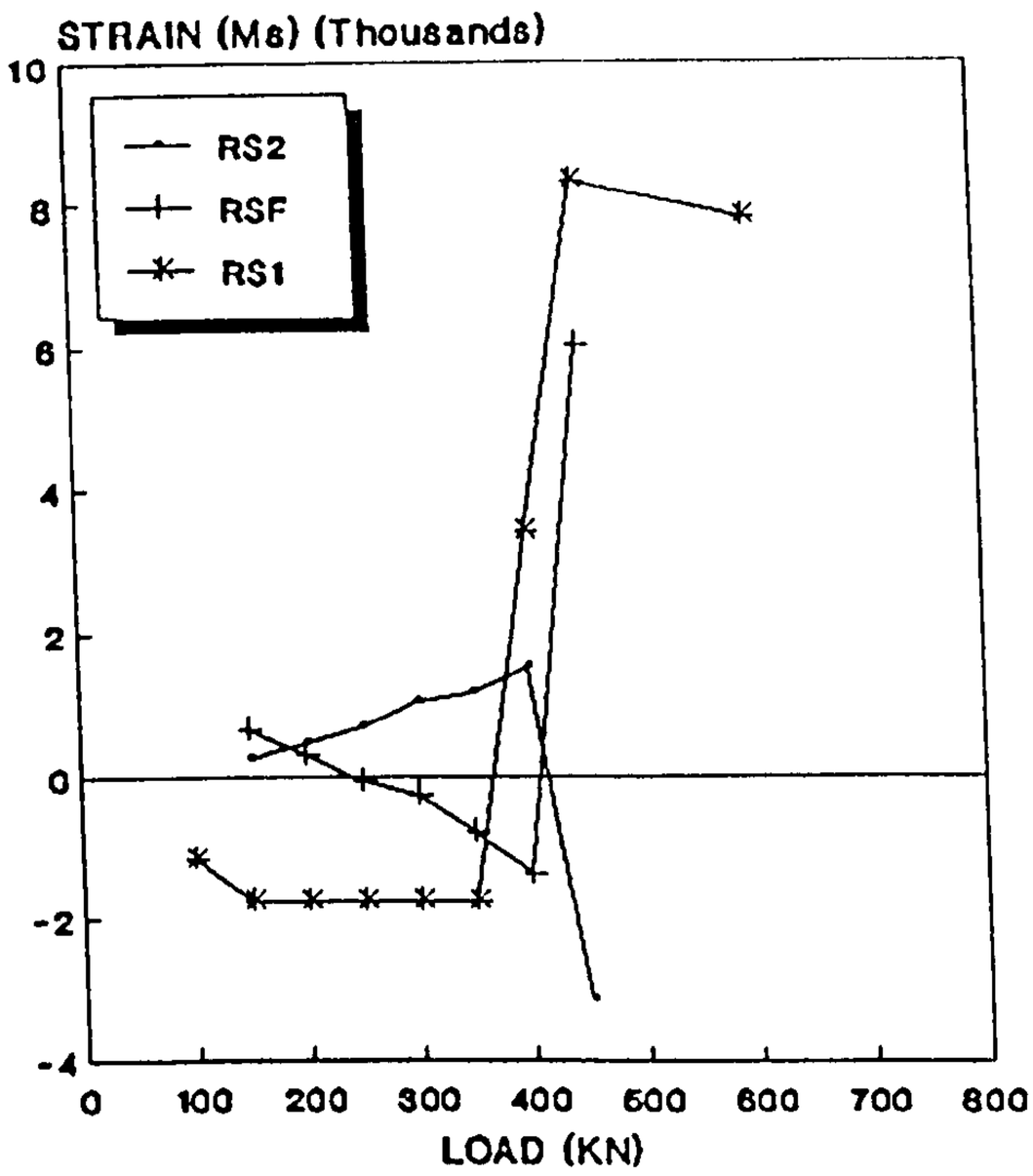

Fig .5.15: LOAD Vs STRAIN
Between Loaded Areas, Point E
Due to Loading P1-For M2

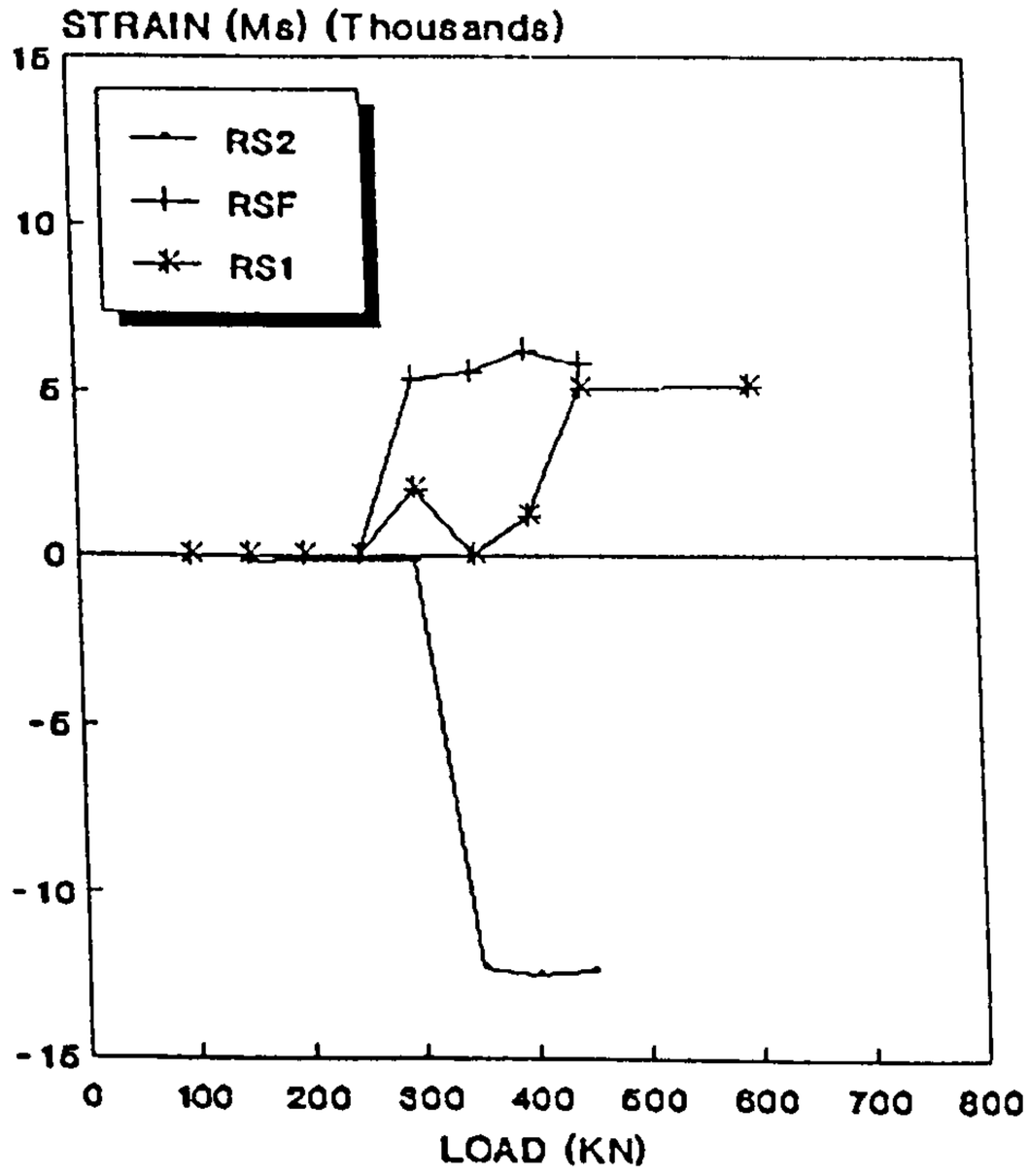

Fig. 5.16: LOAD Vs STRAIN
Inner Loaded Area, Point F
Deu To Loading P1- For M2

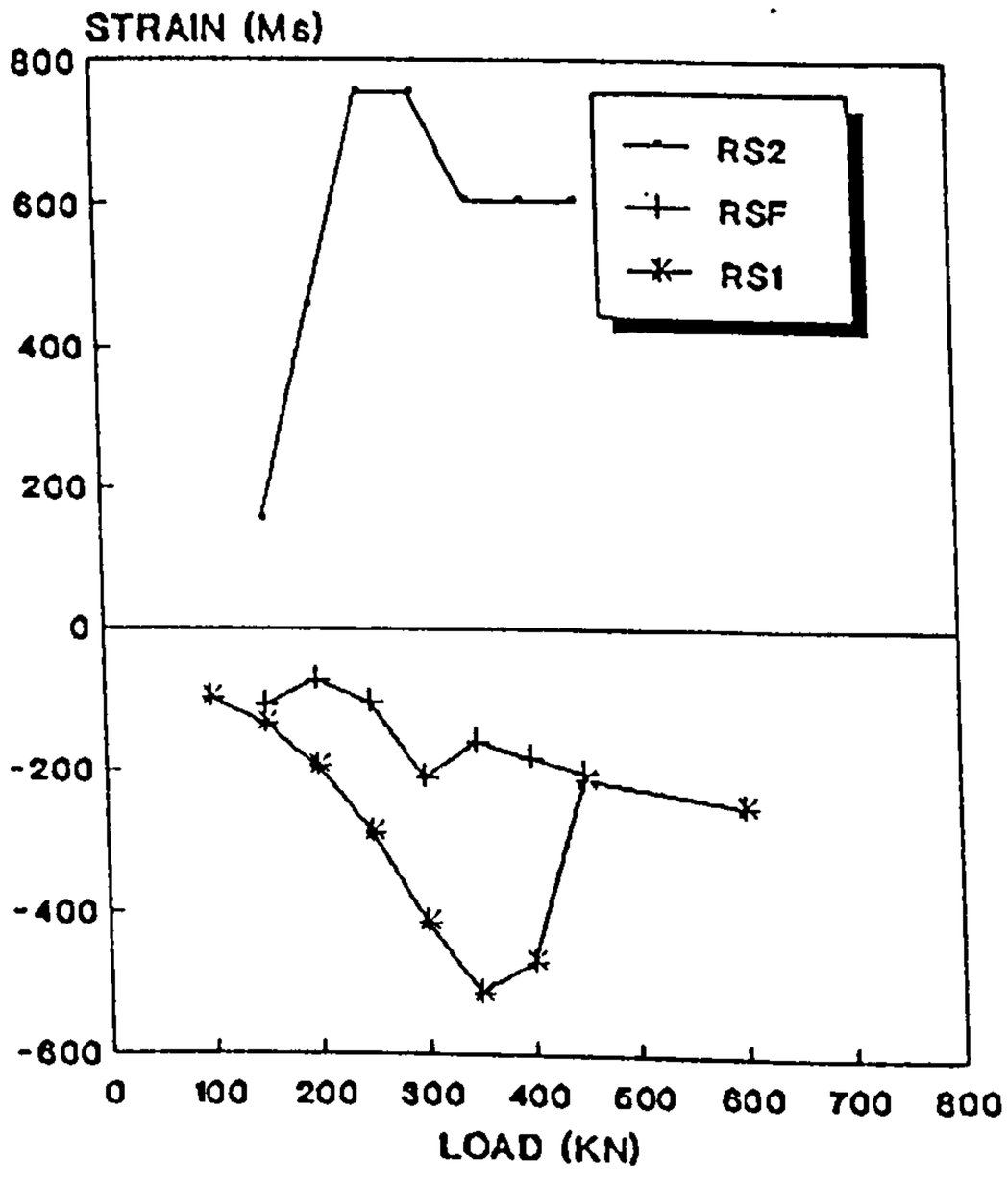

[For Test Rig Notations See Table 4 2 and Fig. 4.4]

Fig. 5.17: LOAD Vs DEFLECTION
Free Corner, Point 14
Due to Loading P3- For M2

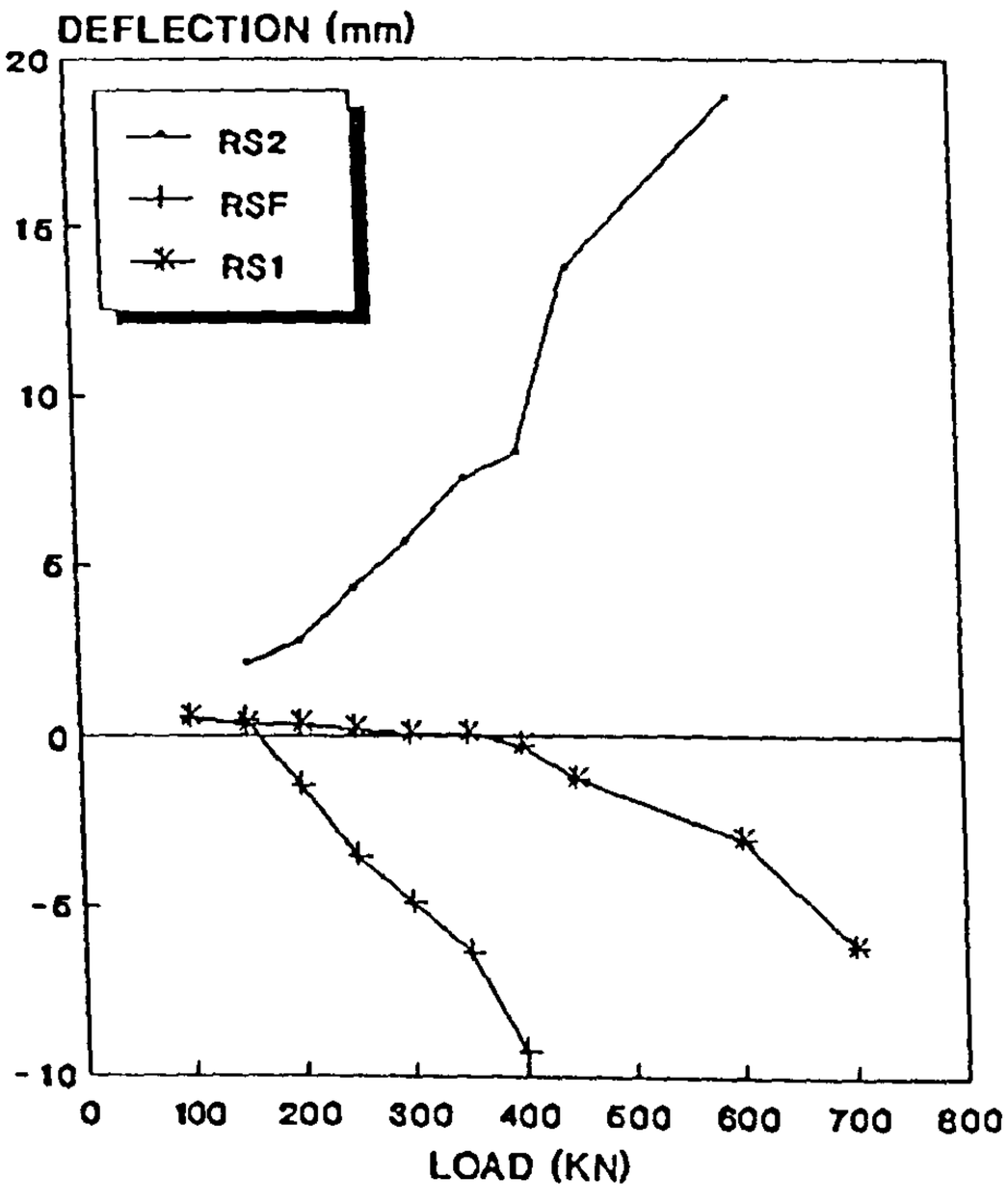

Fig. 5.18: LOAD Vs DEFLECTION
Outer Loaded Area, Point O
Due To Loading P1- For M1

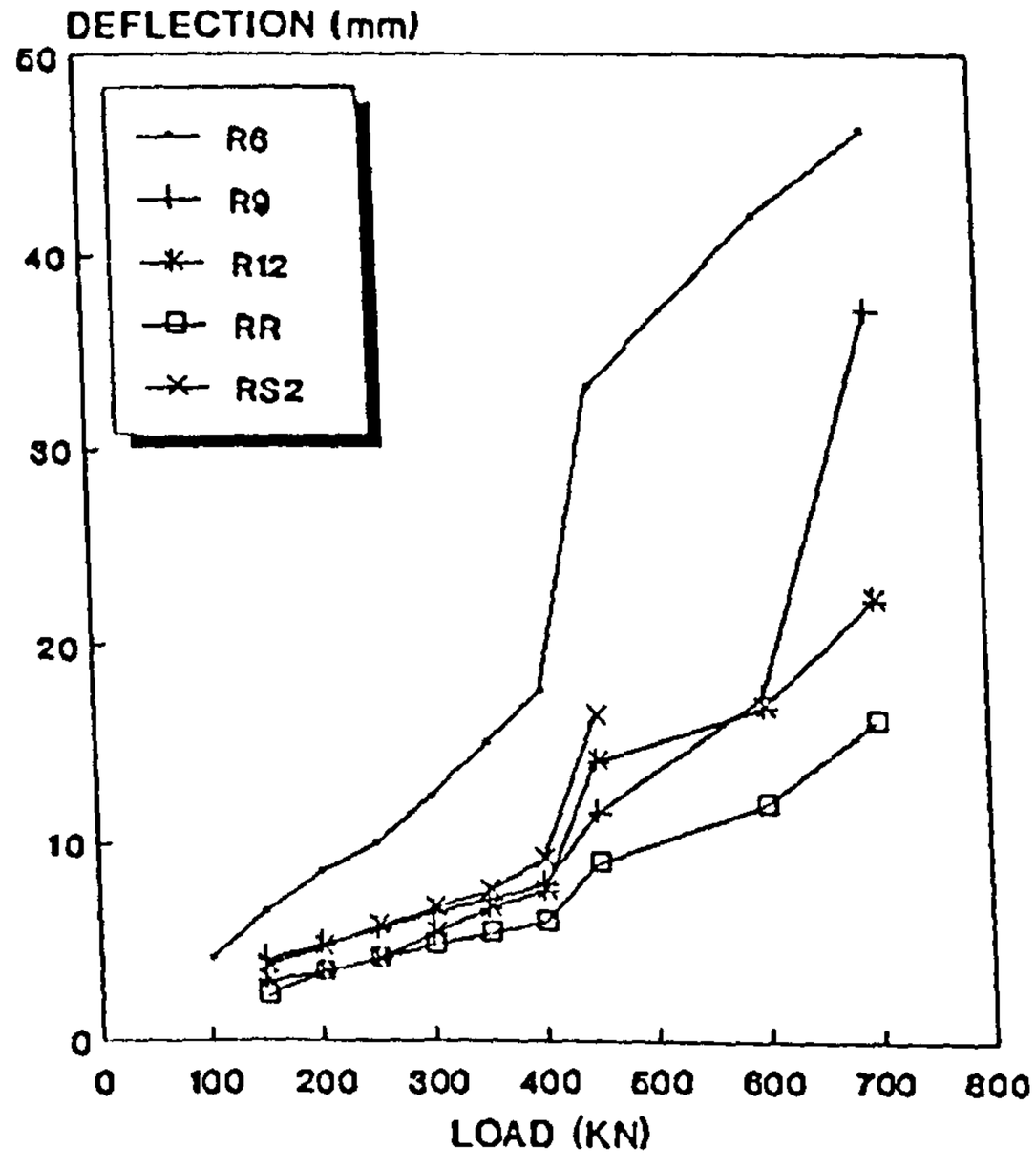

[For Test Rig Notations See Table 4.2 and Fig. 4.4]

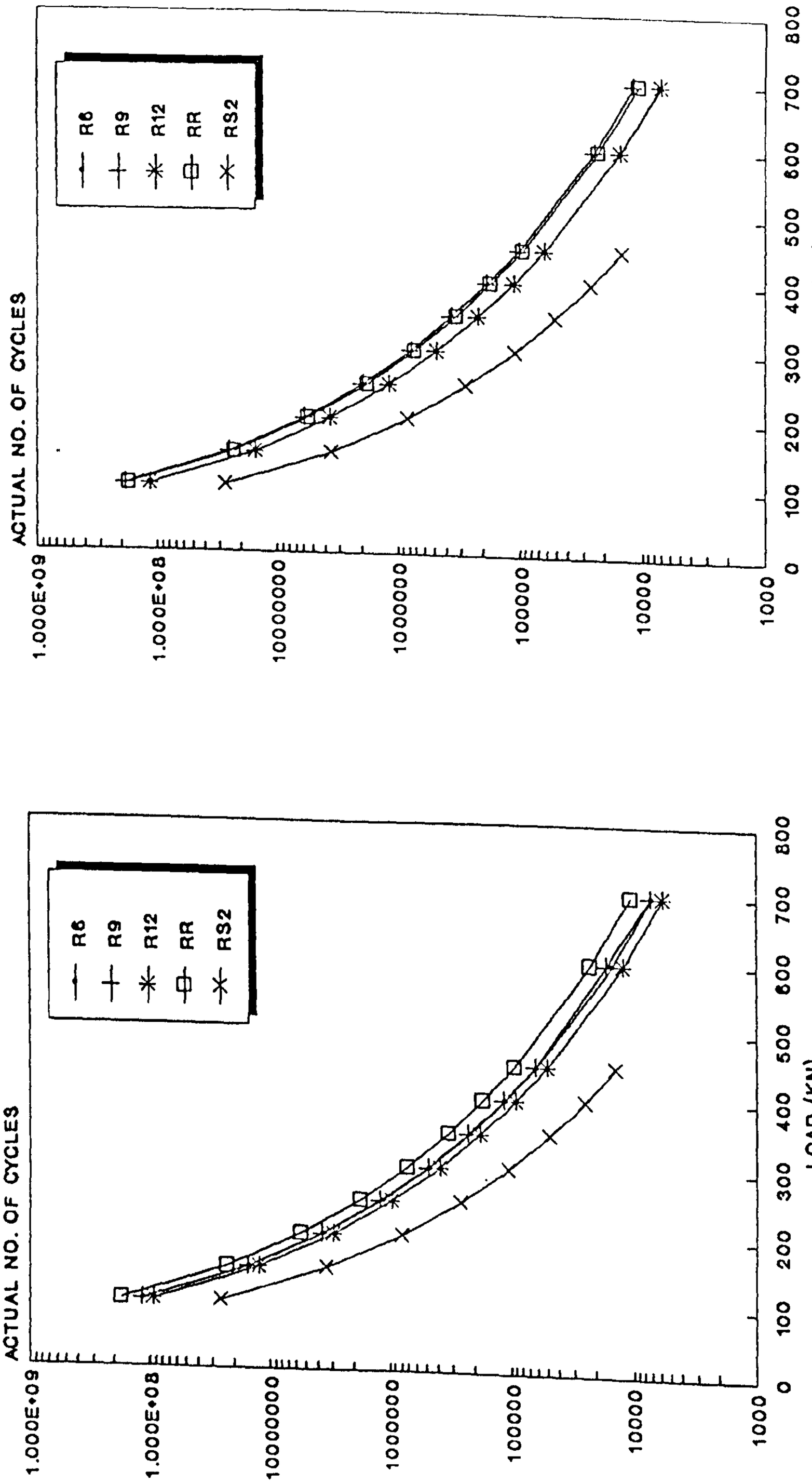

Fig.5.19: LOAD Vs LOAD CYCLES
Due to Loading P1-For M1

[For Test Rig Notations See Table 4.2 and Fig. 4.4]

Fig.5.20: LOAD Vs LOAD CYCLES
Due to Loading P2- For M1

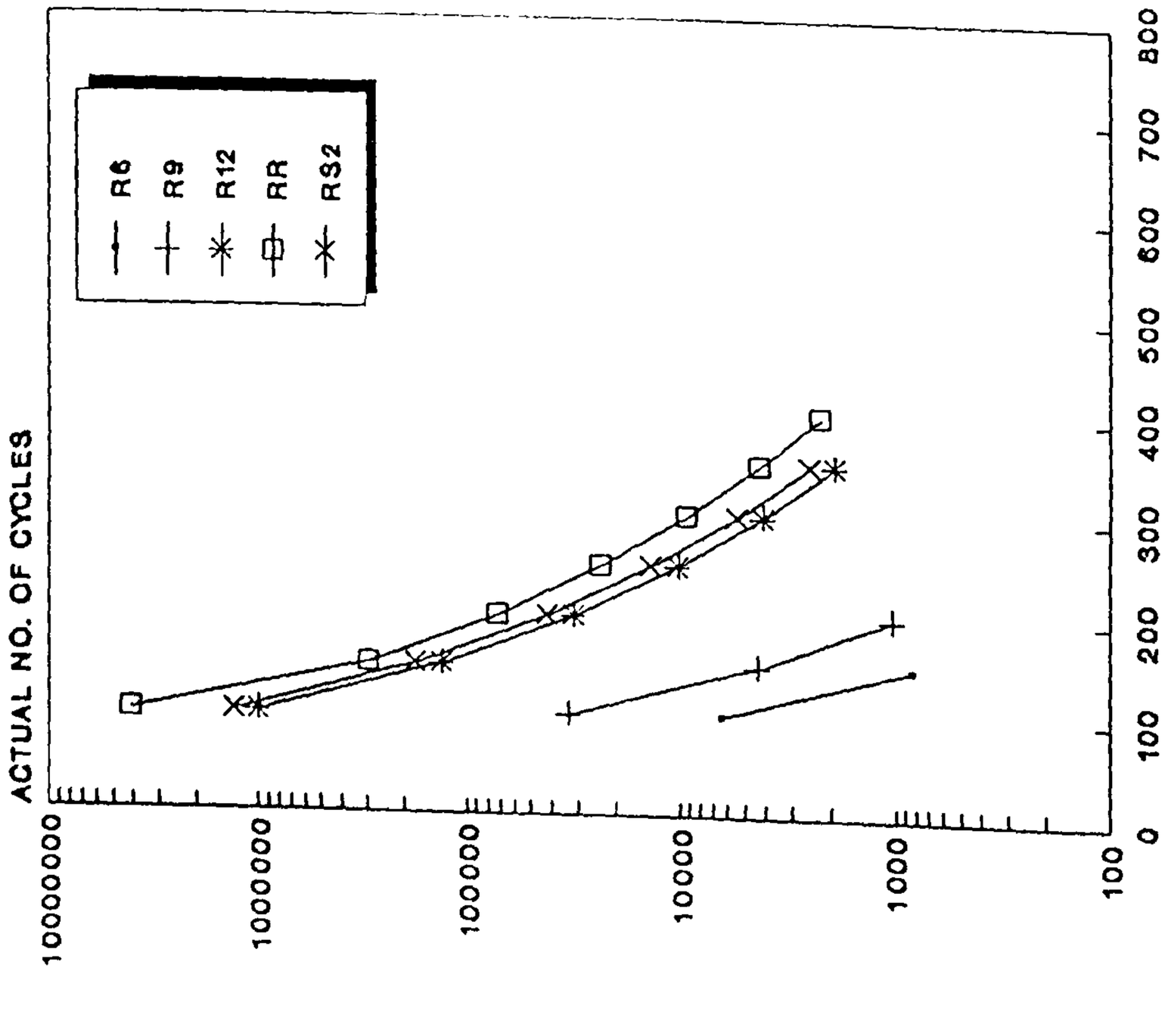

Fig. 5.22: LOAD Vs LOAD CYCLES
Due to Loading P4 - For M1

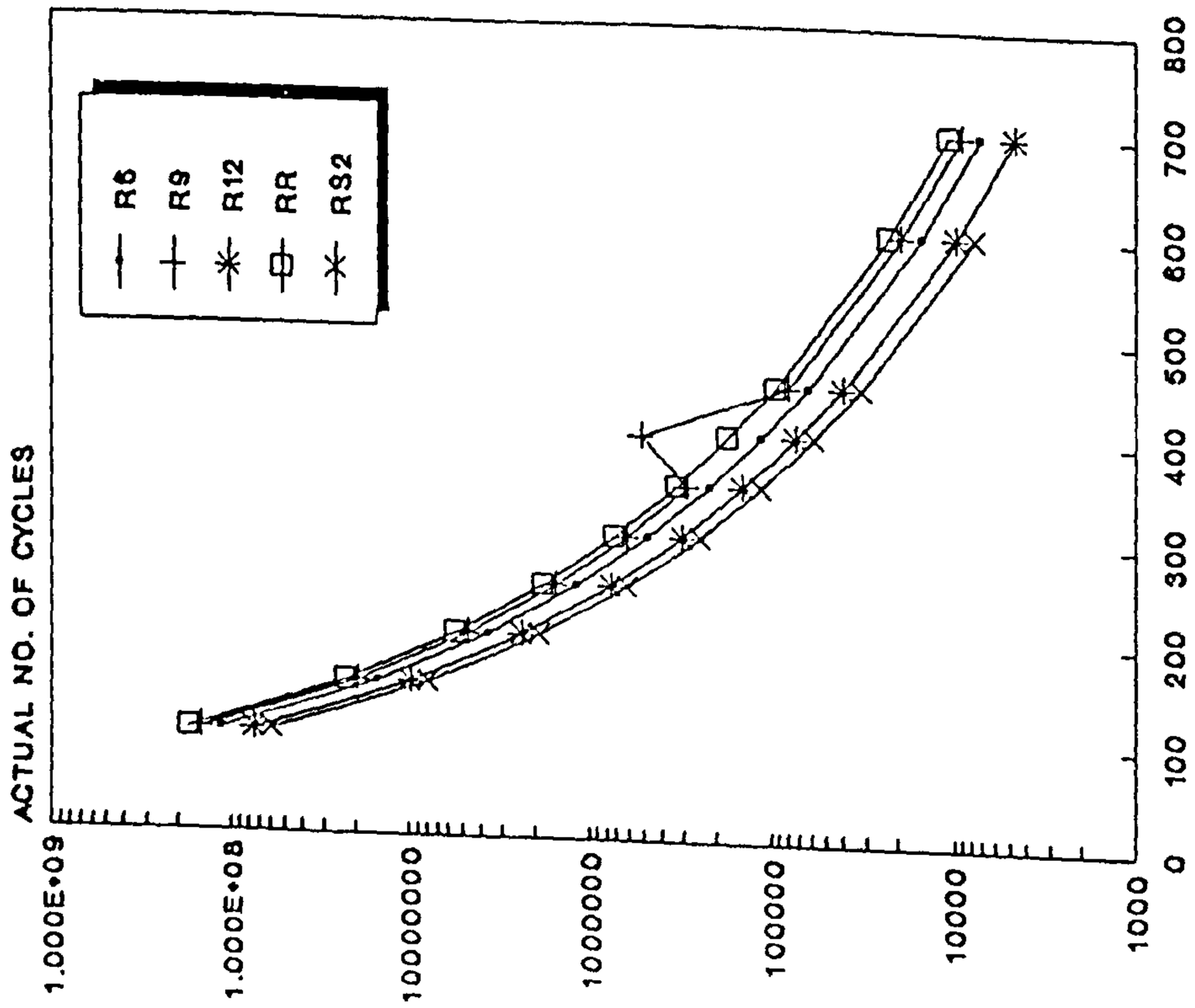

Fig. 5.21: LOAD Vs LOAD CYCLES
Due to Loading P3-For M1

[For Test Rig Notations See Table 4.2 and Fig. 4.4]

Fig. 5.23: LOAD Vs DEFLECTION
Inner Loaded Area - Point 9
Due to Loading P4 - For M2

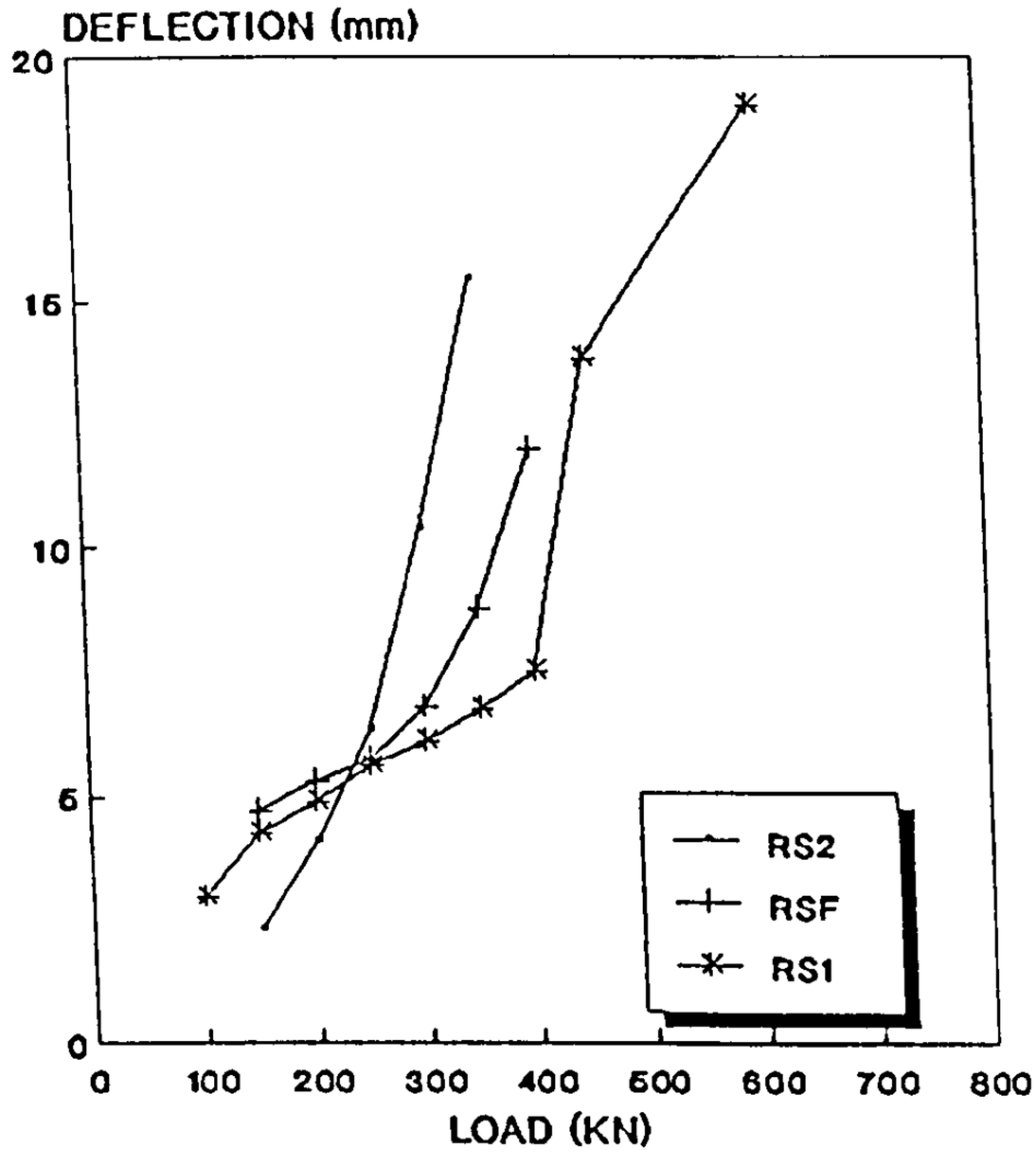

Fig. 5.24: LOAD Vs LOAD CYCLES
Due to Loading P2 - For M2

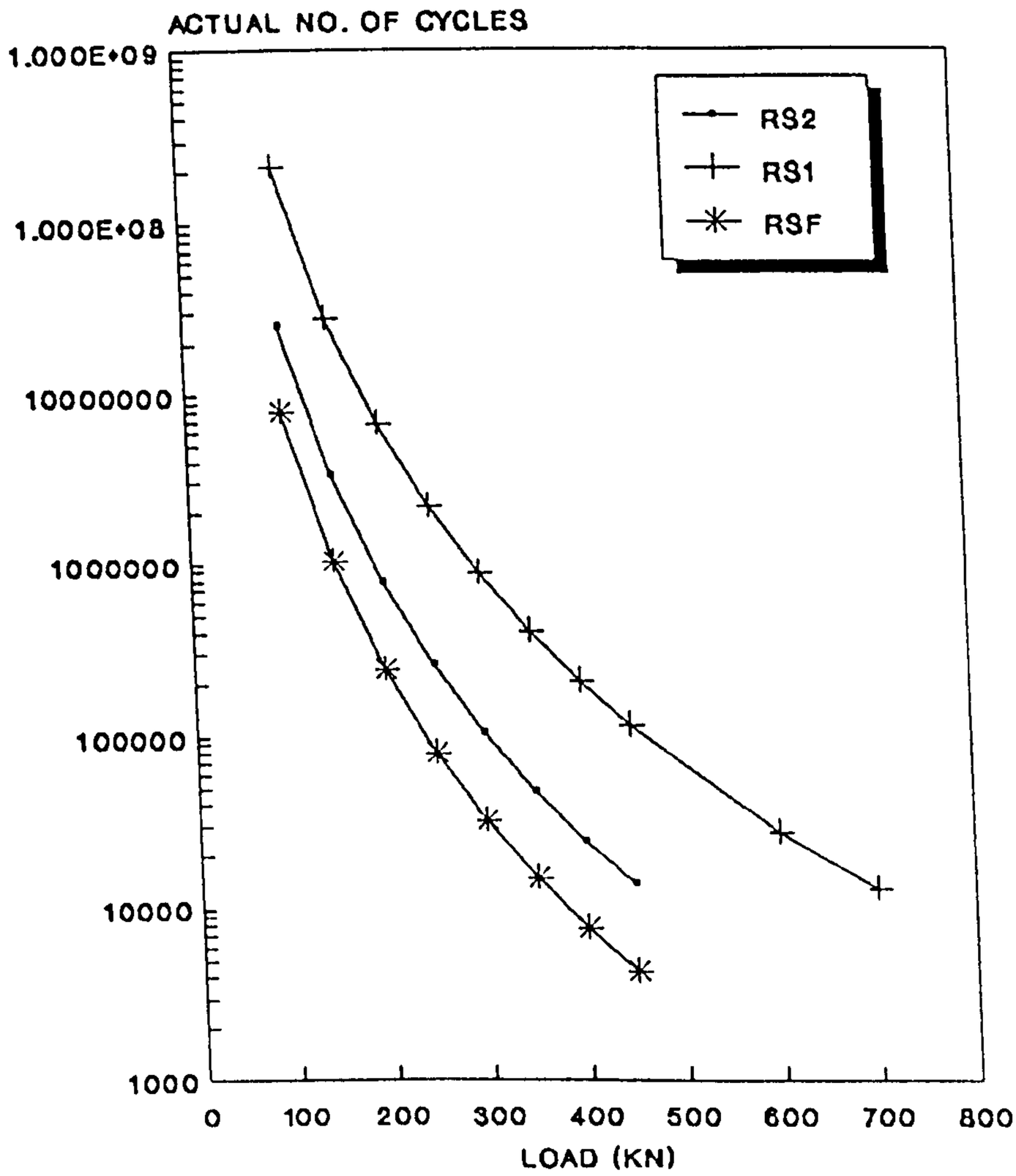

[For Test Rig Notations See Table 4.2 and Fig. 4.4]

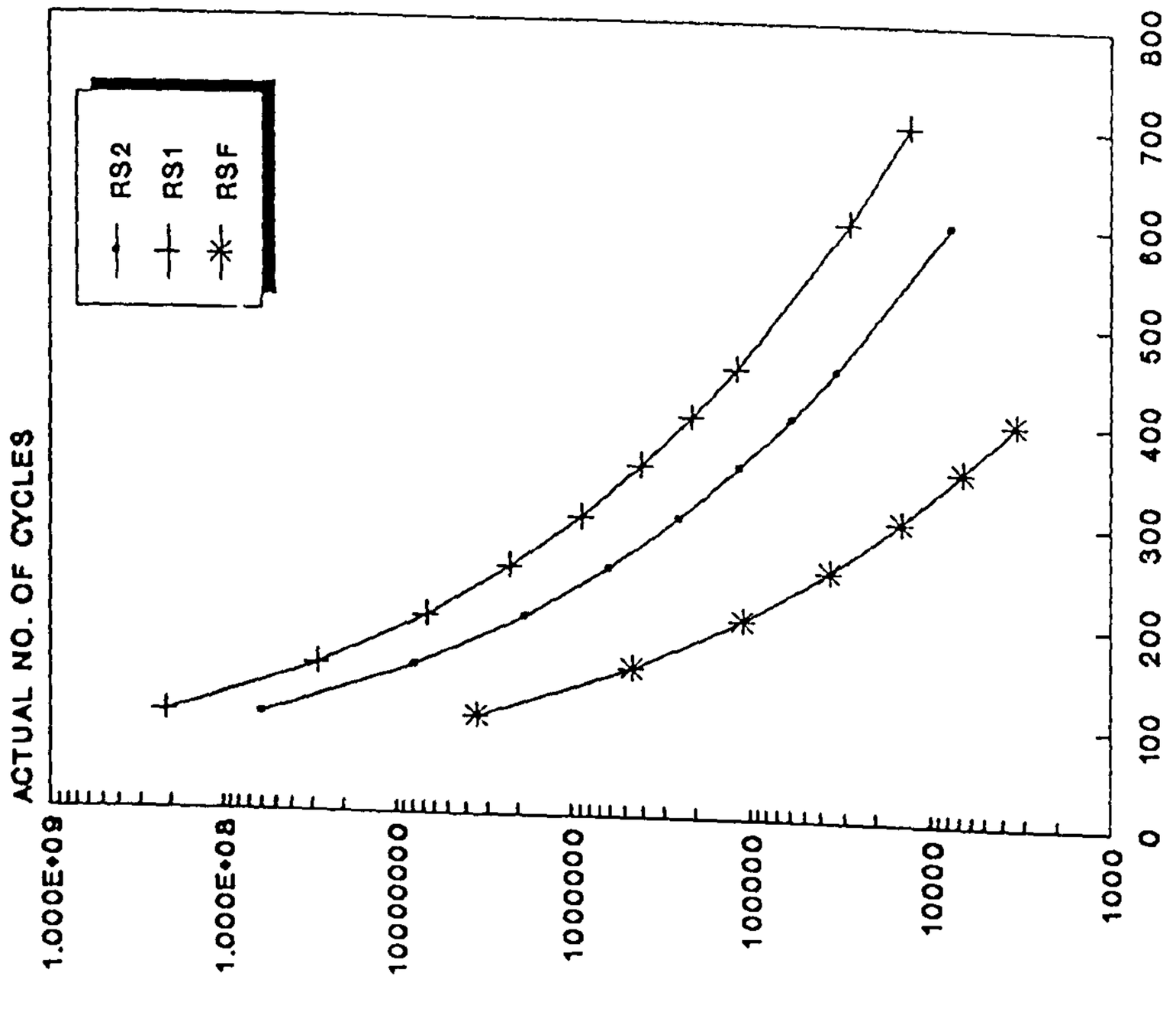

Fig. 5.25: LOAD Vs LOAD CYCLES
Due to Loading P3-For M2

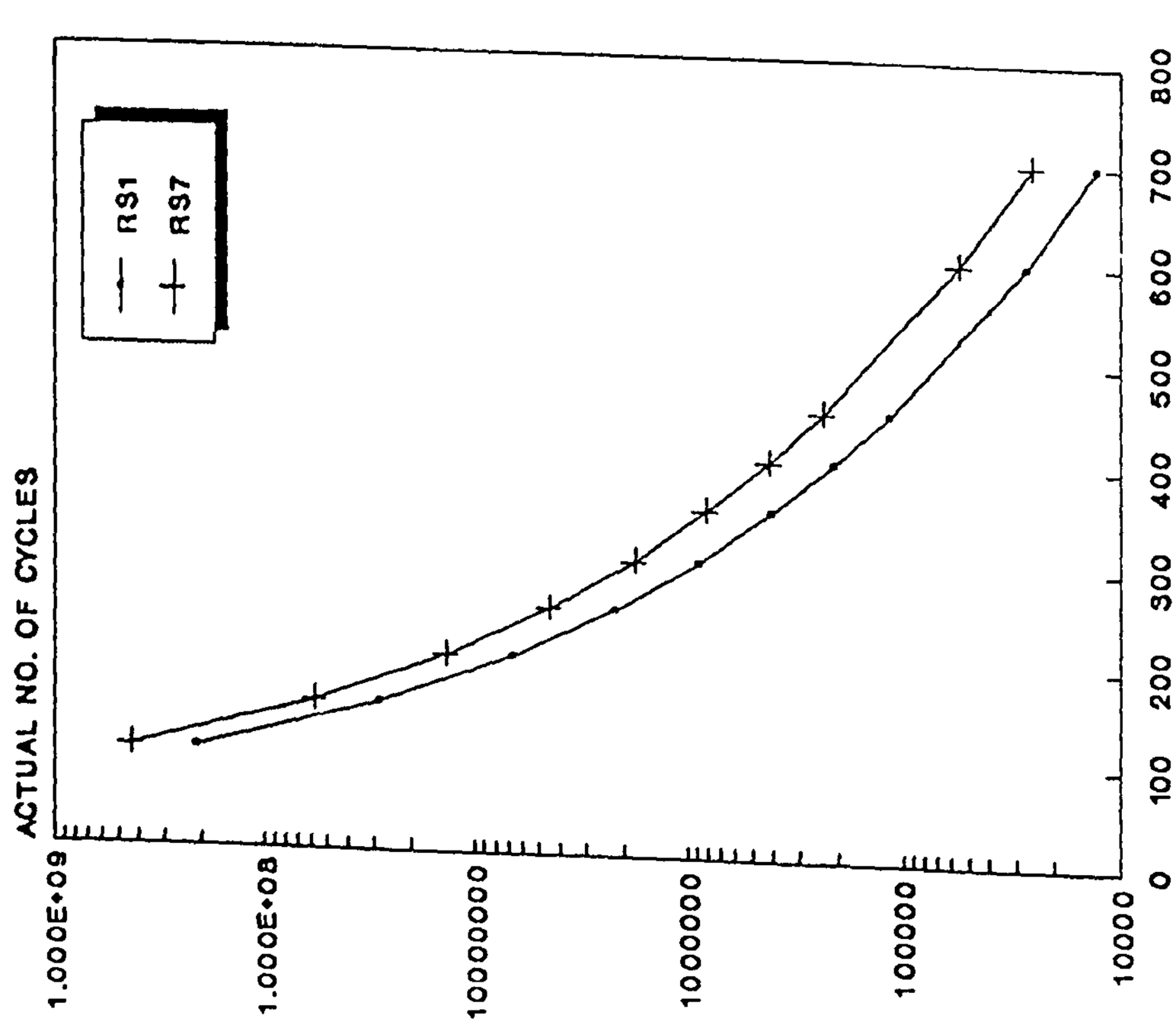

Fig. 5.26: LOAD Vs LOAD CYCLES
Due to Loading P3 - For M3

[For Test Rig Notations See Table 4.2 and Fig. 4.4]

Fig. 6.1: LOAD Vs TOP CRACKS
Due to Loading P1-For M2

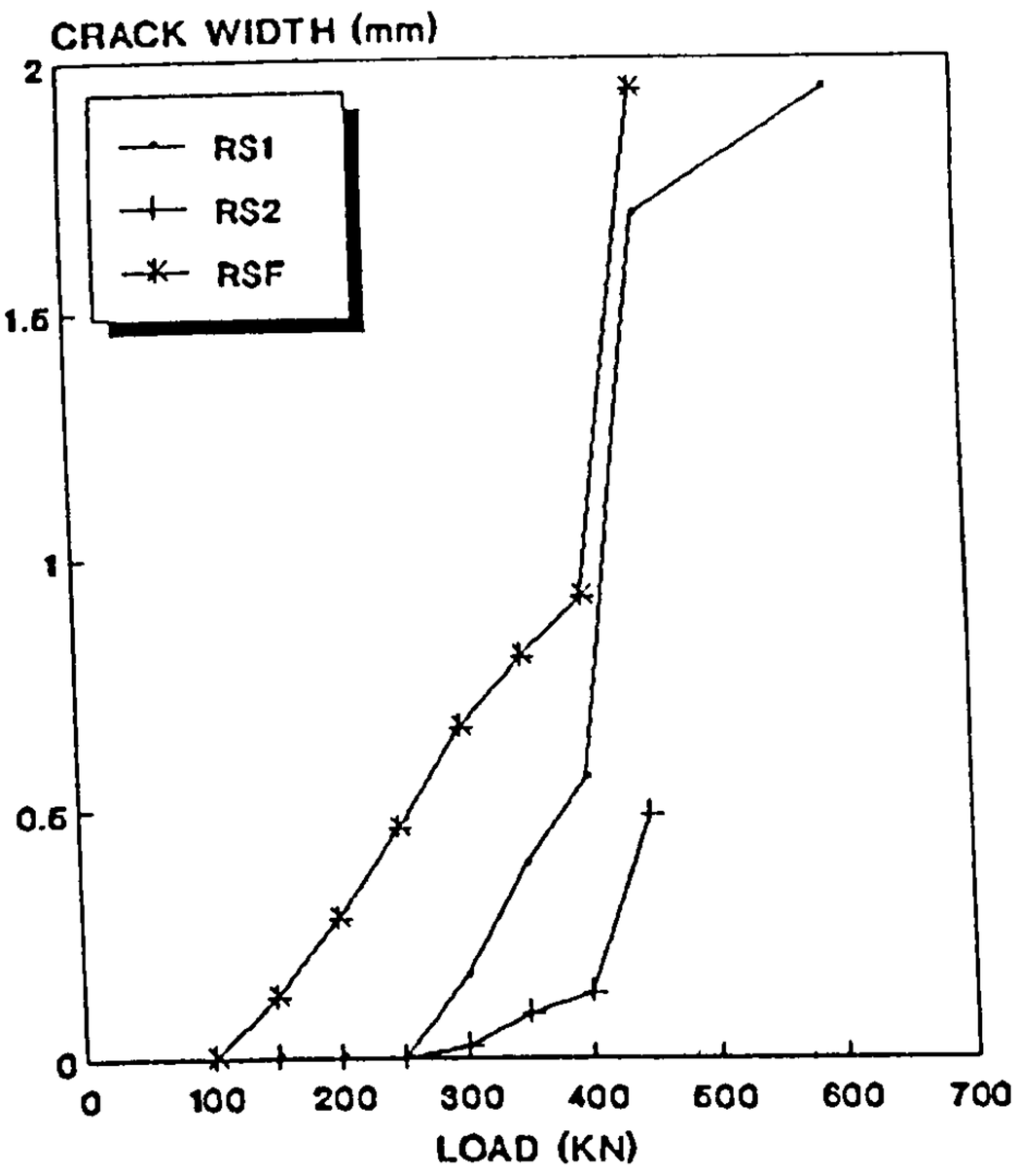

Fig. 6.2: LOAD Vs BOTTOM CRACKS
Due to Loading P1-For M2

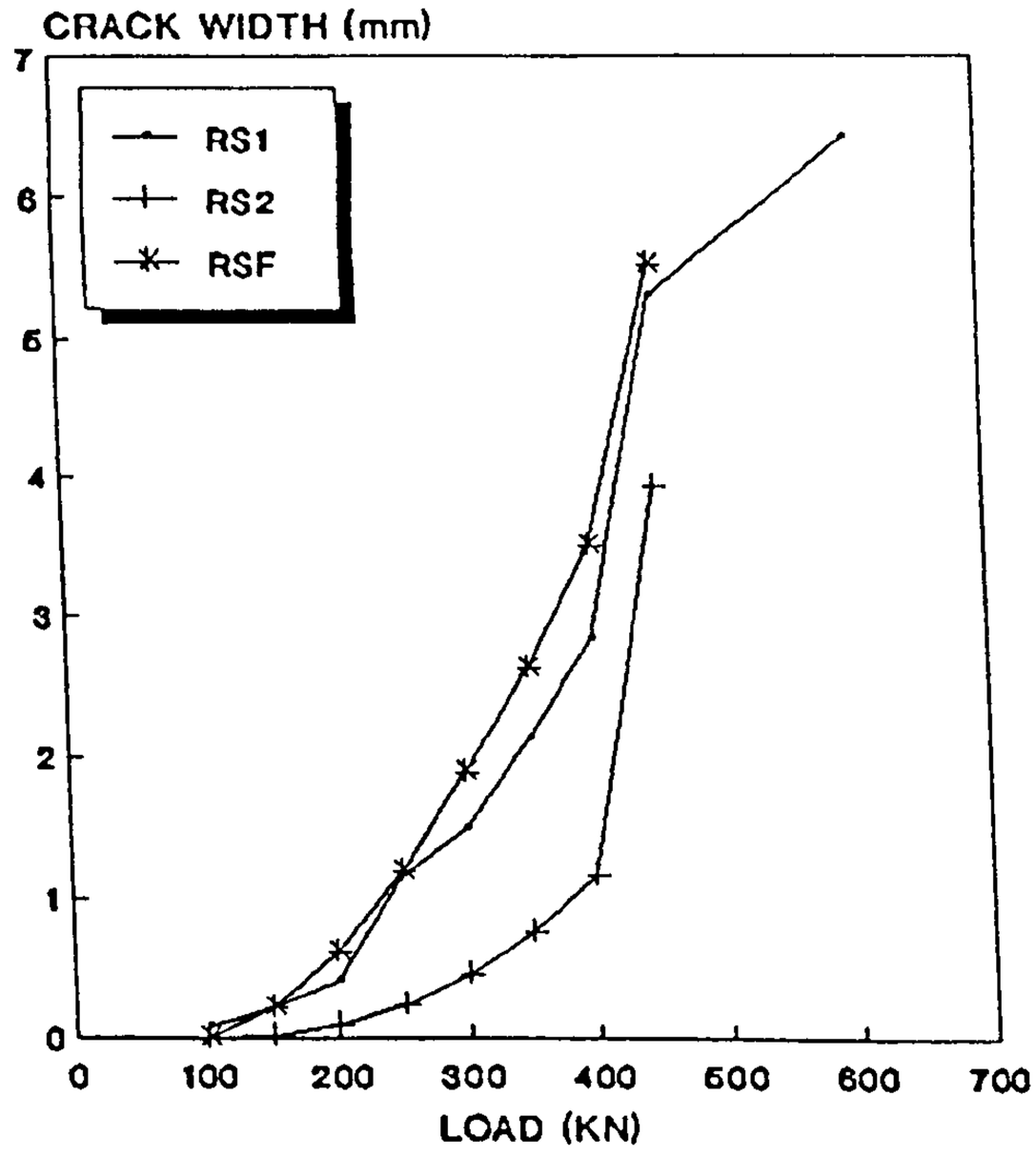

Fig. 6.3: LOAD Vs BOTTOM CRACKS
Due To Loading P1- For M3

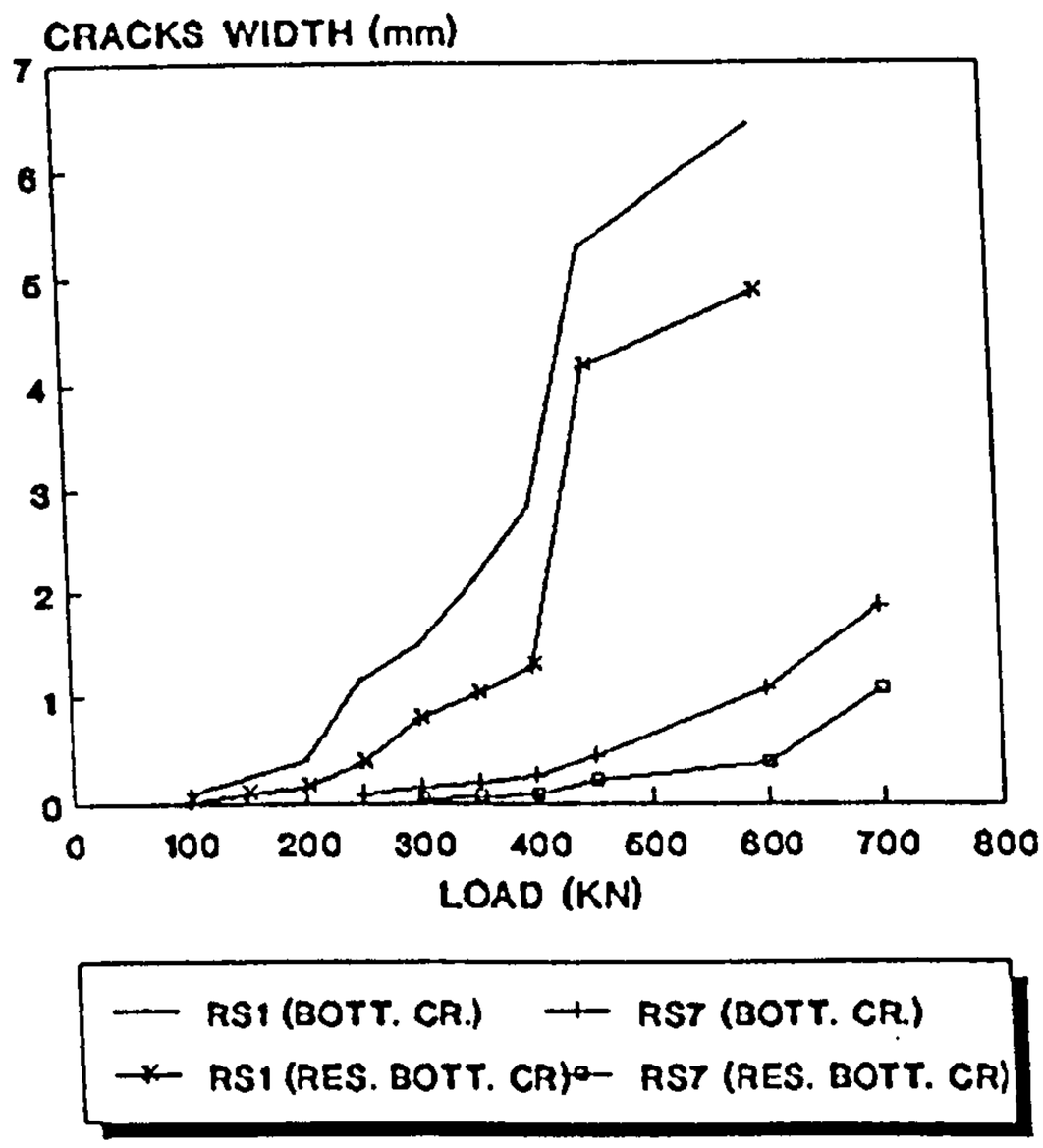

Fig. 6.4: LOAD Vs TOP CRACKS
Due to Loading P1- For M3

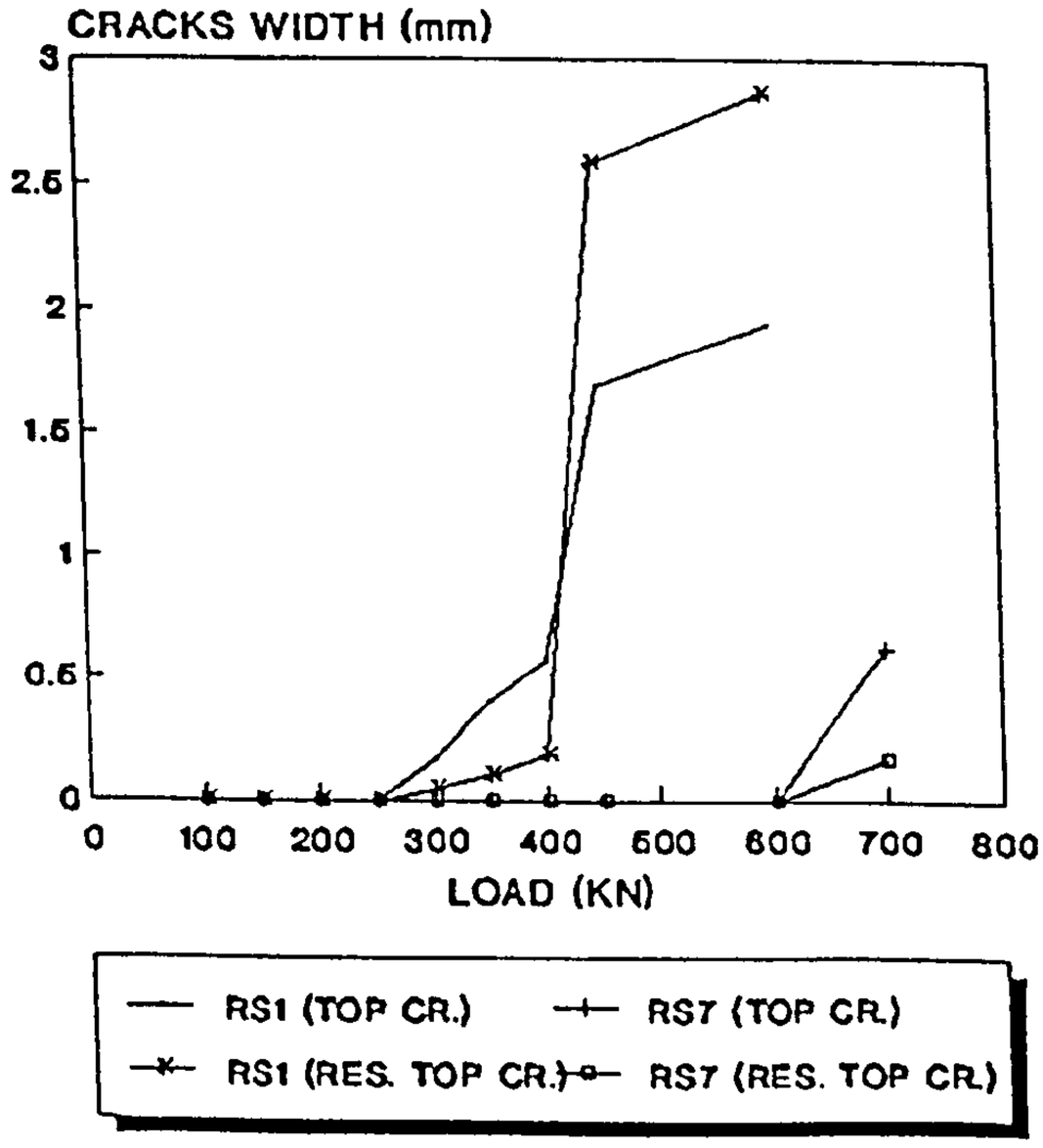

[For Test Rig Notations See Table 4.2 and Fig. 4 4]

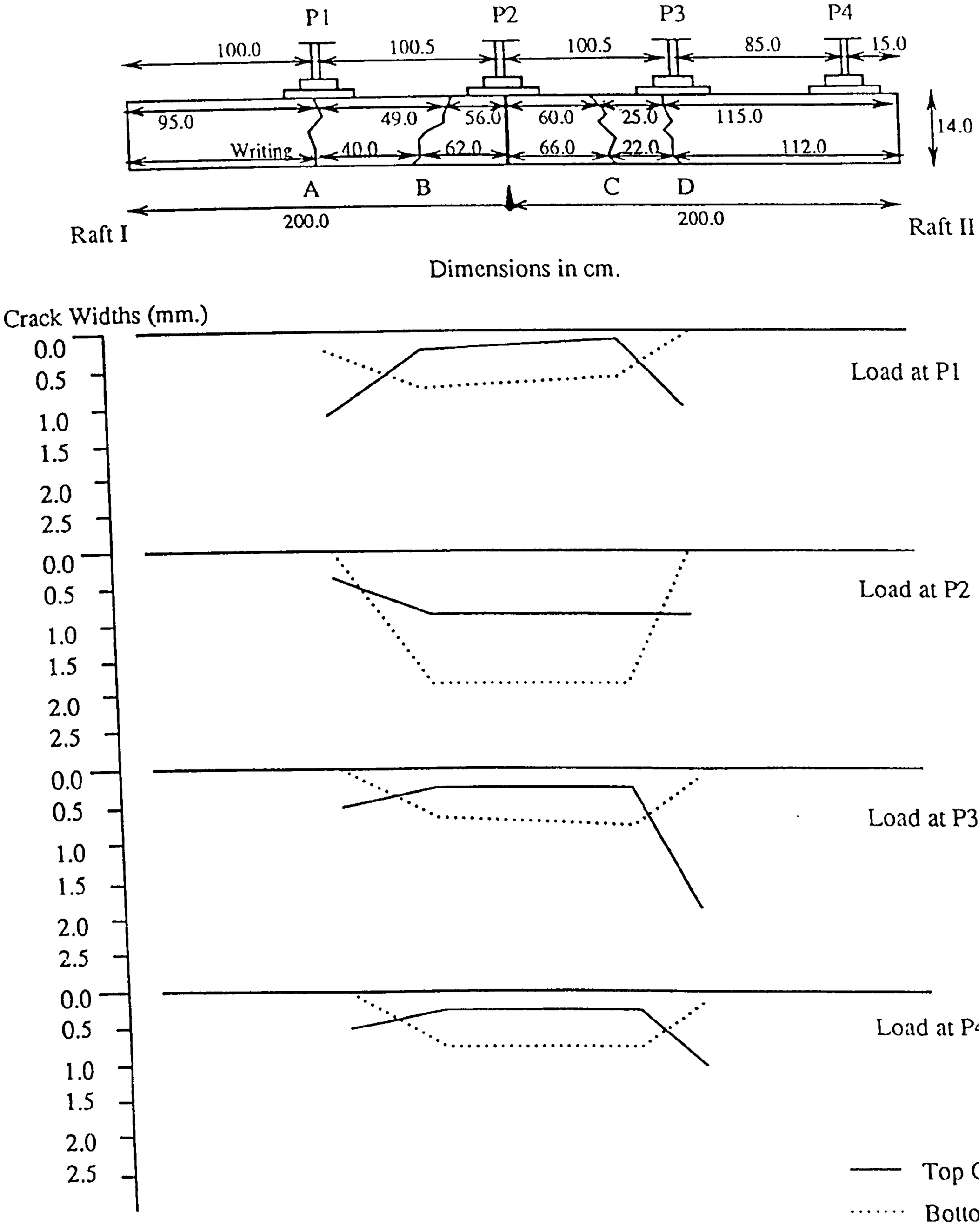

Fig. 6.5: Relationship Between Cracks Widths and Loading Positions For Load 450kN ,Raft unit RS2.

[For Test Rig Notations See Table 4.2 and Fig. 4 4]

Fig. 6.6: LOAD CYCLES Vs BOTTOM CRACKS
For Load 450kN
Due to loading P1- For M2

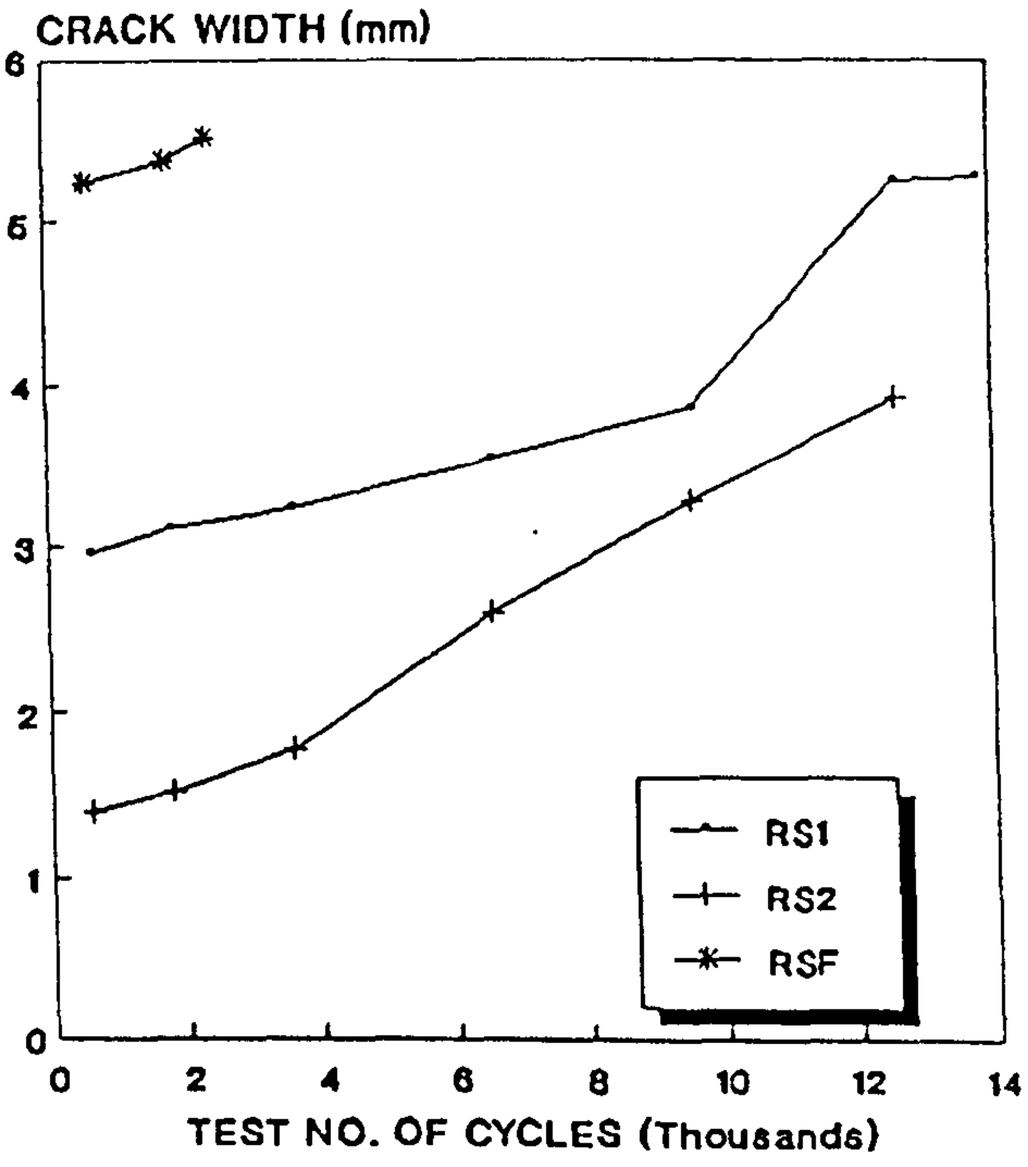

Fig. 6.7: LOAD CYCLES Vs TOP CRACKS
For Load 450kN
Due to Loading P1- For M2

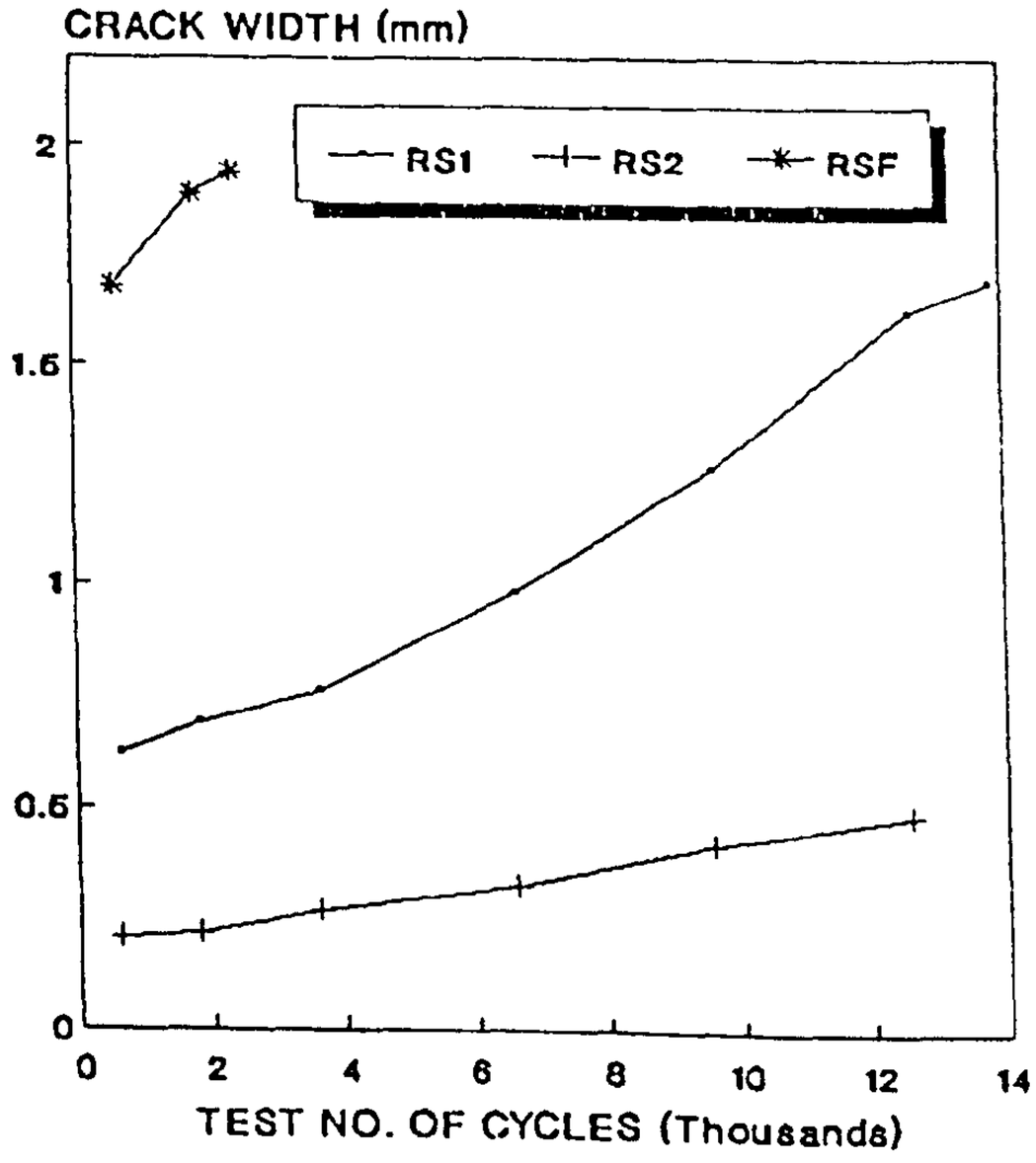

Fig.6.8: LOAD Vs STRAIN
Between Loaded areas, Point K
Due to Loading P3-For M2

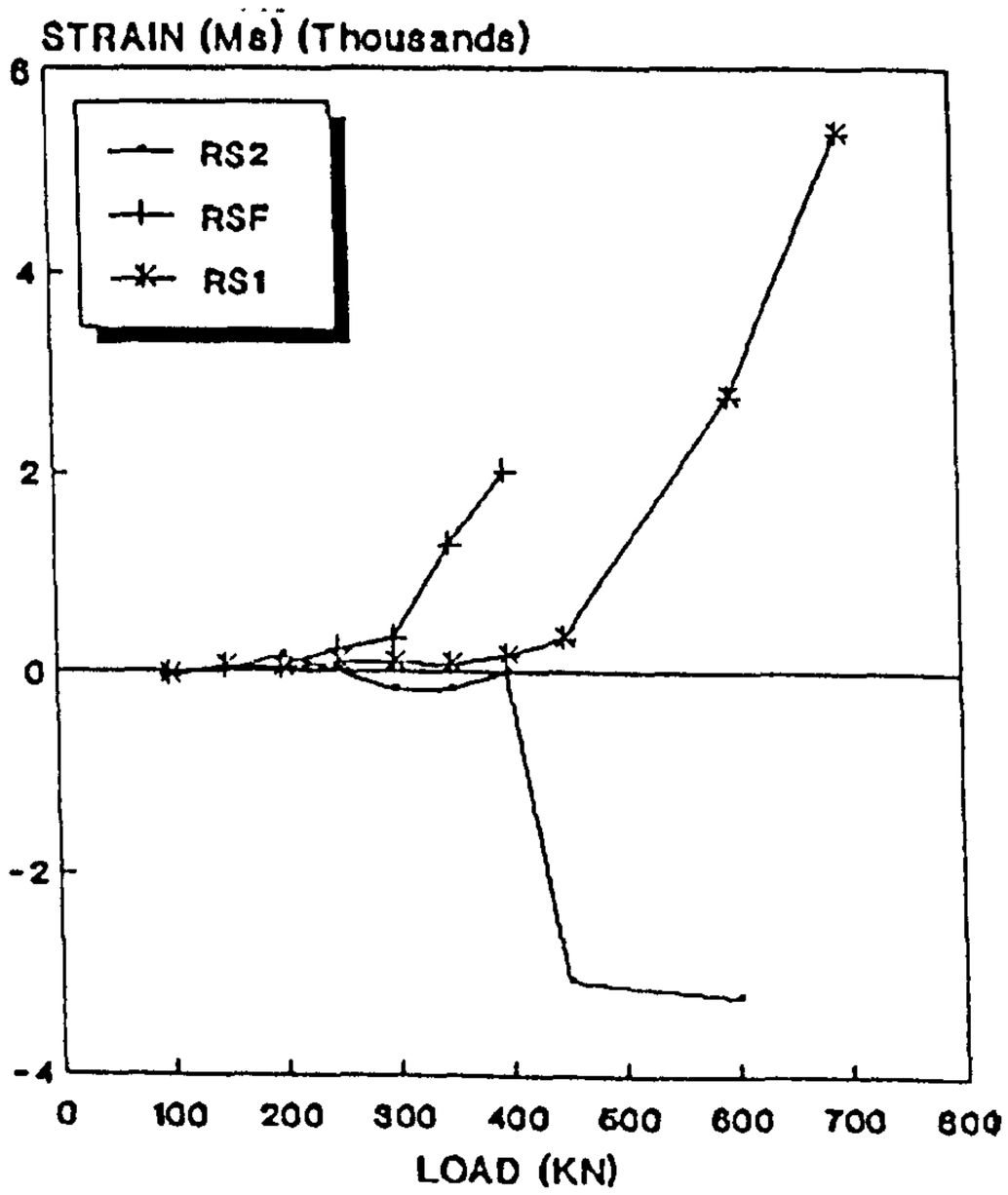

Fig.6.9: LOAD Vs STRAIN
Remote Sections ,Point I
Due to Loading P1-For M2

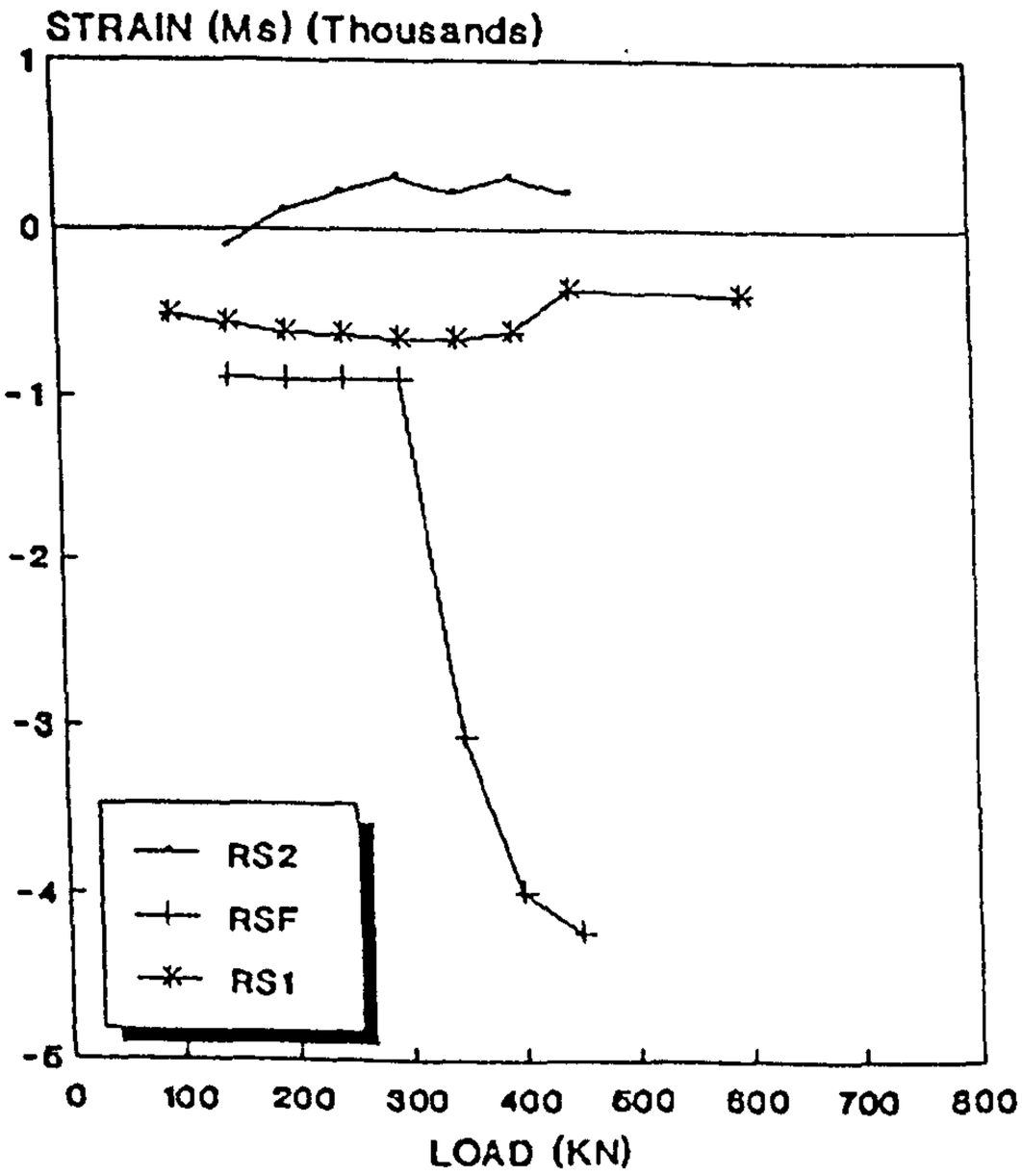

[For Test Rig Notations See Table 4.2 and Fig. 4.4]

Fig. 6.10: LOAD Vs STRAIN
Inner Loaded Area ,Point P
Due to Loading P4- For M2

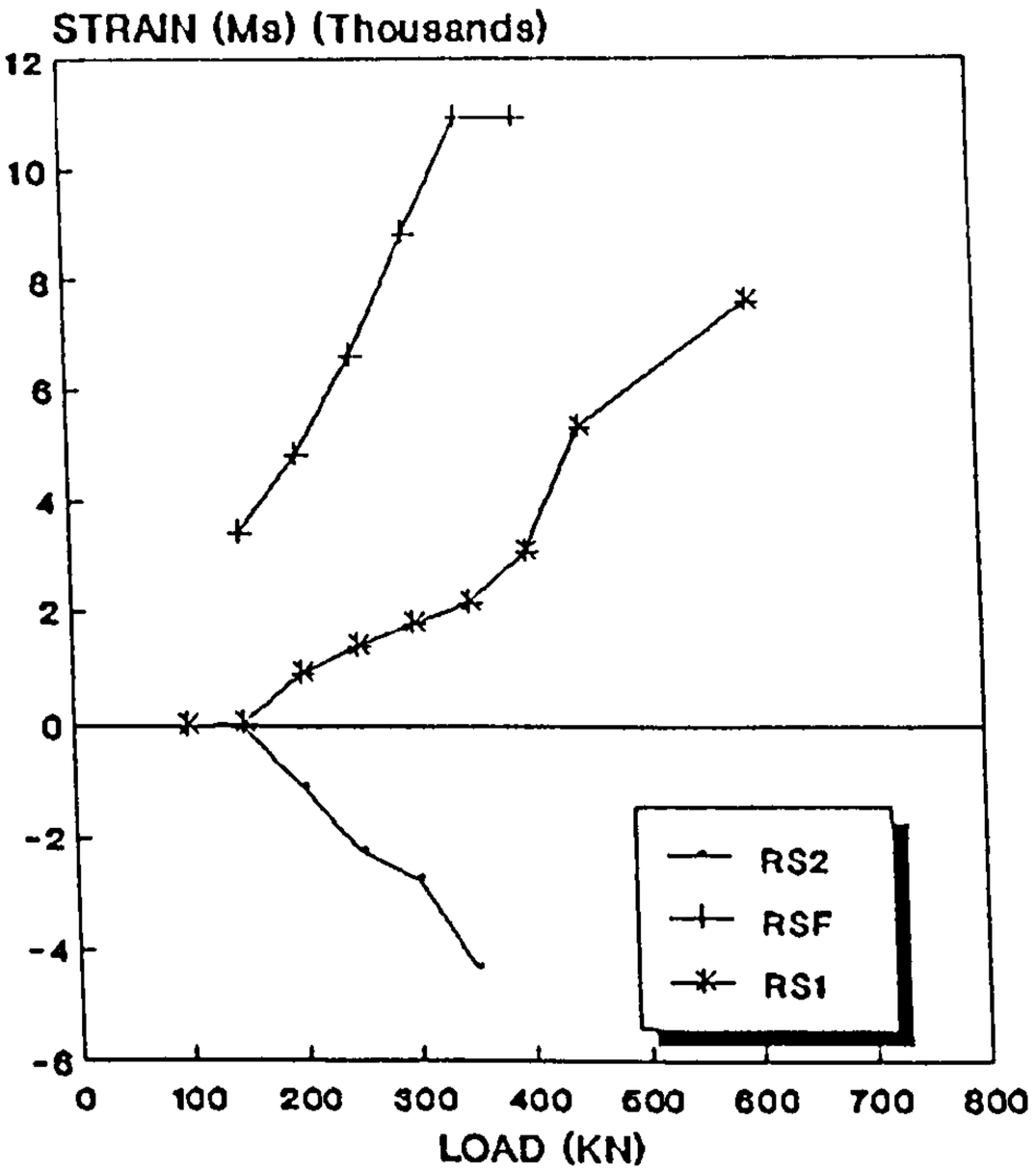

Fig. 6.11: LOAD Vs STRAIN
Outer Loaded Area, Point A
Due To Loading P1- For M1

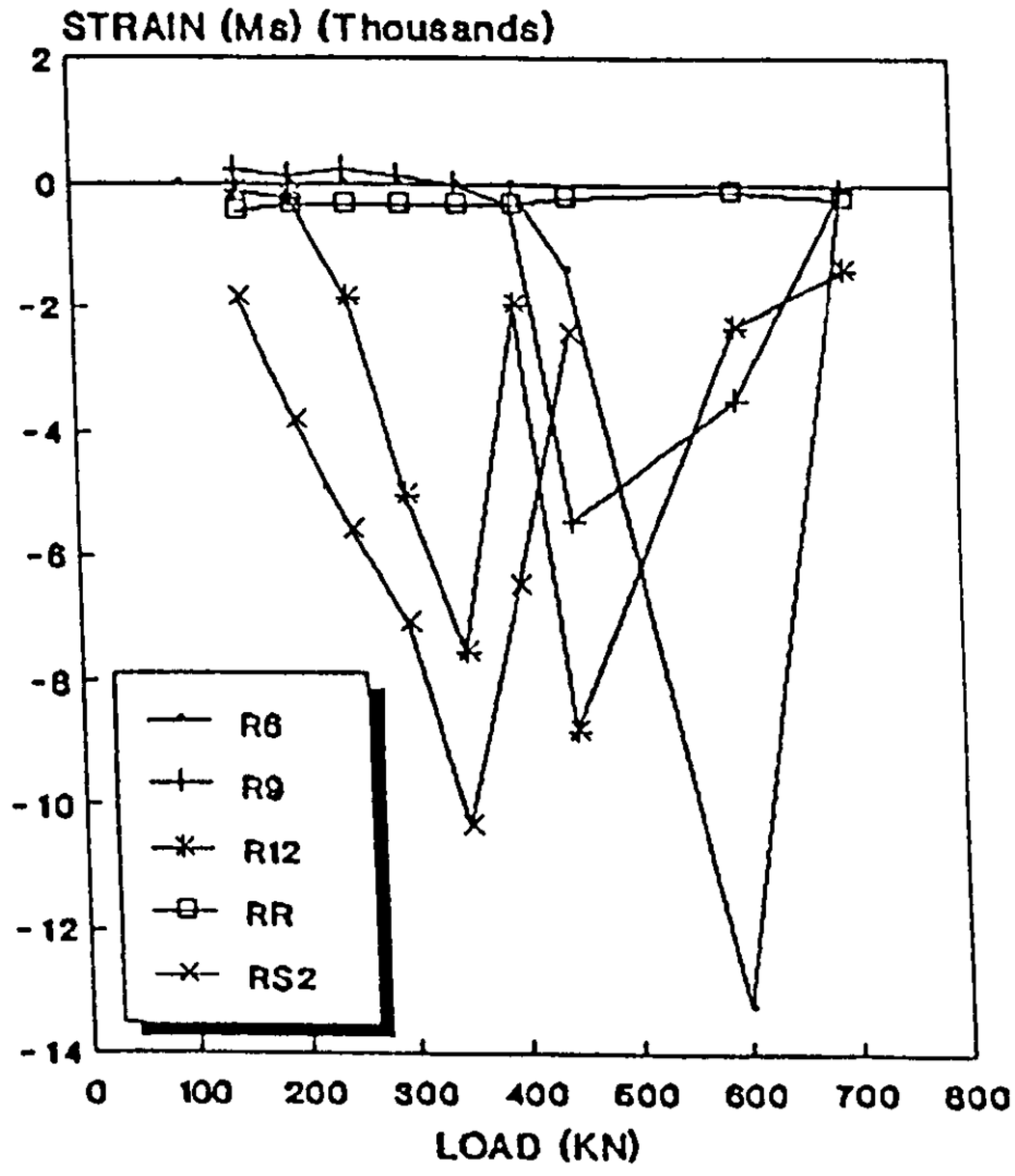

[For Test Rig Notations See Table 4.2 and Fig. 4.4]

Fig. 6.12: LOAD Vs STRAIN
Between Loaded Areas, Point E
Due to loading P1- For M1

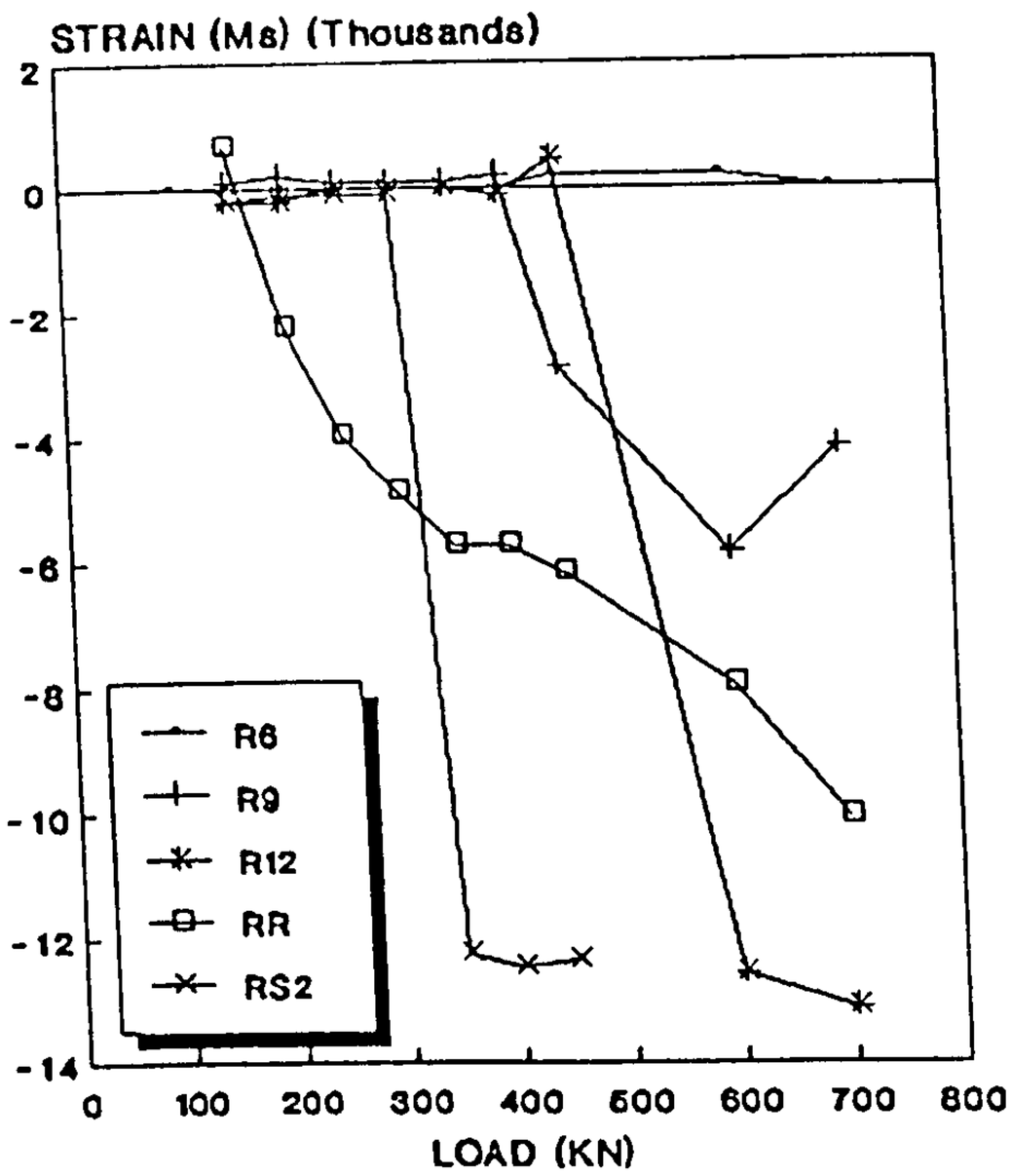

Fig. 6.13: LOAD Vs STRAIN
Inner Loaded Area, Point F
Due to Loading P1-For M1

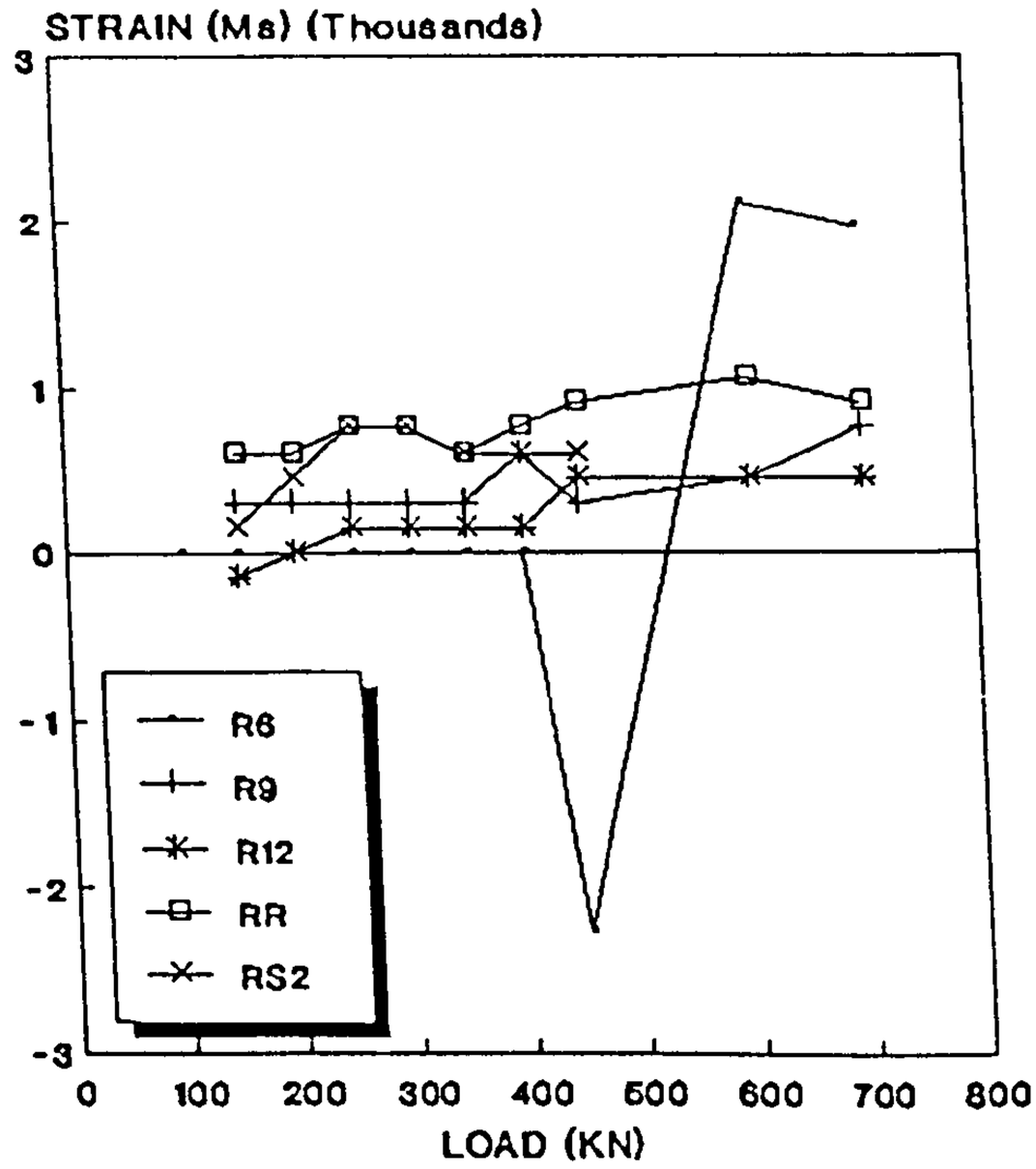

Fig.6.14: LOAD Vs STRAIN
Remote Sections, Point I
Due to Loading P1-For M1

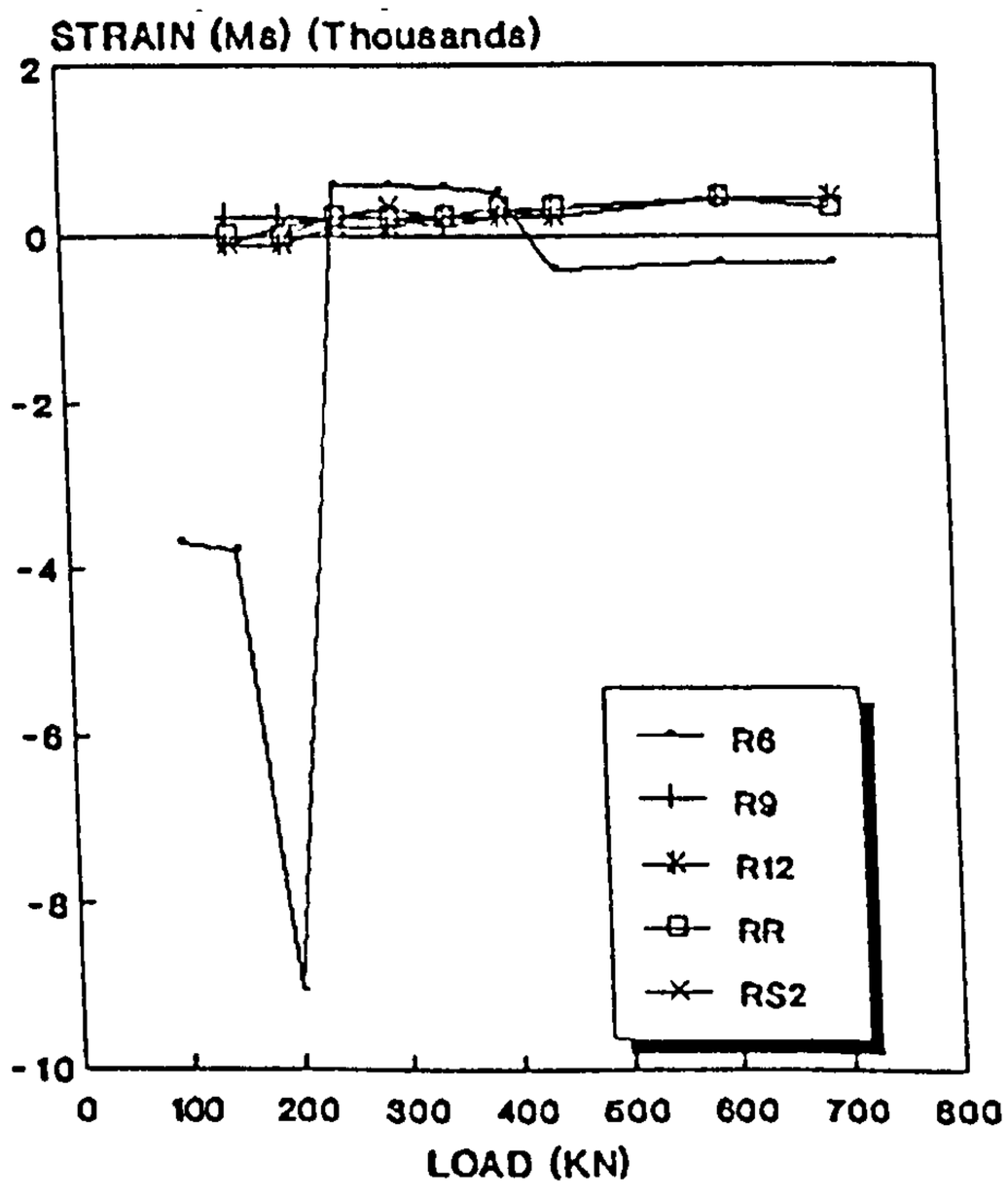

Fig.6.15: LOAD Vs STRAIN
Between Loaded Areas ,Point J
Due to Loading P2-For M1

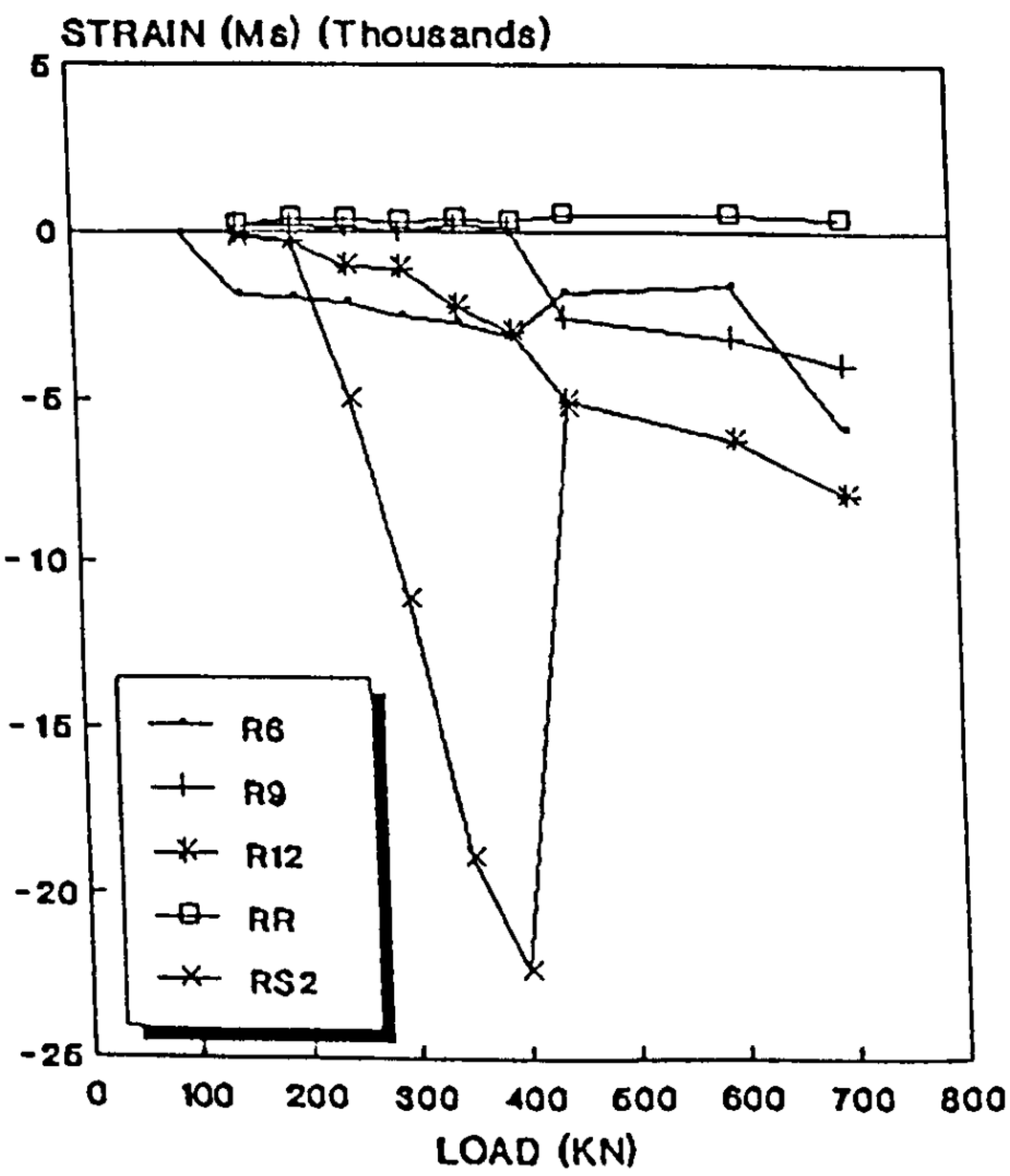

[For Test Rig Notations See Table 4.2 and Fig. 4.4]

Fig. 6.16: LOAD Vs STRAIN
Remote Sections , Point E
Due to loading P2- For M1

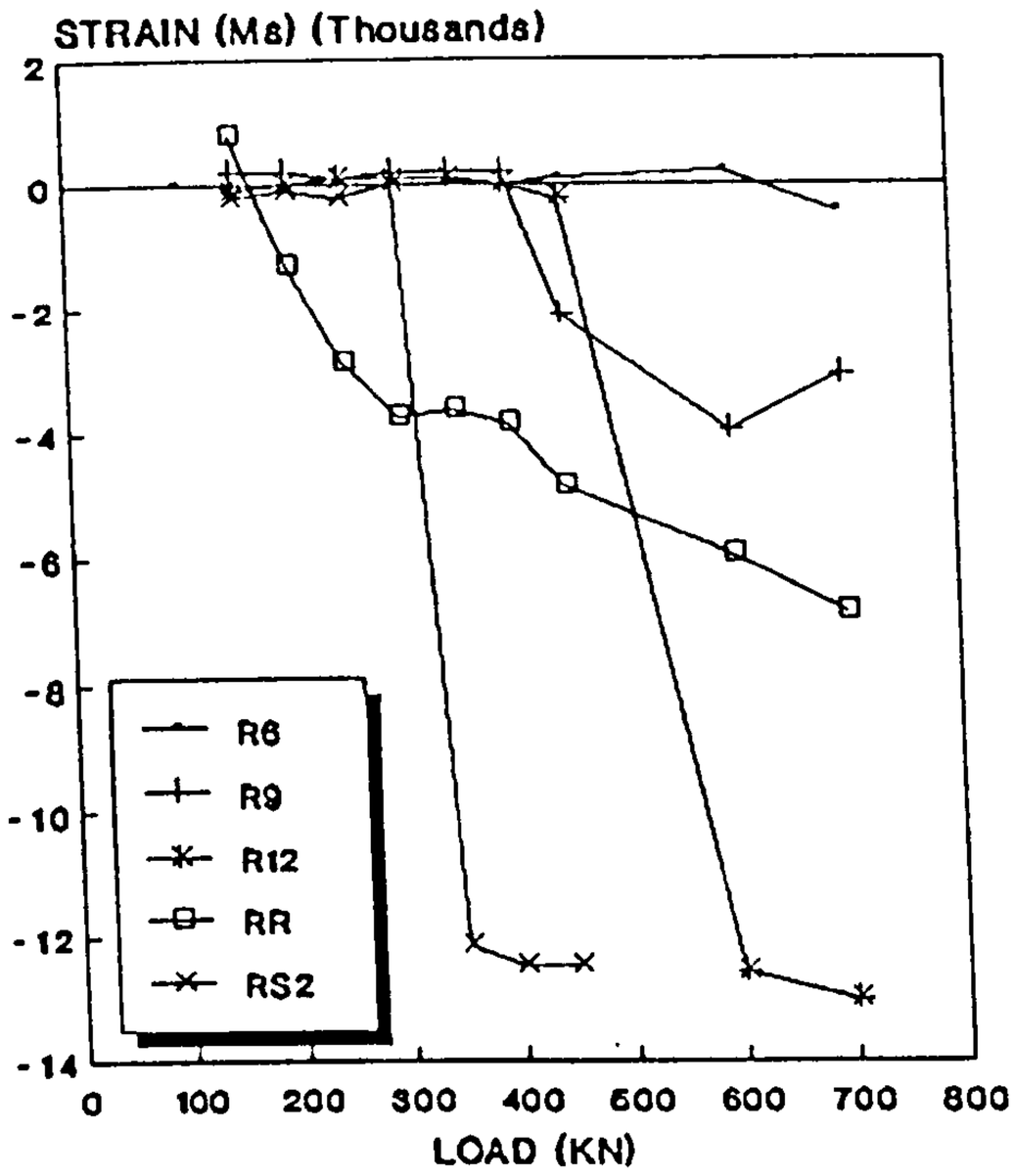

Fig. 6.17: LOAD Vs STRAIN
Remote Sections , Point K
Due to Loading P2-For M1

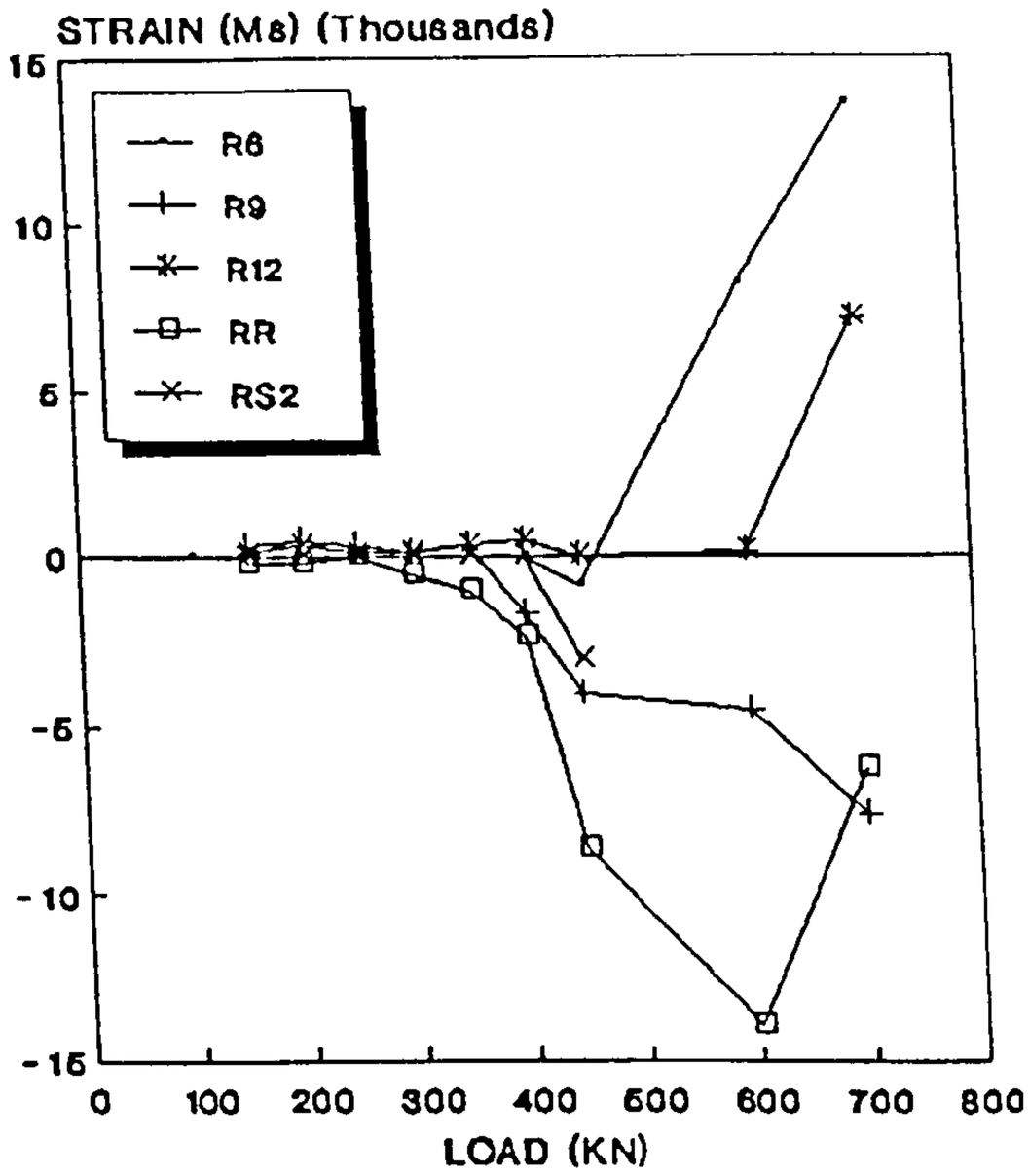

Fig.6.18: LOAD Vs STRAIN
Between Loaded Areas , Point K
Due to Loading P3-For M1

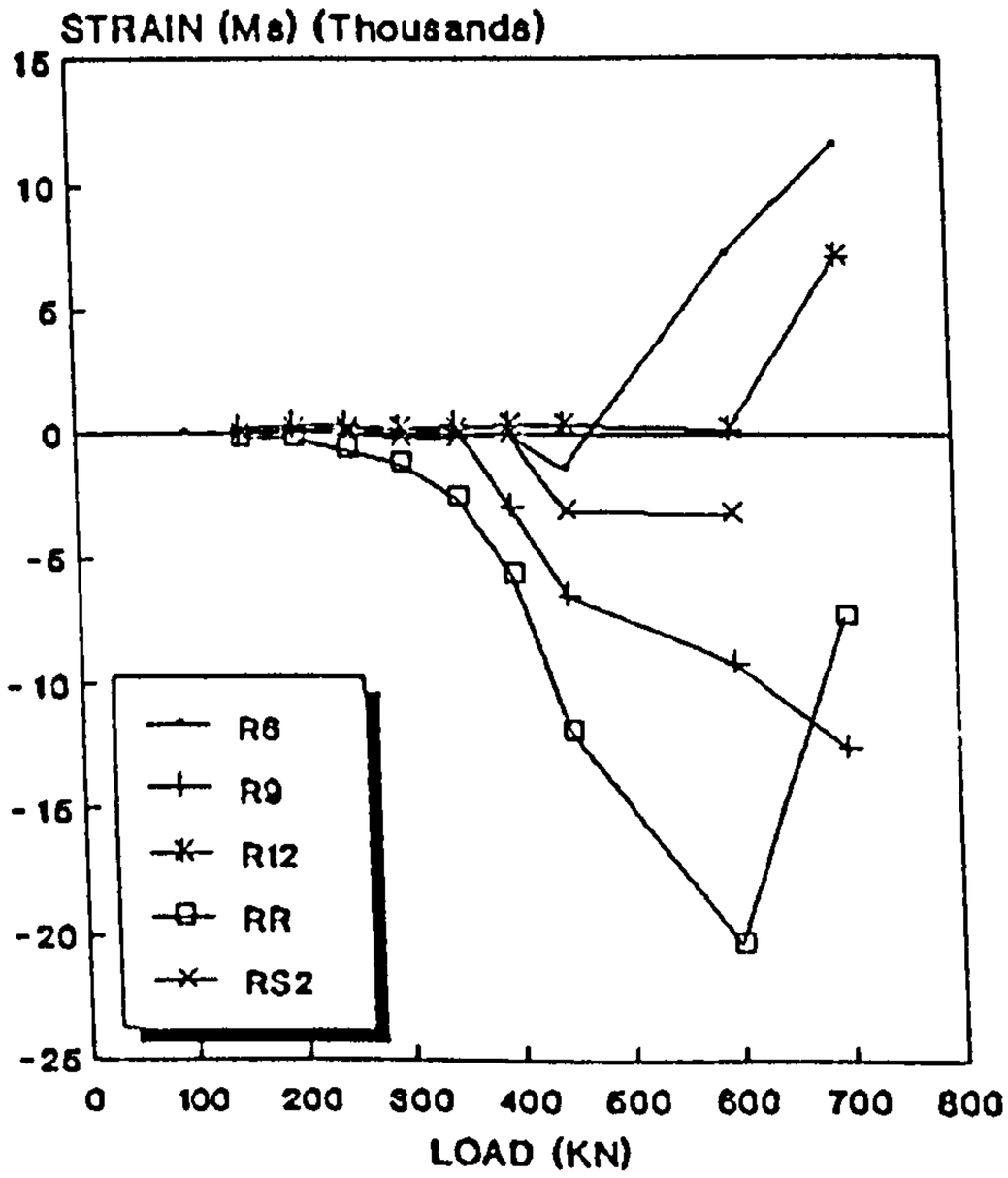

Fig.6.19: LOAD Vs STRAIN
Between Loaded Areas ,Point L
Due to Loading P4-For M1

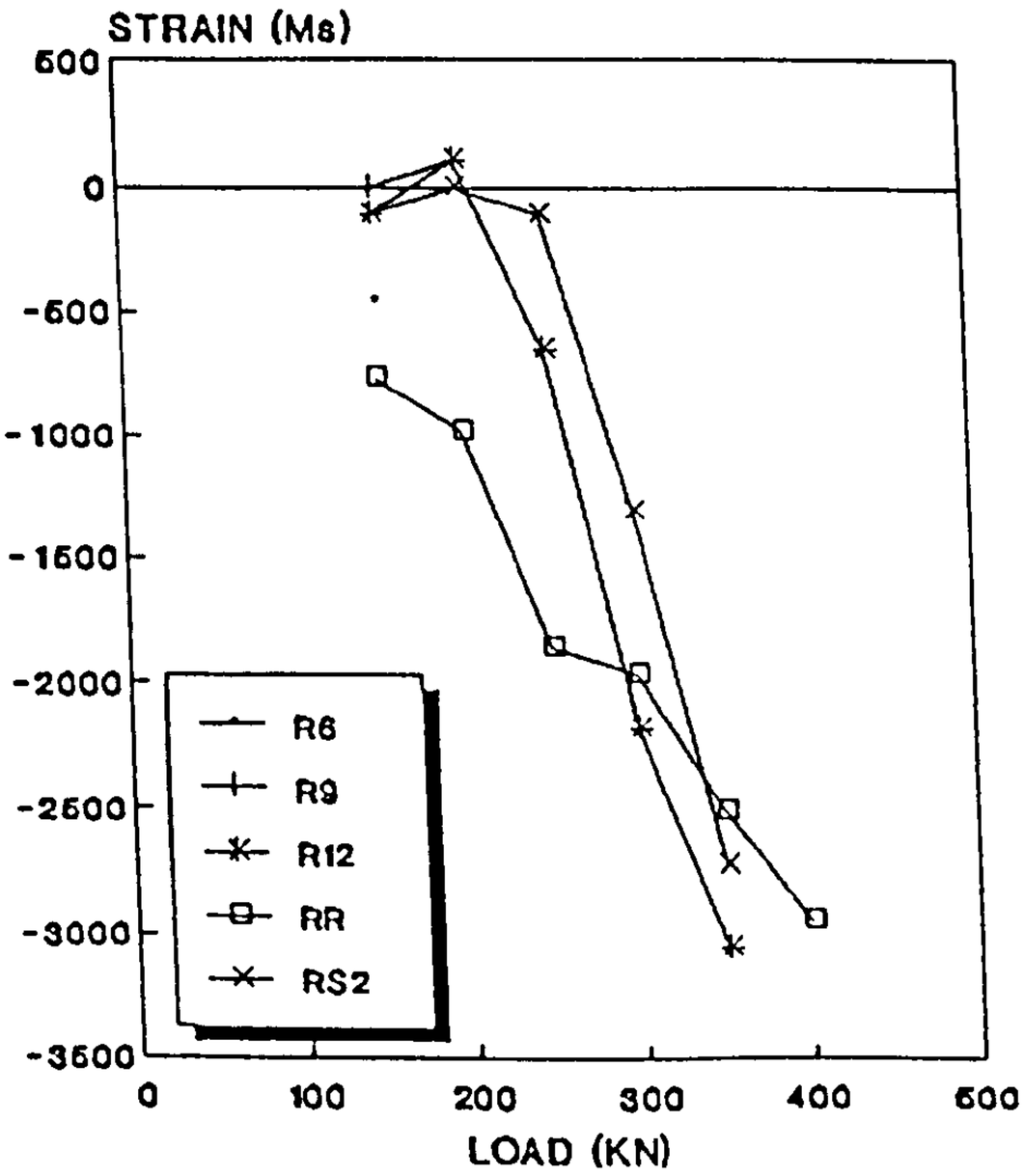

[For Test Rig Notations See Table 4.2 and Fig. 4 4]

Fig. 6.20: LOAD Vs STRAIN
Outer Loaded Area, Point M
Due to loading P3- For M1

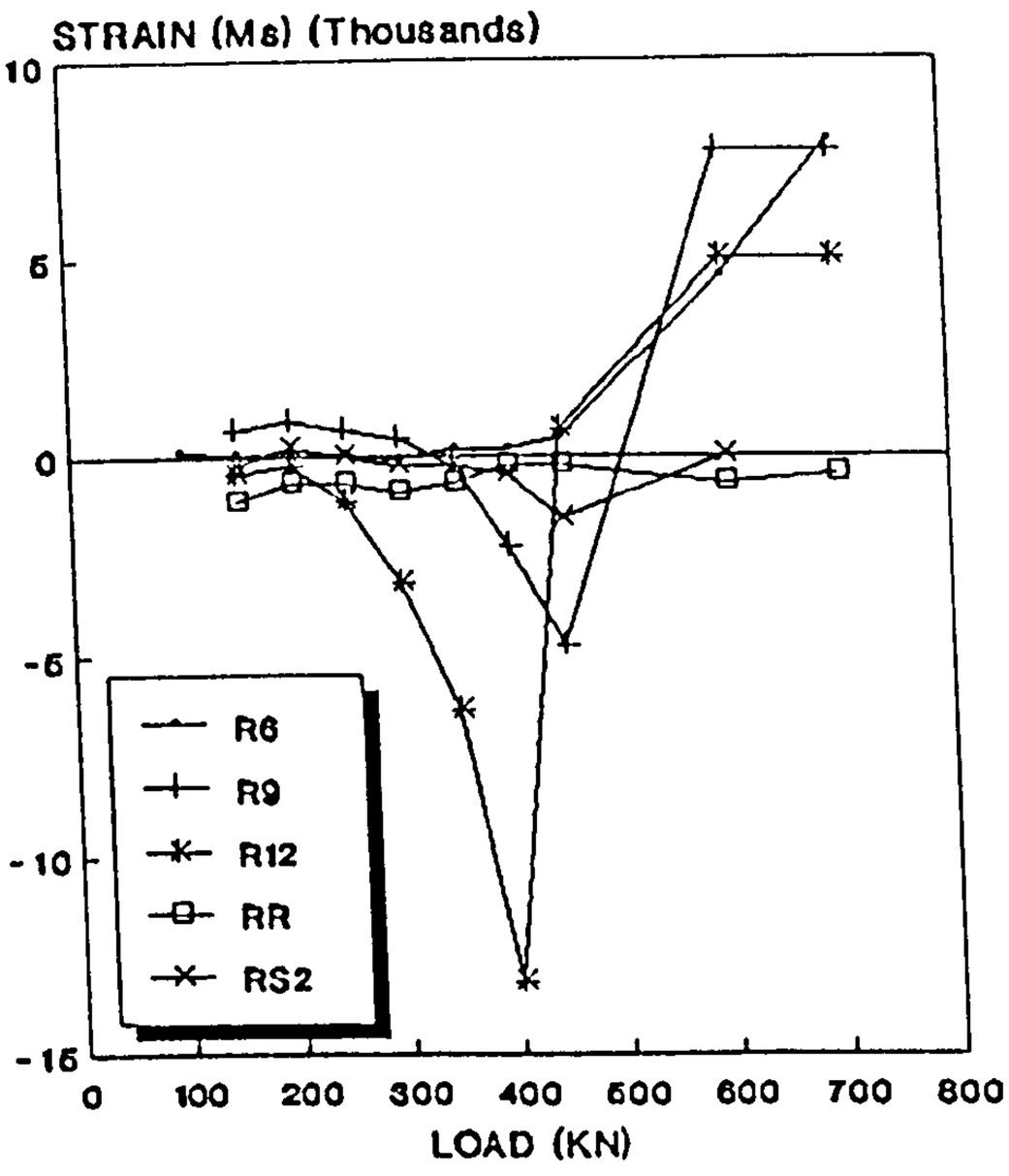

Fig. 6.21: LOAD Vs STRAIN
Inner Loaded, Point P
Due to Loading P4-For M1

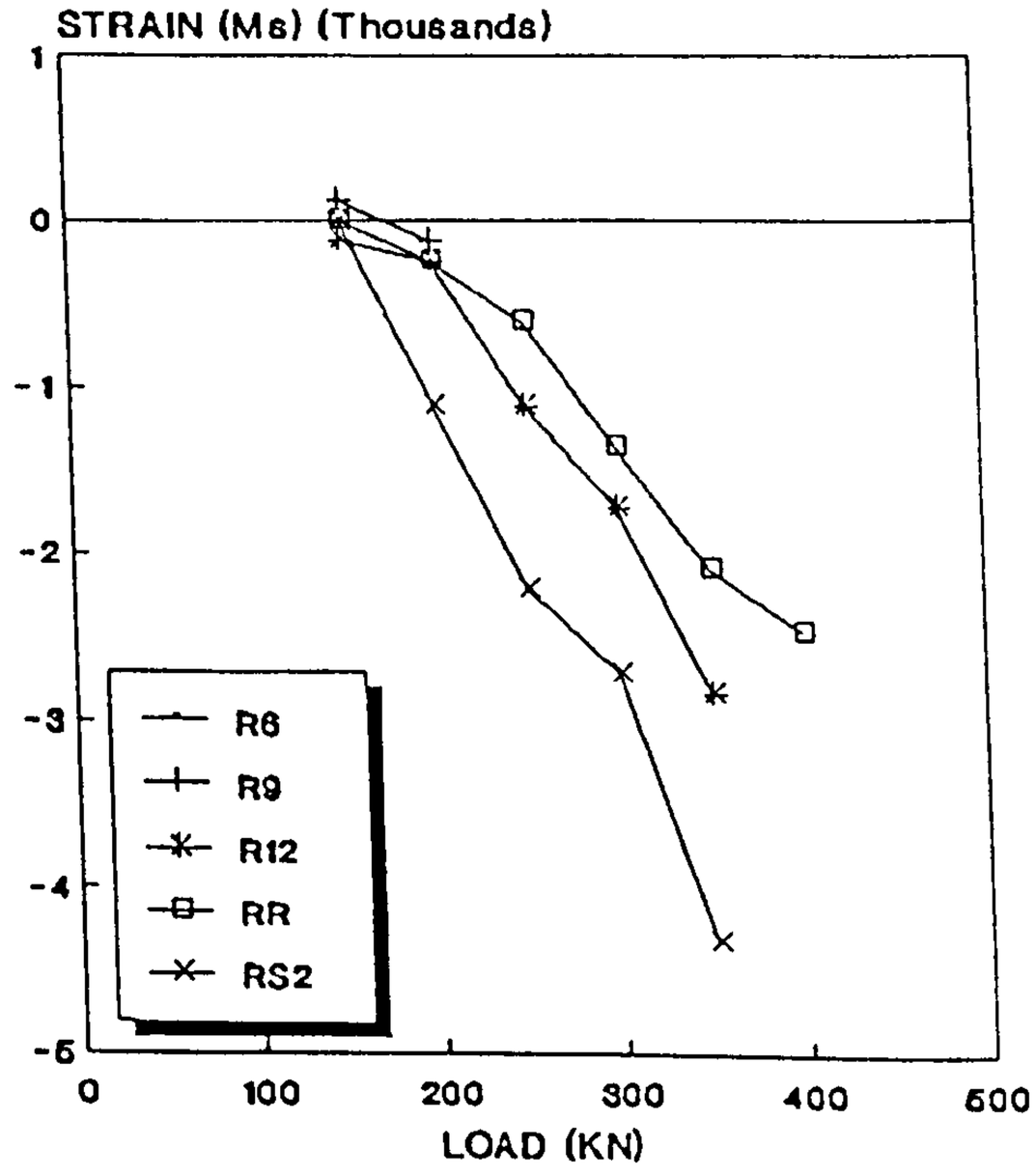

Fig.6.22: LOAD Vs STRAIN
Between Loaded Areas, Point J
Due to Loading P2-For M2

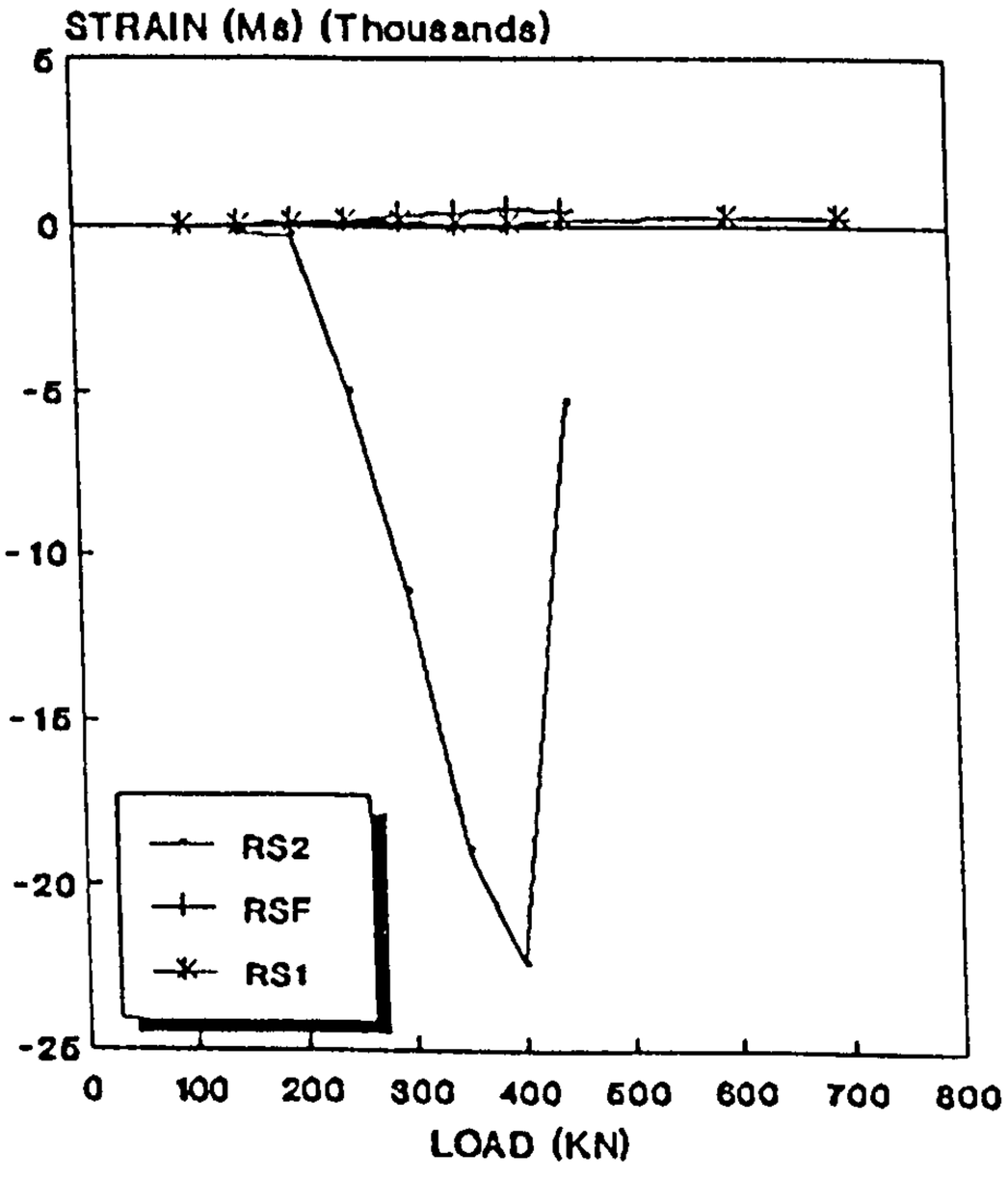

Fig.6.23: LOAD Vs STRAIN
Between Loaded Areas ,Point L
Due to Loading P4-For M2

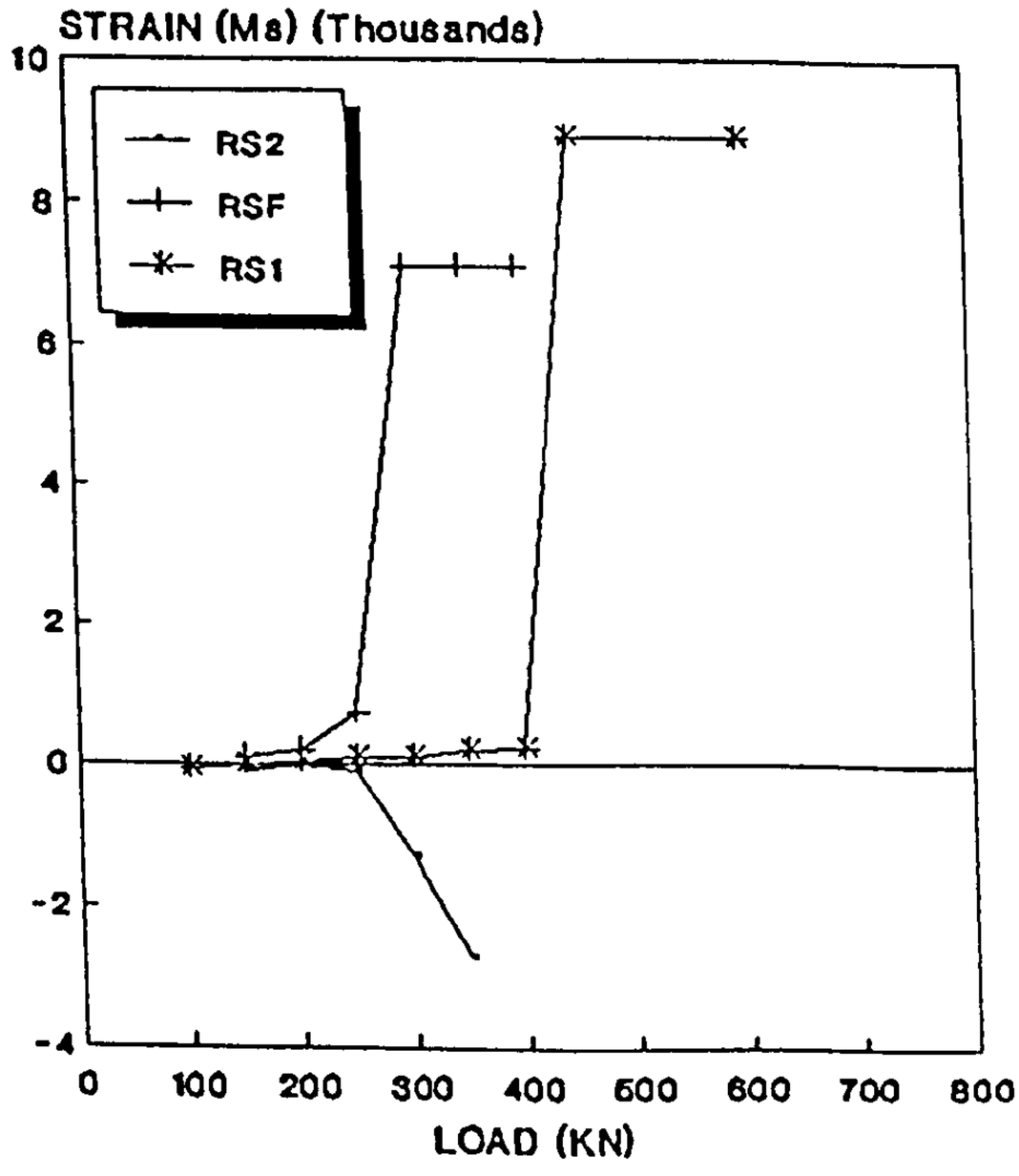

[For Test Rig Notations See Table 4.2 and Fig. 4.4]

Fig. 6.24: LOAD Vs STRAIN
Outer Loaded Areas , Point A
Due to loading P1- For M2

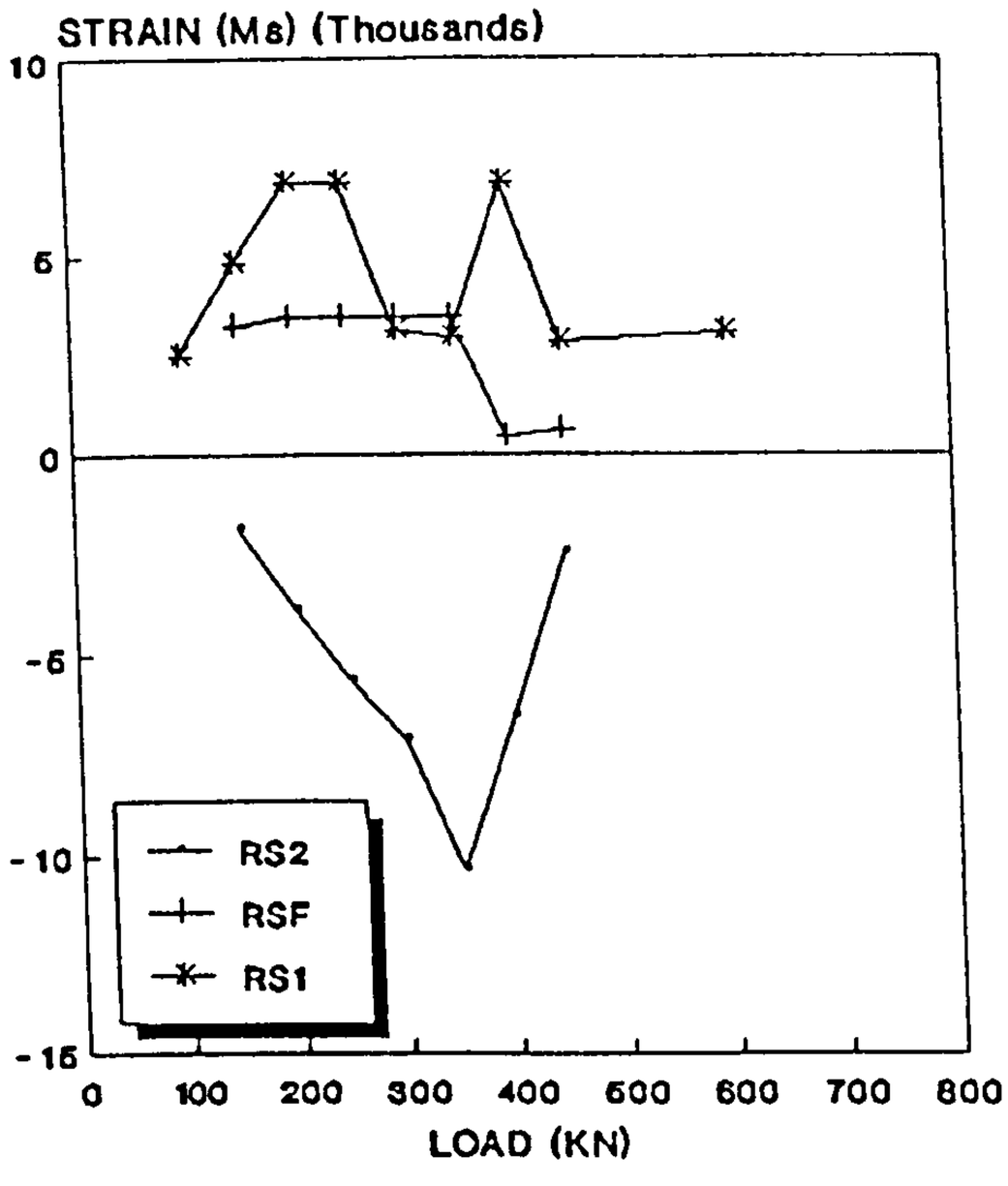

Fig. 6.25: LOAD Vs STRAIN
Between Loaded Areas, Point J
Due to Loading P2-For M3

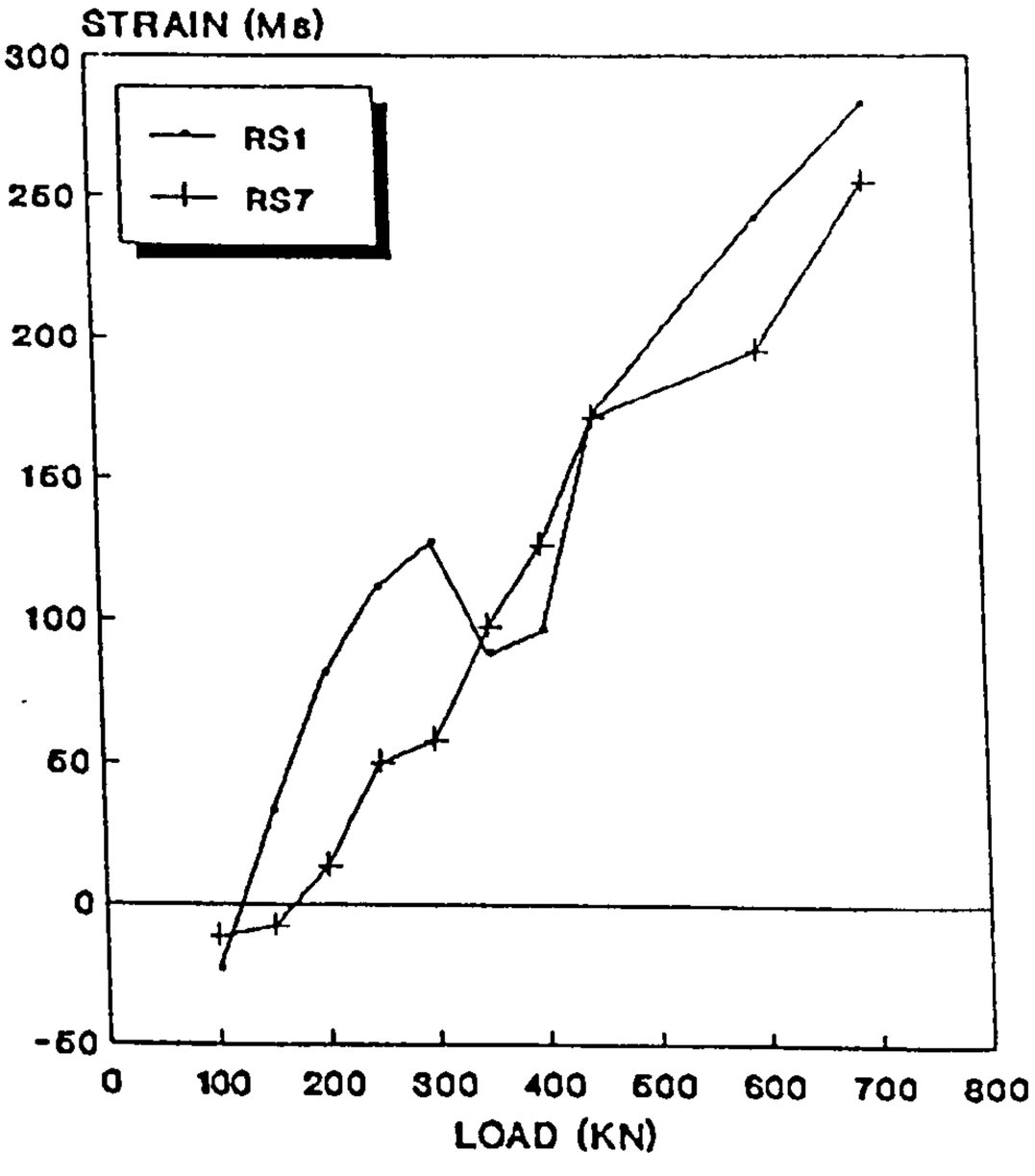

Fig.6.26: LOAD Vs STRAIN
Between Loaded Areas , Point K
Due to Loading P3-For M3

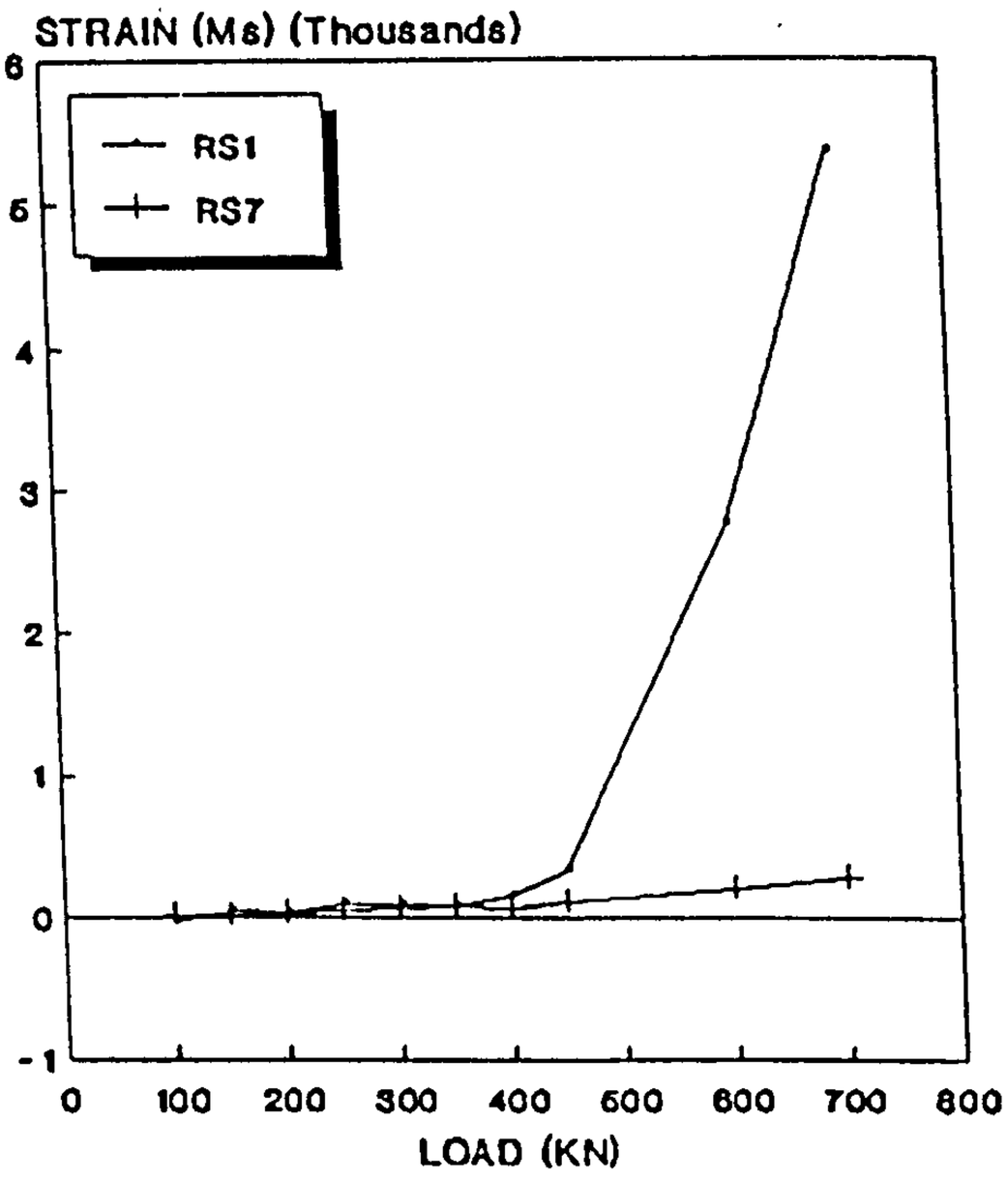

Fig.6.27: LOAD Vs STRAIN
Between Loaded Areas ,Point L
Due to Loading P4-For M3

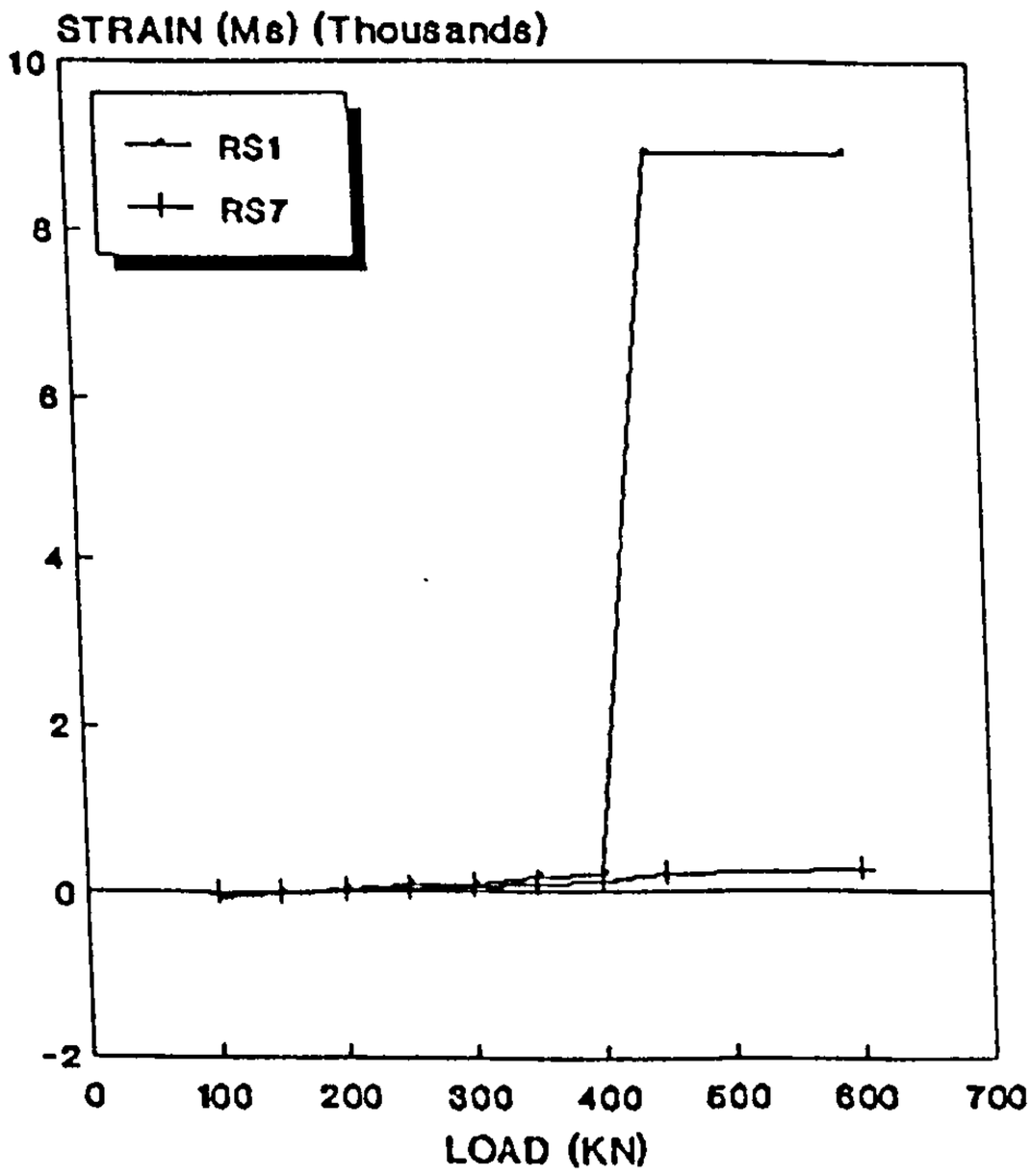

[For Test Rig Notations See Table 4.2 and Fig. 4.4]

Fig. 6.28: LOAD Vs STRAIN
Outer Loaded Area , Point A
Due to loading P1- For M3

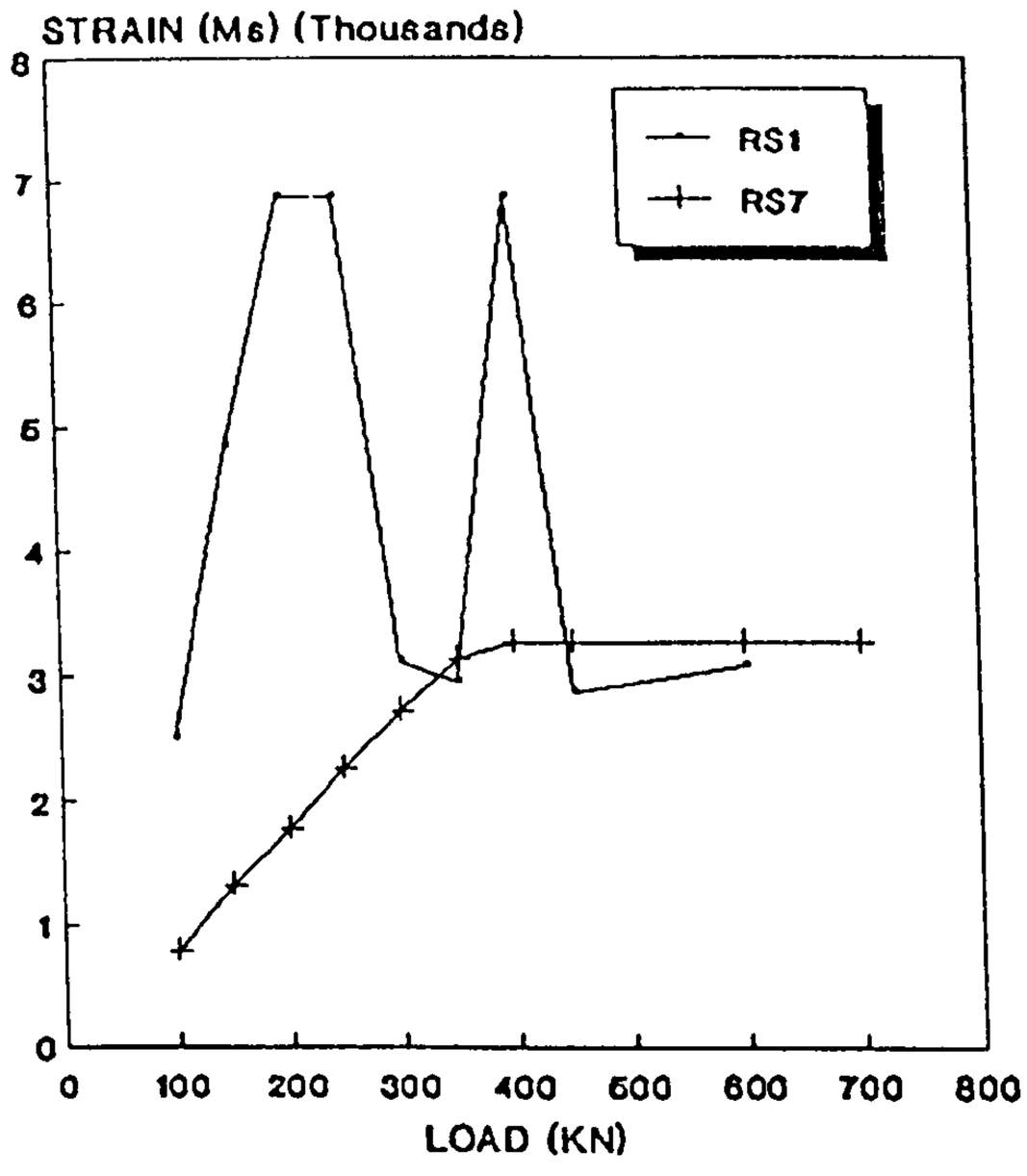

Fig. 6.29: LOAD Vs STRAIN
Inner Loaded Area, Point P
Due to Loading P3-For M3

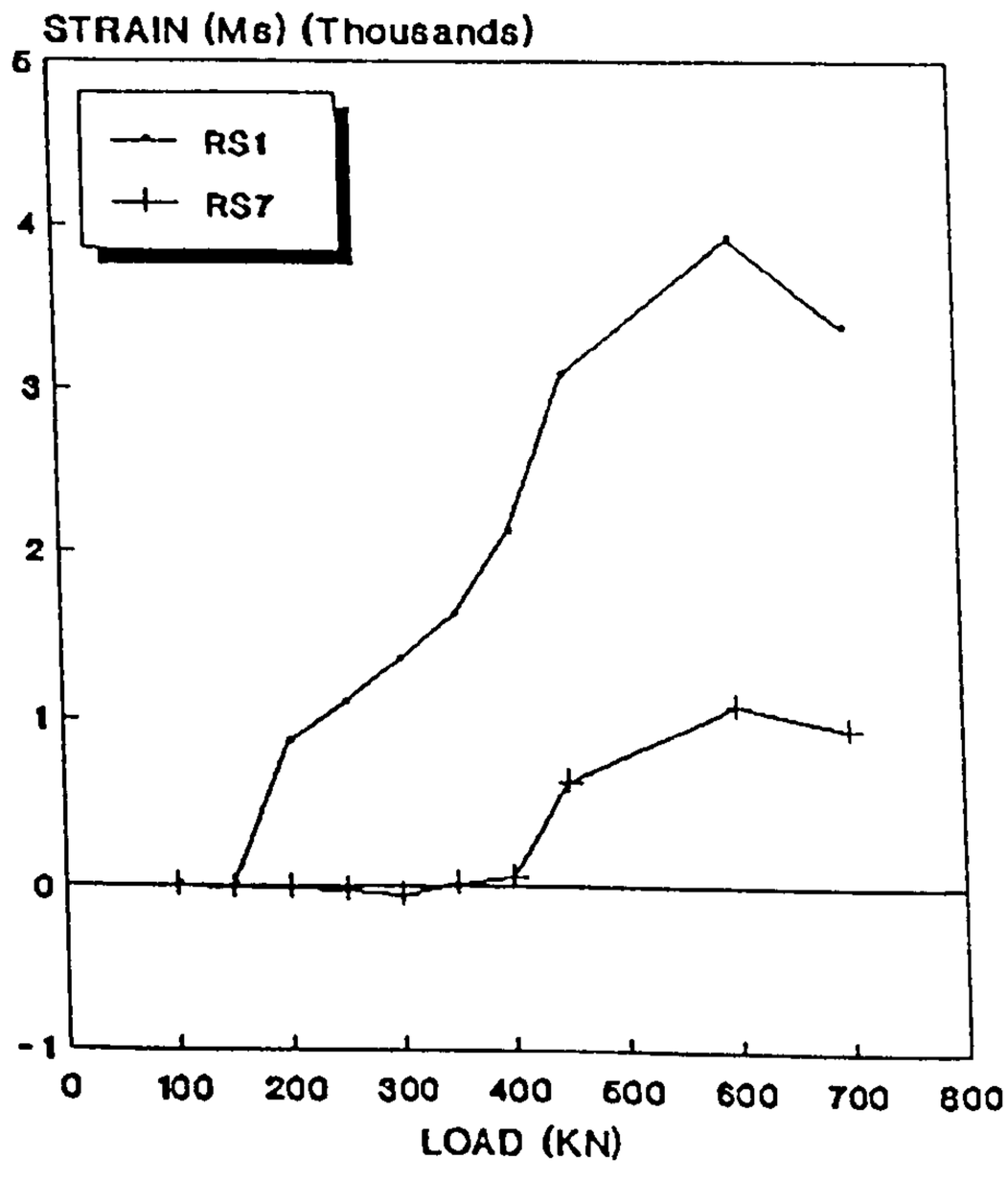

Fig.6.30: LOAD Vs STRAIN
Inner Loaded Area , Point P
Due to Loading P4-For M3

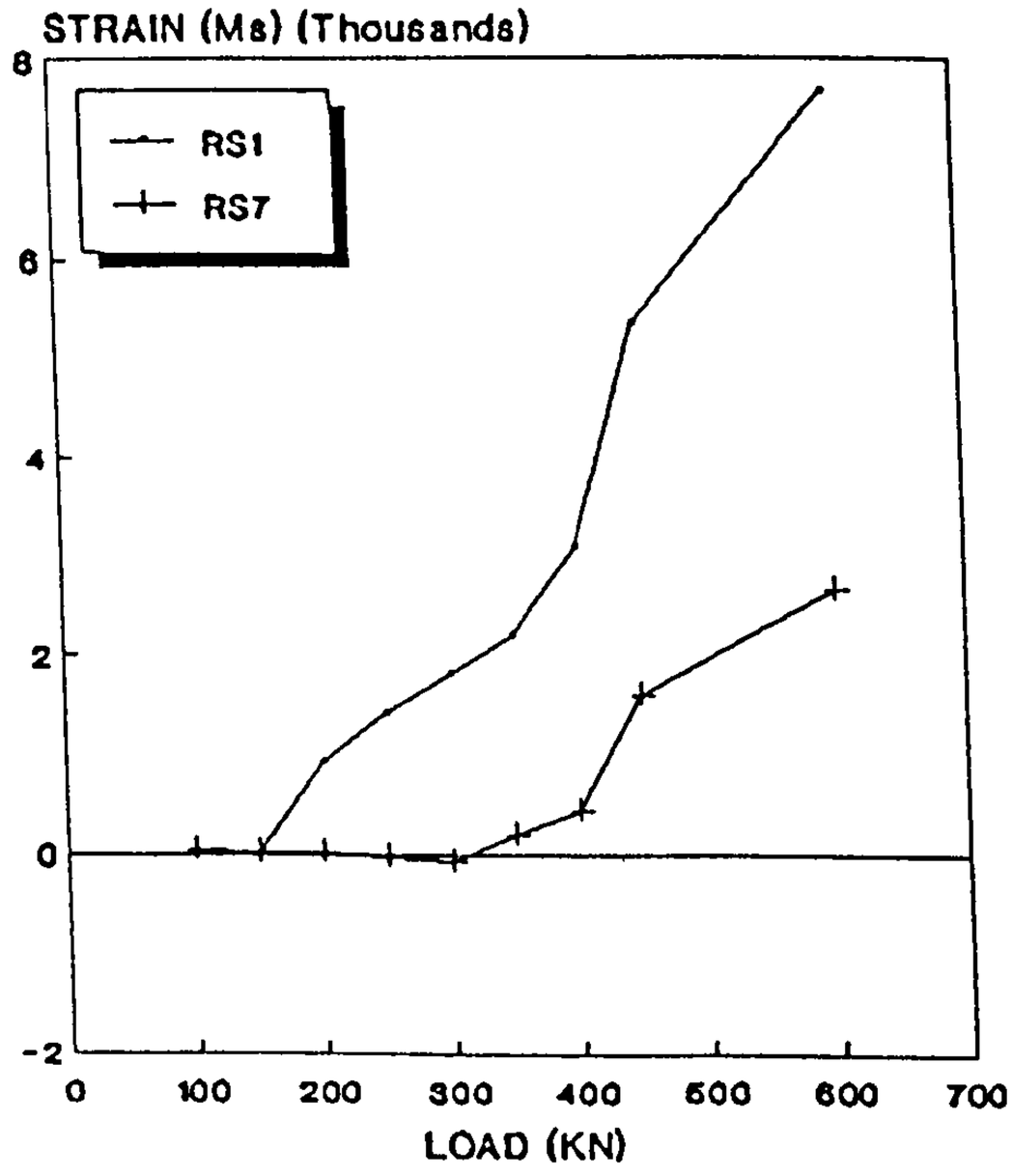

Fig.6.31: LOAD Vs DEFLECTION
Inner Loaded Area ,Point 6
Due to Loading P1-For M1

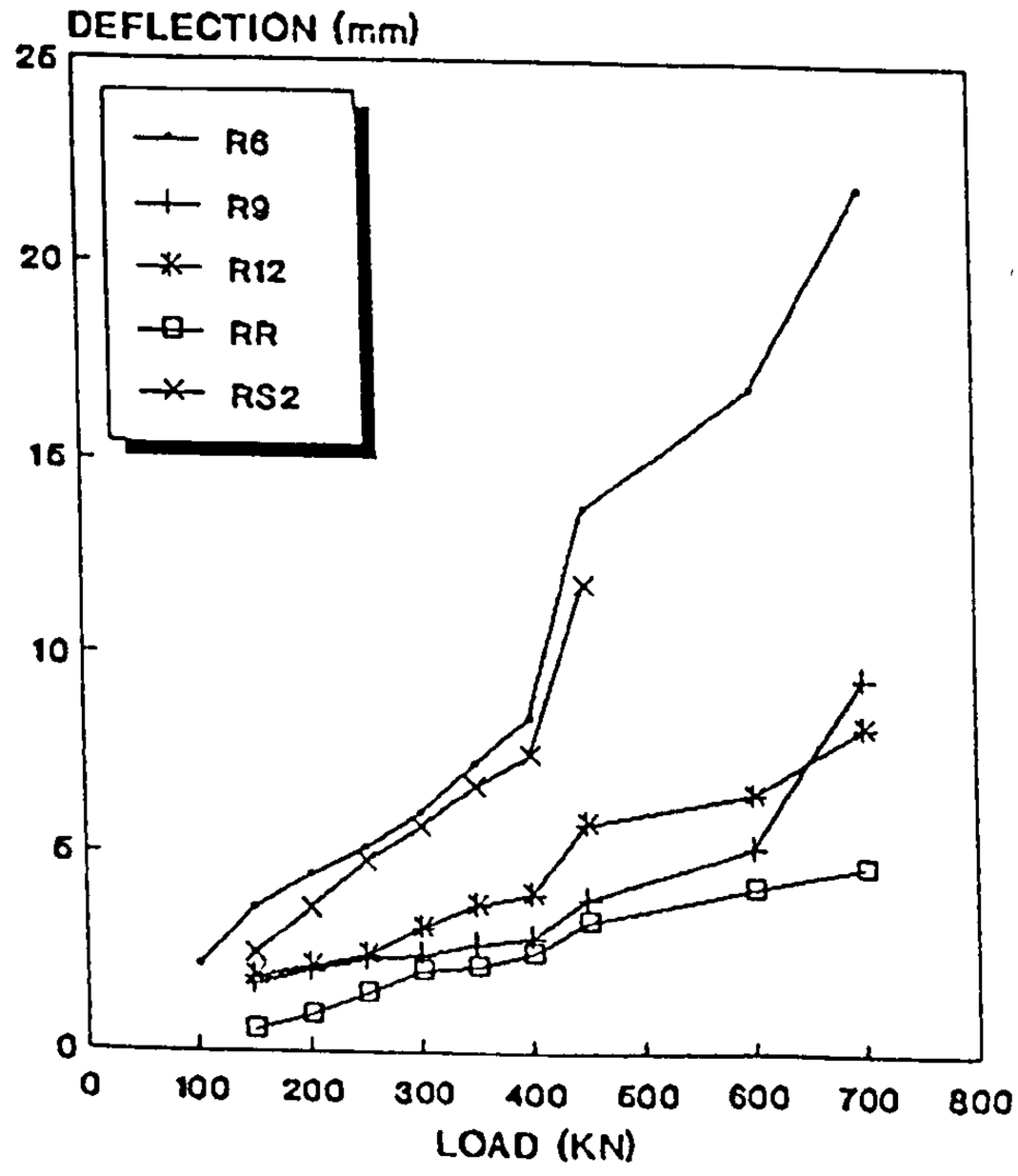

[For Test Rig Notations See Table 4.2 and Fig. 4.4]

Fig. 6.32: LOAD Vs DEFLECTION
At Free Corners , Point 1
Due to loading P1- For M1

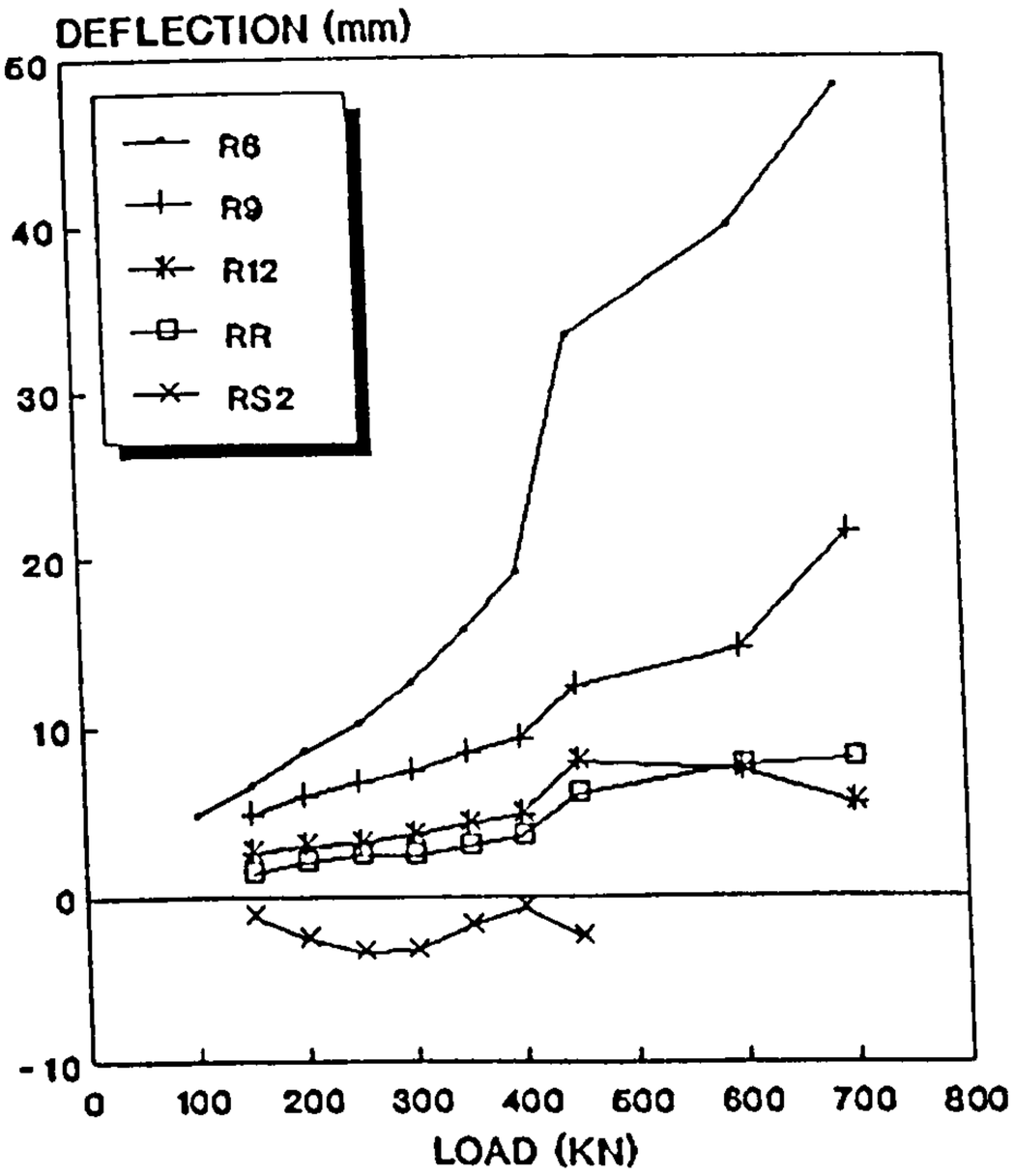

Fig. 6.33: LOAD Vs DEFLECTION
At Free Edge, Point 7
Due to Loading P4-For M1

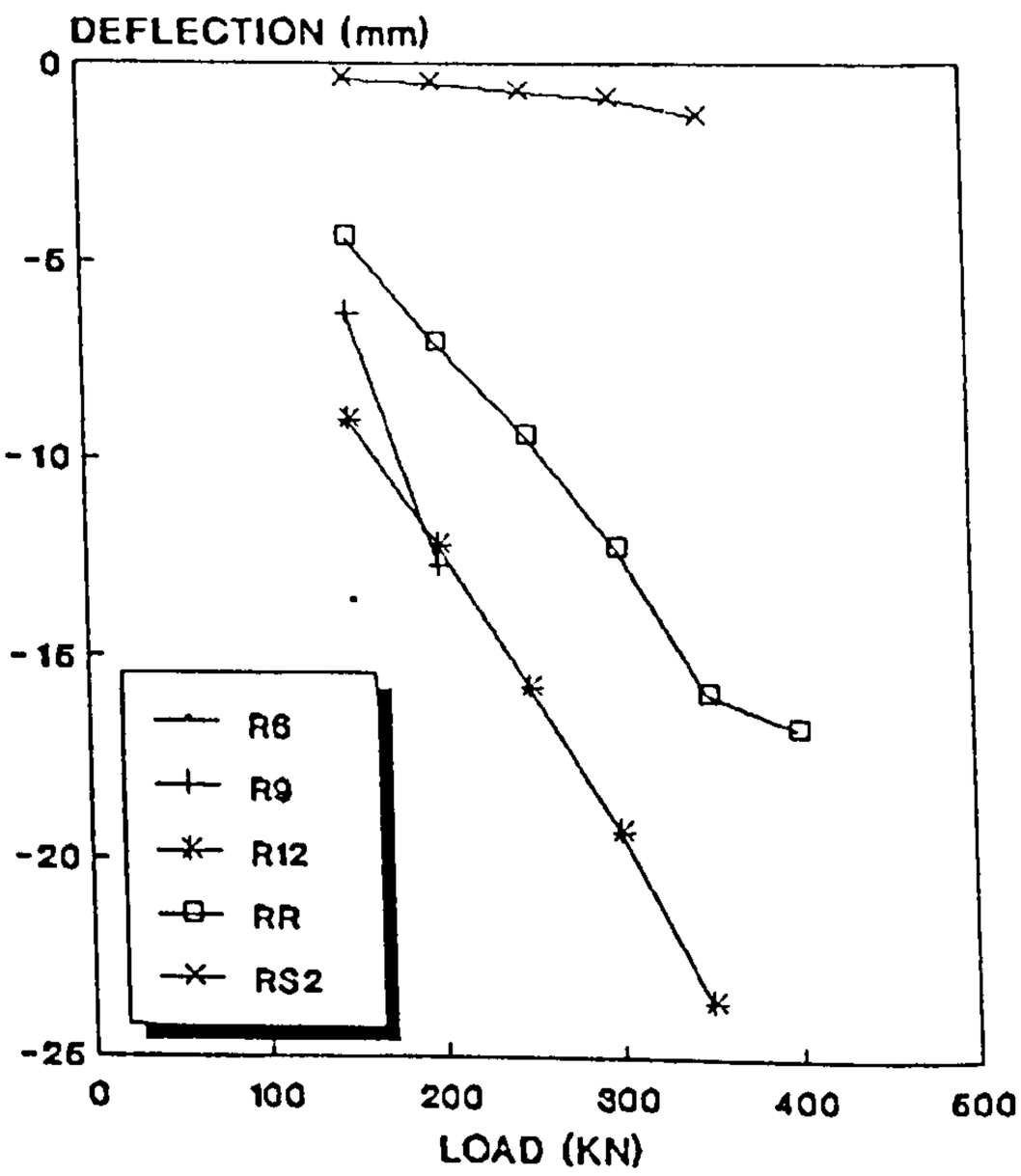

Fig.6.34: LOAD Vs DEFLECTION
At Middle of Tracking Load , Point 13
Due to Loading P1-For M1

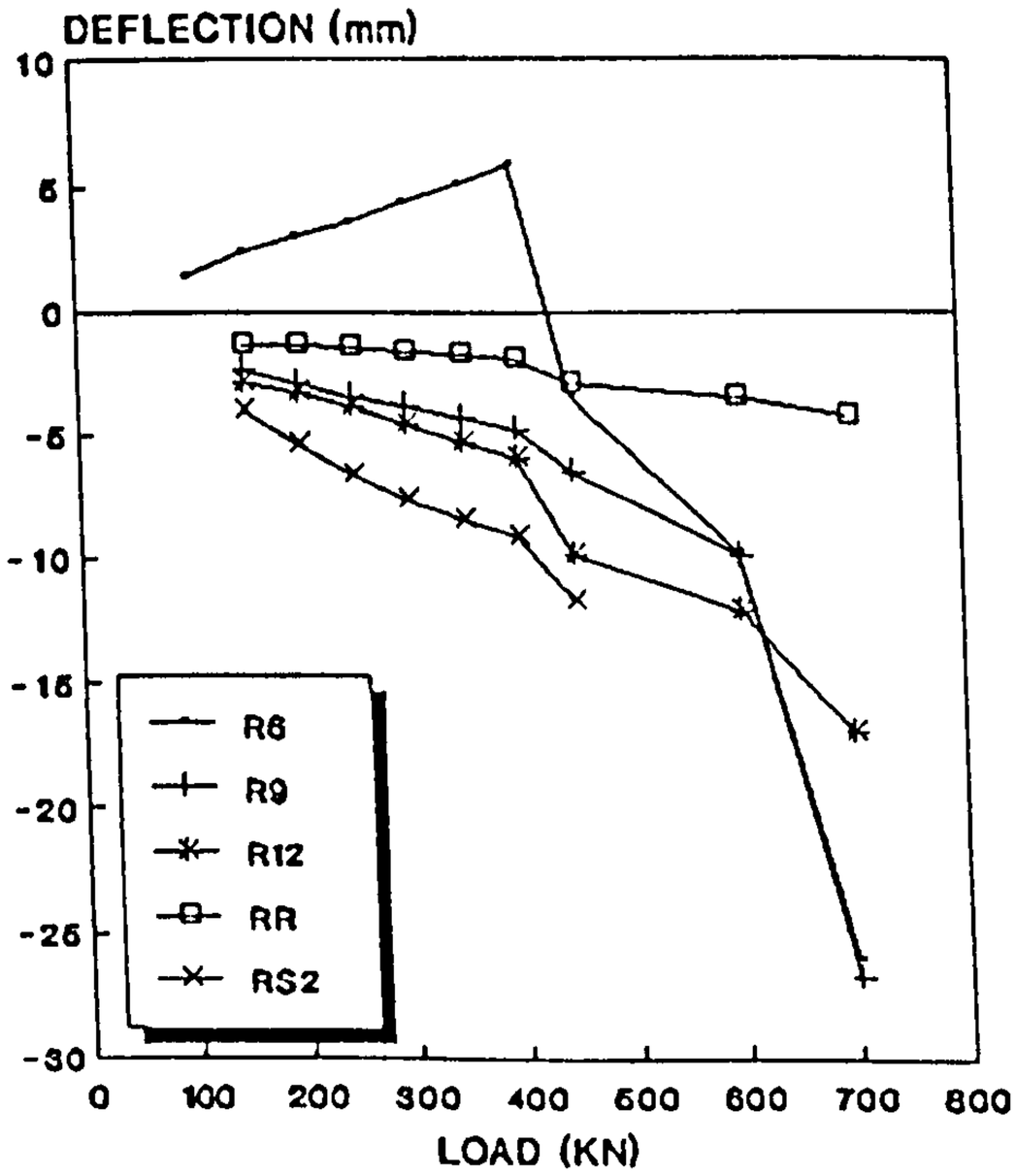

Fig.6.35: LOAD Vs DEFLECTION
At the Free Edge ,Point 9
Due to Loading P2-For M1

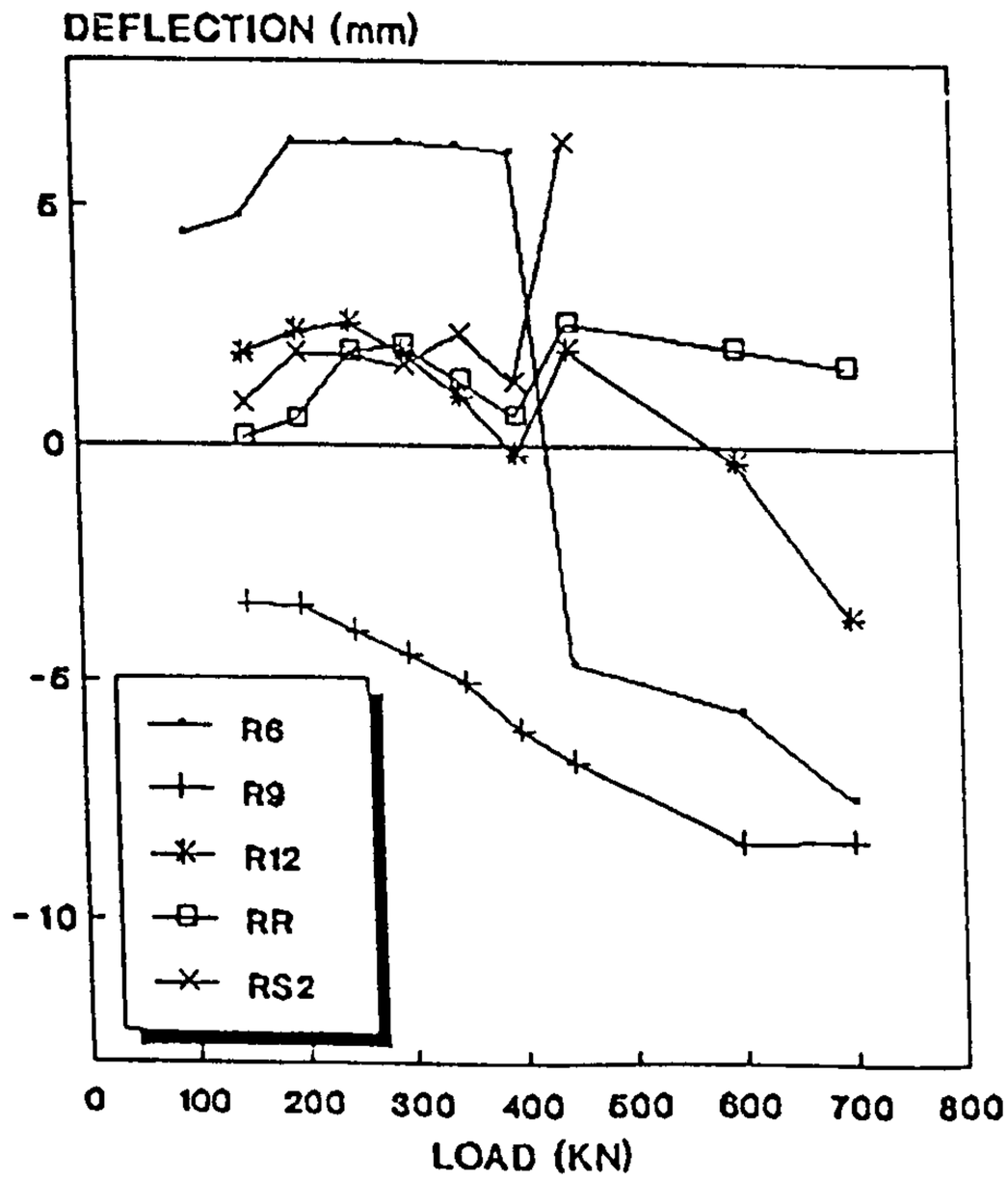

[For Test Rig Notations See Table 4.2 and Fig. 4.4]

Fig. 6.36: LOAD Vs DEFLECTION
Outer Loaded Area , Point 1
Due to loading P2- For M1

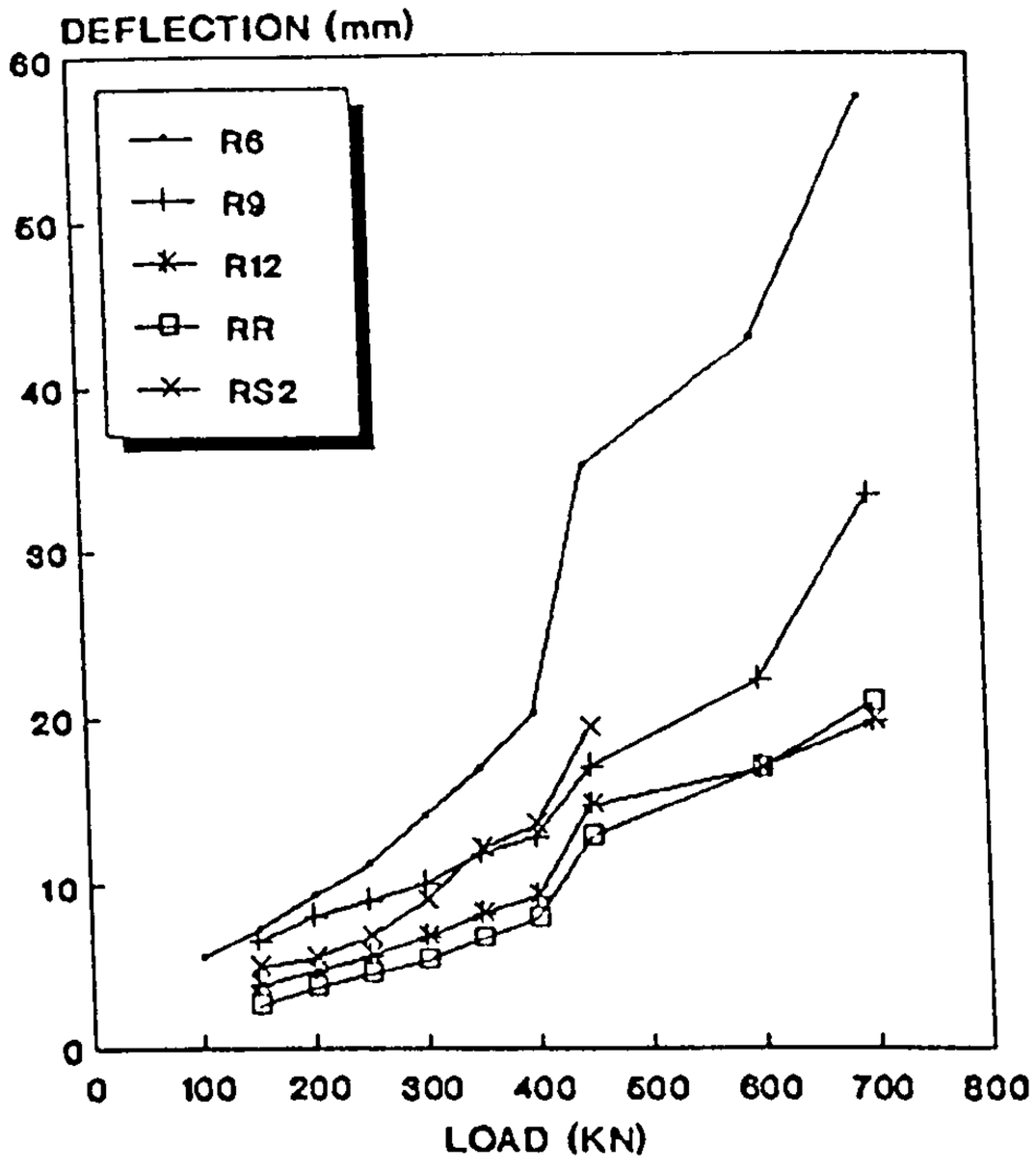

Fig. 6.37: LOAD Vs DEFLECTION
At the Free Edge , Point 2
Due to Loading P4-For M1

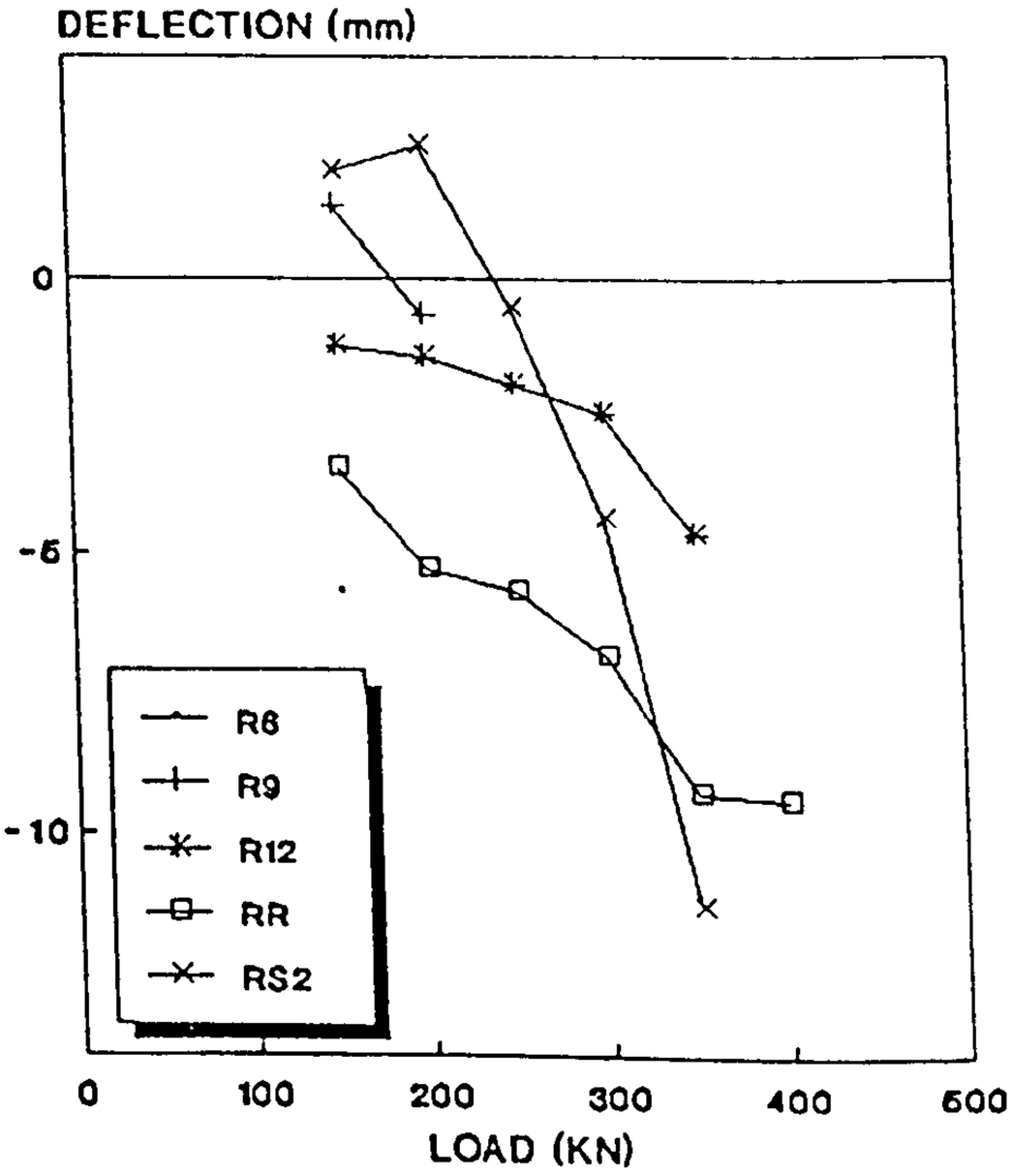

Fig.6.38: LOAD Vs DEFLECTION
At Middle of Tracking Load , Point 13
Due to Loading P1-For M2

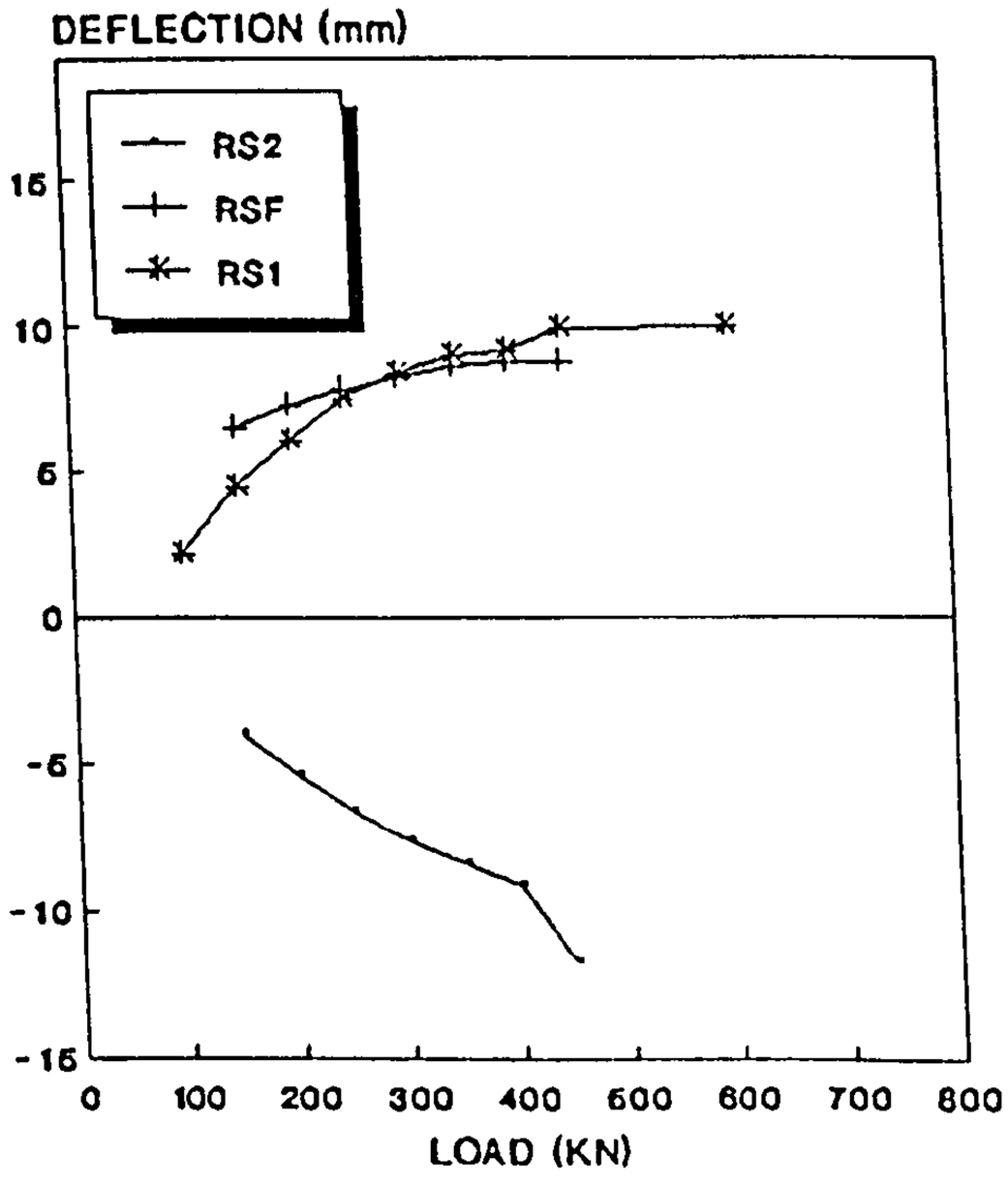

Fig.6.39: LOAD Vs DEFLECTION
At the Free Edge ,Point 15
Due to Loading P2-For M2

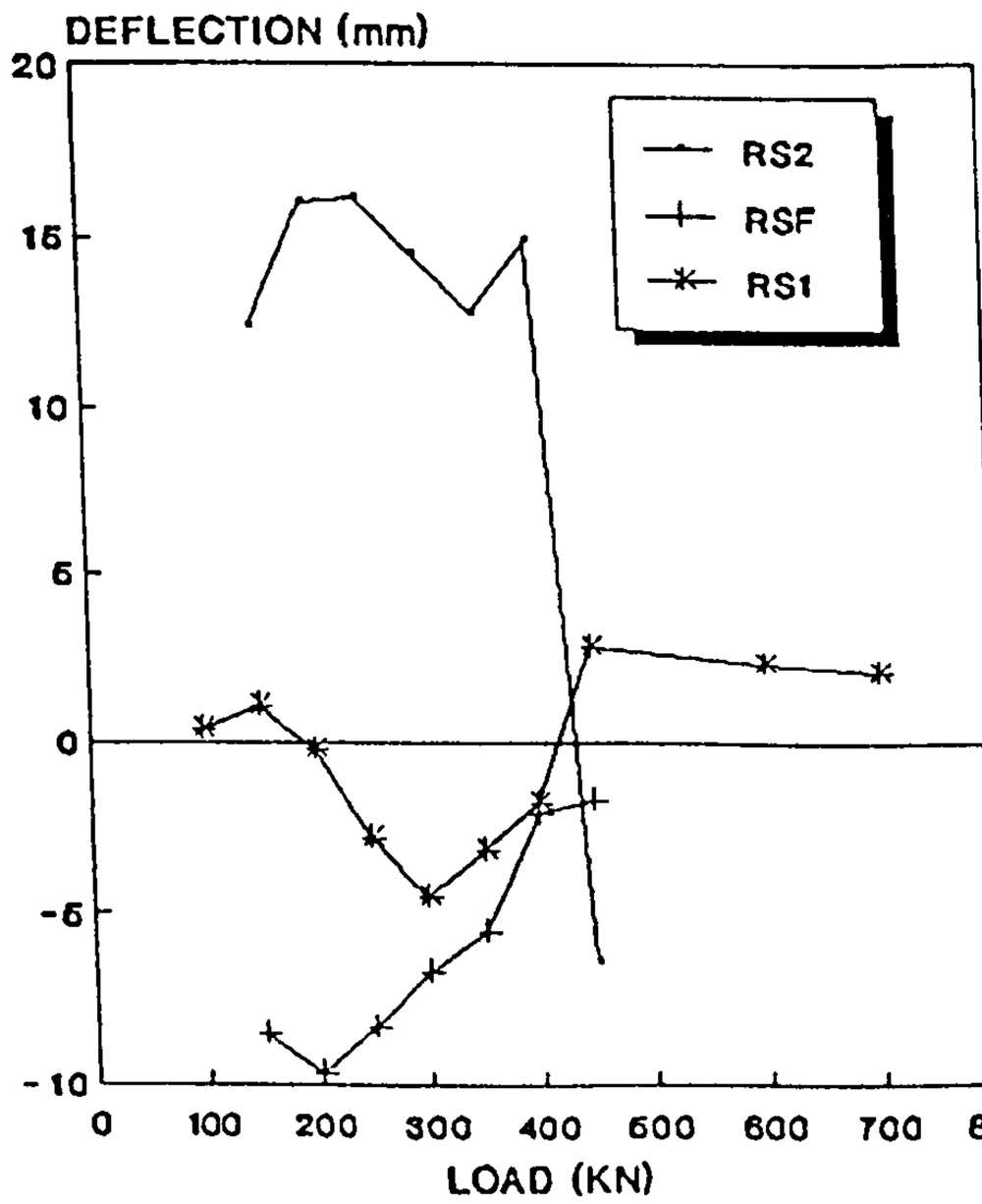

[For Test Rig Notations See Table 4.2 and Fig. 4.4]

Fig. 6.40: LOAD Vs DEFLECTION
Outer Loaded Area , Point 2
Due to loading P2- For M2

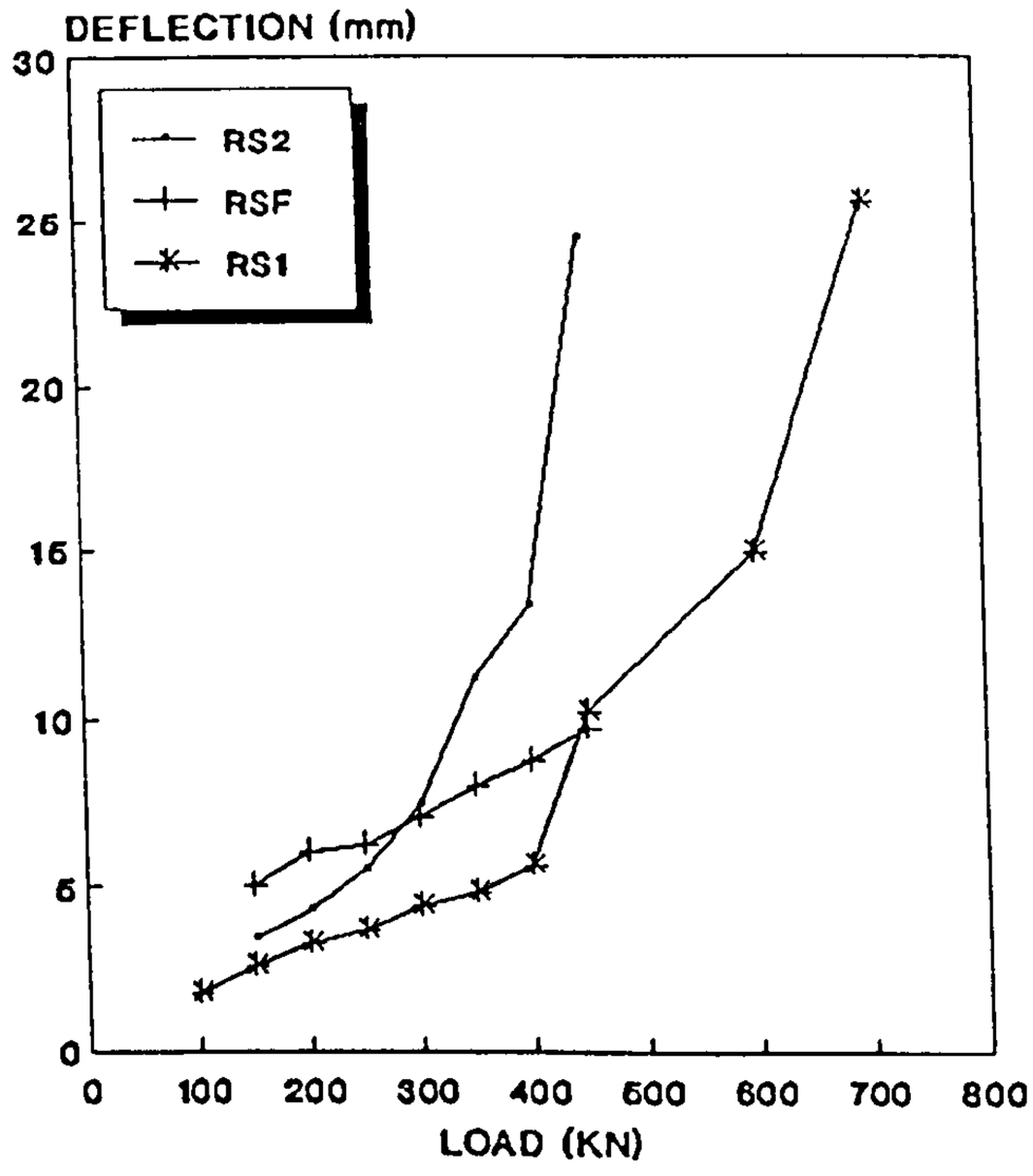

Fig. 6.41: LOAD Vs DEFLECTION
Free Corners, Point 1
Due to Loading P1-For M3

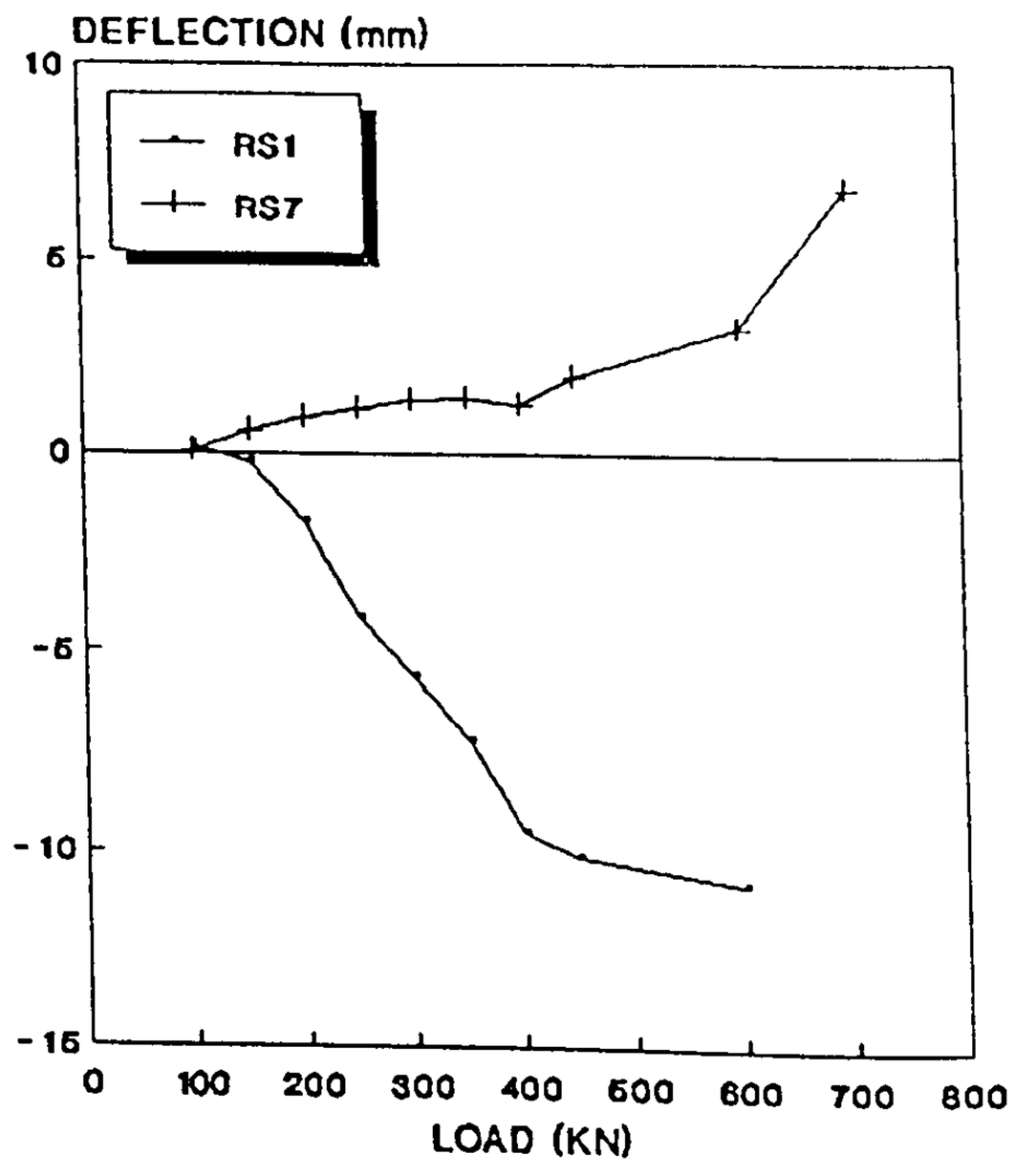

Fig.6.42: LOAD Vs DEFLECTION
Free Edge, Point 2
Due to Loading P4-For M3

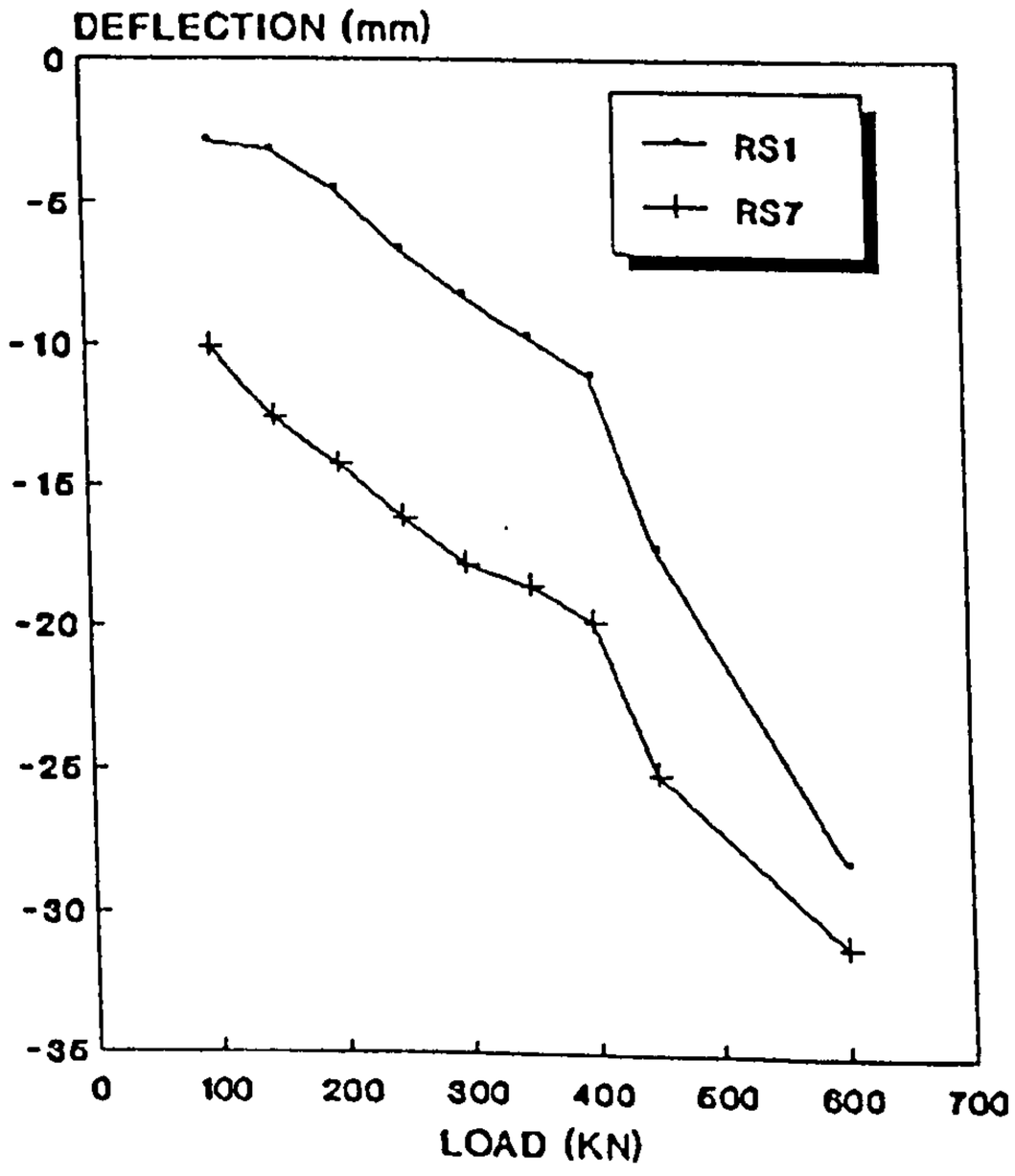

[For Test Rig Notations See Table 4.2 and Fig. 4.4]

Fig. 6.43: LOAD Vs DEFLECTION
Inner Loaded Area,Point 9
Due to Loading P4- For M3

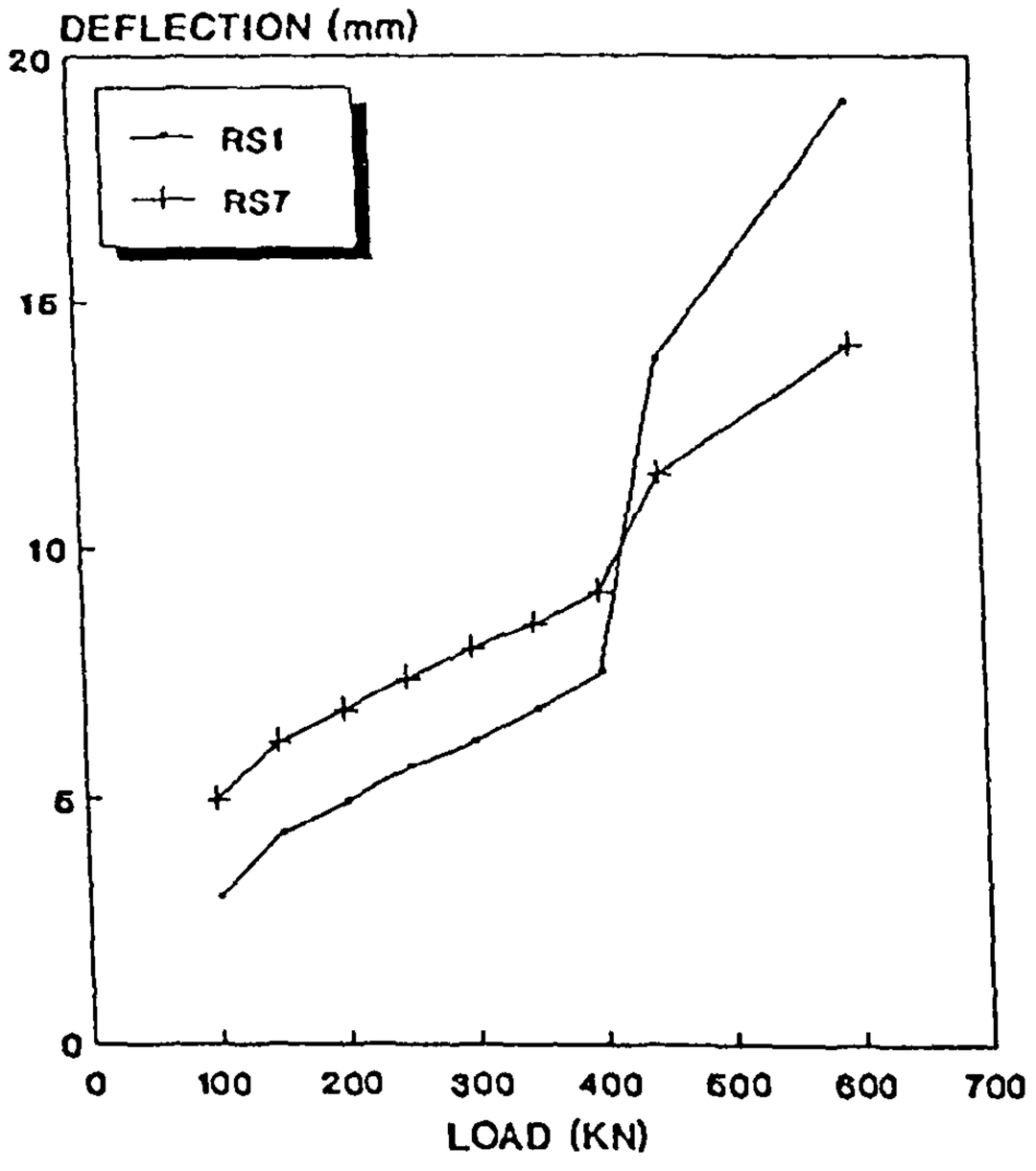

Fig. 6.44: LOAD Vs DEFLECTION
Out er Loaded Area, Point O
Due To Loading P1- For M3

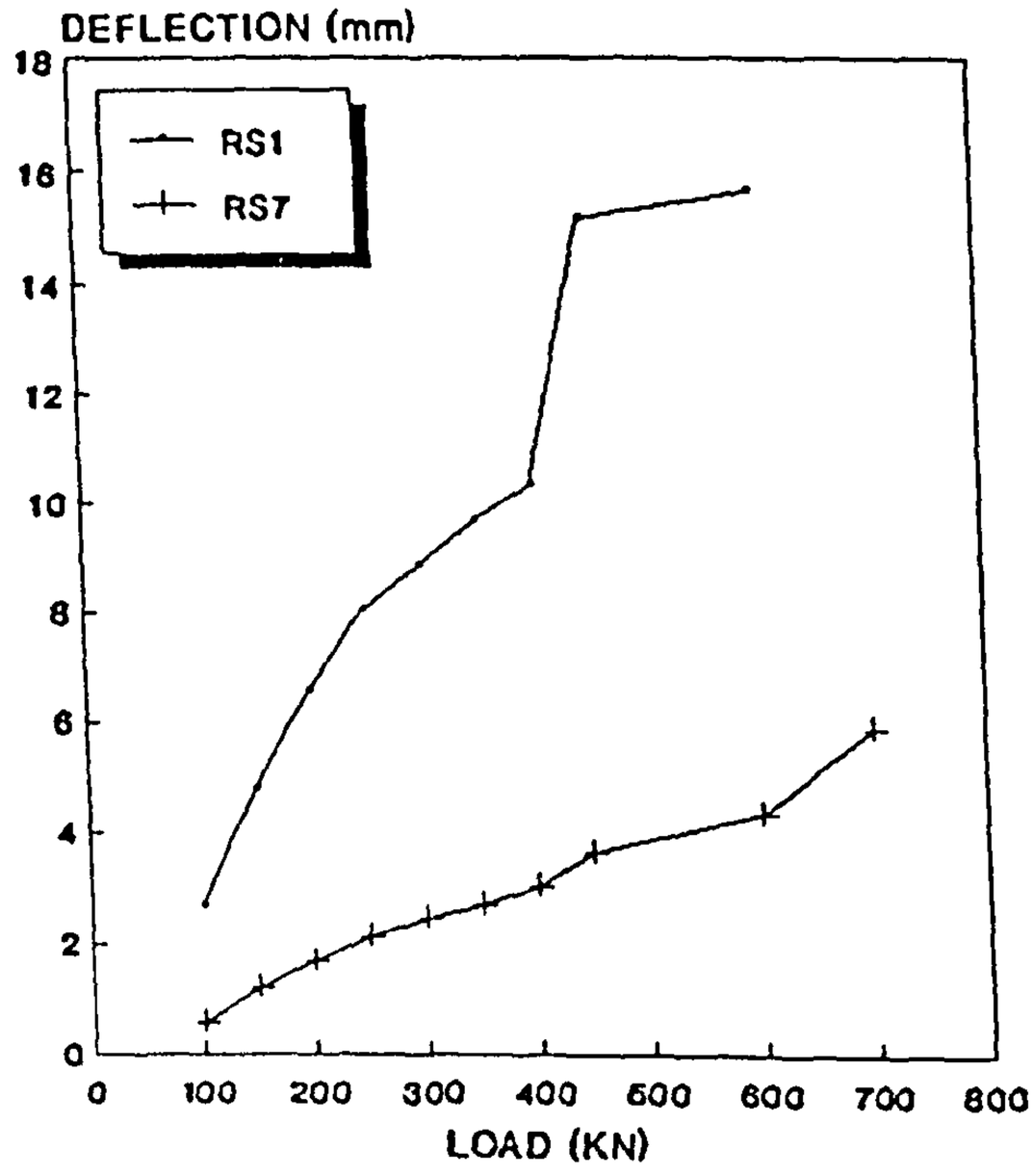

[For Test Rig Notations See Table 4.2 and Fig. 4.4]

$$N_{ed} = \frac{75\% \text{ of the observed load repetitions}}{\text{The predicted load repetions using Bull method}}$$

- P1/P3 are the same positions relative to the edge of a raft unit
- MODULE M1 represents the effect of plan dimensions of raft units.
- The design Charts included 25% F.O.S.

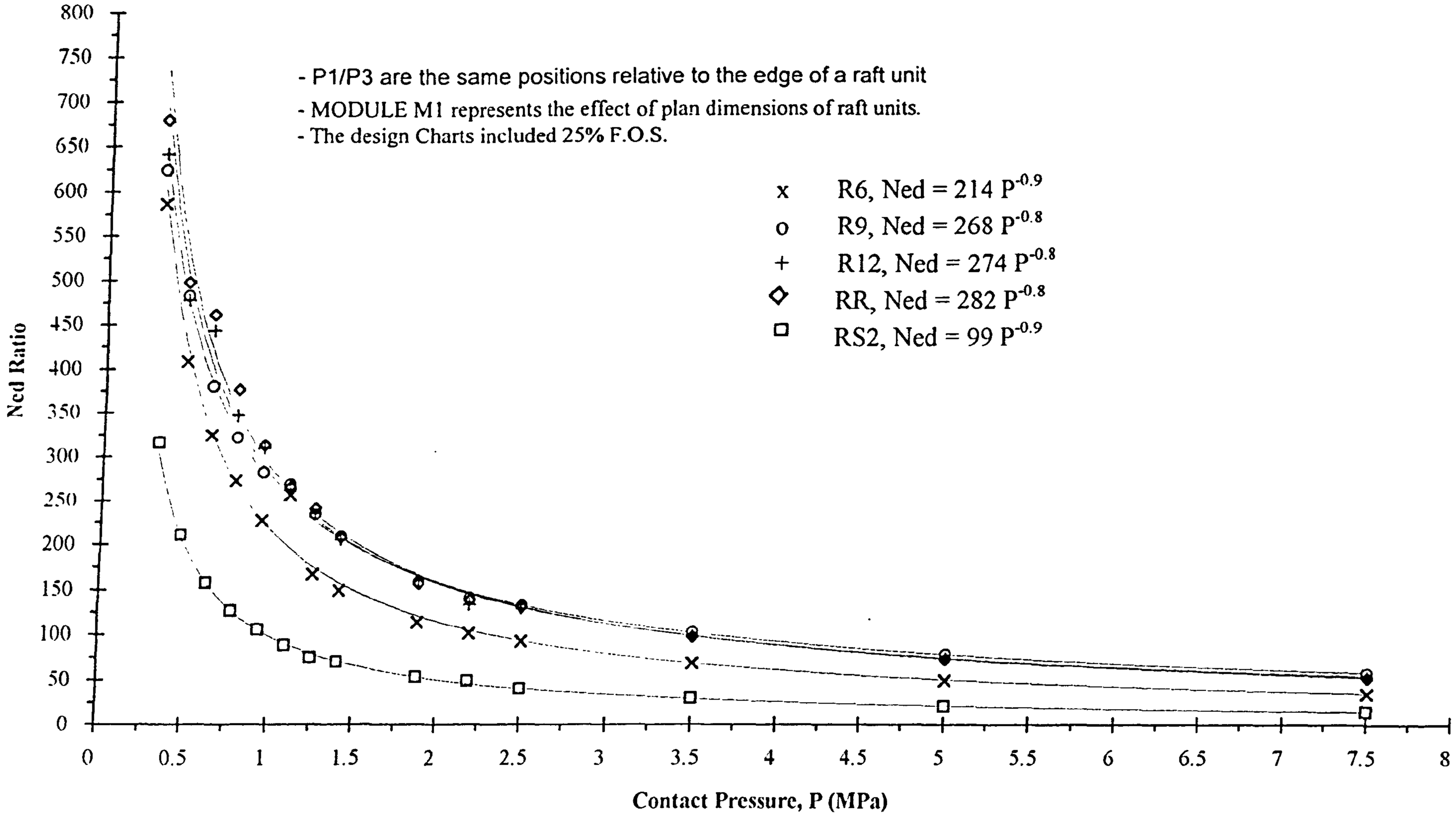

Fig.7.1: LOAD REPETITIONS RATIO **Vs** CONTACT PRESSURE FOR MODULE M1 AT LOADING POSITIONS P1/P3

$$N_{ed} = \frac{\text{75\% of the observed load repetitions using Bull method}}{\text{The predicted load repetions using Bull method}}$$

- MODULE M1 represents the effect of plan dimensions of raft units.
- The design Charts included 25% F.O.S.

x R6, Ned = 16.7 $P^{-1.1}$
o R9, Ned = 16.3 $P^{-1.1}$
\+ R12, Ned = 13 $P^{-1.1}$
◇ RR, Ned = 4.2 $P^{-1.1}$
□ RS2, Ned = 3.4 $P^{-0.99}$

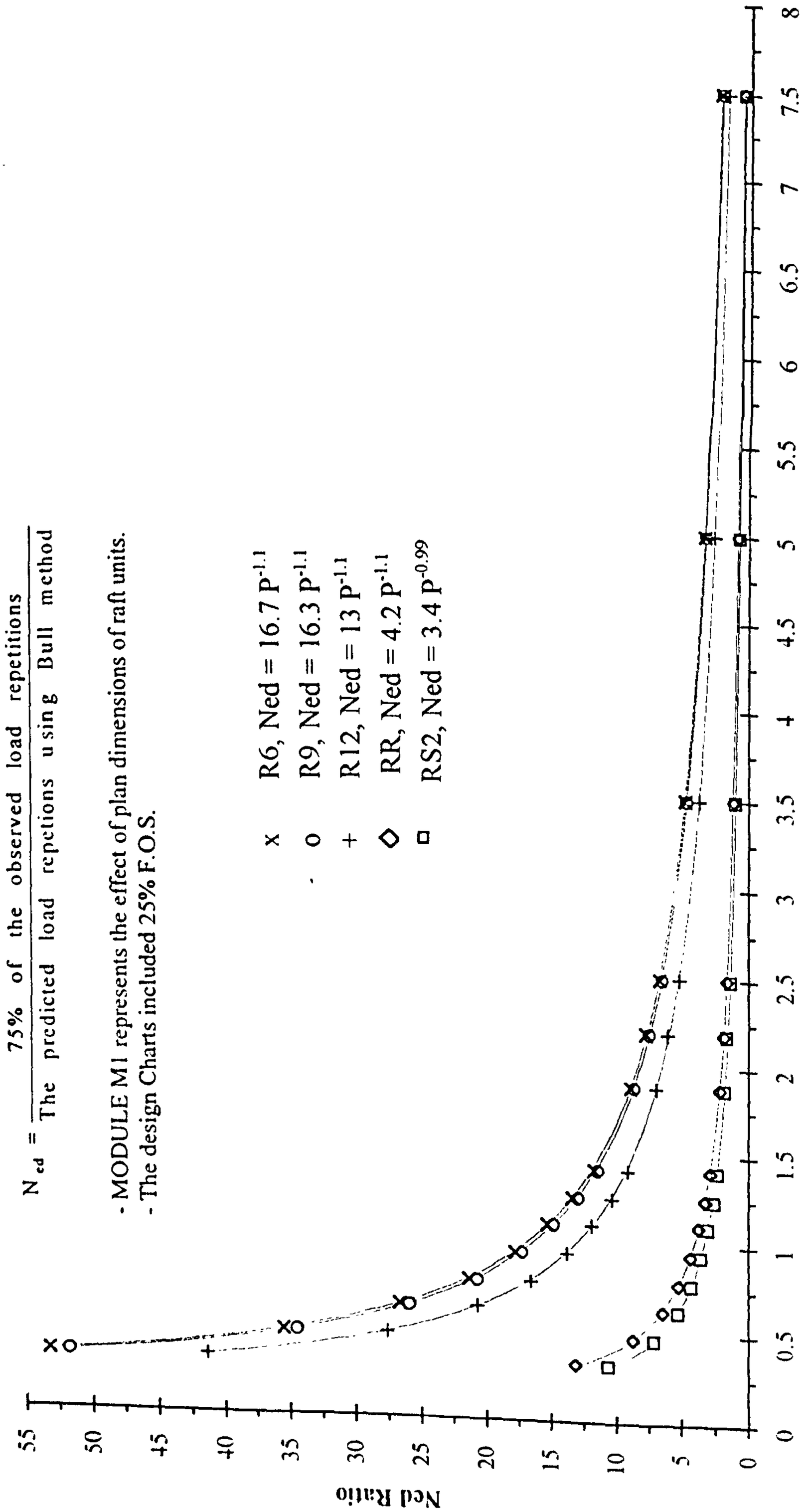

Fig.7.2: LOAD REPETITIONS RATIO Vs CONTACT PRESSURE FOR MODULE M1 AT LOADING POSITION P2

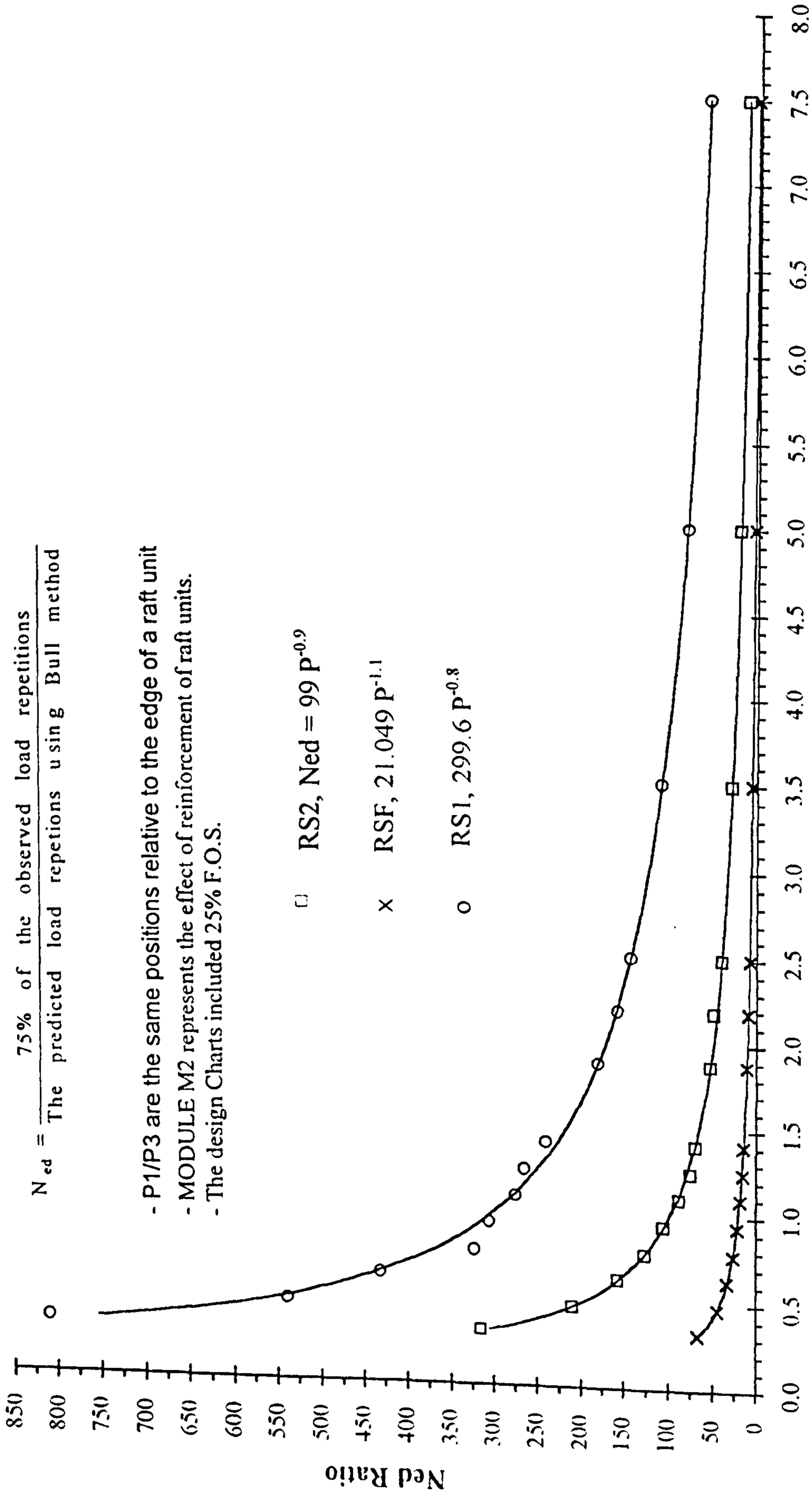

Fig.7.3: LOAD REPETITIONS RATIO Vs CONTACT PRESSURE FOR MODULE M2 AT LOAD POSITIONS P1/P3

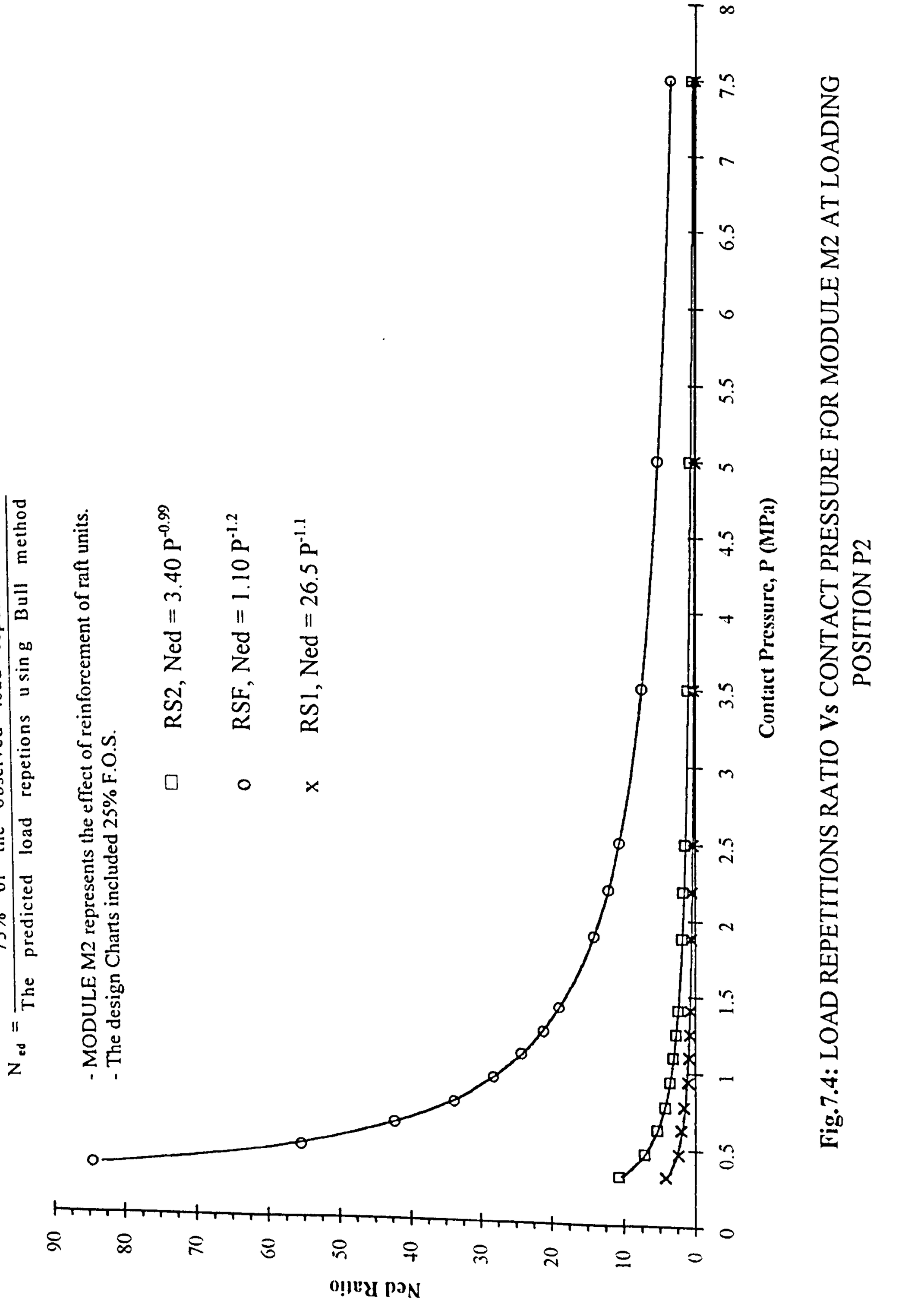

Fig.7.4: LOAD REPETITIONS RATIO Vs CONTACT PRESSURE FOR MODULE M2 AT LOADING POSITION P2

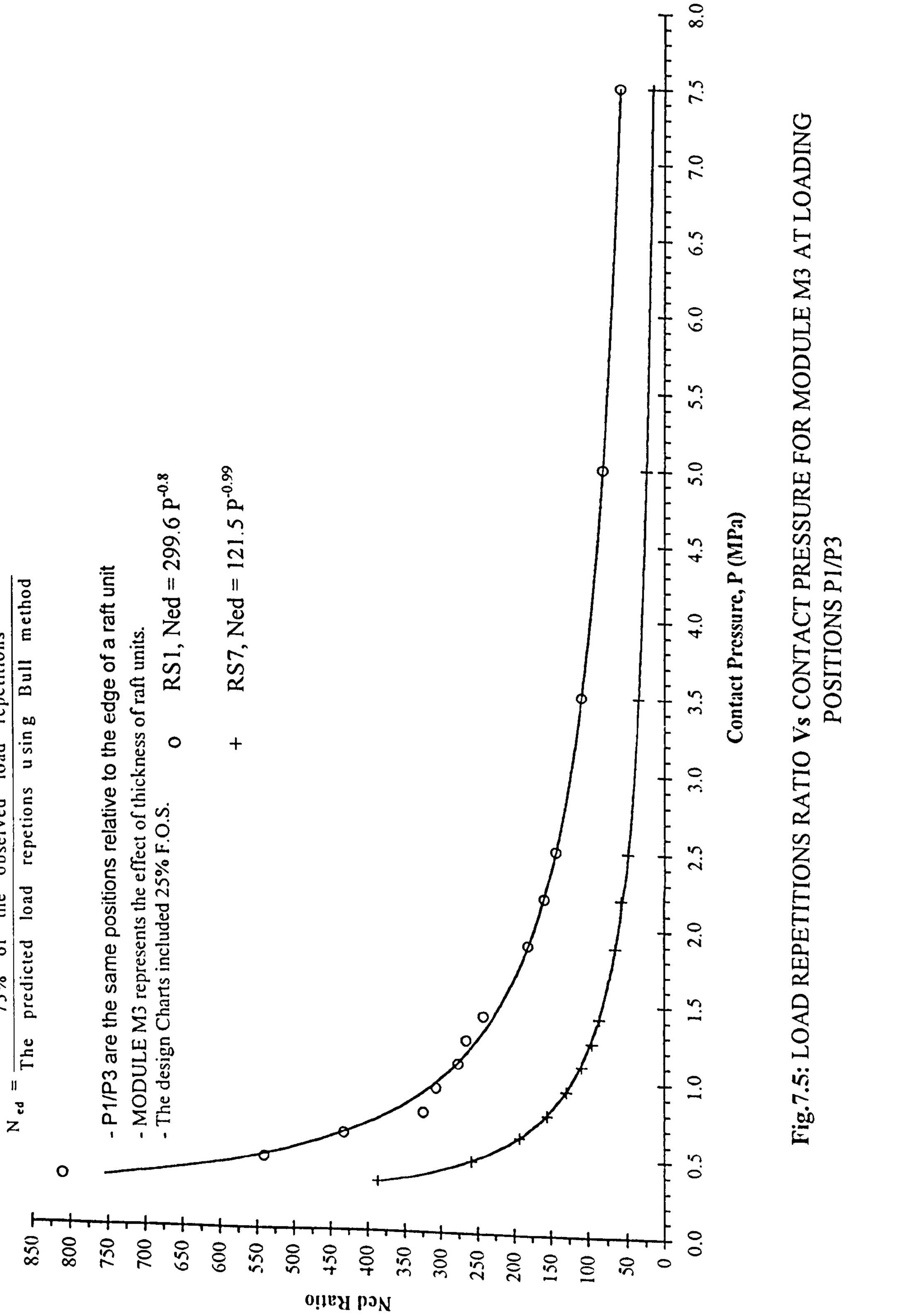

Fig.7.5: LOAD REPETITIONS RATIO Vs CONTACT PRESSURE FOR MODULE M3 AT LOCATIONS P1/P3

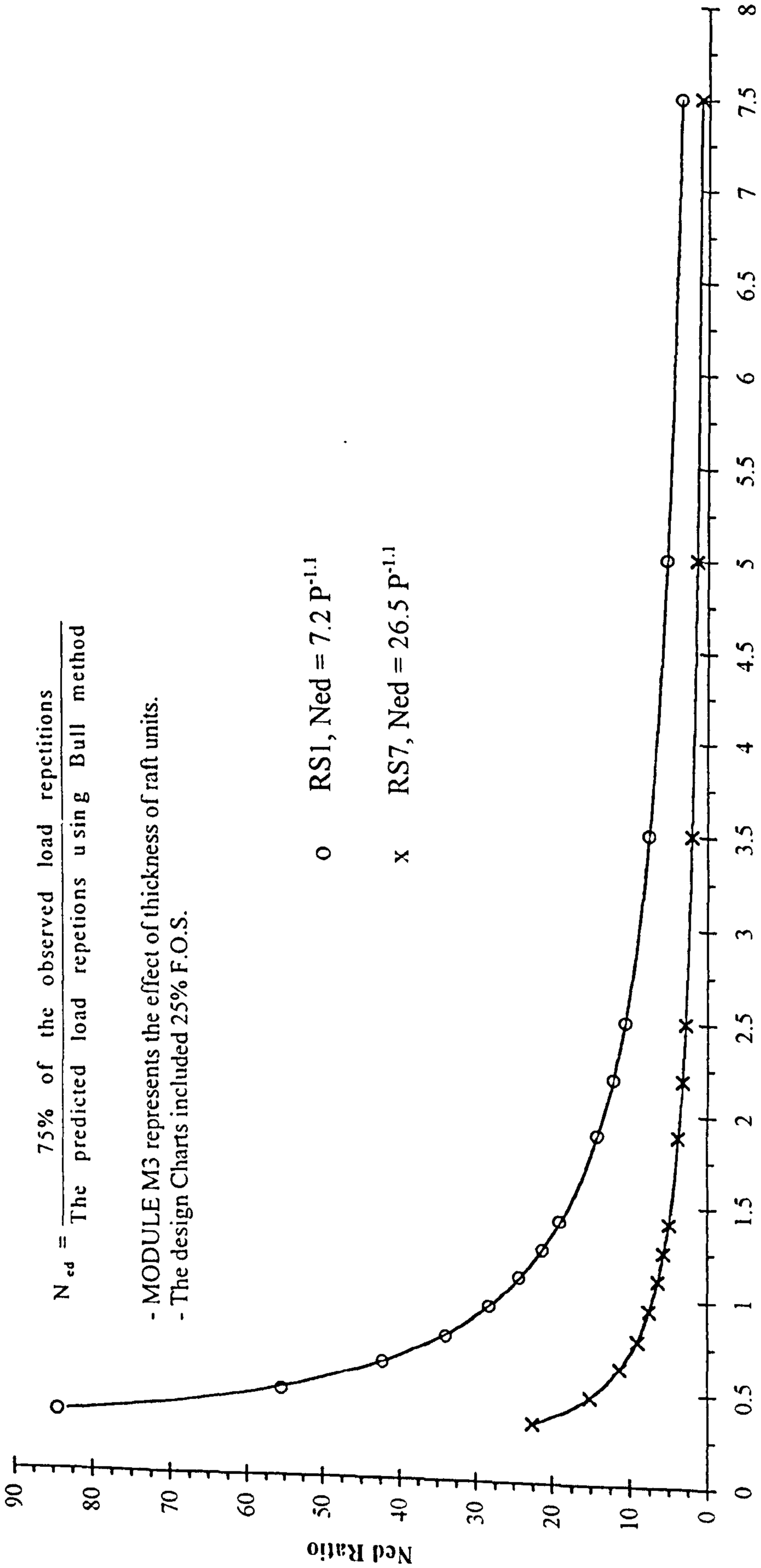

Fig.7.6: LOAD REPETITIONS RATIO Vs CONTACT PRESSURE FOR MODULE M3 AT LOADING POSITION P2

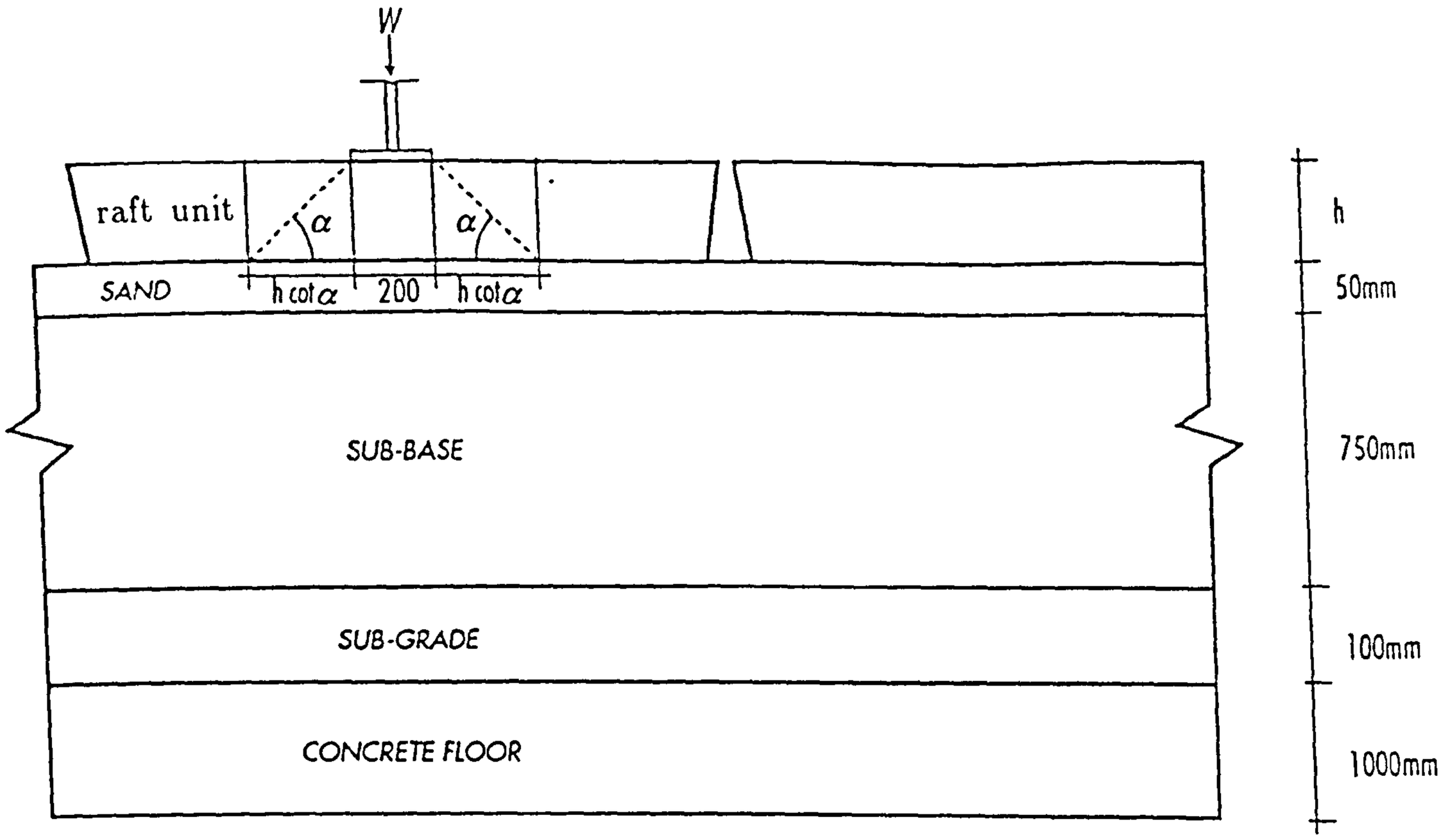

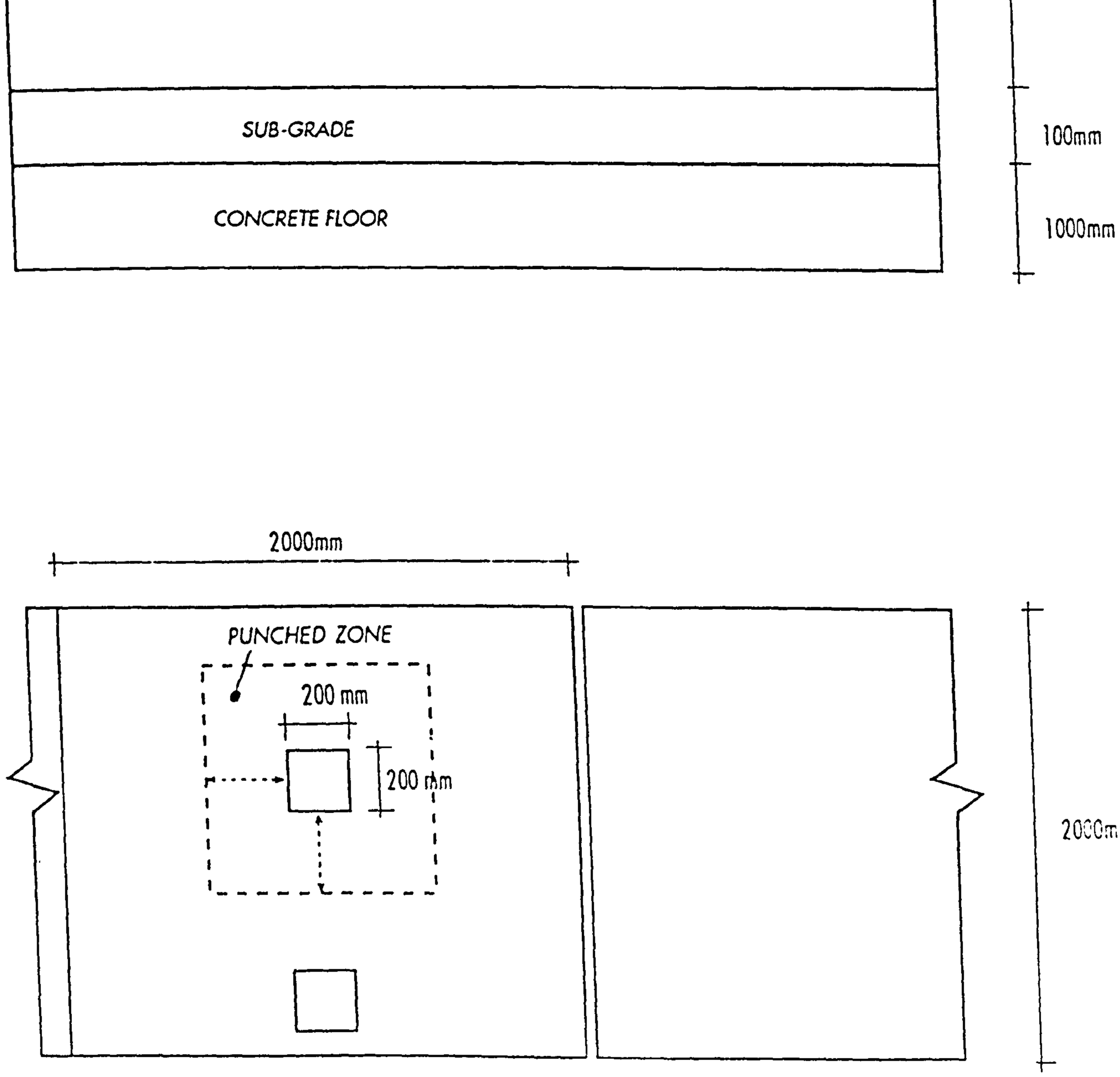

Fig.7.7: Critical Perimeter for Punching Shear

$R = \varepsilon_n / \varepsilon_{450}$,where ε_n is the induced strain on the side of the raft below the loading beam at one third of the thickness from the base due to load n.

- Neq=The number of load cycles that is needed to cause failure for a range of load from 100 kN to 700 kN
- MODULE M1 represents the effect of plan dimensions of raft units.
- The design Charts included 25% F.O.S.

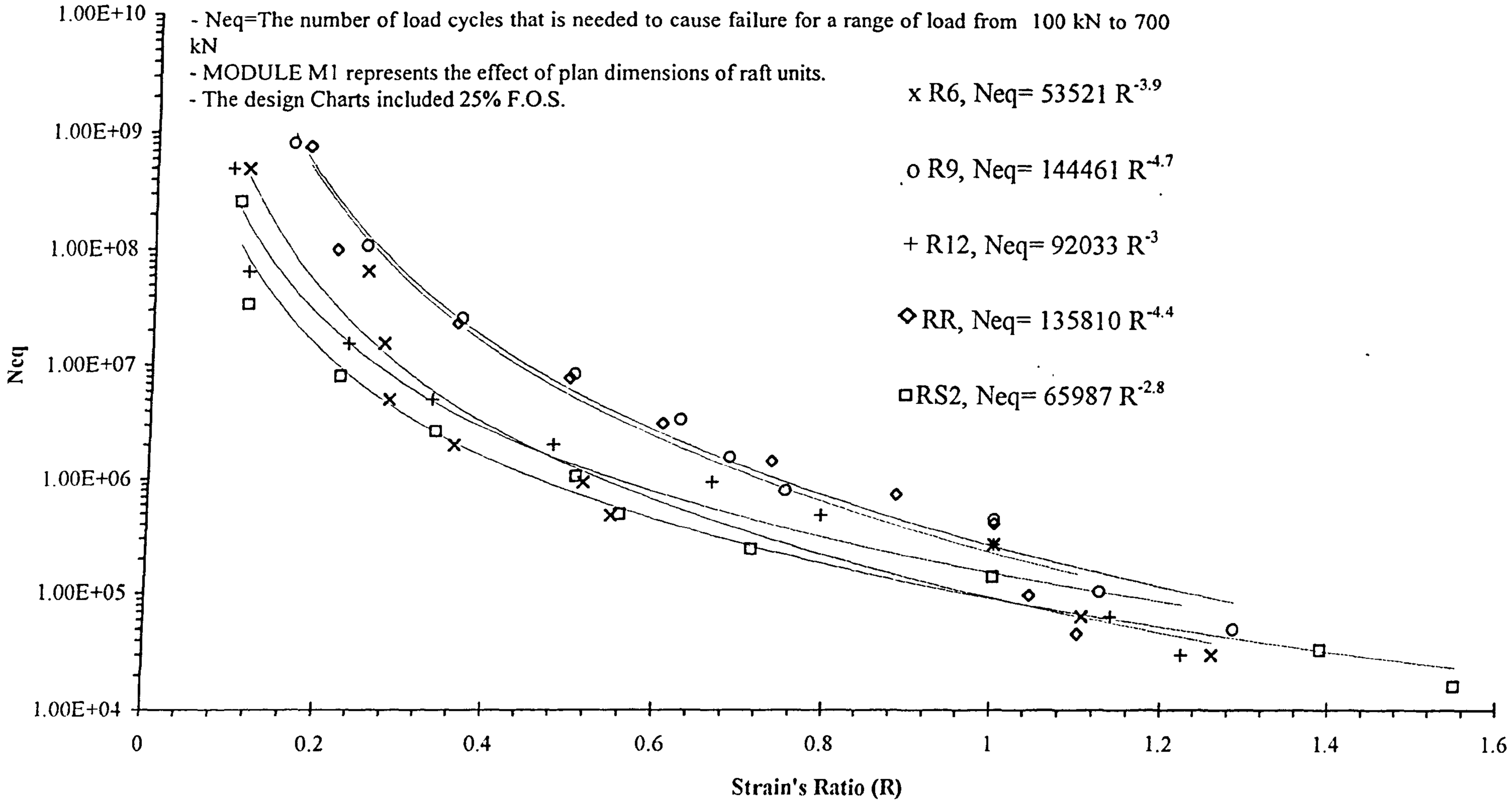

Fig.7.8: Equivalent Number of Load Repetitions **Vs** Strain's Ratio (R) for Module M1

$R = \varepsilon_n / \varepsilon_{450}$,where ε_n is the induced strain on the side of the raft below the loading beam at one third of the thickness from the base due to load n.

- Neq=The number of load cycles that is needed to cause failure for a range of load from 100 kN to 700 kN
- MODULE M2 represents the effect of reinforcement of raft units.
- The design Charts included 25% F.O.S.

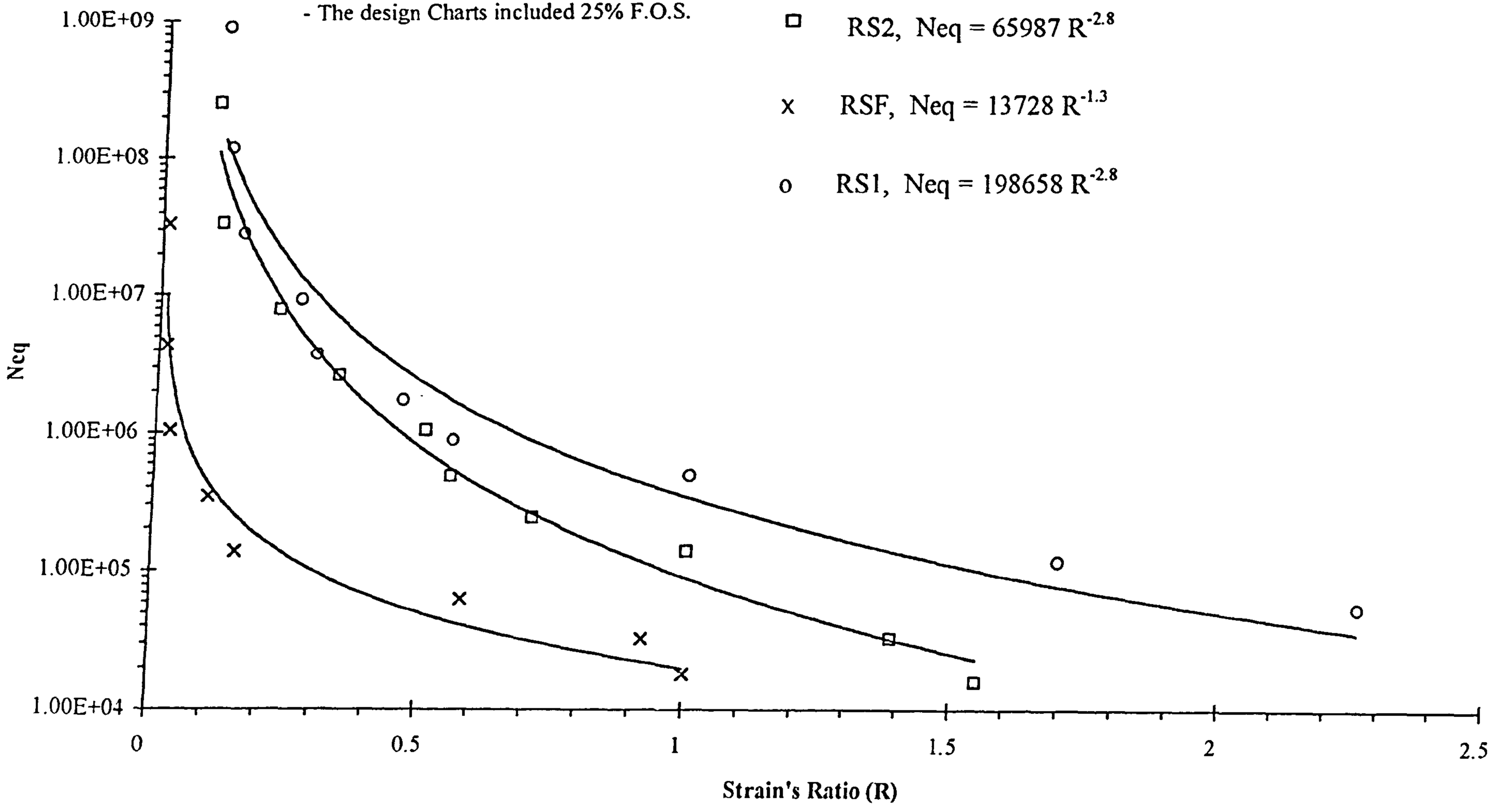

Fig.7.9: Equivalent Number of Load Repetitions **Vs** Strain's Ratio (R) for Module M2

$R = \varepsilon_n / \varepsilon_{450}$,where ε_n is the induced strain on the side of the raft below the loading beam at one third of the thickness from the base due to load n.

- Neq=The number of load cycles that is needed to cause failure for a range of load from 100 kN to 700 kN
- MODULE M3 represents the effect of thickness of raft units.
- The design Charts included 25% F.O.S.

o RS1, $Neq = 198658\ R^{-2.8}$

x RS7, $Neq = 671885\ R^{-2.7}$

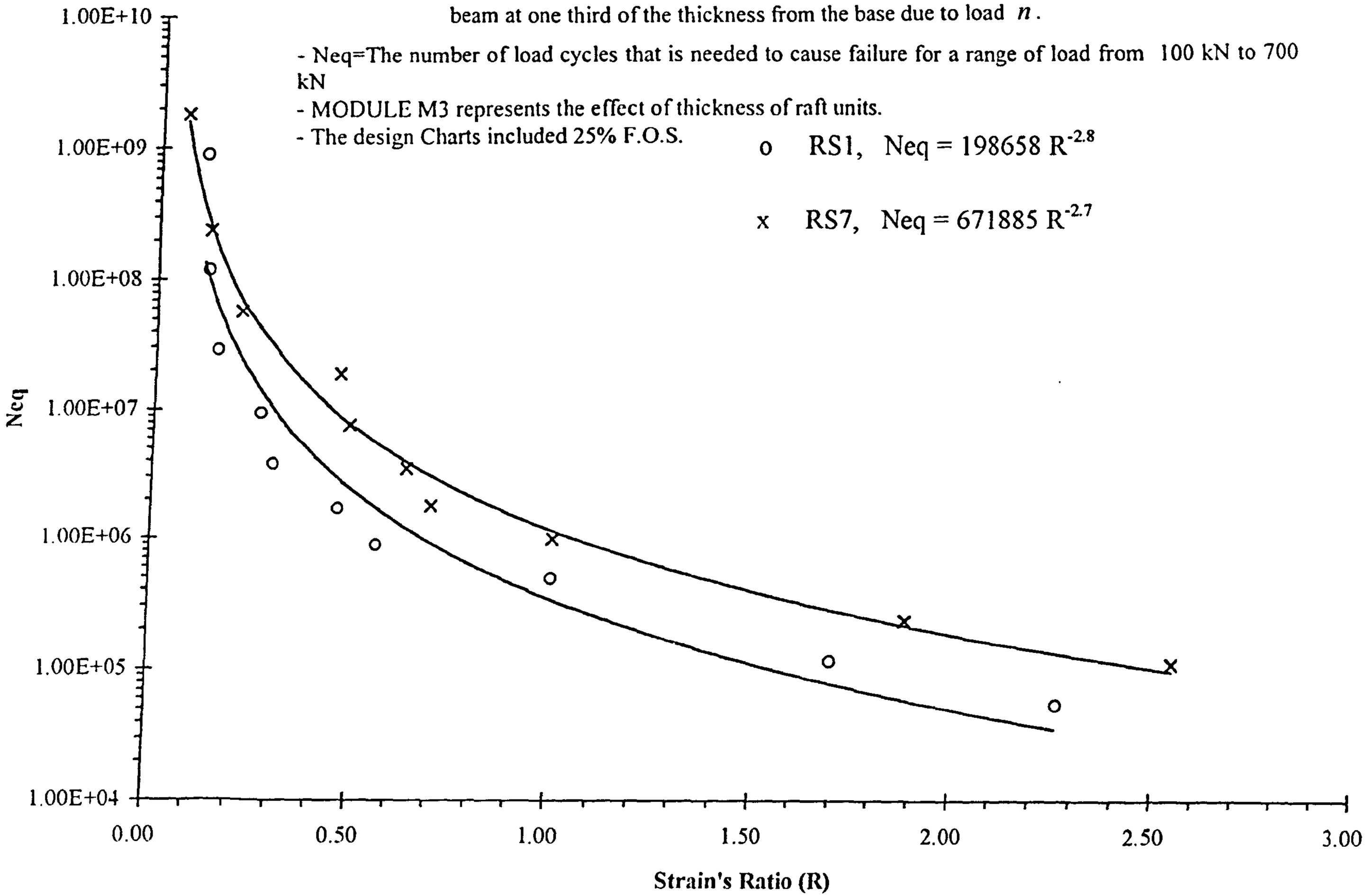

Fig.7.10: Equivalent Number of Load Repetitions **Vs** Strain's Ratio (R) for Module M3

$R = \varepsilon_n / \varepsilon_{450}$,where ε_n is the induced strain on the side of the raft below the loading beam at one third of the thickness from the base due to load n.

- N_{acc} = The number of load cycles with each set of points to failure representing the applied load [from 100 kN to 700kN] that converted to equivalent design load of 450kN
- MODULE M1 represents the effect of plan dimensions of raft units.
- The design Charts included 25% F.O.S.

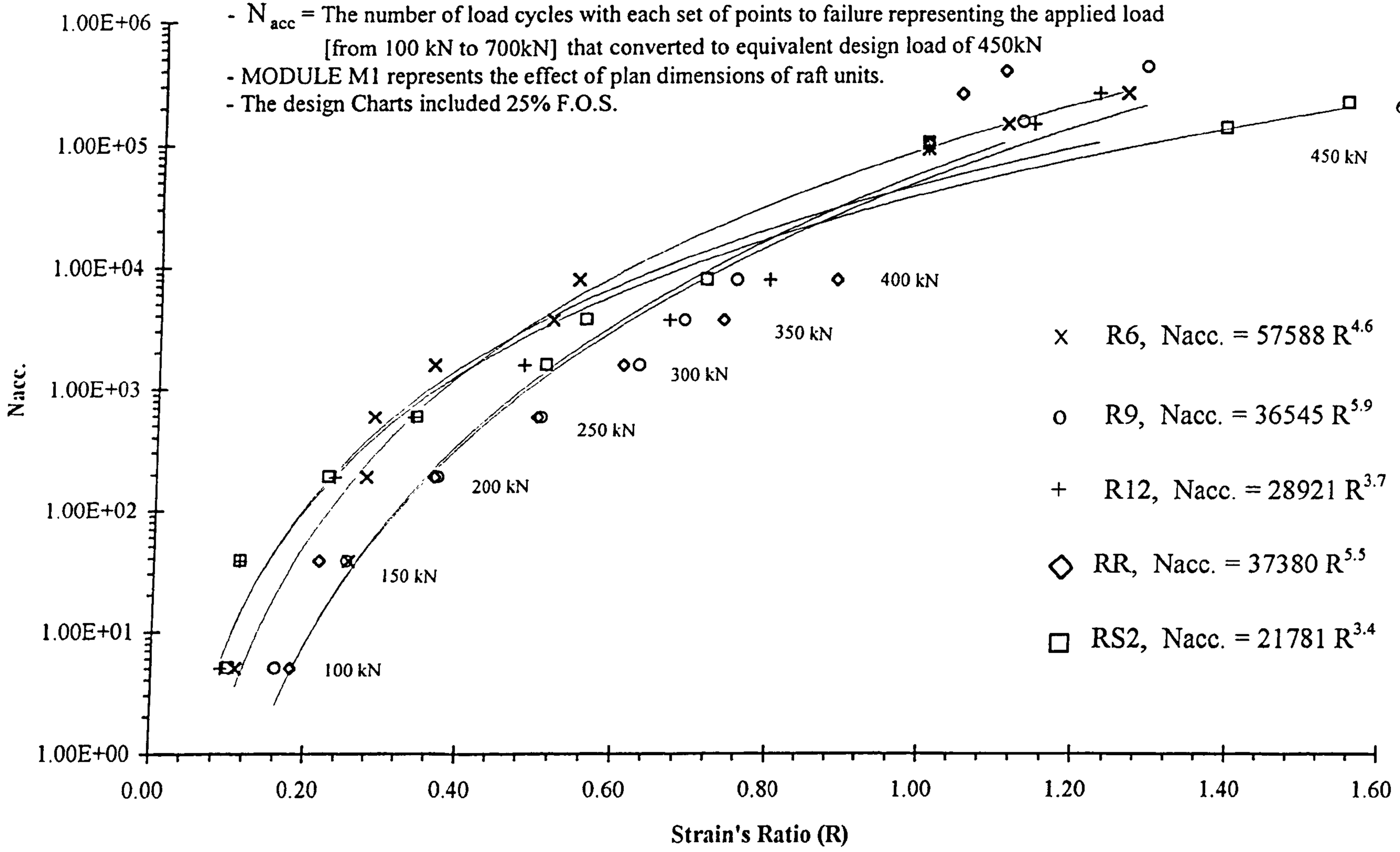

Fig.7.11: Accumulated Number of Load Repetitions **Vs** Strain's Ratio (R) for Module M1

$R = \varepsilon_n / \varepsilon_{450}$,where ε_n is the induced strain on the side of the raft below the loading beam at one third of the thickness from the base due to load n.

- N_{acc} = The number of load cycles with each set of points to failure representing the applied load [from 100 kN to 700kN] that converted to equivalent design load of 450kN
- MODULE M2 represents the effect of reinforcement of raft units.
- The design Charts included 25% F.O.S.

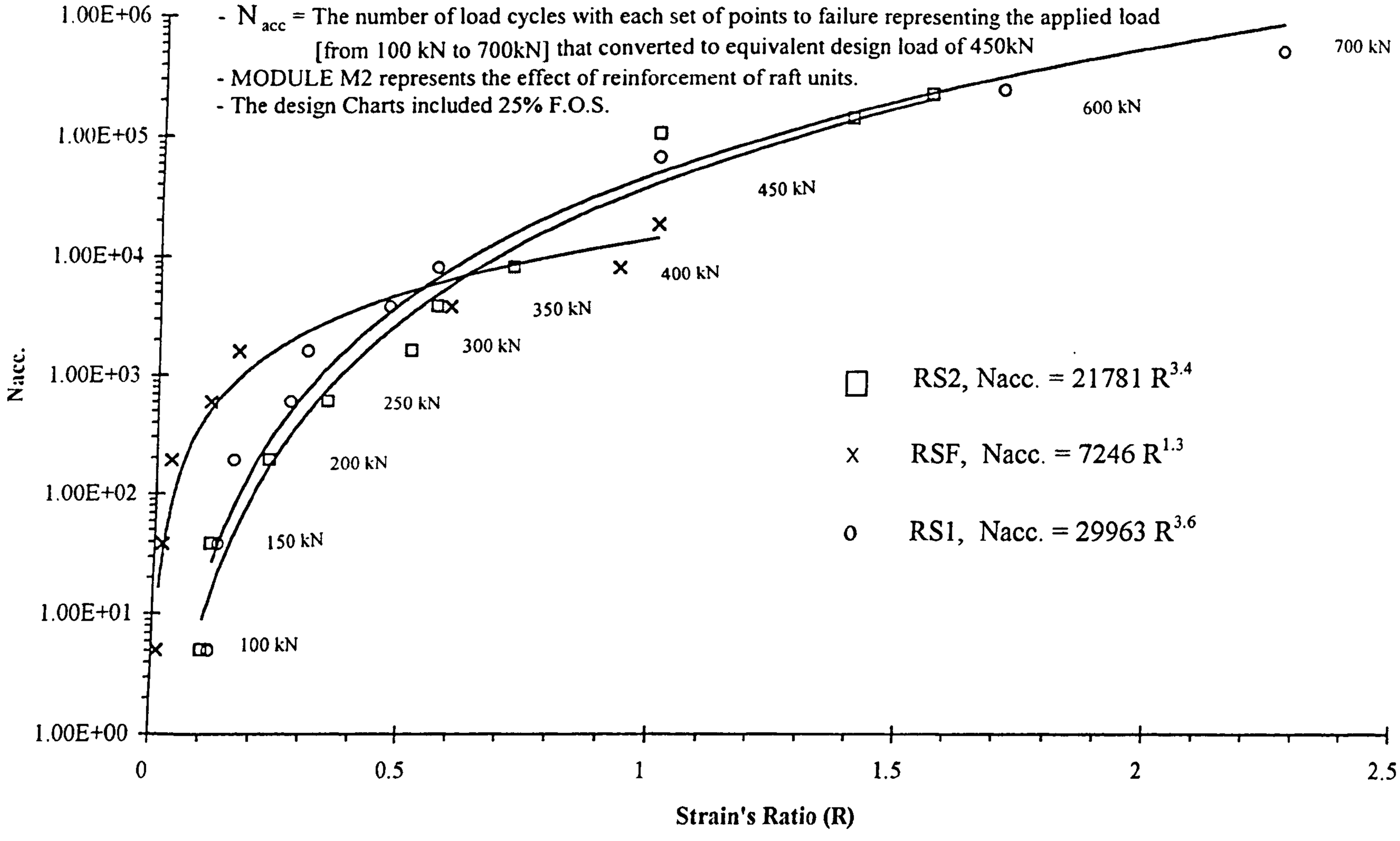

Fig.7.12: Accumulated Number of Load Repetitions **Vs** Strain's Ratio (R) for Module M2

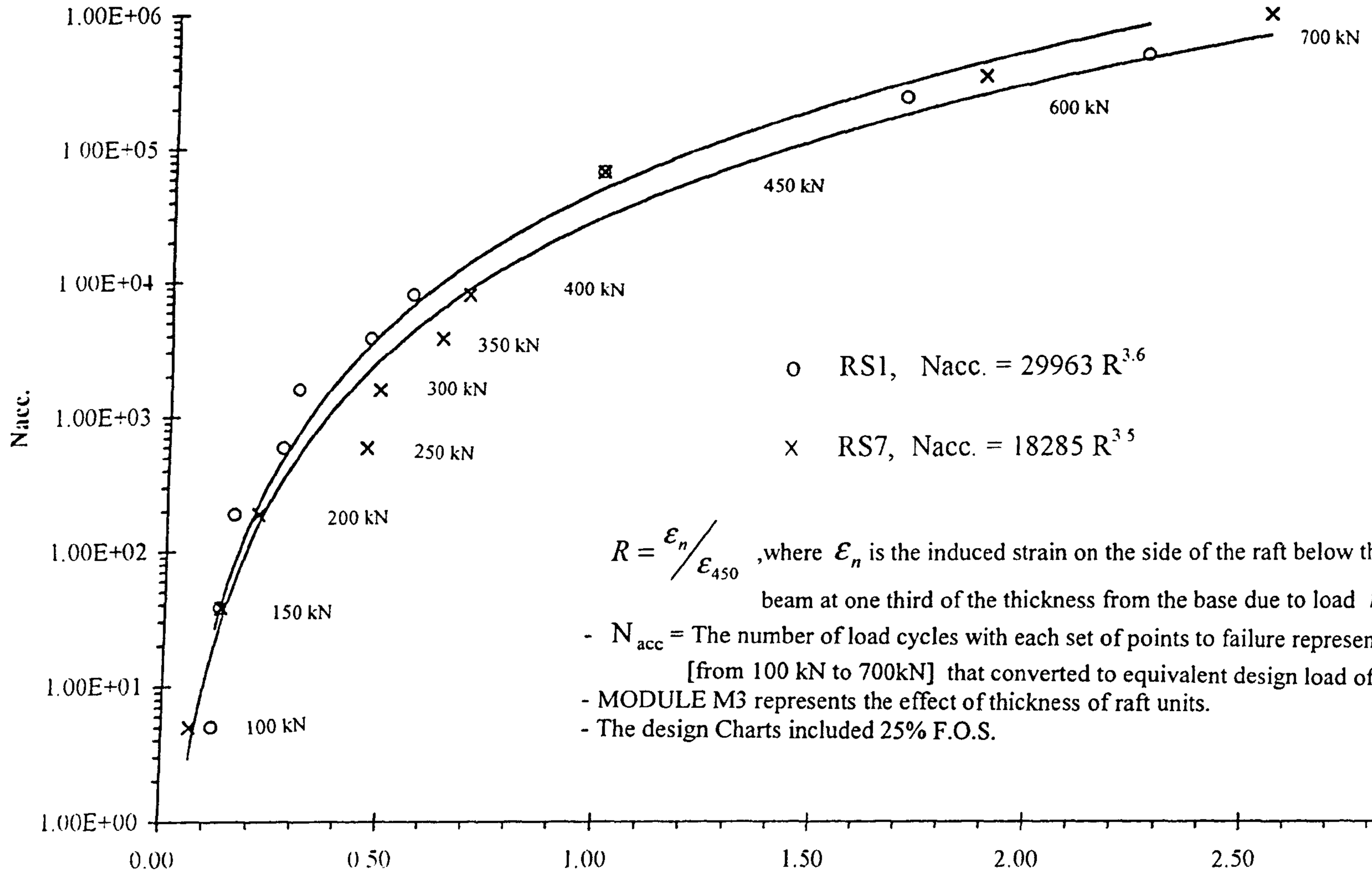

Fig.7.13: Accumulated Number of Load Repetitions Vs Strain's Ratio (R) for Module M3

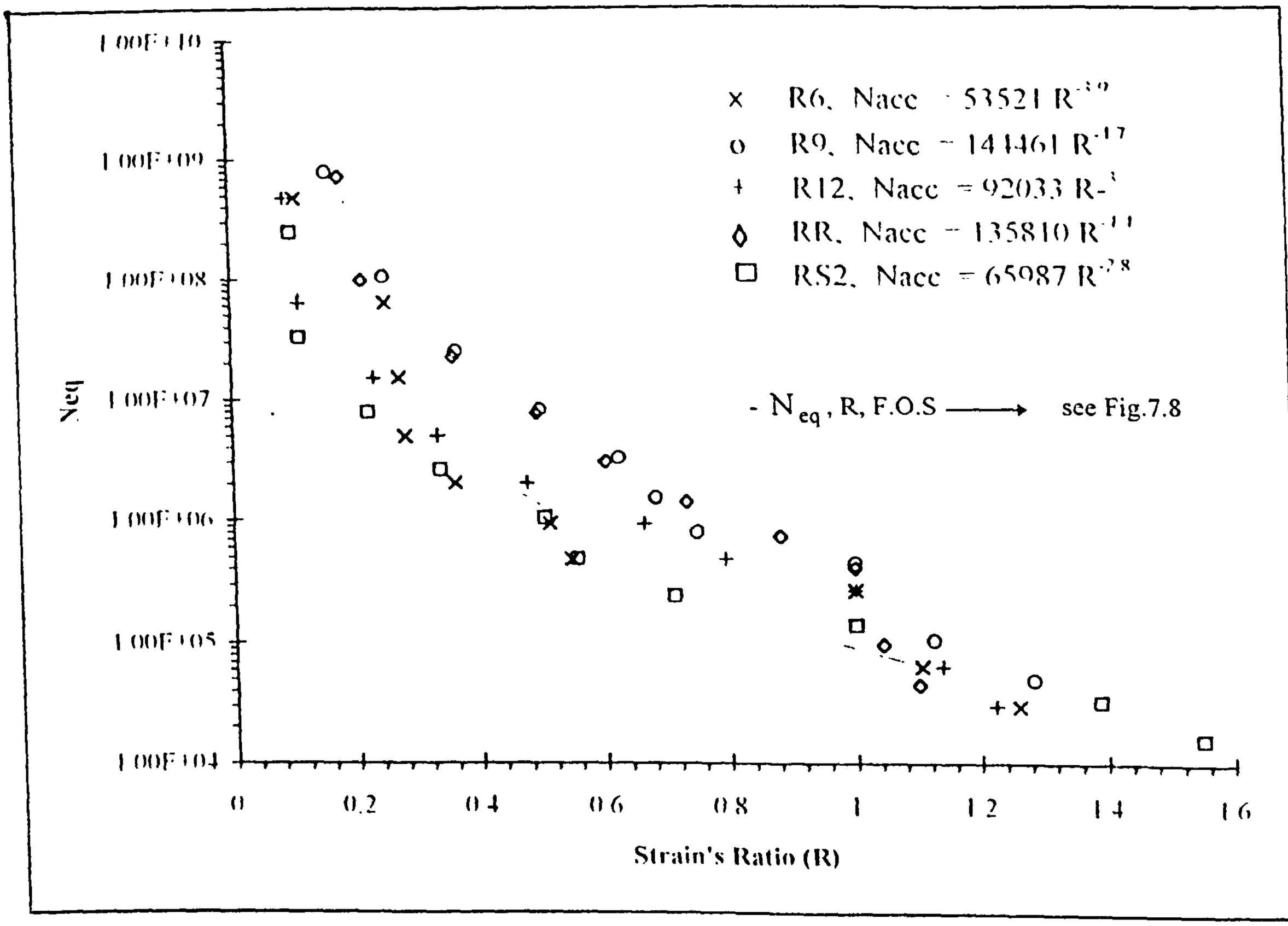

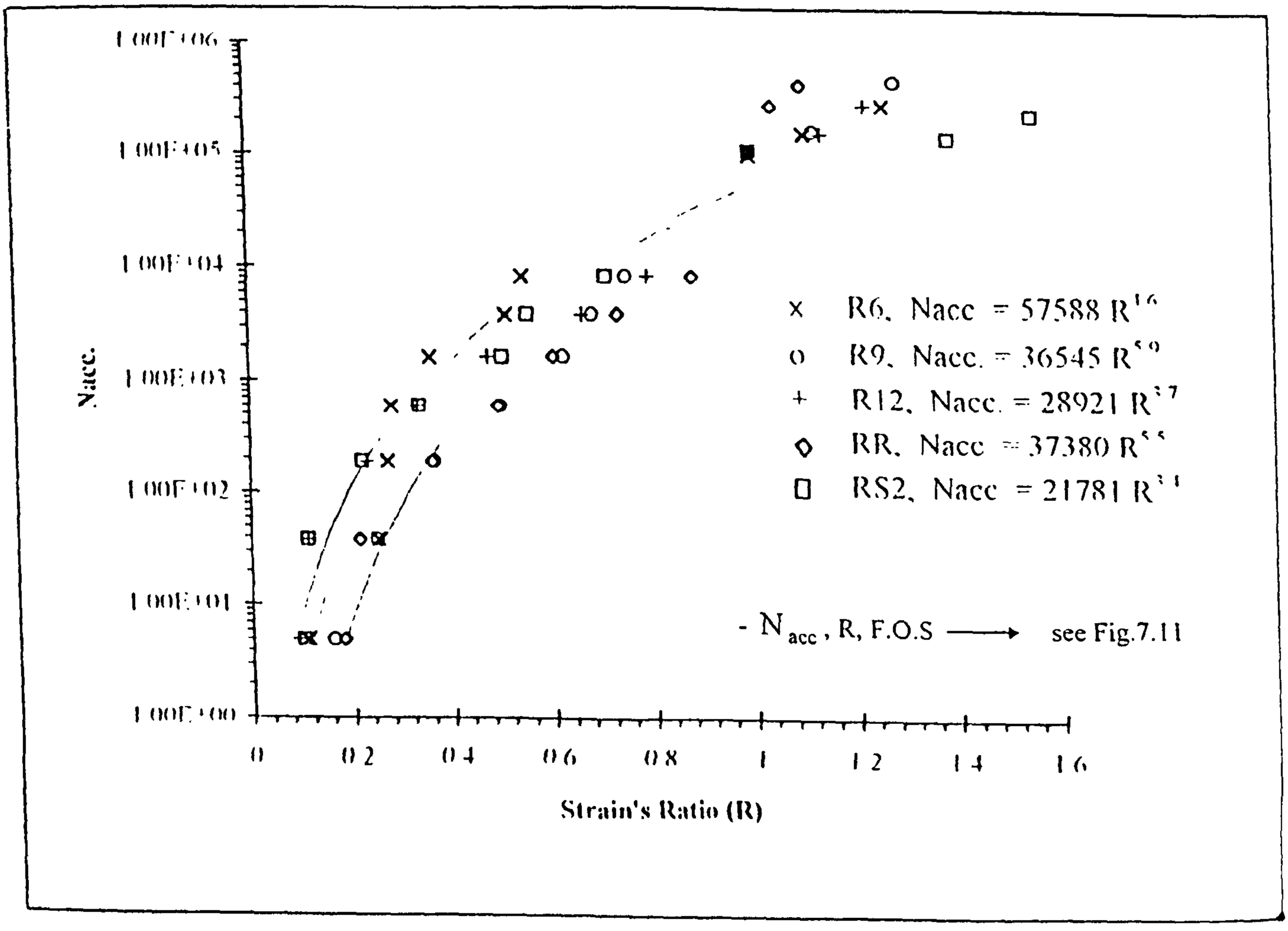

Fig.7.14: Nomograph for the Performance Model of Module-M1

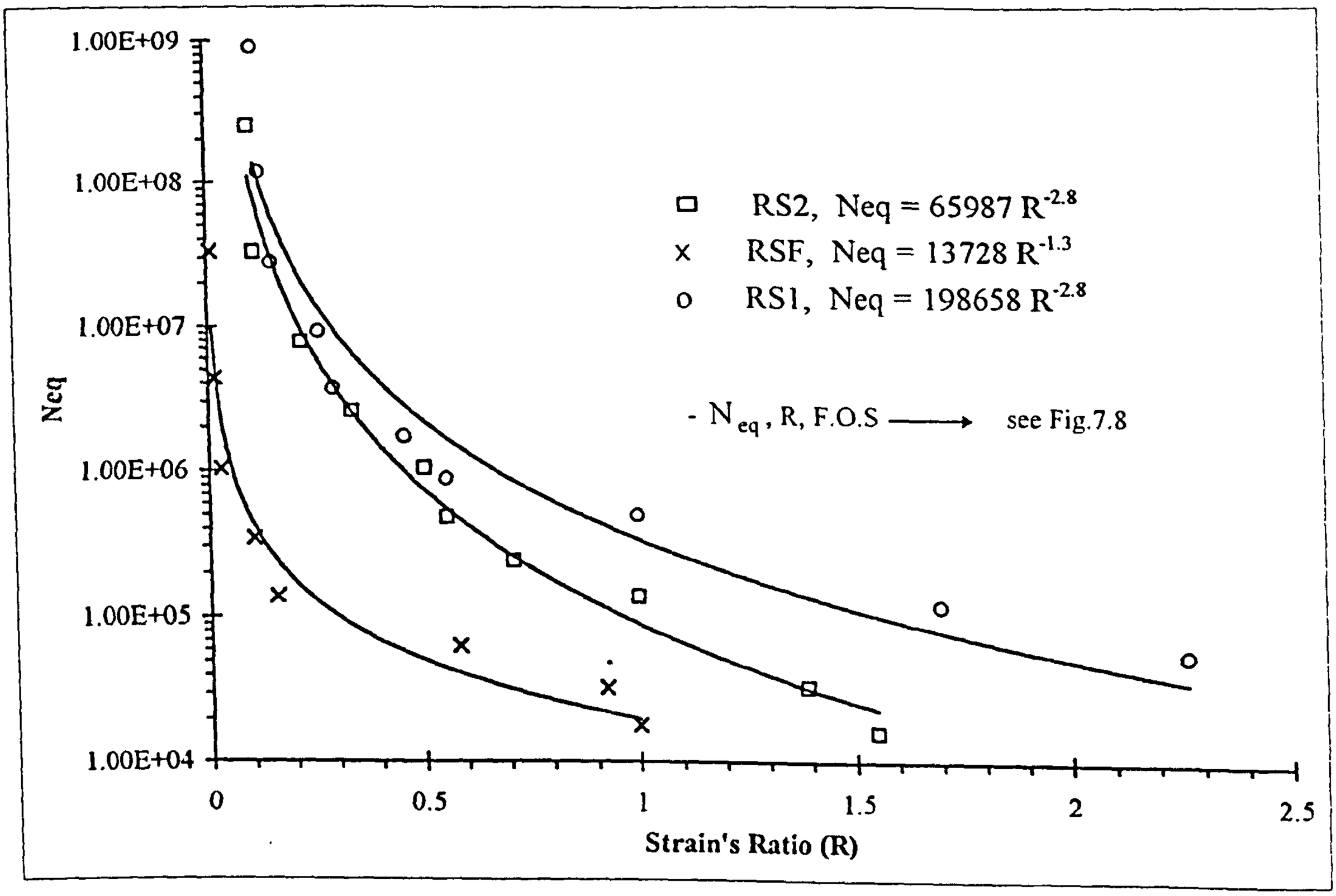

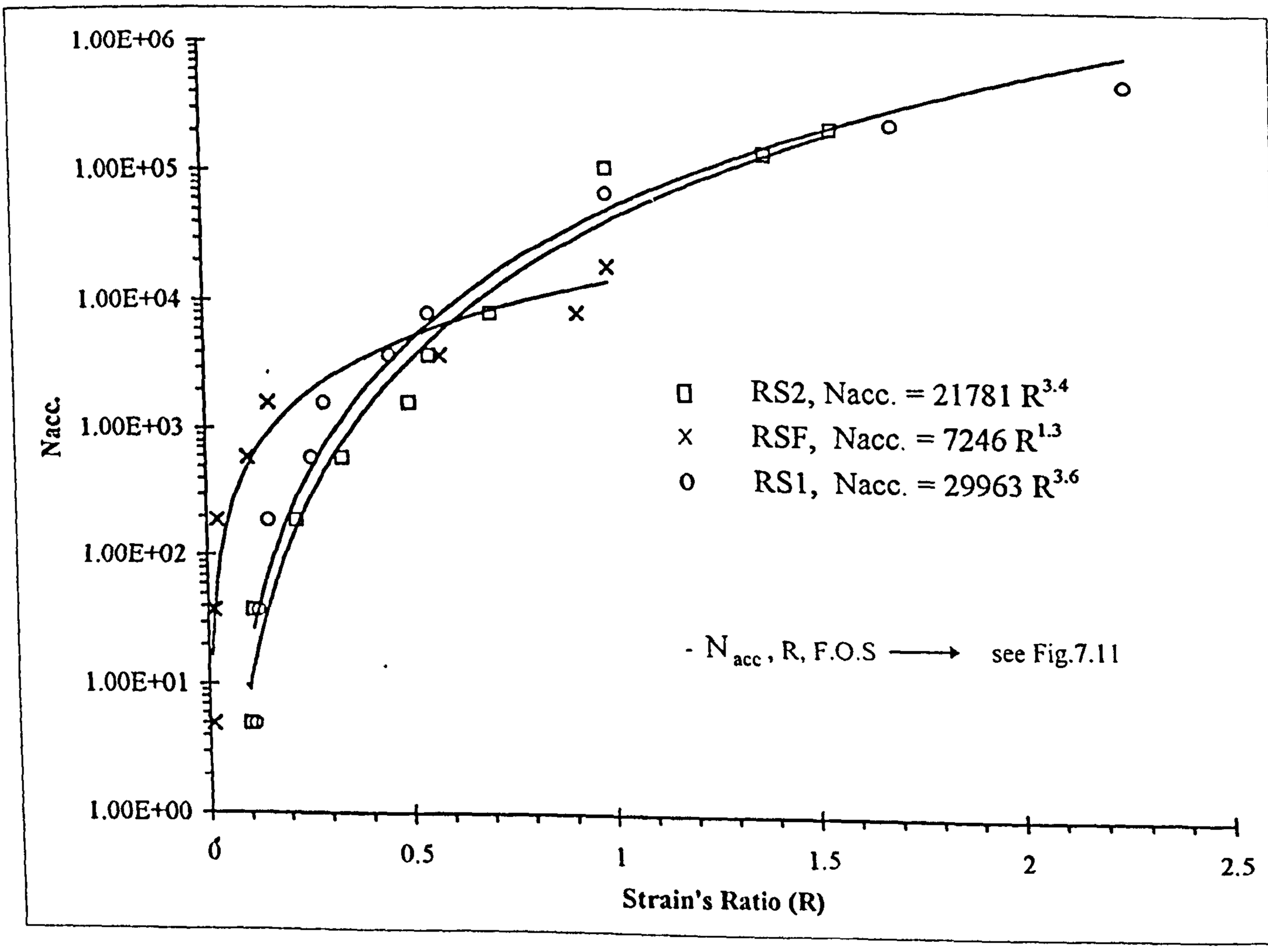

Fig.7.15: Nomograph for the Performance Model of Module-M2

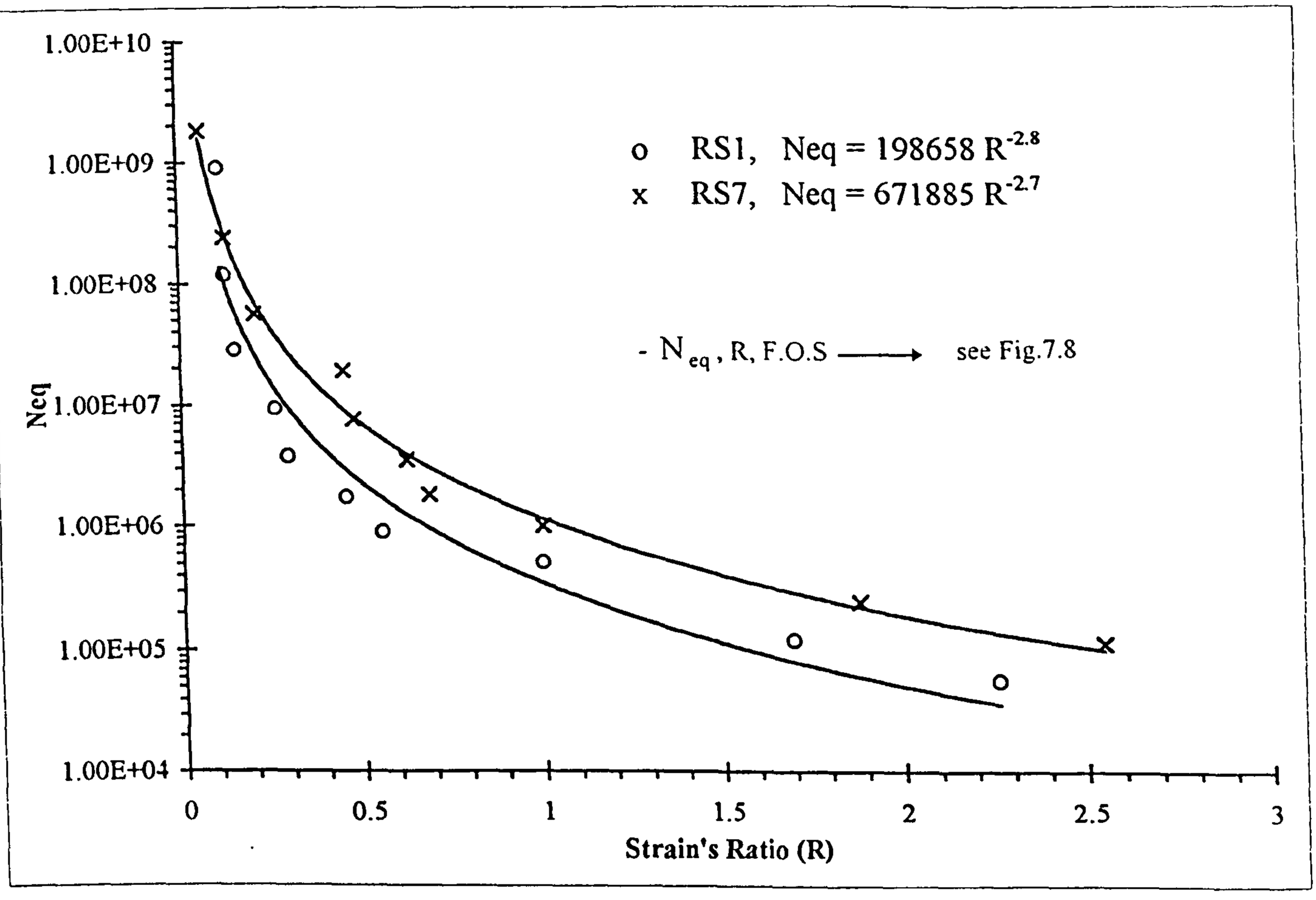

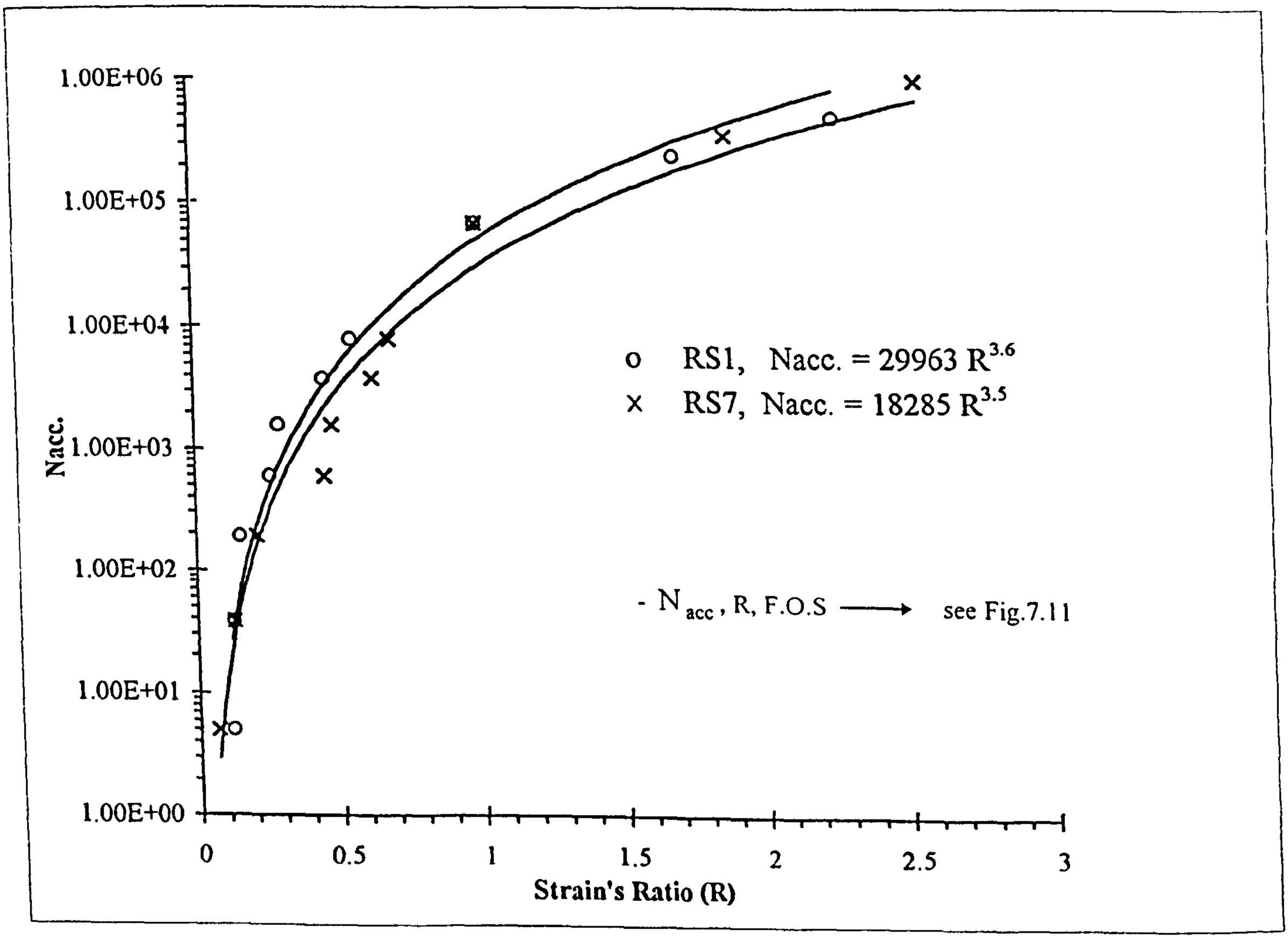

Fig.7.16: Nomograph for the Performance Model of Module-M3

1- Concrete Paving Blocks

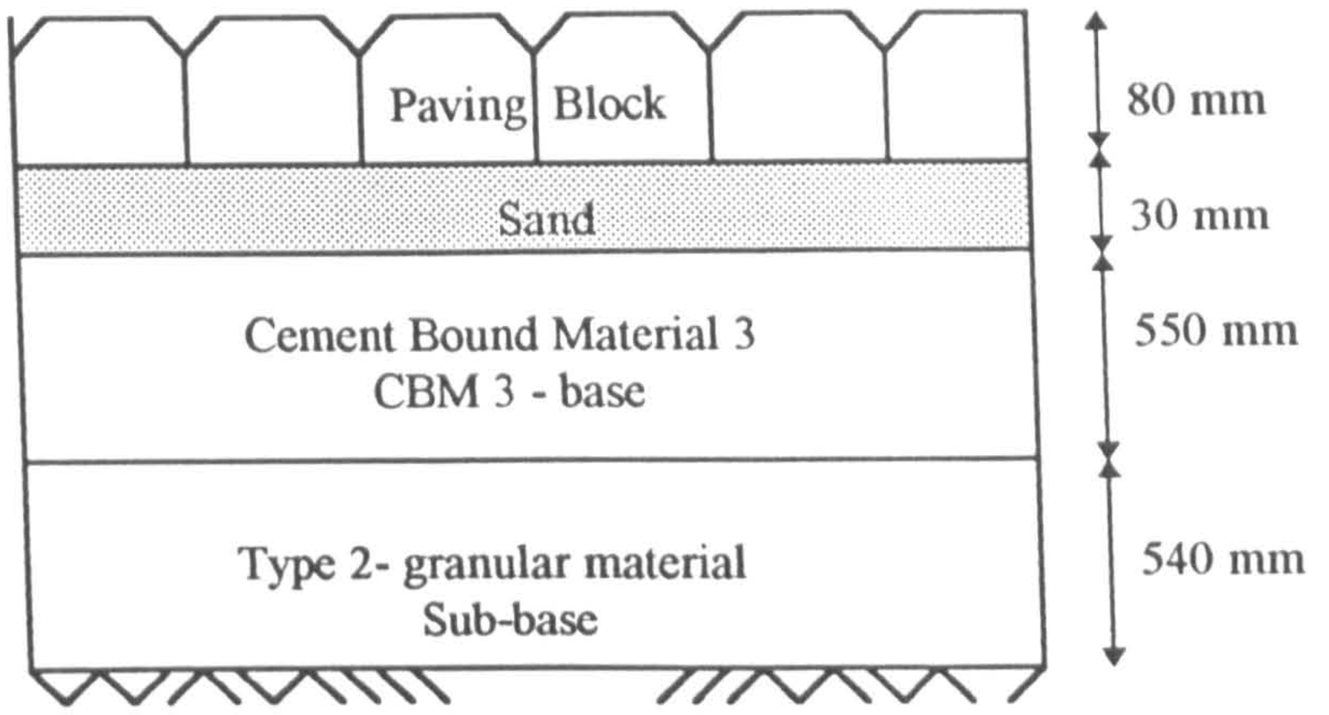

2- Pavement Quality Concrete (PQC)

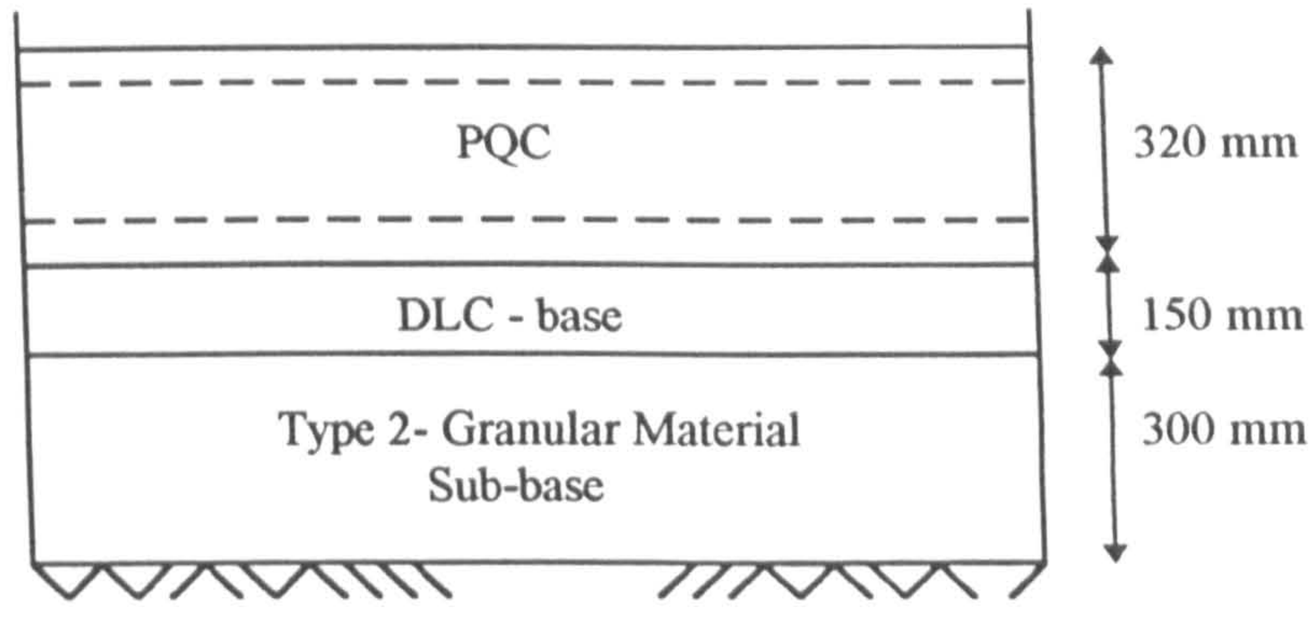

3- Precast Concrete Raft Units

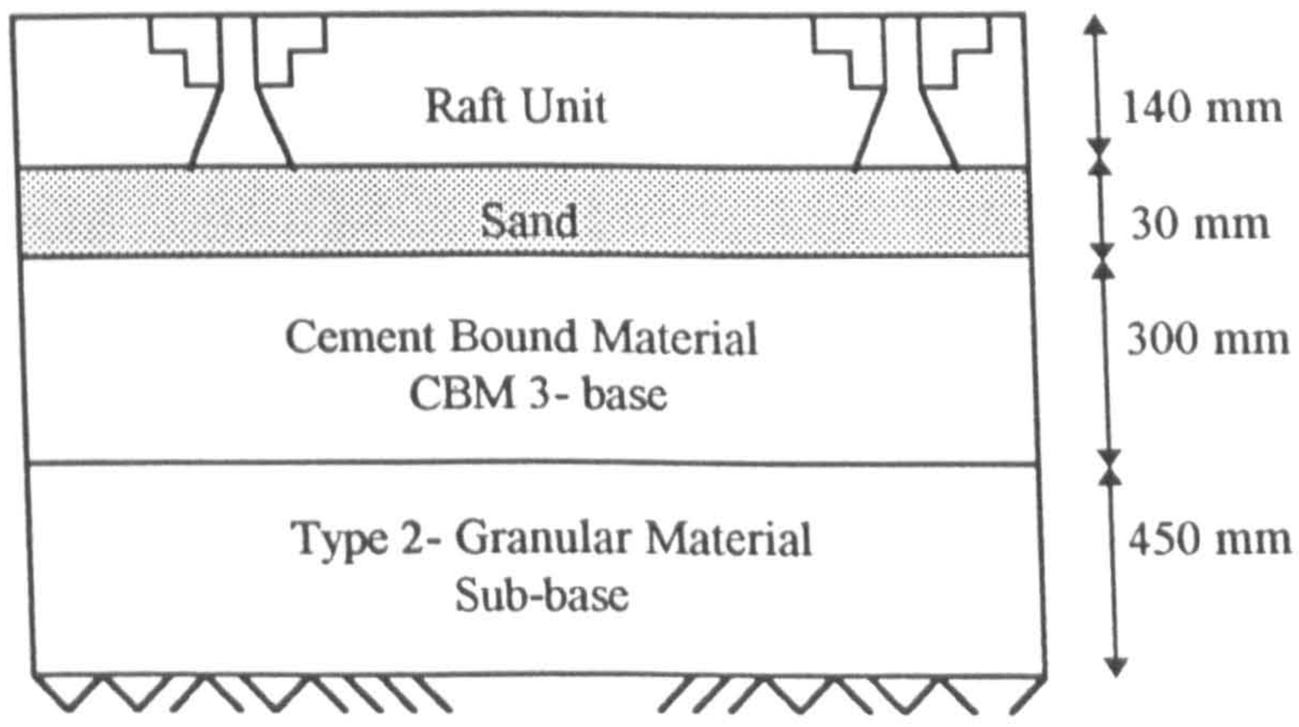

Fig.7.17: Design Cross Sections for the Whole Life Cost Analysis.

PLATE 2.1a : Single Main Landing Gear of a Propellered Engine

(Landing Operation)

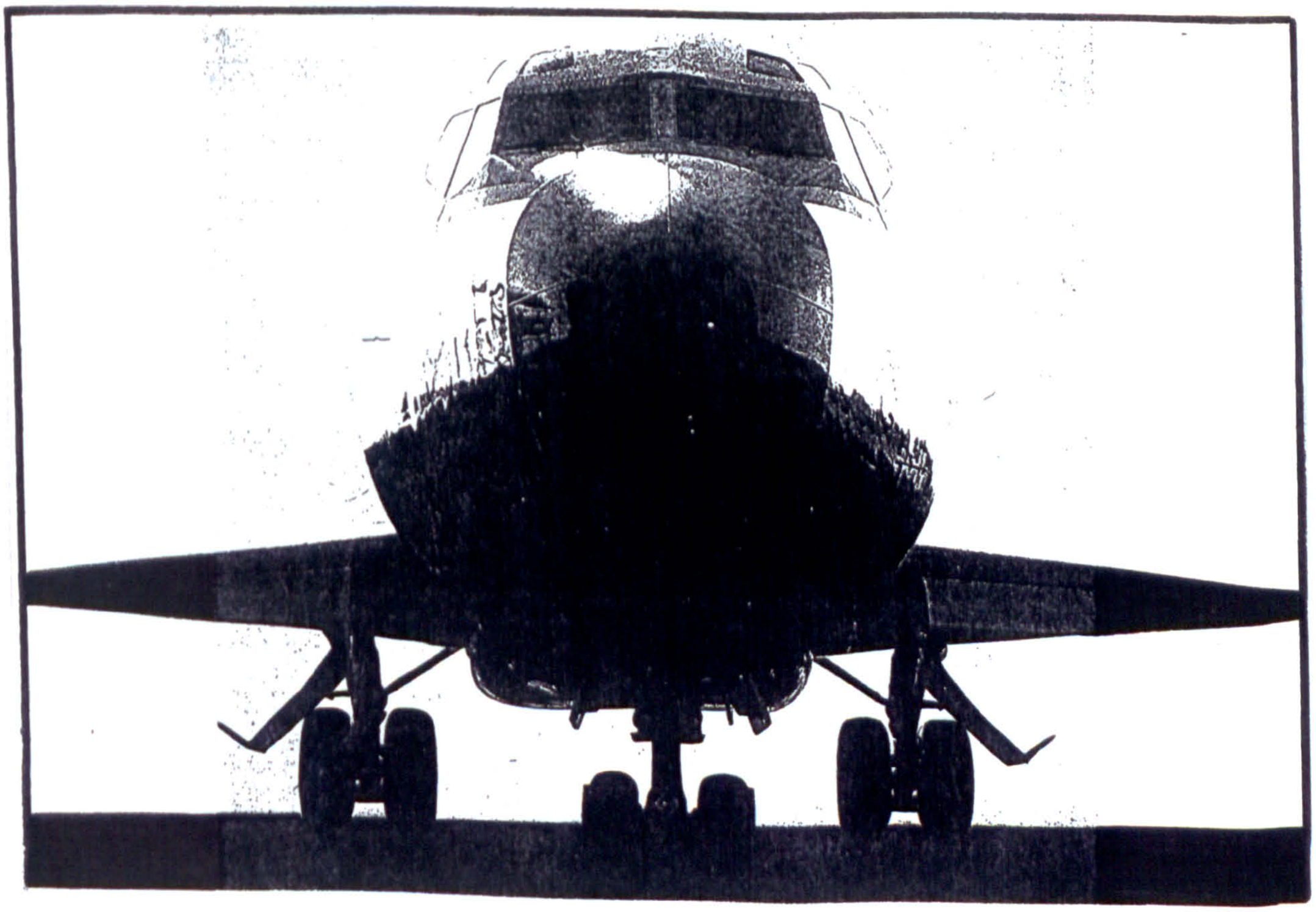

(Taxiing Operation)

PLATE 2.1b : Dual Main Landing Gear of B.727

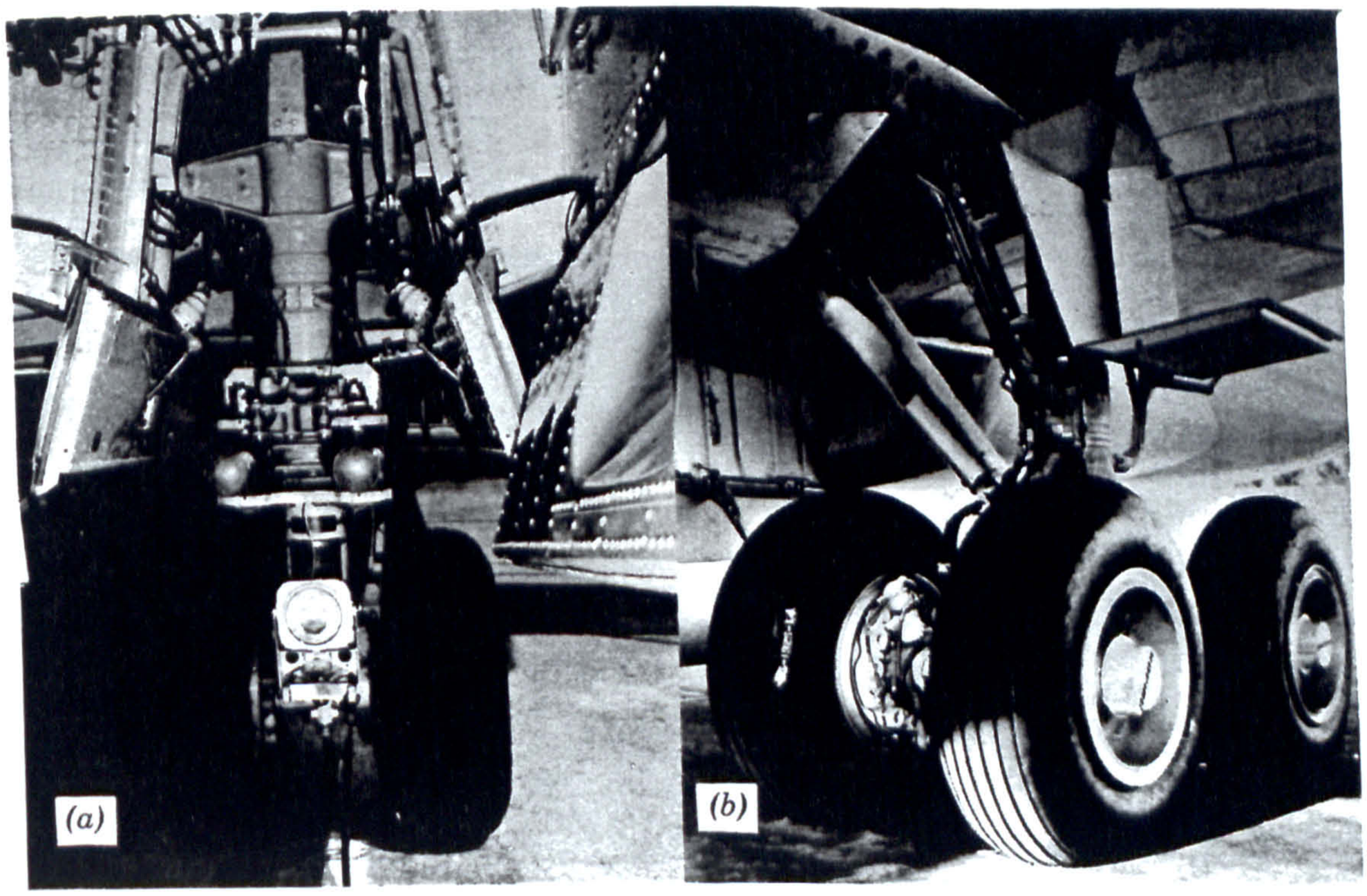

PLATE 2.1c : Dual Tandem Main Landing Gear of B.707

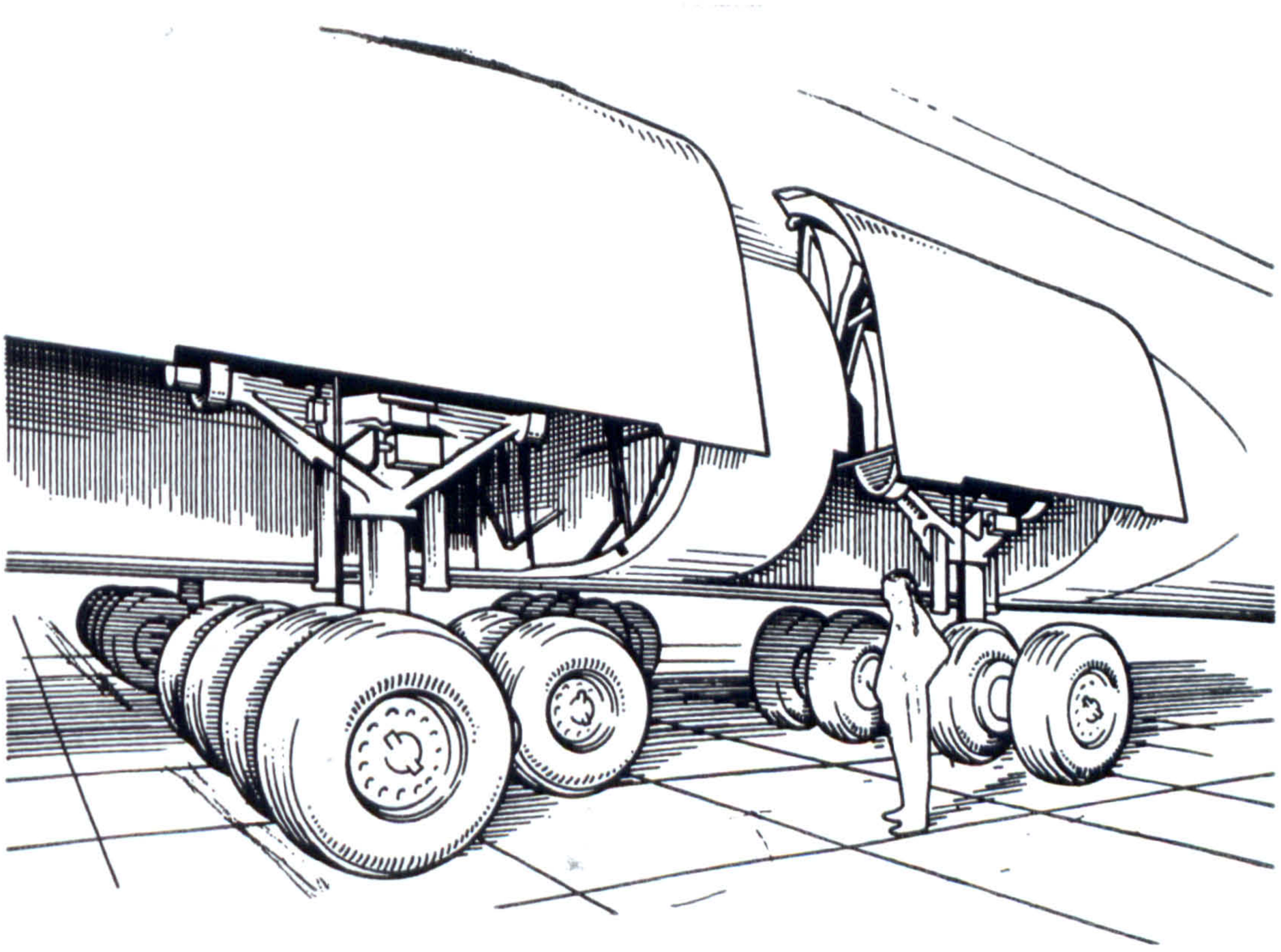

PLATE 2.1d : Complex Main Landing Gear of Lockheed Galaxy
(rotated and lateral spread, triangle footprint)

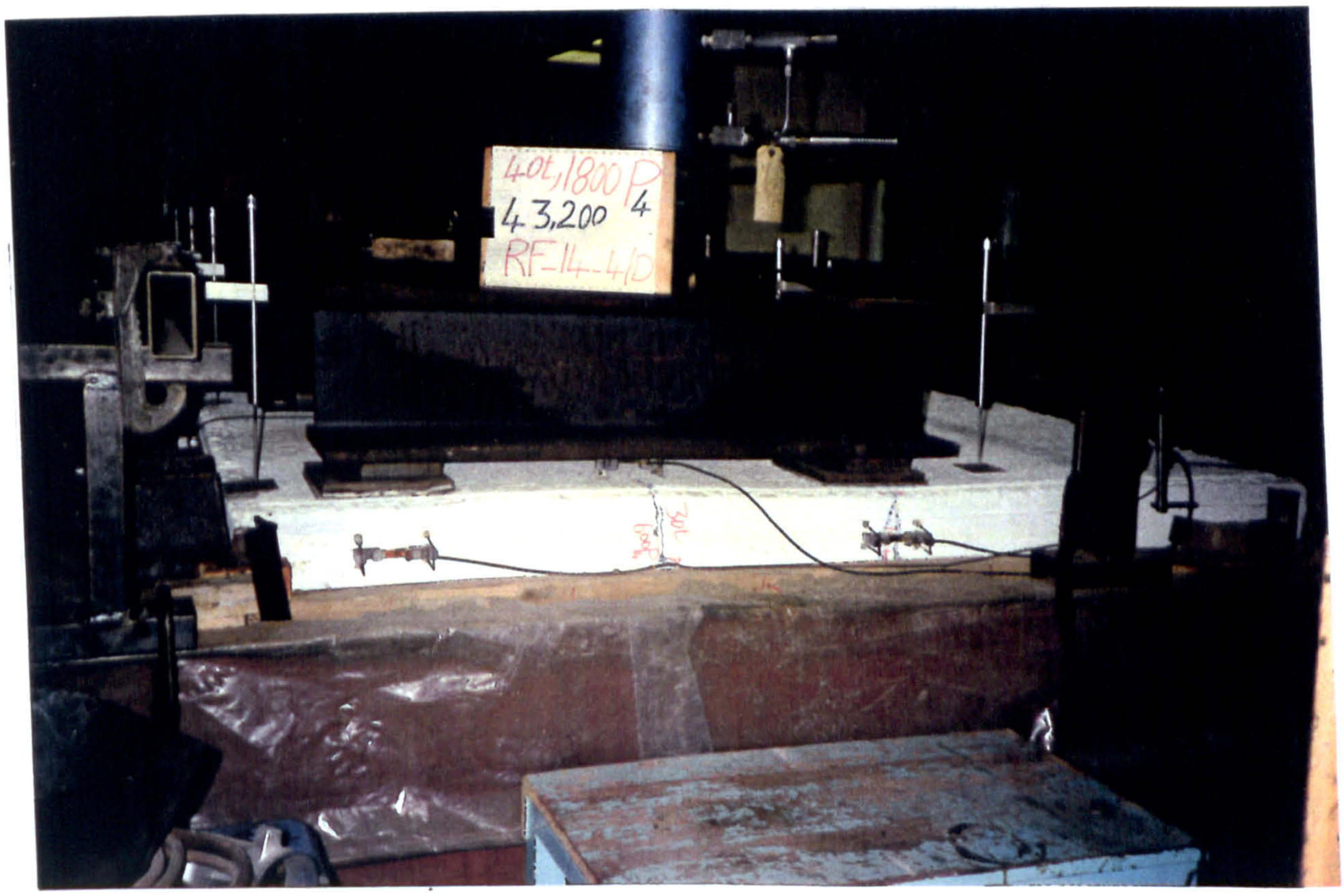

PLATE 4.1 : Mounting the LVDTS Transducers on the Hollow Steel Box-Section

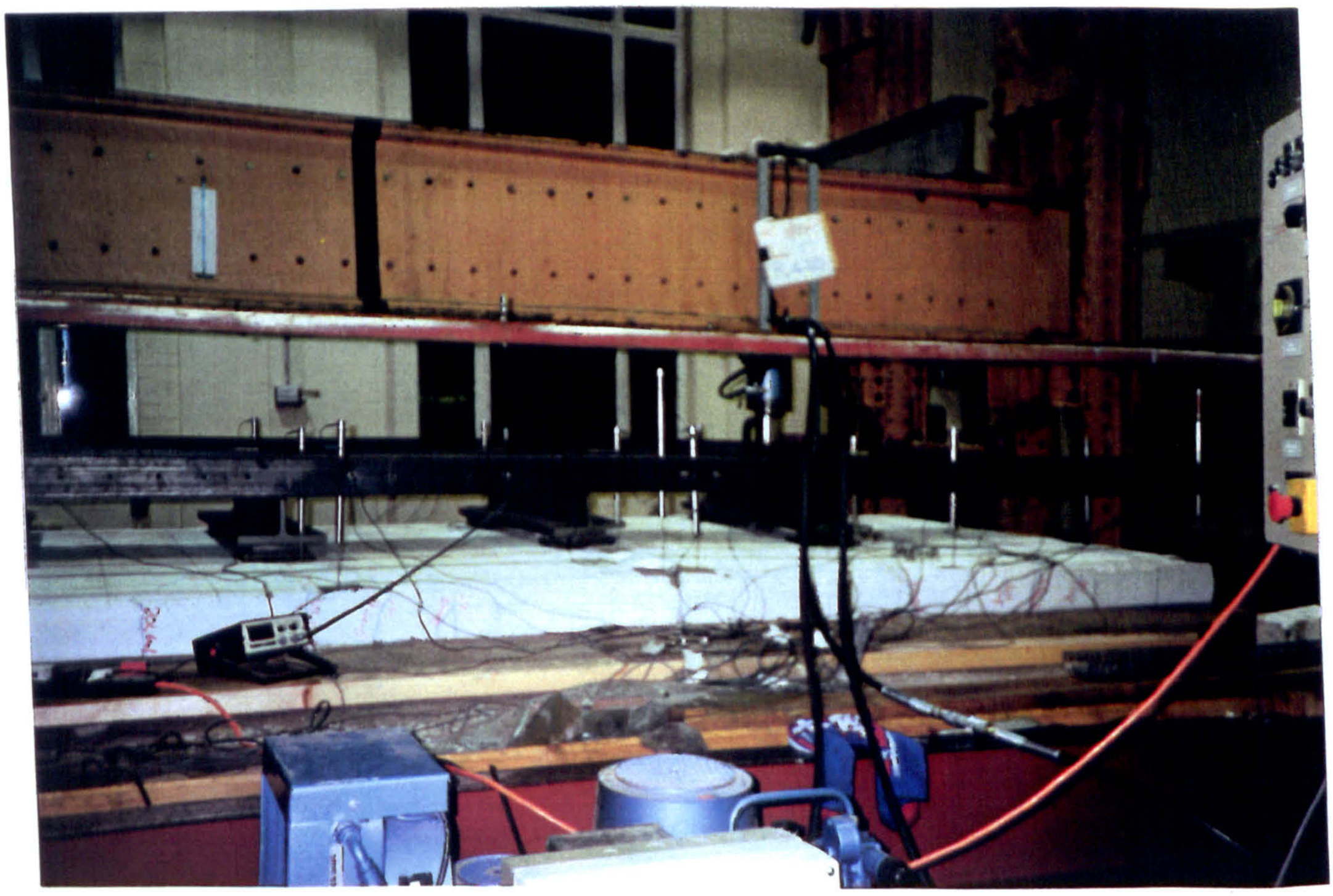

PLATE 4.2 : General Layout for Loading Frame and Test Area

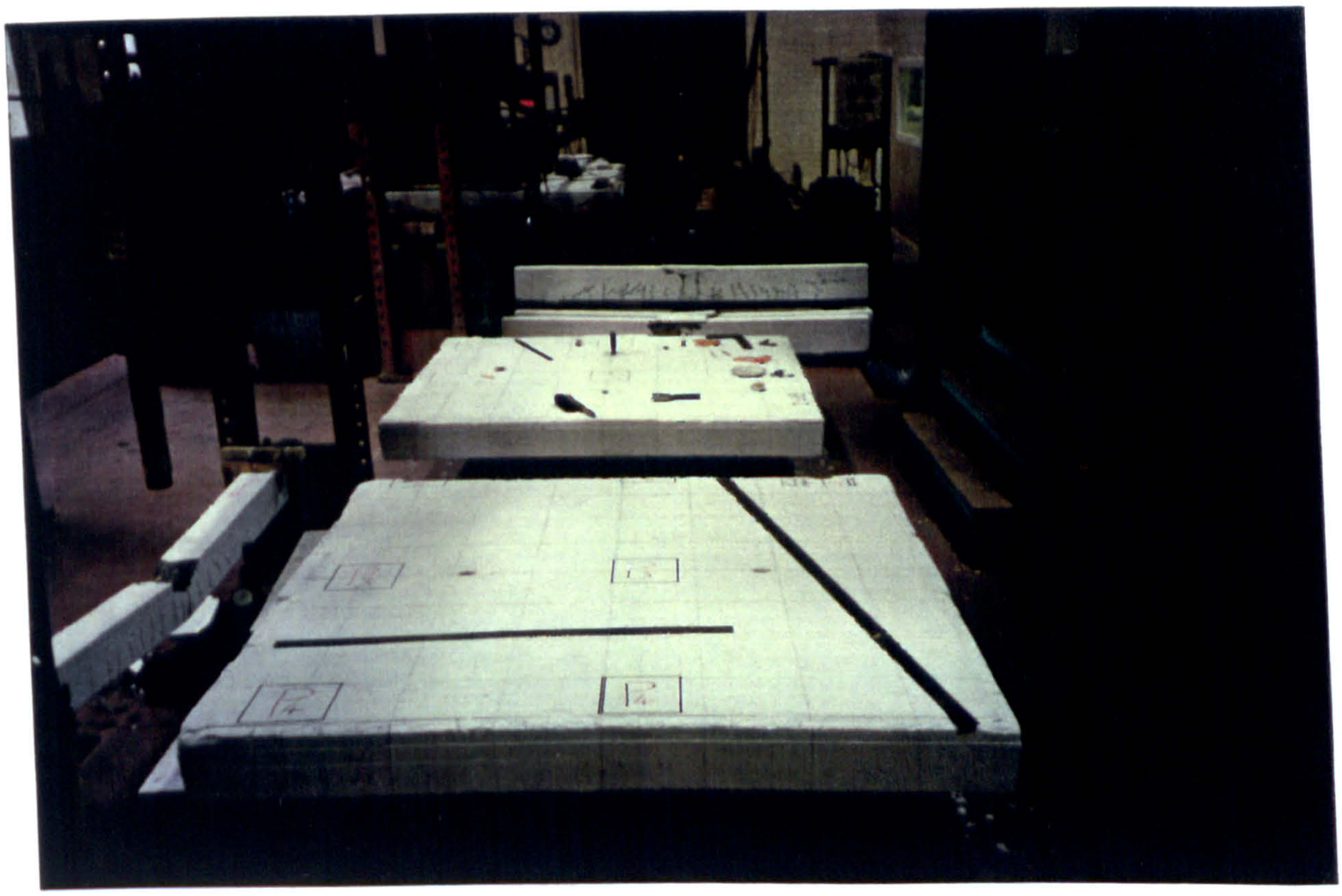

PLATE 4.3 : Before the Test - Preparation of the Raft

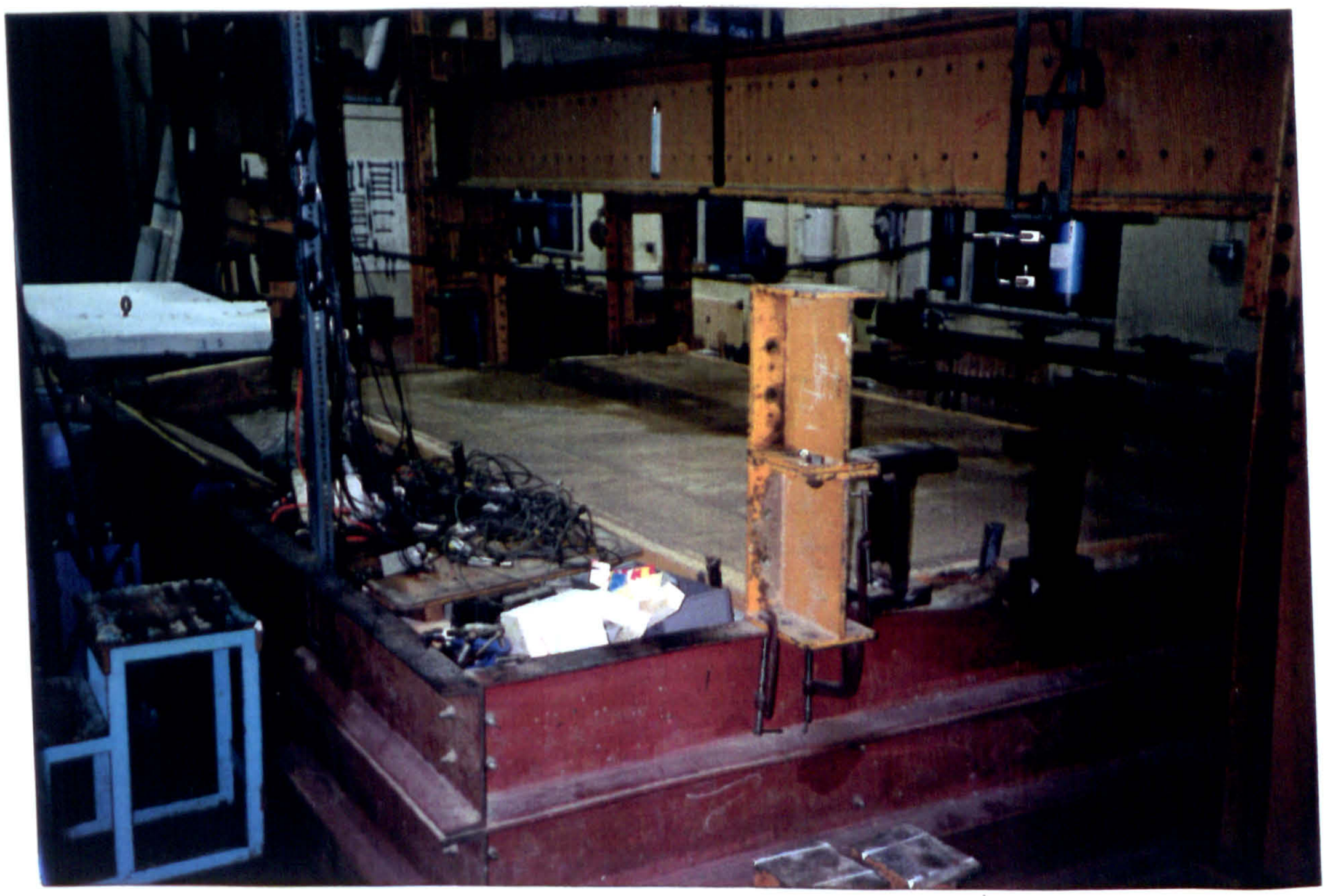

PLATE 4.4 : Sand Screeded and Ready for Laying the Raft

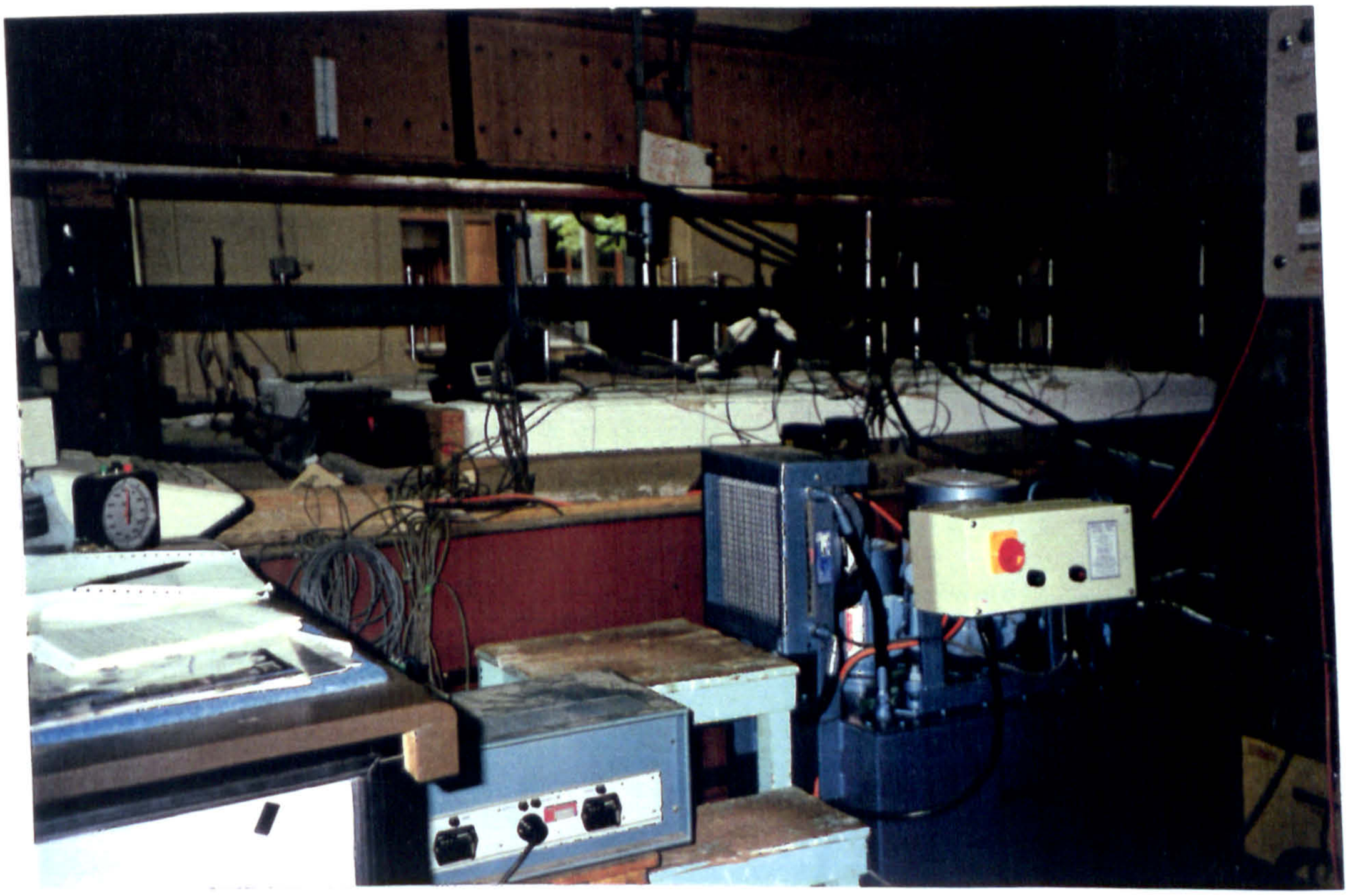

PLATE 4.5 : Work in Progress with Hydraulic Equipment and The Data Logging

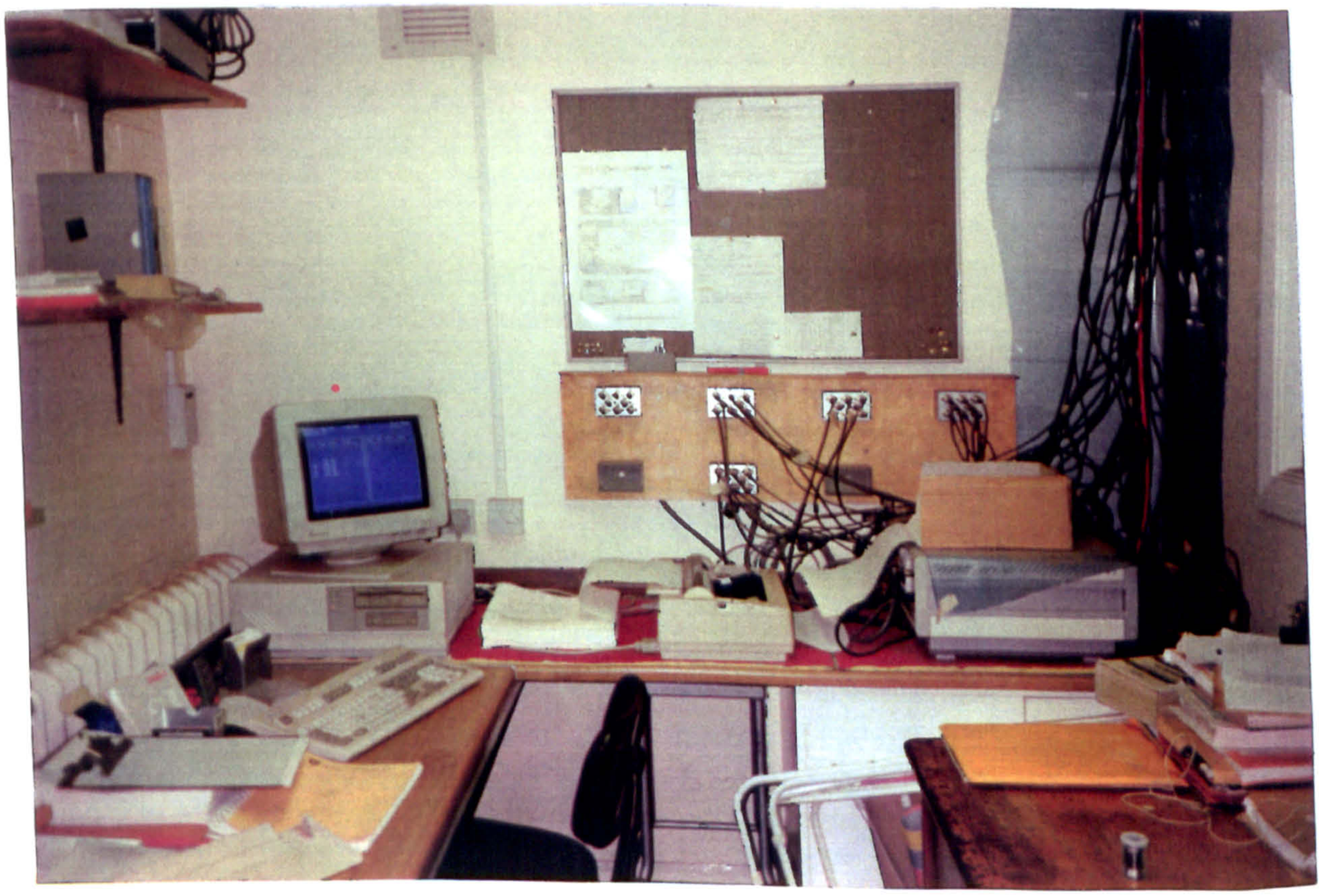

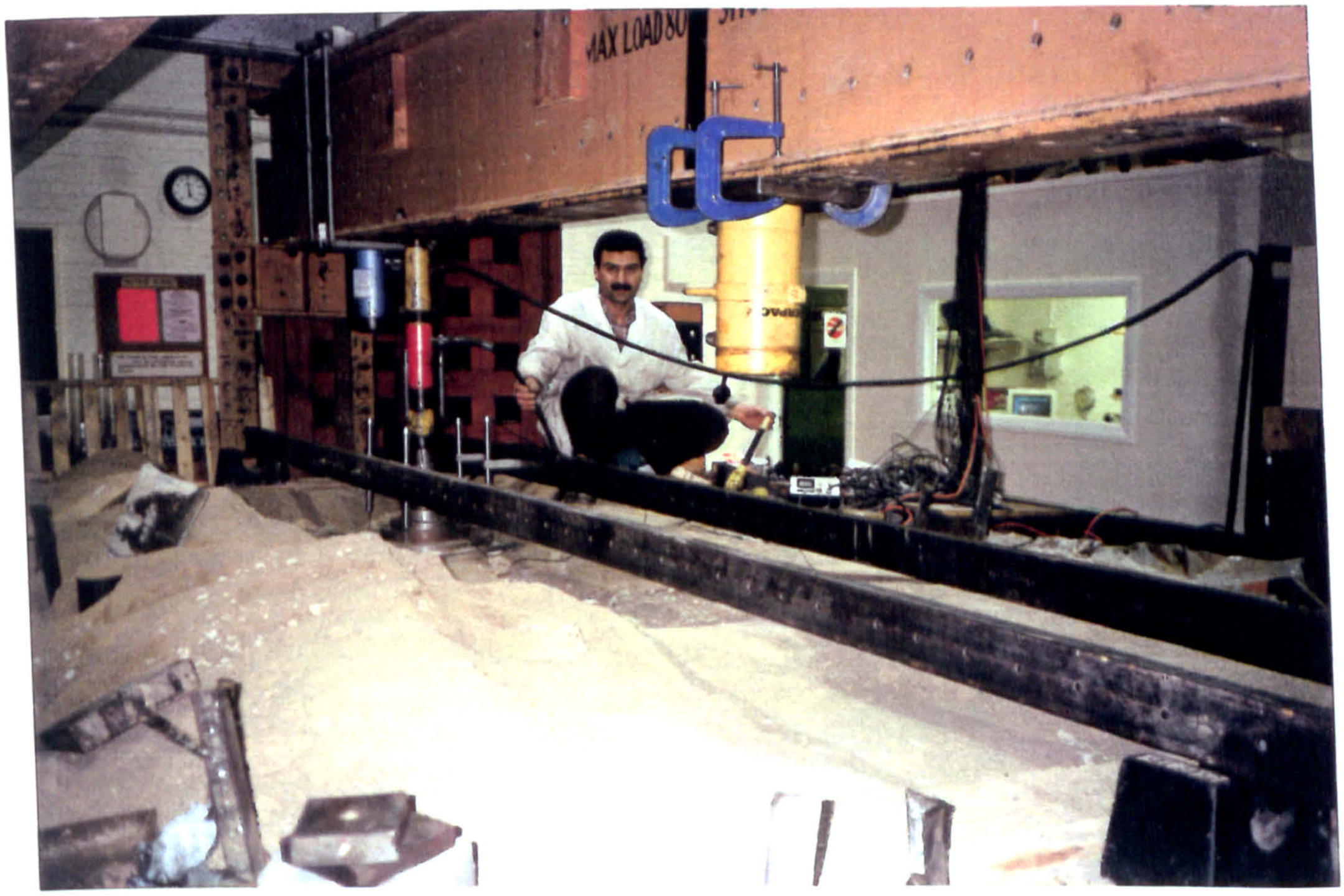

(a) For Sub-Base

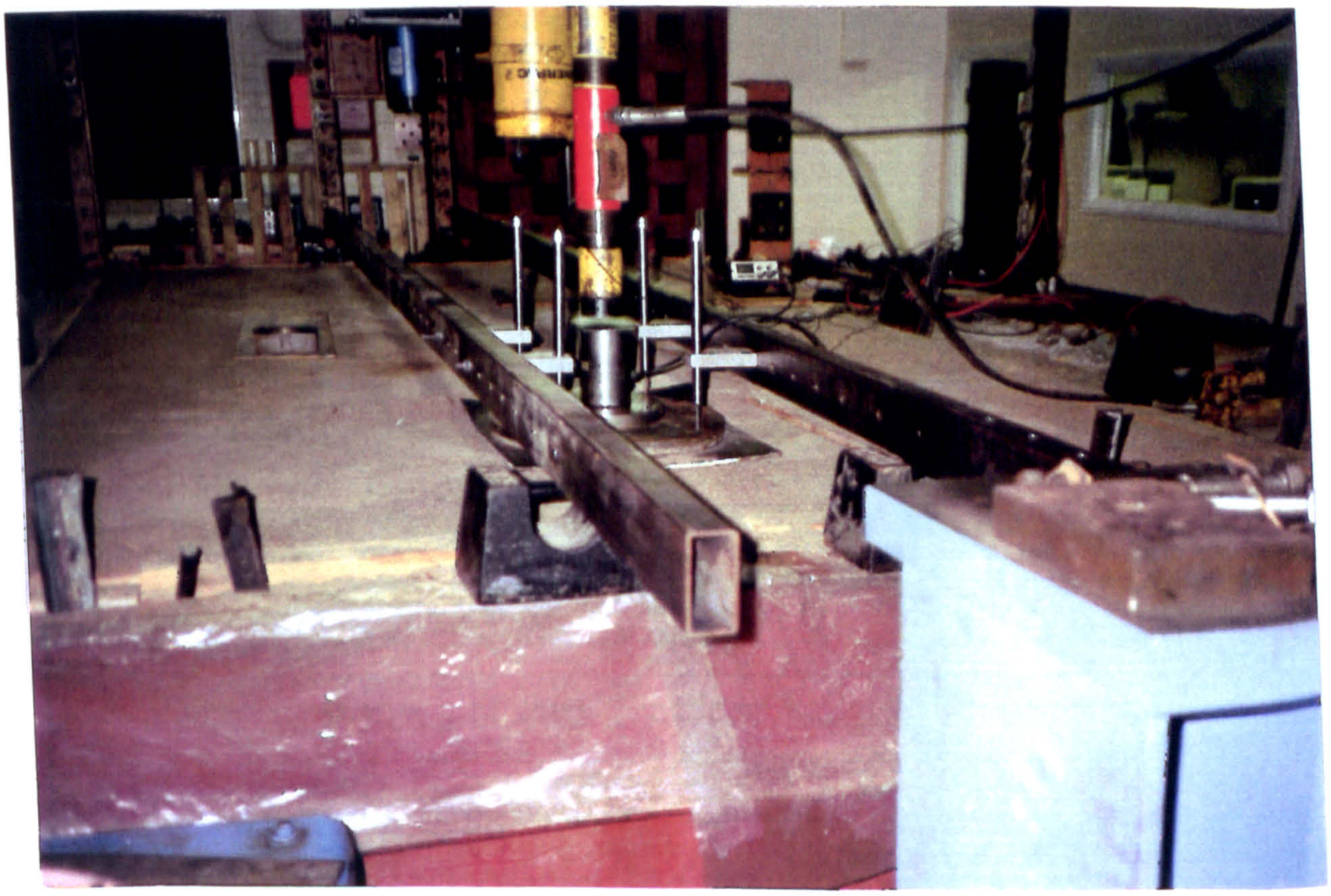

(b) For Bedding Sand

PLATE 4.6 : Plate Bearing Test and Associated Equipments

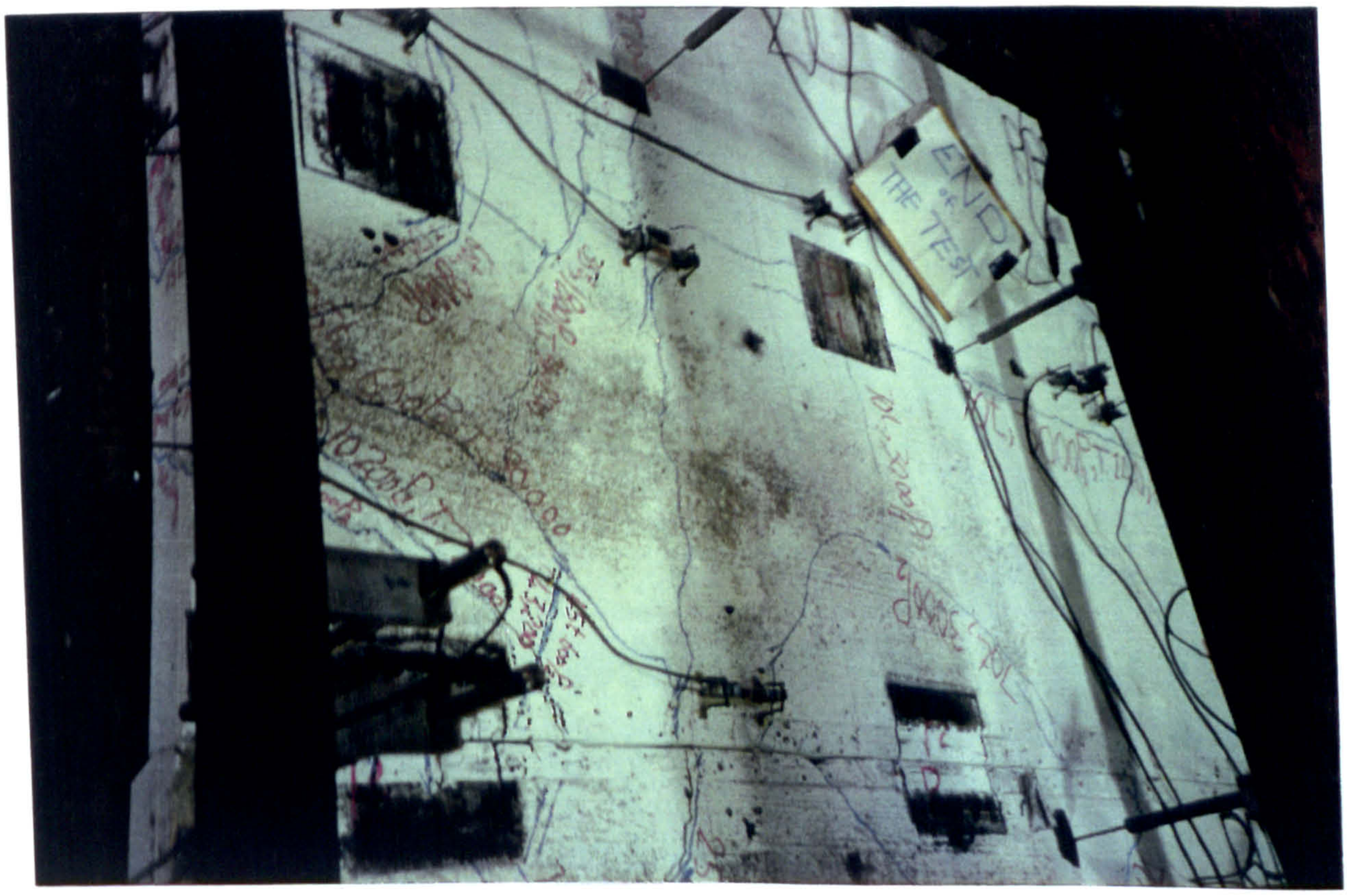

(a) Longitudinal

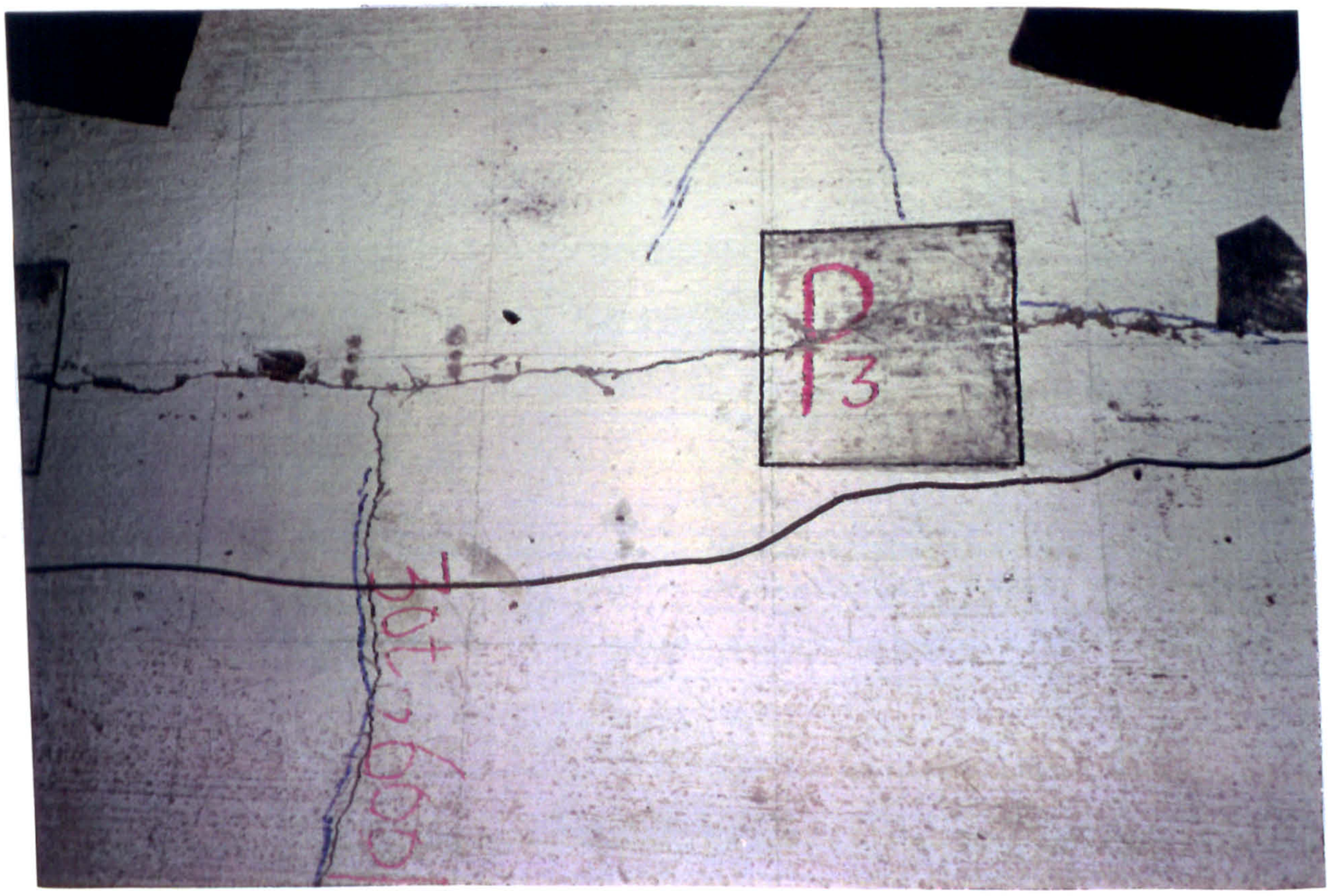

(b) Transverse

PLATE 5.1 : Type of the Main Cracks Observed During the Test

(a) Raft I

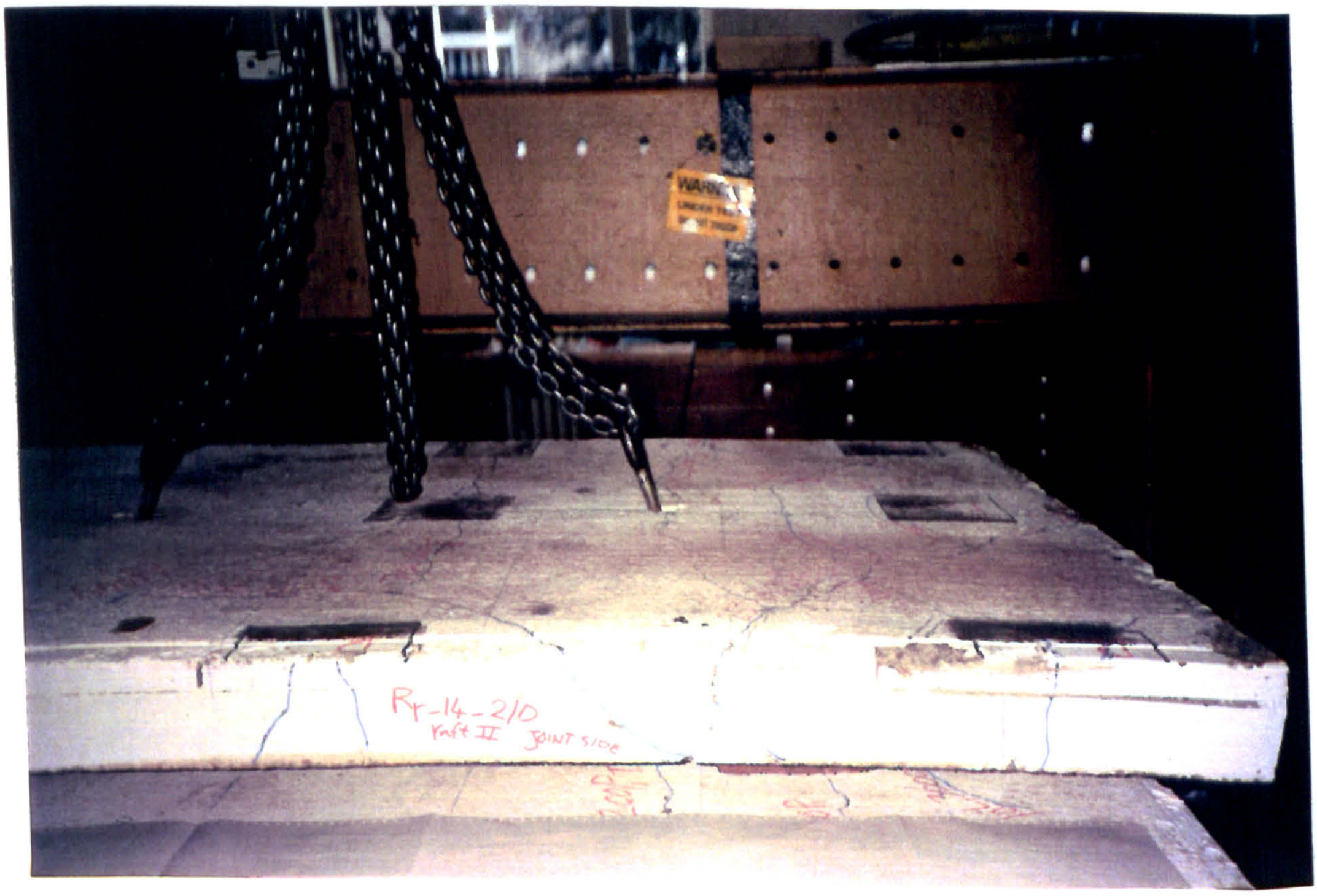

(b) Raft II

PLATE 5.2 : Failure Crack Patterns at the Joint Interface of Raft RR - Module M1

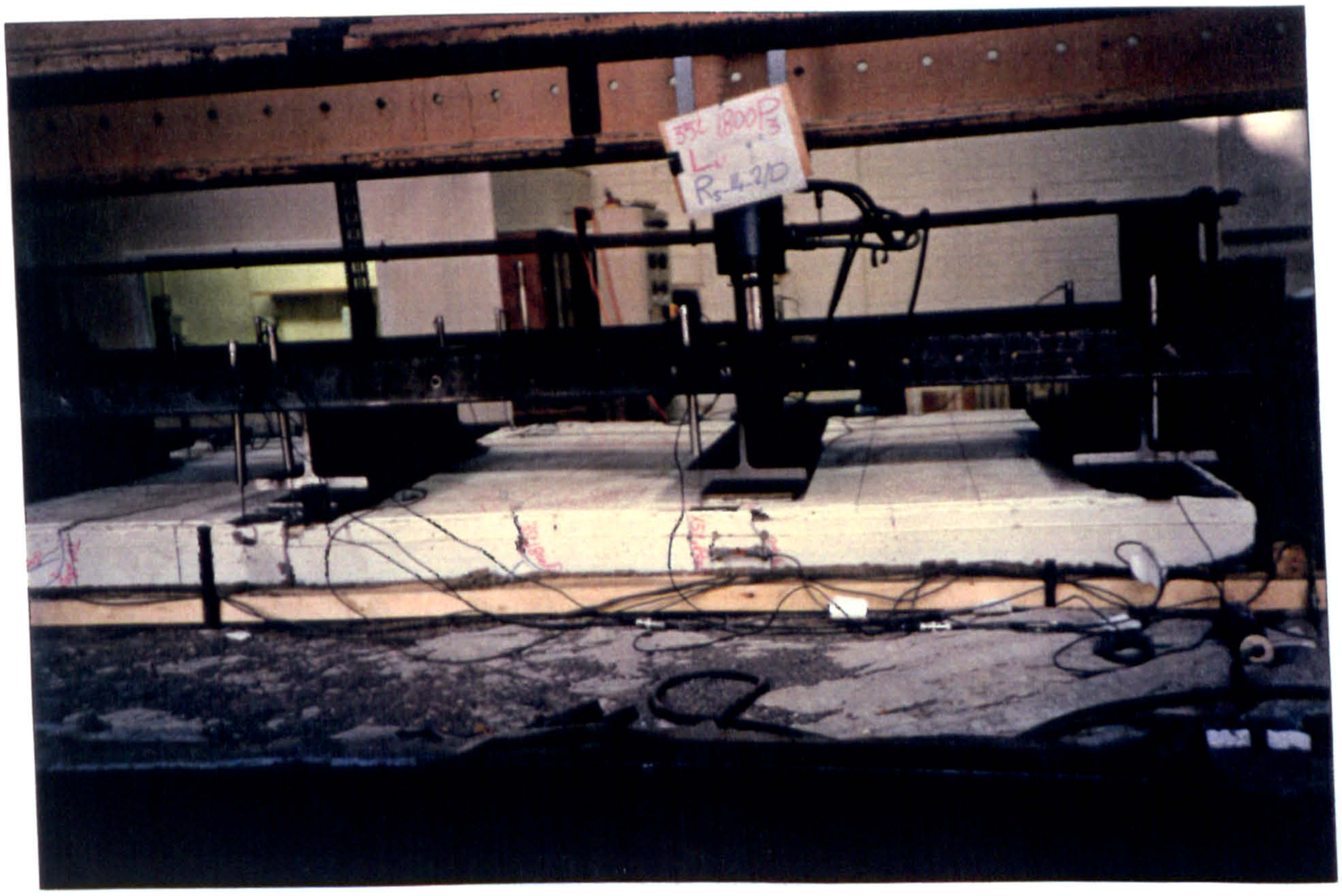

(c) Cross Corner

(d) Delta-Form

PLATE 5.1 (cont.)

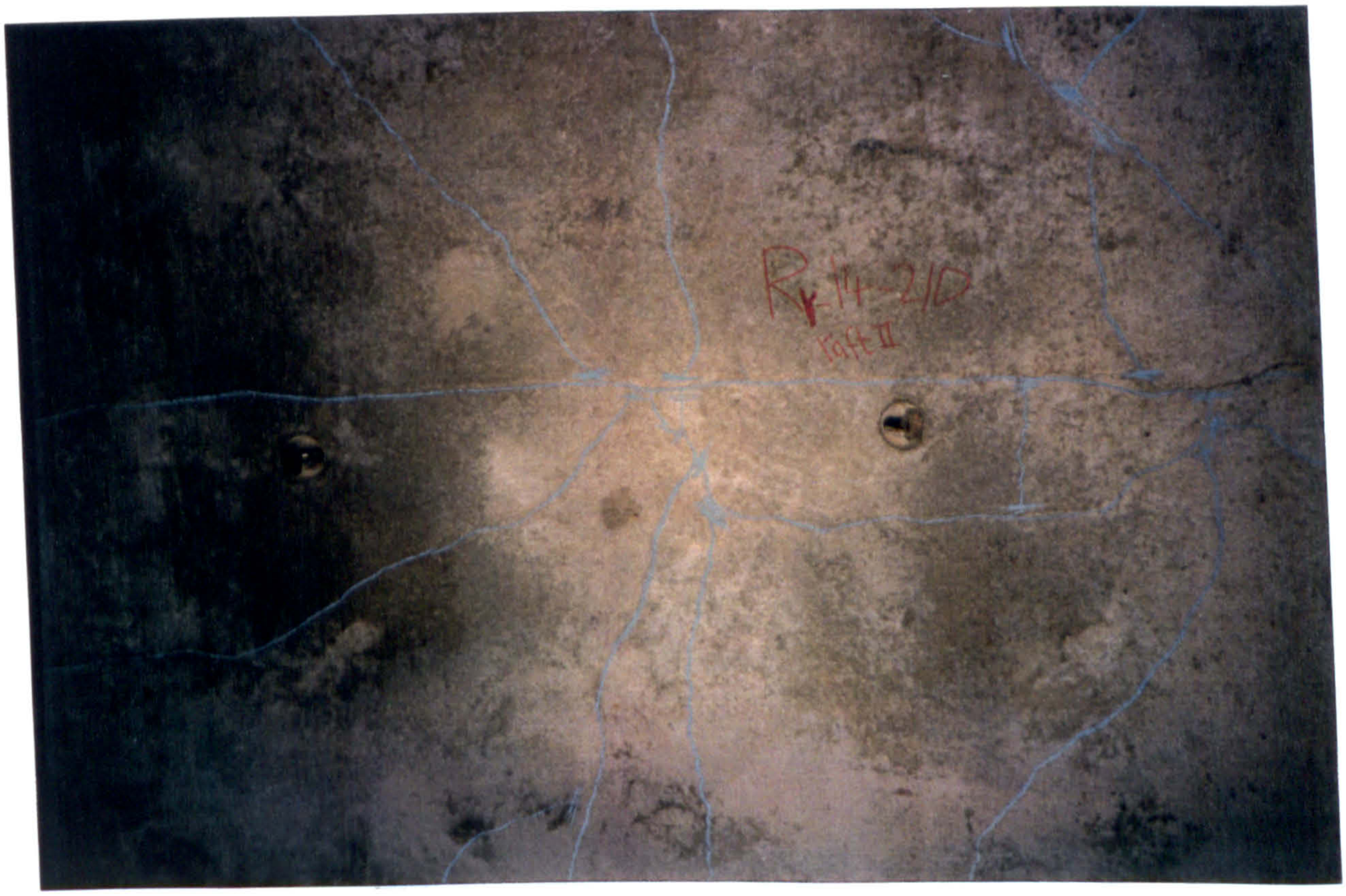

PLATE 5.3 : Bottom Crack Patterns at Failure of Raft RR - Module M1

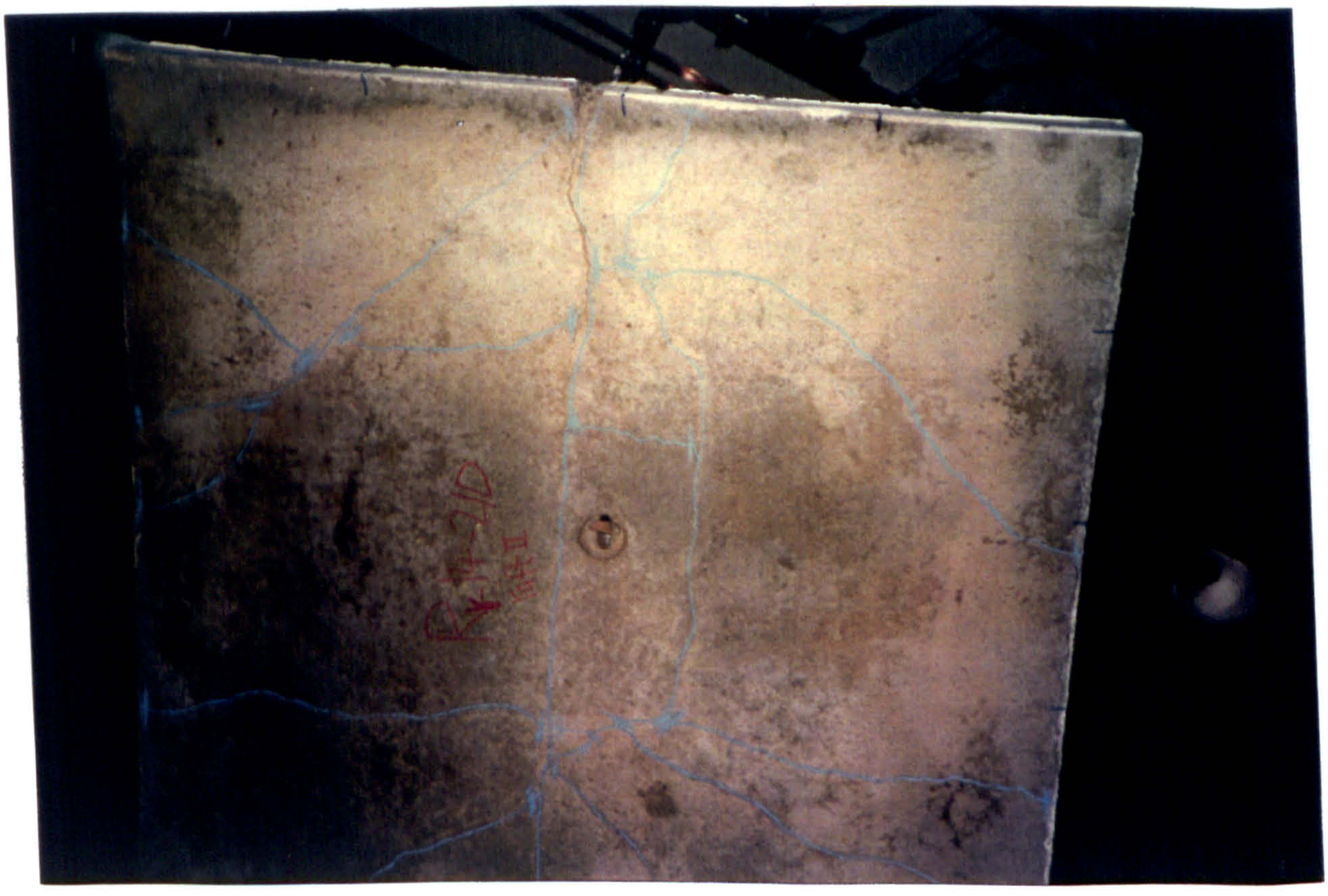

PLATE 5.4 : Full Penetration of the Main Transverse Crack at Failure

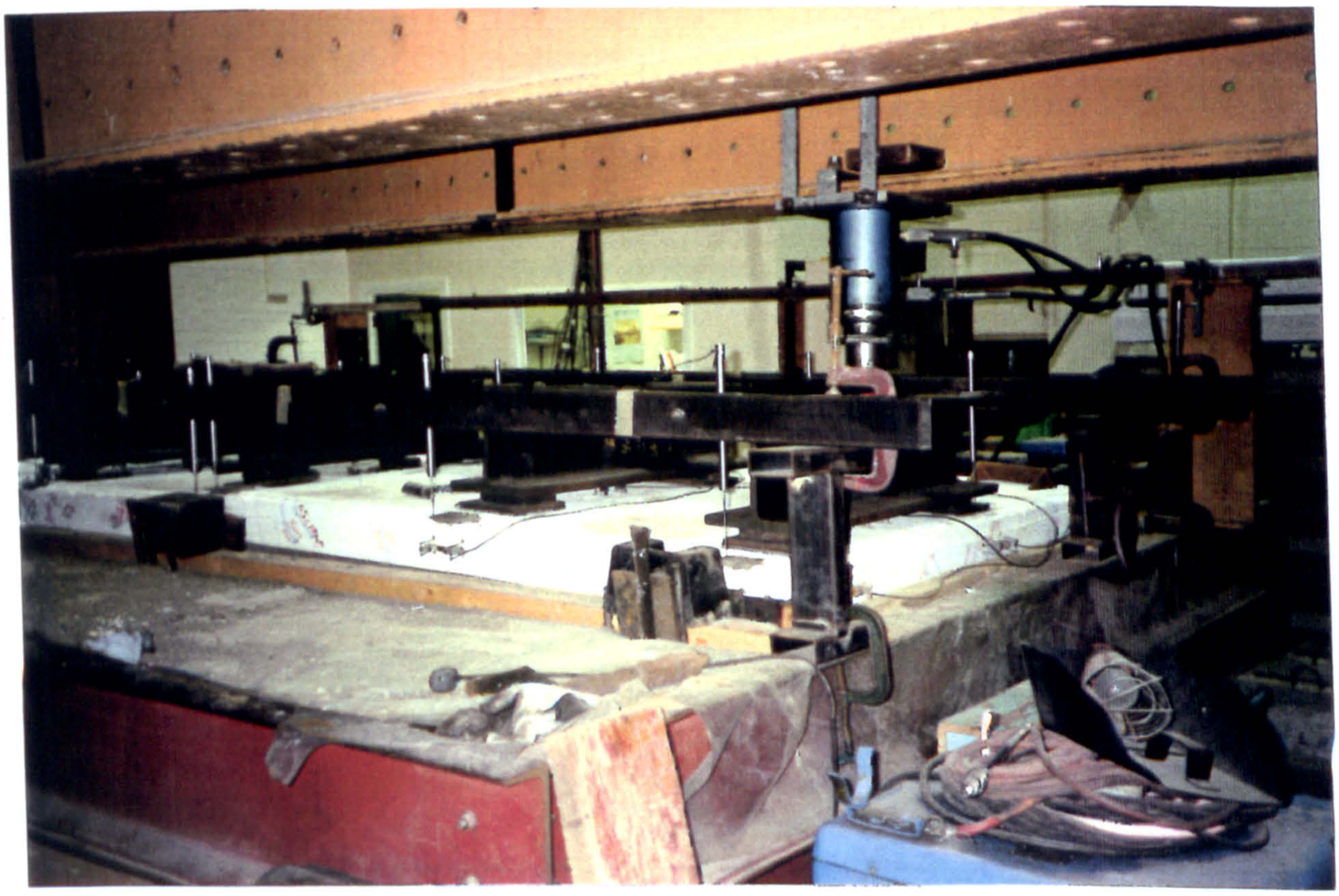

PLATE 5.5 : The Uplift Deflection due to *Loading* Position P4

PLATE 5.6 : The Differential Deflection at the Joint due to Loading P4

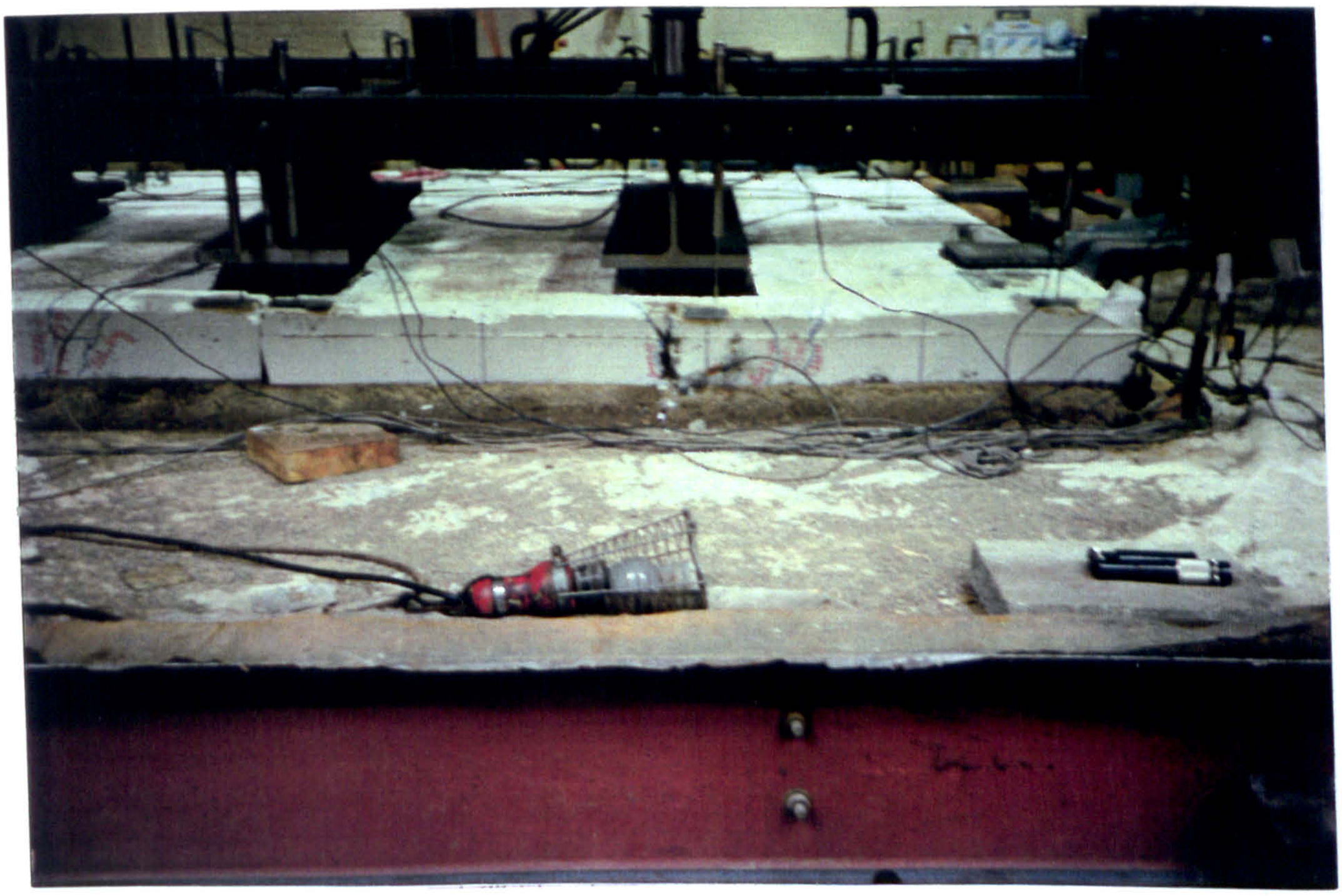

(a) Fatigue Fracture at P3 of Raft RR

(b) Punching Shear at P2 of Raft RS2

PLATE 5.7 : Fatigue Failure Mode of Rafts RR and RS2 - Module M1

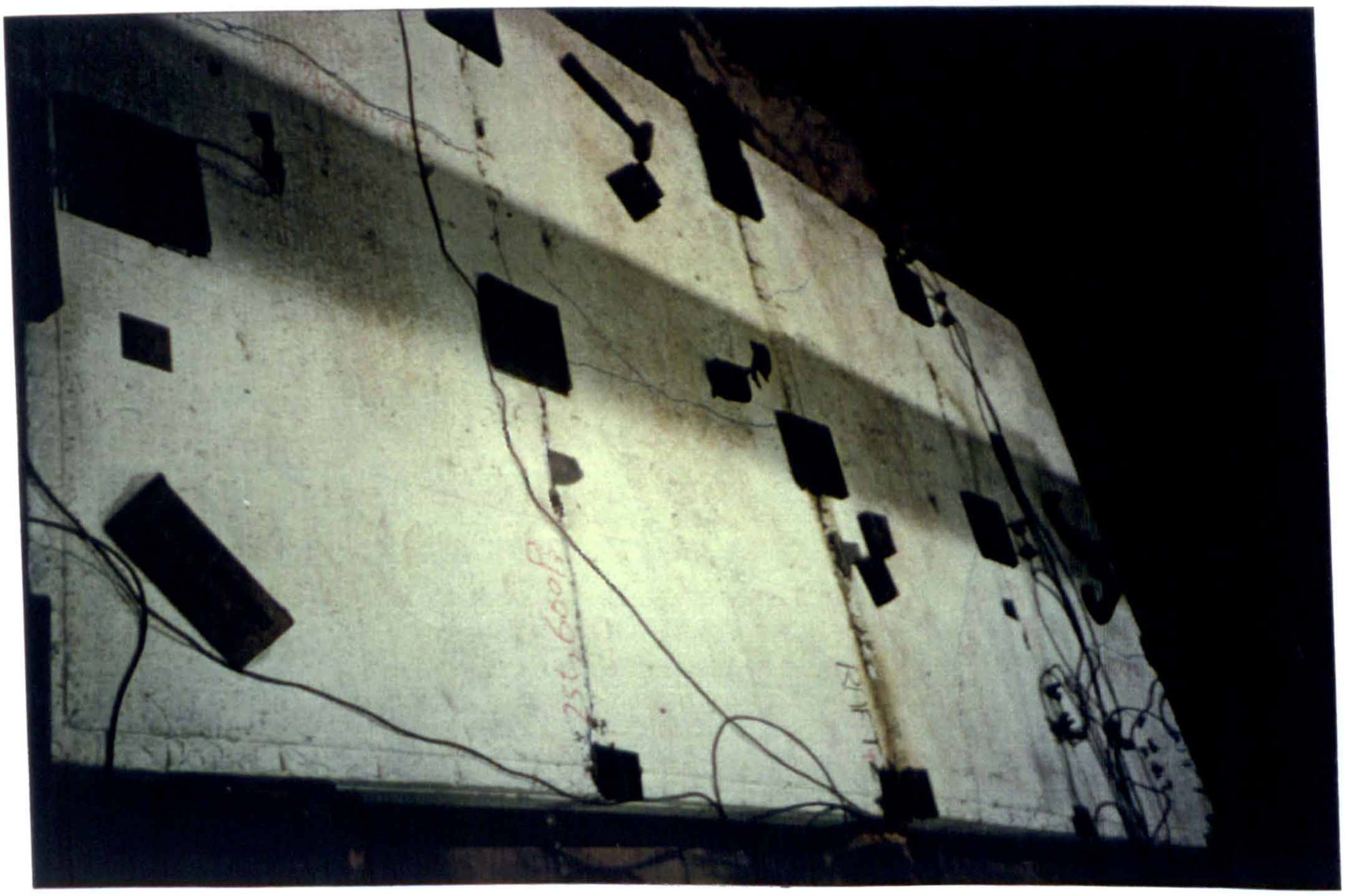

PLATE 6.1 : Top Crack Patterns at Failure of Raft RSF - Module M2

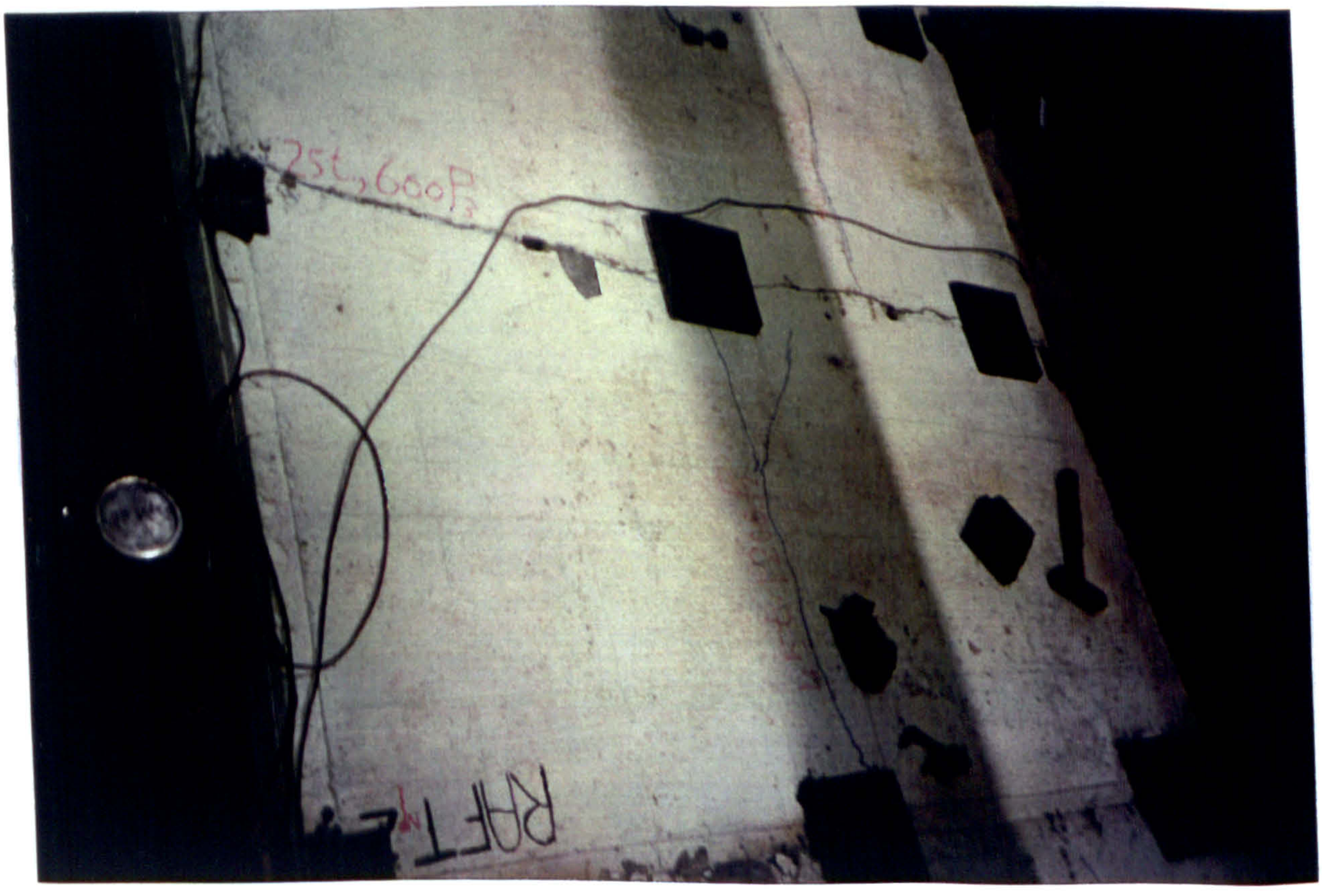

PLATE 6.2 : Transverse Main Crack at Failure, Raft RSF - Module M2

PLATE 6.3 : Bottom Crack Patterns at Failure of Raft RS1 - Module M2

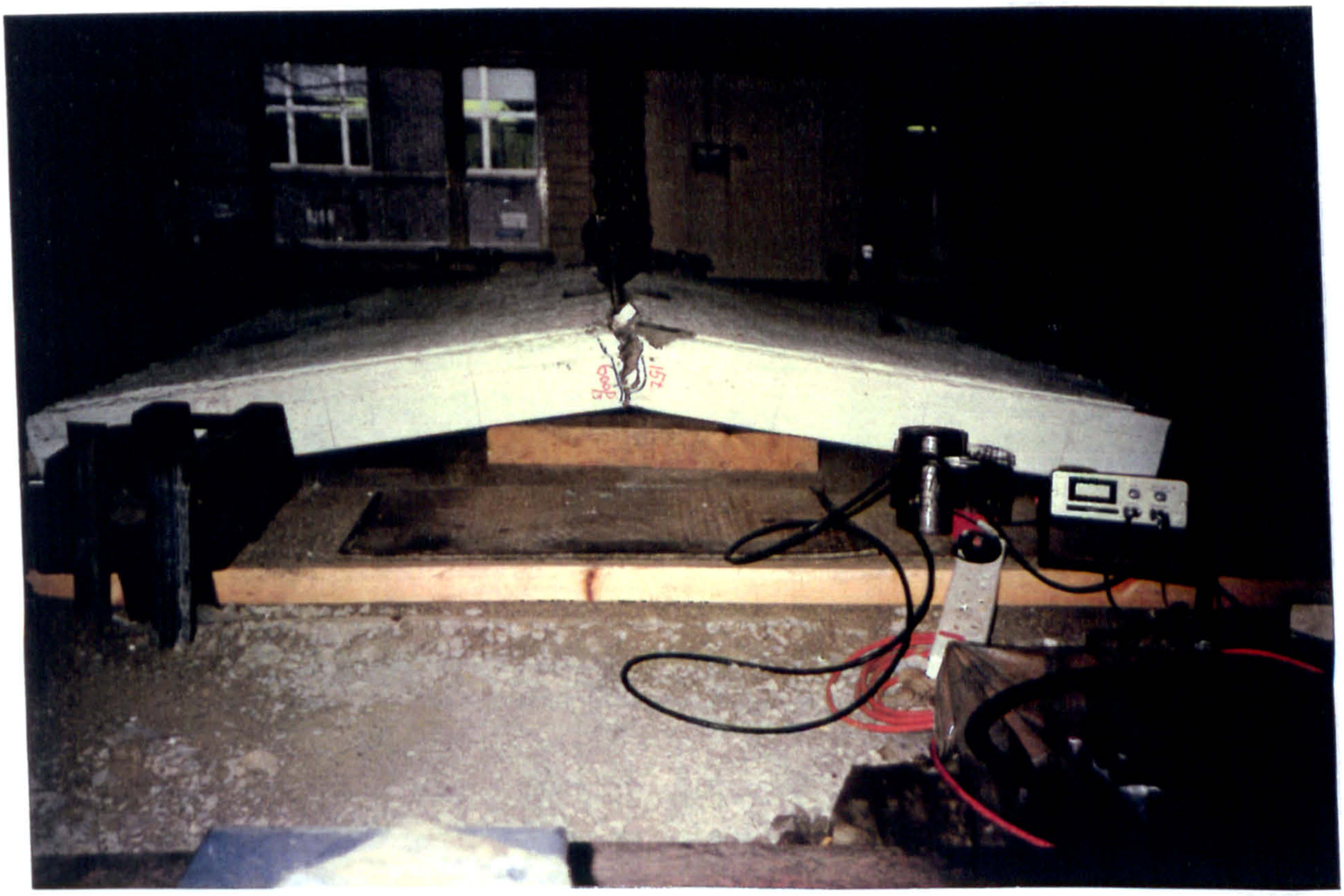

(a)

(b)

PLATE 6.4 : Lifting the Failed Raft of Steel Fibre in Parts - Module M2

(c)

(d)

PLATE 6.4 : Lifting the Failed Raft of Steel Fibre in Parts - Module M2 (cont.)

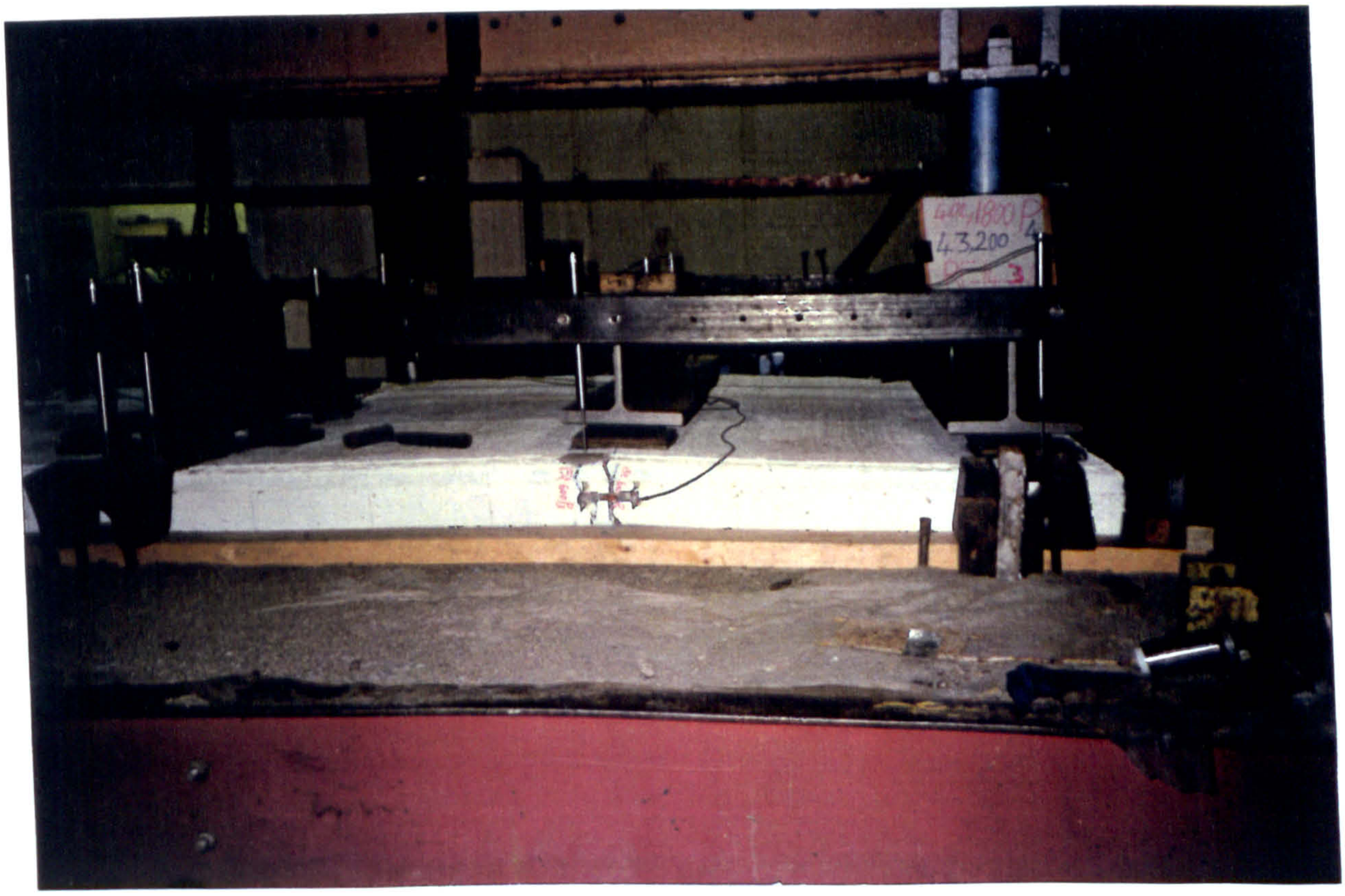

PLATE 6.5 : Effect of Main Transverse Crack in Reducing Uplift Deflection Due to Loading P4 of Raft RSF - Module M2

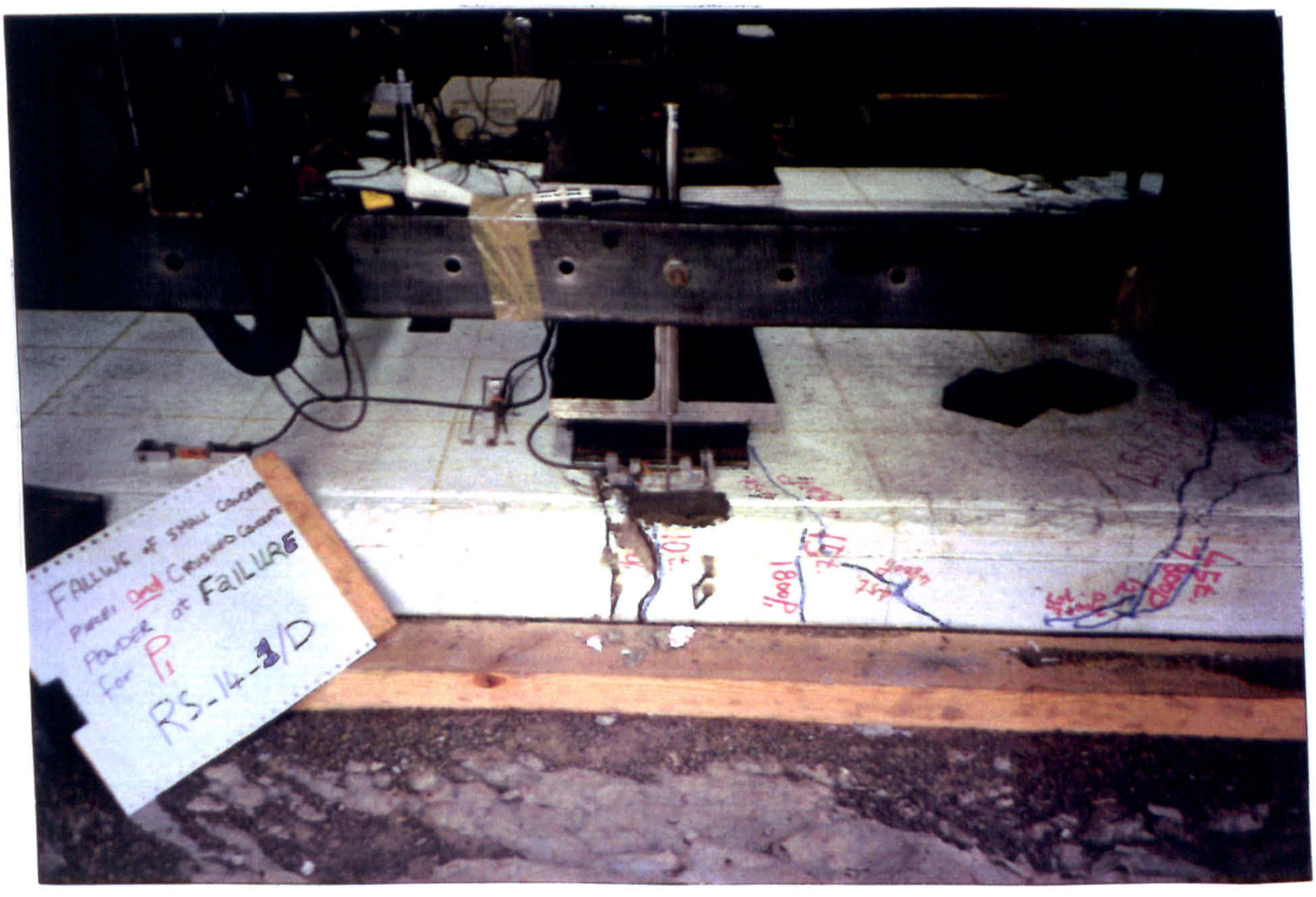

PLATE 6.6 : Falling of Small Concrete Pieces From a Cracked Section at Failure of P1 - Raft RS1

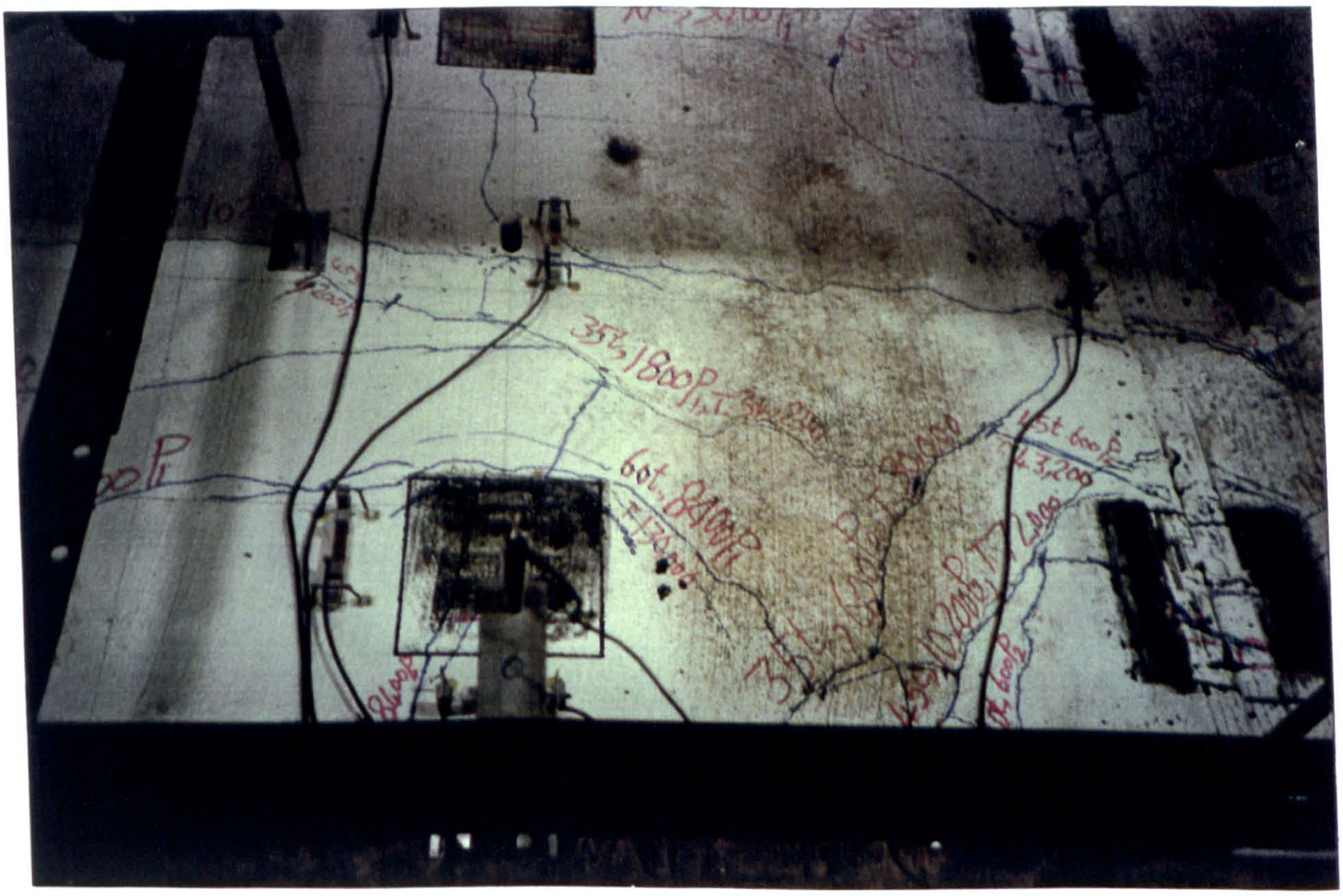

(a) Position P1

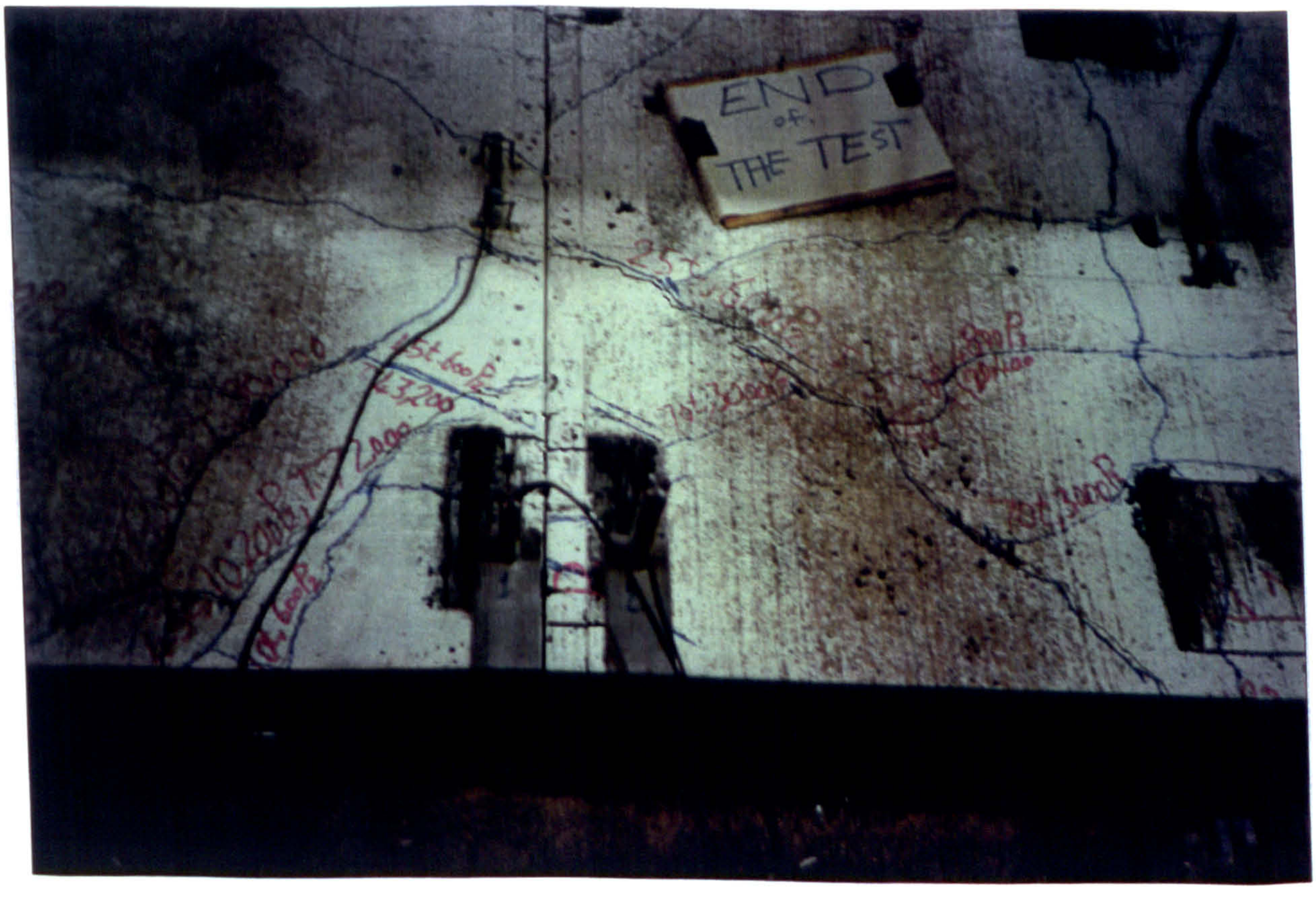

(b) Position P2

PLATE 6.7 : Punching Shear Failure at P1 and P2 of Raft RS1, Module M2

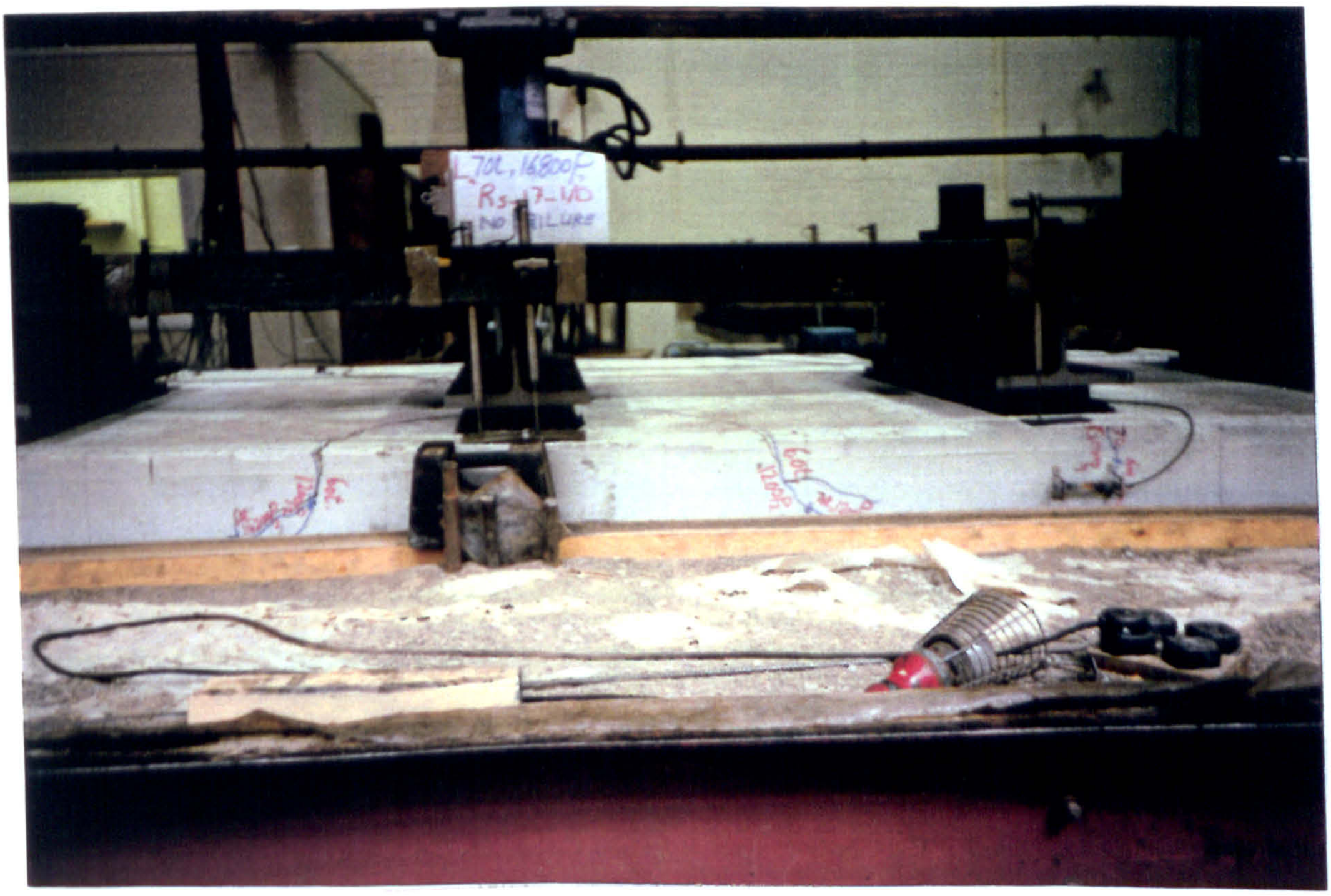

PLATE 7.1 : Crack Patterns - Cross Corner at P2 for RS7 - Module M3

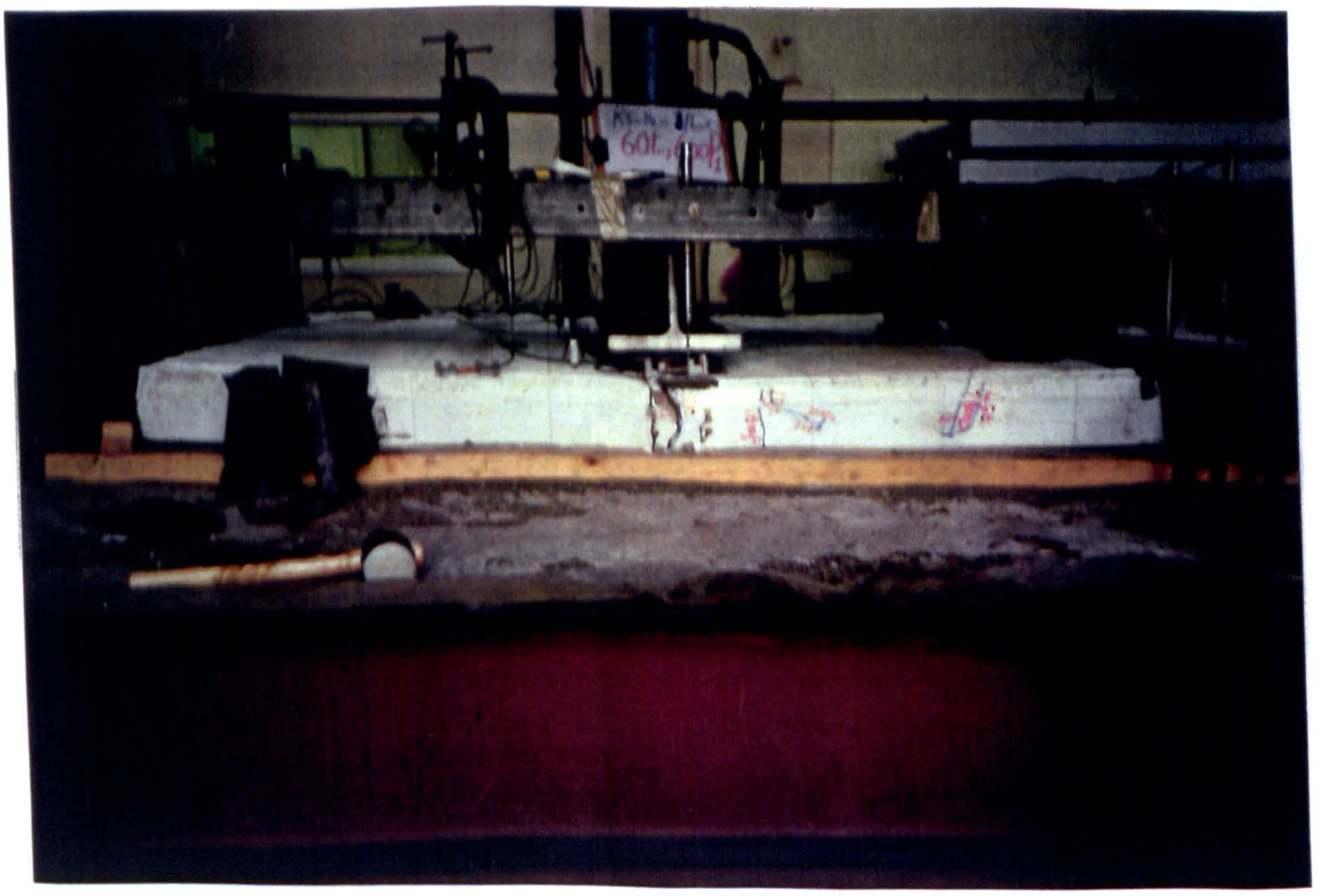

PLATE 7.2 : Fatigue Fracture Failure at P1 of Raft RS1 - Module M3

PLATE 7.3 : Combination of Punching Shear and Fatigue Fracture Failure at P3 of Raft RS1 - Module M3

PLATE 7.4 : Cross Corner Crack at the Joint Interface